Aalborg University
The Study Board for Civil Engineering
Indoor Environmental Engineering, 9th - 10 th semester

Natural ventilation in hospitals

Aabenraa Hospital

Grantham Hospital

Maria Lejsgaard Myrup
Jesper Lundgaard Olesen

2007/2008

Aalborg University
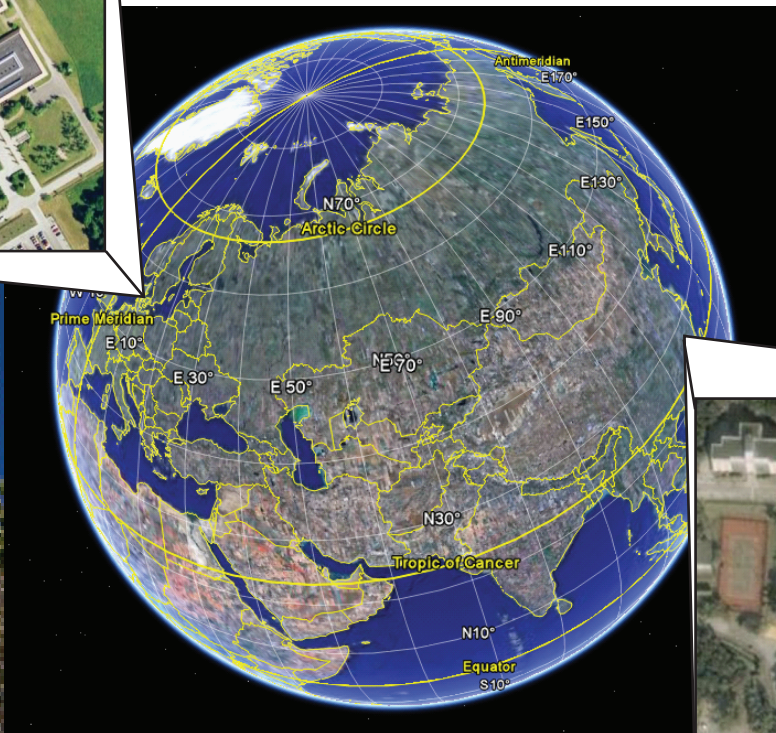
Title:

Natural ventilation in hospitals

Project period:
Master thesis
Indoor Environmental Engineering
September 2nd 2007 - June 11th 2008

Group members:

—————————————

Maria Lejsgaard Myrup

—————————————

Jesper Lundgård Olesen

Supervisor:
Per Heiselberg
Peter V. Nielsen

Co-supervisor:
Yuguo Li
The University of Hong Kong
Hong Kong

Copies: 6

Page count: 416

Abstract:

The aim of this project is to investigate the possibility of using natural ventilation for hospitals.
For the project are looked further into the possibility of using natural ventilation especially for isolation rooms in hospitals. The calculations are based on two cases; Aabenraa hospital in Denmark and Grantham hospital in Hong Kong.
For both Aabenraa and Grantham hospital it is investigated that with the actual layout of the isolation room the natural driving forces are not strong enough to ensure a minimum air change rate of 12 h^{-1} all the time. To ensure a high enough air change rate are made minor changes of the layout of the isolation room and there are used hybrid ventilation.
With local weather data it is calculated from multi zone models that for Aabenraa hospital only 6 % of the time the air change rate is below 12 h^{-1} and for Grantham hospital 5 % of the time after the changes.
For Grantham hospital was also made a CFD simulation to investigate the influence of the local mountain and sea breeze. With the changed layout of the isolation room the average air change rate according to mountain breeze was 37 h^{-1} and for sea breeze 18 h^{-1}.

Preface

This report is the product of the master thesis project *"Natural ventilation in hospitals"* at The Study Board for Civil Engineering with specialization in Indoor Environmental Engineering at Aalborg University. The report is prepared on the 9th - 10th semester from September 2nd 2007 to June 11th 2008.

The report is about using natural ventilation specially for isolation rooms in hospitals. The purpose is to investigate the possibility and reliability of using natural ventilation for isolation rooms to lower the costs compared to mechanical ventilation.

The project is a cooperation between Aalborg University and The University of Hong Kong.

The project is divided into a report, appendix and CD. The report include conditions for the calculations, methods of calculation, results and conclusions. The appendix include used theory and experimental results used for the report. On the CD the used programs and the project in pdf format are located.

References to figures, tables and equations are done by chapter number and number for the figure. For example figure 1 in chapter 2 state the number figure 2.1. References to sources are done by surname and the year for publication and stated in square brackets, for example [Jensen, 2003]. For internet pages the reference is done to the main page and the year for publication and stated in square brackets, for example [bsn.aau.dk, 2008]. The bibliography is placed at the back of the report.

Contents

Chapter 1

Problem statement

To minimize the spread of airborne infections in hospitals ventilation plays an important role. Since the outbreak of SARS in Hong Kong in 2003 the significance of ventilation became even clearer.

To ensure optimal ventilation rates especially in isolation rooms mechanical ventilation is normally used because it is reliable, and deliver a constant supply of outdoor air. One of the drawbacks with mechanical ventilation is the cost of the system. The average price of a bed in an isolation room is about HK$300.000. Because of the strict requirements for the ventilation system according to relatively high air change rates, the need for HEPA filters, negative/positive pressure rooms etc. add up to the cost of installing and running mechanical ventilation in isolation rooms. This means that only relatively small number of such rooms can be made available in a country and it is almost impossible for poor countries to have a sufficient amount of isolation rooms. [LI, 2007]

A way to make it possible to have more isolation rooms is by making the installation and running cost cheaper. This can be done by using natural ventilation instead of mechanical ventilation. Natural ventilation uses the natural forces such as wind pressure and temperature difference to get an airflow through the building where as mechanical ventilation uses a fan.

Since natural ventilation dependents on the weather conditions at the location it has been perceived that it is not as reliability as mechanical ventilation. The advantage of natural ventilation compared to mechanical ventilation is the costs for the systems.

The main purpose for this project is to look into the possibility of using natural ventilation for isolation rooms. The problem statement for the project is therefore:

"Is it possible to use natural ventilation for isolation rooms in hospitals?"

The problem statement include the following point:

- Is it possible to ensure the right airflow rate?

- Is it possible to ensure the ventilation efficiency?

- Is it possible to create the right airflow direction between rooms?

- Is it possible to secure a good comfort level in the isolation room?

The possibilities of implementing natural ventilation for isolation rooms in hospitals located in both Denmark and Hong Kong will be investigated and different solutions will be discussed. The calculations are based on the layout of Aabenraa hospital in Denmark and Grantham hospital in Hong Kong.

Both cases are based on the real layout of the hospital. First the reliability by implementing natural ventilation for the isolation room are discussed. Hereafter are made different solutions to improve the use of natural ventilation. Finally the application of natural ventilation for isolating rooms will be discussed.

The project will be divided into different phases:

- Analysis of different types of ventilation systems in hospitals in Denmark and Hong Kong

- Identification of challenges for implementing natural ventilation in hospitals

- Investigation of the effect of surrounding environments

- Investigation of the potential of implementing natural ventilation for isolation rooms in hospitals

- Design of isolation rooms with use of natural ventilation

Chapter 2

History

With the spread of tuberculosis in Denmark around 1900 the layout of the hospital and the amount of fresh air for the patients became very important. Around 1900 a medical treatment for tuberculosis did not exist and therefore patients with tuberculosis had to follow a treatment that included that the patient had to get a lot of fresh air and a nutrition treatment. The normal treatment included the following points:

- **Air treatment**, Accomplished by staying in fresh air

- **Rest treatment**, Accomplished by laying in a hall or on a veranda

- **Training treatment**, Accomplished by systematic prescribed walks

- **Nutrition treatment**, Aimed to get the single patient on a suitable weight

- **Tempering treatment**, Accomplished by showering and bath

[Vejlefjord, 2007]

Because of the high amount of fresh air for the patients the tuberculosis hospitals were normally located in areas close to a forrest or the water. With this location the air was not as contaminated as closer to the city and with the amount of fresh air necessary for the treatment this had great importance. [Vejlefjord, 2007] [PrivatHospitalet Skørping, 2007]

At the time mechanical ventilation was not installed in the hospitals to ensure enough fresh air for the patients. Therefore to ensure that the patients got enough fresh air many hospitals were designed with a veranda or a balcony. In the summertime the beds with the patients were removed from inside to the veranda or the balcony at dawn and back inside again at the dusk. An outside atrium and balcony with patients are shown in figure 2.1 and 2.2.

Figure 2.1: *Outside courtyard for patients to get fresh air. The bedbound patients were placed in the atrium in their beds. [avisen.dk, 2007]*

Figure 2.2: *Roofed balcony for the patients. [Nasjonalt medisinsk museum, 2007]*

Also hospitals in Hong Kong were designed with a balcony as showed for the Grantham hospital, founded in 1957, in figure 2.3.

Figure 2.3: *Balcony at Grantham hospital in Hong Kong.*

Normally the patients would stay at the hospital for about 6 months until they were at a stage where it was not possible to do anything more for them or they were as well as possible for the time being so they could go home again.

Because of the limited possibilities for mechanical ventilation at the time natural ventilation had great importance. The only way to get fresh air was by using natural ventilation. Already in 1900 it was clear that to reduce the risk for infections the airflow rate had to reach a high level. At the time the solution to this problem was by using natural ventilation and place the patients outside.

Today the treatment of patients with airborne infections has changed a lot and the use of natural ventilation do almost not happen anymore. The following chapter describe the design of a normal bed ward in a hospital in Denmark and Hong Kong today.

Chapter 3

Design of bed wards in hospitals

The purpose of the following chapter is to describe both the design of existing bed wards in hospitals and guidelines on how to design bed wards in both Denmark and Hong Kong.

3.1 Bed wards in Denmark

The average number of beds per bed ward for Denmark is 1,7, while the maximum number of beds per bed ward is for Regionshospitalet Silkeborg with 2,7 beds per bed ward and the minimum number is for Børne- og Ungdomspsykiatisk Regionscenter with 0,8 beds per bed ward [Indenrigs- og Sundhedsministeriet, 2007] .

Most often the bed wards are either located on both side of a corridor with access to the bed wards from the corridor as showed in figure 3.1 or with bed wards on just one side of the corridor and staff area on the other side.
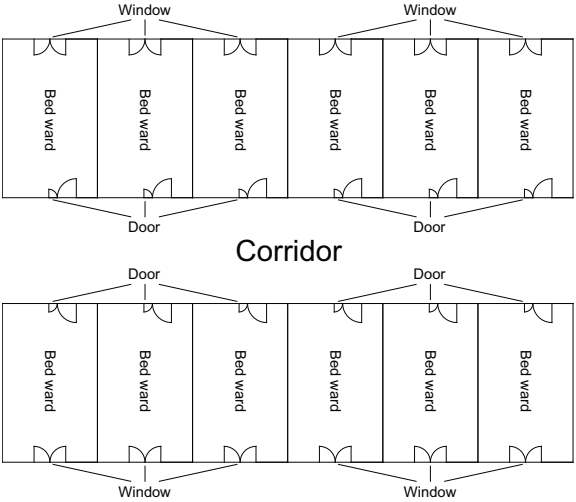
Figure 3.1: *Principle of location of bed wards as often normally designed.*

The bed wards are normally designed with the two beds beside each other as shown in

figure 3.2.

Figure 3.2: *Picture of a bed ward with two beds. [Region Nordjylland, 2007]*

3.1.1 Guidelines for bed wards

For bed wards in Denmark are more often only placed one bed [Larsen, 2007] . For the patients it means that it is possible to stay private and not get disturbed from other patients, and it is possible to get isolated from other ill people.

There are many guidelines that should be followed when a bed ward is designed. The guidelines are only made for normal bed wards and do not take isolation rooms into consideration. The guidelines are made for 1 and 2-bed bed wards where some of the characteristics are listed below:

- It is designed for 1 or 2 patients

- It is designed so it is possible to do some kind of standing and sitting care

- It is designed so it is possible to do manual lifting and lifting with a lift

- There is room for bed, bed table, dinner table and chair, armchair, sink and wardrobe

- There is room for one or two vehicles or other kind of facilities

- There is room for en extra long bed

- There is room to get around with toilet/bath chairs and other equipment

- It is functional

- There are good conditions according to ventilation, heat, sound, calling, alarm, hygiene etc.

- There are good communication conditions for the patients

- It is possible to have a private life and discretion

[Vejle Amt, 2003]

Two examples of a design of a 1-bed bed ward and a 2-bed bed ward from the guidelines are showed in figure 3.3 and 3.4.
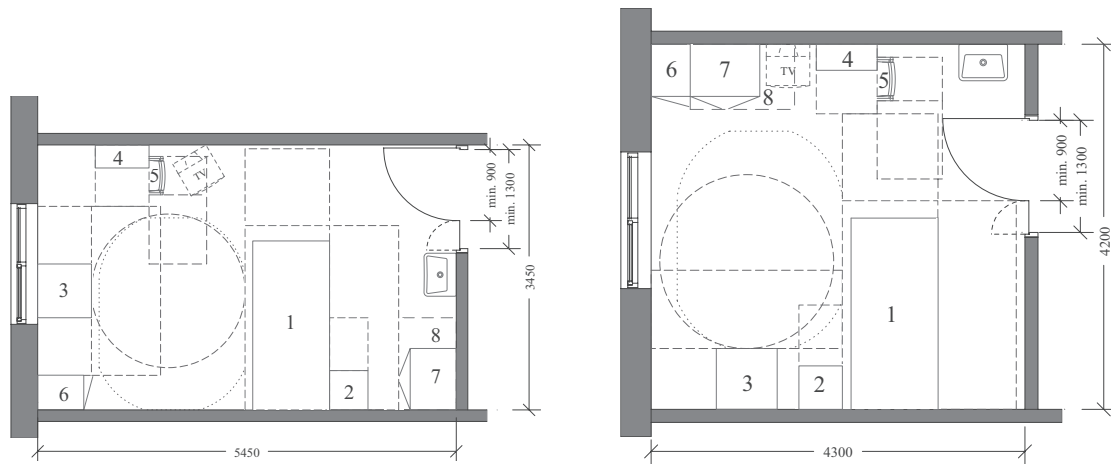
1. Bed, 2. Bed table, 3. Armchair, 4. Table, 5. Chair, 6. Wardrobe, 7. Cupboard for small facilities
8. Parking for transport and training equipment

Figure 3.3: *Examples of design of 1-bed bed ward. [Vejle Amt, 2003]*
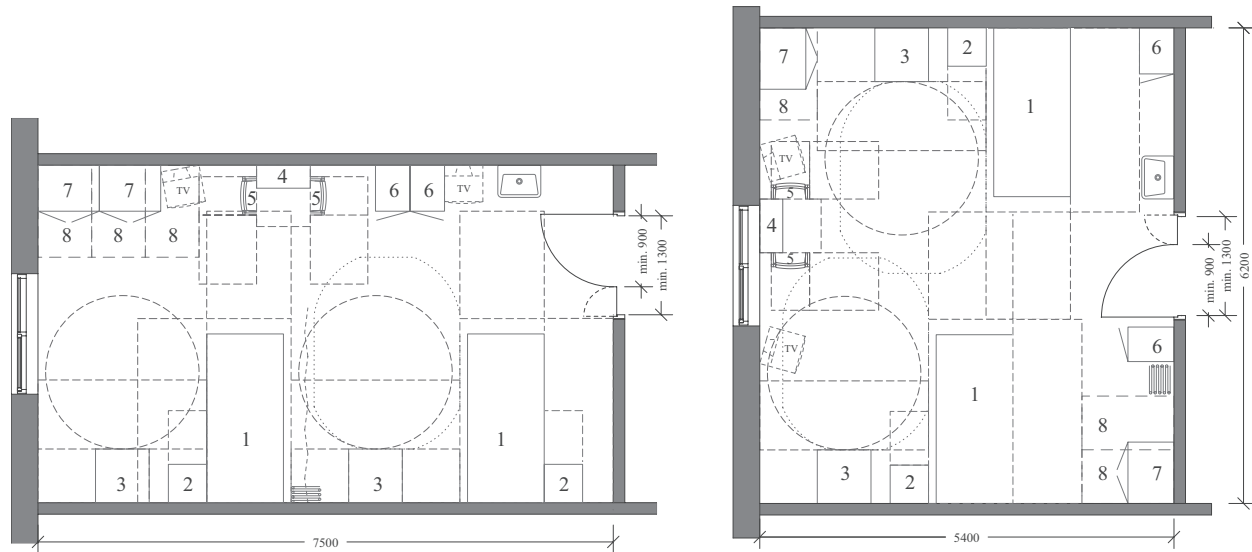
1. Bed, 2. Bed table, 3. Armchair, 4. Table, 5. Chair, 6. Wardrobe, 7. Cupboard for small facilities
8. Parking for transport and training equipment

Figure 3.4: *Examples of design of 2-bed bed ward.   [Vejle Amt, 2003]*

From figure 3.3 and 3.4 it is showed that the bed is located closer to the door and to the corridor than to the window. For designing an isolation room with natural ventilation the best location of the bed is close to the window, so contaminated air is let direct to the outside without crossing other people. To make an isolation room the ventilation system especially has to be taken into consideration. The air change rate per hour and the airflow has to be decided to avoid the spread of contaminant from one patient to another.

3.2   Bed wards in Hong Kong

Compared to Denmark the number of beds for a normal bed ward in Hong Kong is higher. For a normal bed ward the number of beds per ward is about 6-8 compared to about 1-2 for Denmark [Canossa Hospital, 2004] . The beds are normally located opposite each other with the head of the bead closest to the wall as showed in figure 3.5.

Figure 3.5: *Examples of design of 7-bed bed ward. [Canossa Hospital, 2004]*

Because of the resent outbreak of SARS and the higher amount of infected persons with tuberculosis there are designed a greater amount of bed wards with only one or two beds for the purpose of isolations rooms. In table 3.1 are listed the numbers of bed wards with 1, 2 and 4 beds per room for the 9 major acute hospitals in Hong Kong.

Table 3.1: *Number of beds for the 9 major acute hospitals for handling of confirmed and suspected SARS patients. [Health, Welfare and Food Bureau, 2003]*

Hospital	Rooms for confirmed SARS patients No. of beds in room			Rooms for suspected SARS patients No. of beds in room		
	1	**2**	**4**	**1**	**2**	**4**
Princess Margaret Hospital	12	0	24	4	16	12
Tuen Mun Hospital	0	0	12	25	30	14
Alice Ho Miu Ling Nethersole Hospital	2	6	8	42	3	7
Queen Elizabeth Hospital	4	16	0	12	36	10
United Christian Hospital	4	0	12	4	24	0
Pamela Youde Nethersole Eastern Hospital	4	5	9	20	2	12
Queen Mary Hospital	0	11	8	2	0	11
Prince of Wales Hospital	0	8	8	12	24	0
Kwong Wah Hospital	2	0	12	14	6	27

From table 3.1 it is shown that the number of bed wards with only one bed differ from the different hospitals and also for the case if the person is confirmed or suspected SARS patient. From the table it is also seen, that isolation rooms for SARS patients do not always only cover one patient but up to 4 patients in the same room.

As showed in table 3.1 the number of isolation rooms for SARS patients is higher than

the number of isolations rooms for Denmark.

The common design of the hospital in Hong Kong is a narrow hospital where there either are located bed wards on either side of a corridor as for Denmark showed in figure 3.1, or there are located only one room connecting both sides of the floor as showed in figure 3.6.
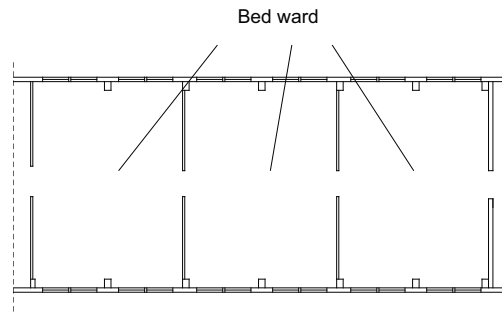
Figure 3.6: *Principle for design of 8-bed bed ward in Hong Kong*

Most of the hospitals in Hong Kong are located between other building and are high rise buildings as the surrounding buildings.

3.2.1 Guideline for isolation room

For the isolation rooms are some strict requirements. Below are listed some design guidelines for isolation rooms. General for both negative and positive isolation rooms are:

- Air handling systems

    - Prevention of air leakages
    - Pressure differentials (negative, positive, neutral)
    - At least 12 air changes per hour

- Rooms

    - Separate bathroom preferred
    - Well-sealed approximately $0,05\ m^2$ leakage
    - Small gap of $1,3\ cm$ under door for sufficient airflow path
    - Monitoring

- Anteroom

    - Can be waived if there is a high quality negative pressure room with robust ventilation system and good pressure differential
    - To ensure appropriate air-balance relationships, help to reduce the escape of droplet nuclei during opening and closing of isolation room door

– Also useful prompt to good infection control technique

– Masking and unmasking should take place in the anteroom

Specially for positive and negative isolation rooms are stated:

Negative pressure isolation rooms:

- Greater exhaust than supply air

- Pressure difference of 2, 5 Pa

- Windows do not open

- Requirements

    – Clean to dirty airflow ie direction of the airflow is from the out side adjacent space (eg. corridor, anteroom) into the room

    – Air from room preferably exhausted to the outside, but may be recirculated if provided through HEPA filter

    – Personal protective equipment for personnel entering these rooms

Positive pressure isolation rooms:

- Greater supply than exhaust air

- Pressure differential of 2, 5–8 Pa, preferably 8 Pa

- Positive airflow relative to the corridor (ie airflows from the room to the outside adjacent space)

- HEPA filtration, if the air is returned

[Asian Intensive Care, 2007]

To avoid the spread of disease in the hospital it is imported that there is the right pressure in the hospital especially in the isolation rooms. The pressure difference is used to control the direction of the airflows.

3.3 The direction of the airflows in the hospital

The idea of the direction airflows in the hospitals is that the air should flow from places with least contaminated air towards places with more contaminated air. To control the air and make sure it always take that path it is necessary to pressurizing the rooms in the hospital's wards. A pressurized room can either have a positive or negative pressure. If there is a positive pressure in a room it is not possible for the air outside the room to get into the room and if there is negative pressure in the room it should not be possible for

the air inside the room to escape it.

To fulfil the idea of how the air should move in the hospital the offices in the ward where the personal stays is supplied with air and air is extracted into the rooms where the patients lies, as shown in figure 3.7.
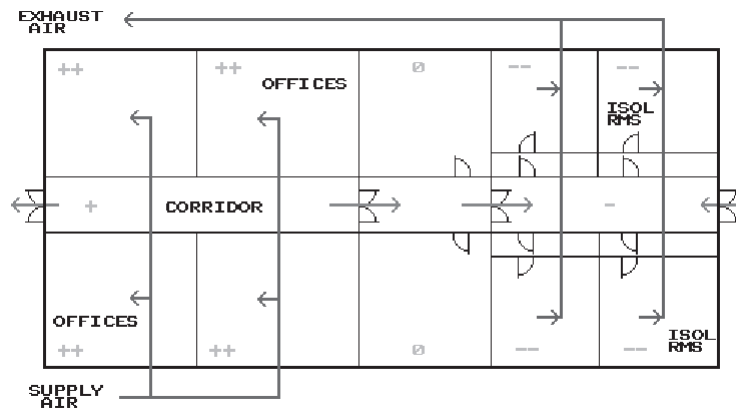
Figure 3.7: *Airflow in a hospital ward [Kowalski, 1996]*

The isolation rooms in the hospital should always be pressurized. Whether the pressure is positive or negative compered to the surroundings depends on the patients who are hospitalized in the isolation rooms. If the patients are particular week and vulnerable to diseases the isolation rooms should have a positive pressure to keep out the pathogenic microorganisms from the surrounding areas, as shown in figure 3.8.
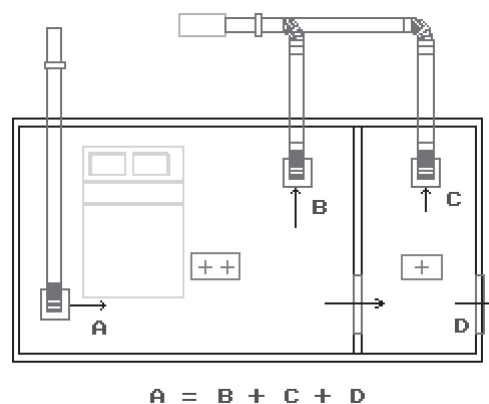
Figure 3.8: *An isolation room with an anteroom that has a positive pressure. The airflows out of the isolation room this means the supply air,A, is equal to the air out of the room B,C and D. [Kowalski, 1996]*

If the patients instead are a sources to airborne diseases the isolation rooms should have a negative pressure to avoid the spread of diseases to the rest of the wards, as shown in

figure 3.9.
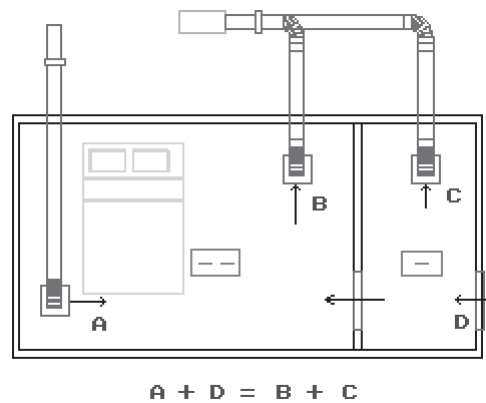
Figure 3.9: *An isolation room with an anteroom that has a negative pressure. The airflows into the isolation room and is exhaust in both the isolation room and the anteroom this means the supply air,A and D, is equal to the air exhaust out of the rooms B and C. [Kowalski, 1996]*

In both cases the idea of air going from a cleaner place to a dirtier place is kept. The anteroom could of cause also have been applied a lower pressure then the corridor and the isolation room. Hereby it would make sure that any contamination entering the anteroom would be exhausted. The anteroom could also have been applied a higher pressure than the corridor and the isolation room. This would mean that no contamination would entering the anteroom.

If the isolation room contains a patient that is a source of an airborne disease the air should move away from the personnel and the other way around if the person is very sensitive towards diseases. This is in the first case done to protect the personnel and in the other case to protect the patient.

If natural ventilation is used it might not be possible to create a constant negative and positive pressure as by mechanical ventilation. This means that it is a great challenge to design a natural ventilation system for a hospital that always will create a sufficient airflow going in the right direction. In the following chapter are an introduction to the spread of infections in hospitals and in chapter 5 are described possibilities of using natural ventilation for isolation rooms and the advantages and disadvantages for natural ventilation.

Chapter 4

Infections in hospitals

In this chapter are an introduction to how infections can happen in hospitals and especially airborne infections. Based on this analyze some solutions are listed on how airborne infections can be avoided.

4.1   Infections

Infections in hospitals is costed by pathogenic organisms. Pathogenic organisms is a therm that covers all disease producing microorganisms. The pathogenic organisms will either be endogenous bacteria which are bacteria from the patient, exogenous bacteria, viruses or fungus. Of these the most dangerous airborne diseases would be tuberculosis and SARS. [Chaddock, 1986]

Most often the infections in hospitals are coursed by endogenous bacteria or exogenous bacteria transferred by contact and therefore not by any airborne pathogenic organisms. This means that there are many infections and diseases in the hospitals that can not be avoided only by the use of ventilation.   [Chaddock, 1986]

A disease coursed by an airborne pathogenic microorganisms normally happens when an infected patient sneezes or coughs and thereby sends out thousands of droplets carrying the pathogenic microorganisms. The largest of the droplets falls to the ground before they evaporate whereas the smaller droplets will evaporate extremely fast in the air into droplet nuclei. The pathogenic microorganisms therefore soon disperse into the atmosphere. Under normal calm conditions it will take a droplet nuclei with a diameter of 2 μm 4,4 hour to fall 2 m. This means that when droplets nuclei are affected by an external force from for instance the ventilation system it is possible for it to travel far around in the hospital. [Beggs, 2002]

4.2   Control of the airborne infection

Since it is possible for the droplets nuclei to travel far around in the hospital they could easily course harm to the people, and especially the patients in the hospital are particularly

vulnerable to the airborne diseases. To avoid that people in the hospital gets infected by air that is polluted with pathogenic microorganisms it is very important to control the concentration of pathogenic microorganisms in the air and the airflows in the building.

The concentration of pathogenic microorganisms in the air can be controlled by diluting the air with fresh air. To save energy it can be an advantage to recirculate some of the air but it require that the finest filter the air is passing through is a HEPA filter where 99,997 % of the pathogenic microorganisms will get trapped.

Displacement ventilation can also be used to ventilate the wards in the hospital. The advantage with displacement ventilation is that the forces from buoyancy and gravity will keep the droplet nuclei concentrated in one layer of the air and hereby not spreading into all the air. This can also be a huge disadvantage because if a healthy person gets into contact with this layer the person will be exposed to a high concentration of the airborne pathogenic microorganisms. Therefore it is necessary to be particulary observant when it is chosen to use displacement ventilation in area containing dangerous airborne diseases.

Another way to minimize the concentration of airborne pathogenic microorganisms is by killing them. This can be done by exposing them to UV irradiation for a sufficient amount of time. The UV irradiation will destroy the pathogenic microorganisms DNA and thereby kill them. The advantage by using the ultraviolet germicidal irradiation field in connection with recycling, the air is that it produce a much smaller pressure drop than the HEPA filter. Hereby it is possible to install a smaller air handel unit that will produce less noise. [Limb, 2002]

Chapter 5

Natural ventilation for isolation rooms

The purpose of the following chapter is to describe the possibilities of using natural ventilation for isolation rooms and which problems this may cause.

The air change per hour for isolating rooms are stated to be 12 h^{-1}. The design criteria for isolation rooms are shown in table 5.1.

Table 5.1: *Design criteria for isolation rooms.* *[ASHRAE, 2003]*

Function	Pressure relationship to adjacent areas	Minimum air changes of outdoor air per hour [h^{-1}]	Minimum total air changes per hour [h^{-1}]	All air exhausted directly to outdoors	Air circulated within room units	Relative humidity [%]	Design temperature [$°C$]
Airborne infection isolation room	Negative	2	12	Yes	No	-	21,1-23,9

From table 5.1 it is seen that the design criteria for isolation rooms are 0strict. The minimum air changes of outdoor air per hour stated in the third column describes the minimum air changes of outdoor air for the room to cover ventilation comfort and odor control. The minimum total air changes per hour state the total minimum air change per hour for the room including the air changes of outdoor air per hour. This air change per hour can be established by both natural and mechanical ventilation. [ASHRAE, 2003]

For the isolation rooms there has to be a negative pressure. It is listed that the exhausted air has to be let direct to the outdoors. If it is not possible to let the exhaust air direct to outdoors this has to be returned through a HEPA filter to an air-handling system

that only service the isolation room. From the table it is also seen that it is not possible to recirculate the air within the room. The temperature for the isolation room has to be between $21, 1 - 23, 9 \, ^\circ C$. Because of the strict criteria for the isolation rooms and the fact that it has to be under pressure mechanical ventilation is normally used for ventilation the rooms.   [World Health Organization, 2007] .

To reduce the risk of infection from one patient to another patient the air change rate per hour has a great influence. In figure 5.1 are listed information about the concentration of droplet nuclei in an enclosed isolation room at different rates and duration of ventilation. For the calculation are made some assumptions:

1. The air change rate remain constant

2. The concentration of droplet nuclei in the enclosed space is uniform
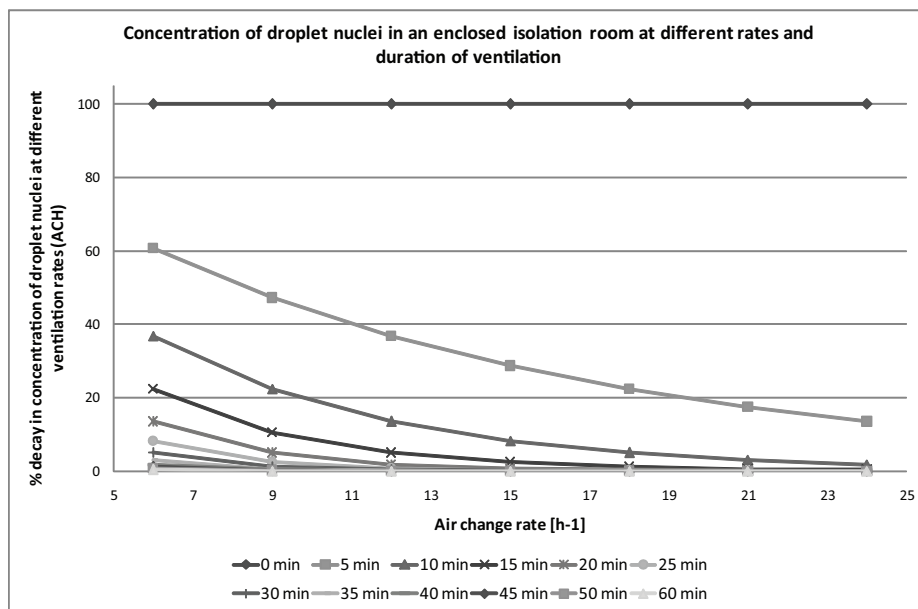
Figure 5.1: *Concentration of droplet nuclei in an enclosed isolation room at different rates and duration of ventilation.   [World Health Organization, 2007]*

From figure 5.1 it is seen that by increasing the ventilation from 12 h^{-1} to 15 h^{-1} the decay in concentration of droplet nuclei gets reduced from $36, 8$ % to $28, 7$ % for a duration of the ventilation of 5 minutes. This shows the great importance of air changes per hour for an isolation room.

5.1   Advantage and disadvantage

To ventilate the hospital there are three main principles:

Mechanical ventilation For mechanical ventilation there are installed fans to create the airflow trough the building. Mechanical ventilation can be combined with air conditioning and filtration systems which is normally done for hospitals and the rooms are pressurized to control the airflow.

Natural ventilation Natural ventilation uses the principle of natural driving forces as thermal buoyancy and wind pressure.

Hybrid ventilation Hybrid ventilation combines mechanical ventilation and natural ventilation. Hybrid ventilation can be installed in different ways.

The main problem with natural ventilation compared to mechanical ventilation is the reliability of the ventilation rate. With mechanical ventilation it is possible to control the ventilation rate and make sure that the exactly amount of air gets trough the room. With natural ventilation the ventilation rate depend on the outside conditions and the location of the building. For natural ventilation it is therefore not possible to control the ventilation rate in the same way as for mechanical ventilation.

The temperature of the inlet air for natural ventilation also depend on the temperature of the outside air. If the air is let directly into the room trough a window without any preheating there will for cold climates be a possibility of cold draught by using natural ventilation. To avoid this problem a solution could be to preheat the air before it is let into the room. Mechanical ventilation is not affected by the outside conditions in the same way because it is possible to preheat and cool the air and is therefore suitable for all weather conditions. To avoid that it gets too cold in the room a suggestion could be to use heat recovery. To avoid any spread of contaminant air there should be a heat recovery unit for every single room because of leakage in the unit.

Because of the natural driving forces the location of the room in the building compared to the wind direction and the temperature in the building has to be taken into consideration to create the desired pressure relation in the room. Because it is possible to control the pressure with mechanical ventilation it is easier and the location of the room do not have any big influence on mechanical ventilation. With mechanical ventilation it is also possible to create a constant pressure for the hole time, with natural ventilation this may variate with the temperature, wind speed and direction.

A benefit for natural ventilation is the cost by both installing it and maintenance. For mechanical ventilation the costs by installing and maintenance are high compared to natural ventilation.

For the occupants in a room it is possible to control the environment in a simple way just by opening a window. For mechanical ventilation this is not possible. To control the environment by mechanical ventilation requires expertise. If a window gets opened when the room is mechanical ventilated this can effect the ventilation rate for the room because it is not designed for natural ventilation and it is therefore not reliably anymore.

It table 5.2 are shown some advantages and some disadvantages for mechanical ventilation and natural ventilation.

Table 5.2: *Advantages and disadvantages for mechanical and natural ventilation. [World Health Organization, 2007]*

| | Ventilation system | |
	Mechanical ventilation	Natural ventilation
Advantages	Suitable for all climates and weather	Lower capital, operational and maintenance costs
	More controlled and comfortable environment	Capable of achieving very high ventilation rate for immediate complete removal of indoor pollutants
	Heat recovery	Possible control of environment by occupants
Disadvantages	Expensive to install and maintain	More difficult to predict, analyze and design
	Requires expertise	Reduces comfort level of occupants when weather is hostile, i.e. too hot, humid or cold
		Risk of exposure to insects or vectors

5.1.1 Operation safety

As listed in section 5.1 there are both advantages and disadvantages with natural ventilation. Some of the major concerns with natural ventilation are:

- The air change per hour is variable with natural ventilation

- It may not be possible to establish a constant pressure difference in an isolation room with natural ventilation

- Controlling the direction of the airflow

From different measurements it is shown that by natural ventilation it is possible to exceed an air changes rate higher than 12 h^{-1}. Two different measurements are shown in

table 5.3 and 5.4.

Table 5.3: *Air change per hour for naturally ventilated clinical rooms in Lima, Peru.* *[Escombe et al., 2007]*

Room condition	Wind speed	
	$< 2 \frac{m}{s}$ ACH $[h^{-1}]$	$> 2 \frac{m}{s}$ ACH $[h^{-1}]$
Closed	2,7	4,1
Partially open	14,1	53,1
Fully open	46,6	82,3

Table 5.4: *Air change per hour for naturally ventilated rooms in China, Hong Kong SAR.* *[World Health Organization, 2007]*

Room condition	ACH $[h^{-1}]$
Completely open window and open door	29,3-93,2
Completely open window and closed door	15,1-31,4
Half-open window and closed door	10,5-24
Closed window and open door	8,8

From table 5.3 and 5.4 it is seen that by natural ventilation it is possible to create an air change rate per hour that extent the prescribed air change rate per hour of 12 h^{-1}. It is shown that only when the window is closed it is not possible to create high enough air change per hour. The calculated air change per hour depend on the location of the room because of the different weather conditions. Therefore the air change per hour may be different for other locations. The air change rates listed in table 5.3 are high compared to the air change rates listed in table 5.4 this can be according to the different climate but also because of different measurement methods. Table 5.3 also shows that the air change rate when the doors and windows are closed are $2, 7 - 4, 1$ h^{-1} this shows that the building is quiet leaky. The Danish Building Regulation state that the leakage for a building with a pressure of 50 Pa may not be higher than $1, 5$ $\frac{l}{s}$ per m^2 heated floor area. From the measurement from Peru it is listed in table 5.3 that the air change rate with closed doors and windows is $2, 7-4, 1$ h^{-1} this means that the leakage will be between $2, 3-3, 4$ $\frac{l}{s}$ per m^2.

As stated in table 5.1 the pressure relationship to the adjacent areas is supposed to be negative for isolation rooms. By natural ventilation it may not be possible to create a constant pressure difference as by mechanical ventilation. To avoid the spread of airborne infection the isolation rooms can be designed for a desired airflow. Figure 5.2 shows an isolation room designed for an airflow going from patient to areas free of transit.
From figure 5.2 it is seen that the airflow is supplied to the room through the door and out through the windows and the toilet exhaust. In this way the air containing pollutant
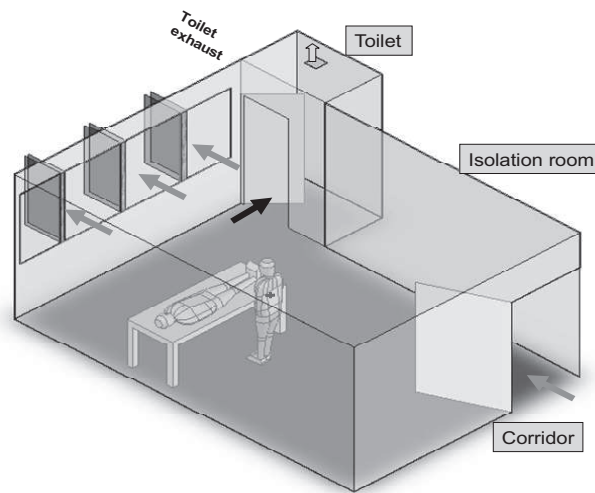
Figure 5.2: *Isolation room designed for a desired airflow from patient to areas free of transit.* *[World Health Organization, 2007]*

is let away from areas with people.

To avoid the spread of pollutant air even further the location of the isolation rooms in the hospital has to be taken into consideration. For the best protecting the isolation rooms should be placed in an area away from other patients and with good exposure to the surroundings. The air from the rooms should be let out to areas that are not often used by people. The patient should be placed in the isolation room as close to the exterior wall as possible and close to a window to avoid the pollutant air to cross the room. [World Health Organization, 2007]

To avoid that the patients are getting infected by other illnesses from disease-carrying insects mosquito nets can be used for the windows.

In chapter 8 are listed some ideas on how to implement natural ventilation for isolation rooms.

5.2 Costs

Because of the strict requirements for isolation rooms as listed in table 5.1 the costs for an isolation room is high. After the SARS outbreak in Hong Kong in 2003 the Hong Kong government spent more than HK\$410 million to retrofit 500 negative pressure isolation rooms. The cost for a single room was HK\$800 000 and for a single bed HK\$300 000. The isolation rooms also consume more energy than general hospital wards do. [LI, 2007]

Because of the high cost for isolation rooms it can be difficult for recourse-limited countries to install these kind of rooms. For other countries the high cost for isolation rooms

means that it is only possible to create a small number of these rooms. For Aalborg hospital there are only installed 2 isolation rooms [Aalborg Sygehus, 2007] .

A way to lower the costs for isolation rooms could be by using natural ventilation instead of mechanical ventilation. The costs of installing natural ventilation compared to mechanical ventilation is shown in figure 5.3.
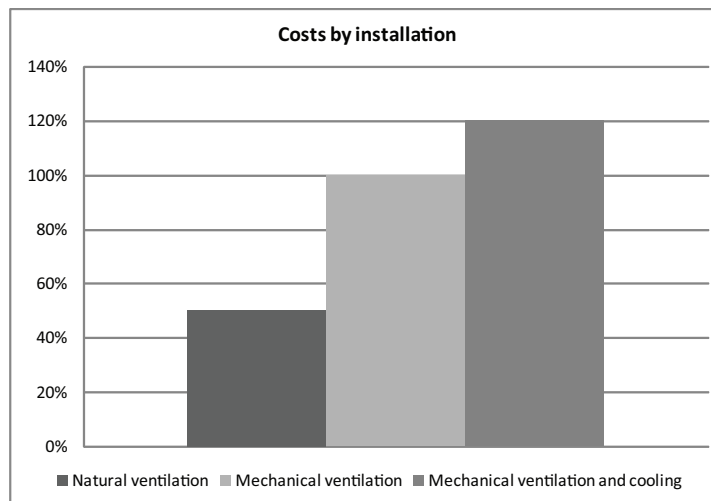
Figure 5.3: *Costs by installation for natural and mechanical ventilation. [Window Master, 2007]*

It is shown in figure 5.3 that generally the cost for mechanical ventilation compared to natural ventilation is twice as high. The graph only show the general costs by installation, because of the high energy demand for isolation rooms the costs can be a bit different to figure 5.3. In figure 5.4 are the running costs for natural and mechanical ventilation showed.
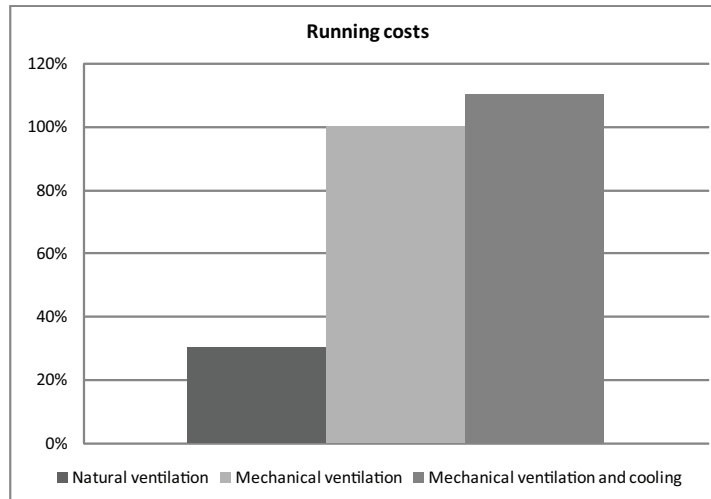
Figure 5.4: *Running costs for natural and mechanical ventilation. [Window Master, 2007]*

From figure 5.4 it is seen that the running costs for natural ventilation is only 30 % of the cost for mechanical ventilation in general. As for the costs of installation the running costs from figure 5.4 may be different for the isolation rooms because of the strict requirements for these.

From the two figures it is showed that in general the costs by natural ventilation compared to mechanical ventilation are about 30-50 % of mechanical ventilation. By using natural ventilation for isolation rooms the costs thereby reduces and it may be possible for recourse-limited countries to install isolation rooms too.

The costs showed in the two figures figure 5.3 and 5.4 are typical for office buildings, therefore there will be a difference to a hospital building. The requirements for mechanical ventilation in special for isolation rooms in a hospital is a lot higher compared to an office building because of the risk of airborne infections, therefore also the costs for mechanical ventilation in hospitals compared to office buildings may be higher. The difference in costs between natural and mechanical ventilation may therefore be greater than shown in the figures. The figures do only give a rough idea about the costs for mechanical ventilation compared to natural ventilation.

5.3   Geographical location and design

Natural ventilation uses the principle of natural driving forces such as thermal buoyancy and wind. According to the geographically location of the hospital this makes some difficulties. For natural ventilation the natural driving forces have a great influence to create the desired ventilation flow in a room or building. For the indoor environmental quality the outside temperature do have great influence because if the air is too cold this can create cold draught and if the air is too hot this can cause that the temperature in the room gets too high. Also the pollutant level in the outside air does have influence on the indoor air

quality. Therefore the weather conditions at the location of the building has to be taken into consideration.

5.3.1 Denmark

The weather conditions for Denmark are measured in the Danish Reference Year, DRY. The weather data in DRY are collected from a 30 year period from 1961-90 and holds information about air temperature, radiation, cloud cover, wind direction, wind speed, air pressure, rain, relative humidity, time etc.

Because of the location of Denmark at 55.66N and 12.57E specially in wintertime the weather becomes pretty cold. In figure 5.5 and 5.6 are the temperature during the year showed.
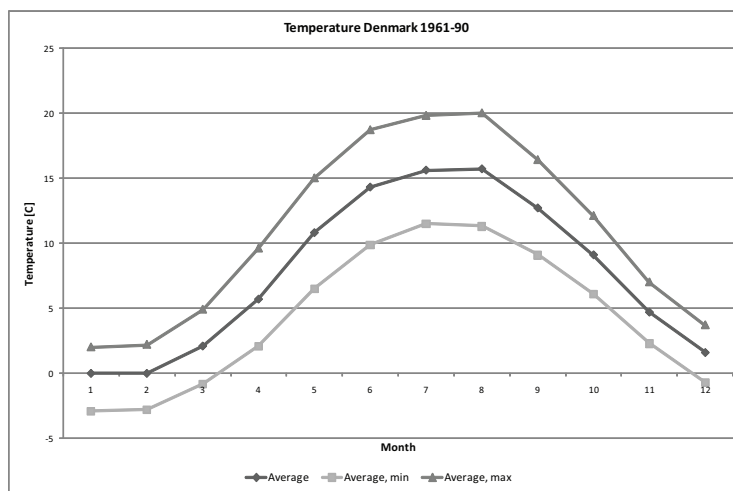
Figure 5.5: *Temperature for Denmark during the period 1961-90. [DMI, 2007]*
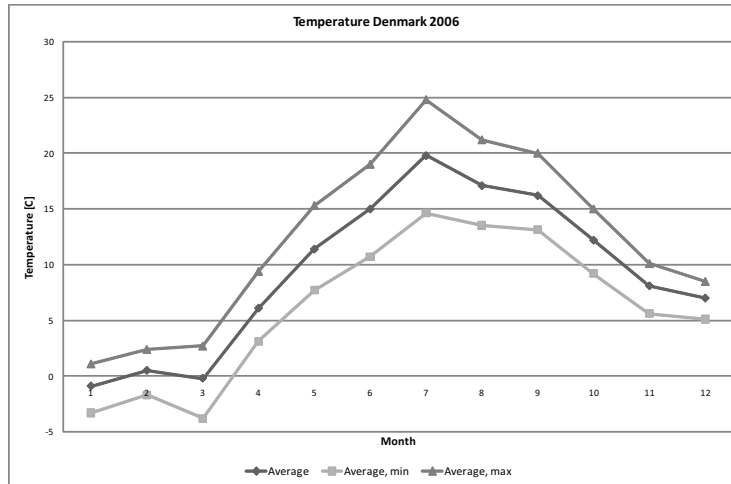
Figure 5.6: *Temperature for Denmark in 2006. [DMI, 2007]*

From the two figures it is shown that the temperature for Denmark during summer rises to a temperature between $10 - 15\ ^{\circ}C$ and for winter the temperature is between $0 - 5\ ^{\circ}C$.

Specially during wintertime draught can be a problem when natural ventilation is used because of the low temperature in Denmark. Therefore it can be necessary to preheat the air before it is let into the room. Because of the higher temperature during summertime draught is not a problem in the daytime. For the summertime the problem can be when the temperature rises a temperature higher than $23,5\ ^{\circ}C$ because the air temperature then gets too high.

When using natural ventilation the wind direction and speed also need to be taken into consideration. In figure 5.7 are shown the wind speed for Denmark.
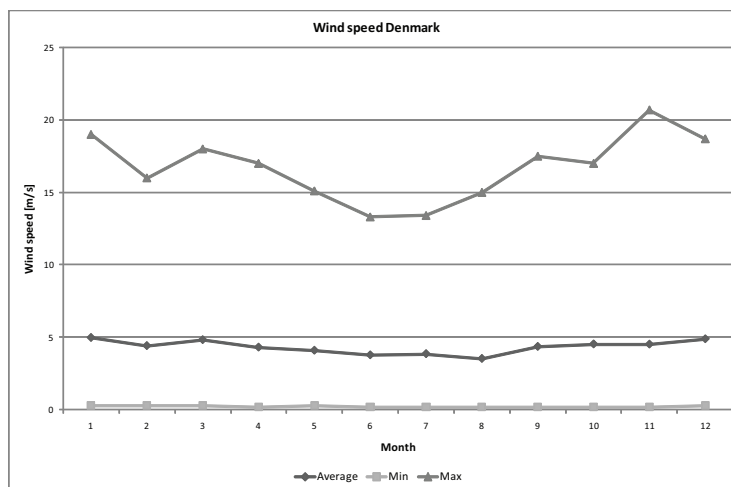
Figure 5.7: *Wind speed for Denmark. [Jensen, 2007]*

From figure 5.7 it is seen that the average wind speed for Denmark during the year is about $3,5 - 5,0 \frac{m}{s}$. From the figure it is also seen that the highest wind speed gets to a level of $15 - 20 \frac{m}{s}$.

To get the most efficient ventilation rate according to natural ventilation the wind direction have great influence too. Therefore the location of the main openings in the building has to be located in the direction of the main wind direction to get the most efficient ventilation rate.

5.3.2 Hong Kong

Hong Kong is located at 22.31N and 114.19E in the tropical zone, which means that the weather can become pretty hot in the summertime. The temperature for Hong Kong are shown in figure 5.8 and 5.9.
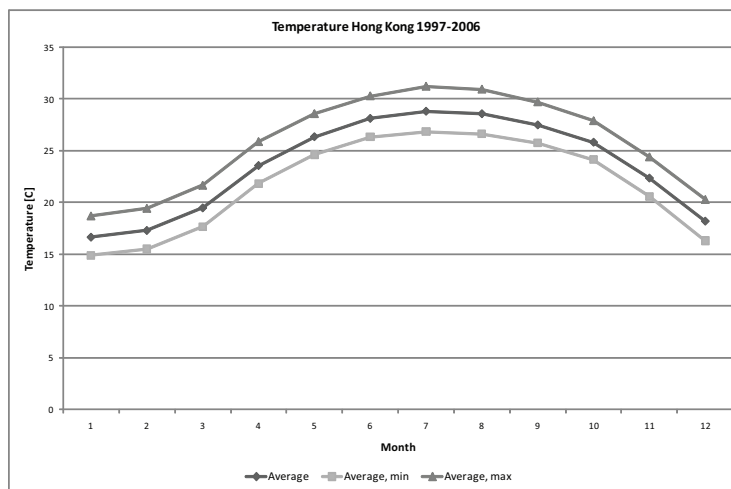
Figure 5.8: *Temperature for Hong Kong during the period 1997-2006. [Hong Kong Observatory, 2007]*
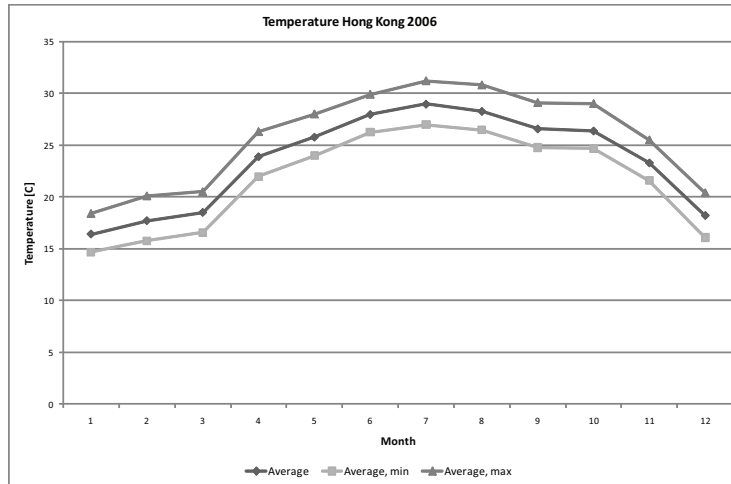
Figure 5.9: *Temperature for Hong Kong for 2006. [Hong Kong Observatory, 2007]*

From the two figures figure 5.8 and 5.9 it is seen that the temperature rises to $25-29\ ^\circ C$ for the summertime and $17-25\ ^\circ C$ for the wintertime. Because of the high outside temperature this can cause problems with overheating the rooms when natural ventilation is used. When natural ventilation is used for ventilation it therefore has to be taken into consideration if the air need to be cooled down before it is let into the room.

The mean wind speed for Hong Kong for a year is showed in figure 5.10.
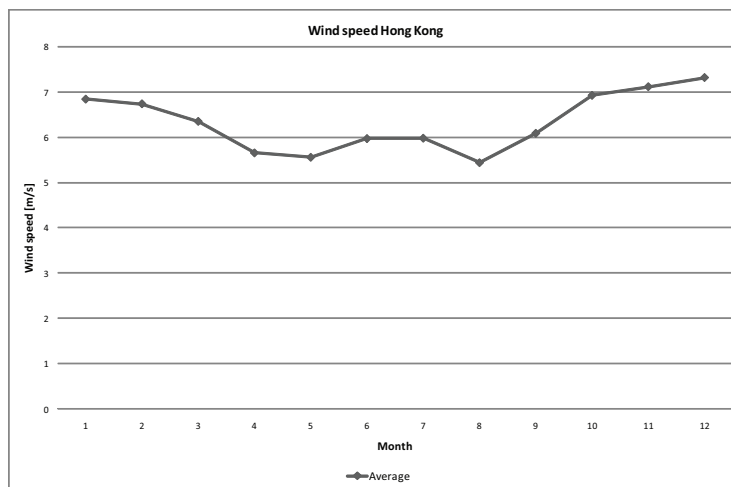
Figure 5.10: *Wind speed for Hong Kong. [Hong Kong Observatory, 2007]*

From figure 5.10 it is seen that the average wind speed is about $5,5-7\ \frac{m}{s}$ which is higher than for Denmark. When the building both the wind speed and the direction of the wind has to be taken into consideration to get the most efficient airflow for the building.

5.3.3 Pollution level

Because natural ventilation uses the outside air for ventilation, the pollutant level of the outside air is important. Especially for hospitals the pollutant level of the air has great importance because the immune systems for some of the patients may not be as good as for a well person. For Denmark the main pollutant in the air is from pollen. In bigger cities car fume may also cause some problems according to the air pollutant.

Because of the high buildings in Hong Kong and the amount of cars especially the pollutant of the outside air is important.

In table 5.5 and 5.6 the emission level for Hong Kong and Denmark are listed.

Table 5.5: *Emission level for Hong Kong and Denmark. [Environmental Protection Department, 2007b] , [Environmental Protection Department, 2007a] , [ENERGINET.DK, 2006] , [Energistyrelsen, 2006]*

	Hong Kong			Denmark
	Emission level in 2005 (ton)	Change in emission level during 1997-2005	Emission reduction target for 2010	Emission level in 2005 (ton)
CO_2	38,1			50,9
SO_2	84 500	+31 %	-40 %	10 300
NO_X	93 500	-15 %	-20 %	45 500
RSP	7 200	-36 %	-55 %	-
VOCs	40 256	-26 %	-55 %	3 700

Table 5.6: *Emission level for Hong Kong and Denmark. [Ables et al., 2006] , [National Environmantal Reseach Institute, Denmark, 2007] , [National Environmental Research Institute, Denmark, 2005]*

	Hong Kong 2005	Denmark 2005
CO $[\frac{\mu g}{m^3}]$	150	Traffic 643,8 Urban background 287
SO_2 $[\frac{\mu g}{m^3}]$	22,5	Traffic 3,5
NO_2 $[\frac{\mu g}{m^3}]$	53,8	Traffic 42,3 Urban background 21,1

From table 5.5 and 5.6 it is seen that the emission from Hong Kong is higher than the emission from Denmark except for CO_2. From the table it is also seen that the emission for Hong Kong from SO_2 did rise in the period 1997-2005 while the emission from NO_X, RSP

and VOCs did get lower. Because of the high pollution load for Hong Kong this has to be taken into consideration when natural ventilation is used for buildings because a too high pollution load inside the building may cause discomfort and illness for people. A way to reduce the inlet of particles into buildings is by using filters to filtrate the particles before the air is let into the building.

In the following chapter are described the location and layout of the two hospitals that are used for further investigations.

Chapter 6

Aabenraa and Grantham hospital

The purpose of the following chapter is to describe the building form, layout etc. for Aabenraa hospital in Denmark and Grantham hospital in Hong Kong. The two hospitals are selected for further investigations on how to implement natural ventilation. Because of the different location of the two hospitals they meet different problems in designing natural ventilation. In section 6.1 are Aabenraa hospital described and in section 6.2 are Grantham hospital described.

6.1   Aabenraa hospital

In January 2002 a renovation of Aabenraa hospital started. The aims for the renovation were:

"to introduce innovative energy efficient design solutions into an existing hospital and to reduce the energy demand of the hospital to a level equivalent to or lower than that of new hospitals and at the same time to ensure an attractive indoor climate"
[Esbensen Consulting Engineers A/S, 2005]

The project about renovation of the hospital were a part of the EU-project Hospitals which included 5 different hospitals in Europe:

- Aabenraa sygehus, Denmark

- Fachkrankenhaus NF, Germany

- MEYER Children's Hospital, Italy

- Torun City Hospital, Poland

- Deventer Ziekenhuis, The Netherlands

The location of the different hospitals are shown on figure 6.1.

Figure 6.1: *Location of the different hospitals in the EU-project Hospitals. [European Commission, 2005]*

For Aabenraa hospital the following points have been taken into consideration:

- Exploitation of passive solar heating and daylight

- Use of active solar collectors for heating of domestic hot water

- Use of hybrid ventilation

- Optimization of heating system

- Installation of a modern computerized Building Management System (BMS)

[Esbensen Consulting Engineers A/S, 2005]

By implementing hybrid ventilation it was measured/estimated that the electricity demand got reduced by 93 % [Esbensen Consulting Engineers A/S, 2005] .

Aabenraa hospital is located in the southern part of Jutland as shown in figure 6.2 with a size of 28000 m^2 according to a medium size hospital. The hospital has 104 beds but space for 145. The beds are divided into three different wards each consisting of 3 floors including a basement. The operation rooms are located in separate buildings from the beds and connected to each other. The hospital is built between 1987 and 1992. In 2002 the health committee of the County of South Jutland decided to renovate the hospital and enlarge the existing hospital by 8000 m^2. [Esbensen Consulting Engineers A/S, 2005]

Figure 6.2: *Location of Aabenraa hospital.   [Esbensen Consulting Engineers A/S, 2005]*

The layout of the hospital is shown in figure 6.3.
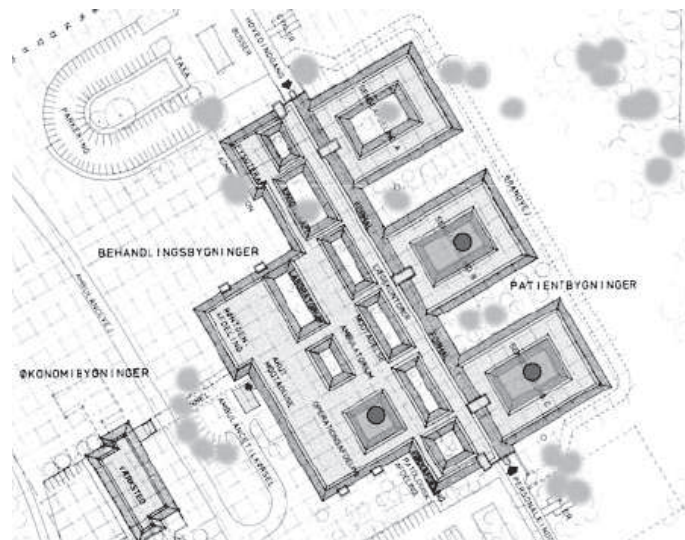
Figure 6.3: *Layout of Aabenraa hospital.   The dots locate the glazed courtyards [Esbensen Consulting Engineers A/S, 2005]*

6.1.1   Hybrid ventilation

For the hospital hybrid ventilation were installed in the common areas in the glazed court-yards and in parts of the addition to the hospital for the beds wards. For the hospital there were used two different ventilation systems for the common areas and the bed wards respectively.

Common areas

The common areas in the glazed courtyards are designed by using displacement ventilation. The inlets for the fresh air are placed at the bottom of the external walls. The fresh air is provided trough these inlets and passes trough the basement of the hospital to get a constant temperature of 16 °C. Before the air gets into the common area it has to pass trough a filter and a convector element to percolate particles. On the roof are placed cowls for the exhaust air. The wind load on the cowls creates an under pressure that ensures an air change rate for the courtyard of about $1,0 - 1,5 \ h^{-1}$.

For the cowls there are also placed assisting fans to ensure the air change rate when the wind pressure is not sufficient. The air change rate is controlled by dampers located in the cowls. For the ventilation system the temperature and CO_2 level are controlled.

The principle for the hybrid ventilation system for the courtyard is shown in figure 6.4.
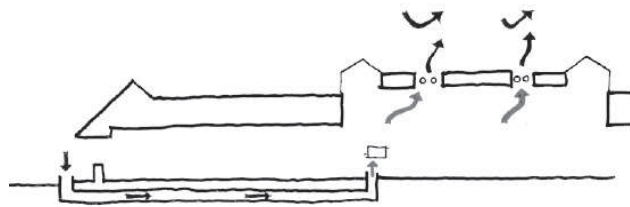
Figure 6.4: *The principle for hybrid ventilation for the glaced area in the courtyard.* [Esbensen Consulting Engineers A/S, 2005]

Bed wards

The bed wards in the new part of the hospital are equipped with hybrid ventilation. For the bed wards there are placed inlets in the bottom of the facade and outlets on the roof. To avoid draught in the bed wards from the inlet air the air is preheated to 18 °C before it is let into the room. The dimensions of the inlet openings are according to the dimensioning opening in the summertime.

The outlets on the roof are wind driven fans with mechanical backup like for the common areas.

In figure 6.5 are shown the principle for the hybrid ventilation for the bed wards.
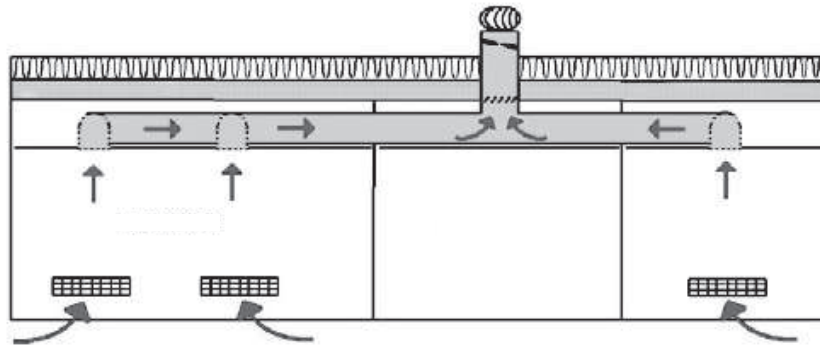
Figure 6.5: *The principle for hybrid ventilation for the bed wards. [Esbensen Consulting Engineers A/S, 2005]*

6.1.2 Building Management System, BMS

To control the ventilation system a new Building Management System (BMS) were integrated. The system makes it possible to:

- change set-point values automatically in accordance with outdoor conditions

- change set point values from a central workstation

- monitor values of importance to the correct functioning of the technical systems and the indoor climate e.g. room temperature, difference between design set point and actual values etc.

- get automatic alarms if actual values differ more than acceptable from design set points

- automatically monitor, store and process energy use data

[Esbensen Consulting Engineers A/S, 2005]

To use the BMS for the hybrid ventilation in the bed wards there are placed censors for the fans in the roof to control the temperature. With the BMS it is possible to control the indoor air quality even better than before and thereby increase the thermal comfort in the bed wards.

6.2 Grantham hospital

In the following section is a presentation of the Grantham hospital in Hong Kong.

The Grantham hospital is located on the south side of Hong Kong island, as shown in figure 6.6.

Figure 6.6: *The location of the Grantham hospital in Hong Kong.*

The hospital is placed close to a mountain with a height of 430 m, as shown in figure 6.7. The hospital utilize the wind and the thermal buoyancy for natural ventilation. Because of the location of the hospital at the bottom of a mountain and close to the South China Sea it can be affected by a land and a sea breeze.
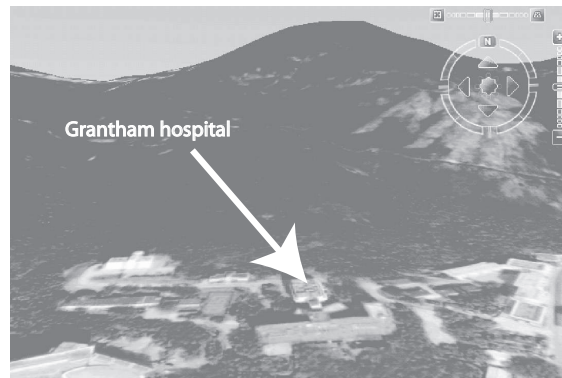
Figure 6.7: *The surroundings of the hospital.*

The hospital was founded in 1957 by the Hong Kong Tuberculosis, Chest and Heart Diseases Association and renamed after Alexander Grantham, a former Governor of Hong Kong. [Grantham Hospital, 2007]

At the time when the hospital was constructed it consisted of 9 different buildings, as shown on figure 6.8. The buildings are showed in figure 6.8 and were:

- Staff buildings

- Administration

- Workshop

- Recreation hall

- Aids quarter

- Main hospital
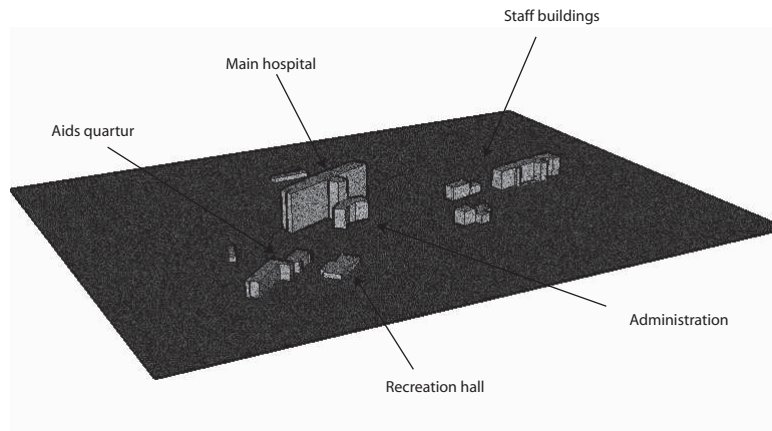
Figure 6.8: *The hospital buildings, at the time when it was constructed.*

Most of the buildings remains from that time, as shown on figure 6.9.
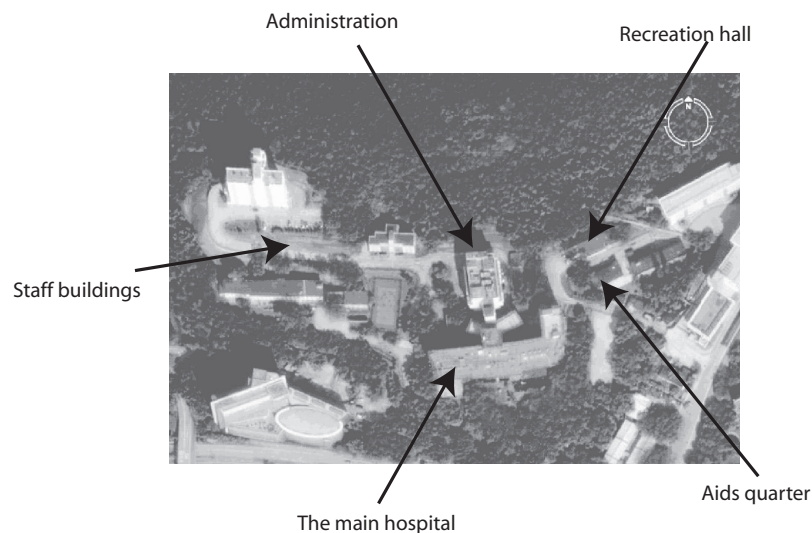
Figure 6.9: *Grantham hospital.*

Today the hospital has 496 beds and about 800 staff. The beds are found in the isolation rooms and the three types of wards. These three types of wards, are a first, a second and a third class of ward. The first class wards, which have only two beds, are placed in the three top floors. The second class wards are found from the ground floor to the fifth floor and the third class wards are placed on all the floors. The second and the third class ward have four and eight beds respectively.

The hospital is developing into a tertiary referral center for treatment of heart and lung diseases, as for instance tuberculose. This means that the hospital has to undertake research that will benefit science. For instance was the hospital the first hospital in Hong Kong that preformed a double-lung transplant. [Grantham Hospital, 2007]

Even though the hospital has developed over time it still remains a natural ventilated hospital. The huge amount of windows in the hospital makes it possibly to utilize single sided ventilation and cross ventilation, as shown on figure 6.10. If the doors to the wards are closed only the third class ward can utilize cross ventilated the others will be single sided ventilated.
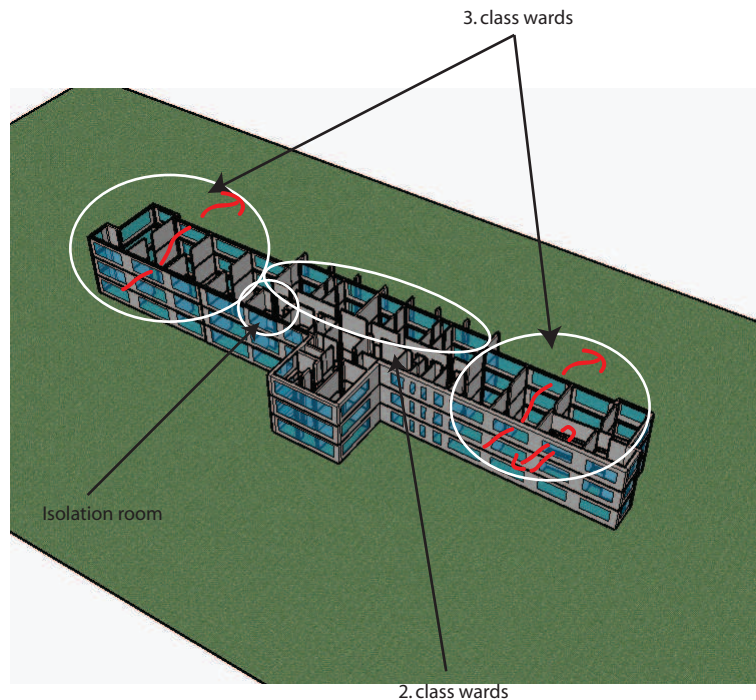
Figure 6.10: *A cross section of the main hospital.*

6.3 Weather conditions and natural ventilation

Both Aabenraa hospital and Grantham hospital utilizes natural ventilation as described above, therefore the weather conditions have great influence on the ventilation system. In the following chapter are analyzed the weather conditions for both Denmark and Hong Kong. For Hong Kong also the special conditions for the hospital because of the location at the bottom of a mountain and close to the sea are analyzed.

In chapter 8 are listed different ideas for natural ventilation and it is discussed how some of the ideas can be implemented for the two hospitals.

Chapter 7

Weather data

In this chapter are the cumulative distributions for the weather data in Hong Kong and Denmark showed. The calculations of the distributions are listed in the subfolder '\Excel\Weather' data on the cd.

The data from Denmark and Hong Kong will be compared to each other to point out the main differences and there meaning for natural ventilation. For the later simulations of the airflow for the hospitals by natural ventilation there are made cumulative normal distributions for the following parameters:

- Relative humidity

- Ambient temperature

- Water content in the air

- Barometric pressure

- Wind speed

- Wind direction

The average values and standard deviations to generate the normal distributions are listed in table 7.1. These values have been found by analyzing data from the design reference year for the two countries.

Table 7.1: *The average value and standard deviation for the weather data in Denmark and Hong Kong.* *[EnergyPlus, 2007]* *[Jensen, 2007]*

		Denmark		Hong Kong	
		Average value	Standard deviation	Average value	Standard deviation
Relative humidity	[%]	82,0	14,8	78,1	12,0
Ambient temperature	[$^\circ C$]	7,76	7,39	23,1	5,29
Water content in the air	[$\frac{g}{kg}$]	5,61	2,78	14,5	4,9
Barometric pressure	[kPa]	101	1,2	101	0,73
Wind speed	[$\frac{m}{s}$]	4,37	3,09	3,08	1,77
Wind direction	[$^\circ$]	179	102	124	85,8

The approximative normal distributions for the relative humidity fits well to the actual data, as shown in figure 7.1.
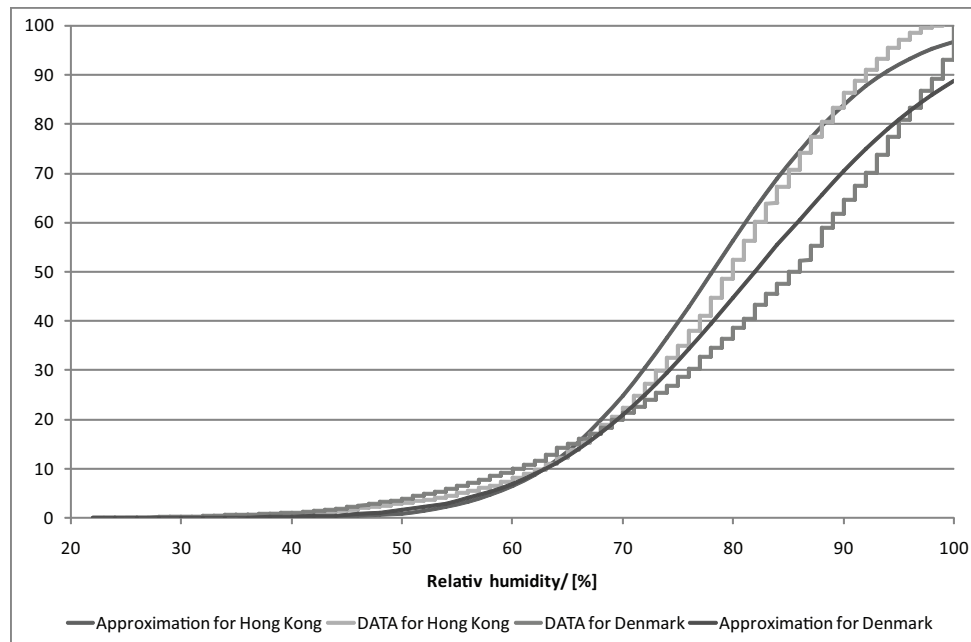
Figure 7.1: *The cumulative normal distribution for the relative humidity in Hong Kong and Denmark compared to the weather data.*

The relative humidity distribution is in both countries almost the same. For the two countries the peeks are at different time of the year, as shown in figure 7.2. In Denmark the relative humidity is highest in the winter period, and lowest in the summer period, whereas it is the opposite for Hong Kong. A reason for this could be that there almost falls the same amount of rain in Denmark every month [DMI, 2007a] , and because of the higher temperatures in the summer period the relative humidity is lower here than in the winter period. For Hong Kong most of the rain falls in the summer period, and even though the

temperatures is higher in the summer period than in the winter period this means that the relative humidity is higher in the summer period, than in the winter period. [DMI, 2007b]
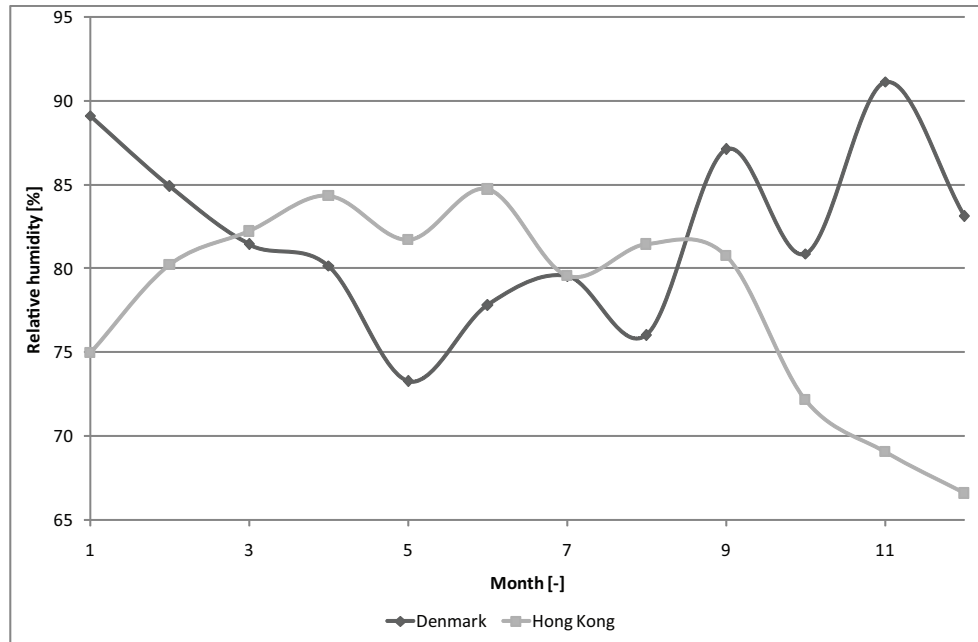
Figure 7.2: *The average relative humidity for Hong Kong and Denmark each month during a year.*

The ambient temperature for Denmark and Hong Kong are shown in figure 7.3. Because of the low ambient temperature for Denmark it is possible to use the outside air for cooling.

Because of the low ambient temperature for Denmark the temperature difference will be higher in Denmark compared to Hong Kong, as shown in figure 7.3. This means that the buoyancy driven natural ventilation system is better suited for Denmark than for Hong Kong.
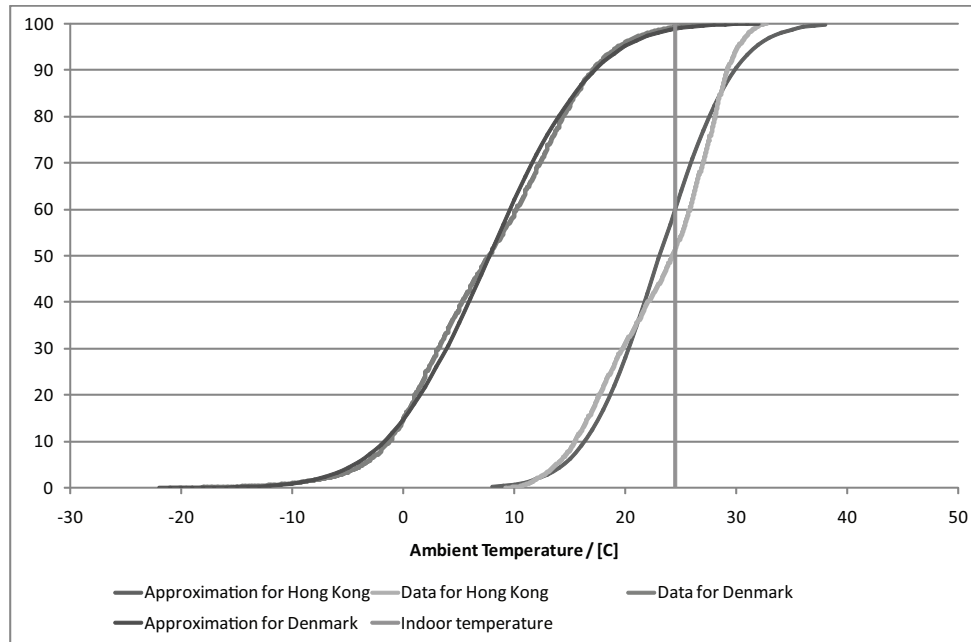
Figure 7.3: *The cumulative normal distribution for the ambient temperature in Hong Kong and Denmark compared to the weather data. The ambient temperatures are also put in relation to an indoor temperature of 24,5 °C.*

As shown in figure 7.4 the water content in the outdoor air is higher in Hong Kong than in Denmark. The reason is that the relative humidity for Hong Kong and Denmark is almost the same but the ambient temperature in Hong Kong is higher than for Denmark.
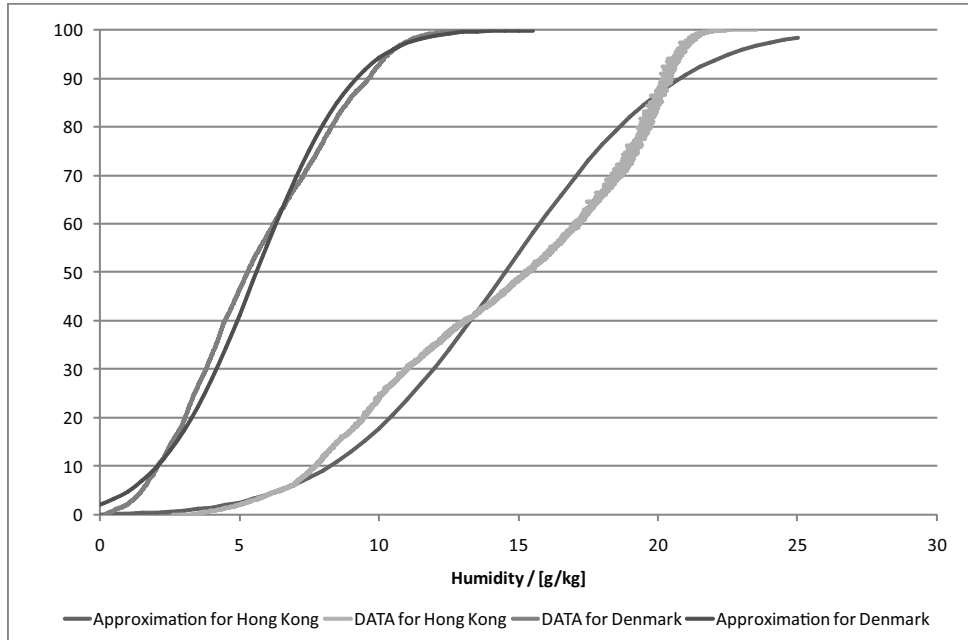
Figure 7.4: *The cumulative normal distribution for the water content in the air in Hong Kong and Denmark compared to the weather data.*

From figure 7.5 it is seen that the barometric pressure is almost the same for both places, but it varies most for Denmark.
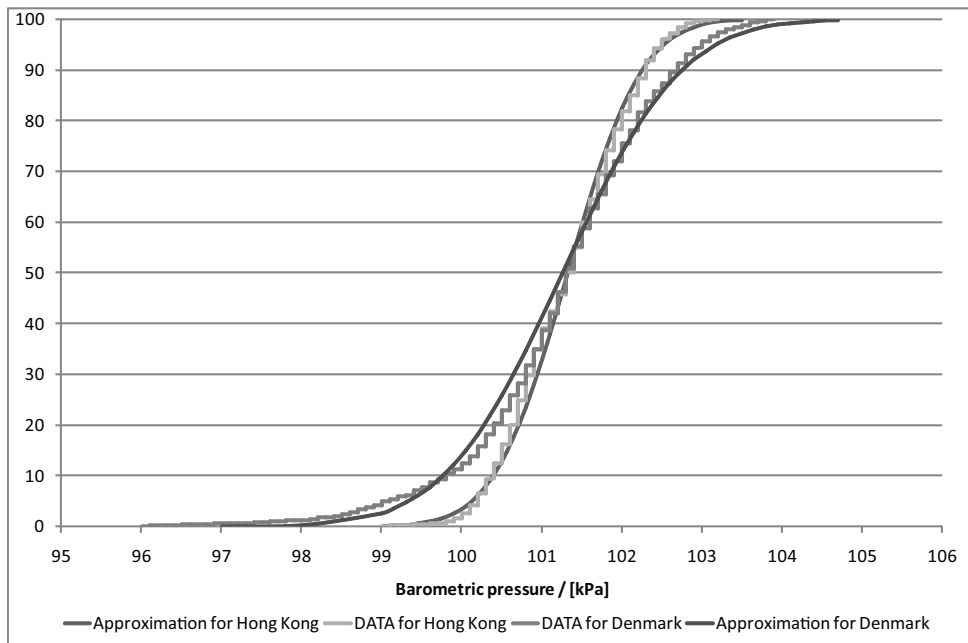
Figure 7.5: *The cumulative normal distribution for the barometric pressure in Hong Kong and Denmark compared to the weather data.*

It is seen from figure 7.6 that for both Denmark and Hong Kong the wind is almost

always blowing. The average wind each month is almost the same, but for Denmark it is a bit lower in the summer period than the rest of the year, as shown in figure 7.7. Since there almost always is a wind present and the average wind speed almost is the same each month, utilizing the wind for natural ventilation can be good.

Even though the cumulative wind speed profiles are close to be the same, the profiles shows that the wind is a bit stronger in Denmark than in Hong Kong. Since the pressure difference between two openings is proportional to wind speed in second power, this makes the effect of using the wind for natural ventilation even greater in Denmark than in Hong Kong than what the graph implies.
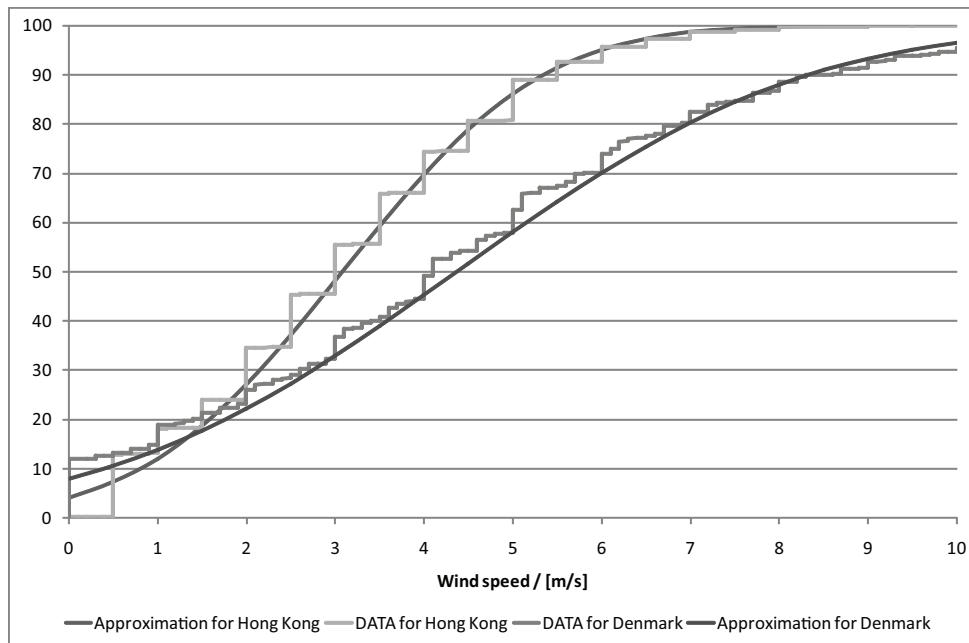
Figure 7.6: *The cumulative normal distribution for the wind speed in Hong Kong and Denmark compared to the weather data.*
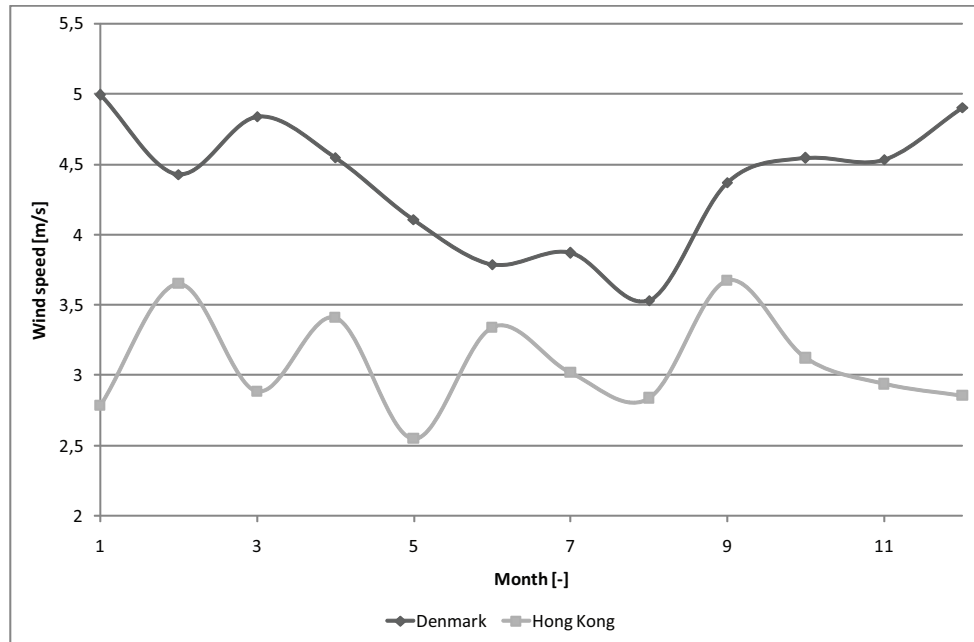
Figure 7.7: *The average wind speed for Hong Kong and Denmark each month during a year.*

The main wind direction for Hong Kong is 80° to 100°, as shown in figure 7.8. This means the wind in Hong Kong mainly is from east, and therefore comes from the South China Sea. To get the highest airflow the openings for natural ventilation should be facing east, unless local conditions dictates otherwise. For Denmark there is not any reel main wind direction, but the strongest wind comes from the west and north west, because of the open sea.
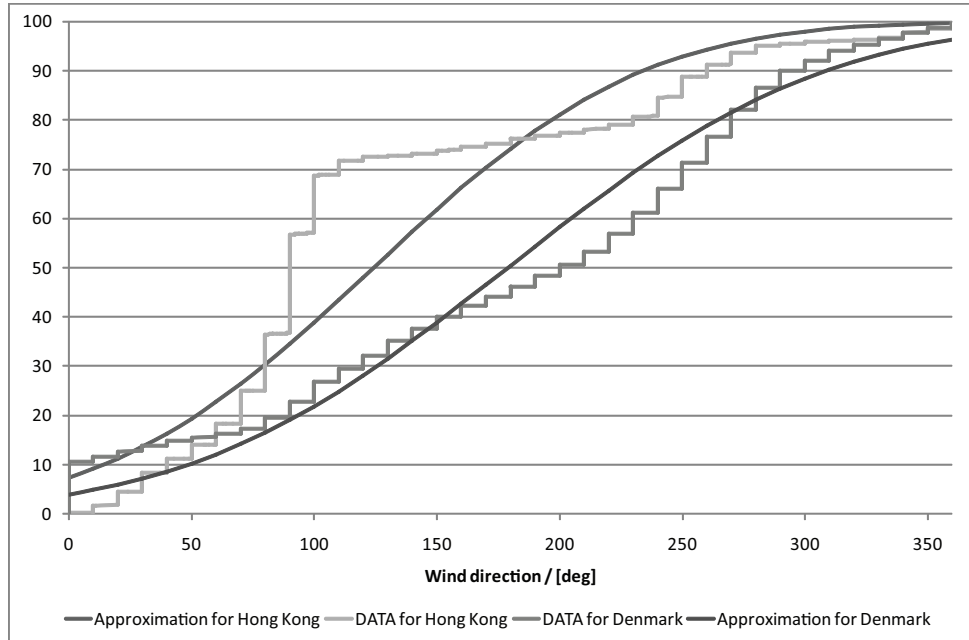
Figure 7.8: *The cumulative normal distribution for the wind direction in Hong Kong and Denmark compared to the weather data.*

The normal cumulative distribution for the wind direction for Hong Kong fits however a bite poorly to the data, as shown in figure 7.8. The wind comes oftener from the east than what the approximative function shows.

7.1 Local weather conditions for Grantham hospital

To efficiently take advantages of the natural driving forces for natural ventilation it is necessary to know the local weather conditions close to the building.

For the simulations of the airflow for and around Grantham hospital the location and the local weather conditions therefore have to be taken into consideration.

As listed in chapter 6.2 Grantham hospital is located on the southern side of Hong Kong Island on Wong Chuk Hang Road in Aberdeen. The location is showed in figure 6.6.

In section 6.2 it is stated that the hospital is located at the bottom of a hill surrounded with threes. In the southern and eastern direction from the hospital is located another hill and in the south-eastern direction is located the South China Sea. The distance from the hospital to the sea is about 1 kilometer. The height of the hill located behind the hospital is about 430 meter high with an average slope of about 9°. In figure 7.9 is showed the cross section of the land where the line is marked in the figure. On the southern and eastern direction of the hospital are located other buildings in a distance of about 200 meter away from the hospital. In the northern and western direction are not located other buildings.
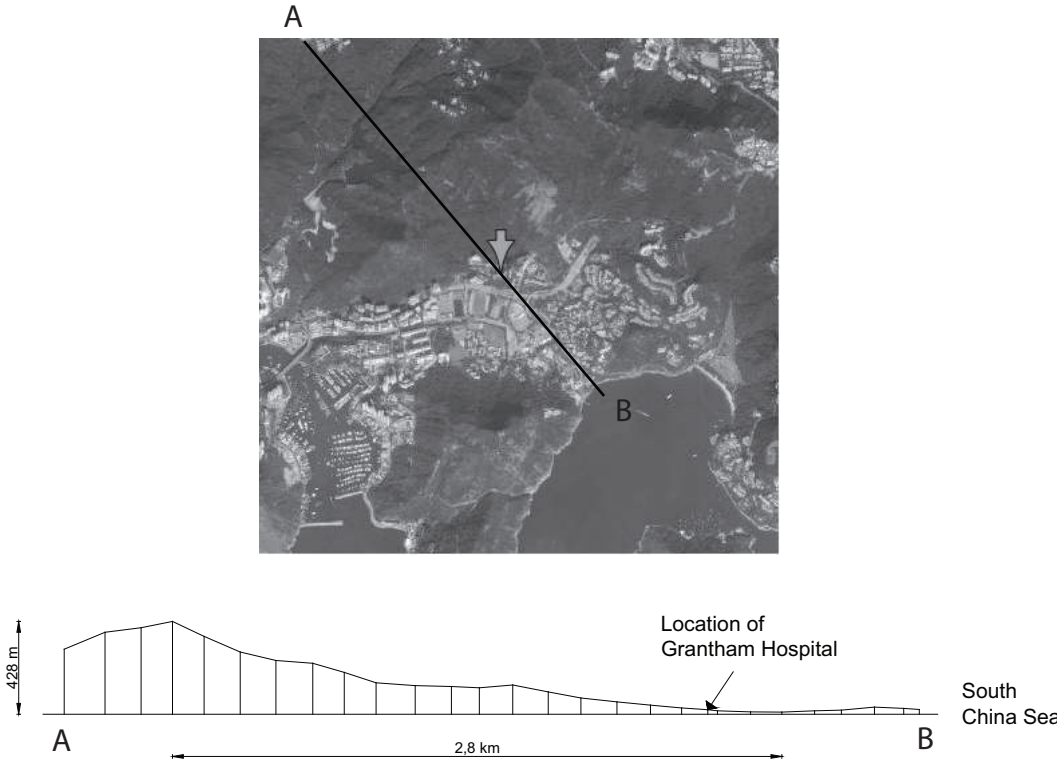
Figure 7.9: *Cross section of the land where the line is marked.*

The airflow for the hospital are investigated for a situation without wind. In this situation the airflow is created only according to thermal buoyancy. In table 7.2 are listed the percentage for the wind speed according to the direction. A calm period is reported when the mean wind speed of the 60 1-minute is $0 \frac{m}{s}$ [Yik et al., 2003] .

Table 7.2: *Percentage frequency of wind speed by direction for Hong Kong in the period 1984-1998. [Yik et al., 2003]*

Direction [°]	Wind speed [$\frac{m}{s}$]										
	0,0–1,5	2,0–3,5	4,0–5,5	6,0–7,5	8,0–9,5	10,0–11,5	12,0–13,5	14,0–15,5	16,0–17,5	18,0–20,5	All speeds
Calm	0,14										0,14
Variable	0,83	0,03									0,86
350–010	1,58	2,23	0,39	0,03	0,00+						4,22
020–040	2,65	3,94	0,96	0,11	0,01	0,00+					7,68
050–070	2,40	5,02	3,29	0,94	0,10	0,05	0,02	0,00+	0,00+		11,82
080–100	3,72	16,36	17,03	4,77	0,54	0,11	0,02	0,01	0,00+	0,00+	42,57
110–130	1,13	2,87	1,68	0,29	0,06	0,02	0,01	0,00+	0,00+		6,06
140–160	0,53	0,85	0,15	0,02	0,01	0,00+					1,57
170–190	0,67	1,97	0,43	0,05	0,00+	0,00+					3,12
200–220	0,52	1,75	0,96	0,18	0,03	0,00+	0,00+				3,45
230–250	1,46	2,45	1,19	0,21	0,02	0,01	0,00+	0,00+		0,00+	5,34
260–280	3,82	4,97	1,62	0,15	0,03	0,01					10,61
290–310	0,78	0,38	0,11	0,02	0,00+	0,00+					1,30
320–340	0,71	0,47	0,06	0,01	0,00+						1,27
All directions	20,94	43,30	27,88	6,78	0,81	0,21	0,05	0,01	0,01	0,00+	100

As showed in table 7.2 a calm period only is 0,14 % of the time. It is also showed that the most common wind speed is $4,0 - 5,5 \frac{m}{s}$ with the direction of $80 - 100$ °.

In figure 7.10 is showed the hours of calm periods over the day.
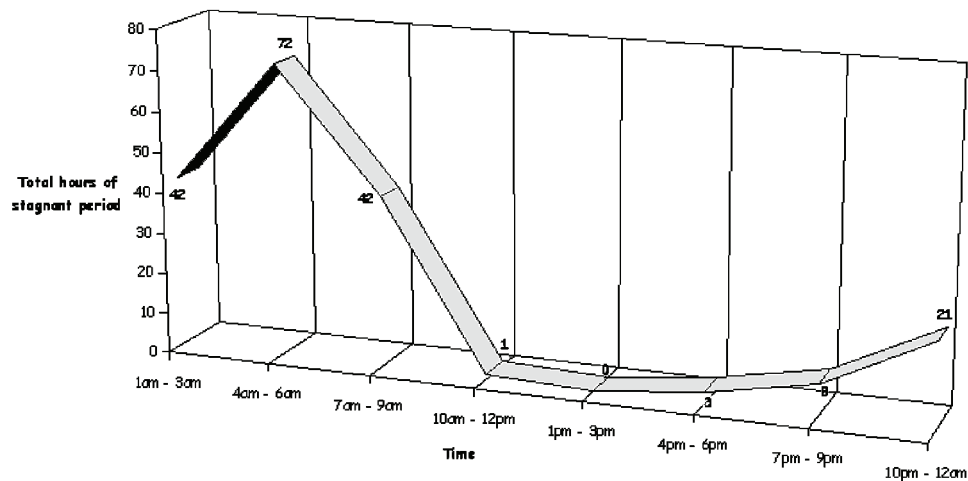
Figure 7.10: *Total hours of calm periods specified for every hour during the day. [Yik et al., 2003]*

From figure 7.10 it is seen that the time where the calm period is most often is for the time 4am - 6am. From 10am - 9pm a calm period is rare.

In figure 7.11 is the monthly total hours of calm periods for Hong Kong showed.
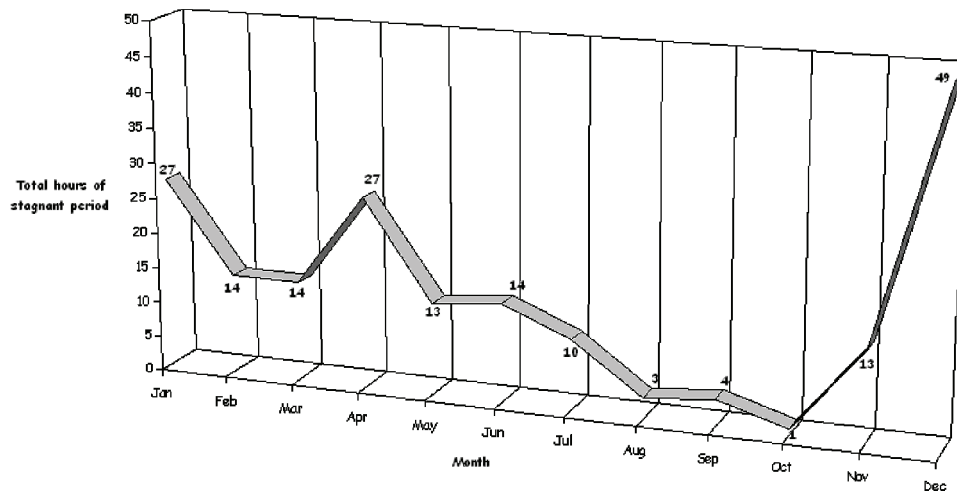
Figure 7.11: *Total hours of calm periods specified for every month during the year. [Yik et al., 2003]*

From figure 7.11 it is seen that from December to January most calm periods is represented. Calm periods for April is also quiet often compared to the other months for the year. For August to October it is most rare with calm periods.

Because of the hilly landscape for Hong Kong the wind direction and wind speed vary a lot. In figure 7.12 is shown the wind direction for The Hong Kong Observatory and at Wong Chuk Hang.
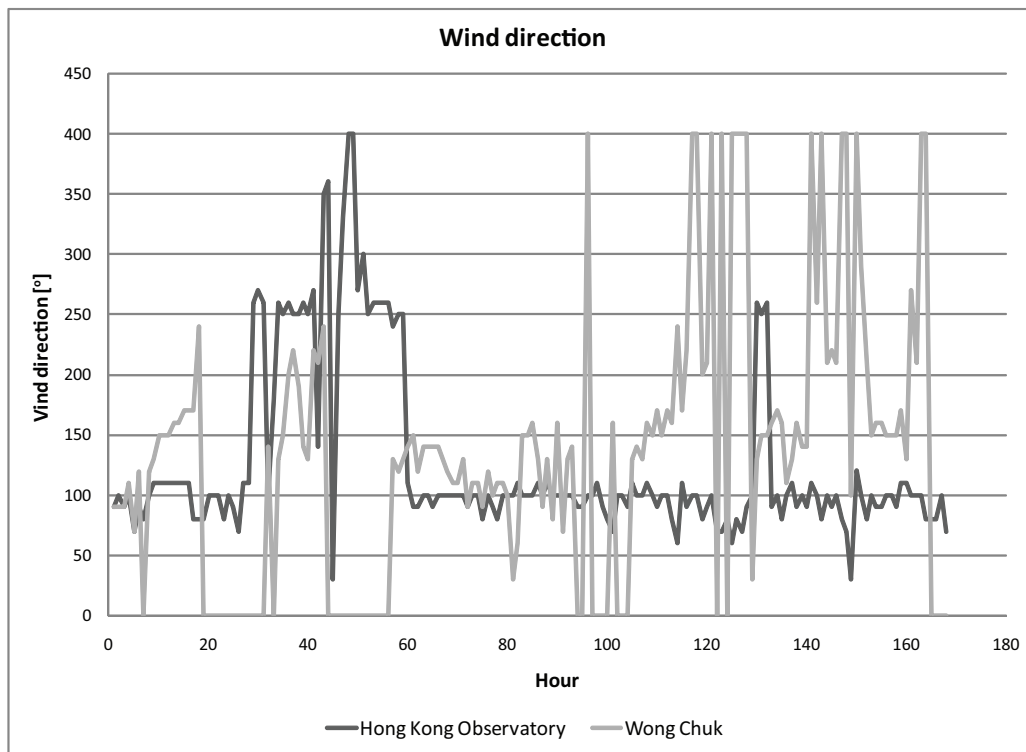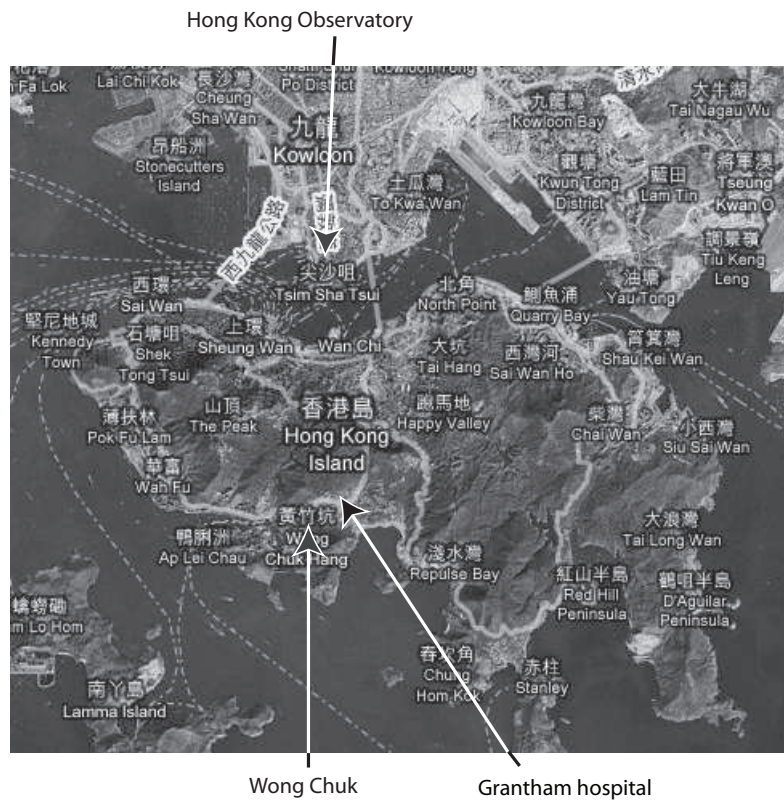
Figure 7.12: *Wind direction for The Hong Kong Observatory and at Wong Chuk hourly from 5th of November to 11th of November 2005. A direction of 400 ° means that no data is available. [Qian, 2005a] , [Qian, 2005b]*

In figure 7.12 is shown that the the wind direction for the two location does vary. For the location of Grantham hospital the actual wind direction therefore may wary from the measured wind direction at The Hong Kong Observatory. From the figure it is also showed that for Wong Chuk more often calm periods occur than for The Hong Kong Observatory.

7.1.1 Mountain and sea breeze

Because of the location of the hospital at the bottom of a hill and near to the sea as showed in figure 7.9 there is a possibility for mountain and sea breeze when the weather is calm. The mountain breeze occur at night when the surface of the mountain is getting cooled, because of radiation, to a lower temperature then the ground surface. Because of the difference in the density of the air according to the temperature there will be an airflow down the mountain and create a mountain breeze. The principle is shown in figure 7.13.
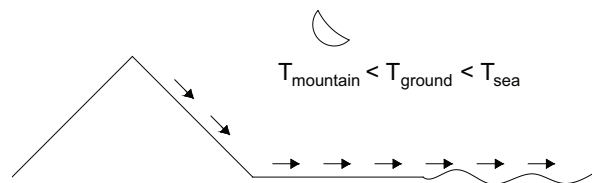
Figure 7.13: *Principle of sea breeze.*

In the daytime when the surface temperature of both the mountain and the ground is higher than the sea there will be an airflow from the sea going op the hill according to the difference in the density of the air. The principle is showed in figure 7.14.
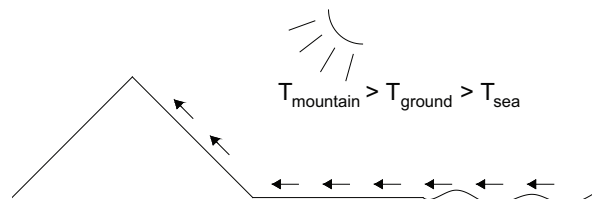
Figure 7.14: *Principle of sea breeze.*

7.1.2 Cases for simulation

To investigate the effect where there is no wind there are made two cases for the simulations:

- Daytime case without wind where the effect from the sea breeze is taken into consideration.

- Nighttime case without wind where the effect from the mountain breeze is taken into consideration

In the daytime situation is used measured temperature corresponding to the temperatures at 15.00 O'clock the 14th of November as boundary conditions in the simulations. In the night time situation is used the temperatures at 23.00 O'clock as boundary conditions in the simulations.

As stated above a calm period is most often in the early morning. The reason for the investigation of the case without wind for the daytime is to see the effect of the sea breeze and investigate the worst case even that it will not happen that often. A reason why there is almost no calm periods in the daytime could also be according to the sea breeze why this is investigated.

For both the daytime and the nighttime case are the worst case investigated. For the daytime case this means the time where the temperature rises to the highest point and for the nighttime case when the temperature gets to the lowest point.

Chapter 8

Ideas for ventilation

In this chapter different natural and hybrid ventilation strategies are explained, and some ideas how they can be used to ventilate an isolation room in a hospital are showed.

The discussed ventilation strategies are:

- Single sided ventilation
- Stack ventilation
- Cross ventilation
- Hybrid ventilation
- Ventilation with earth cooling or heating

8.1 Single sided ventilation

When a room is single sided ventilated the openings in the room are placed in the same side of the building. How well the openings in the building utilize the driving forces of the wind and the thermal buoyancy depends on the configuration of the openings. For instance the more the openings are displaced vertical the more the thermal buoyancy is used as a driving force for ventilation.

For single sided ventilation thermal buoyancy and wind are the driving forces for the airflow. The wind can be subdivided into a steadystate term and two turbulent terms, turbulent eddy and pulsation. The turbulent terms are normally not included in the calculations since most calculations are steadystate calculations. However they do play a great role in ventilating a building with large openings. For large openings it is possible for big eddies to be let through, and the eddies will course an bidirectional airflow. [Heiselberg, 2006]

If only the thermal buoyancy is coursing the airflow through the room the pressure difference across the opening can be found as the difference between the hydrostatic pressure inside and outside. The pressure difference across the opening for this situation is showed in figure 8.1 . [Heiselberg, 2006]
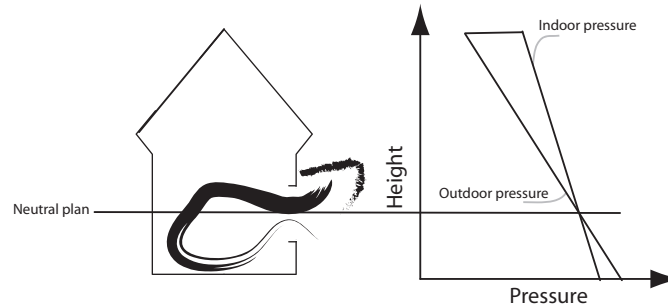
Figure 8.1: *The principle of single sided ventilation.*

To decide whether single sided ventilation is a suitable ventilation solution for the room it is necessary to know the main advantages and disadvantage, as shown in table 8.1.

Table 8.1: *Advantages and disadvantages for single sided ventilation.*

Advantages	Disadvantages
It is a simple solution	The airflow through the room depends on the outside weather conditions
It is a cheap solution which can provide a very high air exchange of the room	It can be difficult to control the direction of the infiltration to the other rooms in a multi zone building, especially when the wind is pulsating
	The penetration depth of the air is low. The room must have a width that maximum is two times the height of the room to have a sufficient penetration depth. [Heiselberg, 2007a]

single sided ventilation is a reliable ventilation system since there almost always are a temperature difference between inside and outside, thus there always will be an airflow through the room. Further more will the wind almost always enhance the airflow through the room.

8.1.1   Single sided ventilation of an isolation room

An idea for using single sided ventilation in a hospital could be letting both the corridor and the isolation room be single sided ventilated, as shown in figure 8.2. Depending on the temperature inside and outside the hospital the air will either come in from the bottom of the window and out at the top or the other way around.

Lower temperature outside than inside

Higher temperature outside than inside
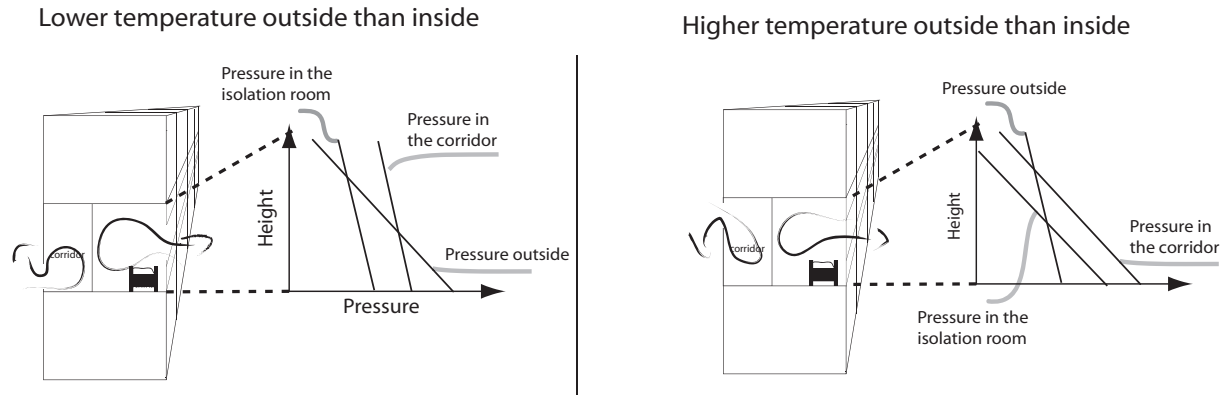
Figure 8.2: *single sided ventilation of a negative pressurized isolation room. The pressure distribution of the corridor, the isolation room and the outside can be seen as well as the airflow through the rooms.*

In the situation without any wind and where the outside temperature is lower than the inside temperature, the outside pressure will be higher than the inside pressure beneath the neutral plane. Above the neutral plane the outside pressure will be lower than the inside pressure as shown in figure 8.2. Since the air is flowing from a higher pressure to a lower pressure, the air will flow into the room from the bottom of the window and out again through the top of the window. However if the outside temperature is higher than the inside temperature in the hospital, the pressure distribution will be the opposite and the flow will go in the opposite direction through the window.

To create a negative pressurized isolation room the pressure in the isolation room has to be lower than in the corridor. When single sided ventilation is utilized this can be achieved with the correct position of the openings. If the outside temperature is lower than the inside temperature the opening in the isolation room should be placed higher than the opening in the corridor, as shown in figure 8.2. If the temperature is higher inside than outside the openings should have the opposite position, to make sure that the pressure in the isolation room is lower than the pressure in the corridor.

To make the ventilation strategy work when there is a wind present, it is necessary that the pressure different between the corridor and isolation room is big. This is because the pulsation from the wind will suddenly create higher or lower pressure in the isolation room and the eddies will hit the walls and create a local high and low pressure in the room.

If there is a sufficient airflow from the room the wind will enhance the airflow independent of which side the openings are facing. However the exploitation of the wind is generally biggest if the opening is facing toward the main wind direction.

8.2   Stack ventilation

Another ventilation principle that uses the thermal buoyancy as a natural driving force to create an airflow is stack ventilation. Compared to single sided ventilation there are at least two openings in the room with a vertical distance. Because of the longer distance between the inflow and the outflow compared to single sided ventilation, stack ventilation will create a greater pressure difference across each of the openings in the building. The principle is shown in figure 8.3. The greater pressure difference across each of the openings means that stack ventilation utilize the driving force from the thermal buoyancy efficiently.
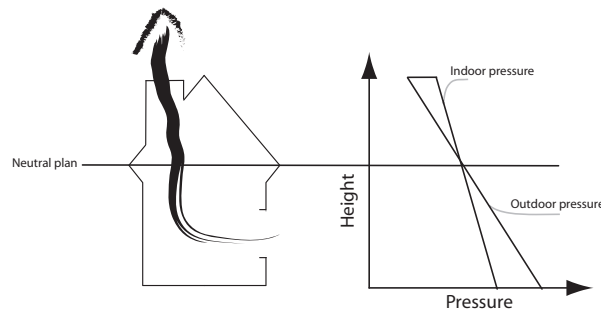
Figure 8.3: *The principle of stack ventilation.*

The height of the neutral plane can be controlled by the sizes of the openings. For a high location of the neutral plane the opening in the top should be bigger than the opening in the bottom and vise versa for a low location of the neutral plane.

The advantages and disadvantages for stack ventilation are listed in table 8.2.

Table 8.2: *Advantages and disadvantages for stack ventilation.*

Advantages	Disadvantages
It is a simple solution	The airflow through the room depends on the outside weather conditions
It is a cheap solution which can provide a very high air exchange of the room	It can be difficult to control the direction of the infiltration to the other rooms in a multi zone building.

Like single sided ventilation it is a reliable system since there almost always is a temperature difference between the ventilated room and the outside.

If the temperature outside primary is colder than inside the air will flow upwards in the chimney. In this case it can be an advantages to use the sun to heat up the air in the chimney and hereby enhance the airflow through the chimney. This could be done by letting the chimney be covered with glass and let this work as a greenhouse to heat up the chimney.

If the chimney is simplified to a cube then it goes that there always will be the lowest C_p value on the top of the cube no matter from which side the wind is coming, as shown in figure 8.4. But the wind is best exploited when the inlet opening is facing toward the wind.
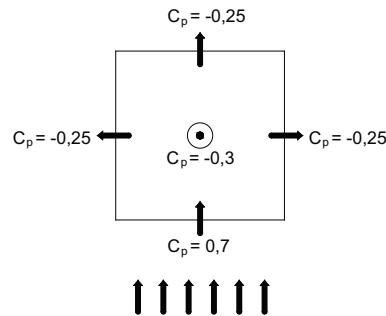
Figure 8.4: *Pressure coefficient for a cube.*

Because the lowest C_p value is on the top, the wind will always enhance the airflow through the chimney, when it is warmer inside the building than outside. When there is the opposite temperature situation the thermal buoyancy will work against the wind. The strongest driving force will then dictate the direction of the airflow.

8.2.1   Stack ventilation of an isolation room

An idea for natural ventilation could be using stack ventilation for an isolation room, located in the lower part of the building, and single sided ventilation for the corridor. The principle is shown in figure 8.5. The location of the isolation room would create the highest pressure difference across each of the openings, and thus the biggest airflow through the room.
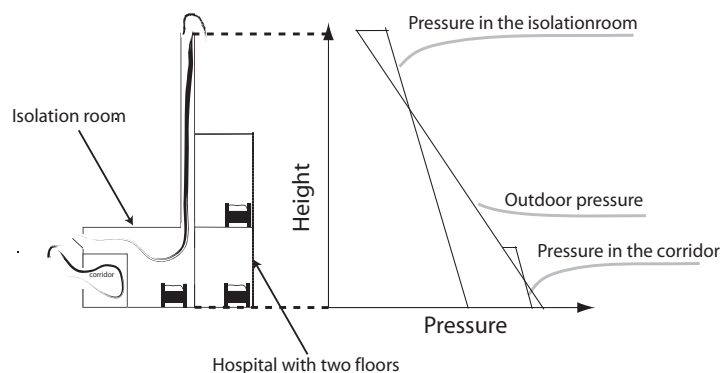
Figure 8.5: *Stack ventilation of a negative pressurized isolation room.*

As mentioned for single sided ventilation, there will be a higher outside pressure than the inside pressure beneath the neutral plane, and the opposite above the neutral plane if the outside temperature is lower than the inside temperature. This means that implementing a chimney in the isolation room will enhance the negative pressure difference between

the isolation room and the outside compared to a single sided ventilated isolation room, when the outside temperature is lower than the inside temperature.

The corridor's neutral plane is located in the middle of the window opening, and the negative pressure difference between the corridor and the isolation room is therefore greater than a single sided ventilated isolation room and a single sided ventilated corridor.

If instead the corridor utilized the chimney and the isolation room was single sided ventilated there would be a positive pressure difference between the corridor and the isolation room. Hereby will the air flow from the isolation room to the corridor.

To avoid the spread of diseases it is necessary that there is a lower pressure in the chimney than in the rooms it is passing by. When there is a higher temperature inside the building than outside, this can be obtained by making sure that the chimney is higher than the building so that the neutral plane is placed above the building. The higher position of the neural plane can also be obtained by having a bigger outlet opening than inlet opening. For a different temperature situation the neutral plane has to be placed as low as possible. This can be done by having a smaller opening at the top of the chimney than at the button.

8.3   Cross ventilation

For a natural ventilated building where the primary driving force is wind pressure cross ventilation might be a solution. Cross ventilation occur when a room has at least two openings to the outside that are not placed in the same side. The wind pressure will create positive and negative pressure areas around the building and the pressure difference will make an airflow through the room, as shown in figure 8.6.
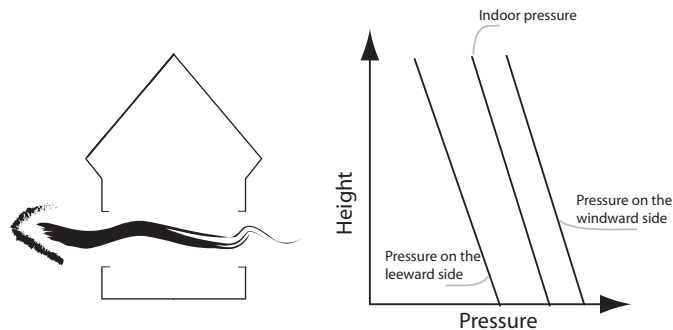
Figure 8.6: *The principle of cross ventilation.*

The advantages and disadvantages for cross ventilation are listed in table 8.3.

Table 8.3: *Advantages and disadvantages for cross ventilation.*

Advantages	Disadvantages
It is a simple solution.	The airflow through the room depends on the wind speed and wind direction outside.
It is a cheap solution which can provide a very high air exchange of the room.	It can be difficult to control the direction of the infiltration to the other rooms in a multi zone building, especially when the wind is pulsating.
Great penetration depth of the airflow into the room. The penetration depth is 2,5 times wider than a single sided ventilated room. [Heiselberg, 2007a]	

How the wind is utilized in the building depends on the configurations of the openings. To get the highest airflow rate through the room the openings should either be placed with one opening in the windward side and the other on the roof or on the leeward side. In this way the highest pressure loss between the openings is provided, as shown in figure 8.7.
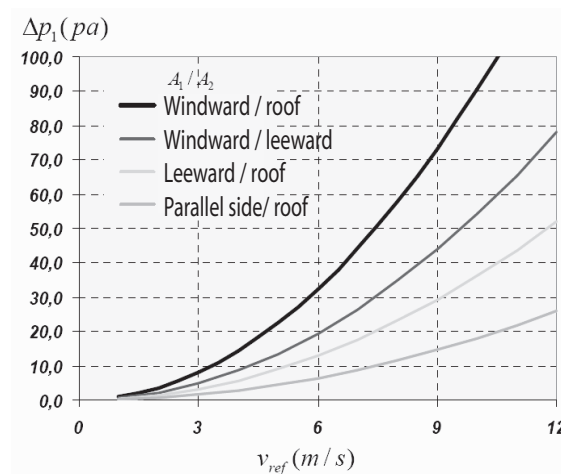
Figure 8.7: *Pressure loss for a squared building with a flat roof. [Heiselberg, 2006]*

The room should be placed in the middle of the building, as shown i figure 8.8 where the highest C_p-value is and thus the highest pressure. The position of the highest C_p-value depends on the direction of the airflow and the shape of the building.
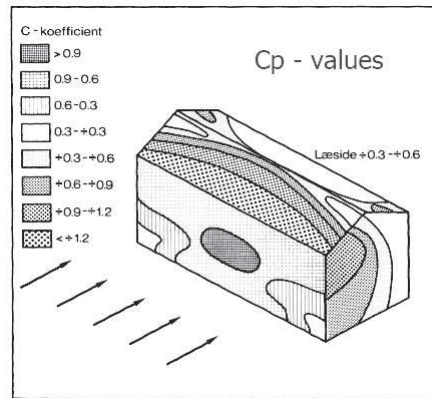
Figure 8.8: *C_p values for a building where the wind is perpendicular to the building [Heiselberg, 2007a] .*

To control the pressure in the building there should be used different openings' sizes. By making the opening bigger in the windward side than in the leeward side the pressure in the building is increased. If the opening in the leeward side is made bigger than the opening in the windward side then the pressure decreases in the building.

8.3.1   Cross ventilation of an isolation room

An idea for using natural ventilation for an isolation rooms could be by letting the isolation room be cross ventilated and the corridor be single sided ventilated.

The first idea is by letting the isolation room be placed in the middle of a very slim building with one of the openings facing in the main wind direction, as shown in figure 8.9. This proposal will take the advantages of a high local C_p value on the facade. Since the openings in the isolation room are placed opposite each other in the main wind direction, they are placed in an efficient position.
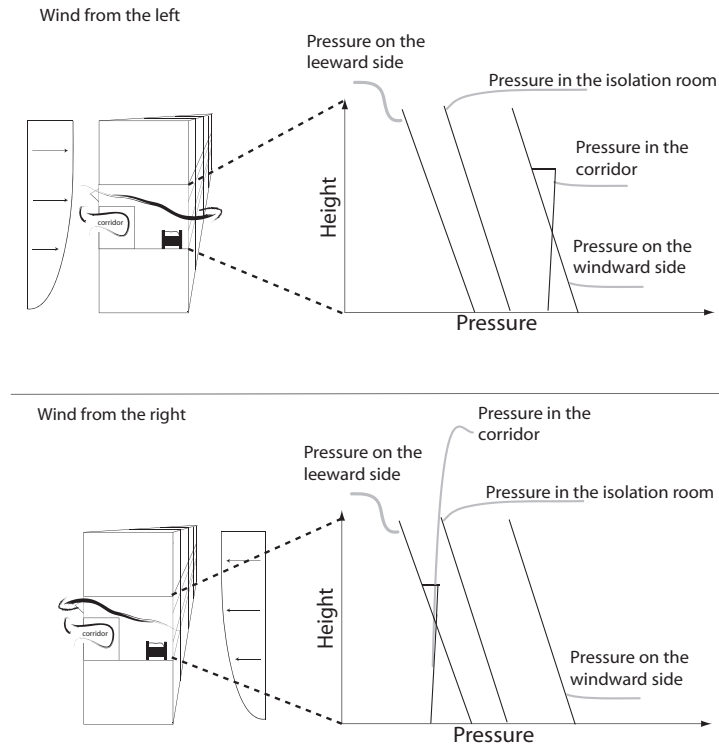
Figure 8.9: *Cross ventilation for a negative pressurized isolation room.*

In the corridor there will be a bidirectional airflow through the opening, because of the positive and negative pressure difference between the outside and the inside above and below the neutral plane, as shown in figure 8.9. The airflow in the isolation room will go right through the room, because of the higher pressure on the windward side and the lower pressure on the leeward side.

The pressure for the isolation room should be lower than for the corridor. The ventilation strategy, shown in figure 8.9, will therefore only work in the situation when the wind is coming from the left. It is therefore necessary to use another ventilation strategy when the wind is coming from the right, for instance single sided ventilation.

Another idea is to place the isolation room in the top of the building. For this location it is possible to locate an opening on the roof and in the windward side. The principle is shown in figure 8.10.

Wind from the left

Pressure on the
roof

Pressure in the isolation room

Height

Pressure in the
corridor

Pressure on the
windward side

Pressure

Wind from the right

Pressure on the
roof

Pressure in the isolation room

Height

Pressure in the
corridor

Pressure on the
leeward side
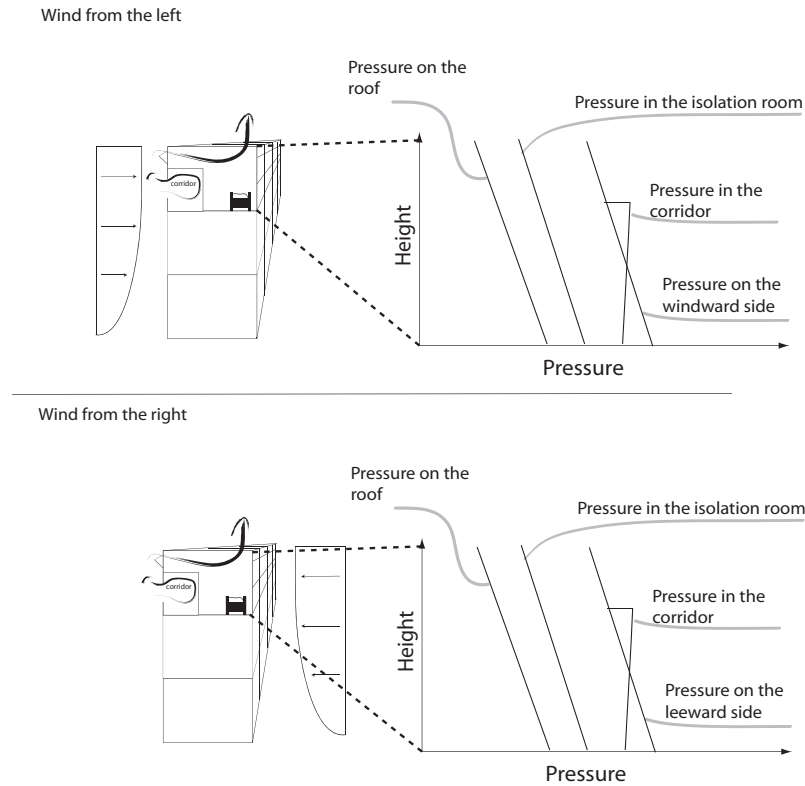
Pressure

Figure 8.10: *Cross ventilation for a negative pressurized isolation room placed in the top of the building.*

The advantages with this ventilation strategy, is that it will ensure that the isolation room always has a lower pressure than the corridor, no matter the direction of the wind.

A last idea could be to let the corridor and the isolation room have a common ventilation system. The principle is shown in figure 8.11. To use this idea it is necessary to be sure that the airflow is flowing in the intended direction from the corridor to the isolation room and then flows out of the building.
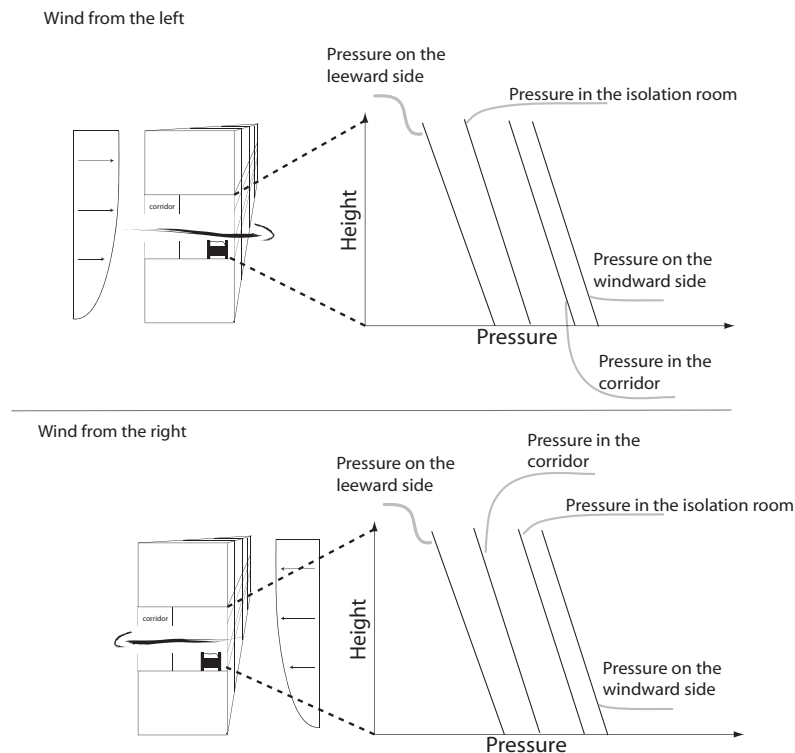
Figure 8.11: *Cross ventilation for a negative pressurized isolation room that has common ventilation with the corridor.*

For the ideas it applies, to create a lower pressure in the isolation room compared to the corridor, the opening for the corridor the wind has to come from the left. Like for the first idea it does not work when the wind is coming from the right, and in that situation it is necessary with a different ventilation strategy to keep the isolation room low pressurized.

The size of the opening in the isolation room have an influence on the pressure in the isolation room. The smaller the opening in the windward side is compared to the opening in the leeward side the closer the pressure distribution in the isolation room will be to the pressure distribution on the leeward side.

8.4 Hybrid ventilation

To make sure that the airflow rate is sufficient and the rooms always is correctly pressurized it can be an advantage to use hybrid ventilation instead of purely natural ventilation.

Hybrid ventilation combines the principle of natural and mechanical ventilation. For hybrid ventilation natural ventilation is used as the main ventilation system. When the natural driving forces are not able to create the desired ventilation rate for the room or building a mechanical driven fan are used to support. With hybrid ventilation it is also possible to control the airflow in the building, which is very important for a hospital. For hybrid ventilation there are three principles showed in figure 8.12.

First principle   Second principle   Third principle
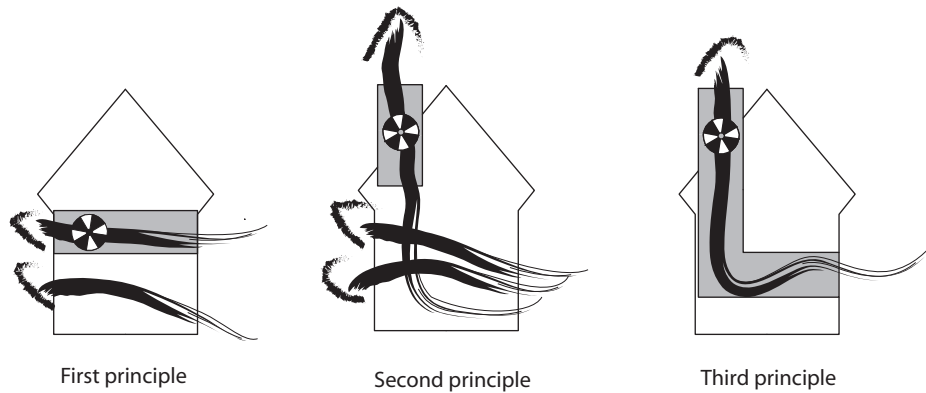
Figure 8.12: *The three principles for hybrid ventilation.*

The three principles are:

First principle Natural ventilation is separated from mechanical ventilation. For this design it is possible to switch between the two systems and use them for different tasks.

Second principle Fan assisted natural ventilation. For this design there are installed a fan for assistance when needed.

Third principle Stack- and wind-assisted mechanical ventilation. This design is based on mechanical ventilation which have a small pressure loss because the natural driving forces create a pressure loss too.

In table 8.4 are listed some advantages and disadvantages for hybrid ventilation.

Table 8.4: *Advantages and disadvantages for hybrid ventilation.   [Heiselberg, 2002]*

Advantages	Disadvantages
Uses the advantages of both mechanical and natural ventilation in one system	Depend on mechanical ventilation
Fulfill high requirements for indoor environment performance	Because of the installation costs for components for mechanical ventilation the costs for hybrid ventilation is higher than for natural ventilation
The combination with mechanical ventilation ensure a ventilation flow when the natural driving forces are not strong enough	When natural ventilation is used the outdoor conditions have influence
Minimizing energy consumption according to mechanical ventilation because of the control system that can switch between natural and mechanical ventilation	Higher energy consumption than natural ventilation
High user satisfaction because of the natural ventilation and the possibility to influence the system	Because of the influence by people this may influence the prescribed indoor air quality
Possible to use hybrid ventilation to cool the building in colder climates	

As listed in table 8.4 there are advantages and disadvantages by using hybrid ventilation. Especially when there are high requirements for the indoor environment performance hybrid ventilation has an advantage according to natural ventilation because it is possible to ensure the desired ventilation rate when the natural driving forces are not strong enough because of the combination with mechanical ventilation.

In table 8.5 are listed a guideline for the probability of success by using hybrid ventilation for a building in the North European climate.

Table 8.5: *Probability of success by using hybrid ventilation.   [Heiselberg, 2002]*

Parameter in question	Probability for success		
Building related	**High**	**Medium**	**Low**
Glass in % of area of facade	30	70	100
Solar protection	Extern shading	Intern shading	No shading
Contaminant emission from surfaces	Low	Intermediate	High
Room height [m]	> 3	2,5-3	$< 2,5$
Room depth [m]	< 6	6-15	> 15
Thermal mass characterization	Heavy	Intermediate	Light
Thermal mass access	Exposed	Partly exposed	Not available
Intake culvert with thermal mass	Yes	Partly	No
Night cooling	Possible	Partly	Not possible
Need for openings in the facade	No	In some periods	Always
Enhanced use of stack effect and wind	Yes	Partly	No
Exhaust air heat recovery important	Not important	Important	Very important
Heat recovery possible	Yes	Partly	No
Activity related			
Internal heat load [$\frac{W}{m^2}$]	< 20	20-30	> 30
High polluting activities	In separate rooms	Partly in separate rooms	Distributed in occupied zones
Typical occupation duration	8 hours	16 hours	24 hours
Air change demand in heating season	< 2	2-4	> 4

8.4.1   Hybrid ventilation for isolation room

An idea for using hybrid ventilation for a negative pressure isolation room is by installing an exhaust fan in the toilet and using doors and windows for inlet or outlet. A way to design this is shown in figure 8.17.
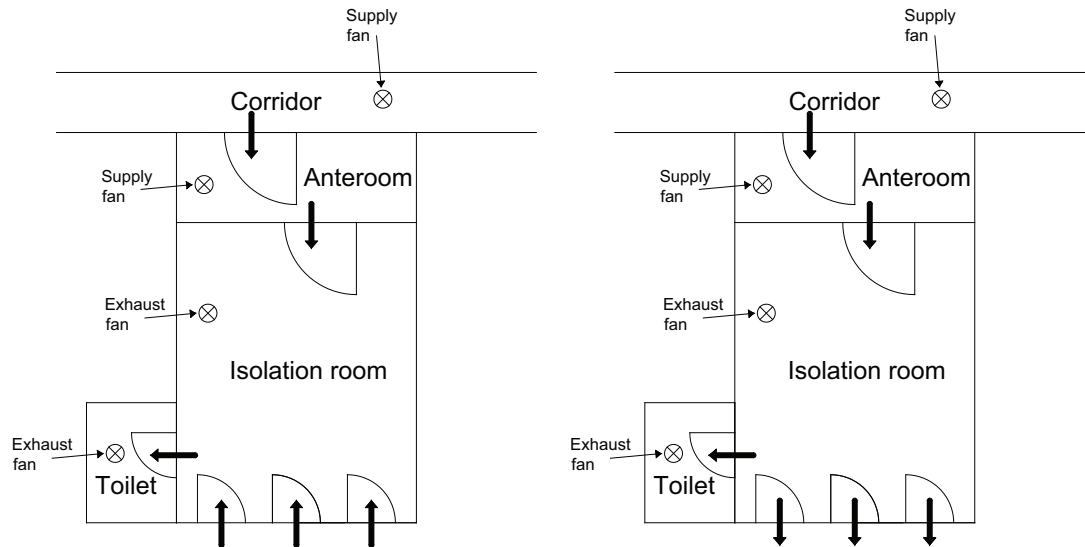
Figure 8.13: *Ideas for hybrid ventilation for a negative isolation room. Airflow is shown by the arrows.*

The first idea for this design is that the air is getting into the room through the windows and the door and let out through the exhaust fan in the toilet. The second idea is that the air is let into the room from the anteroom and out through the windows and the exhaust fan. In this way the principle of natural ventilation is used because of the open windows and door. In the first case the contaminant air is let away from the room through the exhaust fan so it is not getting into other rooms. For the second case some of the contaminant air is also let away by the exhaust fan but also through the windows. For this case the location of the windows has to be taken into consideration so the air is not let out where people are walking by or close to other open windows that are used for inlet. By using a fan it is also possible to ensure the necessary air change rate per hour when the natural driving forces are not strong enough to create this.

For the system the idea is that the mechanical fans are only used when the natural driving forces are not strong enough to create the desired ventilation airflow. Therefore the system is affected by the natural driving forces.

The effect from the thermal buoyancy in two different cases with a higher indoor temperature than outdoor temperature and the opposite is showed in figure 8.14.
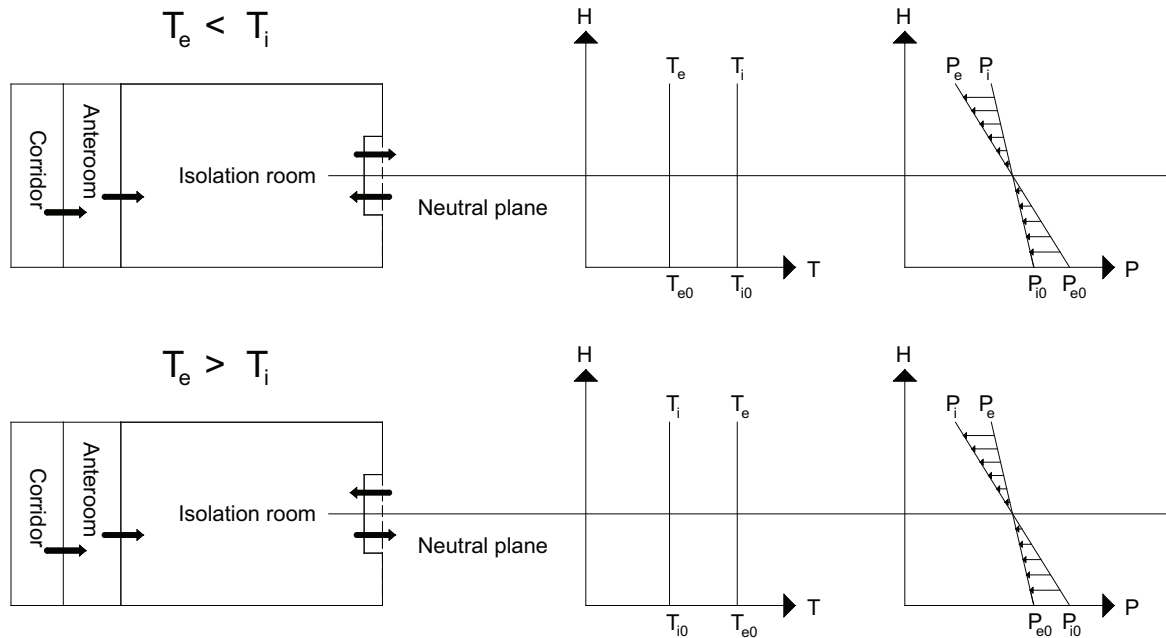
Figure 8.14: *Airflow according to thermal buoyancy in two different situations where the indoor temperature is respectively higher than outdoor temperature and the opposite.*

In the situation where the indoor temperature is higher than the outdoor temperature the airflow is letting into the room through the bottom of the window and out through the top of the window as shown in figure 8.14. For this case where the airflow is only according to thermal buoyancy there will be a negative pressure in the top of the room and a positive pressure at the bottom. In the other case where the outdoor temperature is higher than the indoor temperature the air is getting into the room through the top of the window and out through the bottom and there will be a negative pressure in the bottom of the room and an positive pressure in the top.

The effect on the system of the wind pressure depend on the wind direction. In the situation showed in figure 8.15 where the wind is blowing from left side there will be a negative pressure on the facade where the window is located according to the negative pressure coefficient.
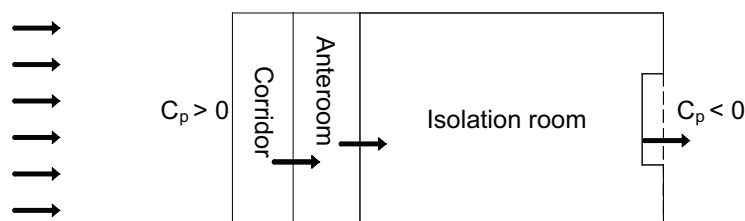
Figure 8.15: *Pressure coefficient according to the wind direction.*

In this situation the airflow for the isolation room will be from the room to the outside as showed in figure 8.15. For a wind direction the opposite way from the east will create

a positive pressure coefficient on the facade where the window is located and a negative pressure coefficient on the other side. In this situation the airflow will be from the outside into the building.

When the wind direction is from left side and the inside temperature is higher than the outside temperature there will be created a negative pressure in the bottom of the room and the location of the neutral plane will be located higher in the room. In this situation it is possible only by natural driving forces to create the desired pressure in the room.

In the situation where the inside temperature is lower than the outside temperature and the wind still from west the location of the neutral plane will move closer to the bottom of the room and the space for negative pressure is lower than for the above case. The two situations are showed in figure 8.16.
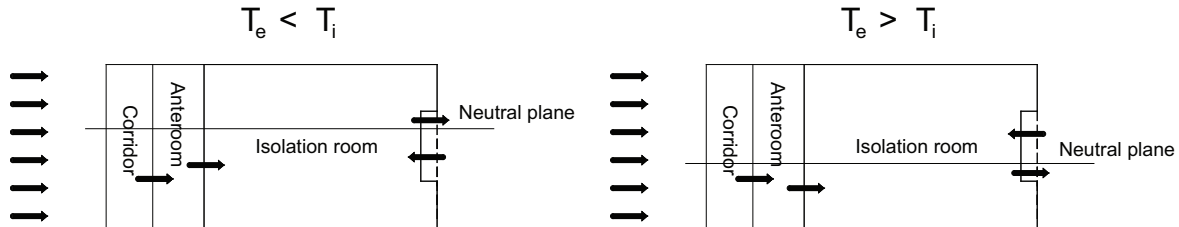
Figure 8.16: *Location of the neutral plane according to the temperature difference between inside and outside.*

From equation (8.1) it is showed that the pressure according to the wind depend on the pressure coefficient and the wind speed while the pressure according to thermal buoyancy depend on the temperature difference and the location of the room according to the neutral plane.

$$\Delta p = \Delta p_w + \Delta p_t = \frac{1}{2} C_p \rho_e v_{ref}^2 - P_i + \frac{\rho_e \Delta T}{T_i} g(H_0 - H) \tag{8.1}$$

With a high wind speed and a low temperature difference the wind has the greatest effect on the room. In this situation there will be created a positive pressure in the room. In the other situation with a high temperature difference and a low wind speed the pressure distribution depend on the temperature distribution as showed in figure 8.14.

When it is not possible to create the desired airflow and pressure only according to natural ventilation the mechanical fans are used to create the desired airflow. Specially when the pressure in the room is desired to be negative and the wind is from right it might be necessary to use the fans to create this pressure. When the wind is from left it will more often be possible to create a negative pressure in the room.

For positive pressure isolation rooms the fan can be used in the opposite way where it is used for inflow when the natural driving forces are not strong enough to create the desired

ventilation flow for the room. For the positive pressure room the windows are still used for inlet while the outlet will be through the door. The idea is showed in figure 8.17.
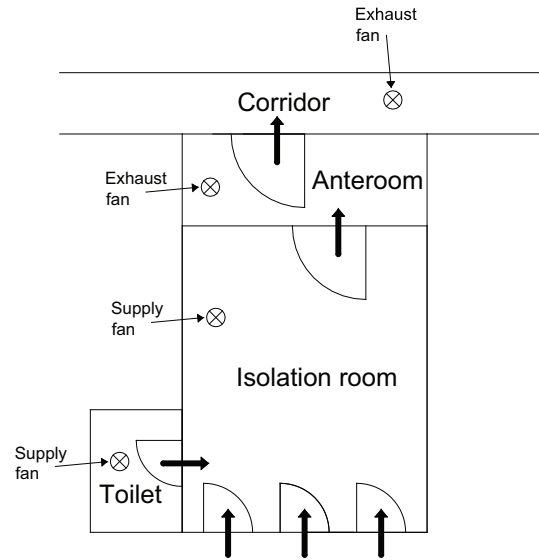
Figure 8.17: *Ideas for hybrid ventilation for a positive isolation room. Airflow is shown by the arrows.*

By the design showed in figure 8.17 the positive pressure and the airflow is ensured by the inlet fan in the toilet. To create the desired airflow and pressure distribution for the isolation room the pressure in the corridor has to be lower than in the isolation room.

8.5 Ventilation with earth cooling or heating

The idea of using earth cooling or heating for the system is to preheat or cool the air before it is let into the room. In this way it is possible to get a more comfortable temperature in the room than when the air is let directly into the room. For earth cooling or heating there are different principles depending on whether the air has to get heated or cooled. The principles are shown in figure 8.18.
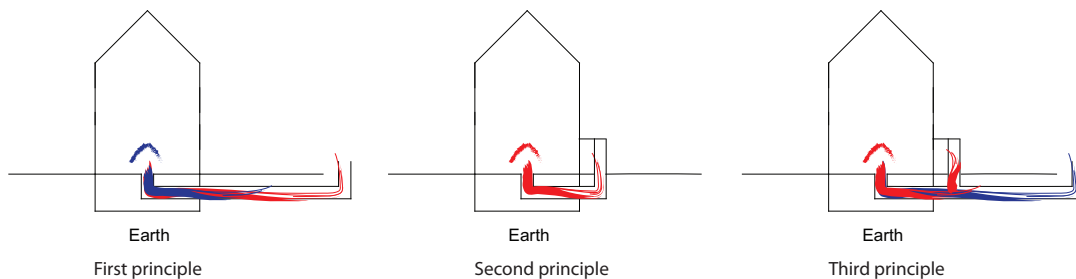
Figure 8.18: *The three principles for earth cooling or heating.*

The three principles are:

First principle Used to cool or heat the air . The warm or cold air is let through a duct in the ground to cool or heat the air before it is let into the building.

Second principle Used to heat the air. The cold air from outside is heated in a glasshouse and lead into the ground to stay at the same temperature and thereafter let into the building. The collected solar energy might also be used to heat the canal so it is possible to improve the heating in the night.

Third principle A combination of heating and cooling. The cold air from outside is mixed with warm air from the glasshouse to get a comfortable temperature before it is let into the building. For use in spring and autumn.

Below are listed how the system might be used for different cases:

- Heating or cooling for the building

- Day and night situation

- Winter, summer and seasons in between

- Combination of glasshouse and canal

Heating or cooling for the building

In the situation where there is a need for heating of the building the system can be used to heat the air before it is let into the building. Depending on how much the air need to be heated either of the principles can be used. The first principle might be used in the case where the desired temperature has to stay almost constant all year around. At a depth of about 5 meters the temperature of the ground stays at the same temperature the hole year. In the winter time the principle can therefore be used to heat the air and in the summertime to cool the air. The first principle does not depend on the solar radiation.

The second principle depend on the solar radiation. On cold days with sunshine this principle can be used to heat the air before it is let into the building. The glasshouse collect heat from the sun radiation and heat the air. The air is thereafter lead through isolated channels in the ground and into the building.

In the mid season where the air often is warmer than winter but not as warm as in the summer and therefore not need to be heated as much as in the winter the third principle can be used. The colder outside air is let through a channel into the building. Before the air is let into the building it is mixed with warmer air from the glasshouse. This principle utilize the ground heat and the heat generated from the solar radiation.

In warm periods specially the first principle can be used to cool the air. Because of the constant temperature of the ground the temperature of the ground will often be lower than the air temperature on warm summer days. This situation can be used to cool the air before it is let into the building.

Day and night situation

Specially for warm days there is a need for cooling in the daytime and heating in the night-time. The cooling can be done as listed above. The night heating can be done in different ways. One principle is to use ground heating as listed above by using the first principle.

Another way is to use the collected solar energy in the daytime to preheat the canal. To use this principle the heat conductivity of the canal need to be high so the energy can be stored in the canal. By nighttime the colder air is let through the canal and is heated in this way.

Winter, summer and seasons in between

Depending on the location the conditions for the summer and winter periods vary. For Denmark the winter is a lot colder than for Hong Kong and for the summertime the temperature for Hong Kong is a lot higher than for Denmark. This might have great influence on the desired principle to use. For Denmark heating is most important therefore the second or third principle might be the best. The second principle can be used in the winter time and the third in the mid seasons where the need for heating is not as high as for the winter time.

For Hong Kong the most important is cooling, therefore the first principle might be the best for this situation. In the winter time there might be a need for heating, in this situation a combination with the third principle might be used.

Combination of glasshouse and canal

As listed above it is also possible to use the collected heat from the glasshouse to preheat the canal. Hereby the air might be let through the canal at nighttime and use the collected heat in the channel to preheat the air.

In table 8.6 are listed some advantages and some disadvantages for ventilation with earth cooling and heating.

Table 8.6: *Advantages and disadvantages for earth cooling or heating.*

Advantages	Disadvantages
Decrease in electrical costs for cooling or heating	Possibility of condensation buildup in the duct work and mold growth
Uses the energy of the earth to cool or heat the air	Ribbed tubing can not be used because of the possibility of mold growth
Keeps the temperature of the air at a almost constant temperature	The air temperature depends on the temperature of the soil
The costs by running the system is lower than a electric driven air conditioner or heater	Limited heating and cooling capacity

From table 8.6 it is shown that there are both advantages and disadvantages for the systems. One of the main advantages is that the variation of the temperature of the soil is low compared to the variation of the air temperature. The temperature of the soil is typically about $10 - 20 \; °C$ for the northern hemisphere all year around [Wikipedia, 2007] . Because the temperature of the soil is lower than the air temperature in hot climate and higher in cold climate it is possible to use the earth for heating in cold climate and cooling in hot climate.

8.5.1 Ventilation with earth cooling or heating for isolation rooms

For the isolation rooms the idea for using earth cooling or heating is designed by ducts under the bed wards. The intake for the air is located in a position where surrounding obstacle do not disturb or shade for the wind. Depending if the air has to get heated or cooled the air will be mixed with hot air. The main idea is shown in figure 8.19.
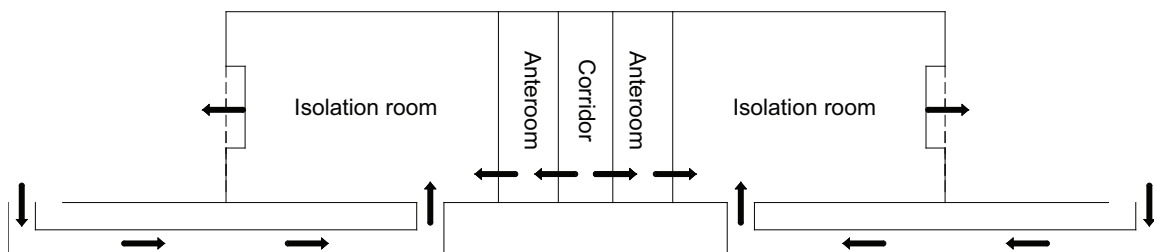
Figure 8.19: *Ideas for earth cooling or heating for isolation room.*

For this design it is possible to preheat or cool the air before it is let into the room. The system is only driven by natural driving forces but it is possible to install a mechanical driven fan in the inlet ducts to ensure the desired ventilation rate when the natural driving

forces are not strong enough. A problem with the design is that the bed wards have to be located relatively close to the ground otherwise the inlet ducts have to be isolated so the air keeps the desired temperature until it reaches the room. Depending on the design of the system the air for the corridor might be supplied through mechanical fans. Another option is to use the same principle for the corridor by letting the air into the corridor through a canal and out through the rooms on either side or an opening in the roof.

Pressure distribution by using earth cooling or heating

To create the desired airflow direction the thermal buoyancy had to be taken into consideration and the neutral plane has to be located in between the inlet duct opening and the outlet window opening. The inlet opening for the duct therefore has to be located lover than the windows. The pressure distribution for this situation where only the thermal buoyancy is acting on the system is showed in figure 8.20. To create the airflow showed in figure 8.20 the pressure in the corridor has to be higher than in the isolation room.
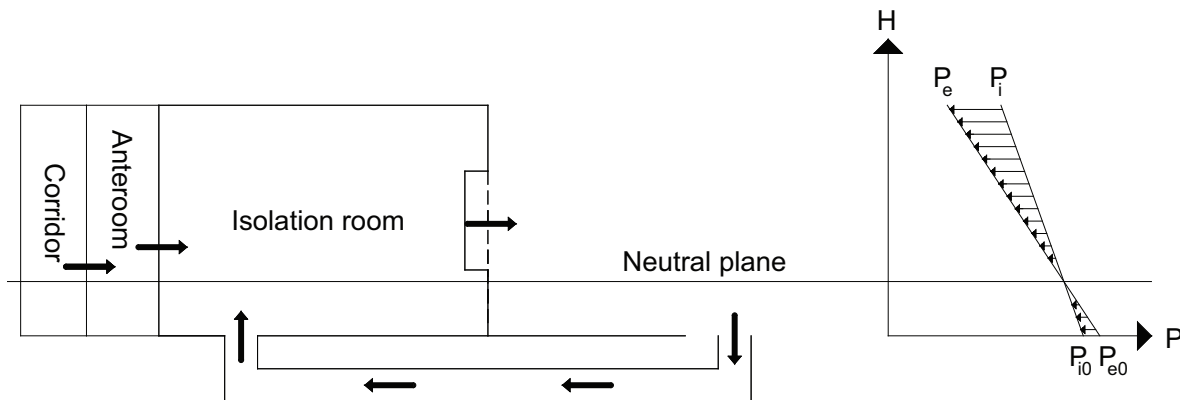
Figure 8.20: *Pressure distribution according to thermal buoyancy. The arrows show the airflow direction.*

To create the desired airflow where the air is let into the room through the duct and out through the windows the inlet for the duct has to be placed in the windward side and the windows has to be placed in the leeward side because of the pressure coefficient showed in figure 8.4.

A way to create the opening in the duct to ensure that the opening always will be in the windward side is by creating a duct with openings for all the sides and locate a sensor to measure the wind direction. From the measured wind direction it is possible to only let the opening in the windward side be open. The principle is shown in figure 8.21.
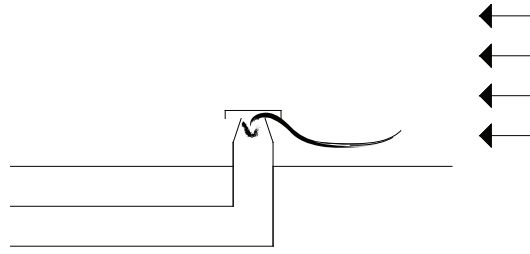
Figure 8.21: *Principle for duct inlet.*

If the location of the opening in the duct is placed in the leeward side the airflow will be from the room to the outside. The duct therefore has to be placed on the other side of the building or in a location where different obstacles do not shade for the wind to ensure that the opening of the duct is in the windward side. To create a negative pressure for the room the pressure coefficient, opening area and wind speed have to be taken into consideration according to equation (8.2).

$$q = C_d A \sqrt{\frac{C_p \rho_e v_{ref}^2 - P_i}{\rho}} \tag{8.2}$$

From equation (8.2) it is showed that the wind speed around the windows, the pressure coefficient and the opening area has great influence on the airflow.

Influence of the local weather conditions

Because the system uses natural driving forces to create the airflow the system is depending on the thermal buoyancy and wind pressure. If there is no difference in the air densities or no wind it is not possible to create the desired airflow only by the natural driving forces. To ensure that there always will be an airflow through the room it is possible to install a fan in the duct inlet to drag air into the room when the natural driving forces are not high enough.

According to the difference in the temperature from Denmark to Hong Kong there will be a difference in the airflow direction according to thermal buoyancy for the two places. For Denmark the outdoor temperature is normally lower than the indoor temperature therefore there will be a positive pressure difference below the neutral plane and a negative pressure above the neutral plane. For Hong Kong the outside temperature is often higher than the inside temperature therefore there will be a negative pressure difference below the neutral plane and a positive pressure difference above the neutral plane. During the day the temperature will rise and the indoor temperature will get to the same point as the outside temperature. In this case there is no temperature difference and and it is not possible to use thermal buoyancy for ventilation. In the nighttime the inside temperature will most often be higher than the outside temperature as for Denmark. The situations are showed in figure 8.22.
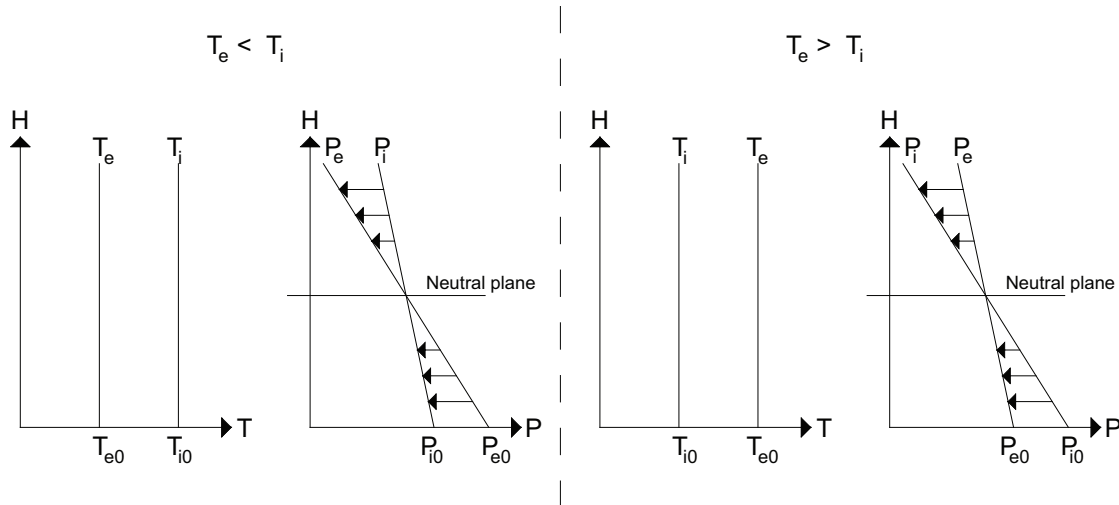
Figure 8.22: *Pressure distribution for two different temperature situations.*

Because the difference in the airflow direction according to the temperature difference for the two locations this has to be taken into consideration. In figure 8.20 it is considered that the outside temperature is lower than the inside temperature. In the case where the inside temperature is lower than the outside temperature the airflow will be in the opposite direction. To ensure that the inlet is still through the duct the opening of this has to be located in a higher position than the window. The pressure distribution for this situation is showed in figure 8.23.
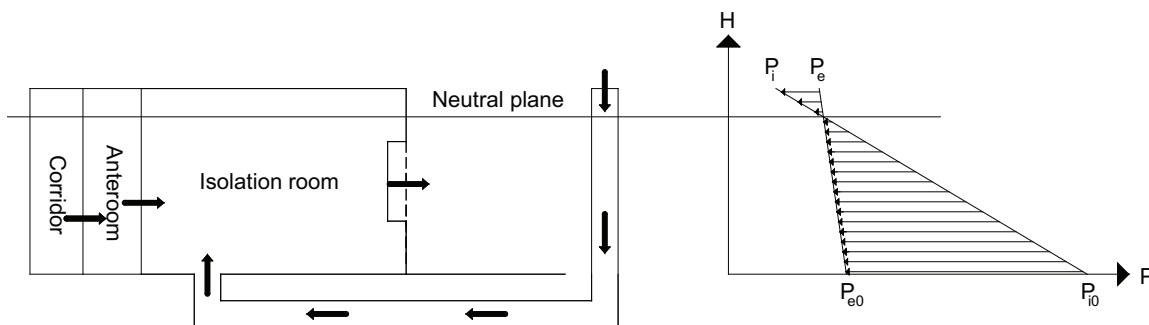
Figure 8.23: *Pressure distribution for the situation where the indoor air is colder than the outdoor air.*

In the case where the inside temperature is higher than the outside temperature and the system is designed as showed in figure 8.23 the airflow according to thermal buoyancy will be in the opposite direction. To create the desired flow direction in this situation the wind pressure has to have a greater influence than the thermal buoyancy. In the case where the wind pressure is not high enough to create the desired airflow a fan can be installed to supply the right amount of air for the room.

8.6 Aabenraa hospital and Grantham hospital

In the following are discussed how to improve the use of natural ventilation for Aabenraa hospital and Grantham hospital.

8.6.1 Aabenraa hospital

As described in section 6.1 there are used hybrid ventilation for the common areas and for the new build bed wards. For the common areas are used a combination of hybrid ventilation with earth heating where the fresh air passes through the basement before the air is let into the area. The exhaust for the common area is through a fan in the roof. For the bed wards are also used hybrid ventilation. The intake is in the bottom of the facade where the air is heated before it is let into the rooms. For the bed wards are also placed fans on the roof for exhaust.

From figure 6.2 in chapter 6.1 it is showed that two of the bed ward are located around a glazed courtyard and the third bed ward are located around an unglazed courtyard all facing north-east. In the south-west are placed administrative buildings. For the bed wards the length and the width is almost the same. For the hole building in general the length and the width is also almost the same.

For Denmark the strongest wind is western wind as listed in chapter 7. Because the bed wards are located facing north-east they are located on the leeward side of the building. To be able to create a positive pressure isolation room the rooms has to be located in the windward side of the building if single sided ventilation is used. Because of the location of the rooms on the leeward side it is possible to create a negative pressure room by using either single sided ventilation or hybrid ventilation according to section 8.1 and 8.4. Even though the strongest wind is from west the wind direction does vary through the time as listed in chapter 7. For the rooms it is possible to install a fan in the roof. The fan can ensure the desired pressure when the wind direction varies and in the situation where the wind is not strong enough to create the pressure in the room. By installing a fan for the room it is also possible to let the air from the room away from other people or other intakes.

The temperature distribution for 2006 for Denmark is showed in figure 5.6 in chapter 5.3, the average temperature was $9, 4\ °C$ [DMI, 2007] . Because of the low temperature this can create problems with draught and people feeling uncomfortable when the windows are open. Therefore because of the low outside temperature a consequence is that people in the room does close the windows. If the windows are closed it is not possible to create the desired pressure by natural ventilation. A way to avoid this is by using earth heating and letting the fresh air into the room through ducts as described in chapter 8.5 because the rooms are located close to the ground or by installing vents behind radiators to heat the air.

Because of the location of the rooms facing north-east and the most common wind direction from west the most efficient and reliable way to create a positive pressure room is by installing hybrid ventilation to create the desired airflow and pressure distribution.

Both the ideas listed above and the already installed system for the hospital uses the principle of hybrid ventilation. The thought with the listed idea is that when the wind is from the desired direction and strong enough only the wind pressure is used to create the desired airflow and the fan is not used. The listed idea thus uses the second principle of hybrid ventilation.

8.6.2   Grantham hospital

As described in chapter 6.2 Grantham hospital is using cross ventilation and single sided ventilation. Cross ventilation utilize the driving force from the wind more effectively than single sided ventilation. It could therefore be an advantages to redesign the single sided ventilated rooms so they can use cross ventilation. The rooms that requires the highest air change rate, as for instance an isolation room, should be located on the top floor of the building, the 8th floor. For this solution they can be connected to a chimney so the thermal driving force is used more effectively.

In Hong Kong the main wind direction is from east. For an isolation room that should be negative pressurized the best position would be in the west side of the building. If the isolation room should have a high pressure the isolation room should be placed in the east side of the building.

For the hospital there are periods where there almost is no wind present to create a driving force. If there at the same time almost is no thermal driving force, the air changes rate for the rooms in the building can end up being too low. To prevent this situation it can be necessary to implement a mechanical ventilation system so the hospital is hybrid ventilated.

The airflow for the rooms in the building is happening through the windows. In Hong Kong there are periods during the year where it is necessary to use cooling to have a comfortable indoor temperature, as written in chapter 7. There are in the bed wards not installed any cooling coils. It could therefore be an advantages to supplement the ventilation system with earth cooling.

In the following chapter are listed more specific ideas on how to use natural ventilation for both Aabenraa hospital and Grantham hospital and the calculated airflow rate for the ideas.

Chapter 9

Analytical calculation of airflow

In the following chapter are made analytical calculations of the airflow for different rooms for both Aabenraa and Grantham hospital. The analytical calculations are made to get a rough idea about the airflow and the air change rate for the rooms. The calculation are also used to get an idea if all the different ventilation principles listed in chapter 8 can be used for the room. Later are made a CFD simulation and multi zone simulations to calculate the airflow for the rooms more accurate.

9.1 Aabenraa hospital

The analytical calculations for Aabenraa hospital are made to investigate if it is possible to use natural ventilation in some part of the hospital's bed wards without a big renovation of the rooms. Based on the results there will be made suggestions on how the natural ventilation system can be improved.

For Aabenraa hospital there are not designed any isolation rooms therefore three of the bed wards with one bed will be changed and redesigned to isolation rooms to investigate the use of natural ventilation for isolation rooms. To investigate how the suggested improvement works are first made analytical calculations.

For the calculations the rooms are considered to be single zones with either single sided, cross or stack ventilation. This means that the airflow for the rooms are not infected by other rooms and thereby airflow between the rooms and infiltration are not taken into consideration. This is a simplification to the real surroundings where the airflow for the single rooms will be influenced by the other rooms. This means that the analytical calculations only can be used to give a rough estimate of the airflow and air change rate.

The purpose of the calculations are to investigate if the different ventilation strategies can supply the rooms with a sufficient air changes rate. For the calculation average values of the weather data from the Danish design reference year are used. For the calculations the summer period are defined as the 6 warmest months of the year and the winter period are defined as the 6 coldest months of the year. For the warmest and coldest month are

used July and February respectively. The calculations are made in the Excel spreadsheet simple calculations for Aabenraa.xls.

The calculations are made for the south eastern part of the hospital, shown in figure 9.1.
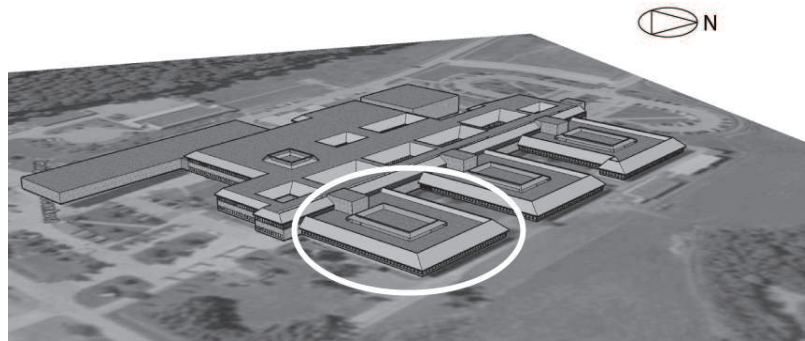
Figure 9.1: *The south eastern part of the hospital for which the calculations are made.*

In the south eastern part of the hospital are 23 bed wards with two beds and three with one bed. The rooms are placed close to the building's facade, as shown in figure 9.2.
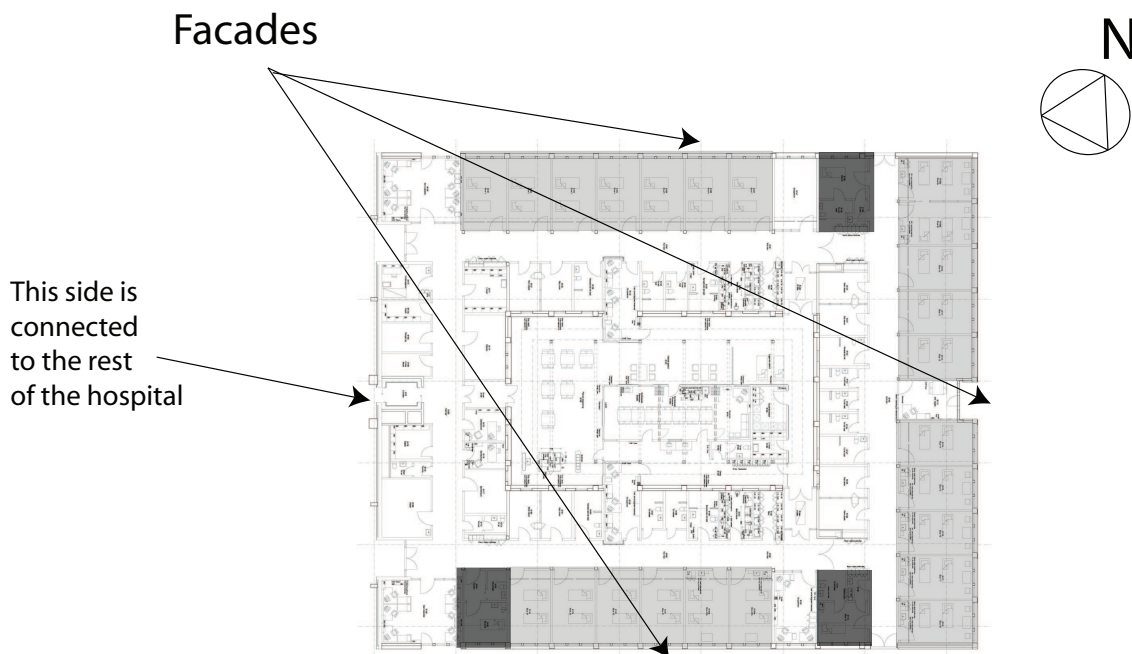
Figure 9.2: *The dark gray hatch shows the bed wards with one bed and the light gray hatch shows the bed wards with two beds.*

The construction of the bed wards with two beds are almost completely alike, the only differences is the position of the doors. The design of the bed wards with two beds are shown in figure 9.3.

Section A-A

0,94m 0,93m 0,63m

A

23,4 m²   A

1,03 m
0,40 m
1,04 m
0,50 m
2,50 m
0,05 m

0,25 m
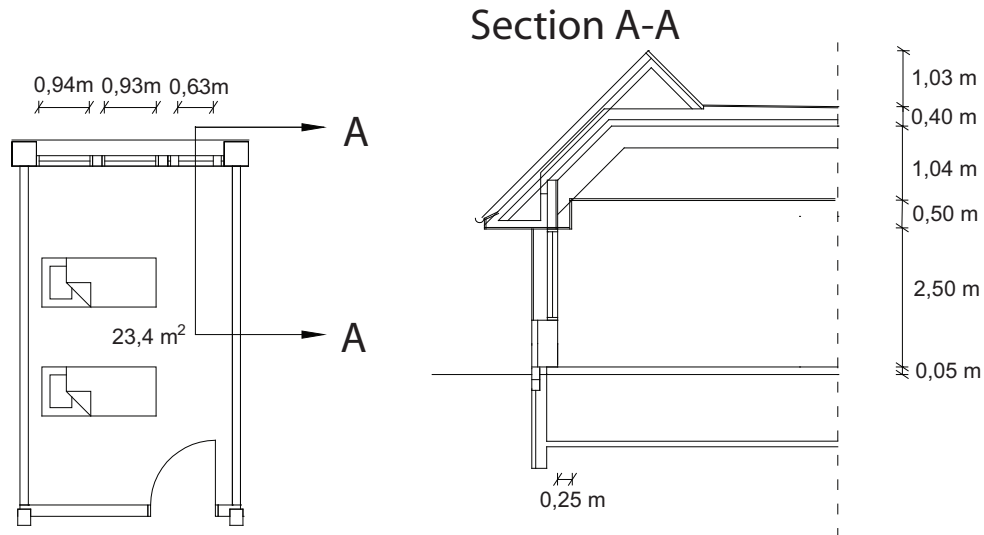
Figure 9.3: *Dimensions of the bed wards with two beds.*

The dimensions of the bed wards are listed in table 9.2.

Table 9.1: *Dimensions of the bed ward.*

Area	$[m^2]$	23,4
Height	$[m]$	3,0
Volume	$[m^3]$	70,2

The bed wards with one bed are not all constructed in the same way, it is therefore chosen only to do the calculations for the bed ward close to the north east facade. The design of the room is shown in figure 9.6.
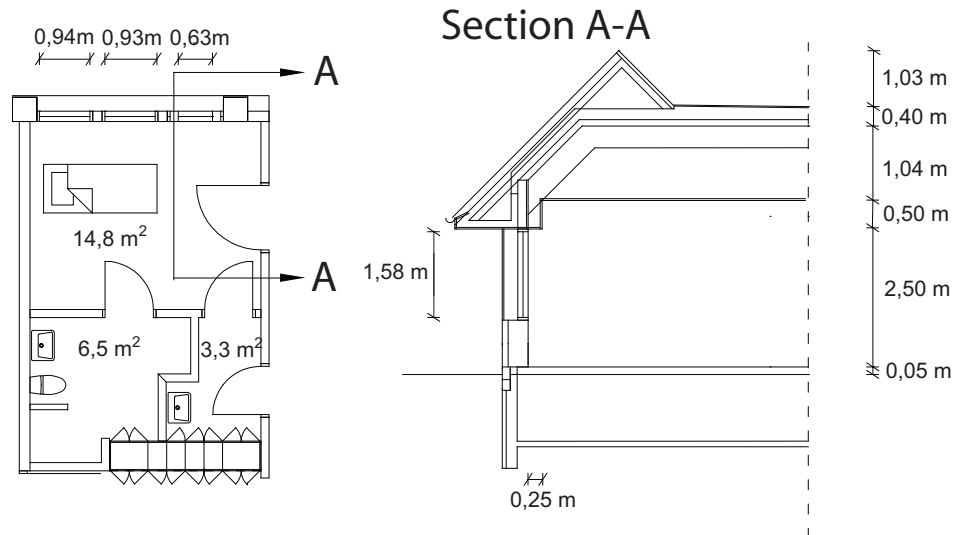
Figure 9.4: *Dimensions the bed ward with one bed.*

The bed ward consist of a toilet with a bath, a main room with a bed and an extra room. For the calculations all the rooms have a common ventilation system. The dimensions of the rooms for the bed ward are listed in table 9.2.

Table 9.2: *Dimensions of the bed ward with one bed.*

Area of the toilet	$[m^2]$	6,5
Height of the toilet	$[m]$	3,0
Volume of the toilet	$[m^3]$	19,5
Area of the main room	$[m^2]$	14,8
Height of the main room	$[m]$	3,0
Volume of the main room	$[m^3]$	44,4
Area of the extra room	$[m^2]$	3,3
Height of the extra room	$[m]$	3,0
Volume of the extra room	$[m^3]$	9,9

9.1.1   Location and weather data

The calculations are made in four different situations; summer, winter, July and February. The used weather data are listed in table 9.3.

Table 9.3: *Weather data used for the calculations.*

		Winter period	Summer period	February	July
Ambient temperature	$[°C]$	2,00	13,4	-1,02	16,4
Wind speed	$[\frac{m}{s}]$	4,71	4,03	4,43	3,87
Wind direction	$[°]$	167	195	129	205
Density of ambient air	$[\frac{kg}{m^3}]$	1,30	1,23	1,30	1,22

The wind from the atmosphere is at the surface slowed down by friction. This means that it is necessary to convert the average wind speed for the Danish reference year to a reference wind speed that affects the building. This is done by using the equation:

$$V_{ref} = V_{10} \cdot k \cdot h^\alpha \tag{9.1}$$

[Heiselberg, 2007b]

where

V_{10}	:	Meteorological wind speed in open land measured at 10 m height $[\frac{m}{s}]$
h	:	Actual height above ground for the building $[m]$
k and α	:	Terrain coefficients $[-]$

The hospital is assumed to be placed in an environment corresponding to country with scattered stand. The used terrain coefficients and height of the building are listed in table 9.4.

Table 9.4: *Terrain coefficients and height of the building.*

Height, h	$[m]$	6,0
k	$[-]$	0,52
α	$[-]$	0,20

From the values listed in table 9.3 and table 9.4 the reference wind speed are calculated and listed in table 9.5.

Table 9.5: *Reference wind speed.*

		Winter period	Summer period	February	July
V_{ref}	$[\frac{m}{s}]$	3,50	3,00	3,29	2.88

The C_p-value for a surface depends on the angle by which the wind hits the surface. The C_p-values for a squared building in an exposed environment can be found in literature [Heiselberg, 2007a] . The C_p-values are given for the angle, θ, between the normal of a facade and the wind direction. The C_p-values are listed in table 9.6.

Table 9.6: *The c_p-values for the building.   [Heiselberg, 2007a]*

		Winter period	Summer period	February	July
Surface 2	[-]	-0,2	-0,4	-0,2	-0,4
Roof	[-]	-0,6	-0,6	-0,6	-0,6

For the calculations are used an indoor temperature of $24,5\ ^\circ C$ in the summer period and $22\ ^\circ C$ in the winter period. These temperatures corresponds to the average thermal comfort levels in the periods [DS474, 1994] . All the openings in the rooms are assumed to have a discharge coefficient of 0,61, which correspond to a standard discharge coefficient for a sharp-edged opening [Heiselberg, 2006] .

9.1.2   Air changes rate for the bed wards

As written in chapter 4 the minimum requirement for the air changes rate in an isolation room is $12\ h^{-1}$. For a bed ward the minimum air change rate is $6\ h^{-1}$. For the bed wards it is therefore investigated if it is possible to get an air change rate of minimum $6\ h^{-1}$ in all the four situations.

For both bed wards only the windows in the facade are used for natural ventilation. The ventilation principle for the bed wards are shown in figure 9.5.
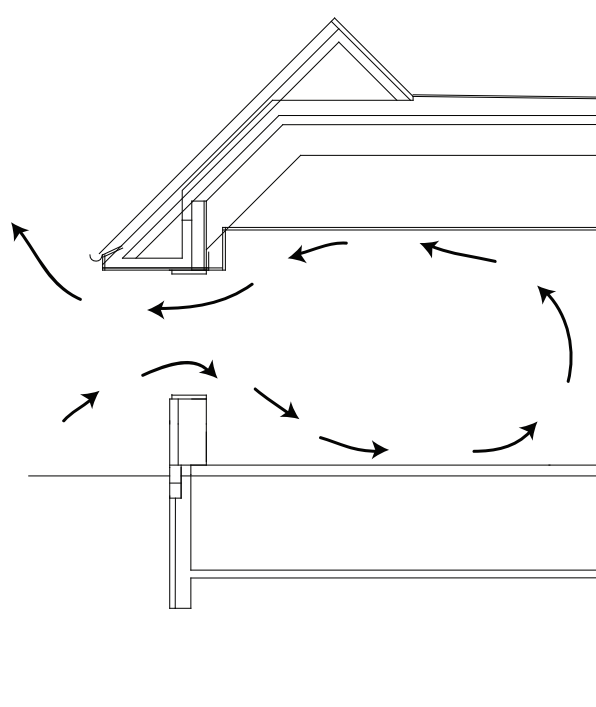
Figure 9.5: *The ventilation principle for the bed wards.*

The airflow for the two bed wards according to both thermal buoyancy and wind pres-

sure and only by thermal buoyancy are calculated from equation (A.11) and (A.10). The airflows and the air changes rates for the two bed wards are calculated and listed in table 9.7.

Table 9.7: *Airflows and air changes rates for the bed wards.*

Bed ward with one bed		Winter period	Summer period	February	July
Airflow coursed by thermal buoyancy	$[\frac{m^3}{s}]$	0,49	0,36	0,53	0,31
Air changes rate coursed by thermal buoyancy	$[h^{-1}]$	24,1	17,8	26,0	15,2
Airflow coursed by wind and thermal buoyancy	$[\frac{m^3}{s}]$	0,28	0,22	0,29	0,20
Air changes rate coursed by wind and thermal buoyancy	$[h^{-1}]$	13,6	10,9	14,3	9,8

Bed ward with two bed					
Airflow coursed by thermal buoyancy	$[\frac{m^3}{s}]$	0,49	0,36	0,53	0,31
Air changes rate coursed by thermal buoyancy	$[h^{-1}]$	25,4	18,7	27,3	16,0
Airflow coursed by wind and thermal buoyancy	$[\frac{m^3}{s}]$	0,28	0,22	0,29	0,20
Air changes rate coursed by wind and thermal buoyancy	$[h^{-1}]$	14,3	11,5	15,0	10,4

The results in table 9.7 shows that the wind has a negative effect on the air changes rates in all the situations. This is not a problem since both bed wards have an acceptable air changes rate according to the minimum air change rate for a bed ward in all four situations with and without wind as a driving force. However there would in the winter period probably be thermal comfort problem in the rooms since the air through the windows are not heated. To avoid this problem it could be an advantage to let the air through an opening under the windows and let it pass by a convector before it enters the room. To avoid that the opening gets too big it can be necessary to use cross and stack ventilation for the rooms.

9.1.3   Design for isolation rooms

To investigate the possibilities of using natural ventilation for isolation rooms, the three bed wards with one bed are redesigned to isolation rooms. The design of the isolation rooms are shown in figure 9.6. The toilet and the main room in the isolation room have a common

ventilation system. The extra room in the bed wards are in the isolation rooms changed to an anteroom. It is only possible to access the isolation rooms through the anteroom to avoid spread of diseases.
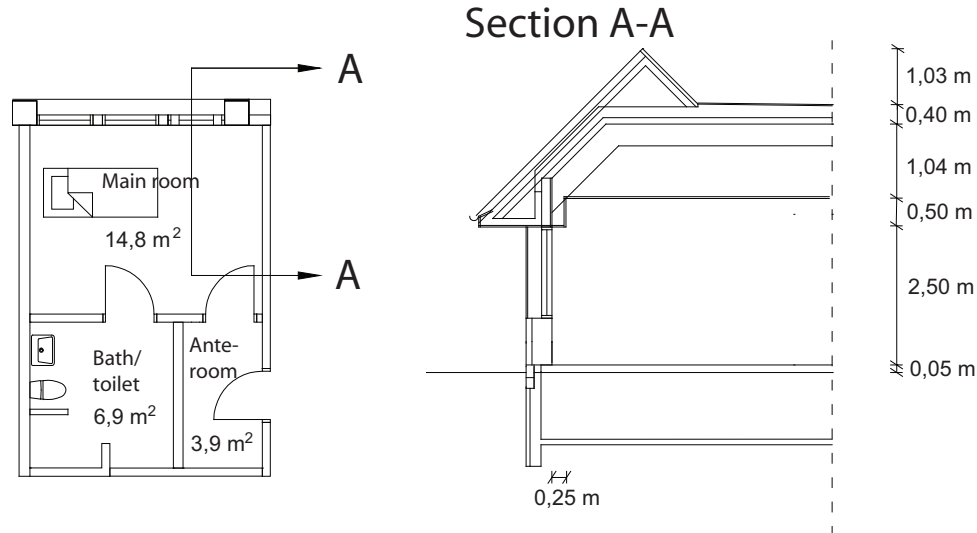
Figure 9.6: *The design of the isolation rooms.*

The dimensions for the isolation rooms are listed in table 9.8.

Table 9.8: *Dimensions of the isolation room and the anteroom.*

Area of the isolation room	$[m^2]$	21,7
Height of the isolation room	$[m]$	3,0
Volume of the isolation room	$[m^3]$	65,1
Area of the anteroom	$[m^2]$	3,9
Height of the anteroom	$[m]$	3,0
Volume of the anteroom	$[m^3]$	11,7

9.1.4 Single sided ventilation

For the first suggestion the rooms are assumed to be single sided ventilated. For the rooms the airflow and the air change rate are investigated.

For the bed wards and the isolation rooms are located a vertical opening beneath the windows used for ventilation, as shown in figure 9.7.

The anterooms are placed inside the building, and do not have a direct access to the facade. It is therefore chosen to ventilate the anterooms through a horizontal opening in the roof, as shown in figure 9.7.
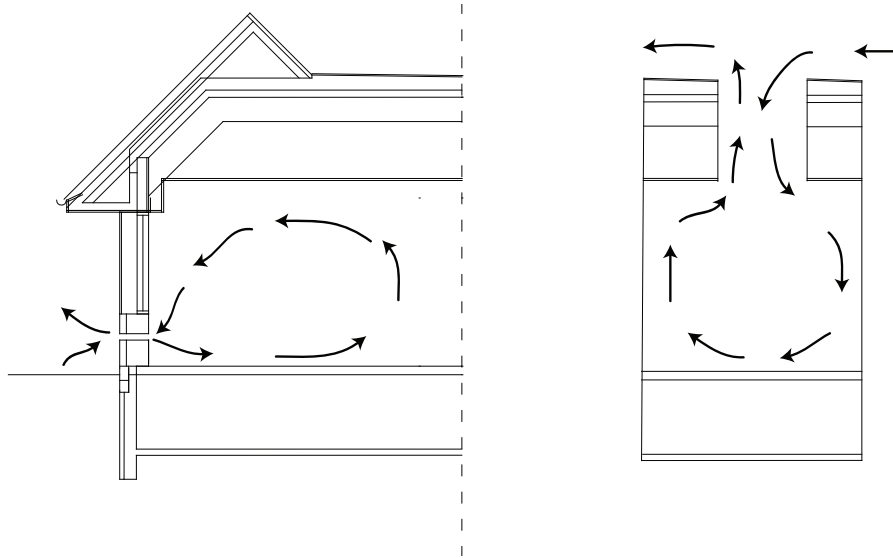
Figure 9.7: *The single sided ventilation principle for the bed wards and the part of the isolation rooms containing the main room and the toilet are shown at the left. The single sided principle for the anterooms are shown to the right.*

The airflow through the openings in the isolation rooms and the bed wards are calculated from equation (A.11) and (A.10) from appendix A. The airflows and the air changes rates for the two rooms in the four situations are listed in table 9.9.

Table 9.9: *Opening's sizes, airflows and air changes rates through the isolation rooms and the bed wards.*

Isolation rooms		Winter period	Summer period	February	July
Height of the opening	$[m]$	0,66	0,78	0,64	0,84
Length of the opening	$[m]$	2,50	2,50	2,50	2,50
Area of the opening	$[m^2]$	1,6	2,0	1,6	2,1
Airflow coursed by thermal buoyancy	$[\frac{m^3}{s}]$	0,37	0,35	0,38	0,34
Air changes rate coursed by thermal buoyancy	$[h^{-1}]$	20,6	19,5	21,3	18,6
Airflow coursed by wind and thermal buoyancy	$[\frac{m^3}{s}]$	0,22	0,22	0,22	0,22
Air changes rate coursed by wind and thermal buoyancy	$[h^{-1}]$	12,0	12,0	12,0	12,0

Bed wards					
Height of the opening	$[m]$	0,41	0,48	0,40	0,52
Length of the opening	$[m]$	2,50	2,50	2,50	2,50
Area of the opening	$[m^2]$	1,03	1,2	1,01	1,29
Airflow coursed by thermal buoyancy	$[\frac{m^3}{s}]$	0,18	0,17	0,19	0,16
Air changes rate coursed by thermal buoyancy	$[h^{-1}]$	9,4	8,7	9,8	8,3
Airflow coursed by wind and thermal buoyancy	$[\frac{m^3}{s}]$	0,12	0,12	0,12	0,12
Air changes rate coursed by wind and thermal buoyancy	$[h^{-1}]$	6,0	6,0	6,0	6,0

Like in the situation when the windows were used for natural ventilation the wind have a negative effect on the airflow through the rooms.

From table 9.9 it is seen that it is possible to use the openings beneath the windows for ventilation for both the isolation room and bed ward. The best solution for single sided ventilation is to have an opening with the dimensions corresponding to the one used in the winter period. For the summer period, when there are no thermal comfort problems, the opening's sizes can be enhance by using the windows.

The anterooms are ventilated through an opening in the roof. The ventilation of the rooms are coursed by the density difference of the inside and the outside air. The heavier colder air outside will make a buoyancy driven downward flow and to ensure the mass

balance this will create an outflow of warmer air from the room [Heiselberg, 2006] . For the calculation of the airflow equation (A.14) in appendix A is used. The input and output are listed in table 9.10.

Table 9.10: *Opening's sizes, airflows and air changes rates through the anterooms.*

		Winter period	Summer period	February	July
Thickness of the opening, h	$[m]$	1,44	1,44	1,44	1,44
Diameter, D	$[m]$	0,54	0,75	0,52	0,88
Length of the sides	$[m]$	0,48	0,63	0,46	0,78
Area	$[m^2]$	0,23	0,40	0,21	0,61
Airflow	$[\frac{m^3}{s}]$	0,040	0,041	0,040	0,042
Air changes rate	$[h^{-1}]$	12,0	12,0	12,0	12,0
Condition for the calculation 0,4<h/D<3,25		2,64	2,01	2,79	1,64

From table 9.10 it is seen that it is possible to create a sufficient air change rate with the opening in the roof.

9.1.5 Cross ventilation

For the second solution the airflow rate is investigated in the case where cross ventilation is used for the bed wards and isolation room.

The bed wards and the isolation rooms have direct access to the outside through one of the building's facades and the roof. It is therefore chosen to have an opening in the facade under the window and in the roof. The anterooms are only connected to the outside through the roof, it is therefore not looked further into if it is possible to use cross ventilation for the anteroom. The ventilation principle for the bed wards and isolation rooms are shown in figure 9.8.
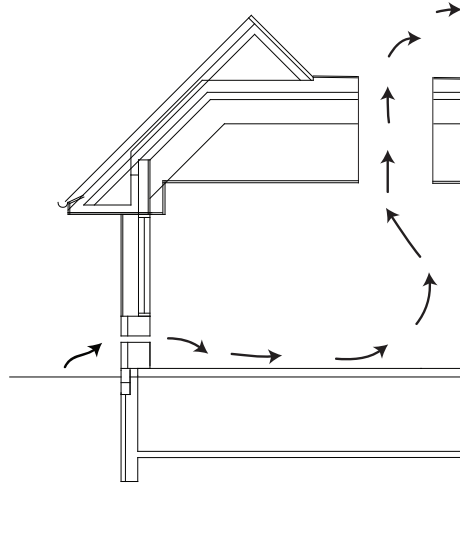
Figure 9.8: *The cross ventilation principle for the bed wards and the isolation rooms.*

The airflow through the rooms are calculated by equation (A.30) in appendix A.1. The neutral plane and intern pressure in the rooms are calculated by iteration of the mass balances in equation (A.20) and (A.26) in appendix A.1. The input and output for the calculation of the air changes rate are listed in table 9.12 and table 9.11.

Table 9.11: *Opening's sizes, airflows and air changes rates through the isolation room.*

		Winter period	Summer period	February	July
Height of the inlet	$[m]$	0,06	0,10	0,06	0,10
Width of the inlet	$[m]$	2,5	2,5	2,5	2,5
Inlet area	$[m^2]$	0,15	0,25	0,15	0,25
Outlet area	$[m^2]$	0,15	0,25	0,15	0,25
Position of inlet's center	$[m]$	0,53	0,53	0,55	0,55
Position of outlet's center	$[m]$	5,0	5,0	5,0	5,0
Location of neutral plan	$[m]$	2,64	2,71	2,64	2,72
Airflow coursed by thermal buoyancy	$[\frac{m^3}{s}]$	-0,167	-0,199	-0,179	-0,169
Air changes rate coursed by thermal buoyancy	$[h^{-1}]$	9,2	11,0	9,9	9,3
Internal pressure coursed by wind	$[pa]$	-3,11	-2,77	-2,76	-2,52
Airflow coursed by wind	$[\frac{m^3}{s}]$	-0,14	-0,15	-0,14	-0,14
Air changes rate coursed by wind	$[h^{-1}]$	8,4	8,2	7,9	7,8
Internal pressure with wind and thermal buoyancy	$[pa]$	-3,64	-2,8	-3,12	-2,5
Airflow through the outlet coursed by wind and thermal buoyancy	$[\frac{m^3}{s}]$	-0,23	-0,25	-0,22	-0,22
Air changes rate coursed by wind and thermal buoyancy	$[h^{-1}]$	12,4	13,7	12,0	12,0

Table 9.12: *Opening's sizes, airflows and air changes rates through the bed wards.*

		Winter period	Summer period	February	July
Height of the inlet	$[m]$	0,04	0,05	0,04	0,06
Width of the inlet	$[m]$	2,5	2,5	2,5	2,5
Inlet area	$[m^2]$	0,10	0,13	0,10	0,13
Outlet area	$[m^2]$	0,10	0,13	0,10	0,13
Position of inlet's center	$[m]$	0,52	0,53	0,52	0,53
Position of outlet's center	$[m]$	5,0	5,0	5,0	5,0
Location of neutral plan	$[m]$	2,63	2,69	2,63	2,71
Airflow coursed by thermal buoyancy	$[\frac{m^3}{s}]$	-0,112	-0,100	-0,120	-0,102
Air changes rate coursed by thermal buoyancy	$[h^{-1}]$	5,7	5,1	6,12	5,2
Internal pressure coursed by wind	$[pa]$	-3,11	-2,76	-2,76	-2,52
Airflow coursed by wind	$[\frac{m^3}{s}]$	-0,10	-0,07	-0,10	-0,08
Air changes rate coursed by wind	$[h^{-1}]$	5,2	3,8	4,9	4,3
Internal pressure with wind and thermal buoyancy	$[pa]$	-3,12	-2,76	-3,12	-2,52
Airflow through the outlet coursed by wind and thermal buoyancy	$[\frac{m^3}{s}]$	-0,15	-0,12	-0,15	-0,13
Air changes rate coursed by wind and thermal buoyancy	$[h^{-1}]$	7,7	6,4	7,4	6,8

From table 9.11 and 9.12 it is seen that it is possible to use cross ventilation in the four investigated periods of the year. It is also seen that the driving forces in all four situations work together to ensure a sufficient air changes rate for the rooms.

9.1.6 Stack

To ensure a high air change rate for the isolation room the effect of a chimney is investigated. The position of the openings and the size correspond to those previous found for an isolation room in the winter situation. The effect of the chimney for the four situations are shown in figure 9.9.
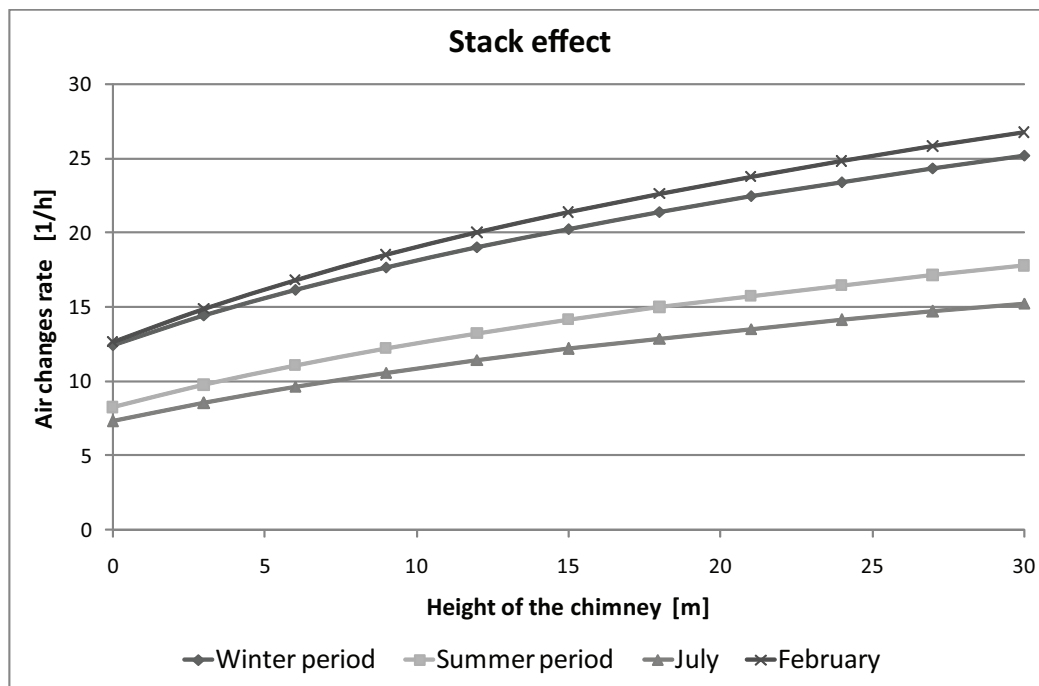
Figure 9.9: *The effect of placing a chimney on the roof on the isolation room.*

From figure 9.9 it is seen that the chimney enhance the air changes rate for the isolation room in all four weather situations.

9.1.7 Choice of ventilation system

From the above calculations it is seen that it is possible to create a sufficient air changes rate in the bed wards and the isolation rooms in the four weather situations with both single sided ventilation and cross ventilation. However the calculations showed that the optimal solution was to combine cross ventilation with a chimney for both the bed wards and the isolation rooms therefore this principle is chosen for further investigations. The most obvious ventilation principle for the anteroom is a horizontal opening therefore also this principle will be further investigated. The different principles are shown in figure 9.10.
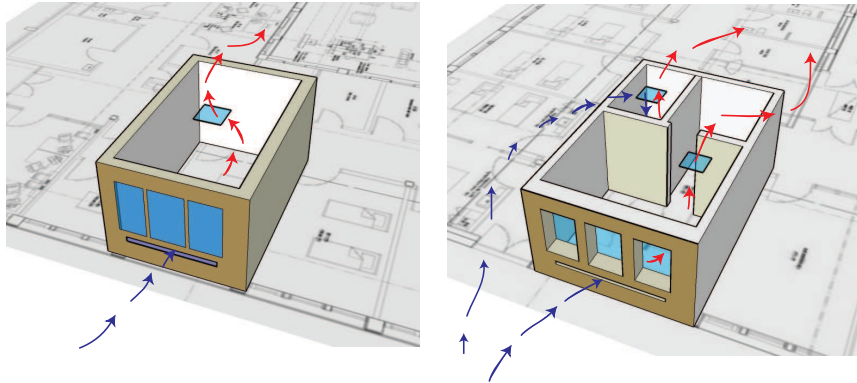
Figure 9.10: *The chosen ventilation strategies for the bed wards, the isolation rooms and the anterooms.*

Beside getting the right airflow for the isolation room, it is also necessary that the isolation room has the right pressure, to create the intended airflow between the isolation room and anteroom. For a low pressurized isolation room the airflow has to be from the anteroom to the isolation room, as shown in figure 9.11.
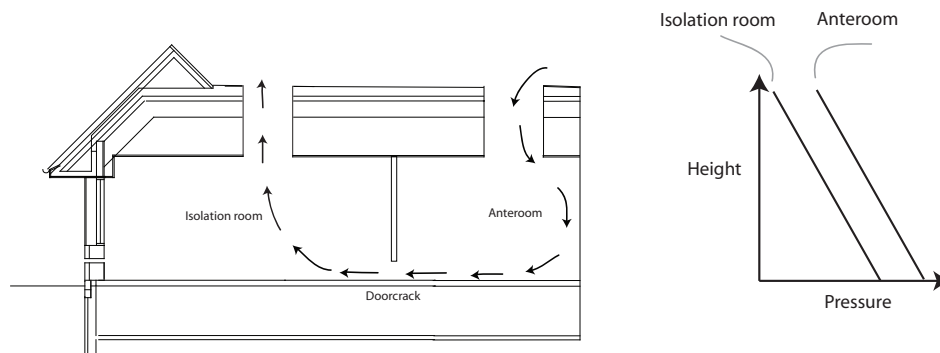
Figure 9.11: *The airflow between the anteroom and the isolation room, when the isolation room is low pressurized.*

For a high pressurized isolation room the airflow have to be from the isolation room into the anteroom, as shown in figure 9.12.
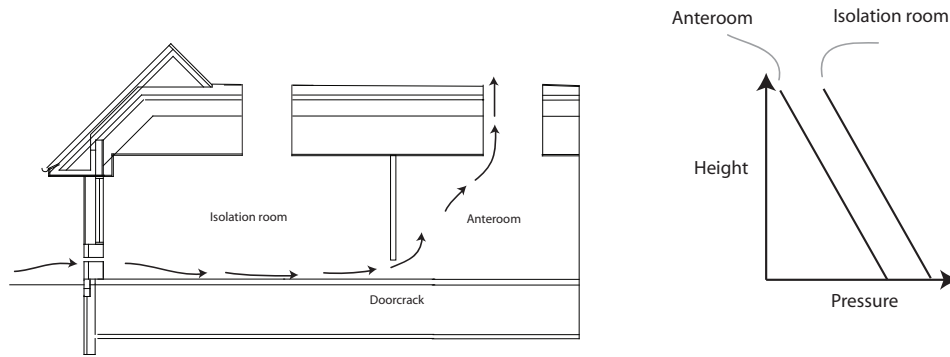
Figure 9.12: *The airflow between the anteroom and the isolation room, when the isolation room is high pressurized.*

The further investigation of the ventilation principle will consist of a multi zone model in which the data from the Danish design reference year will be used for a year simulation. The final design of the ventilation system will be decided thus there during a year always are a sufficient air changes rates in the rooms as well as sufficient pressure in the isolation rooms and the anterooms.

9.2 Grantham hospital

As for Aabenraa hospital there are also made analytical calculations for Grantham hospital to investigate the air change rate for the third class bed ward and the isolation room. Grantham hospital is showed in figure 9.13.
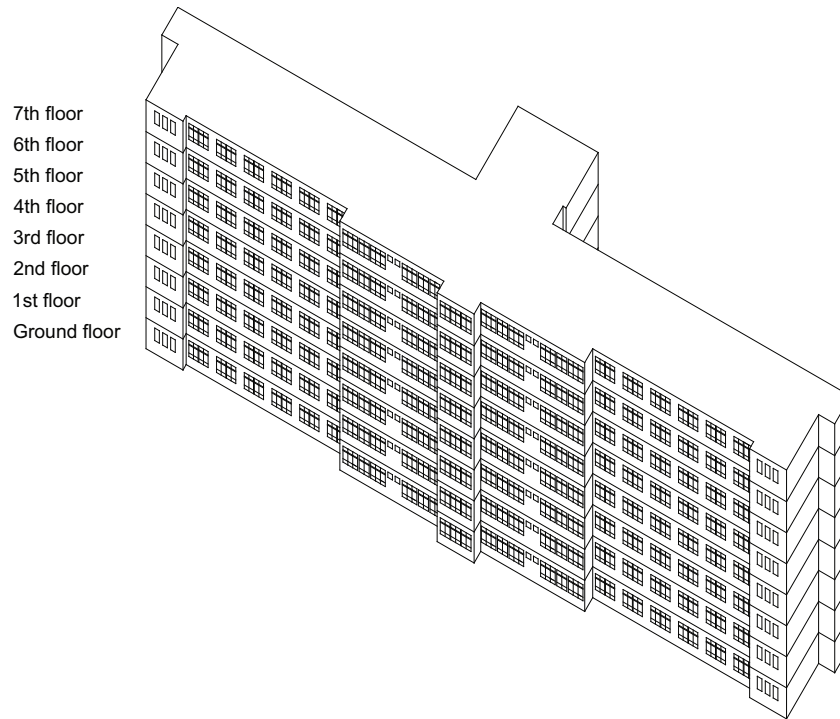
Figure 9.13: *Grantham hospital.*

The floor plan of the 1st, 2nd and 4th floor of Grantham hospital is showed in figure 9.14.
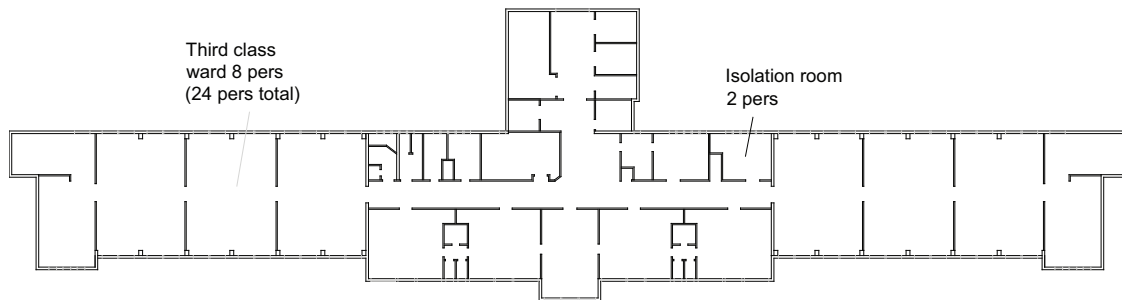
Figure 9.14: *Floor plan of the 1st, 2nd and 4th floor of Grantham hospital.*

For the floor are calculated the airflow rate for one of the third class ward and for the isolation room. The two rooms are showed in figure 9.15.
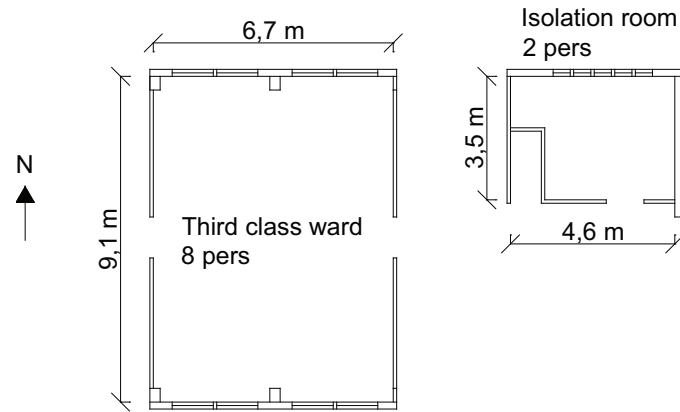
Figure 9.15: *Third class ward and isolation room.*

The floor and window area of the two rooms are listed in table 9.13.

Table 9.13: *Detailed information of the two rooms.*

	Third class ward	Isolation room
Room dimensions		
Length $[m]$	6,7	4,6
Width $[m]$	9,1	3,5
Height $[m]$	3,4	3,4
Area $[m^2]$	61,5	16,1
Volume $[m^3]$	206,2	54,1
Window dimensions		
Height $[m]$	1,3 + 0,4	1,4
Width $[m]$	1,2	0,4
Number $[-]$	4	5
Total area $[m^2]$	7,6	3,0
Discharge coefficient $[-]$	0,7	0,7
Height above ground bottom $[m]$	1,0	1,3
Height above ground top $[m]$	2,8	2,8

In table 9.14 are listed the indoor and outdoor temperature and the wind speed used for the calculations. For the calculations are used weather data for July, January, an average of the 6 summer months and an average of the 6 winter months. July and January are chosen because these months are the warmest and the coldest month respectively for Hong Kong. The average of the summer and winter months are chosen to get an average calculation of the airflow.

The calculations can be found in the spreadsheet 'Analytical calculations, Grantham.xls' on the CD.

Table 9.14: *Indoor and outdoor temperature and wind speed.*

Temperature	
Indoor temperature, summer [$°C$]	24,5
Indoor temperature, winter [$°C$]	22,0
Outdoor temperature, July [$°C$]	29,0
Outdoor temperature, January [$°C$]	16,4
Outdoor temperature, summer [$°C$]	27,2
Outdoor temperature, winter [$°C$]	19,6
Wind speed	
July [$\frac{m}{s}$]	6,3
January [$\frac{m}{s}$]	6,1
Summer [$\frac{m}{s}$]	6,1
Winter [$\frac{m}{s}$]	6,5
Reference wind speed, July [$\frac{m}{s}$]	5,0
Reference wind speed, January [$\frac{m}{s}$]	4,9
Reference wind speed summer [$\frac{m}{s}$]	4,9
Reference wind speed winter [$\frac{m}{s}$]	5,1

9.2.1   Single sided ventilation

For both the third class ward and the isolation room are calculated the airflow rate according to single sided ventilation. For both situations it is assumed that the neutral plane is located in the middle of the opening. This is done because all the openings for the room are located in the same height and it is assumed that the room is not influenced by any other rooms, as for the calculations for Aabenraa hospital. Therefore also the calculations for Grantham hospital can only be used to get a rough estimate of the airflow. The airflow for the rooms are calculated by equation (A.10) in appendix A.1. The airflow rate and air change rate for the two rooms in the summer and winter situation are listed in table 9.15.

Table 9.15: *Airflow rate and air change rate for the two bed wards in the summer and winter situation according to thermal buoyancy.*

	Third class ward	Isolation room
Airflow rate, July [$\frac{m^3}{s}$]	3,11	1,14
Airflow rate, January [$\frac{m^3}{s}$]	3,68	1,34
Airflow rate, summer [$\frac{m^3}{s}$]	2,39	0,87
Airflow rate, winter [$\frac{m^3}{s}$]	2,43	0,88
Air change rate, July [h^{-1}]	54,4	75,5
Air change rate, January [h^{-1}]	64,3	89,3
Air change rate, summer [h^{-1}]	41,7	58,0
Air change rate, winter [h^{-1}]	42,3	58,8

In chapter 5 it is listed that the air change rate for an isolation room has to be minimum 12 h^{-1}. The simple calculation of the air change rate according to only thermal buoyancy shows that with the temperatures listed in table 9.14 for all the situations the air change rate is higher than the minimum value.

The ventilation rate according to both thermal buoyancy and wind in the case of single sided ventilation is calculated from equation (A.12) and equation (A.13) in appendix A.1. The airflow rate and air change rate are listed in table 9.16.

Table 9.16: *Airflow rate and air change rate for the two rooms in the summer and winter situation according to both thermal buoyancy and wind pressure.*

	Third class ward	Isolation room
Airflow rate, July $[\frac{m^3}{s}]$	0,24	0,12
Airflow rate, January $[\frac{m^3}{s}]$	0,69	0,26
Airflow rate, summer $[\frac{m^3}{s}]$	0,35	0,15
Airflow rate, winter $[\frac{m^3}{s}]$	0,60	0,23
Air change rate, July $[h^{-1}]$	4,1	7,9
Air change rate, January $[h^{-1}]$	12,0	17,6
Air change rate, summer $[h^{-1}]$	6,1	10,0
Air change rate winter $[h^{-1}]$	10,5	15,6

From table 9.16 it is showed that for the summer situation for both the third class ward and the isolation room the air change rate is lower than the minimum air change rate for a bed ward of 6 h^{-1} and an isolation room of 12 h^{-1} respectively. For the winter situation the air change rate is high enough in both situations.

A reason for the lower air change rate in the situation with both thermal buoyancy and wind pressure compared to the situation with only thermal buoyancy is because the thermal buoyancy and the wind pressure act against each other.

9.2.2 Cross ventilation

From figure 9.15 it is seen that for the third class ward there is placed windows on both the north and the south side. For the third class ward it is therefore possible to use cross ventilation to ventilate the room. For the isolation room it is showed in figure 9.15 that there only are windows on the north side. To use cross ventilation for this room it is therefore necessary to open the door and thereby use the windows on the south facade for cross ventilation. For an isolation room where the infection is spread by the air it is very important that the air is not let from the isolation room into other rooms. Therefore it is decided that it is not possible to use cross ventilation for the isolation room.

The pressure difference according to thermal buoyancy is calculated from equation (A.16) in appendix A.1. The airflow rate is calculated by:

$$q = C_d A \sqrt{\frac{2\Delta p}{\rho}} \tag{9.2}$$

The pressure difference and airflow rate according to thermal buoyancy are listed in table 9.17.

Table 9.17: *Pressure difference, airflow rate and air change rate according to thermal buoyancy.*

Pressure difference	
July $[Pa]$	-0,15
January $[Pa]$	0,20
Summer $[Pa]$	-0,09
Winter $[Pa]$	0,08
Airflow rate	
July $[\frac{m^3}{s}]$	-2,66
January $[\frac{m^3}{s}]$	3,04
Summer $[\frac{m^3}{s}]$	-2,04
Winter $[\frac{m^3}{s}]$	2,00
Air change rate	
July $[h^{-1}]$	-46,5
January $[h^{-1}]$	53,0
Summer $[h^{-1}]$	-35,7
Winter $[h^{-1}]$	34,9

From table 9.17 it is seen that by only thermal buoyancy the air change rate is higher for both summer and winter situation than the minimum air change rate for an isolation room.

The pressure difference according to wind pressure is calculated from equation (A.22) in appendix A.1. Because there is only two openings for the room and it is assumed that the discharge coefficient and air density for the two openings are the same the internal pressure is calculated from:

$$P_i = \frac{1}{2}\rho_e v_{ref}^2 \frac{A_1^2 C_{p1} + A_2^2 C_{p2}}{A_1^2 + A_2^2} \tag{9.3}$$

The used pressure coefficient and internal pressure are listed in table 9.18.

Table 9.18: *Pressure coefficient and internal pressure.*

	Pressure coefficient
Leeward $[-]$	-0,3
Windward $[-]$	0,06
	Internal pressure
July $[Pa]$	-1,77
January $[Pa]$	-1,73
Summer $[Pa]$	-1,64
Winter $[Pa]$	-1,93

The pressure difference and airflow rate according to wind pressure are listed in table 9.19.

Table 9.19: *Pressure difference, airflow rate and air change rate according to wind pressure.*

Pressure difference	
July $[Pa]$	2,65
January $[Pa]$	2,59
Summer $[Pa]$	2,46
Winter $[Pa]$	2,89
Airflow rate	
July $[\frac{m^3}{s}]$	11,18
January $[\frac{m^3}{s}]$	11,07
Summer $[\frac{m^3}{s}]$	10,78
Winter $[\frac{m^3}{s}]$	11,68
Air change rate	
July $[h^{-1}]$	195,2
January $[h^{-1}]$	193,2
Summer $[h^{-1}]$	188,2
Winter $[h^{-1}]$	204,0

From table 9.19 it is seen that the air change rate for both summer and winter is a lot higher than the minimum air change rate of $12\ h^{-1}$. A reason for the high air change rate can be the value of the pressure coefficient. The pressure coefficient is estimated from table values for a building with a length two times the width, exposed and up to three stories. This is an estimate and not the correct values for the building. A reason for the high air change rate could therefore be according to the pressure coefficient or the reference wind speed.

The pressure difference according to both thermal buoyancy and wind pressure is calculated from equation (A.29) and are listed in table 9.20.

Table 9.20: *Pressure difference, airflow rate and air change rate according to both thermal buoyancy and wind pressure.*

Pressure difference	
July $[Pa]$	2,80
January $[Pa]$	2,79
Summer $[Pa]$	2,55
Winter $[Pa]$	2,98
Airflow rate	
July $[\frac{m^3}{s}]$	11,49
January $[\frac{m^3}{s}]$	11,48
Summer $[\frac{m^3}{s}]$	10,97
Winter $[\frac{m^3}{s}]$	11,85
Air change rate	
July $[h^{-1}]$	200,7
January $[h^{-1}]$	200,3
Summer $[h^{-1}]$	191,5
Winter $[h^{-1}]$	206,9

From table 9.20 it is again seen that the air change rate is high compared to the minimum air change rate for an isolation room. The reason might be as stated above for the situation with wind only.

For all the listed cases above there only is a problem with the air change rate in the summer period with single sided ventilation where both thermal buoyancy and wind are acting. For all the other cases the air change rate is higher than the minimum air change rate for an isolation room. It is also showed that the air change rate by cross ventilation is higher than for single sided ventilation.

The used weather data for the calculations are mean values from Hong Kong for 2006. Since it is mean values there might be situations that are more critical than the one listed above. Therefore there might be problems in other situations specially for the single sided ventilation.

For the calculations it is also stated that the discharge coefficient for all the windows are 0,7. This one might vary for the windows depending on the type of the opening.

To ensure the right air change rate all the time it is possible to use a fan to assist when the natural driving forces are not high enough to create the desired air change rate as listed in section 8.4.

Another idea listed in section 8.5 is to use earth cooling and heating to pre-heat or cool the air. For this solution the best location of the rooms are close to the ground so it is

not necessary to create canals from ground level to upper levels. By doing this it is also important that the canals are isolated in a proper way so the air in the canal does not loose or gain energy before it reach the desired room. Because of the high location of the rooms in the building ventilation by using earth cooling or heating may not be the best solution.

Because of the layout of the building it is concluded that single sided or cross ventilation is the best solution.

9.2.3 Isolation room

In chapter 3.2 are listed some guidelines for an isolation room. It is stated that for the optimal isolation room there have to be an anteroom to:

- Ensure the right air-balance relationship

- Help to reduce the escape of droplet nuclei during opening and closing of the isolation room door

- Masking and unmasking of the nursing people and doctors

For the isolation room for Grantham hospital showed in figure 9.15 it is seen that the room does not have en anteroom. In figure 9.16 are showed a layout for the isolation room where there is implemented an anteroom. The outer dimensions for the isolation room showed in figure 9.16 are the same as for the original isolation room showed in figure 9.15.
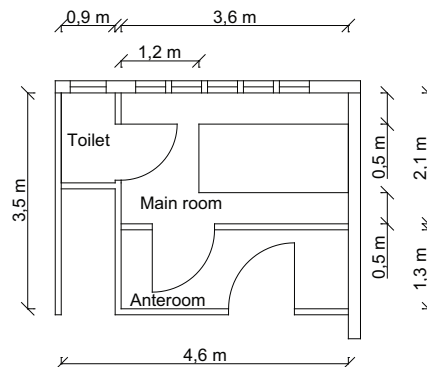
Figure 9.16: *Floor plan of the isolation room after the changes.*

For the isolation room is also located a window in the toilet. Before the change there was no window in the toilet. Because of the position of the isolation room in the building as showed in figure 9.14 it is argued that the best ventilation principle for the isolation room is single sided ventilation. The ventilation principle for the room is showed in figure 9.17.
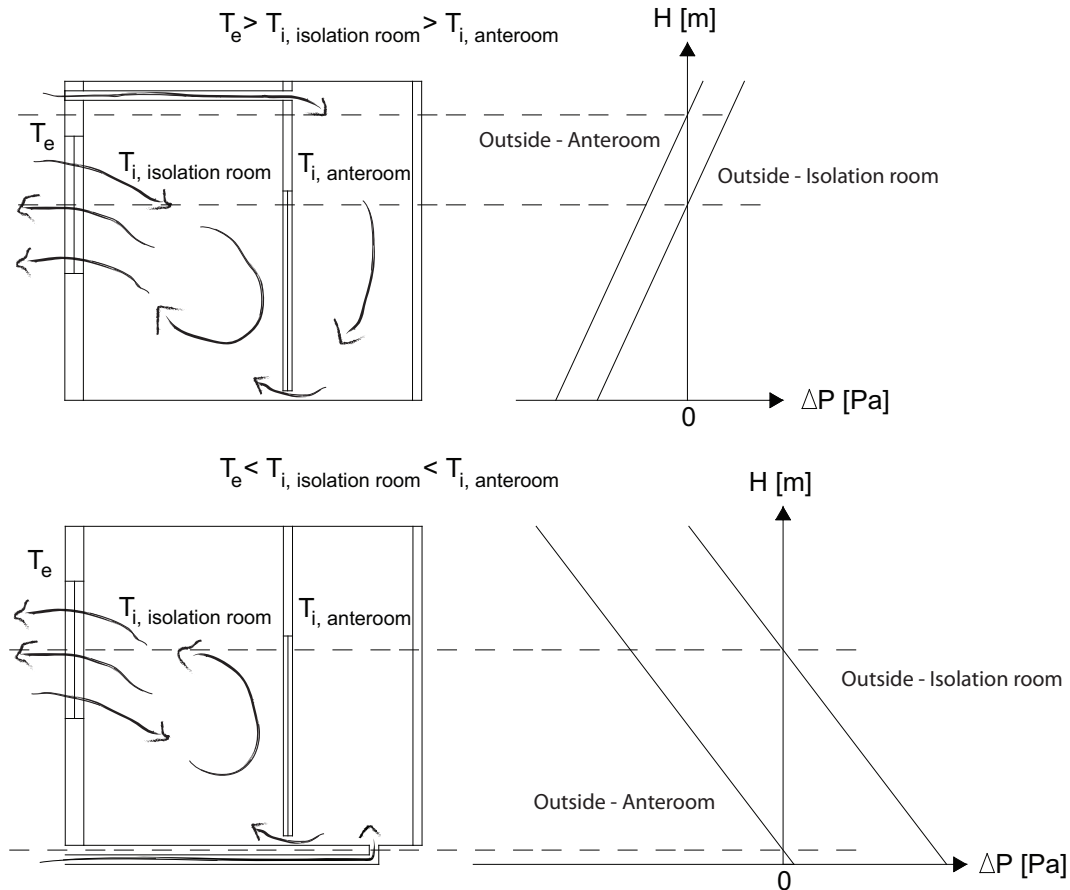
Figure 9.17: *Ventilation principle for the two cases where the outside temperature is higher than the inside temperature and opposite.*

In figure 9.17 are showed two principles for the ventilation system for the isolation room and the anteroom. For the ventilation principles it is assumed that the temperature in the anteroom in the wintertime is higher than the outside temperature and for the summertime lower than the outside temperature.

In the first principle in figure 9.17 the temperature in the anteroom is higher than the outside temperature. For this principle the air from outside is lead into the anteroom through a pipe in the top of the room. From the anteroom the air i lead into the isolation room through a crack under the door into the isolation room. From the isolation room it is lead outside through the window. For the isolation room alone the air is lead into and out of the room through the window. By letting the fresh air into the anteroom and thereafter into the isolation room it is ensured that the bacteria from the sick person is not spread into other rooms.

For the other situation where the temperature in the anteroom is lower than the outside temperature the fresh air is let from outside through a pipe under the floor and into the anteroom. From the anteroom the air is let into the isolation room through the crack under

the door and out again.

To ensure the right airflow in the two situations the neutral plane for the two situations have to be located in different height according to the pressure difference.

In figure 9.18 are the mean outside temperature compared to the inside comfort temperature showed.
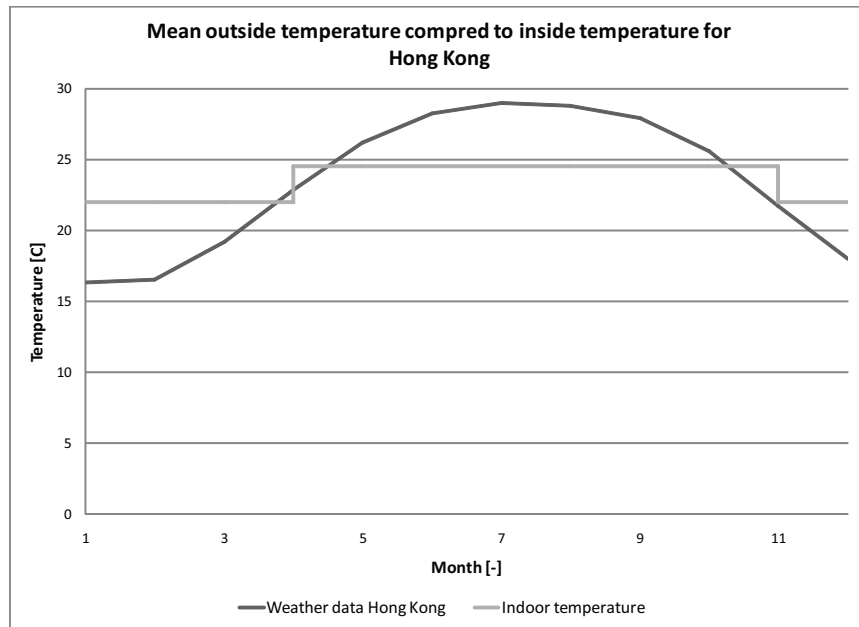
Figure 9.18: *Mean outside temperature compared to inside comfort temperature.*

In figure 9.18 it is seen that for most of the time the mean outdoor temperature is higher than the inside temperature. Because the outside temperature often is higher than the inside temperature there will only be looked further into the first situation showed in figure 9.17. To ensure the right airflow in the case where the inside temperature is higher than the outside temperature there have to be installed a fan.

Single sided ventilation for the isolation room

In the following is the opening area calculated for the redesigned layout of the isolation room. The opening areas are calculated for an air change rate of 12 h^{-1}. The opening area are calculated in the summer situation since it is seen in figure 9.18 that it is only for the summer time the outside temperature is higher than the inside temperature. For the winter time the average outside temperature is lower than the inside temperature and to guarantee there is the necessary airflow for the isolation room a fan are installed.

For the calculations are made two cases shown in figure 9.19. A case where the airflow is coming from the outside through the pipe and into the anteroom. From the anteroom the air is let into the isolation through a crack under the door and out through the windows.

For the other case only the airflow for the isolation room are taken into consideration. In this situation the air is let into the room through the window and out again through the window. The two situations are showed in figure 9.19.
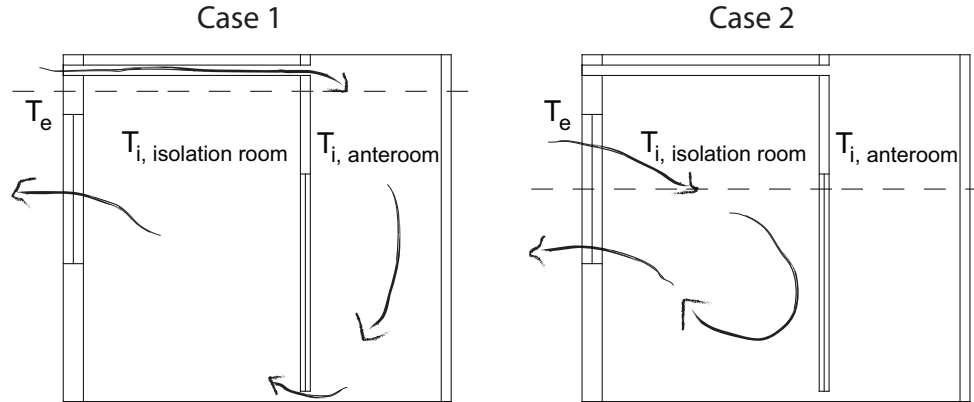
Figure 9.19: *The two cases for the isolation room for which the opening areas are calculated according to the air change rate.*

For the calculation it is assumed that the temperature in the isolation room is the average of the outside temperature and the temperature in the anteroom. The different temperatures are listed in table 9.21.

Table 9.21: *Outside temperature, temperature for the isolation room and temperature for the anteroom.*

Room	Month	Temperature $[^{\circ}C]$
Outside	July	29,0
	Summer	27,2
Isolation room	July	26,8
	Summer	25,8
Anteroom	July	24,5
	Summer	24,5

The dimensions of the two rooms are listed in table 9.22.

Table 9.22: *Dimensions of the two rooms.*

Room		Dimension
Isolation room	Length	$3,6\ m$
	Width	$2,1\ m$
	Height	$3,4\ m$
	Volume	$25,7\ m^3$
Anteroom	Length	$3,6\ m$
	Width	$1,3\ m$
	Height	$3,4\ m$
	Volume	$15,5\ m^3$

The air change rate for the isolation room is set to $12\ h^{-1}$. With a volume of the isolation room of $25,7\ m^3$, as listed in table 9.22, this correspond to a volume flow rate of $0,09\ \frac{m^3}{s}$. For the calculations of the opening area for the changed isolation room are used the same weather data as for the calculations of the air change rate before the changes listed in table 9.14.

For the first case there are two openings located above each other on the same side of the room as showed in figure 9.19. For this situation the opening area of the pipe in the top of the room and the opening area of the crack under the door is calculated from equation (A.18) in appendix A.1. The pressure difference is calculated from equation (A.17). The opening area is calculated for the openings according to an airflow of $12\ h^{-1}$ for the single openings. In the second case there is only located one opening for the room. For this case the opening area is calculated from equation (A.10).

The height of the neutral plane and the height of the openings are listed in table 9.23.

Table 9.23: *Height of neutral plane and location of the openings.*

	Height above floor $[m]$
Neutral plane	3,0
Pipe	3,2
Crack	0,05
Window middle	2,1
Window top	2,8
Window bottom	1,3

The pressure difference according to thermal buoyancy for the two cases and the calculated effective opening areas are listed in table 9.24.

Table 9.24: *Pressure difference and effective opening area for the two cases according to thermal buoyancy.*

		Case 1	**Case 2**
Pressure difference			
Pipe	July	$0,43\ Pa$	
	Summer	$0,25\ Pa$	
Crack	July	$-6,20\ Pa$	
	Summer	$-3,65\ Pa$	
Window	July		$-1,20\ Pa$
	Summer		$-1,17\ Pa$
Effective opening area			
Pipe	July	$0,10\ m^2$	
	Summer	$0,13\ m^2$	
Crack	July	$0,03\ m^2$	
	Summer	$0,03\ m^2$	
Window	July		$0,23\ m^2$
	Summer		$0,30\ m^2$

For the openings are used a discharge coefficient of $0,7$ as listed in table 9.13. The opening area and the dimensions for the different openings according to thermal buoyancy are listed in table 9.25.

Table 9.25: *Opening area and dimensions of the different openings according to thermal buoyancy.*

		Case 1	**Case 2**
Opening area			
Pipe	July	$0,14\ m^2$	
	Summer	$0,17\ m^2$	
Crack	July	$0,04\ m^2$	
	Summer	$0,05\ m^2$	
Window	July		$0,34\ m^2$
	Summer		$0,43\ m^2$
Dimension			
Diameter pipe	July	$0,43\ m$	
	Summer	$0,49\ m$	
Height crack		$0,1\ m$	
Width crack	July	$0,38\ m$	
	Summer	$0,49\ m$	
Height window			$1,44\ m$
Width window	July		$0,23\ m$
	Summer		$0,30\ m$

The opening area according to wind pressure for the first case is calculated from equation (A.27) in chapter A.1. For the calculation the opening area of the pipe from the calculation according to thermal buoyancy is used. In this case only the opening area of the crack is calculated. The effective opening area of the crack is listed in table 9.26.

Table 9.26: *Effective opening area of the crack according to wind pressure for case 1.*

		Effective opening area $[m^2]$
Leeward	July	0,07
	Summer	0,08
Windward	July	0,15
	Summer	0,16

The effective opening areas and dimensions for the two cases according to both thermal buoyancy and wind pressure are listed in table 9.27. The effective opening area for the first case is calculated from equation (A.30) in appendix A.1 where again only the opening area of the pipe according to thermal buoyancy is used. For the second case the opening area according to both thermal buoyancy and wind pressure is calculated from equation (A.12) in appendix A.1.

Table 9.27: *Effective opening area and dimensions of the different openings according to both thermal buoyancy and wind pressure.*

		Case 1	Case 2
Effective opening area			
Crack	Leeward, July	$0,02\ m^2$	
	Leeward, summer	$0,07\ m^2$	
	Windward, July	$0,03\ m^2$	
	Windward, summer	$0,02\ m^2$	
Window	July		$1,11\ m^2$
	Summer		$1,04\ m^2$
Area			
Crack	Leeward, July	$0,02\ m^2$	
	Leeward, summer	$0,10\ m^2$	
	Windward, July	$0,05\ m^2$	
	Windward, summer	$0,03\ m^2$	
Window	July		$1,58\ m^2$
	Summer		$1,50\ m^2$
Dimension			
Height crack		$0,1\ m$	
Width crack	Leeward, July	$0,24\ m$	
	Leeward, summer	$1,03\ m$	
	Windward, July	$0,48\ m$	
	Windward, summer	$0,30\ m$	
Height window			$1,44\ m$
Width window	July		$1,01\ m$
	Summer		$1,04\ m$

From table 9.24, 9.26 and 9.27 it is seen that the opening area for the first case are biggest for the situation with only wind pressure. For the situation with only thermal buoyancy and the case with both thermal buoyancy and wind pressure the openings area are almost the same. According to the openings areas it is seen that the thermal buoyancy have the greatest influence for the ventilation for the room. In the second case it is seen that the thermal buoyancy also have the greatest influence.

Before the change of the layout for the isolation room it is seen in table 9.15 and 9.16 that the highest airflow rate is in the situation with only thermal buoyancy compared to the situation with both thermal buoyancy. This state that for this situation too the thermal buoyancy have the greatest influence.

Since the airflow rate is lower in the situation with both thermal buoyancy and wind

pressure than the case with only thermal buoyancy the wind pressure have a negative effect on the ventilation system when there is a temperature difference for the room and outside.

The opening areas calculated after the change of the isolation room is also seen to be smaller than before the change. Before the change it was seen that the air change rate was high compared to the necessary air change rate of $12 \ h^{-1}$.

9.3 Detailed calculation of airflow

For both Aabenraa and Grantham hospital were made analytical calculations of the air change rate for different rooms. For both hospitals it is showed that it is possible to create a sufficient air change rate for selected rooms.

To create a better isolation room were for both hospitals designed an anteroom that connect the isolation room to the corridor. The purpose of the anterooms were to create a buffer zone between the isolation rooms and the corridor. For the new design the opening areas for the isolation room was calculated to ensure a sufficient air change rate.

The calculations were done by simplified analytical equations and therefore the calculations can only be used to give a rough estimate of the air change rate. In the following are therefore made more detailed investigations of the airflow and air change rates for the rooms for the two hospitals.

The following chapters are divided into calculations first for Aabenraa and thereafter Grantham hospital. Finally the calculations for the two hospitals are analyzed together and the different results are discussed.

For Aabenraa hospital the calculations are divided into the following sections:

Multi zone simulation of a section of Aabenraa hospital. The calculations are used to investigate the airflow between selected rooms and the air change rate for the selected rooms.

CFD simulation for the hospital. The CFD simulation are used to calculate the pressure coefficient for the hospital.

Multi zone simulation with pressure coefficients from CFD. The calculated pressure coefficients from CFD are used for the multi zone model to get a more accurate picture of the airflow between the selected rooms and the air change rate for the selected rooms. The results from the multi zone model with the calculated pressure coefficients are compared to the first multi zone model with pressure coefficients from literature.

For Grantham hospital the calculations are divided into the following sections:

CFD simulation of the influence of mountain and sea breeze. The CFD simulation are used to investigate the mountain and sea breeze and the influence of these on the airflow and air change rate for an isolation room.

Single zone simulation of an isolation room. For the single zone simulation are made a year simulation of the air change rate for the isolation room.

Multi zone simulation of a section of Grantham hospital. The multi zone simulation are used to investigate the airflow between the rooms and the air change rate for an isolation room under different weather conditions.

Chapter 10

Multi zone calculation of Aabenraa hospital

In the following chapter are made a multi zone model of Aabenraa hospital to calculate the airflow for the hospital. For the model infiltration between the rooms are not taken into consideration except the airflow through the door cracks between the rooms. This means that the different rooms are not influenced by infiltration between the rooms and from outside air. The actual airflow path may therefore differ to the calculated airflow path because of infiltration. For tight buildings the difference may not be big because the influence from infiltration on the airflow path is small compared to the airflow through openings. For leaky buildings the influence is bigger. The maximum infiltration is stated in the Danish Building Regulations for $0,13 \frac{l}{s}$ pr. m^2 heated floor area [Erhvervs- og Byggestyrelsen, 2008] .

In the multi zone model are made an investigation of the airflows through the bed wards, the anterooms and the isolation rooms, when the openings sizes from the analytical calculations are used. The position of these rooms in the south east part of Aabenraa hospital is showed in figure 10.1. In the figure the bed wards are marked with a light gray hatch while the isolation rooms and anterooms are marked with a dark gray hatch.
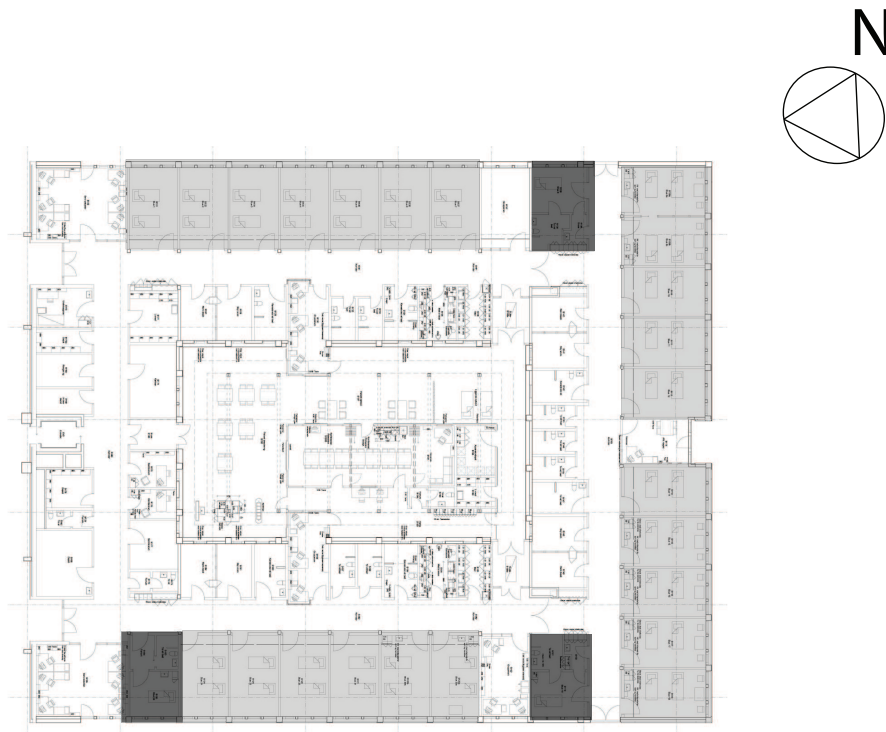
Figure 10.1: *Floor plan of the south east part of Aabenraa hospital, where the bed wards, anterooms and the isolation rooms are highlighted.*

For the model only the south eastern part of the hospital are simulated. This means that connections from the south eastern part of the hospital to the rest of the hospital are not taken into consideration. For the south eastern part of the hospital only the west wall are connected to the rest of the hospital. For the simulation therefore only the west wall would be influenced by the rest of the hospital. None of the investigated rooms are located near this wall which means that the simplification does not have direct influence on these rooms.

Based on an analyze of the results from the multi zone model, the sizes of the openings are decided, thus the bed wards and isolation rooms have a sufficient air changes rate. Both the air change rate and the airflow path for the different rooms are calculated to ensure the right airflow path between the rooms. The requirements to the air changes rate in the rooms and the direction of the airflows between the anterooms and the isolation rooms have to be fulfilled for a hole year.

10.1   Layout of the multi zone model

In the hospital sections there are rooms which are balanced mechanical ventilation this means that the mechanical driven inflow of air to the rooms are equal to the mechanical driven outflow of air from the rooms. For the balanced mechanical ventilated rooms only the infiltration will course an exchange of air to other rooms. [Heisselberg, 2008]

Only infiltration through door cracks are included in the model. This means that if a room only is connected one other room via one door crack then there will in a multi zone model not be an airflow through the door crack as shown in figure 10.2. If the balanced ventilated room was connected to two rooms via door cracks there will be an airflow through the door cracks.

1 door crack in a room that is
balanced ventilated:

Ventilation system
m_1 m_2

m_3

Door crack

Mass flows:

$$m_1 = m_2$$
$$m_3 = 0$$

2 door cracks in a room that is
balanced ventilated:

Ventilation system
m_1 m_2

m_4 m_3

Door crack   Door crack

Mass flows:

$$m_1 = m_2$$
$$m_3 = m_4$$
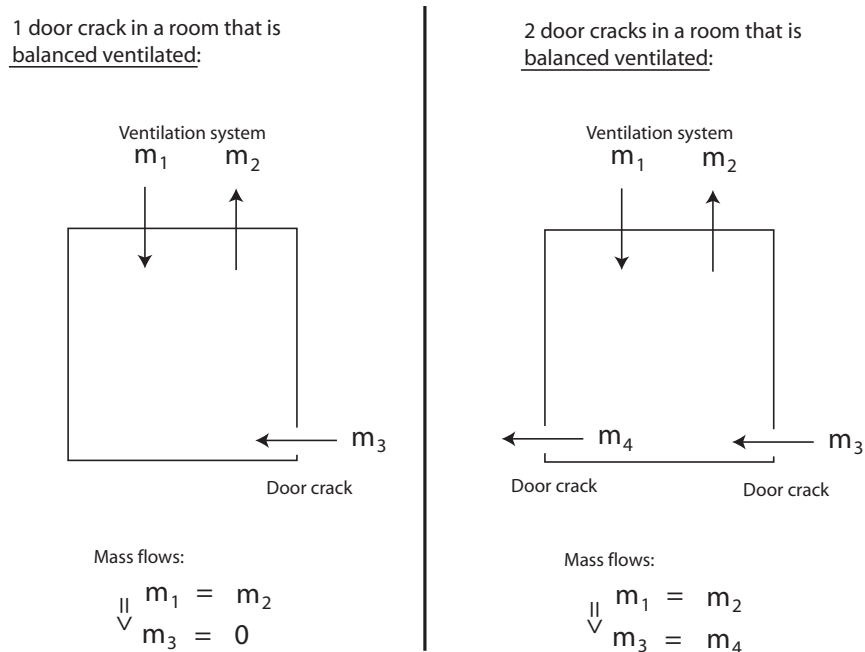
Figure 10.2: *Mass flows in a rooms with a balanced ventilation system.*

For the multi zone model it is assumed, that there is a balanced mechanical ventilation in the following rooms:

- Group rooms

- The service offices

- Medicine room

- Conversation room

- Seminarial rooms

- Cleaning rooms

- Depots

In the multi zone model mechanical balanced ventilated rooms with two door cracks are included in the model. The mechanical balanced ventilated rooms with only one door crack are not included in the model, since they will not affect the airflows in the model of the hospital. The black hatched rooms in figure 10.3 are not included in the model.
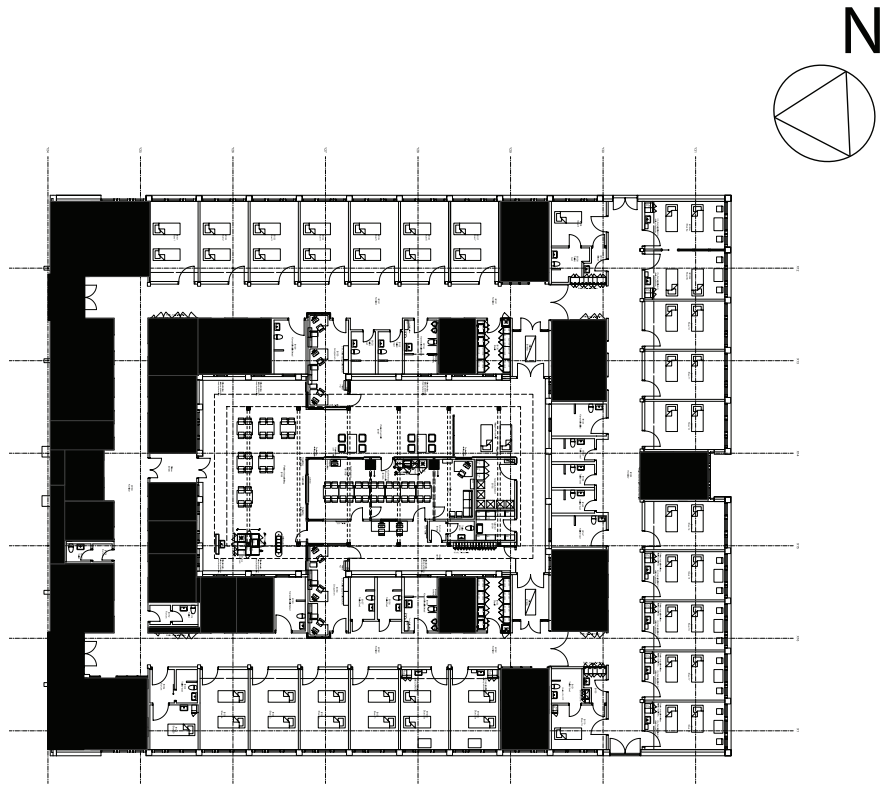
Figure 10.3: *Floor plan of the south east part of the hospital. The highlighted rooms are mechanical balanced rooms.*

The rooms with the greatest influence for the airflow in the hospital are the natural ventilated rooms, the toilets, the kitchen and the sterile rooms. The resent for this is that they do not have a mechanical balance ventilation system, and there are therefore an airflow between these rooms and the nearby rooms.

In the toilets and the kitchen are created a mechanical low pressure, while for the sterile rooms are a mechanical over pressure to keep it sterile.

The division of the rooms in the south east part of the hospital is shown in figure 10.4. The black coloured rooms are the balanced mechanical ventilation rooms that are not included in the model. The green coloured rooms are the rooms that are natural ventilated. The blue coloured rooms are the rooms that have a mechanical low pressure and the red coloured rooms are the rooms that have a mechanical high pressure. The white coloured rooms which primary is the corridor are connecting the different rooms to each other. In the model the corridor also include the small rooms before some of the toilets and the sluice. Inside the corridor there are no closed doors. The brown coloured path is a pipe which is supplying the common room in the center with fresh air.
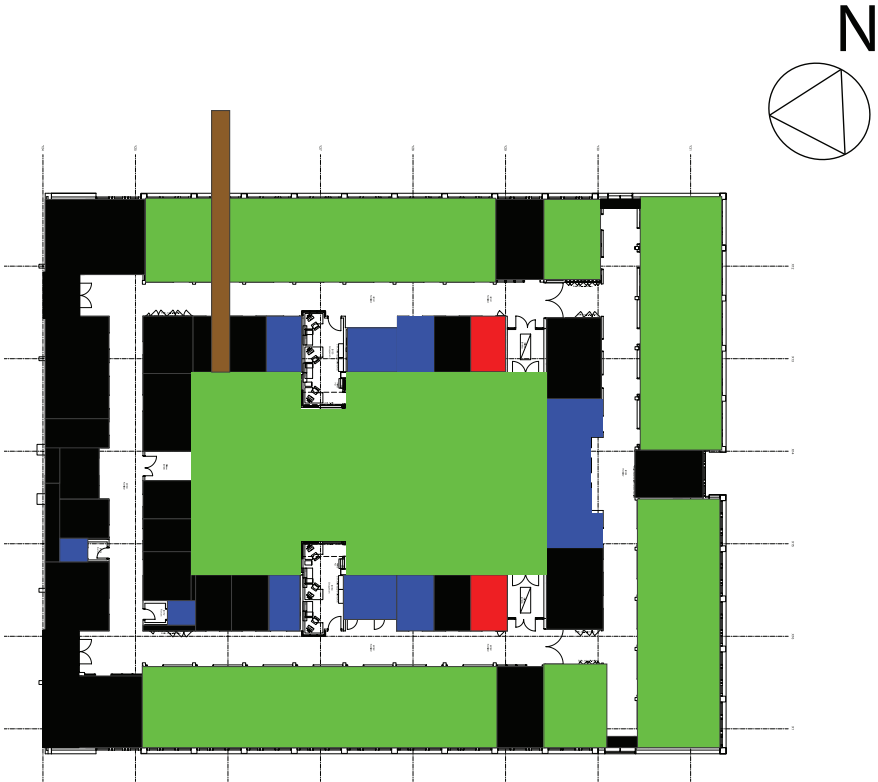
Figure 10.4: *The multi zone model.*

In figure 10.5 are shown the nodal network for the multi zone model in figure 10.4. The black filled circles represent a nodal to the outside and the white filled circles represent a nodal in a zone inside the building. The square represent a resistance where there either will be a pressure increase or a decrease. The white square represent an opening and the grey square a fan.
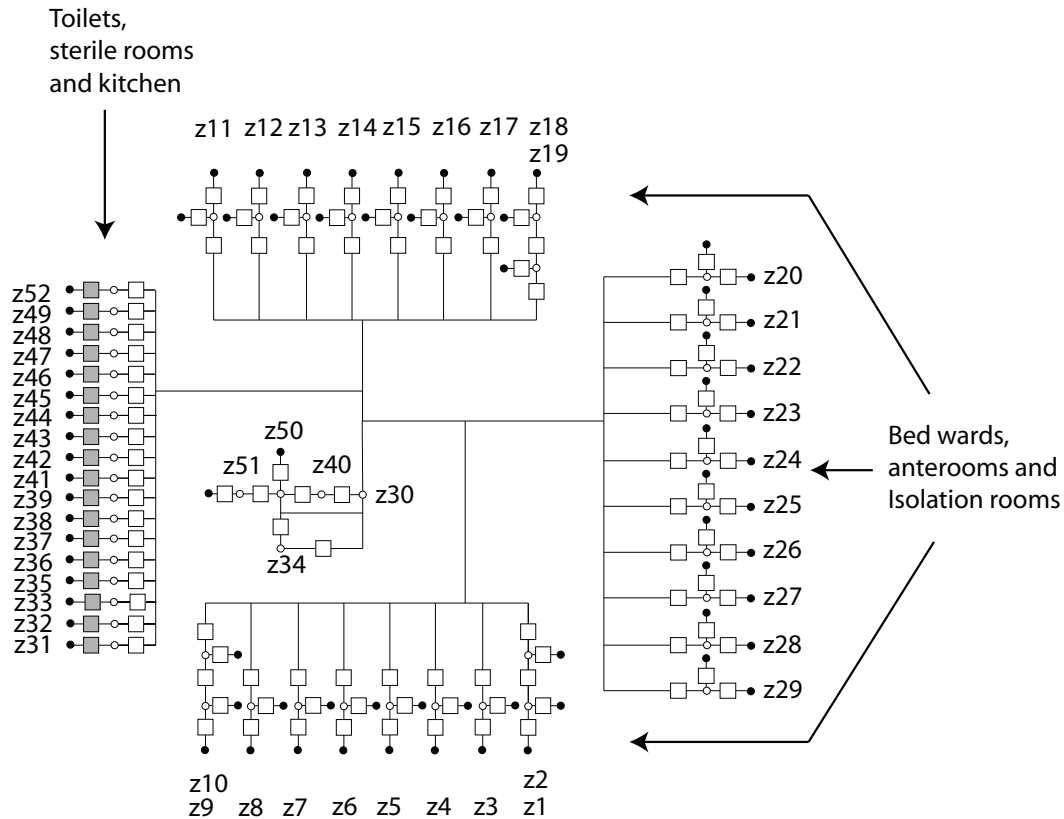
Figure 10.5: *Layout of the multi zone model represented in a 2d nodal network. The numbers in the figure corresponds to the zones used in COMISexcel.*

From figure 10.5 it is seen that there are 52 zones and a resistance between all the zones. It is also seen that most of the zones are connected to the zone in the center which is the the corridor in the hospital.

Since a lot of the rooms are similar both regarding C_p values, indoor temperature, size and ventilation rate many of the natural ventilated rooms can be added together so there are fewer zones in the model, as shown in figure 10.6.
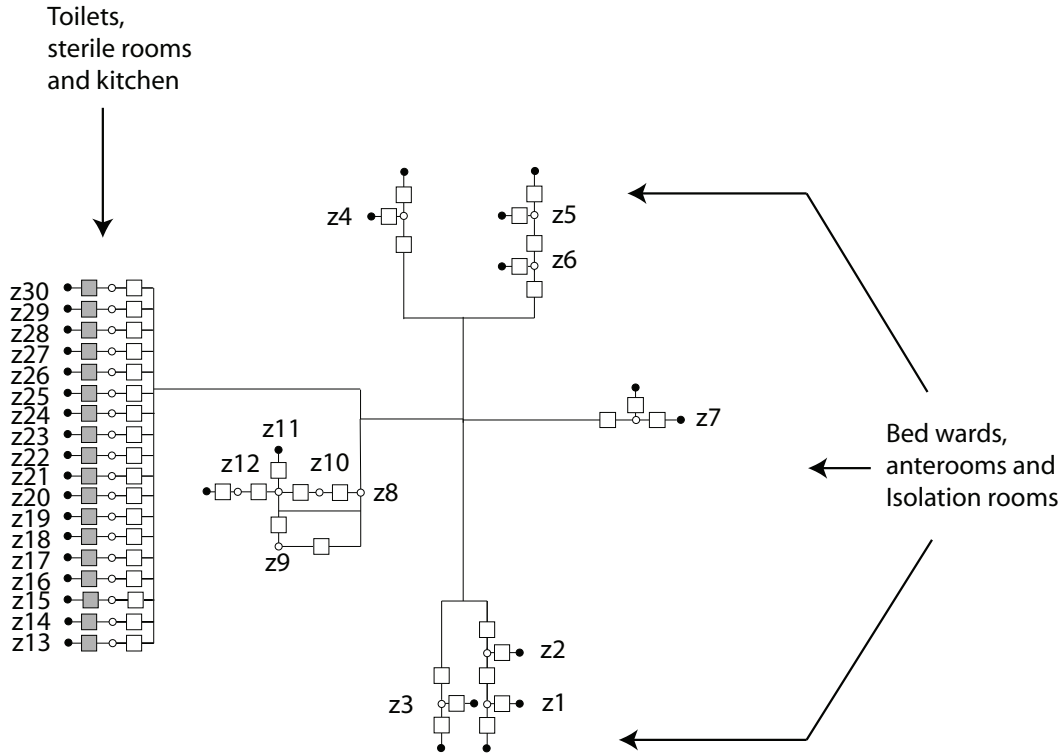
Figure 10.6: *Layout of a more simple multi zone model represented in a 2d nodal network.*

By making a simpler model some computer power can be saved. However even though it is possible to save some computer power by making the simpler multi zone model, it is still chosen to make the more complex model. This is done because the same model then can be reused in simulations where the local C_p values for the openings for natural ventilation are known.

10.1.1 The building and its environment

Like for the analytical calculations in chapter 9.1 it is assumed that the building is placed in an environment corresponding to country with scattered stand. The location of Aabenraa hospital is listed in table 10.1.

Table 10.1: *Geographic position of Aabenraa hospital [Google Maps, 2007a] .*

Latitude $[°N]$	Longitude $[°E]$	Altitude $[m]$
55,06	9,38	75,45

For the first simulations it is assumed that the building have a square shape, like in the analytical calculation, and the same C_p-values are therefore used. To ensure that the right C_p-values are used, the inclination for the facades of 28,9° are listed in the program.

10.1.2   Air changes rate for the toilets

For residences it is stated in the Danish Building Regulations that the airflow from rooms with both toilets and a bath have to be 15 $\frac{l}{s}$, and 10 $\frac{l}{s}$ for rooms with only a toilet [Erhvervs- og Byggestyrelsen, 2008] .

To make sure that the toilets have a high service level there is made an investigation of how high the airflows should be for the toilets to make sure that they almost do not have any pollution left after half an hour.

It is decided that the pollution level only should be 1 % half an hour after a person has left the toilet. To calculate the necessary air changes rate the dilution equation is used:

$$c_{op} = \frac{1}{\varepsilon_{op}} \cdot \left(\frac{q}{n \cdot V_r} \cdot (1 - e^{-n \cdot \tau}) + (c_0 - c_i) \cdot e^{-n \cdot \tau} + c_i \right) \qquad (10.1)$$

[Hansen et al., 1997]
where

$$\begin{array}{lll}
q & : & \text{Pollution generated in the room}[\frac{m^3}{m^3}] \\
V_r & : & \text{Volume of the room } [m^3] \\
n & : & \text{Air change rate for the room } [h^{-1}] \\
\tau & : & \text{Time } [h] \\
c_0 & : & \text{Initial concentration } [\frac{m^3}{m^3}] \\
c_i & : & \text{Pollution concentration in the inflow air } [\frac{m^3}{m^3}] \\
\varepsilon_{op} & : & \text{Ventilation efficiency } [-]
\end{array}$$

For the calculation of the air change rates for the toilets it is assumed that there are nobody using the toilets for the time period and therefore no generation of pollution in the toilets. The ventilation efficiency is set to 100 % and a 100 % pollution concentration in the toilets in the beginning. It is assumed that there are no pollution in the outdoor air. The reduced dilution equation is:

$$c_{op} = e^{-n \cdot \tau} \qquad (10.2)$$

To have a pollution concentration of 1 % in the room after half an hour the air changes rates for the rooms should be 9 h^{-1}.

For the smallest toilets in the hospital, this corresponds to an airflow of 22,5 $\frac{l}{s}$. For the even bigger toilets the airflows will be higher. Since the airflows based on the pollution level in the toilets are higher than the ones given in the Danish Building Regulations these airflows are used for the toilets.

10.1.3   Air changes rate for the kitchen

For residences it is stated in the Danish Building Regulations that the airflow from kitchens have to be minimum 20 $\frac{l}{s}$ [Erhvervs- og Byggestyrelsen, 2008] . This corresponds to a

minimum air changes rate for the 1,2 h^{-1} for the kitchen. However like for the toilets there are done the same consideration regarding pollution in the kitchen and it has been decided that the air changes rate for the kitchen should be 9 h^{-1}.

10.1.4 Openings for natural ventilation

From the analytical calculations in chapter 9.1, it was calculated that the openings in the rooms had to be biggest in July to create the desired air changes rate for the rooms. Because July was the most critical situation it is chosen to use the values of the ventilation openings from this situation in the first simulations in the multi zone model. The sizes of the openings are listed in table 10.2.

Table 10.2: *The sizes of the natural ventilation openings in the first simulations.*

Bed ward	$[m^2]$	0,15
Isolation room	$[m^2]$	0,25
Anteroom	$[m^2]$	0,61

COMISexcel uses the power law to describe the connection between the airflow and the pressure drop through an opening. The power law is give by:

$$q_v = C_m \cdot \Delta P^n \tag{10.3}$$

[Heiselberg, 2006]

where

$$
\begin{array}{lll}
q_v & : & \text{Air flow rate } [\frac{m^3}{s}] \\
C_m & : & \text{Characteristic flow coefficient } [-] \\
n & : & \text{Dimensionless exponent } [-]
\end{array}
$$

The characteristic flow coefficient is in Comis defined as:

$$C_m = \frac{C_s \cdot A}{l} \tag{10.4}$$

[Helmut E. Feustel and Brian V. Smith, 2001]

where

$$
\begin{array}{lll}
C_s & : & \text{Air flow coefficient } [\frac{m^3}{s}] \\
A & : & \text{Areal of the openings } [-] \\
l & : & \text{Length of the openings } [-]
\end{array}
$$

The flow coefficient and dimensionless exponent are calculated by setting the power law equal to the orifice model. The orifice model is, like the power law, a model that describe the connection between the airflow and the pressure drop through an opening:

$$q_v = C_d \cdot A \cdot \sqrt{\frac{2 \cdot \Delta p}{\rho}} \tag{10.5}$$

[Heiselberg, 2006]

where

q_v :   Air flow rate $[\frac{m^3}{s}]$

A :   Geometrical opening area $[m^2]$

C_d :   Discharge coefficient $[-]$

Δp :   Pressure difference across the opening $[Pa]$

ρ :   Air density of the air passing through the opening $[\frac{kg}{m^3}]$

The orifice model are used to describe the airflow through windows and other large openings, whereas the power law often is used to describe the airflow through ventilation components [Heiselberg, 2006] . In the calculation of the flow coefficient and the dimensionless exponent there are used a length of the cracks of 1 m and the average outdoor air density during a year.

$$
\begin{array}{ccc}
\text{Orifice model} & \& & \text{Power model} \\
C_d \cdot A \cdot \sqrt{\frac{2 \cdot \Delta p}{\rho}} = q_v & \& & q_v = C_s \cdot \frac{A}{l} \cdot \Delta p^n \\
C_d \cdot A \cdot \sqrt{\frac{2 \cdot \Delta p}{\rho}} & = & C_s \cdot \frac{A}{l} \cdot \Delta p^n \\
A \cdot \frac{C_d \cdot \sqrt{2}}{\sqrt{\rho}} \cdot \Delta p^{0,5} & = & C_s \cdot \frac{A}{l} \cdot \Delta p^n \\
A \cdot \frac{0,61 \cdot \sqrt{2}}{\sqrt{1,2645}} \cdot \Delta p^{0,5} & = & C_s \cdot \frac{A}{1} \cdot \Delta p^n \\
A \cdot 0,77 \cdot \Delta p^{0,5} & = & A \cdot C_s \cdot \Delta p^n
\end{array}
$$

10.1.5   Door cracks

Except the pipe between the common room and the outside all the rooms in the multi zone model are connected to each other via door cracks.

The used values for the door cracks are listed in table 10.3.

Table 10.3: *Airflow coefficient and dimensionless exponent used for the door cracks [Helmut E. Feustel and Brian V. Smith, 2001] .*

Air flow coefficient, C_s [$-$]	Dimensionless exponent n [-]
0,03	0,6

The cracks under the doors are assumed to have a length of 90 cm and a height of 1 cm. The area of the door cracks are hereby 0,009 m^2.

The airflow through the door cracks can be calculated as:

$$q_v = 0,009 \cdot 0,03 \cdot \Delta p^{0,6} \tag{10.6}$$

The airflow coefficient for the door cracks are low compared to the one for the natural ventilated openings. This means if the two type of opening had the same size there would come lesser air through the door crack. In a hospital the direction of the airflows are controlled by pressurization. Should this strategy fail then it is practical that the doors are very airtight.

10.1.6 Airflow for sterile rooms

In the sterile rooms are installed fans to create an overpressure to keep the rooms sterile. The overpressure will create a velocity of $1 \frac{m}{s}$ through the crack under the door. With an area of the crack of $0,009 \ m^2$ the flow rate from the room is $0,009 \ \frac{m^3}{s}$.

There is a risk that the overpressure on the door is too big and will affect the door so that it is inconvenient to use it. It is therefore investigated how the overpressure will affect the use of the door. It is assumed that there is a hydrostatic pressure distribution in both of the rooms, and the slope of the distributions are the same because of the same temperature in the two rooms, as shown in figure 10.7.
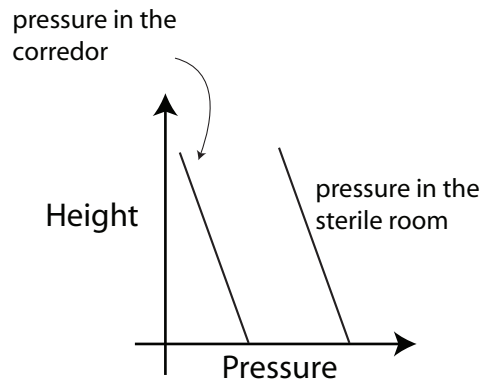
Figure 10.7: *Pressure distribution in the sterile room and the corridor.*

The overpressure on the door will hereby correspond to the pressure drop across the door crack between the corridor and the sterile room.

By using the power law from equation (10.4), and the characteristic flow coefficient and dimensionless exponent for a door from table 10.3, the pressure drop across the door crack can be found.

$$q_v = C_m \cdot \Delta P^n$$
$$\Delta P = \sqrt[n]{\frac{q_v}{C_m}}$$
$$\Delta P = \sqrt[0,6]{\frac{0,009}{0,03 \cdot 0,009}}$$
$$\Delta P = 345 \text{ Pa}$$

The door is assumed to have an area of 1,9 m^2, the force that is affecting the door, can be found to have a size of 656 N. 656 N is a big force and correspond to lift 67 kg and it can therefore be assumed that the overpressure in the room will have a big effect on the use of the door.

10.1.7 Openings for common room

In the common room in the middle of the hospital section there are installed a hybrid ventilation system, as written in chapter 6. The principle for the ventilation system is showed in figure 10.8. The idea is that the airflows from the outside comes through a pipe to the common room and out again through the openings in the roof.
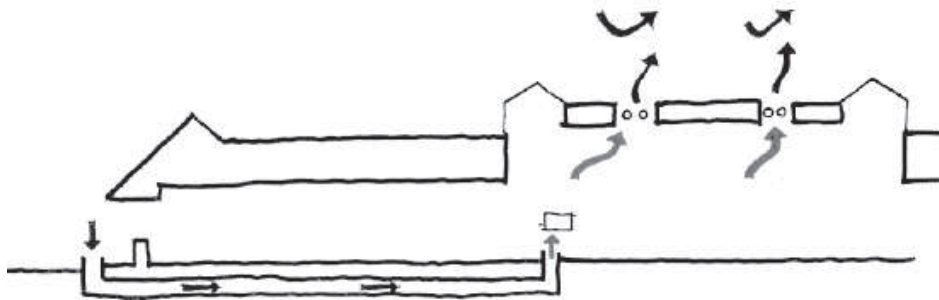
Figure 10.8: *The principle for hybrid ventilation for the bed wards. [Esbensen Consulting Engineers A/S, 2005]*

As written in chapter 6, the hybrid ventilation system is designed, thus that it will provide the room with an air changes rate between 1 h^{-1} and 1,5 h^{-1}. Since there are no available data for the construction of the hybrid ventilation system it is chosen to make the room purely natural ventilated.

The sizes of the ventilation openings in the model are like for the other natural ventilated rooms found by assuming that the room is a single zone. The single zone model of the common room is simplified thus that there only are two openings. The center of the inlet opening is placed in a height of 0,5 m and the outlet opening is placed in the roof of the room in a height of 5,8 m. The air is not let through the window in the facade but through ducts under the building. In the ducts where the air is let through before it enter the common room there is a resistance which will course a pressure loss. This pressure loss has in the calculations not been taking into consideration.

Like for the other natural ventilated rooms, the chosen design weather data are the average weather data from July in the Danish design reference year. The calculations of the openings' sizes can be found in the excel spreadsheet 'simple calculations for Aabenraa.xls'. Some of the input and results from the calculations are listed in table 10.4. In the model both openings are pointing straight up into the sky, and there are therefore used the same C_p-value for both openings. It is therefore assumed that the wind will not contribute to the

ventilation of the room, it is therefore only the driving force from the thermal buoyancy that will do it. In reality this is not the case which will be investigated in a CFD simulation later.

Table 10.4: *Opening's sizes, positions, location of the neutral plane and the air changes rates through the common room.*

Volume	$[m^3]$	1154
Inlet area	$[m^2]$	0,65
Outlet area	$[m^2]$	0,65
Position of inlet's center	$[m]$	0,5
Position of outlet's center	$[m]$	5,8
Location of neutral plan	$[m]$	3,11
Air changes rate	$[h^{-1}]$	1,5

10.1.8   Fan characteristics

For a fan the pressure is a function of the flow. In the calculations there are used a fan characteristic which will insure a constant mass flow no matter the pressure difference [Brohus, 2003] . It is estimated that this is an acceptable assumption for fans used in mechanical ventilation. This is because changes in the pressure difference over the fan from the weather outside normally only will have a little influence on the mass flow from the fan, as shown in figure 10.9 . For a fan in hybrid ventilation this will however not be an acceptable assumption, because the pressure change coursed by the weather outside will have a big influence on the mass flow from the fan.
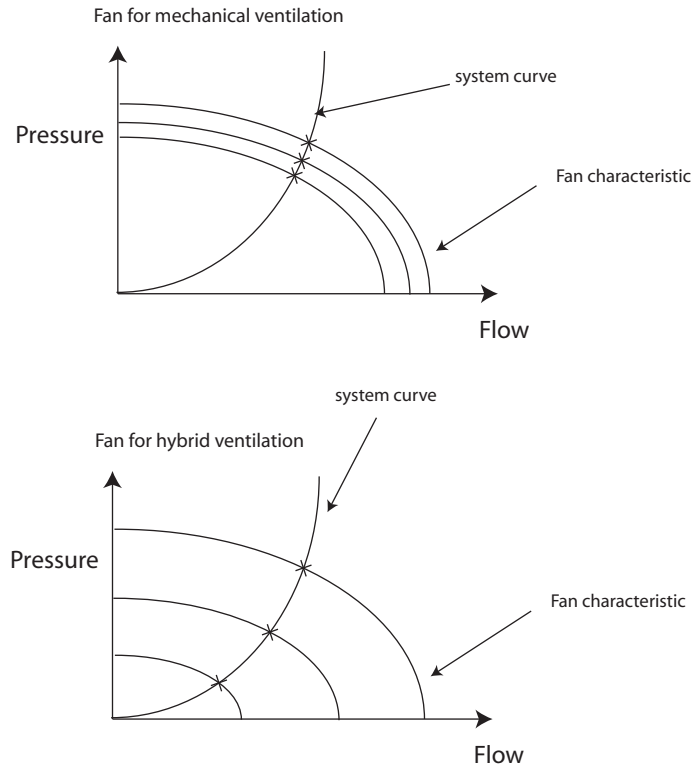
Figure 10.9: *Fan characteristics and system curve for a mechanical ventilation system.*

In the calculations of the mass flows from the fans there are used different densities of the outdoor air depending the simulations in which the fan are used. The used densities are listed in table 10.5.

Table 10.5: *The used densities in the different type of simulation.*

Hole year $\left[\frac{kg}{m^3}\right]$	Winter period $\left[\frac{kg}{m^3}\right]$	Summer period $\left[\frac{kg}{m^3}\right]$	July $\left[\frac{kg}{m^3}\right]$
1,265	1,297	1,232	1,219

For the rooms are used different fans because of the the different volume for the rooms. The fans for the different rooms are listed in table 10.6.

Room	Volume $[m^3]$	Air changes rate $[h^{-1}]$	Air flow rate $[\frac{m^3}{s}]$
Sterile room			0,009
Kitchen	62	9	0,16
Toilet 1	9	9	0,023
Toilet 2	18	9	0,05
Toilet 3	19	9	0,048
Toilet 4	31	9	0,078
Toilet 5	32	9	0,08

10.2   Check of model

To check the model the mass balances are checked for three rooms and there are checked two pressure loop. For the calculations are used average weather data from July from the Danish reference year. The used weather data are listed in table 10.7. The results from the calculation are found in the COMISexcel spreadsheet 'Control2.xls'.

Table 10.7: *Weather data used for the control of the multi zone model.*

Wind speed $[\frac{m}{s}]$	Wind direction $[°]$	Temperature $[°C]$	Humidity $[\frac{g}{kg}]$	Barometric pressure $[kPa]$
3,868	205	16,4	9,33	101,0

To check the model it is chosen to check different types of room that are placed in different parts of the building. The checked rooms are:

- An isolation room

- A bed ward

- A toilet

The rooms are showed in figure 10.10.
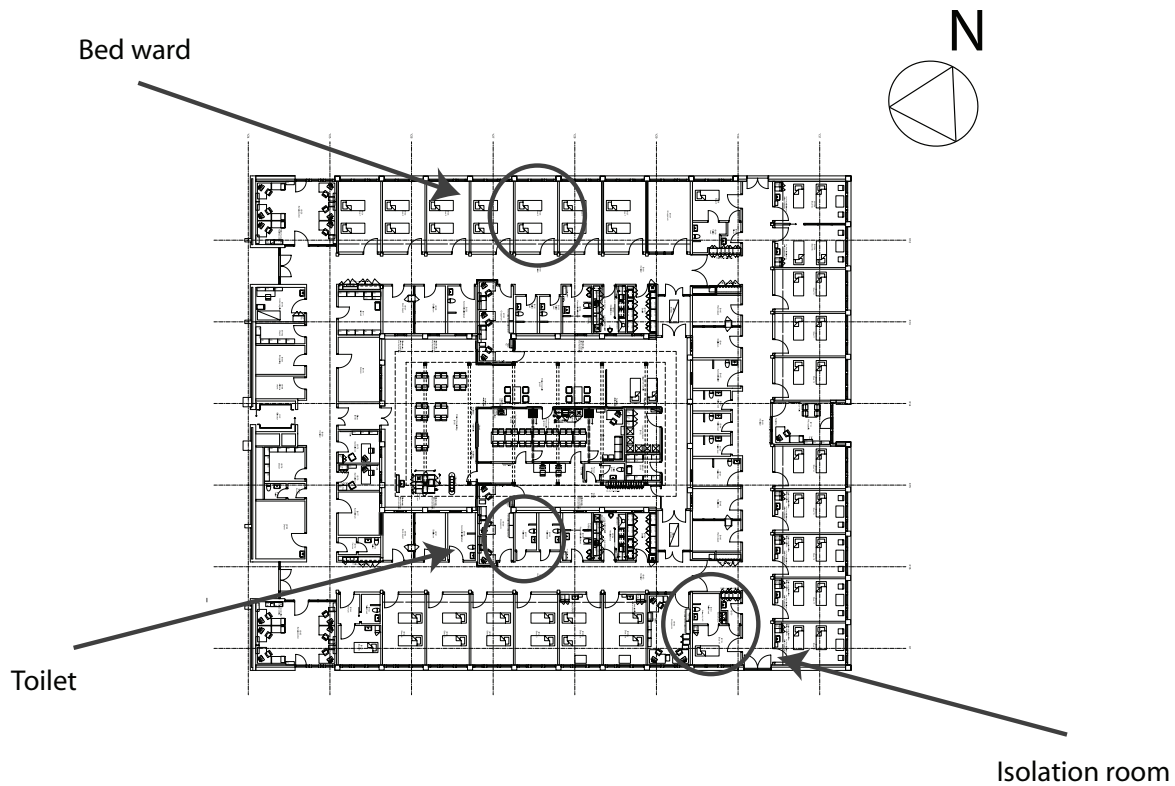
Figure 10.10: *The rooms for which the check is made.*

The location of the openings for three rooms are:

- The isolation room has an opening through the southern part of the building's facade, through the roof and the door crack.

- The bed ward has an opening through the northern part of the building's facade, through the roof and the door crack.

- The toilet has an opening through the roof and the door crack. The opening in the roof is where the fan is placed.

By using the results of the mass flows from the multi zone calculation, the mass balance for the rooms are set up. For the mass balance the inflow and outflow for the rooms should be the same. To set up the mass balances, it is assumed that the mass flows are positive toward the rooms, and negative out of the rooms. The mass balances are listed in table 10.10.

Table 10.8: *Mass balance for the three rooms.*

		Isolation room	Bed ward	Toilet
Opening in the facade	$\left[\frac{kg}{s}\right]$	0,403	0,173	
Opening in the roof	$\left[\frac{kg}{s}\right]$	-0,402	-0,135	-0,0909
Door creak	$\left[\frac{kg}{s}\right]$	-6,54 ·10^{-4}	-0,0387	0,0909
Mass balance	$\left[\frac{kg}{s}\right]$	-5,37 ·10^{-05}	-8.00 ·10^{-05}	0

From the table it is seen that the mass balances are close to zero in all the three rooms. The mass conservations for the three rooms can hereby be assumed to be kept in the multi zone model.

In addition to the check of the mass balance three pressure loops are checked. A pressure loop follows a possible flow path from nodes to nodes. For the pressure loop the sum of pressures have to be equal to zero. The pressure increases and decreases are coursed by wind, thermal buoyancy, fans and the openings where airflows through. It goes that the driving forces in the pressure loop has to be equal to the pressure drops. The general pressure loop equation is:

$$\sum \Delta P_{ij} \quad = \sum \Delta P_{stack,ij} + \sum \Delta P_{wind,ij}$$

$$\sum \Delta P_{ij} \quad = g \cdot \sum \rho_{ij} \cdot \Delta H_{ij} + (\Delta C_p) \cdot 0,5 \cdot \rho_{out} \cdot v_{ref}^2$$

[Heiselberg, 2006]
where

$$\Delta P_{ij} \quad : \quad \text{Pressure losses } [Pa]$$
$$\rho_{ij} \quad : \quad \text{Air density in the zone where the changes of height is happening } [\frac{kg}{m^3}]$$
$$\Delta H_{ij} \quad : \quad \text{The differences in height}[m]$$
$$\Delta C_p \quad : \quad \text{Sum of the pressure coefficients } [-]$$

The pressure losses in the general loop equation are positive for flows in the loops direction, except for the pressure contribution from the fan. The difference in height which is used in the calculation of the driving force from the thermal buoyancy is positive for increase in height in the flow direction and negative when decreased in the flow direction. The C_p value which is used in the calculation for the driving force from the wind is added when the loop is from the outside and into the building and subtracted when the loop is from the inside of the building and to the outside. The indexes in the symbols indicates the two nodes between which the values of the symbols are found.

To check the program two pressure loops in the building are checked. The two pressure looks the same, and have the shape shown in figure 10.11. For the pressure loop the air comes through the inlet opening in the facade and out through the opening in the roof.
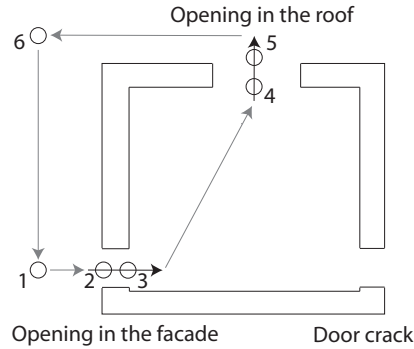
Figure 10.11: *The checked loop.*

The pressure loops for the isolation room and bed ward are set up as:

$$P_{wind,2} - \Delta P_{2,3} - \Delta P_{stack,3,5} - \Delta P_{4,5} - P_{wind,5} + \Delta P_{stack,6,1} = 0$$

$$\Leftrightarrow$$

$$P_{wind,2} - \Delta P_{2,3} - g \cdot \rho_{in} \cdot \Delta H_{3,5} - \Delta P_{4,5} -$$
$$P_{wind,5} + g \cdot \rho_{out} \cdot \Delta H_{6,1} = 0$$

In the calculations of the pressure loops the output from COMISexcel of the wind pressure on the building's surfaces are used, the values are listed in table 10.9. From the table it is noticed that the only value that is negative is the facade toward the south, where the wind is coming from. It is therefore estimated that the positive value from COMISexcel correspond to a low pressure on the building's surfaces and the negative values corresponds to a high pressure on the surfaces.

Table 10.9: *Wind pressure on the building's surfaces from COMISexcel.*

North	[Pa]	1,28232
East	[Pa]	2,51986
South	[Pa]	-3,95461
West	[Pa]	2,90094
Roof	[Pa]	3,5421

The input and the results from the two pressure loops through the isolation room and the bed ward are listed in table 10.10.

Table 10.10: *The pressure loops which flows through the isolation room and the bed ward.*

Input		Isolation room	Bed ward
g	$\left[\frac{m}{s^2}\right]$	9,82	9,82
ρ_{in}	$\left[\frac{kg}{m^3}\right]$	1,186	1,186
ρ_{out}	$\left[\frac{kg}{m^3}\right]$	1,219	1,219
$-\Delta H_{3,5}$	$[m]$	-4,4	-4,4
$\Delta H_{6,1}$	$[m]$	4,4	4,4
$P_{wind,2}$	$[Pa]$	3,95	-1,28
$-\Delta P_{2,3}$	$[Pa]$	-4,47	-2,30
$-\Delta P_{stack,3,5}$	$[Pa]$	-51,2	-51,5
$-\Delta P_{4,5}$	$[Pa]$	-4,45	-1,39
$-P_{wind,5}$	$[Pa]$	-(-3,54)	-(-3,54)
$\Delta P_{stack,6,1}$	$[Pa]$	52,7	52,9
Result	$[Pa]$	$1,34 \cdot 10^{-2}$	$1,30 \cdot 10^{-2}$

From table 10.10 it is seen that the results from both pressure loops are good, since the total pressure are close to 0 Pa. The mass conservations are kept for the rooms and the results of the pressure loops are good, the multi zone model is estimated to be acceptable.

10.3 Winter and summer situation

For the hospital are made simulations of the winter and summer period in Denmark. In both periods the data from the Danish design reference year are used. For some situations the measured wind direction in the Danish reference year is listed as 990 °. The value indicate that it was not possible to measure the value or the wind direction vary a lot. Since an exact value was not given in these hours, it has been decided not to include the hours in the simulations.

The spreadsheets and the results of the simulations for every half year can be found in the folder '\Comis \Aabenraa' on the cd. At that place there is a folder called processed data which contains the Excel spreadsheets where the needed data are exported to and analyzed.

For the first simulations the mass flow between the different zones in the winter and summer period are calculated. The simulations are made with a focus on the bed wards, the isolation rooms and the anterooms.

For each of the sides of the building there is only given one C_p value. This means that the bed wards on each side are exposed to the same driving forces from the wind and are constructed in the same way. Therefore it is chosen only to look at one bed ward from each

side of the building, this means a bed ward from the south, east and north. The same goes for the isolation rooms and anterooms therefore there is only looked at an isolation room and anteroom facing south and north.

The chosen bed wards corresponds to zone 5, 15 and 25, and the isolation rooms and the anterooms corresponds to zone 1, 18, 2 and 19. The zones are marked in the 2d nodal network shown in figure 10.12.
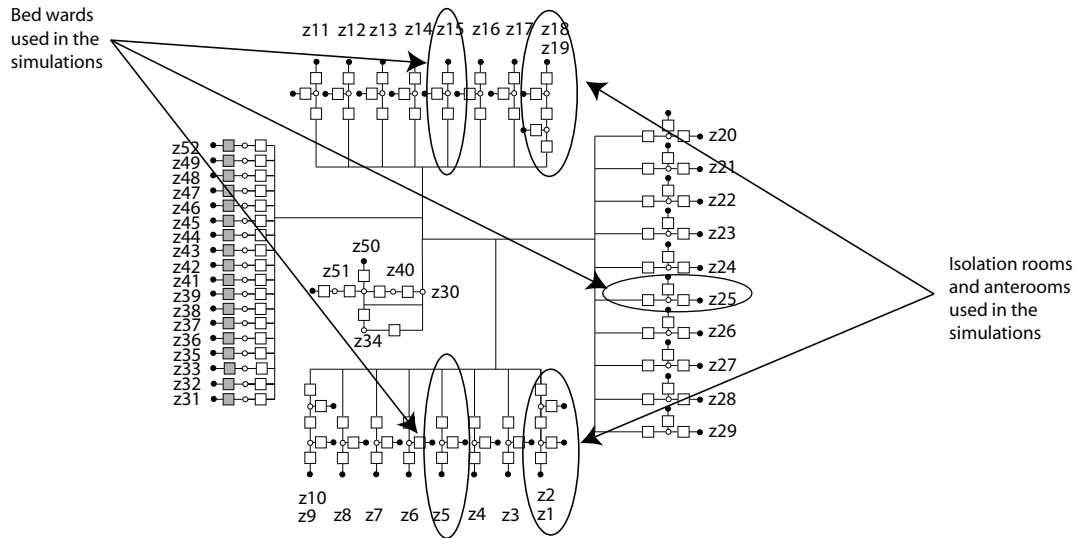
Figure 10.12: *Layout of the multi zone model represented in a 2d nodal network. The numbers in the figure corresponds to the zones used in COMISexcel.*

10.3.1   Air changes rate for bed wards

In figure 10.13 and 10.14 are showed the air change rate for the bed wards in the winter and summer period.
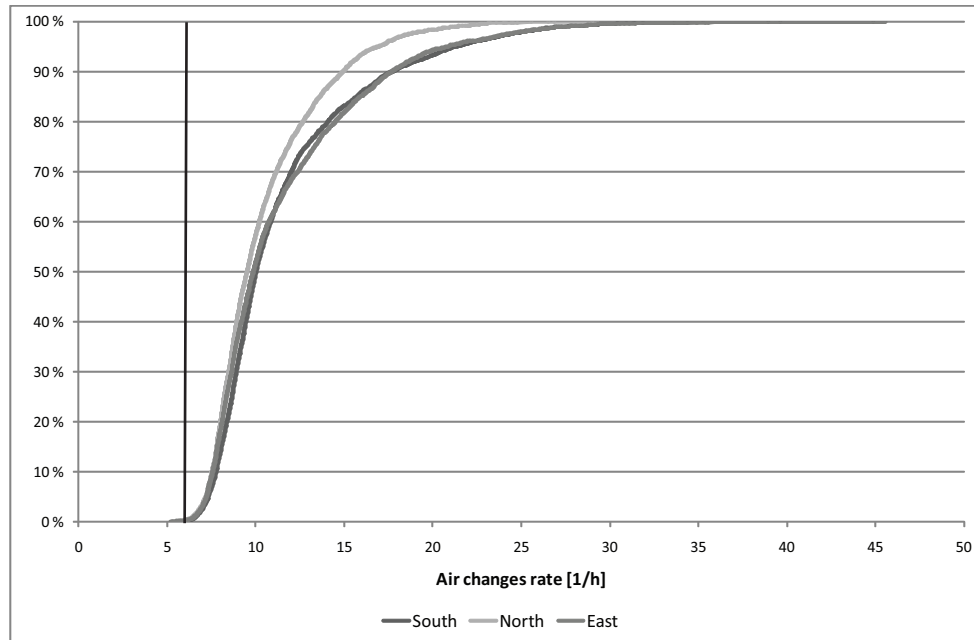
Figure 10.13: *Air changes rate of the bed wards in the winter situation.*
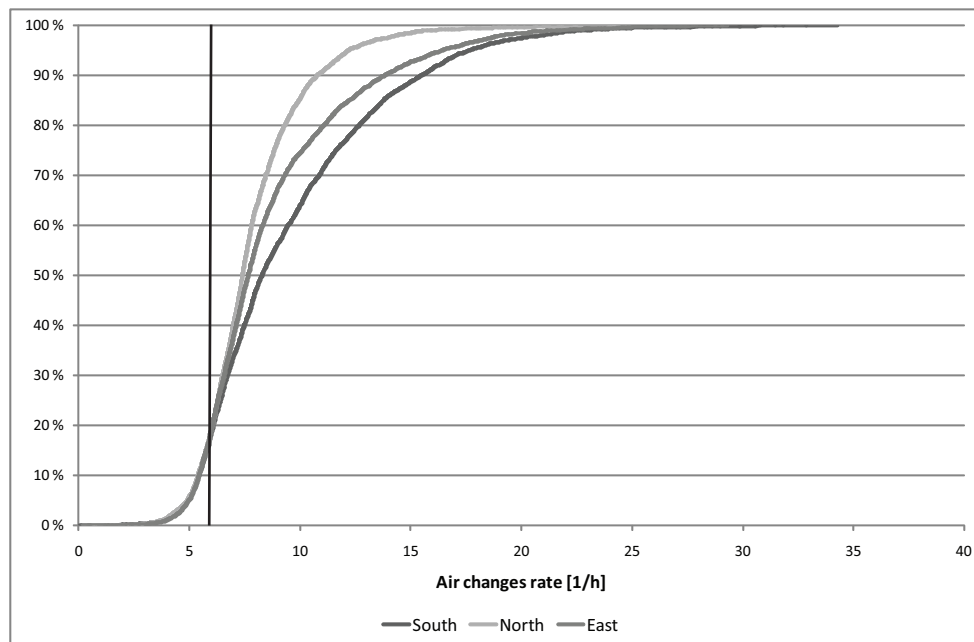
Figure 10.14: *Air changes rate in the bed wards in the summer period.*

From figure 10.13 and 10.14 it is seen that the openings in the bed wards are big enough in the winter period to create a sufficient air changes rate. The openings are however not big enough in the summer period to create a sufficient air changes rate of 6 h^{-1} more than 80 % of the time. This is not acceptable and the air change rate for the rooms have to be increased.

Higher air changes rate in the bed ward

To increase the air changes rate the size of the openings are made twice as big. The size of the openings are hereby increased to $0,30 \ m^2$. This redesign of the openings increases the air changes rate of the bed wards as shown in figure 10.16 and 10.15.
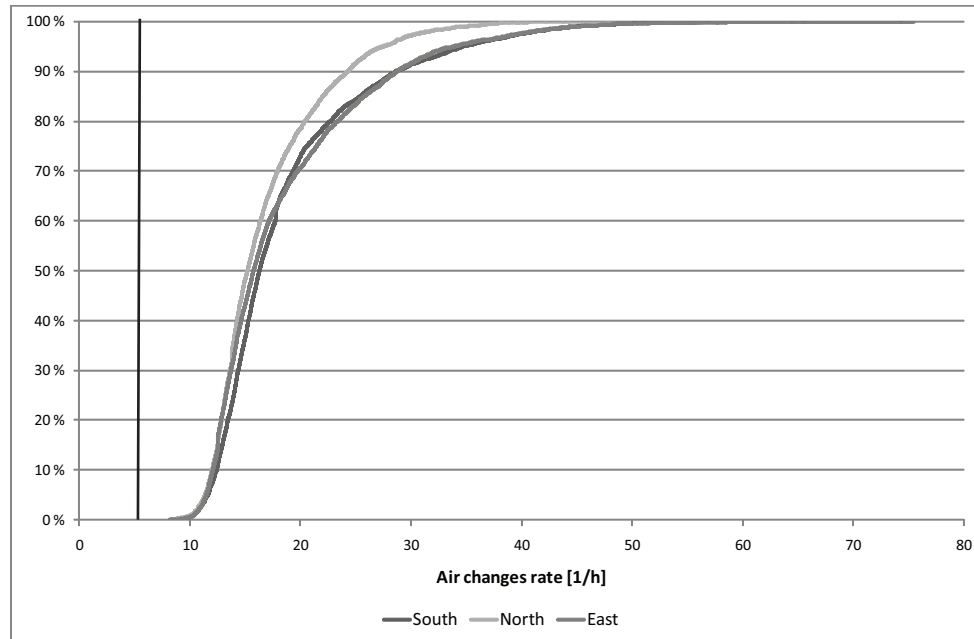
Figure 10.15: *Air changes rate in the bed wards in the winter period when the area of the openings' sizes each are 0,3 m^2, corresponding to that they are made twice as big.*
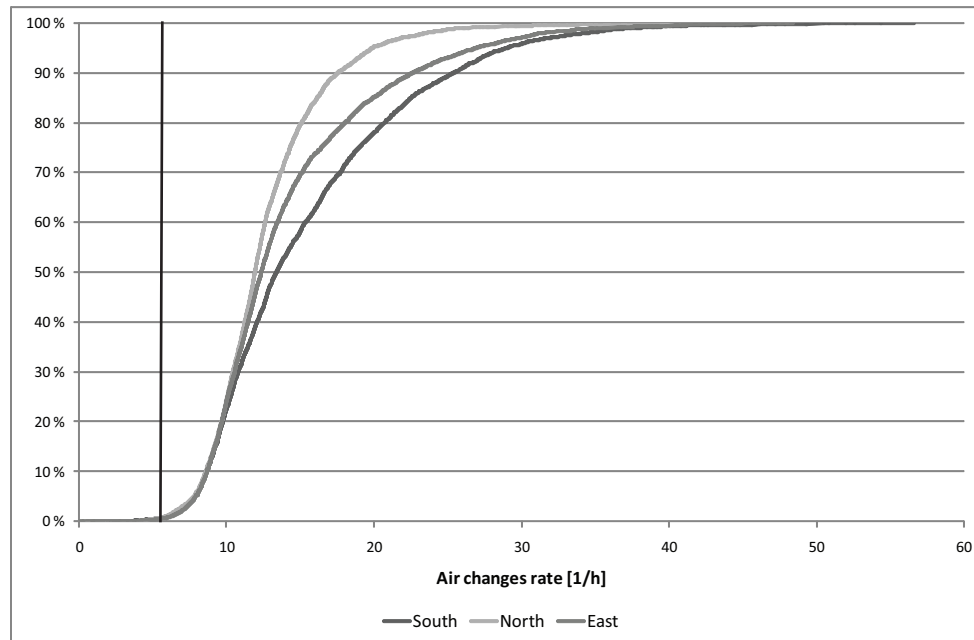
Figure 10.16: *Air changes rate in the bed wards in the summer period when the area of the openings' sizes each are 0,3 m², corresponding to that they are made twice as big.*

From figure 10.15 and 10.16 it is seen that there still are about 1 % of the time where the natural driving forces are too small to create a sufficient air change rate in the summer period for the room. It is therefore estimated that it is necessary to to use a fan to ensure a sufficient air changes rate all the time in the summer period.

10.3.2 Air changes rate for isolation rooms

The air change rate for the isolation rooms for the winter and summer period is showed in figure 10.17 and 10.18.
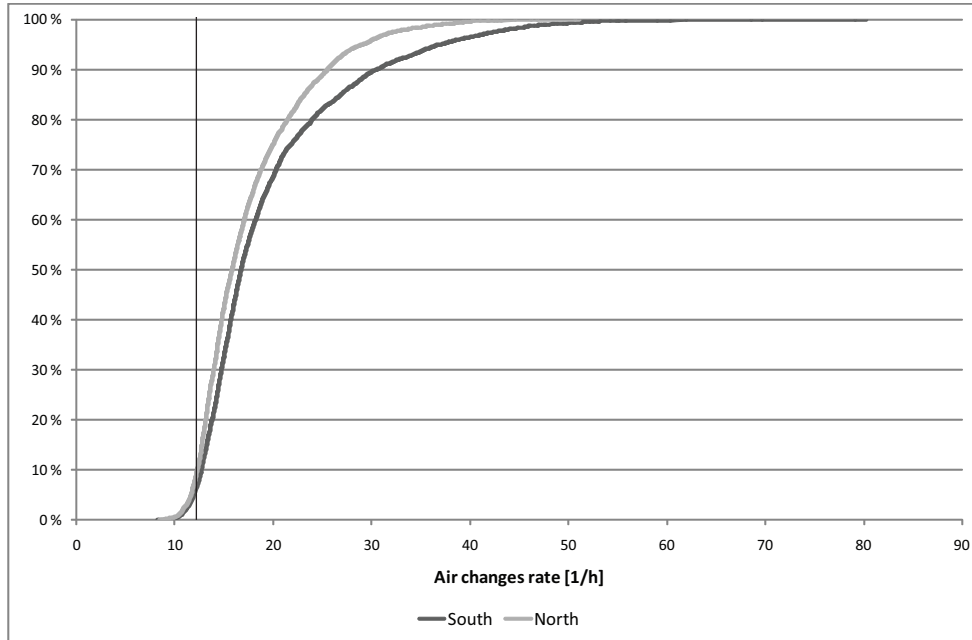
Figure 10.17: *Air changes rate of the isolation rooms in the winter period.*
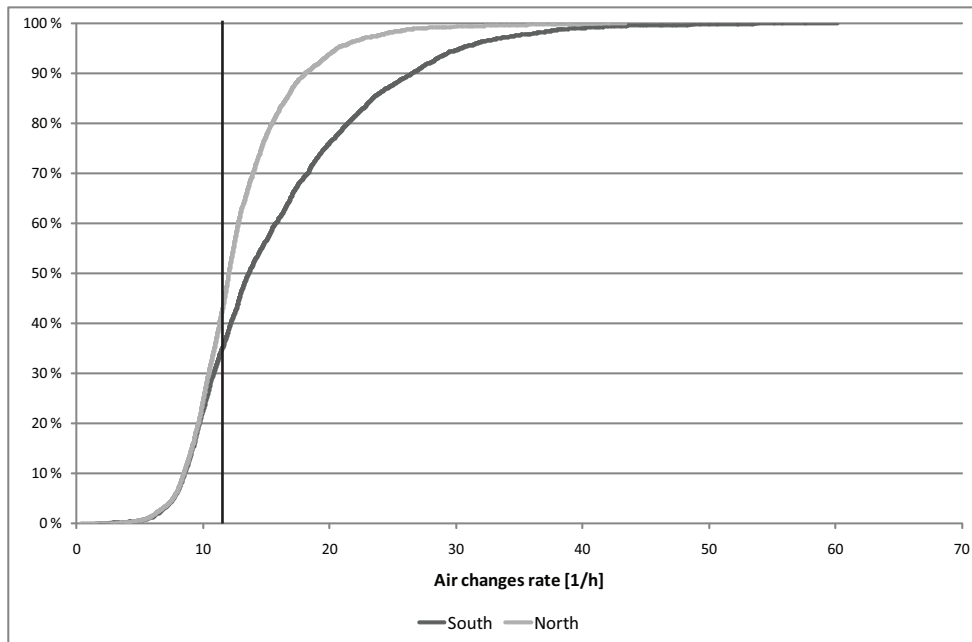
Figure 10.18: *Air changes rate of the isolation room in the summer period.*

For the isolation room facing north it is seen in figure 10.17 that for the winter period there are a sufficient air change rate 95 % of the time. In the summer period the air change rate is above 12 h^{-1} for only about 60 % of the time as seen in figure 10.18, this is not acceptable. To create a sufficient air change rate for the isolation room it is therefore necessary to make some changes for the openings for natural ventilation.

For the isolation rooms it is not just a question about making the openings bigger but also about creating the right pressure in the room.

10.3.3 Airflow between anteroom and isolation room

If the isolation rooms have a positive pressure compared to the anterooms the airflows will flow from the isolation room to the anteroom, whereas if the isolation rooms have a negative pressure the airflows is the opposite direction. The positive direction of the airflow is shown in figure 10.19.
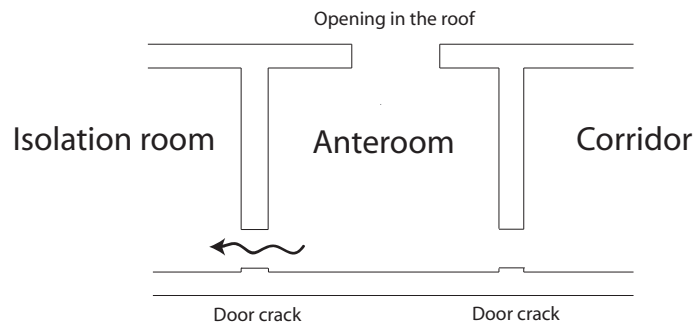
Figure 10.19: *A cross section of the hospital that shows the positive direction of the airflow.*

In figure 10.20 and 10.21 the mass flow between the isolation room and anteroom are showed.
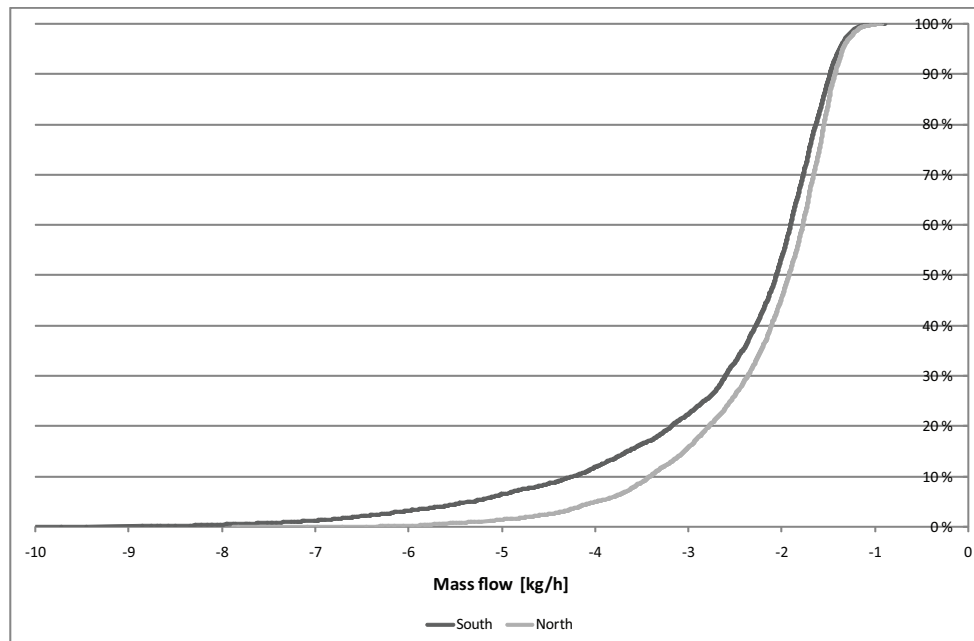
Figure 10.20: *Mass flow from the anteroom to the isolation room in the winter period.*
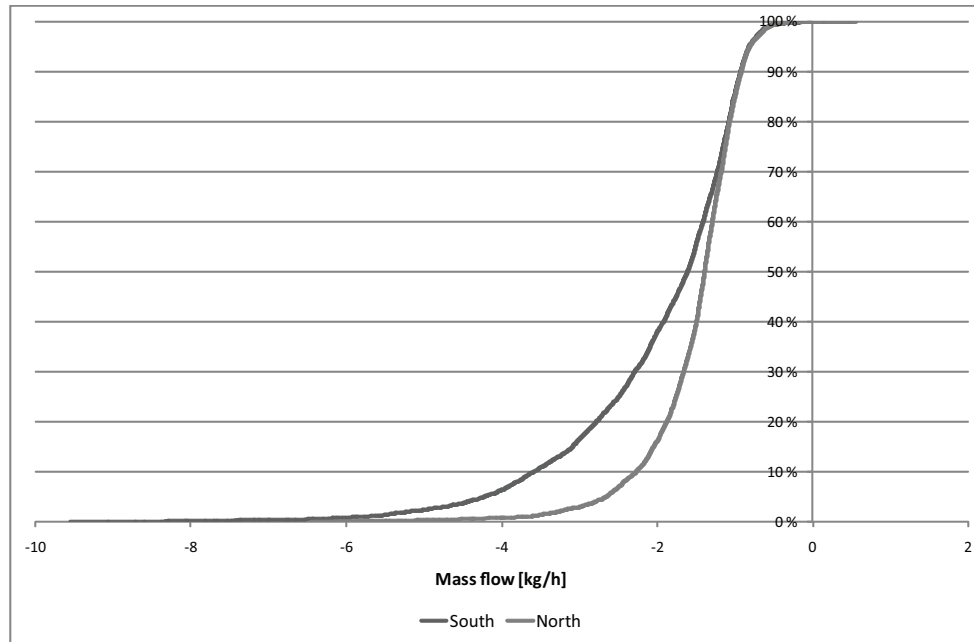
Figure 10.21: *Mass flow from the anteroom the the isolation room in the summer period.*

In figure 10.20 and 10.21 the mass flows are negative when the flow is from the isolation rooms to the anterooms, and positive when the flow is in the opposite direction. From the figures it is therefore seen that the air always flow from the isolation rooms to the anterooms in the winter period. The airflows have the same direction in the summer period, except for a few hours. The airflow out of the isolation rooms to the anterooms are in many of the situations estimated to be coursed by the mechanical ventilation in the toilets and the kitchen.

10.3.4   Airflow between corridor and anteroom

A positive airflow between the anteroom and the corridor means that the airflows from the corridor to the anteroom and a negative flow mens that the airflow is in the opposite direction. The positive direction of the airflow is shown in figure 10.22.
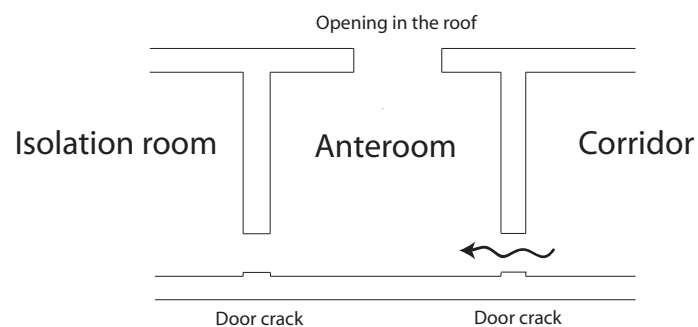
Figure 10.22: *A cross section of the hospital that shows the positive direction of the airflow.*

The mass flow between the corridor and the anteroom for the winter and summer period are showed in figure 10.23 and 10.24.
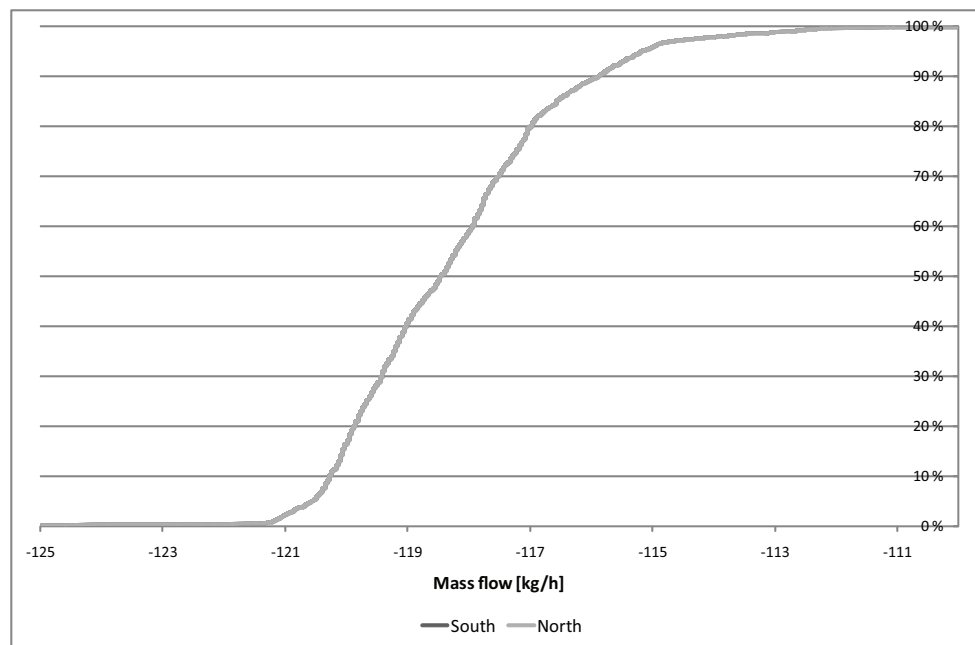
Figure 10.23: *Mass flow from the corridor to the anteroom in the winter period.*
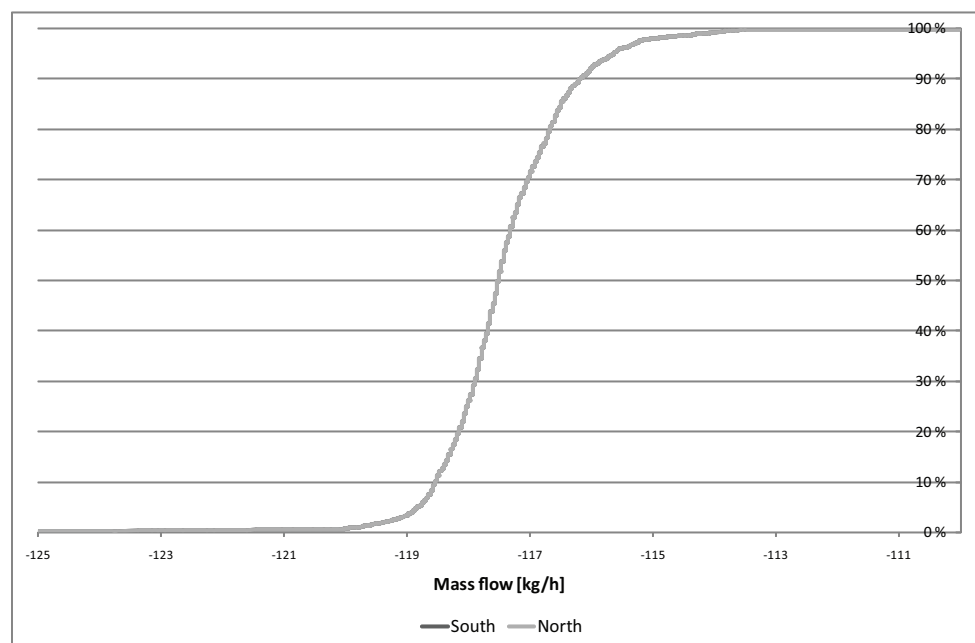
Figure 10.24: *Mass flow from the corridor to the isolation room in the summer period.*

Compared to the airflow between the isolation rooms and the anterooms, the airflow between the corridor and the anterooms are big, as shown in the figures 10.23 and 10.24.

It is also worth noticing that the airflow from the anteroom in the south is the same as the airflow from the anteroom to the north. The direction and the sizes of the airflow is like for the airflow between the anterooms and the isolation room estimated to be coursed by the mechanical ventilation system in the toilets and the kitchen.

10.4 High pressurized isolation room

From figure 10.20 and 10.21 it is seen that the air almost always flows from the isolation room to the anteroom. However there are a few hours in the summer period where the airflows are in the opposite direction. Therefore there have to be made a change of the construction of the isolation rooms to avoid that the air flows from the anterooms to the isolation rooms these few hours.

By looking at the data it is found that the outside temperature is higher than the inside and there almost are no wind. This means that to make the isolation room a high pressurized isolation room in these few hours it is necessary to rise the neutral plan in the room. This can be done by placing a bigger opening in the roof than under the window or use a chimney on the roof. Another solution is to make the system a hybrid ventilation system, thus there is placed a fan in either the isolation room or the anteroom to create the necessary pressure when needed.

It is preferable to use the natural ventilation solution because this would save the electrical energy for a fan. This solution can help the problem regarding the direction of the airflow between the isolation room and the anteroom as well as increasing the isolation room's air changes rate. However if the natural driving forces simply are too low only a fan in the isolation room could ensure a sufficient air changes rate.

From figure 10.17 and 10.18 it is seen that the driving forces were not able to create a sufficient air changes rate all the time in both the winter and the summer situations. Like for the bed wards it might therefore be necessary to make the openings bigger.

10.4.1 Increase of air changes rate

It is now tried to see if it is possible to increase the air changes rate for the isolation rooms by making both openings twice as big which are $0, 5 \ m^2$. In figure 10.25 are showed the air change rate for the isolation room after the change.
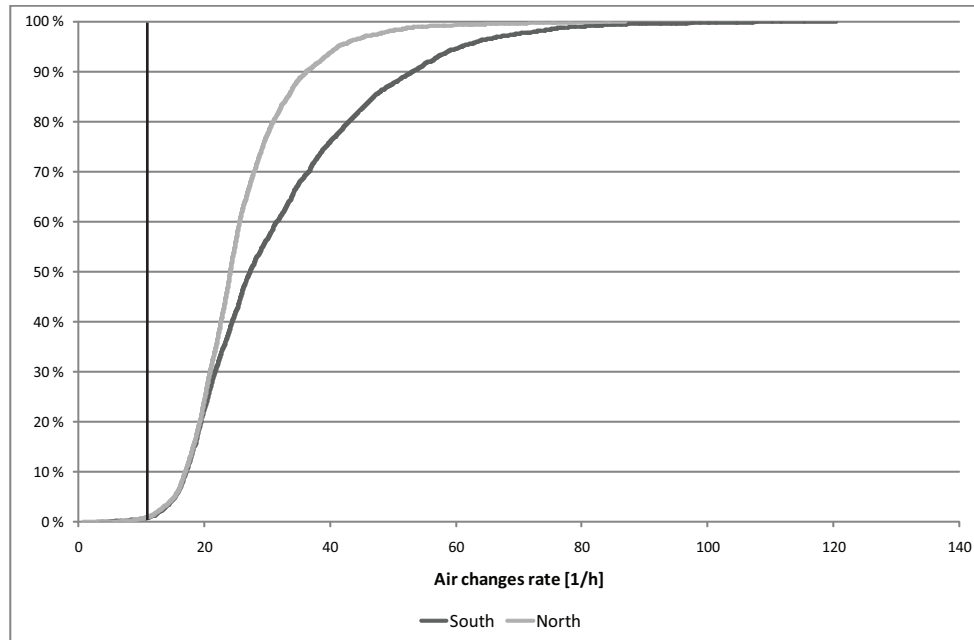
Figure 10.25: *Air changes rate of the isolation room in the summer period when the areas of the openings are made twice as big. With an area of 0,5 m²*

It is seen from figure 10.25 that the reconstruction of the size of the openings for the isolation rooms have the intended effect. The hours which have an air changes rate less than 12 h^{-1} is now only a few percents, as shown in figure 10.25. Since the changes of the air changes rate for the last few percent were very small it is estimated that the driving forces are so small, that it is going to be difficult to get a sufficient air changes rate these hours. This is not acceptable and it is therefore estimated that it is necessary to use a mechanical ventilation system, to make sure there always is a sufficient air changes rate in the isolation room.

For the high pressurized isolation room there are two problems. The first problem is regarding the direction of the airflow between the anteroom and the isolation room the other problem is regarding the air changes rate of the isolation room. It is estimated that it not possible to over come these problems only by the use of natural ventilation. It is therefore decided to make the isolation room hybrid ventilated and place a fan in the isolation room. The fan will make sure there always is a sufficient air changes rate and a high pressure in the isolation room.

The opening under the window is a long slim opening it is estimated that a fan because of the geometry of the opening could not be placed there. The opening in the roof has a more suitable geometry for a fan. It is therefore chosen to place the fan in the opening in the roof.

10.5 Low pressurized isolation room

For the low pressurized room the air has to flow from the isolation room to the anteroom all the time, and there has to be a sufficient air changes rate all the time.

10.5.1 Utilization of a chimney

In the first investigation there is placed a 10 m high chimney on the roof of the isolation rooms. The idea with a chimney on the roof of the isolation room is to lower the pressure in the isolation room, as showed in figure 10.26. The chimney will also be able to increase the air changes rate of the isolation room because of a higher driving force from the thermal buoyancy.

Figure 10.26: *The idea to put a chimney on the roof of the isolation room to create a negative pressure.*

The airflow for the isolation room with the chimney are showed in figure 10.27.
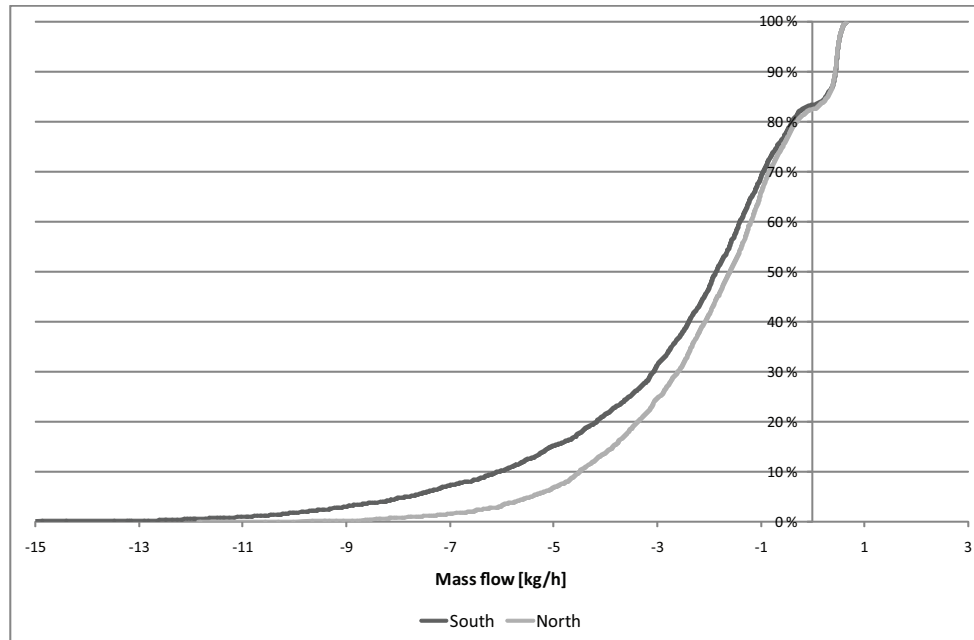
Figure 10.27: *Mass flow from the anteroom to the isolation room in the winter period when there is placed a chimney on the roof. When the mass flow is positive it will flow from the anteroom to the isolation room.*

From figure 10.27 it is seen that for 18 % of the time the airflow is in the intended direction. The amount of time in the winter period the airflow is in the opposite direction as intended is not acceptable.

The mass flow between the isolation room and the anteroom for the summer period is shown in figure 10.28.
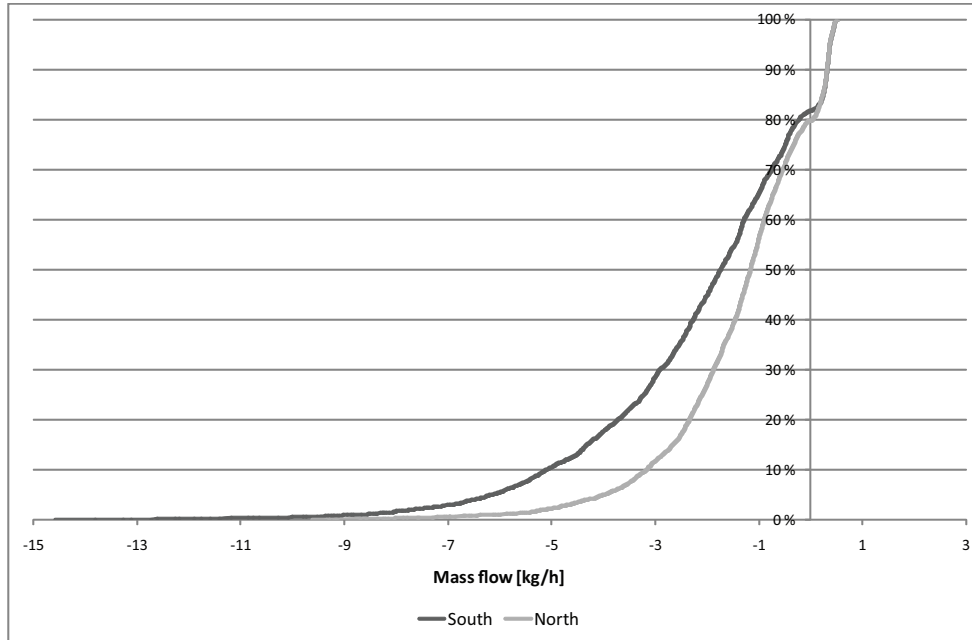
Figure 10.28: *Mass flow from the anteroom to the isolation room in the summer period when there is placed a chimney on the roof. When the mass flow is positive it will flow from the anteroom to the isolation room.*

It is seen in figure 10.28 the for the summer period around 20 % of the time the airflows in the intended direction from the anteroom to the isolation room. This is not acceptable it is therefore necessary to make a different ventilation system.

10.5.2   Combination of openings' sizes and a chimney

To achieve an even lower pressure in the isolation rooms at the floor level it is chosen to make the opening in the chimney 6 times bigger than the opening under the window. The opening under the window has the size of $0,25$ m^2 and the opening in the chimney hereby gets a size of $1,5$ m^2.

The new idea is showed in figure 10.29. The figure illustrate the intended effect of placing a chimney on the roof and making the opening in the roof bigger than the opening under the windows.

Before the changes:
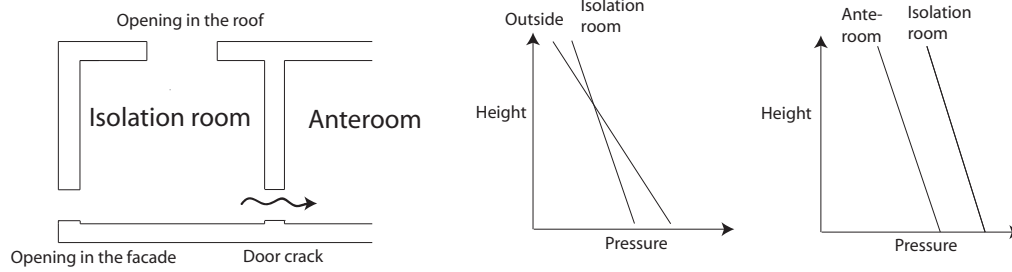
After the changes:
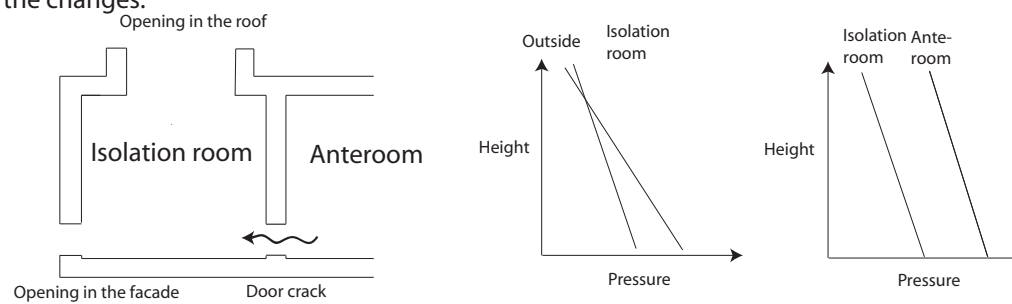
Figure 10.29: *The idea is to put a chimney on the roof of the isolation room and make the opening in the chimney bigger than the opening under the windows. This construction is made to create a negative pressure.*

The mass flow for the isolation room in this situation is showed in figure 10.30.
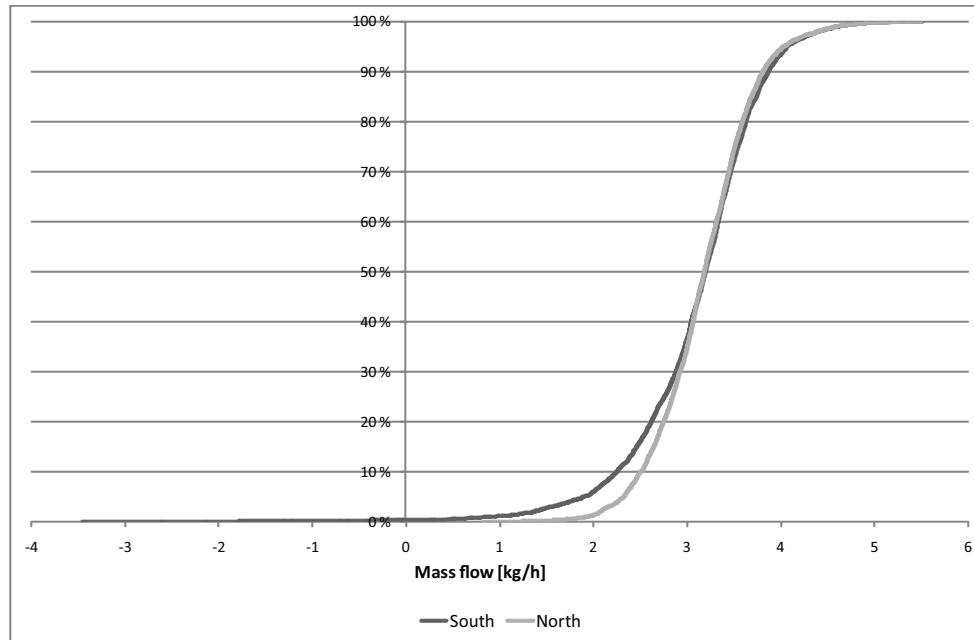
Figure 10.30: *Mass flow from the anteroom to the isolation room when there is placed a chimney on the roof and the opening area in the roof is twice as big as the opening area under the window. When the mass flow is positive it will flow from the anteroom to the isolation room.*

From figure 10.30 it is seen that this construction create such a low pressure near the floor that it is only a few hours during the winter period that the air will flow from the isolation rooms to the anterooms.

The airflow for the same solution are hereafter investigated in the summer situation. The mass flow for the isolation room in the summer period is showed in figure 10.31.
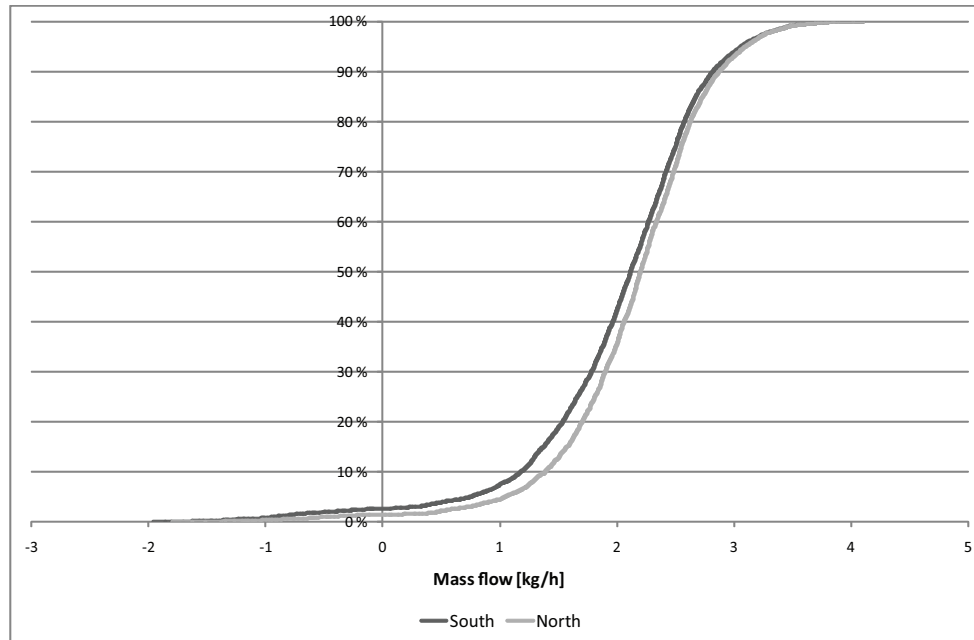
Figure 10.31: *Mass flow from the anteroom to the isolation room in the summer period, when there is placed a chimney on the roof and the opening area in the roof is twice as big as the opening area under the window. When the mass flow is positive it will flow from the anteroom to the isolation room.*

From figure 10.31 it is seen that the ventilation system also works well in the summer period. It is also seen that for a few hours the airflow direction is the opposite as intended for both the isolation rooms. It is therefore estimated that it is necessary to supply the natural ventilation system with a mechanical ventilation systems to always have a sufficient low pressure in the isolation rooms, thus the air flows from the anteroom into the isolation room.

After the system has been design, thus the isolations room have an acceptable pressure it is investigated if there is a sufficient air changes rate in the isolation rooms. The air change rate for the isolation rooms in the winter and summer period are showed in figure 10.32 and 10.33.
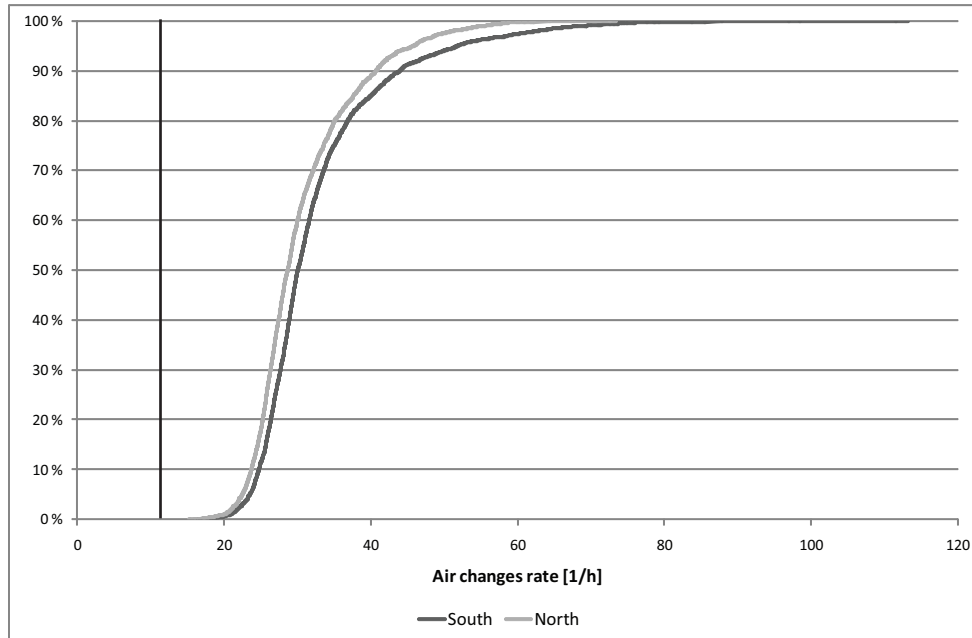
Figure 10.32: *Air changes rate in the isolation room in the winter period when there is placed a chimney on the roof and the opening area in the roof is made six time as big as the area of the opening under the window.*
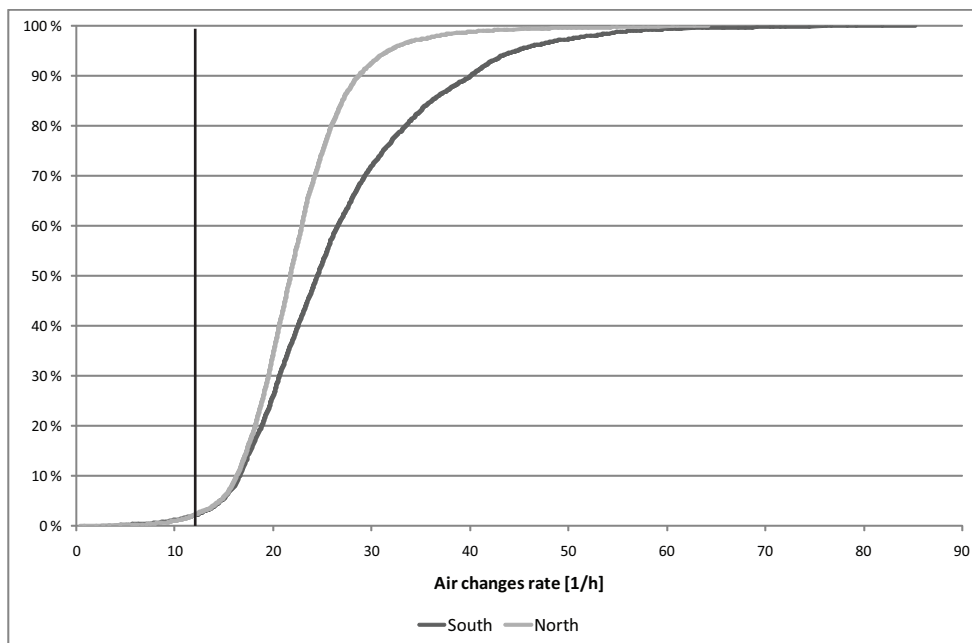
Figure 10.33: *Air changes rate of the isolation room in the summer period when there is placed a chimney on the roof and the opening area in the roof is made six time as big as the area of the opening under the window.*

From figure 10.32 it is seen that the air change rate always are higher than 12 h^{-1} in the winter period. For the summer period it is seen from figure 10.33 that there are a few

hours where the natural driving forces are too low to create a sufficient air change rate for the room. It is therefore necessary to have a mechanical ventilation system in the isolation rooms to create a sufficient air changes for this period.

From the above calculations of the airflow path and air change rate for the bed wards and isolation rooms in the hospital it is concluded that it is necessary to have a hybrid ventilation system to create a sufficient airflow.

10.6 Concise conclusion

There was made a multi zone model of the south east part of the Aabenraa hospital. The model was simplified so the only infiltration that was includes in the model was the one through the door cracks between the rooms. This simplification will cause that the airflow will differ a bit from the real airflows. From the multi zone model it was found that

- The openings in the bed ward have to have a size of $0,3$ m^2 and there should be placed a fan in the roof to ensure the air changes rate of minimum 6 h^{-1} .

- The openings in the high pressurized isolation rooms have to be $0,5$ m^2, and for the opening in the roof there should be placed an inlet fan. The fan also has to ensure an air change in the isolation room of minimum 12 h^{-1}.

- For the low pressurized isolation rooms it is necessary to place a 10 m high chimney on the roof, with an opening size of six times the size of the opening under the windows. The size of the opening in the chimney hereby is $1,5$ m^2 and the opening under the windows $0,25$ m^2. In the chimney are placed a exhaust fan to make sure there always is a sufficient pressure, and air changes rate in the isolation rooms.

In both the bed wards and the high pressurized and low pressurized isolation rooms it was necessary with a fan. To make the hybrid ventilation strategies work it is therefore necessary to have a control system for the fans. For the bed wards there can be used equipment that can measure the speed of the air extracted from the room and this way make sure there is a sufficient air changes rate of the rooms. For isolation rooms this approach can also be used to ensure there is a sufficient air changes rate in the rooms. It is however also important to make sure there is a sufficient pressure in the isolation rooms. Pressure sensors are not very useful to do this because they need a too high pressure to work properly. It is therefore necessary to use another strategy to make sure there is the correct pressure in the isolation rooms. One approach could be to have a fan that if the isolation room was high pressurized supplied more air to the isolation room than it would leak because of infiltration and the opposite if the room was low pressurized.

In these multi zone simulation were used C_p-values from a squared building for all the openings. To get more precise values of the C_p-values, and hereby the effect of the driving force of the wind are made a wind tunnel simulation in a CFD-program for different wind

direction for the hospital. These C_p-values are then used in a new series of multi zone calculations.

Chapter 11

CFD simulation of Aabenraa hospital

For the multi zone model of Aabenraa hospital in chapter 10 were used average C_p values from the literature. For the multi zone model were used the same C_p values for all the openings on the same side. To make the model more correct there are made wind tunnel simulations of Aabenraa hospital in the commercial CFD program Flovent to find the openings' C_p-values for different wind directions.

In the commercial CFD program Flovent, the only two equation turbulence model is the standard $k - \epsilon$ turbulence model. It is therefore chosen to use this turbulence model in the wind tunnel simulation of the Aabenraa hospital. To get an idea of how good this turbulence model is there is first looked on a benchmark case.

11.1 Benchmark model

For the benchmark case there exist measured C_p values for a cube. By making a CFD simulation of the benchmark case it is possible to compare the results from the simulation to the measured values and see how much they differ from each other.

11.1.1 Identification and formulation of the problem

As stated above the purpose is to figure out how accurate the standard $k - \epsilon$ turbulence model is.

Beside of evaluate the turbulence model the simulation of the benchmark case will also give a qualified guess for the position of the first grid point near the surfaces in the wind tunnel simulation of the Aabenraa hospital.

11.1.2 Specification of geometry and grid

In the commercial CFD program Flovent it is only possible to use Cartesian grid, and therefore this grid is used. In the CFD simulation of the cube it is chosen to place the cube so:

- The area in front of the cube has a length corresponding to the 5 times the height of the cube

- The area to the side of the cube has a length corresponding to the 3 times the height of the cube

- The area behind the cube has a length corresponding to the 10 times the height of the cube

- The height of the model is 40 m

The size of the model is shown in figure 11.1. The model is symmetric around the dotted line. To save computer power there is inserted a vertical symmetric plan through the line. This means that it is only the lower half in the xz-plan that is used in the model.

Figure 11.1: *Outline of the CFD model. Measurements in* $[m]$*.*

For the model the finest grid is located close to the surface and areas where changes in the airflow is expected. An example of the used grid is shown in figure 11.2. For the grid the distance from the first grid points to the ground are 3 cm and the distance from the first grid points to the cube's surfaces are 1 cm.

Figure 11.2: *The grid used in the benchmark model*

To estimate if the chosen grid structure is acceptable it is necessary that the dimensionless length y^+ lies in the interval from 30 to 500 [Brohus, 2007a] . It is also important that the results from the simulations are independent of the grid. These two demands can first be checked after the simulation is performed.

11.1.3 Specification of physical models and boundary conditions

To be able to compare the calculated C_p values from the CFD simulation to the measured values it is necessary they are done under the same conditions. The used condition in the CFD model are listed in table 11.1.

Table 11.1: *Input in the CFD model.*

Used values
Isothermal model
Uniform wind profile
Wind speed of 2,5 $\frac{m}{s}$
Gravity acceleration of 9,81 $\frac{m}{s^2}$
Density of the air 1,19 $\frac{kg}{m^3}$

The boundary conditions for the benchmark model are listed in table 12.10.

Table 11.2: *Boundary condition for the benchmark model.*

Surface	Boundary condition
Right side	Open plane
Left side	Placed a fan
Top	Open plane
Back	Open plane
Middle	Symmetry

11.1.4 Solution

The simulation is found in the zipped Flovent file 'A Cube y0,03 y0,01'. From figure 11.3 it is seen that the CFD model of the benchmark case is converged because the residuals for the calculated values in the program are below 1.
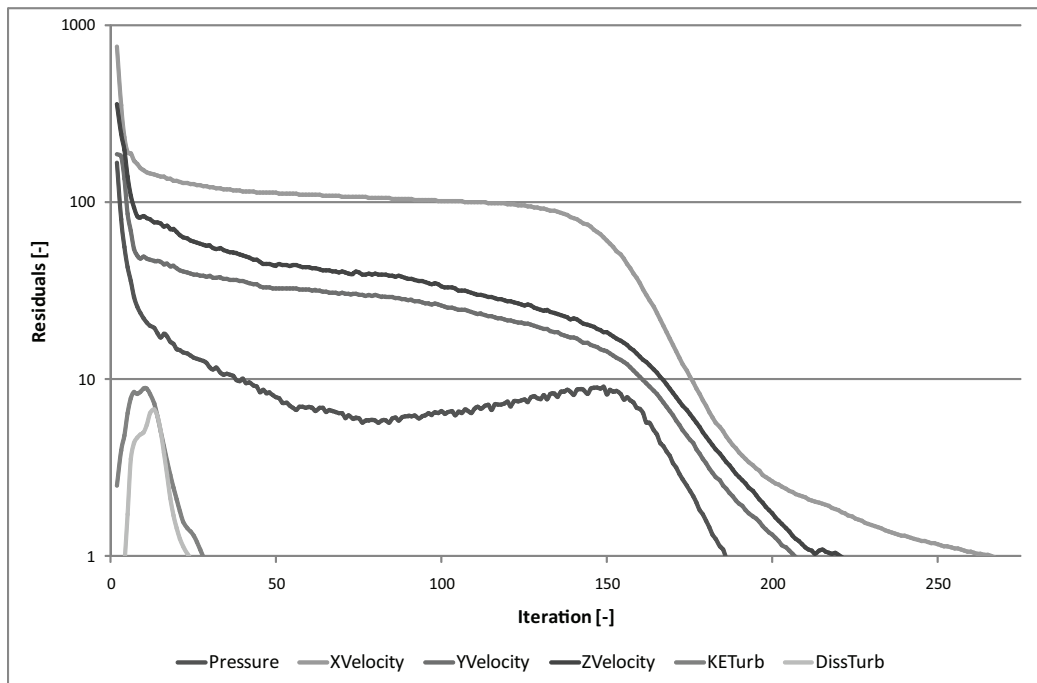
Figure 11.3: *The grid used in the benchmark model*

After the simulation the y^+ values are calculated to determine if the distances between the surfaces and the first grid points are acceptable. The calculations of the y^+ values are located in the Excel spreadsheet 'A Cube y0,03 y0,01 y+.xls' and all the grid points near the surfaces are checked. It is found that y^+ values lies in the interval from 17 to 386, some of the y^+ values are therefore too low they can however still be accepted [Nielsen, 2008] . The procedure for calculation the y^+ values is shown in appendix A.3.

After the acceptable distances to the first grid points are found, it is necessary to check that the results are independent of the grid. This is done by making simulations with

either a much coarser or a finer grid. If the results from the new simulations do not differ significantly from the previous results, the results from the simulations are independent of the grid.

It is chosen to check that the results are independent of the grid by making two extra simulations with a finer grid, the sizes of the grids are listed in table 11.4.

Table 11.3: *The sizes of the grid in the simulations*

Simulation	Number of cells
Simulation A	125496
Simulation B	401636
Simulation C	903968

Model B and C are located in the zipped Flovent files 'B Cube y0,03 y0,01' and 'C Cube y0,03 y0,01'. To check the convergency for the models are showed the residuals for the models in figure 11.4.

Simulation B
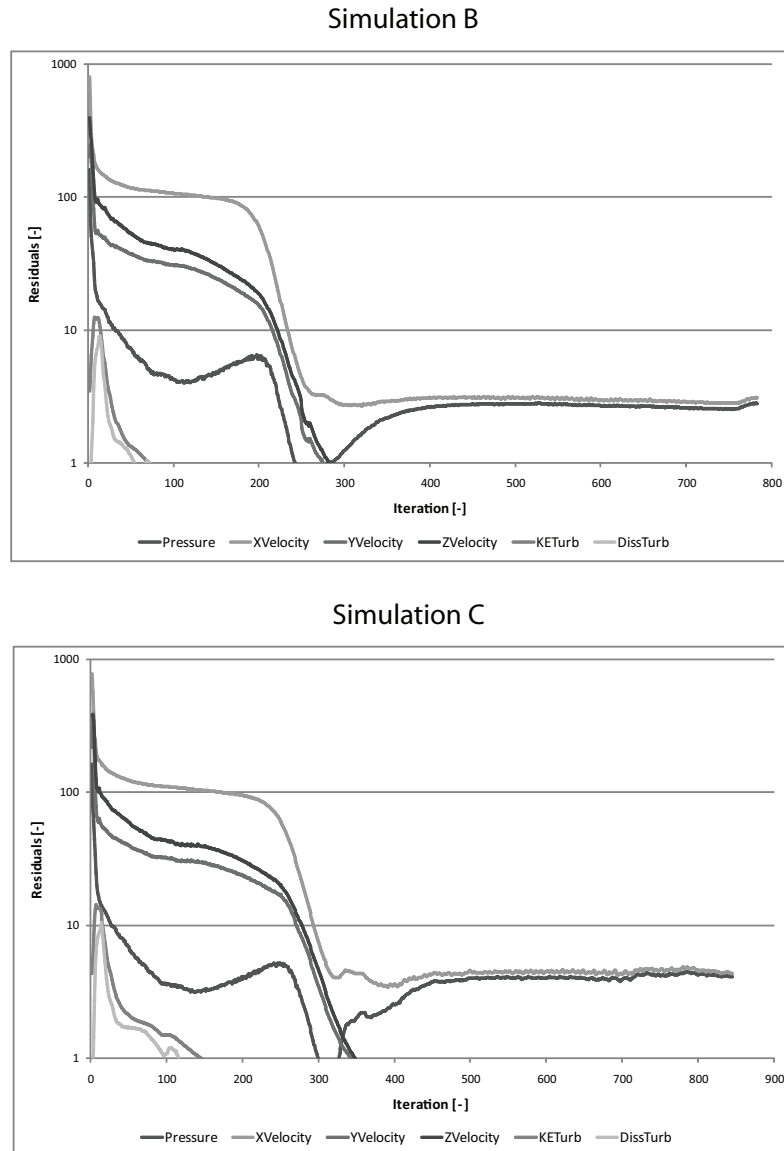
Simulation C

Figure 11.4: *Residuals from the two CFD simulations B and C.*

From figure 11.4 it is seen that the values of residuals are the same during the last iterations, and that the residues are below 50. This means that the models are low level stable.

Since they are low level stable it is necessary to use error fields and monitor points to estimate if the simulations are converged [Brohus, 2007a] . There are therefore placed four monitor points close to the surfaces of the cube and a monitor point in the air behind the cube, where there will be a big eddy.

The error fields only show some errors near the edges, and they are therefore accepted. The values from the monitor points are stable, as shown in figure 11.5. It is hereby estimated that the simulations are converged.

Simulation B
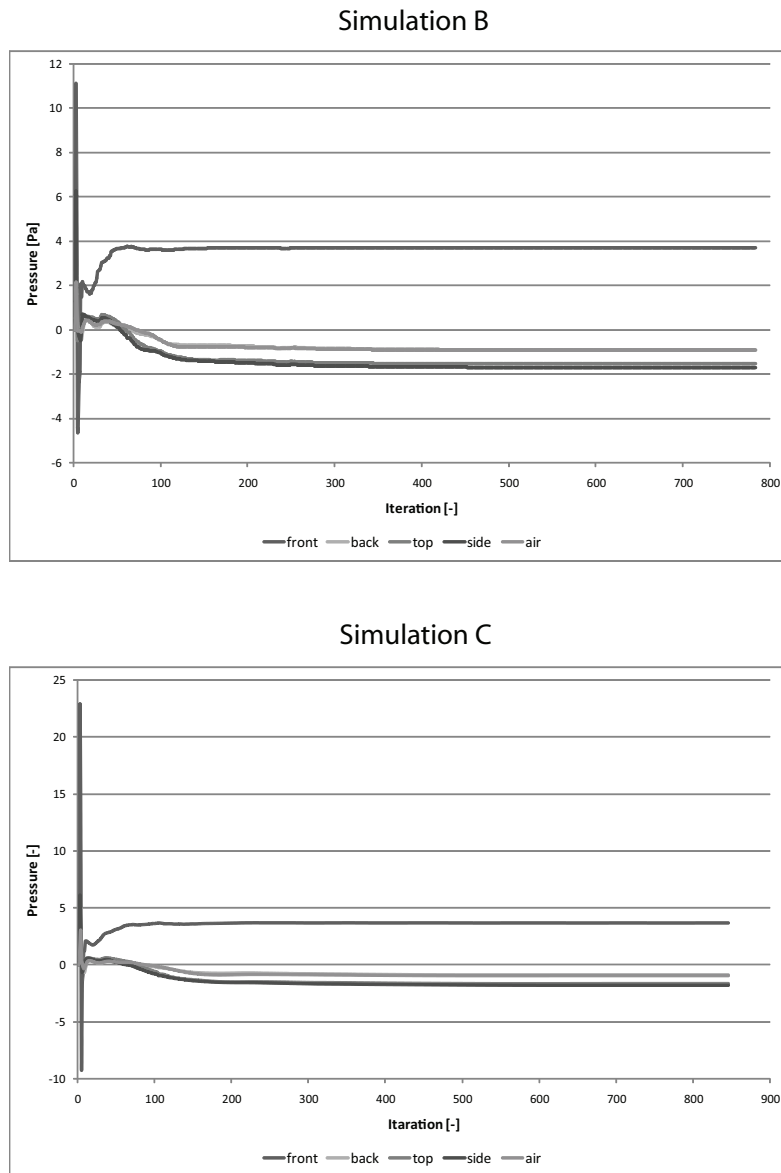
Simulation C

Figure 11.5: *The pressure from the two monitor points B and C*

Like for the first simulation the y^+ values have to be calculated for the two models. But unlike the first model it is chosen only to check the models in four points. The four points are shown in figure 11.6. It is chosen only to check four points because the commercial program Flovent is not very suitable to calculate the y^+ values in. However since it is chosen not to check all the first grid points near the surfaces there is a risk that there are areas in the models where the y^+ values do not have an acceptable value.
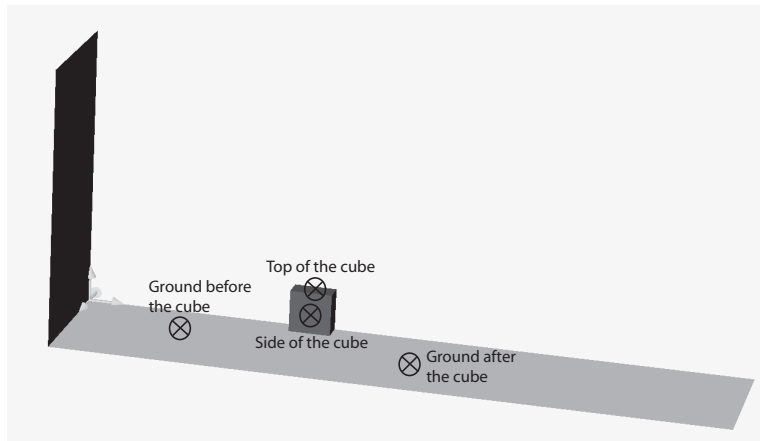
Figure 11.6: *The position of the points where the y^+ values are calculated.*

The results of the calculations of the y^+ values are listed in table 11.4. All the y^+ values are inside the acceptable interval and the distance to the first grid points are therefore accepted.

Table 11.4: *The sizes of the grid in the simulations.*

	Ground before the cube	Ground after the cube	Top of the cube	side of the cube
Simulation B	161,9	145,5	91,9	103,7
Simulation C	171,4	151,9	105,2	110,9

To determine if the results from the CFD simulations are grid independent the results from the three simulations are compared. It is chosen first to compare the results from the monitor point in the air behind the cube, the results are shown in figure 11.7.
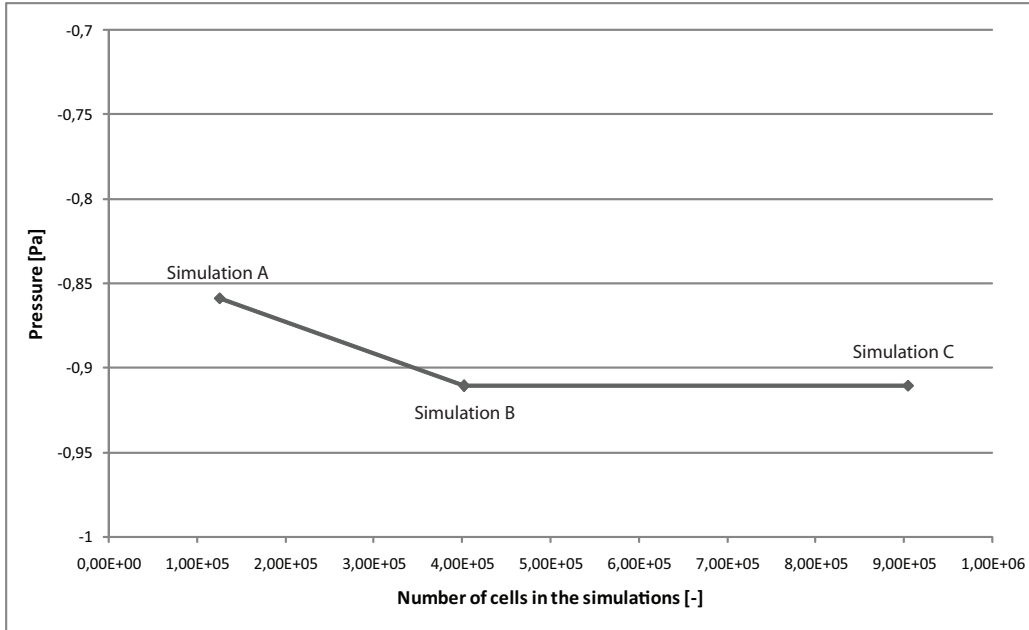
Figure 11.7: *The results from the monitor point behind the cube.*

In figure 11.7 it is seen that the results from simulation B and C are almost the same whereas the results from simulation A differ a bit from the two others. It can therefore be estimated that the results from simulation B and C appear to be independent of the grid.

To ensure that the results are independent of the grid it is also chosen to compare the C_p values in the lines on the cube where there exist measured values. The six lines are seen in figure 11.8.
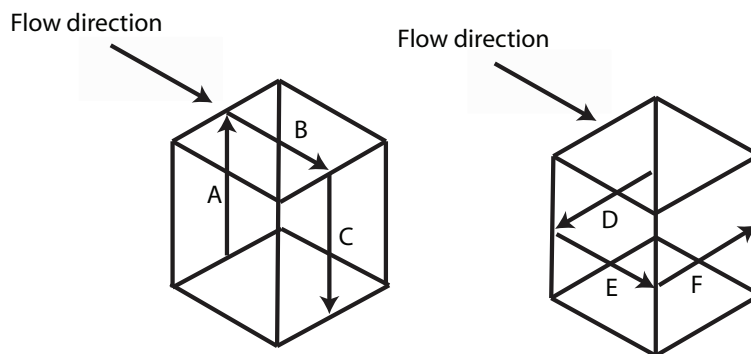
Figure 11.8: *The lines on the surface of the cube where there exist measured $C_p$values.*

From the CFD simulations the pressure for the lines are calculated. The C_p values can then be calculated as:

$$C_p = \frac{P}{0,5 \cdot \rho \cdot v_{ref}^2} \tag{11.1}$$

where

P : Pressure $[Pa]$

v_{ref} : Reference wind speed $[\frac{m}{s}]$

The calculations of the C_p values are listed in the Excel spreadsheet 'Cube Cp values.xls'. The results from the calculations are shown in figure 11.9.
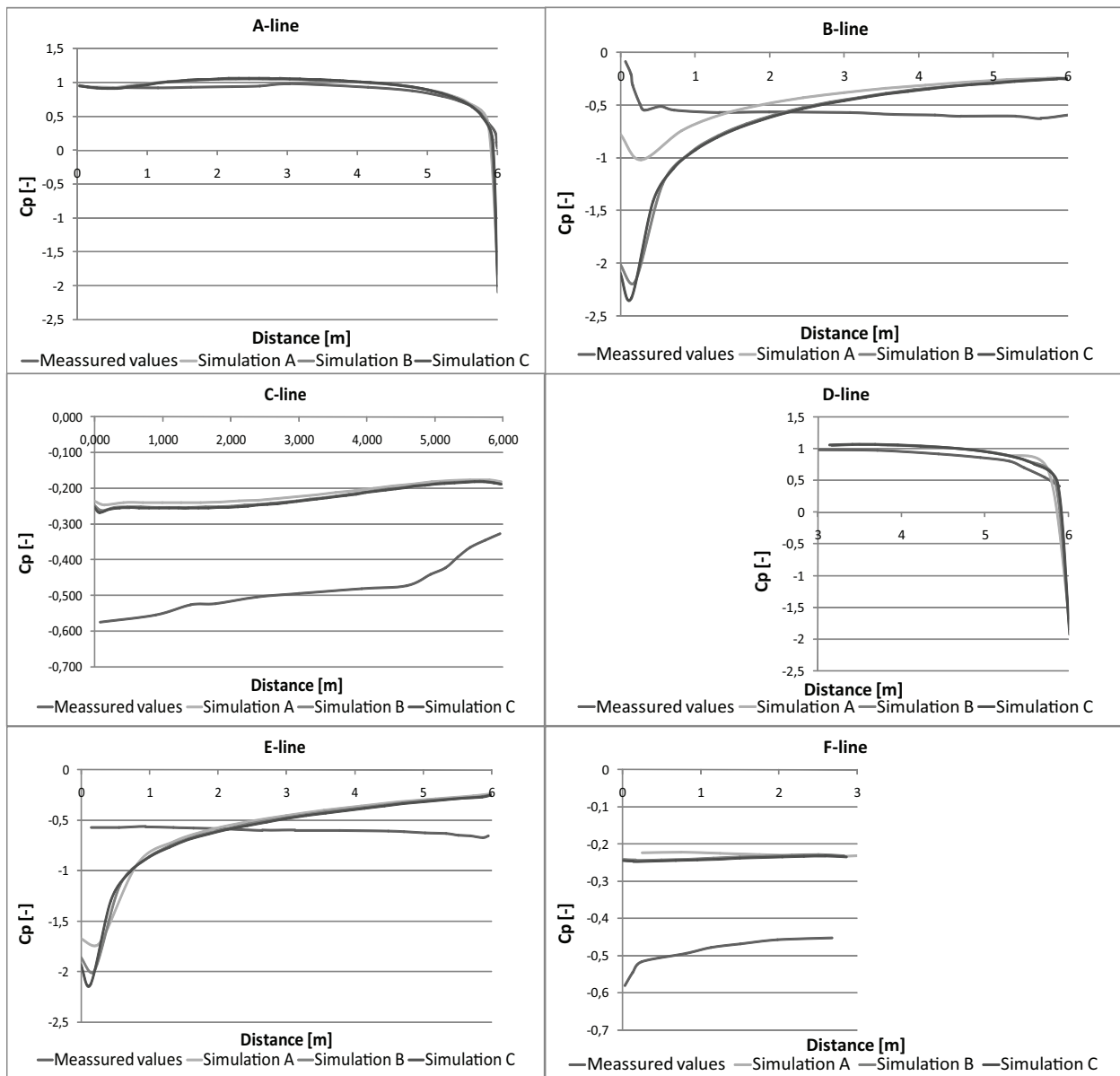
Figure 11.9: *The measured C_p values and the calculated C_p values from the three CFD simulations in the six lines on the cube.*

From figure 11.9 it is seen that the results from simulation A as expected differ a bit from the simulations B and C, whereas the results from simulation B and C are almost the same.

In figure 11.9 it is also seen that the measured values and the values found from the simulations are very much alike in the lines A and D. In the other lines the calculated values are not so close to the measured values. It can therefore be concluded that the standard k-ϵ turbulence model will not give the exact values, but acceptable values.

11.2 CFD simulation for Aabenraa hospital

To calculate more correct C_p values for the section of Aabenraa hospital with natural ventilation there are made wind tunnel simulations. In the simulations the wind is coming from four different direction, north, east, south and west. The processed data from the CFD simulations can be found in the Excel spreadsheet 'Aabenraa CFD.xls'

11.2.1 Identification and formulation of the problem

As stated above the purpose is to make a wind tunnel simulation of the Aabenraa hospital to get more precise C_p values for the Aabenraa hospital. These C_p values can then be used in a new multi zone calculation.

11.2.2 Specification of geometry and grid

In the commercial CFD program Flovent it is only possible to use Cartesian grid, and this grid is therefore used. Inspired by the benchmark model it is chosen that the model of the hospital should be placed so:

- The area in front of the hospital has a length of around 75 m, corresponding to 5 times the height from the ground to the top of the hospital's chimneys.

- The area to the side of the hospital has a length of around 45 m, corresponding to 3 times the height from the ground to the top of the hospital's chimneys.

- The area behind the hospital has a length of around 150 m, corresponding to 10 times the height from the ground to the top of the hospital's chimneys.

- The height of the model is 55 m.

The model is constructed so it is most detailed close to the natural ventilated hospital section and the longer the distance is to this section the lower the detail level is, as shown in figure 11.10. That the detail level is higher close to the natural ventilated hospital section can be seen by it is chosen to keep the nearby courtyards as well as the elevator tower and the vegetation around the hospital section.
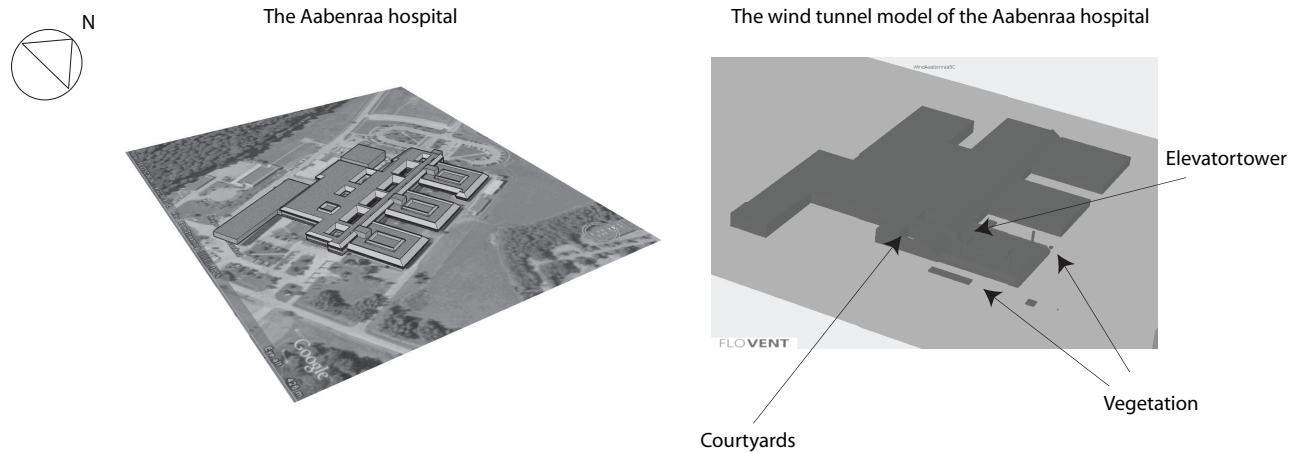
Figure 11.10: *Aabenraa hospital compared to the wind tunnel model of the Aabenraa hospital.*

It is chosen not to let the hole hospital have a high detail level to avoid that the model gets too complex and hereby demands too much computer power to find a solution that converge. It is also done under the assumption that the construction details fare away from the area of interest only will have a little influence on the results in that area compared to the constructions details close to it.

The grid in the CFD models are constructed so that it is coarse fare away from the hospital and the closer it is to the natural ventilated hospital section the finer it is, as shown in figure 11.11. Inspired by the benchmark case it is chosen to let the first grid points be 1 *cm* near the surfaces of the hospital and 3 *cm* above the ground. After the simulations it is determent if this is an acceptable distance.
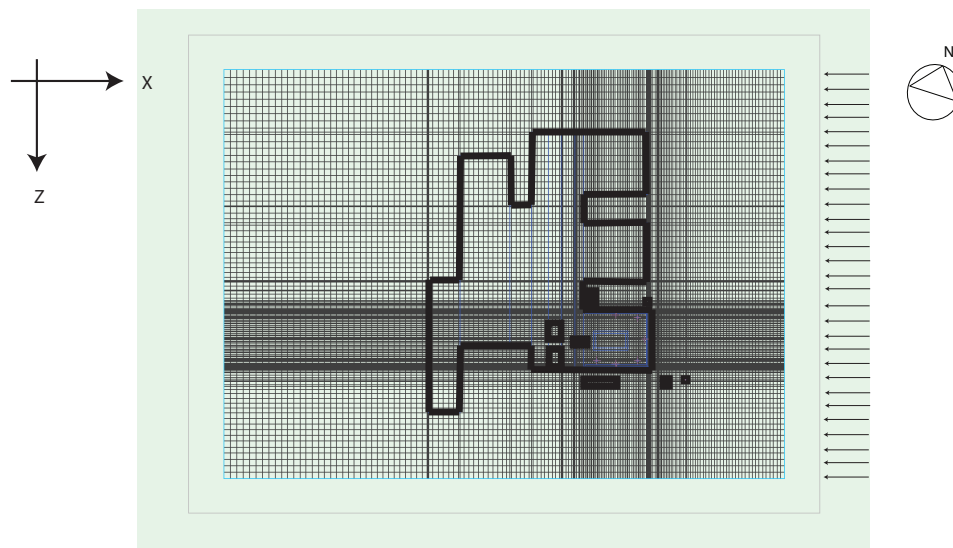
Figure 11.11: *The grid structure for the XZ plan used in the wind tunnel simulations, when the wind is coming from the east.*

11.2.3 Specification of physical models and boundary conditions

Except of the wind velocity profile, the input in the wind tunnel simulations are the same as in the benchmark case. The wind velocity profile is no longer uniform. Instead it is described with the power function in equation (9.1) in chapter 9. In the function there are used terrain coefficients for country with scattered stand, the input in the function are listed in table 11.5.

Table 11.5: *Terrain coefficients.*

V_{10}	$[\frac{m}{s}]$	2,5
k	[-]	0,52
α	[-]	0,20

For the commercial CFD program Flovent it is not possible to model the wind profile exact. Instead are made an approximation of the wind velocity profile. The wind profile is made of sections at the boundary and have the smallest intervals closest to the ground, because it is there the biggest changes in the velocities are. Because the wind velocity profile at the boundary is made of sections it is not smooth, however after the wind has moved a certain distance it will be more smooth, as shown in figure 11.12.
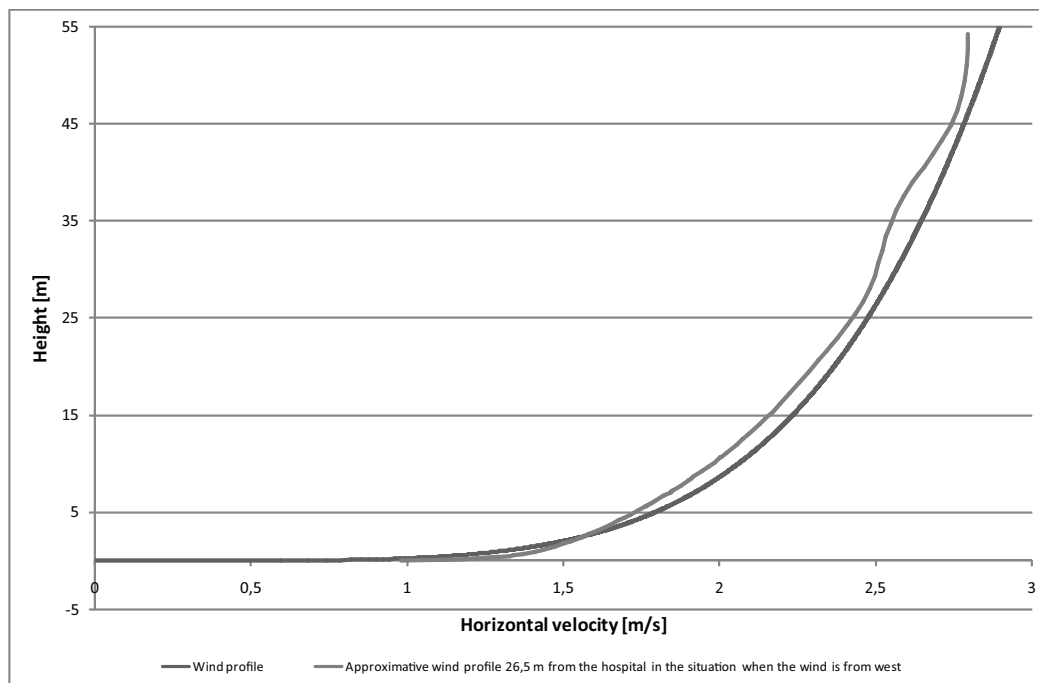
Figure 11.12: *The approximative wind profile used in the simulation when the wind is from west compared to the real wind profile.*

In figure 11.12 it is seen that the two wind velocity profiles are not completely alike they differ a bit from each other. However the approximative wind velocity profile almost have the intended shape. It is therefore estimated that the approximative wind velocity profile used in the wind tunnel simulations is acceptable.

11.2.4 Solution

The wind tunnel simulations for the four wind directions are found in the folder '\CFD \Floventfiles \Windtunnel' on the cd. For all the simulations it goes that they are low level stable with some oscillation. As an example is in figure 11.13 shown the residuals for the situation when the wind is coming from west.
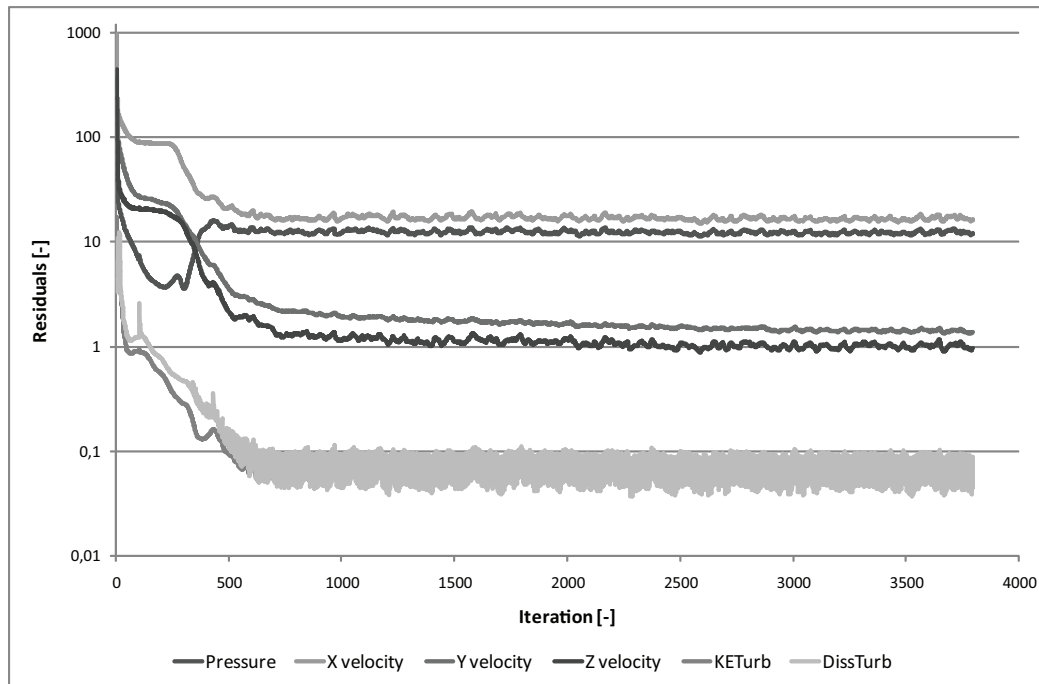
Figure 11.13: *The residuals for the wind tunnel simulation when the wind is coming from west.*

Since the simulations are low level stable with some oscillations it is necessary to look at the error fields in the models and the monitor points. The error fields do only show some problems close to the edge and are therefore fine. The results for the monitor points for the simulation when the wind is coming from the west is shown in figure 11.14. Based on the stable values for the monitor points in the models it is estimated that the model is converged.

Figure 11.14: *The monitor points for the wind tunnel simulation when the wind is coming from west.*

For the different models the y^+ values for all grid points near the surface needs to be checked. However since the commercial CFD program Flovent is not very suitable to calculate the y^+ values it is chosen only to calculate the y^+ values in five different points. These points are chosen so that three of them are close to the hospital section with natural ventilation and the last two are placed a bit further away. The location of the five points where the y^+ values are checked are shown in figure 11.15.
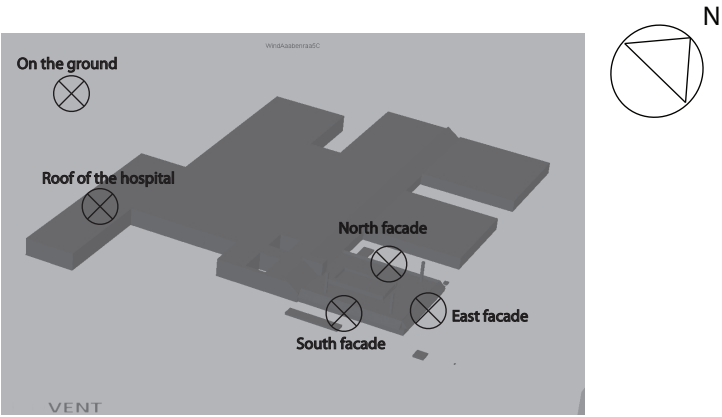
Figure 11.15: *The points where the y+ values are controlled.*

The y^+ values for the five points for the four wind tunnel simulations are listed in table 11.6.

Table 11.6: *The y^+ values in the four wind tunnel simulations for the five points.*

	On the ground	Roof of the hospital	South facade	North facade	East facade
Wind from West	106	54,7	23,8	31,8	15,5
Wind from South	144	50,8	35,1	14,6	33,0
Wind from East	125	37,8	30,5	31,0	31,2
Wind from North	149	45,4	12,9	31,5	32,9

It is seen that all the y^+ values are between 10 and 500 and the position of the first grid points are therefore estimated to be placed in an acceptable distance.

After it is found that the y^+ values lie inside an acceptable interval the simulations have to be checked for grid independency. However to save computer power this is chosen only to be done for one simulation. It is chosen to check the simulation where the wind is coming from west. For this situation there are made two extra simulations, these simulations is found in the folder '\CFD \Floventfiles \Windtunnel \Check' on the cd. The amount of cells for the three simulations of the wind coming from the west are listed in table 11.7.

Table 11.7: *The number of cells that are used in the simulations to check the models for grid independence.*

First simulation	2 596 877 cells
Second simulation	2 075 469 cells
Third simulation	1 834 694 cells

The results from five monitor points are compared to each other, as shown in figure 11.16. It is seen that the results do not vary much from each other but they are not completely stable in all the cases. However it is chosen not to do a simulation with a higher number of cells because it is estimated that such a model will demand too much computer power.
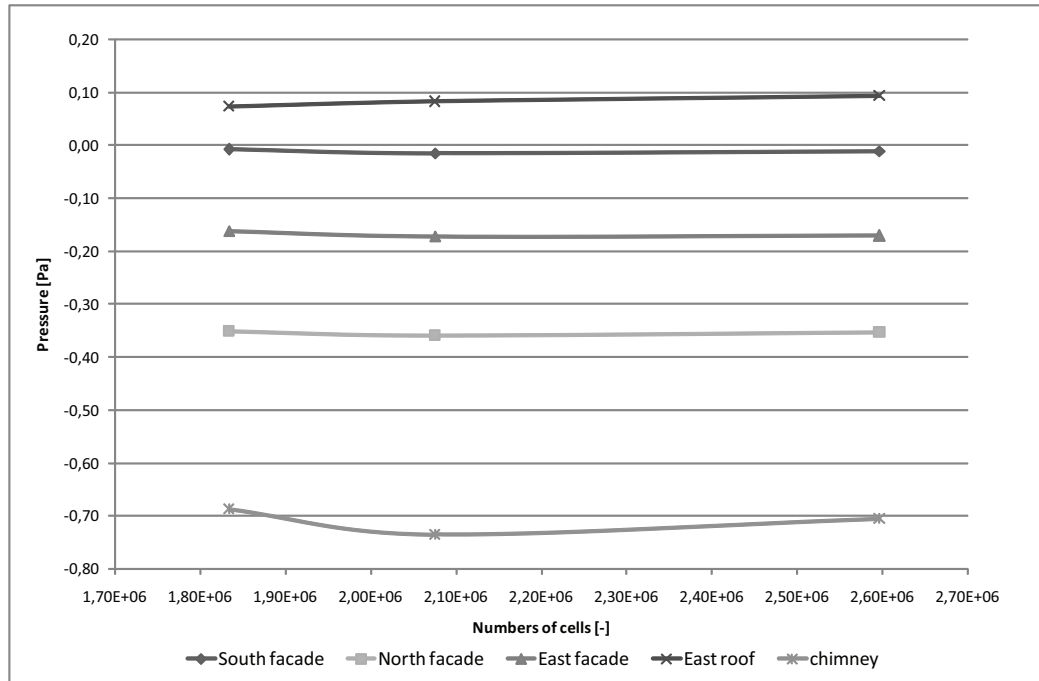
Figure 11.16: *The results from monitor points with the wind coming from west in three different simulations.*

Based on the check of grid independency for the wind tunnel simulation of the wind coming from west it is estimated that the results almost are independent of the grid. So it could be considered to use the model with the lowest amount of cells. It is however chosen to use the biggest model with around 2,6 millions cells in all the wind tunnel simulations.

The C_p values are now calculated for the openings in the natural ventilated hospital section. The openings for natural ventilation are placed near the shown arrows in figure 11.17.
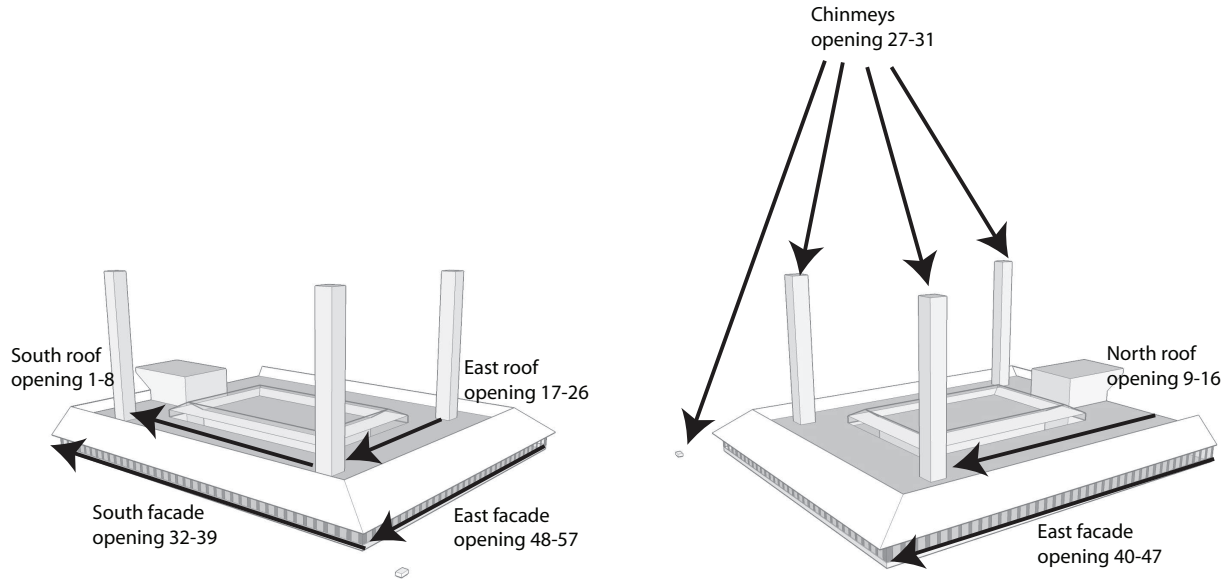
Figure 11.17: *The position of the openings in the natural ventilated hospital section.*

Like for the benchmark case the C_p values for the openings are calculated by using equation (11.1). In the calculations of the C_p values the reference height for the wind is set to 4,95 m which corresponds to the height of the roof on the natural ventilated hospital section.

The C_p values from the wind tunnel simulations are compared to the C_p values found in the literature for a squared low rise building with different surroundings, as shown in figure 11.18.
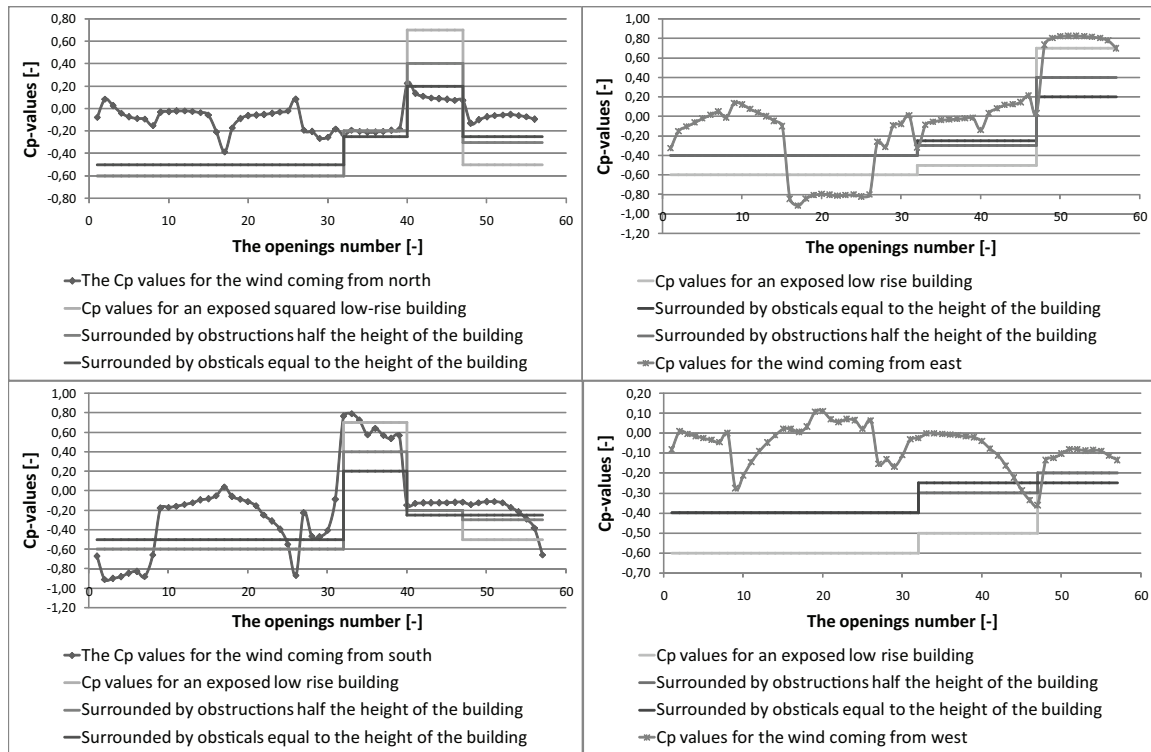
Figure 11.18: *The C_p values from the wind tunnel simulations compared to the C_p value from the literature.*

It is found that when the wind is coming from the south or the east the best fits from the literature is a building in an exposed environment. Whereas if the wind is coming from the north or the west the best fits are estimated to be a building placed in an environment with obstacles with an equal height as the building itself.

It is also found that the C_p values from the CFD simulations vary a lot over the different surfaces on the building. Especially on the roof where there are a lots of obstacles are there big variations between the C_p values from the literature and the C_p values from the wind tunnel simulations. That there is a big variation in pressure field on the roof of the hospital section can also be seen in figure 11.19.
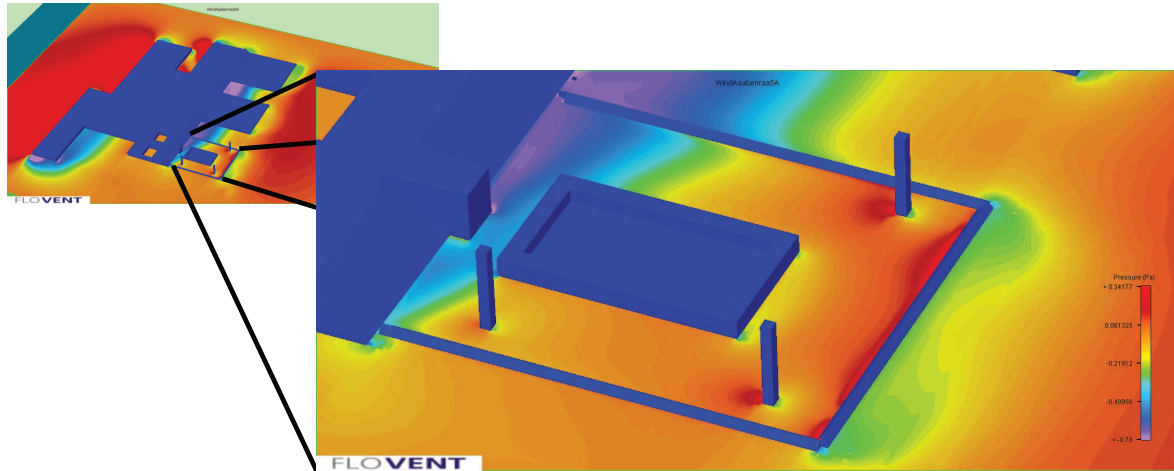
Figure 11.19: *The pressure field in the height of the hospital's roof when the wind is coming from west.*

The difference between the C_p values from the literature used in the multi zone model and the C_p values from the wind tunnel simulations will results in a different air changes rate for the natural ventilated rooms in the hospital. These natural ventilated rooms except the anterooms are shown in figure 11.20.
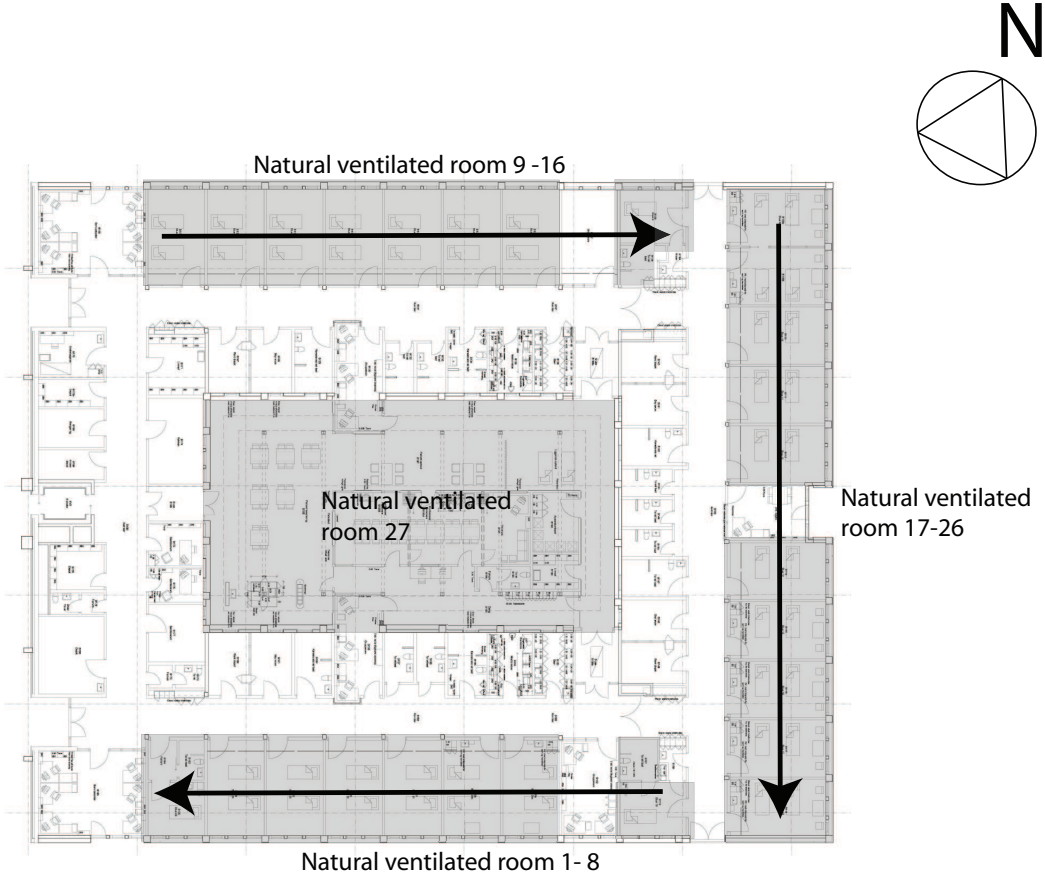
Figure 11.20: *The natural ventilated rooms in the hospital except the anterooms.*

The driving force for the wind and hereby the air changes rate for a room depends on ΔC_p for the openings in the room. An example of how ΔC_p is found is shown in figure 11.21.
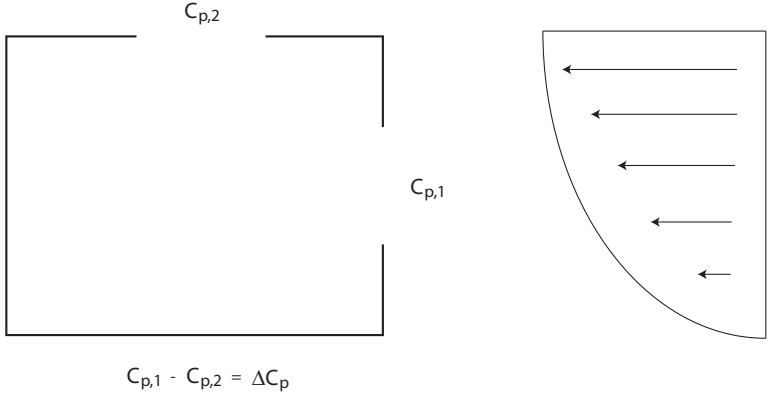
Figure 11.21: *How ΔC_p is found for the isolation rooms and the bed wards.*

To get an idea of how the changes from the C_p values from the literature to the C_p values from the wind tunnel simulations affects the air changes rate for the rooms in the

natural ventilated hospital section, ΔC_p in the two situations have to be calculated and compared to each other, as shown in figure 11.22.
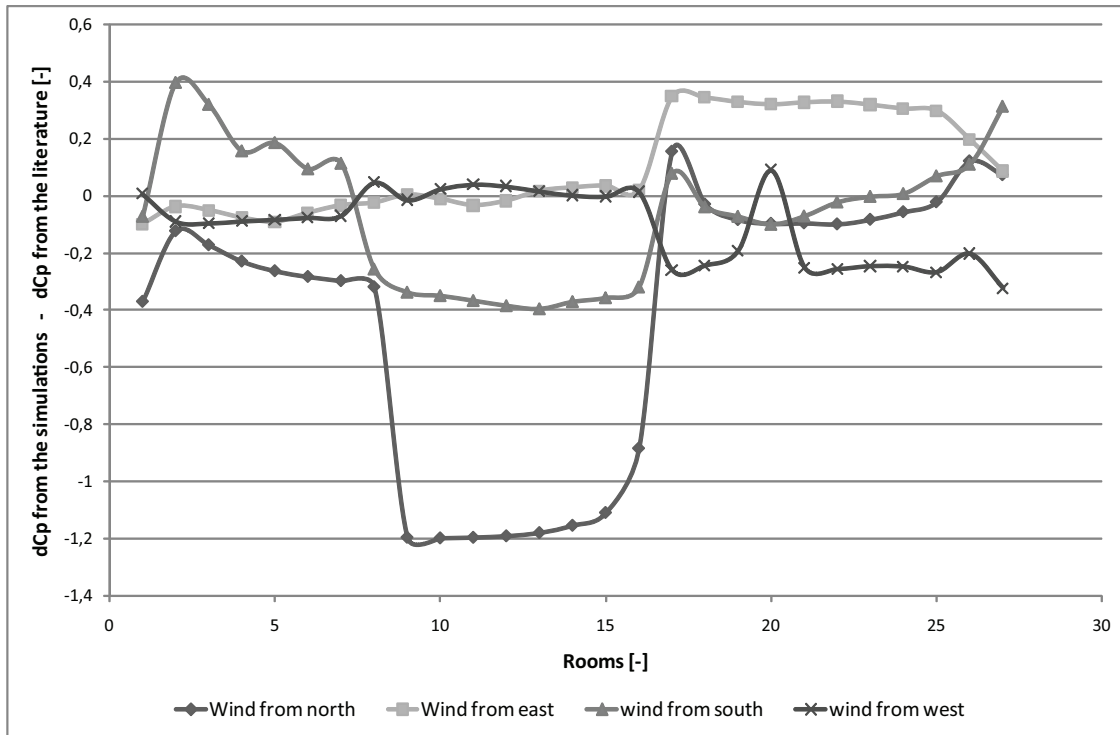
Figure 11.22: *The ΔC_p values from the literature compared to the ΔC_p values from the wind tunnel simulations.*

It is found that $\Delta C_{p,simulation}$ - $\Delta C_{p,literature}$ in general are negative. This means that the driving forces from the wind in the natural ventilated rooms in general are lower when the C_p values from the wind tunnel simulations are used instead of the C_p values from the literature. It is therefore expected that the air changes rate for the rooms will be lower.

To see the more precise effect of the changes in the C_p values there is made another simulation in Comis for the low pressurized isolation rooms. It is chosen only to make the simulation in the summer period since this was the period that was the most critical regarding both the direction of the airflows and the air changes rate for the rooms.

In the Comis simulation it is necessary to know the C_p values for eight wind directions. The last four wind directions are found by interpolation between the C_p values from the wind tunnel simulations.

In the multi zone simulation it is found that for the isolation rooms there are still a sufficient air changes rate of minimum 12 h^{-1}. But as expected the air changes rates are lower with the C_p values from the wind tunnel simulation than with the C_p values from the literature, as shown in the figures 11.25 and 11.26.
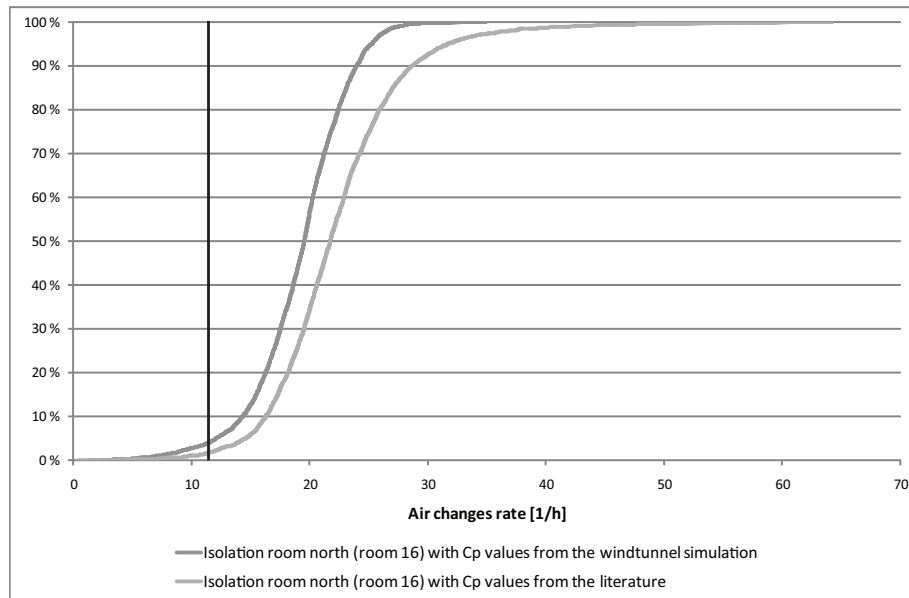
Figure 11.23: *Air changes rate of the isolation room with an opening toward the north in the summer period*
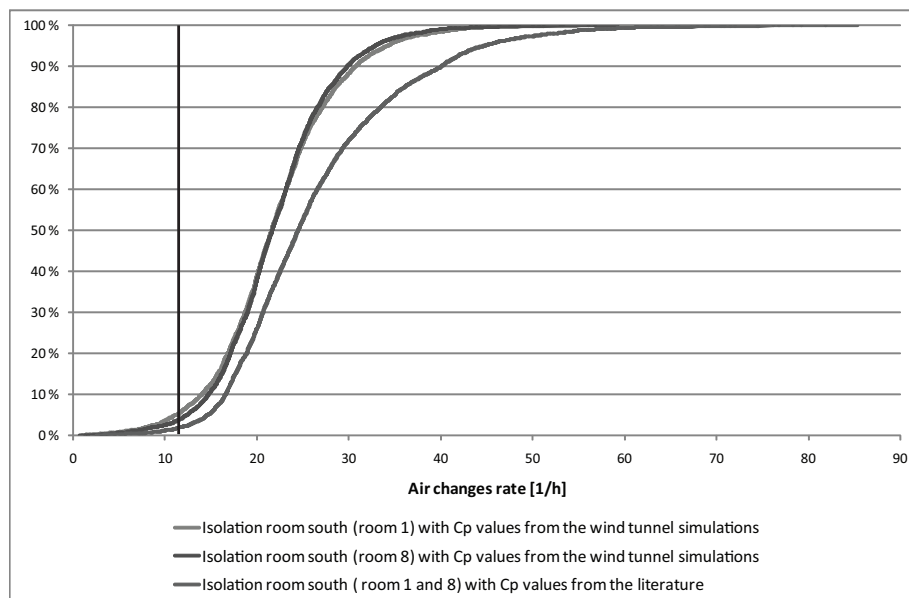
Figure 11.24: *Air changes rate of the isolation rooms with an opening toward the south in the summer period*

The C_p values from the wind tunnel simulations have however a bigger influence on the airflow directions between the isolation rooms and the anterooms. Especially for the isolation room with an opening toward the north.
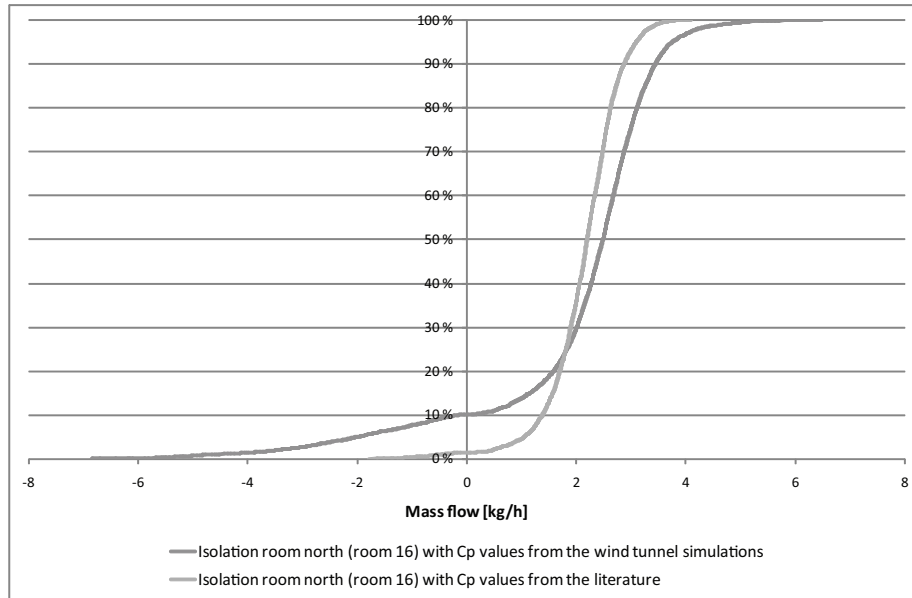
Figure 11.25: *The mass flow from the isolation room with an opening toward the north and anteroom in the summer period.*
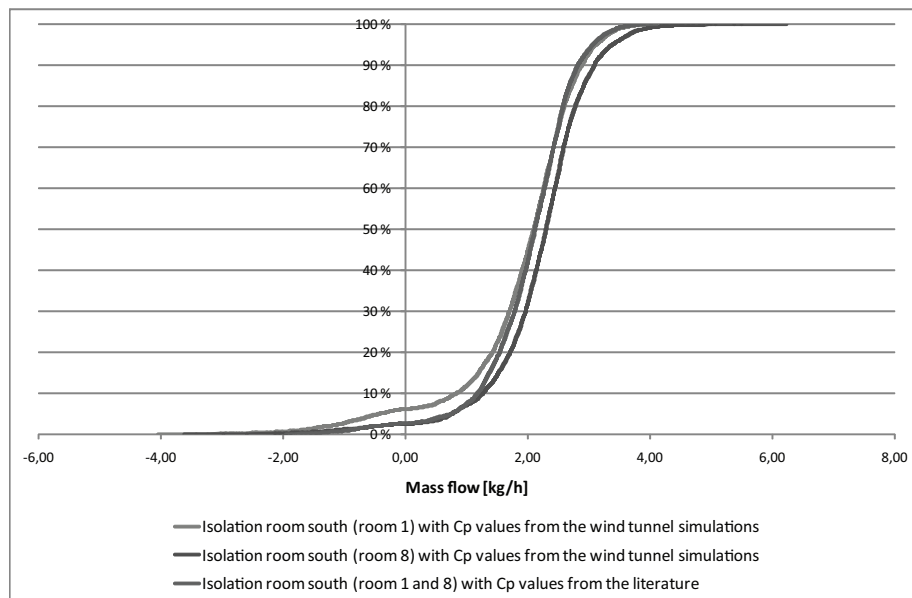
Figure 11.26: *The mass flow from the isolation room with an opening toward the south and anteroom in the summer period.*

When the calculated C_p values from the wind tunnel simulations are used this will as expected have an influence on the directions of the air flows in the hospital as well as the air changes rates for the rooms. It is now possible to have an air changes rate for the isolation room of minimum 12 h^{-1} at least 95 %. The flow direction is at least 90 % of the time in the right direction, from the anteroom to the isolation room.

Chapter 12

CFD simulation of Grantham hospital

In chapter 8 are listed different ventilation principle for natural ventilation and ideas for using natural ventilation for both Aabenraa and Grantham hospital are discussed. In chapter 9 are made a simple analytical calculation of the air change rate according to single sided ventilation and cross ventilation for two rooms of Grantham hospital. The calculation shows that especially by single sided ventilation the natural driving forces might not be strong enough to create the desired air change rate of minimum 12 h^{-1}. The calculations were done with average weather data for Hong Kong.

In chapter 7.1 are stated that there are some special weather conditions for Grantham hospital because of the location of the hospital. Specially for calm periods the mountain and sea breeze have influence on the airflow for the hospital.

In the following chapter the influence of the mountain and sea breeze for the airflow in an isolation room of the hospital is investigated. The calculation procedure and the assumptions are listed below. The calculations are done in the commercial CFD program Fluent.

12.1   2D model

To calculate the velocity profile according to mountain and sea breeze are made a 2D model. The model and the results are described in the following.

12.1.1   Identification and formulation of the problem

As stated in chapter 7.1 the simulations of Grantham hospital are done without wind in two cases:

- Daytime case with sea breeze

- Nighttime case with mountain breeze

For the cases only the thermal buoyancy is taken into consideration. To investigate the wind distribution only according to thermal buoyancy there are made a simple 2D model in Fluent to calculate the wind profile. For the simple model only the hill behind the hospital and the sea is taken into consideration. An outline of the model is showed in figure 12.1.
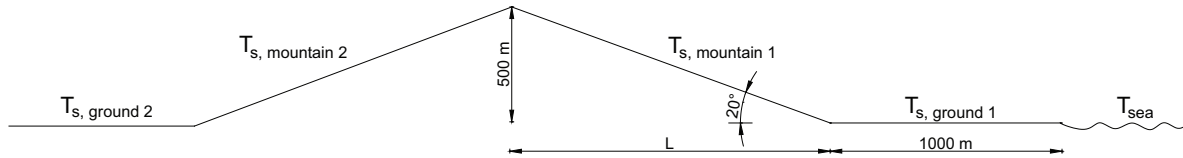
Figure 12.1: *Outline of the model for the simulations to calculate the wind profile according to thermal buoyancy.*

Because of the simplifications of the mountain and the fact that the surrounding obstacles are not taken into consideration the calculated profile will vary to the real profile. Because there are no obstacles for the simulation and the surfaces are smooth this means that circulation for the airflow might not be calculated for the simulation.

The model showed in figure 12.1 is used for the CFD modeling to calculate the wind distribution from mountain and sea breeze according to thermal buoyancy.

The calculated wind profile for the two cases are used to simulate the airflow and pressure distribution for the hospital in a 3D case. The 3D case with the building is simulated in a smaller scale, this means that the domain for the simulation is smaller for the 3D case compared to the 2D case so it is possible to calculate the airflow for the building.

12.1.2 Specification of geometry and grid

The model used to calculate the wind profile is shown in figure 12.2.
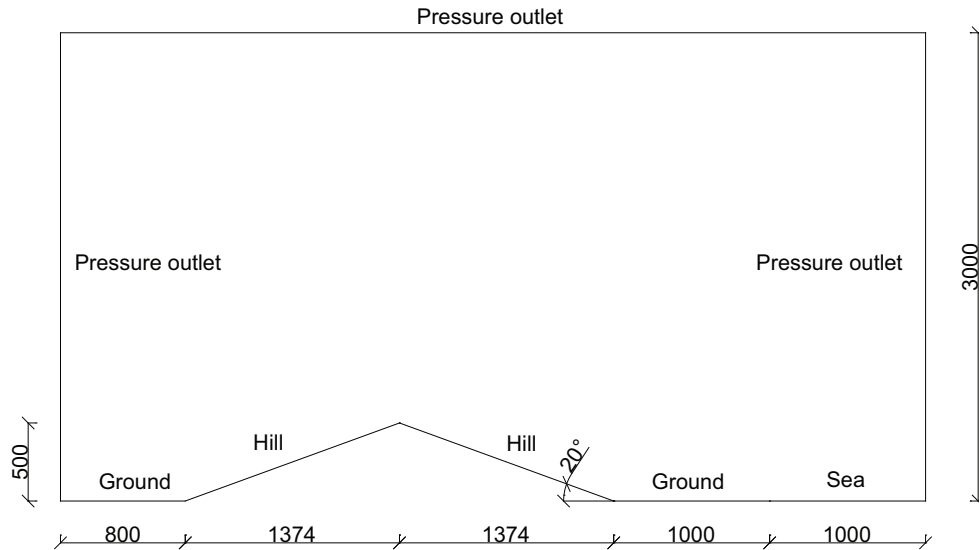
Figure 12.2: *Model from Fluent to calculate the wind profile. Measurements in* [m].

In figure 12.2 it is seen that the hill is modeled as a triangle with a hight of 500 m and a slope of 20 °. On the left side of the hill is the ground with a length of 800 m. On the right side is first the ground with a length of 1000 m and thereafter the sea with a length of 1000 m. The height of the model is 3000 m.

For the simulation the surface of the different faces are modeled as smooth. This is a simplification compared to the real surface. For the mountain there are placed trees on the surface with a hight of about $2 - 5$ m and the ground is not smooth either. For the calculations this means that the boundary layer for the simulation with a smooth surface compared to the real situation is thinner.

Grid layout

Because of the slope of the mountain showed in in figure 12.2 the best grid for the model is the BFC grid. With the BFC grid compared to the cartesian grid it is possible to get the grid to follow the slope because the two side opposite each other for the grid does not need to be the same size as listed in chapter A.3. In figure 12.3 are showed the principle of the grid layout for the slope of the mountain with both the cartesian grid and the BFC grid.
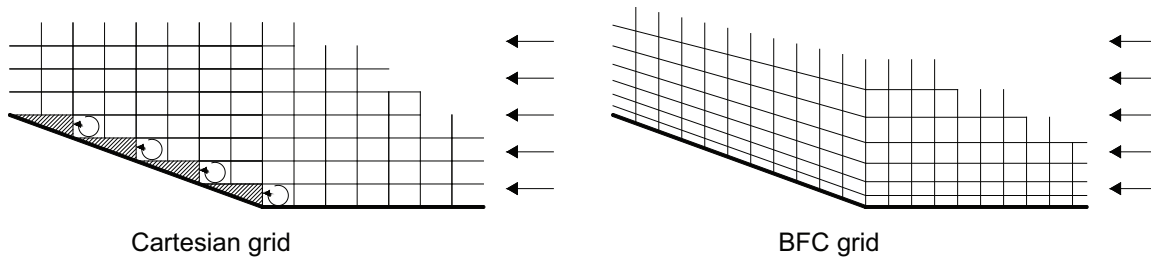
Figure 12.3: *Principle of the grid layout for the slope with the cartesian and the BFC grid.*

It is seen from figure 12.3 that with the cartesian grid it is not possible to follow the shape of the slope. As smaller the grid size is the better the fit will be. With the cartesian grid therefore some circulation is created in the corners that will not happen in the real world. With the BFC grid it is possible to follow the slope of the hill and therefore the turbulent regions that is created with the cartesian grid is not created with the BFC grid. Specially when the buoyancy effects are taken into consideration the use of the cartesian grid compared to the BFC grid for a slope might create significant errors. Both the cartesian grid and the BFC grid used the finite volume method for the calculations.

For the model the grid nodes are finest at the surface. The grid size increases with the height of the model. For the model are made different grid structures for the different surfaces. For the left side of the mountain the grid structure is more coarse than for the right side because the right side is where the hospital is located and therefore the most important side. For the 2D model are used a quadrilateral grid.

To examine the grid the y^+ value is calculated for the model. For the model are used the enhanced wall treatment to get the most exactly calculation of the airflow close to the boundary layer. For this model the most ideally value of the y^+ is in the order of $y^+ = 1$. However a higher value of the y^+ is acceptable as long as it is well inside the viscous sub-layer as showed in figure A.10 in appendix A.3. This means that the y^+ has to be lower than 4-5; $y^+ < 4 \sim 5$. [Fluent Inc., 2005]

12.1.3 Specification of physical models and boundary conditions

In Fluent are implemented the following turbulence models:

- Spalart-Allmaras model

- Standard $k - \varepsilon$ model

- Renormalization-group (RNG) $k - \varepsilon$ model

- Realizable $k - \varepsilon$ model

- Reynolds stress model (RSM)

- Large eddy simulation (LES) model

The Spalart-Allmaras model is a one equation model that only solves the modeled transport equation for the kinematic eddy viscosity. The Spalart-Allmaras model was designed specially for aerospace applications. Because the model is only a one equation model it is criticized for the instability to accommodate changes in length scale as might be necessary when the flow changes abruptly from a wall-bounded to a free stream. [Fluent Inc., 2005]

The Standard $k - \epsilon$ model is a two equation model as stated in appendix A.3. The model is a semi-empirical model. [Fluent Inc., 2005]

The basic of the Renormalization-group (RNG) $k - \varepsilon$ model is similar to the standard $k - \varepsilon$ model. The difference to the standard $k - \varepsilon$ model are:

- The model has an additional term in its ε equation that significantly improves the accuracy for rapidly strained flow

- The effect of swirl on turbulence is included in the RNG model, enhancing accuracy for swirling flows

- Provides an analytical formula for turbulent Prandtl numbers, while the standard $k - \varepsilon$ model uses user-specified, constant values

- The standard $k - \varepsilon$ model is a high-Reynolds-number model, the RNG theory provides an analytically-derived differential formula for effective viscosity that accounts for low-Reynolds-number effects

[Fluent Inc., 2005]

Because of the refinements for the RNG model compared to the standard $k - \varepsilon$ model the model is more accurate and reliable.

The Realizable $k - \varepsilon$ model is also based on the same model as the standard $k - \varepsilon$ model. The difference from the standard $k - \varepsilon$ model and the Realizable $k - \varepsilon$ model is:

- The realizable $k - \varepsilon$ model contains a new formulation for the turbulent viscosity

- A new transport equation for the dissipation rate, ε, has been derived from an exact equation for the transport of the mean-square vorticity fluctuation

[Fluent Inc., 2005]

The benefit of the realizable $k - \varepsilon$ model is that the model more accurate predicts the spreading rate.

For Fluent the most detailed model is the Reynolds stress model (RSM). For the Reynolds stress model the transport equation for the Reynolds stress and an equation for

the dissipation rate is solved as listed in appendix A.3. The model is better to give accurate predictions for complex flows because it can handle an-isotropic turbulence.   [Fluent Inc., 2005]

For the model the RNG $k - \varepsilon$ model is used for the simulation. This is used according to the advantages of the model compared to the Spalart-Allmaras and the standard $k - \varepsilon$ model and because it does not take as much CPU time as the more accurate models. Because the RNG $k - \varepsilon$ model is refined according to the ε equation, the effect of swirl on turbulence and an analytical formula for turbulent Prandtl number the model require more CPU time than the standard $k - \varepsilon$ model. For the Reynolds Stress model four equations are solved in the 2D case and seven equations in the 3D case therefore this model takes more CPU time than the RNG $k - \varepsilon$ model.   [Fluent Inc., 2005]

For the near wall treatment the enhanced wall treatment is used because it solves the boundary layer more accurate than the other wall models.

The first model is used to calculate the velocity profile created by the thermal buoyancy. This model is a 2D model as showed in figure 12.2. The simulation is a steady case where the influence of the time is not taken into consideration.

The operating pressure for the model is 101325 Pa and there is used a gravitational acceleration of $-9,82$ $\frac{m}{s^2}$.

Boundary conditions

For the model is used the boundary condition listed in table 12.1.

Table 12.1: *Boundary condition for the model.*

Surface	Boundary condition
Ground left side	Wall, stationary wall, No slip
Ground right side	Wall, stationary wall, No slip
Hill left side	Wall, stationary wall, No slip
Hill right side	Wall, stationary wall, No slip
Sea	Wall, stationary wall, No slip
Right side	Pressure outlet, intensity and length scale, turbulent intensity 10 %, turbulent length scale 210 m
Left side	Pressure outlet, intensity and length scale, turbulent intensity 10 %, turbulent length scale 210 m
Top	Pressure outlet, intensity and length scale, turbulent intensity 10 %, turbulent length scale 388 m
Air	Boussinesq model, density $1,225$ $\frac{kg}{m^3}$, thermal expansion coefficient $0,00343$ K^{-1}

For all the surfaces is used wall as the boundary condition. For the surfaces are used a

temperature boundary condition to set a fixed temperature for the surface. The surfaces is modeled as a non slip surface. The temperature for the different surfaces are listed in table 12.2. The used temperatures are the measured temperatures from the experiment at The Peak in Hong Kong listed in appendix B.

Table 12.2: *Temperature for the different boundary.*

Surface	Temperature [$°C$]	
	Daytime	**Nighttime**
Ground left side	28	18
Ground right side	28	18
Hill left side	33	15
Hill right side	33	15
Sea	20	20
Air	25	20

Because of the temperature difference of the surface and the air an airflow will be created. According to the higher surface temperatures than air temperature for the daytime situation a sea breeze will be created. The airflow from the sea breeze from the ground towards the hill is characterized as a free boundary layer current. The free boundary layer current is created because of the temperature difference of the air.

In the nighttime the surface temperatures are lower than the air temperature and therefore a mountain breeze will be created. Down the hill a convective boundary layer current will be created according to temperature differences and gravitational acceleration. At the bottom of the hill the airflow will transform into a gravity current and pass by the ground.

For the sides are used the pressure outlet boundary condition because this can be used to define a free boundary for an external flow. For the pressure outlet the following parameter are defined:

- Total pressure

- Static pressure

- Total temperature

- Turbulence method

The total pressure for an incompressible fluid is defined as:

$$p_0 = p_s + \frac{1}{2}\rho|v|^2 \tag{12.1}$$

where

p_0 : Total pressure $[Pa]$
p_s : Static pressure $[Pa]$

The static pressure is defined as:

$$p_s = -\rho_1 gh \tag{12.2}$$

where

ρ_1 : Density according to the temperature at the point $[\frac{kg}{m^3}]$
g : Gravity acceleration $[\frac{m}{s^2}]$
h : Height $[m]$

For the calculation the gauge pressure has to be defined. The gauge pressure is given by the pressure difference between the system and the surrounding atmosphere. The gauge pressure is defined as:

$$p_s' = \rho_0 gh + p_s \tag{12.3}$$

where

p_s' : Gauge pressure $[Pa]$

For the model is used the same temperature for the same height inside the model and outside the model. Therefore the gauge pressure is equal to zero because $\rho_0 = \rho_1$ and thereby:

$$p_s' = \overbrace{(\rho_0 - \rho_1)}^{=0} gh = 0$$

The total pressure is $101325\ Pa$ and the temperature is set for the same as for the air temperature.

For the pressure outlet the turbulence method is specified. For the flow the following models are included:

- $k - \varepsilon$

- Intensity and length scale

- Intensity and viscosity ratio

- Intensity and hydraulic diameter

[Fluent Inc., 2005]

For the $k - \varepsilon$ model the turbulent kinetic energy and the turbulent dissipation rate has to be defined.

For the intensity and length scale the turbulent intensity and the turbulent length scale has to be defined. The turbulent intensity is defined as the ratio of the root-mean square of the velocity fluctuations to the mean flow velocity. The turbulent length scale is related to the large eddies that contain the energy. The turbulent length can be calculated from:

$$l = 0,07L \tag{12.4}$$

where

l : Turbulent length scale $[m]$
L : Turbulent intensity $[\%]$

For the intensity and viscosity ratio the turbulent intensity and turbulent viscosity ratio has to be defined.

For the intensity and hydraulic diameter method the intensity and the hydraulic diameter has to be specified. The hydraulic diameter is defined by:

$$D_h = 4\frac{A}{C} \tag{12.5}$$

where

D_h : Hydraulic diameter $[m]$
A : Area $[m^2]$
C : Circumference $[m]$

For the model is used the intensity and length scale. This is done because the flow involve a turbulent boundary layer. [Fluent Inc., 2005]

For calculating the density of the air the Boussinesq model is used. In the model the temperature is set for a constant value for all the equations except the buoyancy term in the momentum equation. The Boussinesq model can be used when calculating natural convection inside a closed domain. The model can also be used for steady-state problems where the change in the temperature is small. [Fluent Inc., 2005]

When the Boussinesq model is used the temperature is specified at $20°C$ and the thermal expansion coefficient is set to $0,00343\ K^{-1}$.

Solution control

For the solution control is specified the discretization schemes for the pressure, momentum, pressure-velocity coupling, energy, turbulent kinetic energy, turbulent dissipation rate and energy. The selected schemes are listed in table 12.3.

Table 12.3: *Discretization schemes.*

	Discretization scheme
Pressure	Body force weighted
Pressure-velocity coupling	SIMPLE
Momentum	Second order upwind
Energy	Second order upwind
Turbulent kinetic energy	Second order upwind
Turbulent dissipation rate	Second order upwind
Energy	Second order upwind

The under-relaxation factors are listed in table 12.4.

Table 12.4: *Under-relaxation factors. [Fluent Inc., 2005]*

	Under-relaxation factor
Pressure	0,3
Density	1
Body forces	0,4
Momentum	0,5
Turbulent kinetic energy	0,4
Turbulent dissipation rate	0,4
Turbulent viscosity	1
Energy	0,6

The under-relaxation factors control the the change of the dependent factor for the discretization scheme. The values listed in table 12.4 are chosen on background of the default values from Fluent. Compared to the default values from Fluent the under-relaxation factor for the body force, momentum, turbulent kinetic energy, turbulent dissipation rate and energy have been decreased. This is done due to instability of the model according to the natural convection.

Grashof, Reynolds and Archimedes number

To evaluate the velocity distribution according to the ratio of the buoyancy forces to the viscous forces and the motion of the fluid due to density differences are the Grashof and Archimedes number calculated for the model.

The Grashof number evaluate the buoyancy forces to the viscous forces and is given by:

$$Gr = \frac{buoyant\ force}{viscous\ force} = \frac{|g \cdot \beta \cdot \Delta t \cdot l^3|}{\nu^2} \tag{12.6}$$

where

g :   Acceleration due to gravity $[\frac{m}{s^2}]$

β :   Volumetric thermal expansion coefficient $[K^{-1}]$

Δt :   Temperature difference between fluid and wall $[K]$

l :   Characteristic length $[m]$

ν :   Kinematic viscosity $[\frac{m^2}{s}]$

For the Grashof number is stated that when $Gr \gg 1$ the viscous forces is negligible compared to the buoyancy and inertia forces. When the buoyancy forces starts to be greater then the viscous forces the flow will transfer into the turbulent region. For a flat plate in a vertical orientation this will occur around $Gr = 10^9$. [Hoy and Ross, 2005]

To calculate the Grashof number for the model are used the height of the mountain as the characteristic length as this height is parallel to the gravity. The values used for the calculation are listed in table 12.5.

Table 12.5: *Values for calculating the Grashof number.*

	Value	
	Daytime	**Nighttime**
Acceleration, g	$9,82 \ \frac{m}{s^2}$	$9,82 \ \frac{m}{s^2}$
Volumetric thermal expansion coefficient for air, β	$3,37 \cdot 10^{-3} \ K^{-1}$ (25 °C)	$3,43 \cdot 10^{-3} \ K^{-1}$ (20 °C)
Temperature difference between fluid and wall, Δt	$25 \ °C - 33 \ °C$	$20 \ °C - 15 \ °C$
Characteristic length, l	$500 \ m$	$500 \ m$
Kinematic viscosity for air, ν	$15,58 \cdot 10^{-6} \ \frac{m^2}{s}$ (25 °C)	$15,11 \cdot 10^{-6} \ \frac{m^2}{s}$ (20 °C)

From the values listed in table 12.5 the Grashof number for the model in the two cases is calculated from equation (12.6) to:

- Daytime $Gr = 1,36 \cdot 10^{17}$

- Nighttime $Gr = 9,22 \cdot 10^{16}$

It is seen that in both cases this number is higher than 1 this means that for the flow the viscous forces are negligible. For both cases the Grashof number is higher than $Gr = 10^9$. For the model the slope of the plate is 20 ° which means that the turbulent flow might occur for a higher Grashof number than $Gr = 10^9$. The calculated Grashof number for the model is $Gr = 1,36 \cdot 10^{17}$ for the daytime case and $Gr = 9,22 \cdot 10^{16}$ for the nighttime case which is a lot higher than $Gr = 10^9$ this means that the flow might have transferred into the turbulent regime.

From the calculation of the Grashof number for the two cases it is also seen that the magnitude of the number is highest for the daytime case. For the daytime case the temperature difference between fluid and wall is higher than for the nighttime case. This means

that for the two cases the buoyant forces have the greatest influence for the daytime case. For both cases the buoyant forces have a higher impact on the flow than the viscous forces.

To evaluate the flow for the two cases the Reynolds number is calculated. The Reynolds number is used to state if the flow is turbulent or laminar and if forced convection or free convection is dominant for the flow. The Reynolds number is given by:

$$Re = \frac{Inertial\ forces}{Viscous\ forces} = \frac{v \cdot l}{\nu} \tag{12.7}$$

For a flow over a flat plate it is stated that the flow becomes turbulent with a Reynolds number in the order of $10^5 - 10^6$. Usually for a flat plate the characteristic length is set as the length of the plate therefore for the calculations are used the length of the model of $5550\ m$. [Wikipedia, 2008]

For the two situations; daytime and nighttime, the boundary between the laminar and turbulent flow is given for a velocity of:

- Daytime $v = 0,00028\ \frac{m}{s}\ -\ 0,0028\ \frac{m}{s}$

- Nighttime $v = 0,00027\ \frac{m}{s}\ -\ 0,0027\ \frac{m}{s}$

It is seen that for both situations the velocity have to be low to get the flow in the laminar region. The flow will therefore be in the turbulent region. To state if forced convection or free convection is dominating for the flow the following can be used:

- $Gr \ll Re^2$ Forced convection is dominating

- $Gr \gg Re^2$ Free convection is dominating

[Brorsen, 2005]

With a velocity for the two cases of about $0,1 - 2,5\ \frac{m}{s}$ the Reynolds number is:

- Daytime $Re = 3,5 \cdot 10^7 - 8,8 \cdot 10^8$, $Re^2 = 1,2 \cdot 10^{15} - 7,8 \cdot 10^{17}$

- Nighttime $Re = 3,6 \cdot 10^7 - 9,1 \cdot 10^8$, $Re^2 = 1,3 \cdot 10^{15} - 8,3 \cdot 10^{17}$

It is seen that in both situations the magnitude of Gr compared to Re^2 varies depending on the velocity of the flow. For a low velocity $Gr \gg Re^2$ and therefore in this situation the free convection is dominating. In this situation the flow in the boundary layer is forced by density difference according to temperature difference. For a high velocity $Gr \ll Re^2$ therefore in this case the forced convection is dominating. This flow is driven by the flow outside the boundary layer and density differences does not have any influence.

To evaluate the motion of the fluid due to density differences the Archimedes number is calculated. The Archimedes number is given by:

$$Ar = \frac{Gravitational\ force}{Viscous\ force} = \frac{g \cdot l^3 \cdot \rho_l \cdot (\rho - \rho_l)}{\mu^2} \tag{12.8}$$

where

ρ_l : Density of the fluid $[\frac{kg}{m^3}]$
ρ : Density of the body $[\frac{kg}{m^3}]$
μ : Dynamic viscosity $[\frac{kg}{s \cdot m}]$

For a small Archimedes number that might be due to a small number of $\rho - \rho_l$ or the characteristic length the influence of the buoyancy does not influence the flow much. For a great Archimedes number the buoyancy have a great influence on the flow. [Hansen et al., 1997]

To calculate the Archimedes number for the model are used the values listed in table 12.6.

Table 12.6: *Values for calculating the Archimedes number.*

	Value	
	Daytime	**Nighttime**
Acceleration, g	$9,82\ \frac{m}{s^2}$	$9,82\ \frac{m}{s^2}$
Characteristic length, l	$500\ m$	$500\ m$
Density of air, ρ_l	$1,186\ \frac{kg}{m^3}$ $(25\ °C)$	$1,205\ \frac{kg}{m^3}$ $(20\ °C)$
Density of earth, ρ	$5,25\ \frac{kg}{m^3}$	$5,25\ \frac{kg}{m^3}$
Dynamic viscosity, μ	$18,37 \cdot 10^{-6}\ \frac{kg}{s \cdot m}$ $(25\ °C)$	$18,27 \cdot 10^{-6}\ \frac{kg}{s \cdot m}$ $(20\ °C)$

From the values listed in table 12.6 the Archimedes number for the two cases is calculated from equation (12.8) to:

- Daytime $Ar = 1,75 \cdot 10^{19}$

- Nighttime $Ar = 7,33 \cdot 10^{20}$

It is seen that the calculated Archimedes number is high for both the cases, this means that for the flow the gravitational force has a great influence. For the two cases the Archimedes number is highest for the nighttime case, this means that for this case the gravitational force is higher than for the daytime case.

12.1.4   Solution

For the model is used the air temperature for the boundary at the right side as the initial guess. The used Fluent files is located in the subfolder 'Fluent files\2D' on the cd. The values for the initial guess is listed are table 12.7.

Table 12.7: *Values for the initial guess.*

	Daytime	Nighttime
Gauge pressure	$0\ Pa$	$0\ Pa$
X velocity	$0\ \frac{m}{s}$	$0\ \frac{m}{s}$
Y velocity	$0\ \frac{m}{s}$	$0\ \frac{m}{s}$
Turbulent kinetic energy	$0\ \frac{m^2}{s^2}$	$0\ \frac{m^2}{s^2}$
Turbulent dissipation rate	$0\ \frac{m^2}{s^3}$	$0\ \frac{m^2}{s^3}$
Temperature	$298\ K$	$293\ K$

To state when the case had converged were showed the residuals for every iteration and the mass flow rate for the boundary at the left and the right side. The residuals for the daytime case is showed in figure 12.4.
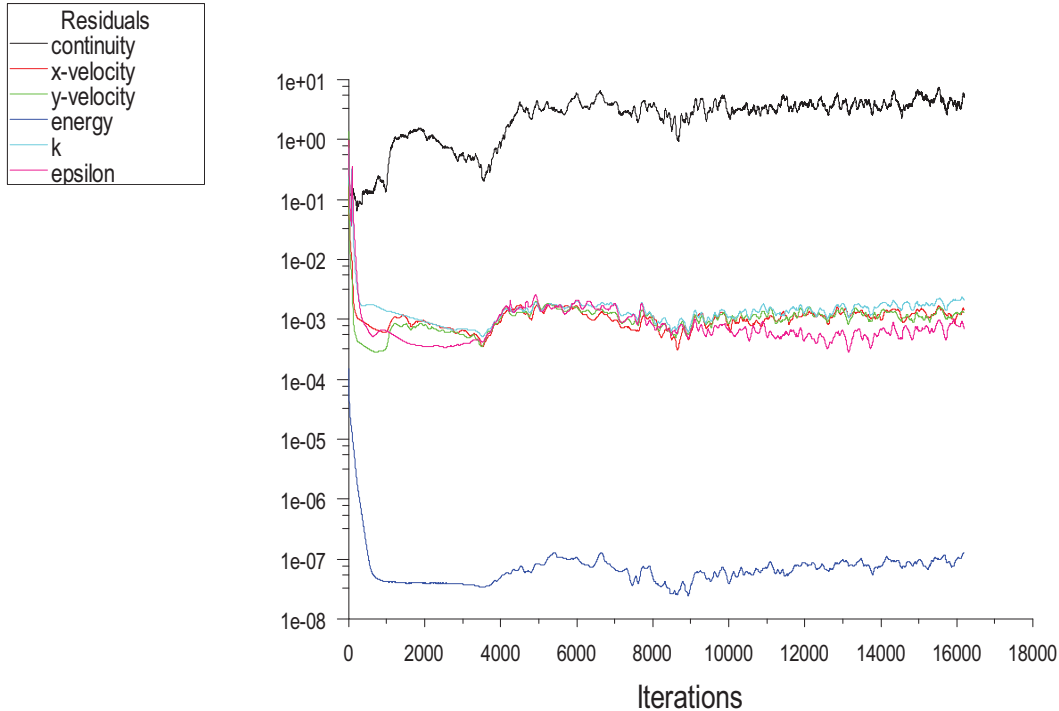
Figure 12.4: *Graph of the residuals for the daytime case.*

From figure 12.4 it is seen that the residuals for the X velocity, Y velocity, energy, k and epsilon all decreases with a factor 3 or more. The continuity residual stays between $1 - 1^1$. It is also seen that the residuals varies with the iterations and does not stay stable. This can either mean that the model has not converged yet or it is not stable. To check the convergence of the model are made two monitoring points for the average mass flow rate for the right side of the model and for the left side of the model. The monitoring points are showed in figure 12.5.
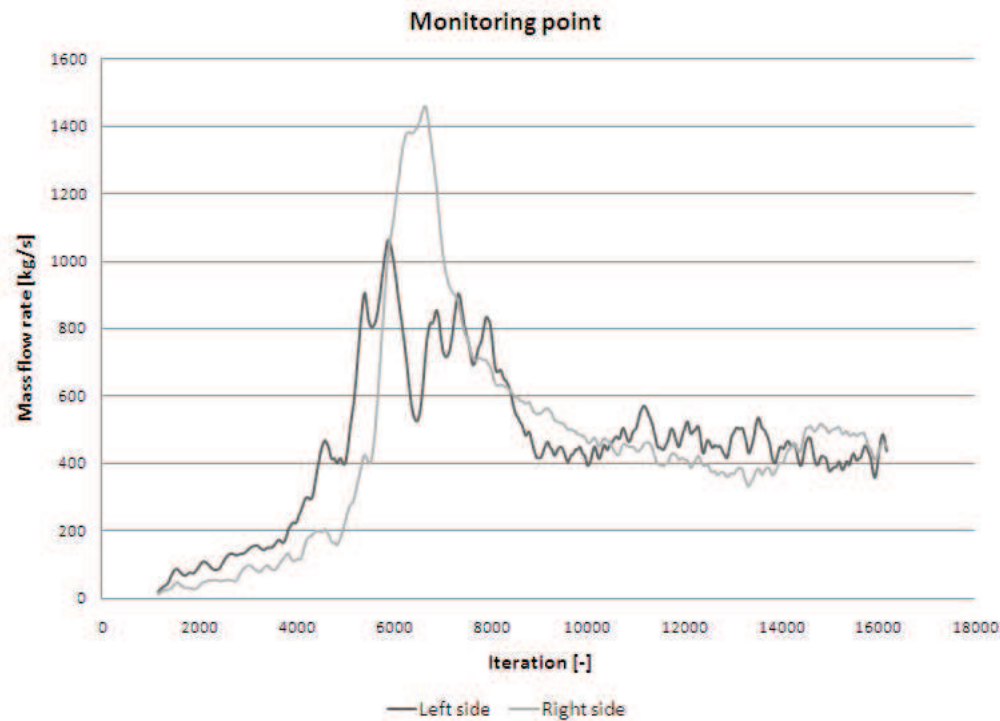
Figure 12.5: *Monitoring point for the average mass flow rate for the left and right side of the model for the daytime case.*

In figure 12.5 it is seen that the monitoring points for both the left and the right side varies. After about 9000 iterations the variation of the points reduces to about 100 $\frac{kg}{s}$ and stays at this level. To ensure that the solution is converged the points have to stay at the same level. Therefore by the monitoring points shown in figure 12.5 it is not possible to ensure that the solution is converged.

The convergence of the solution is also checked by the mass flow rate for the different sides for the model. The mass flow rate for the model is listed in table 12.8.

Table 12.8: *Mass flow rates for the different sides for the model.*

Side	Mass flow rate $\left[\frac{kg}{s}\right]$
Left side	438,5
Right side	449,4
Top	-888,4
Net	-0,6

From table 12.8 it is seen that the net mass flow rate is not 0 but $-0,6 \frac{kg}{s}$. Compared to the magnitude of the mass flow rate for the other sides it is stated that a difference in the mass flow rate of less than 1 the solution has converged.

Even though the mass flow rate listed in table 12.8 shows that the solution has converged the residuals in figure 12.4 and the monitoring points in figure 12.5 shows that the solution has not converged. Since both the residuals and the monitoring points stays at the same point for many iterations and only with a small variation the model might not be stable. In figure 12.6 is showed the magnitude of the velocity, the static pressure and the turbulent kinetic energy.
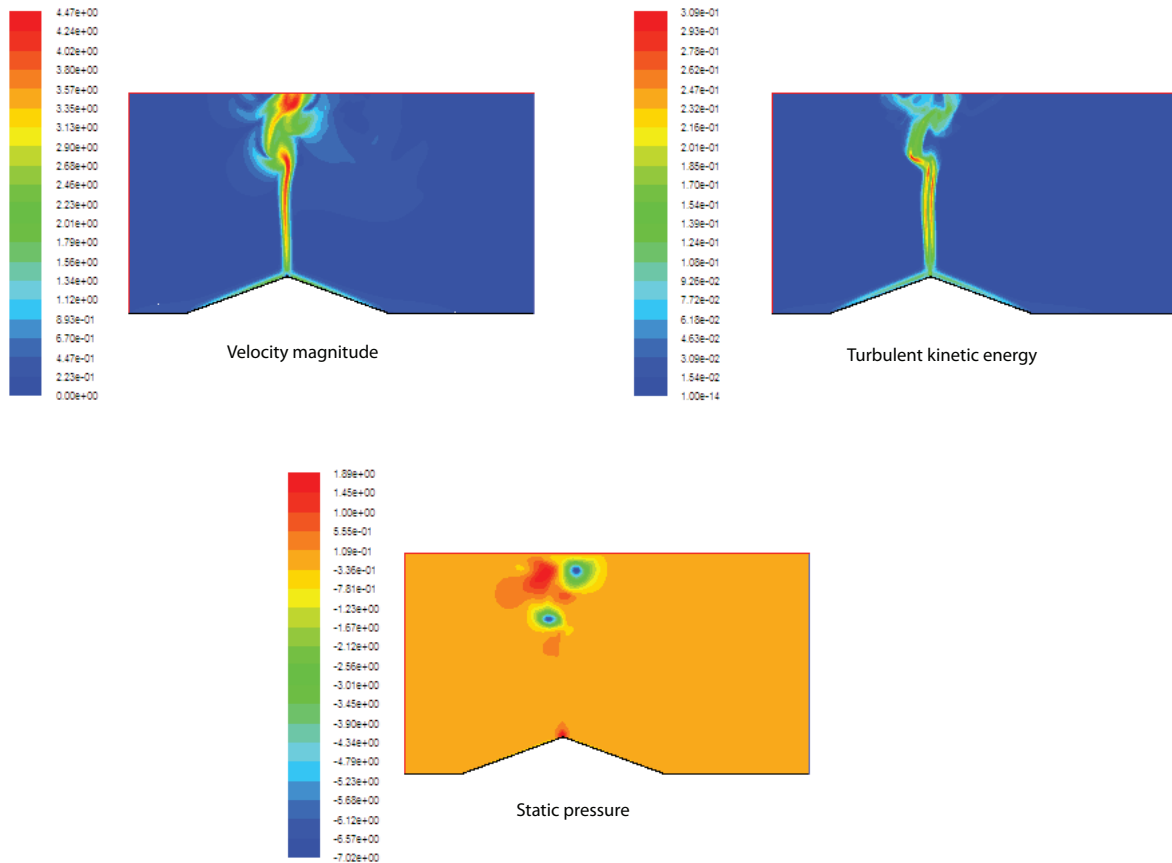
Figure 12.6: *Contour plot of the velocity magnitude, the turbulent kinetic energy and the static pressure for the daytime model.*

It is seen in figure 12.6 that for both the velocity magnitude, the turbulent kinetic energy and the static pressure these are stable close to the bottom and stays stable until about half the height of the model. In the upper half of the model it is seen that for all three situations the model is unstable because the variation. If the model had been stable the velocity magnitude and the turbulent kinetic energy had to stay in a line. Because the difference in densities according to temperature difference the static pressure have to be lower where the plume are.

To get the model stable it is tried to both increase and decrease the height of the model. In both situations the model does not get stable. For both situations the model stays unstable in the top of the model. For the model it is also tried to both increase and decrease the grid size but this does not help either. It is therefore concluded that the

model is unsteady. To get the model to converge it is therefore necessary to do an unsteady simulation of the model.

The purpose of the model is to calculate the velocity profile according to the sea breeze and use the calculated velocity profile for a 3D model in a smaller scale. Since the model is unstable in the upper half of the domain and stable in the lower half the model is used for calculating the velocity profile, because this is calculated in the lower stable part of the domain.

The residuals for the nighttime case are showed in figure 12.7.
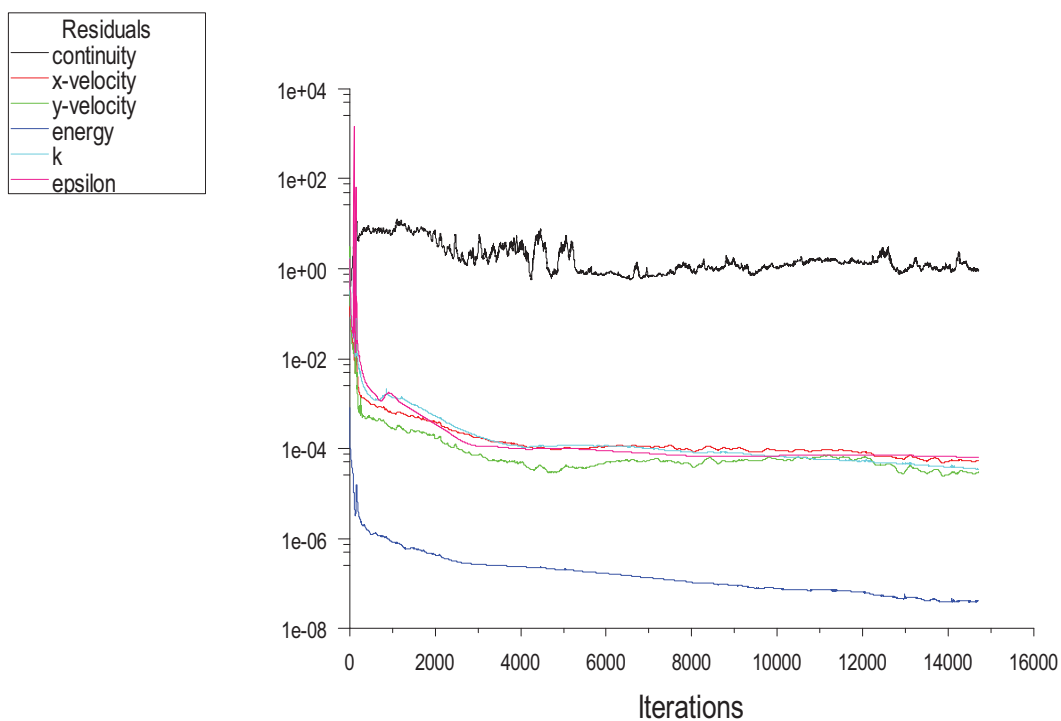
Figure 12.7: *Graph of the residuals for the nighttime case.*

From figure 12.7 it is showed that the residuals for X velocity, Y velocity, energy, k and epsilon all decreases with a factor 3 or more. The continuity residual stays at a value of 1.

To check the grid dependence there are made different models with the same boundary conditions but with different grid. When the results does not change for three simulations in a row where the grid sizes are changed it is said that the model is grid independent. For the actual model the grid independence is checked by calculating the velocity profile for three different locations:

1. 100 meter from the top of the hill

2. On the middle of the hill

3. 100 meter from the bottom of the hill

The locations are also showed in figure 12.8.
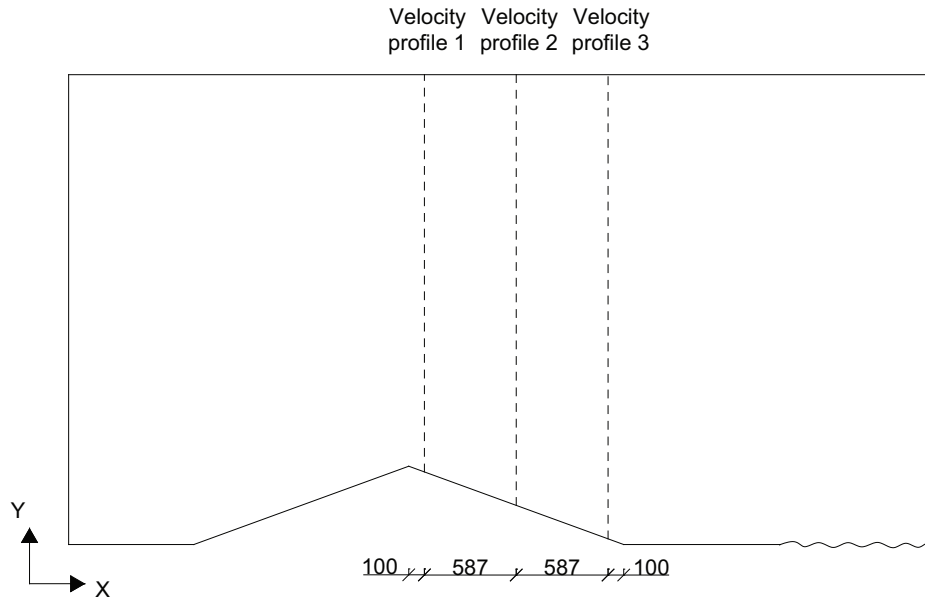
Figure 12.8: *Location of the velocity profiles for checking the model. Measurements in meters*

For the grid check are used the nighttime case, for the daytime case are used the same model setup and grid size as for the nighttime case. To check the model are made 6 models with different grid size. To evaluate the model the grid size and simulation time is also taken into consideration. For all the models the y^+ value is checked to be under 4-5. In figure 12.9 are showed the velocity profile 100 meter from the top of the hill for the 6 models.
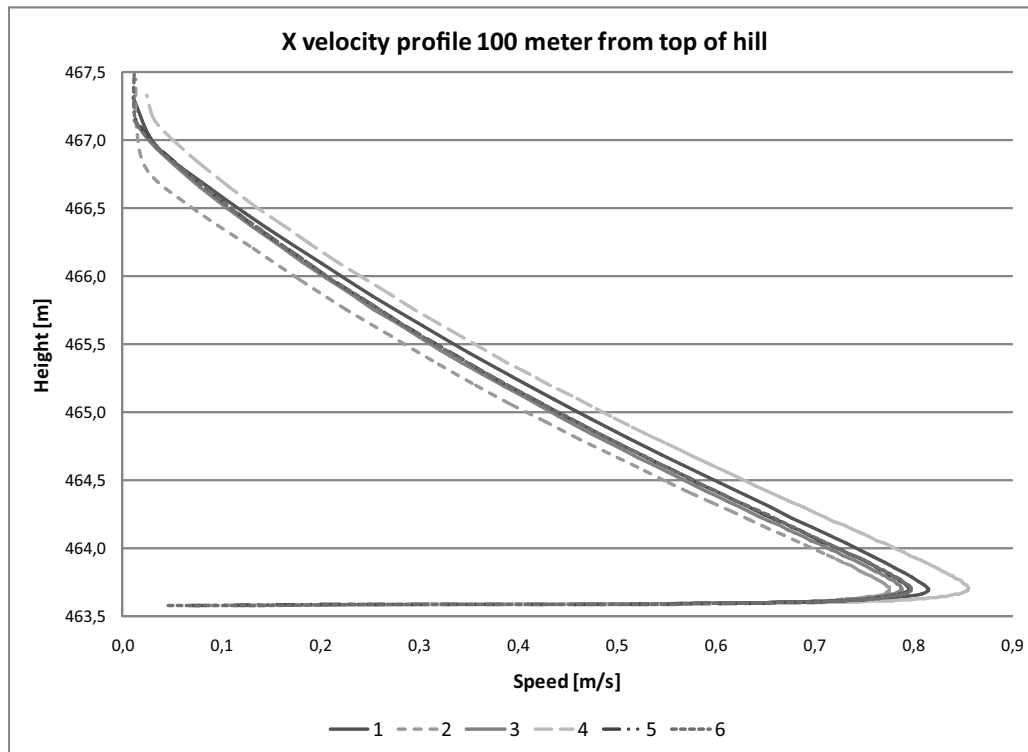
Figure 12.9: *X velocity profile for the first location.*

From figure 12.9 it is seen that the velocity profiles for all 6 models almost are the same and does not vary much from each other. In figure 12.10 is the velocity profiles for the 6 models for the second location on the middle of the hill showed.
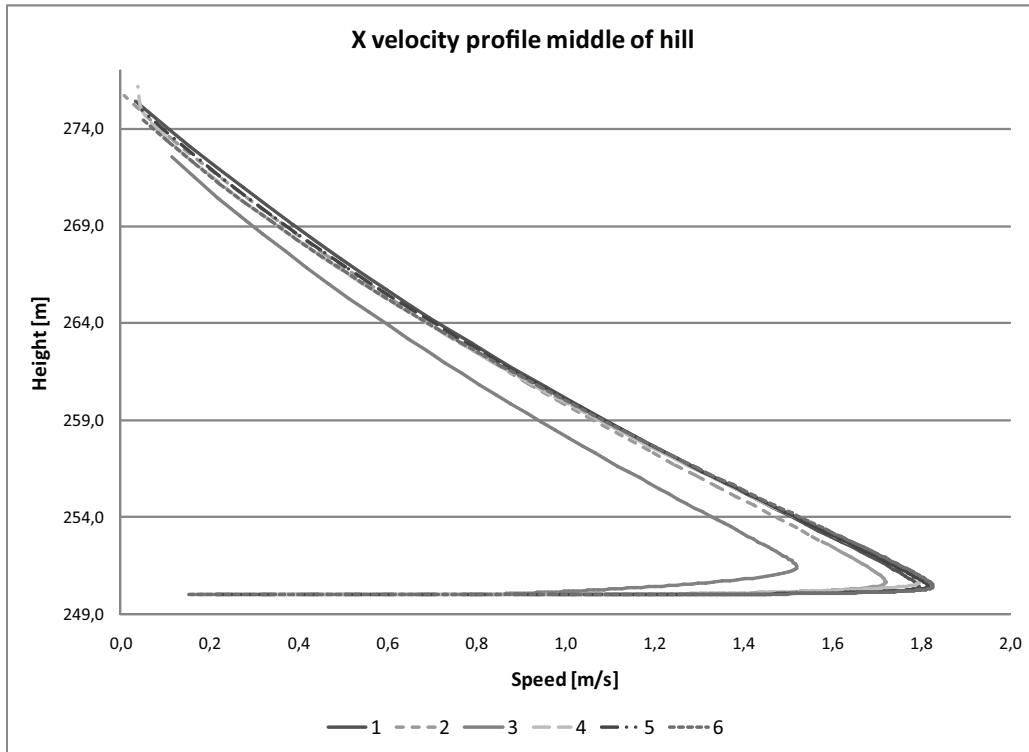
Figure 12.10: *X velocity profile for the second location.*

In figure 12.10 it is seen that velocity profiles vary more than from the first location. Specially velocity profile 3 vary from the other velocity profiles. For all the profiles it is seen that the variation is bigger than for the first location. In figure 12.11 is shown the velocity profiles for the last location 100 meter from the bottom of the hill.
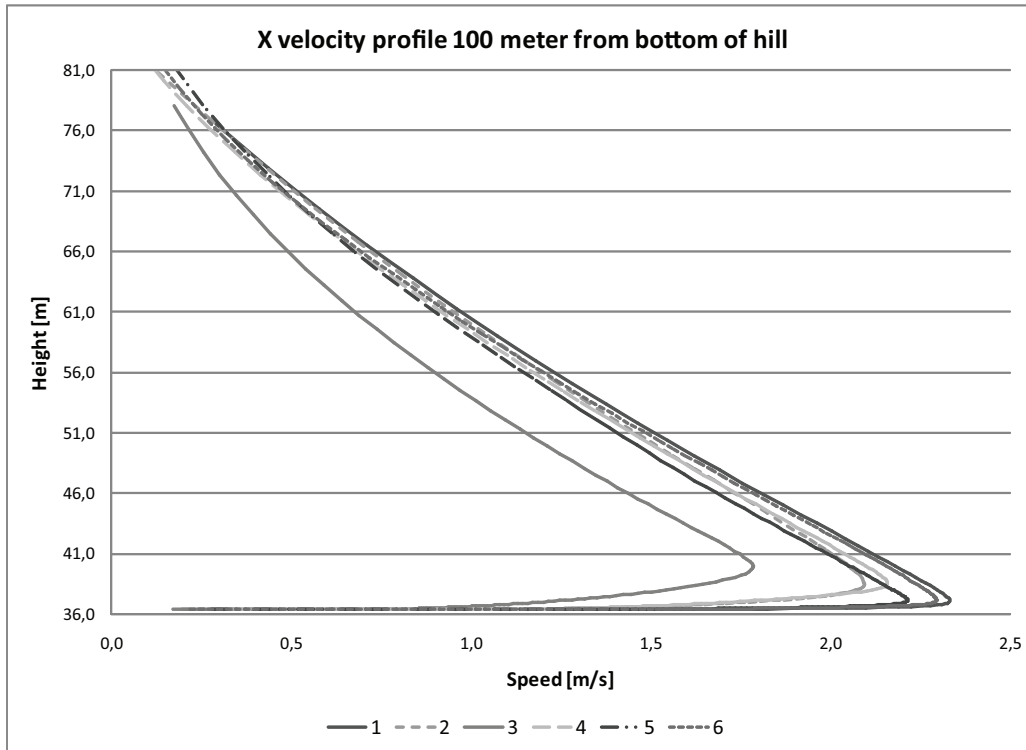
Figure 12.11: *X velocity profile for the third location.*

For the last location of the velocity profiles showed in figure 12.11 it is seen that there is a variation too. For this location also velocity profile 3 vary most from the other profiles.

In figure 12.12 are the simulation time for 100 iterations showed for the different models.
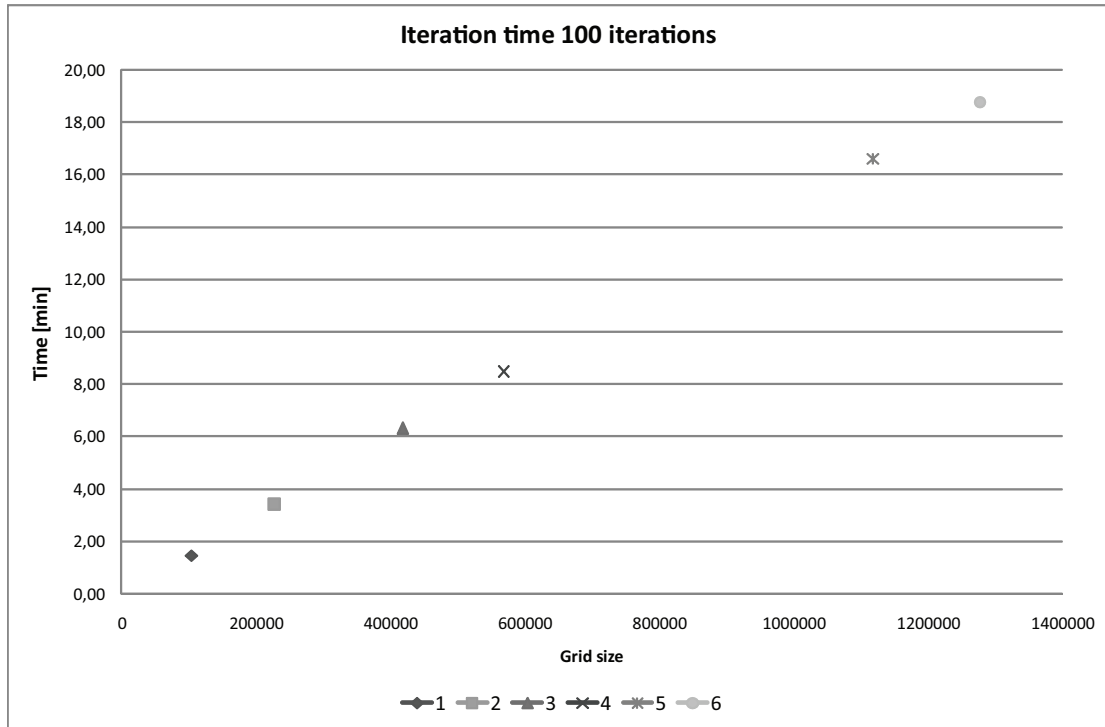
Figure 12.12: *Simulation time for 100 iterations for the different models.*

From figure 12.12 it is seen that the simulation time is linear dependent on the grid size. The time is only calculated for 100 iterations for a higher number of iterations the the time may not be linear dependent on the grid size. The time for more iterations are not measured because this is time consuming. Therefore the graph is only used to get an estimate on the iteration time between the different models. The iteration time is also different on other computers according to the CPU of the computer.

From the figures 12.9, 12.10 and 12.11 it is seen that the velocity profiles vary when the grid size change. From the figures it is also seen that the velocity profiles for all the models have the same shape. For all the figures it is seen that the velocity profile for model 3 differ most from the other profiles. In table 12.9 are stated the maximum values for the velocity profiles.

Table 12.9: *Maximum velocity.*

	Model					
	1	**2**	**3**	**4**	**5**	**6**
Velocity profile 1 $\left[\frac{m}{s}\right]$	0,82	0,78	0,79	0,86	0,80	0,80
Velocity profile 2 $\left[\frac{m}{s}\right]$	1,79	1,72	1,52	1,80	1,82	1,83
Velocity profile 3 $\left[\frac{m}{s}\right]$	2,33	2,10	1,79	2,16	2,22	2,30

From table 12.9 it is seen that the highest value of the velocity is for model 1. It is also

seen that for the first two velocity profiles model 5 and 6 are close to each other but does vary more for velocity profile 3. To ensure that the model i grid independent the velocity has to be the same for three different models. It is seen that for the last two models the velocity profile gets closer to each other but does still vary. To ensure that the model is grid independent the number of grid cells have to be even bigger. According to the time for simulation and the computer available it is chosen to use model 5 to calculate the velocity profile. It is argued that the variation is small for the greater model and according to the simulation time model 5 is chosen.

The velocity profile for the x-direction, y-direction and the velocity magnitude for model 5 in both the daytime and nighttime case is showed in figure 12.13 and 12.14. The velocity is calculated in a distance of $135\ m$ from the bottom of the hill on the right side.
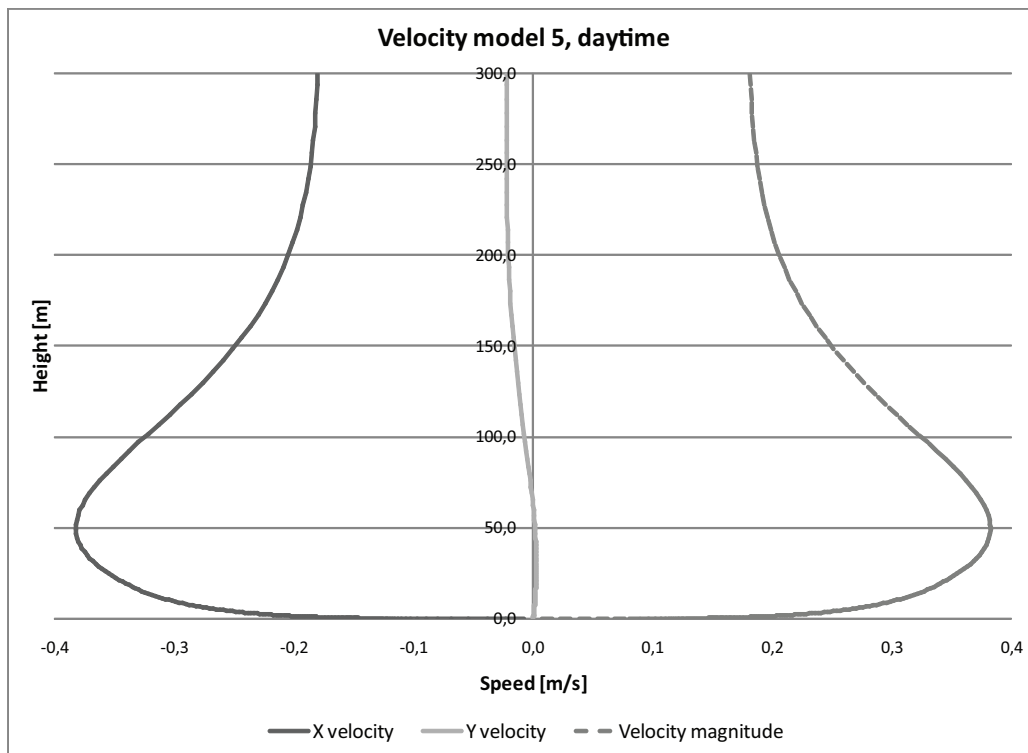
Figure 12.13: *Velocity profiles for model 5 for daytime.*

For the daytime case it is seen in figure 12.13 that the velocity for the x-direction is negative and with a maximum numerical value of about $0,4\ \frac{m}{s}$. The velocity for the y-direction is about 0 for the bottom $100\ m$ and rises to a value of $-0,02\ \frac{m}{s}$ with the height. The magnitude of the velocity does almost follow the velocity for the x-direction but with opposite sign. In the daytime case the most important component for the velocity is therefore the velocity in the x-direction.
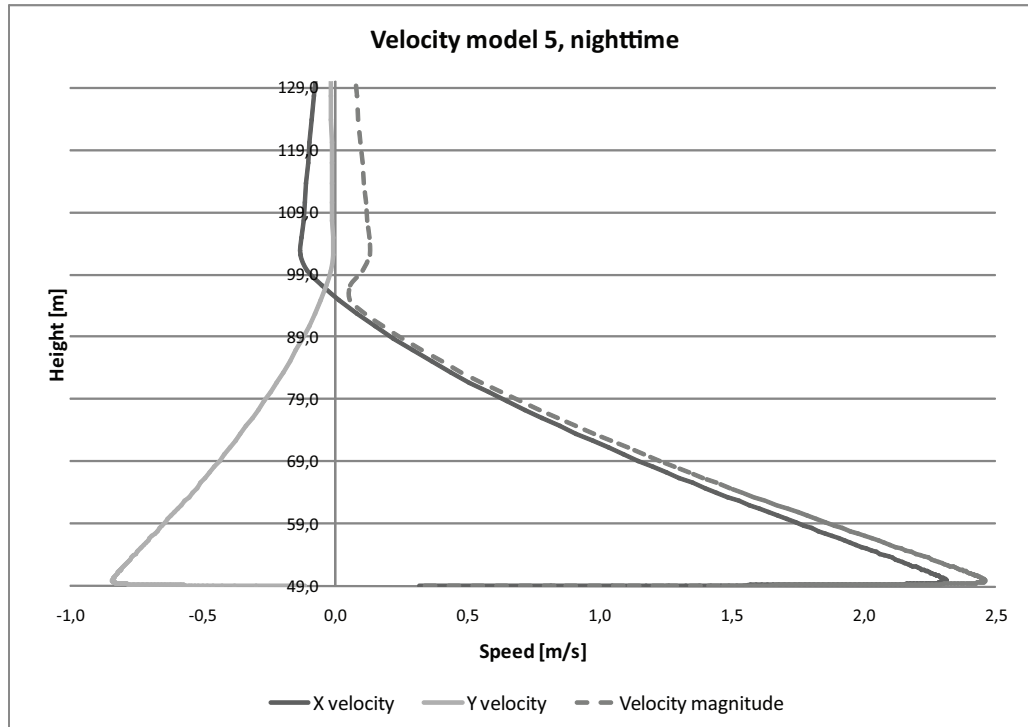
Figure 12.14: *Velocity profiles for model 5 for nighttime.*

From figure 12.14 it is seen that the velocity profile for the x-direction is positive and with a maximum speed of $2,3 \frac{m}{s}$. For the y-direction the speed is negative and with a minimum value of $-0,8 \frac{m}{s}$. The velocity magnitude follow the profile for the x-direction but with a higher value of the maximum speed of $2,5 \frac{m}{s}$. The higher value for the profile for the velocity magnitude compared to the x-direction is because of the addition of the speed for the y-direction.

Because of the higher magnitude of the velocity for the nighttime case compared to the daytime case it is seen that for the nighttime case the forced convection is dominating and for the daytime case the free convection is dominating.

12.1.5 Validation

To check the results these are evaluated according to literature about gravity current. For the evaluation are used the document "Stratified flow in rooms with a cold vertical wall". [Heiselberg, 1994]

For a surface with a lower temperature than the surroundings the layer of air adjacent to the wall is cooled by conduction to the wall. Because of the cooler wall buoyancy forces are generated and force the airflow downward. The layer close to the wall where the vertical motion is created is called the natural convection boundary layer. [Heiselberg, 1994]

For the boundary layer it is characteristic that it starts with zero thickness at the top of the wall and increase the thickness in the downward direction.

The development of the x-velocity profile for model 5 is showed in figure 12.15.
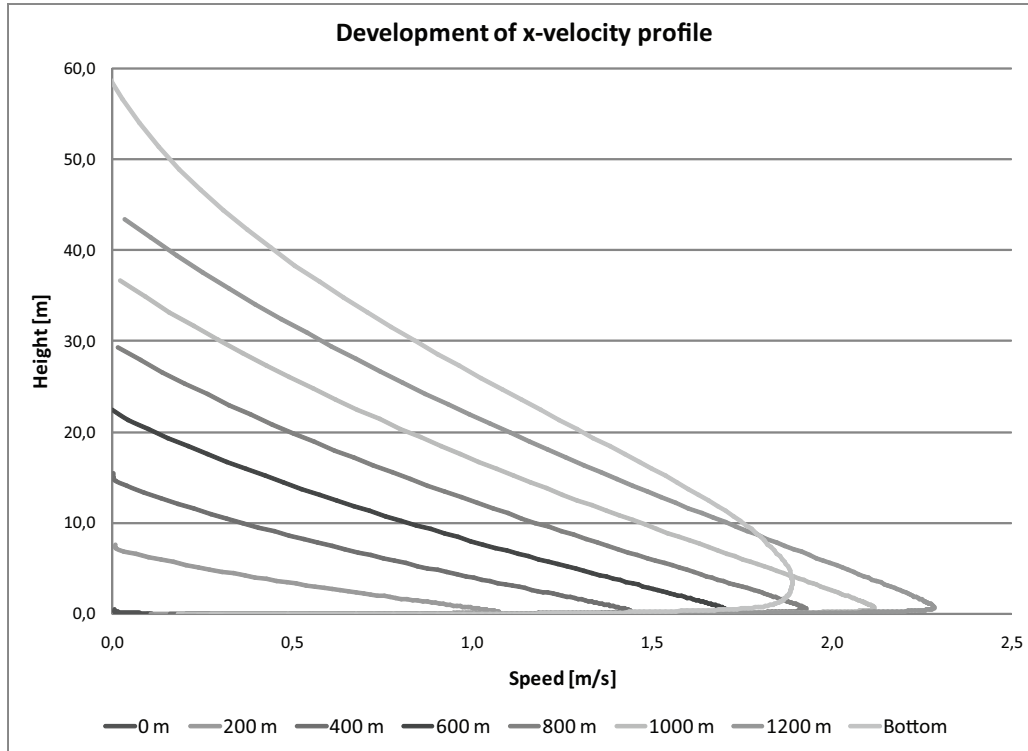
Figure 12.15: *Development of the x-velocity profile for model 5.*

From figure 12.15 it is seen that the thickness of the velocity profile is smallest at the top of the mountain and increases for the other profiles and gets the highest thickness at the bottom of the hill. Even though the hill is not vertical the development of the velocity profile is having the same characteristic as for the development of the velocity profile for a vertical surface as stated above.

The maximum velocity at the bottom of the cold surface can be calculated from:

$$U_{max} = k\sqrt{h\Delta t} \tag{12.9}$$

where

U_{max} : Maximum velocity $\left[\frac{m}{s}\right]$
k : Constant between 0,052-0,10
Δt : Temperature difference between surface and air $[°C]$

The height of the hill in the model is 500 meter and the temperature between the surface and the air is 5 $°C$. The maximum velocity according to equation (12.9) is therefore:

$$U_{max} = 0,055 \cdot \sqrt{500m \cdot 5°C} = 2,75\frac{m}{s}$$

From the model the maximum velocity at the bottom of the hill is calculated to $1,89 \ \frac{m}{s}$. This velocity is lower than the velocity calculated from equation (12.9). The maximum velocity calculated from equation (12.9) assume that the cold surface is vertical. For the model the slope of the hill is only 20 ° this could be the reason why the calculated velocity is different from the velocity found in the model.

From literature it is stated that the wind speed for a land breeze is normally $< 5 \ \frac{m}{s}$ and with a depth of $< 100 \ m$ [Panel on Coastal Meteorology et al., 1992] . From the calculation of the speed for the mountain breeze it is seen that this speed is lower then $5 \ \frac{m}{s}$ and thereby in the normal interval for a land breeze.

At a distance of $0,2 - 0,8 \ m$ from the bottom of the vertical surface the airflow can be calculated as an isothermal wall jet flow given by:

$$\frac{U(y)}{U_{max}} = A \left(\frac{y}{\delta}\right)^{\frac{1}{7}} \left[1 - erf \left(B \left(\frac{y}{\delta}\right)\right)\right] \tag{12.10}$$

[Heiselberg, 1994]
where

$U(y)$	:	Velocity at point y $[\frac{m}{s}]$
A	:	Constant equal to 1,48 $[-]$
B	:	Constant equal to 0,68 $[-]$
y	:	Distance from surface $[m]$
δ	:	Characteristic length, distance from the all where the velocity has decreased to half its maximum value $[m]$
erf	:	Error function

In figure 12.16 are showed the velocity profile from the model at a distance of $0,5 \ m$ from the hill compared to the velocity profile calculated from equation (12.10).
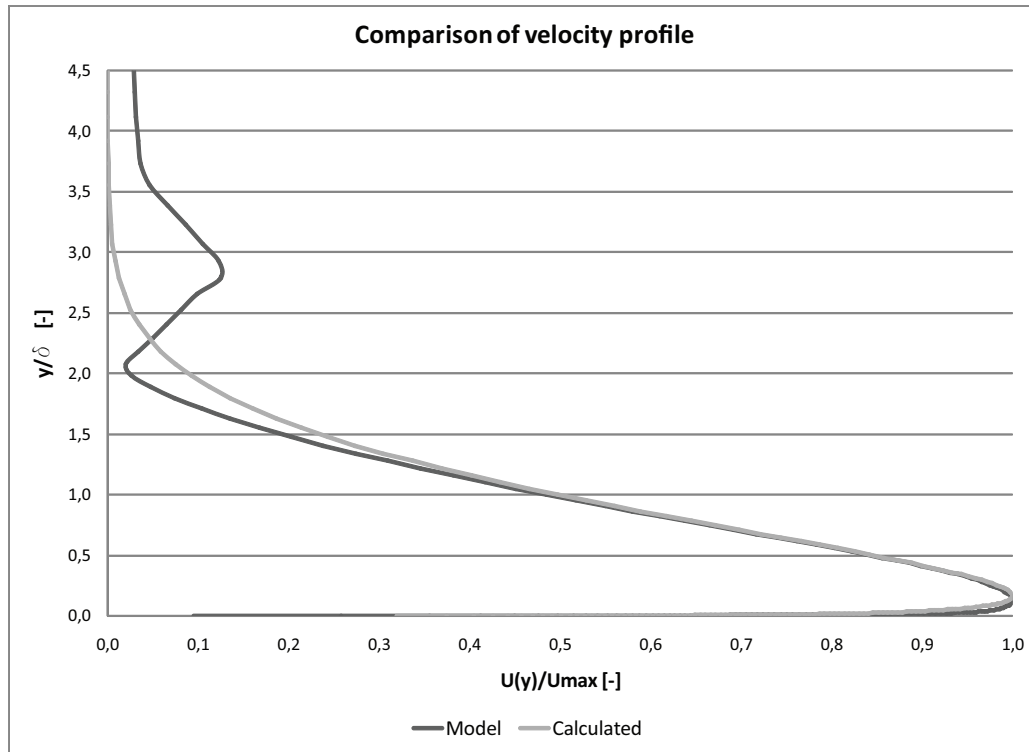
Figure 12.16: *Comparison of velocity profile calculated from the CFD model and by equation (12.10).*

From figure 12.16 it is seen that the velocity profile from the CFD model does fit good with the velocity profile calculated from equation (12.10).

12.2 Benchmark model

To verify the results from the CFD simulations are made a benchmark model. The results from the benchmark model are compared to measured values. For the benchmark model it is checked that the results from the CFD simulations fits with the measured values. The setup for the benchmark model is as close to the same as the setup for the measured values.

12.2.1 Identification and formulation of the problem

As stated above the model is used to check the results. The checked values are the pressure coefficient for a cube. The pressure coefficient are compared to measured values of the pressure coefficient to validate the results. To get the most accurate results the grid size for the model is changed to get close to the measured results. When the pressure coefficients from the model is close to the measured values the grid distance for the first grid point is noted and this distance is used for the final model.

The setup for the benchmark model is the same as used for Aabenraa hospital in chapter 11.1. The benchmark model are also used to validate the turbulence models used. It is

therefore also checked that the results from the model fits with the measured values with the used turbulence model.

For the final model are used the same turbulence model and scale of the domain as for the benchmark model.

12.2.2   Specification of geometry and grid

The 3D benchmark model is showed in figure 12.17.
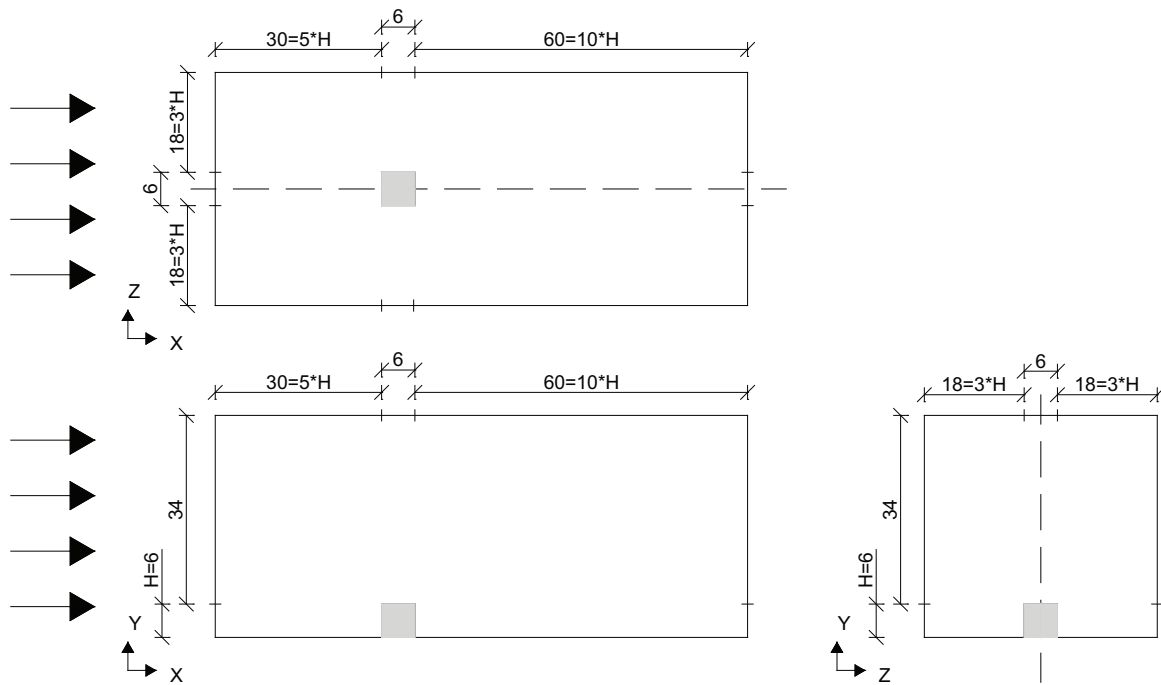
Figure 12.17: *Outline of the benchmark model. Measurements in* [*m*].

As showed in figure 12.17 the model consists of a domain and a cube. The size of the cube is 6 *m*. The length of the domain in front of the cube is 5 times the height of the cube and behind the cube the length is 10 times the height of the cube. The total length of the domain is 96 *m*. The width of the domain is 42 *m* with a length on either site of the cube of 18 *m* which correspond to 3 times the height of the cube. The total height of the domain is 40 *m*.

From figure 12.17 it is seen that the model is symmetric about the dotted line. For the simulations are therefore made a model that only consists of one half of the model showed in figure 12.17.

For the model is used the BFC grid because it is possible to locate a fine grid close to the cube with this grid as listed in appendix A.3. For the model the grid is finest closest to the cube and get coarser further away.

For the calculations the thermal buoyancy is not taken into consideration, therefore the y^+ value have to be in the range of $y^+ > 30 \sim 60$ when the wall function is used. To get the best results it is most desirable that the y^+ value is close to the lower bound, that means a y^+ value of about $y^+ \approx 30$.   [Fluent Inc., 2005]

12.2.3   Specification of physical models and boundary conditions

For the model the RNG $k - \epsilon$ turbulence model is used. This is the same turbulence model as used for the 2D model and the same as will later be used for the final model. For the model the enhanced wall treatment function is used. This is done to get a more accurate result around the cube where the grid is fine. The enhanced wall treatment function improves the accuracy of meshes that can only be resolved to the buffer region.

The model is steady state therefore the time is not taken into consideration.

The operating pressure is set to 101325 Pa and the gravitational acceleration is $9,82 \frac{m}{s^2}$.

Boundary condition

The boundary condition for the benchmark model is listed in table 12.10.

Table 12.10: *Boundary condition for the benchmark model.*

Surface	Boundary condition
Ground	Wall, stationary wall, No slip
Right side	Pressure outlet, intensity and length scale, turbulent intensity 10 %, turbulent length scale 3 m
Left side	Constant velocity inlet, magnitude $2,5 \frac{m}{s}$, intensity and length scale, turbulent intensity 10 %, turbulent length scale 3 m
Top	Pressure outlet, intensity and length scale, turbulent intensity 10 %, turbulent length scale 7 m
Back	Pressure outlet, intensity and length scale, turbulent intensity 10 %, turbulent length scale 7 m
Middle	Symmetry
Air	Constant density $1,225 \frac{kg}{m^3}$,

For the benchmark model the thermal buoyancy is not taken into consideration. Therefore there is not specified any temperatures for either the air or any of the surfaces.

Solution control

The discretization scheme for pressure, pressure-velocity coupling, momentum, turbulent kinetic energy and turbulent dissipation rate are the same as for the 2D model listed in table 12.3. The under-relaxation factors are also the same as for the 2D model and listed in table 12.4.

12.2.4 Solution

As initial guess for the model is used the velocity magnitude for the left side. The values for the initial guess are listed in table 12.11. The Fluent files are located in the subfolder 'CFD\ Fluent files\3D Control' on the cd.

Table 12.11: *Values for the initial guess for the benchmark model.*

Gauge pressure	$0\ Pa$
X velocity	$2,5\ \frac{m}{s}$
Y velocity	$0\ \frac{m}{s}$
z velocity	$0\ \frac{m}{s}$
Turbulent kinetic energy	$0\ \frac{m^2}{s^2}$
Turbulent dissipation rate	$0\ \frac{m^2}{s^3}$

To state when the model is converged are used the same criteria as for the 2D model, that state that the residuals have to decrease with a factor 3 or more and stay at a constant level, this means that the value of the residual have to be lower or equal to 10^{-3}. The residuals for the model are showed in figure 12.18.
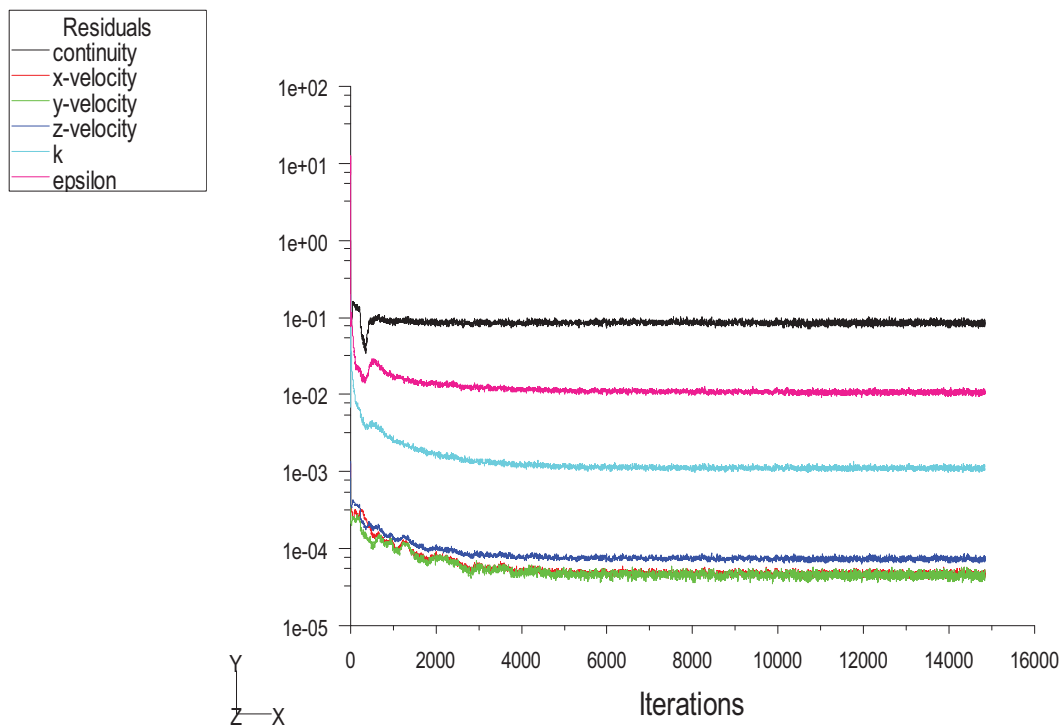
Figure 12.18: *Graph of the residuals.*

From figure 12.18 it is seen that the residuals for x-velocity y-velocity and z-velocity all do decrease with a factor 3 of more from the starting point. The continuity residual does not decrease with a factor 3 or more but stays at a level of 10^{-1}. The ϵ residual decreases

to about 10^{-2} and the k residual decreases to about 10^{-3}. It is seen that the k and ϵ residual do not decrease with a factor 3 which was stated as the convergency criteria. For all the residuals it is seen that these decrease from the starting point and after about 4000 iterations they stay at the same level.

To check the convergency the average mass flow rate at the top of the model and at the outlet of the model is checked too and is plotted on a monitoring point. The monitoring points are showed in figure 12.19.
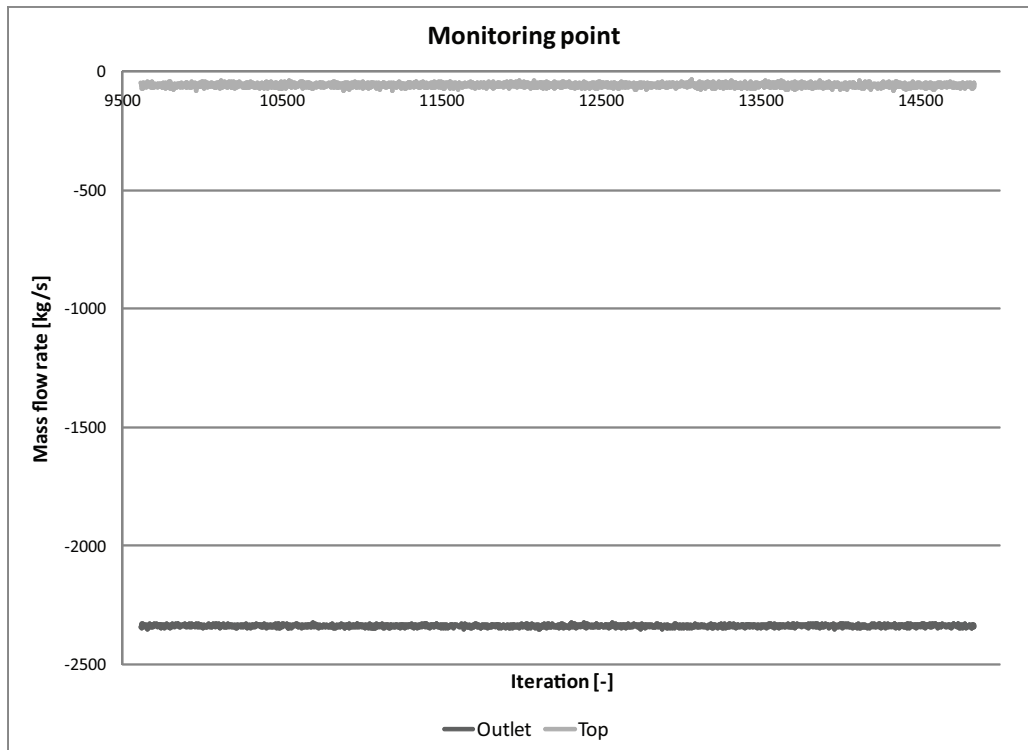
Figure 12.19: *Graph of the monitoring points for the last 5000 iterations.*

From the monitoring points showed in figure 12.19 it is seen that both the monitoring point stays at almost the same level during the simulations. Because the monitoring points almost stays at the same level and the variation is only small it is concluded that the simulation has converged.

To check the convergency even further the total mass balance for the model is calculated. In table 12.12 are listed the mass flow rate for the different sides.

Table 12.12: *Mass flow rates for the different sides for the benchmark model.*

Side	Mass flow rate $[\frac{kg}{s}]$
Back	-177,4
Inlet	2572,5
Outlet	-2339,1
Top	-52,2
Net	3,8

From table 12.12 it seen that the net mass flow rate is not 0 but $3,8 \frac{kg}{s}$. The main airflow for the model is from the left side to the right side and compared to the magnitude of the mass flow rate for these two side this number is small.

To check the grid independence for the model are made 3 different models with different grid size. For all the models the y^+ value is calculated and it is checked that the value is in the right interval. For the comparison the pressure coefficient for 6 different lines are calculated. In figure 12.20 are the different line showed.
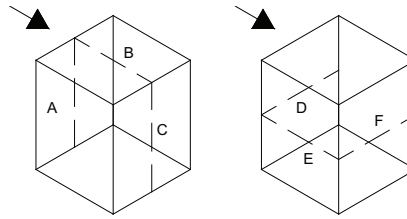
Figure 12.20: *The 6 lines for which the pressure coefficient is calculated.*

In figure 12.21 is showed the pressure coefficient for the lines A-F for the different models.
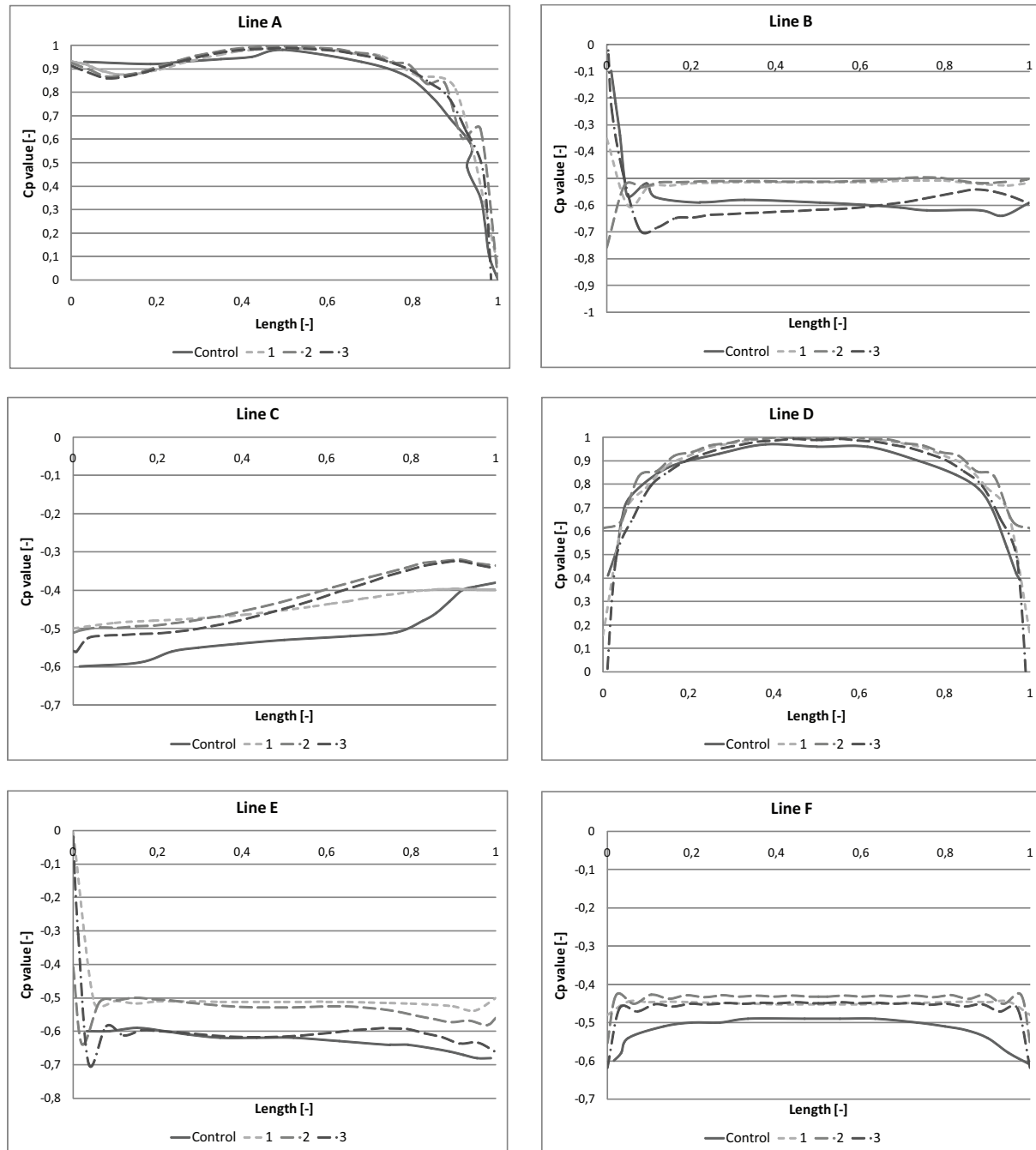
Figure 12.21: *Pressure coefficient for line A-F showed in figure 12.20 for the different models.*

In figure 12.21 are showed the pressure coefficient for the 3 models and the pressure coefficient for the different lines that later are used for check.

From the figure it is seen that there is a small variation for the different models. The greatest variation is for the line B and E that is the line located on the side of the cube. For line B and E the two models 1 and 2 do almost follow each other while there is a greater variation to model 3. From the figure it is also showed that the models have the same shape for the different lines for the pressure coefficient. To ensure that the model is grid independent the results for three models in a row have to be the same. Because of the grid size of the different models according to the accuracy for the model it is chosen not to increase the grid even further because this will take long time with the computer power available. The model 3 is chosen even that this one vary the most from the other models because it is the model with the results closest to the benchmark model.

In figure 12.22 to 12.25 are the pressure coefficient for the different faces for the cube shown.
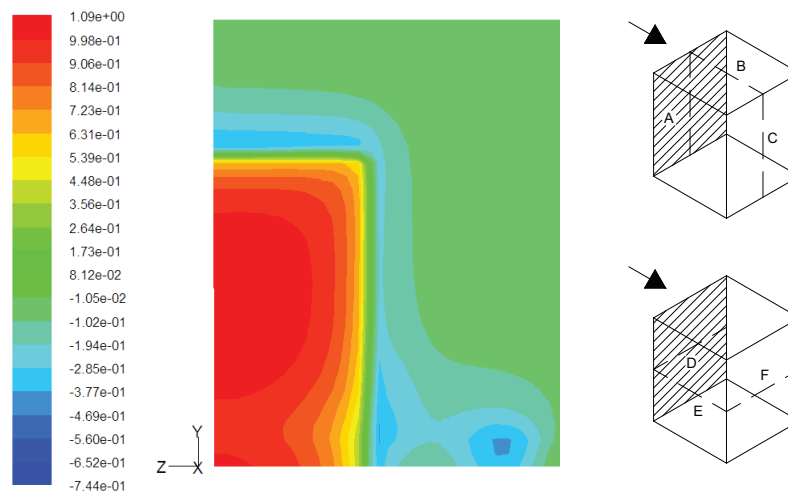
Figure 12.22: *Pressure coefficient for the surface where line A and D are located as shown in figure 12.20.*

For the face showed in figure 12.22, which is the front face of the cube, it is seen that the pressure coefficient is highest just above the middle of the face. From the middle the pressure coefficient gets smaller as closer it gets to the edges. It is also seen that at the bottom the pressure coefficient is as high as for the middle.
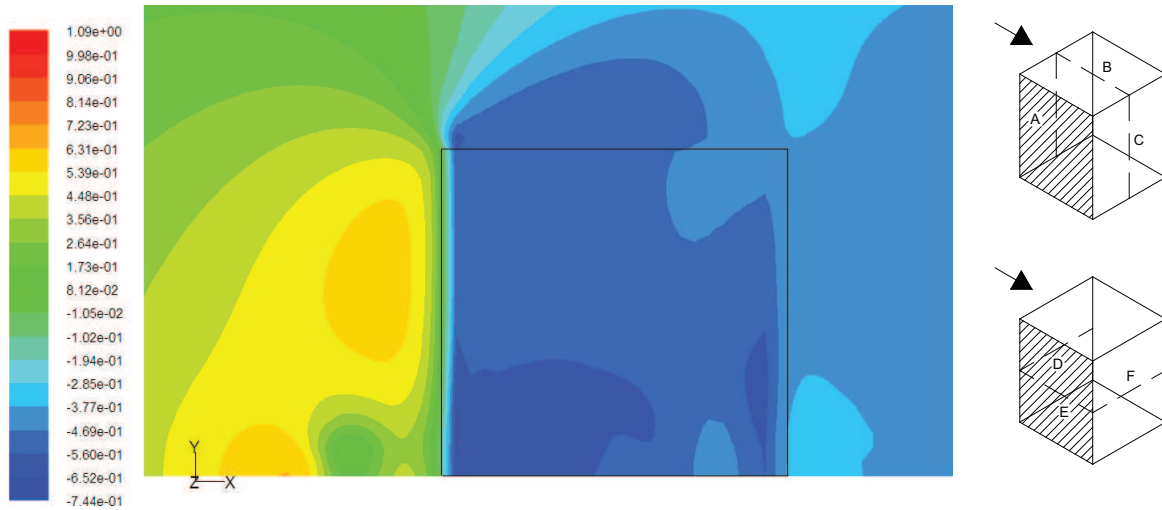
Figure 12.23: *Pressure coefficient for the surface where line E are located as shown in figure 12.20.*

In figure 12.23 are shown the distribution of the pressure coefficient for the side of the cube. From the figure it is seen that the pressure coefficient is lowest in the lower left corner and highest in the upper right corner. It is seen that the pressure coefficient decreases with the distance to the velocity inlet boundary.
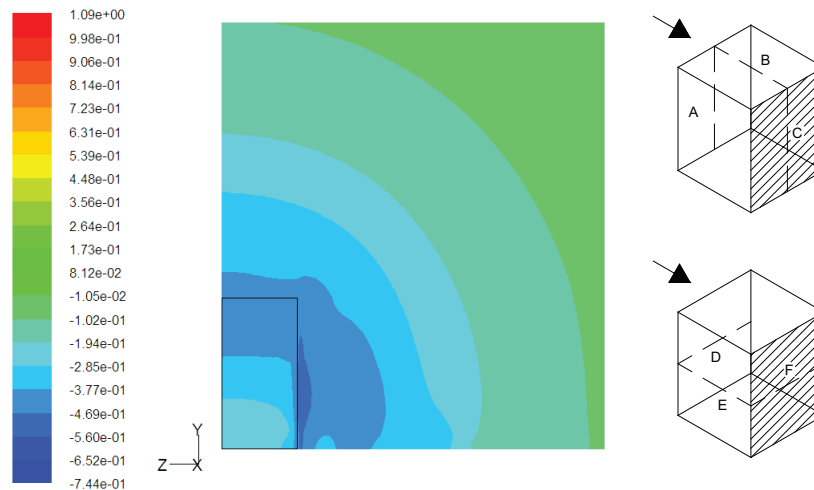
Figure 12.24: *Pressure coefficient for the surface where line C and F are located as shown in figure 12.20.*

The distribution of the pressure coefficient for the back side of the cube is showed in figure 12.24. As for the front side of the cube the numerical pressure coefficient for the back is highest just above the middle of the cube.

Figure 12.25: *Pressure coefficient for the surface where line B are located as shown in figure 12.20.*

For the top of the cube the pressure coefficient is showed in figure 12.25. From the figure it is seen that the pressure distribution is highest closest to the front of the cube and decreases with the distance to the front.

12.2.5   Validation

To verify the results the calculated pressure coefficient for the model is compared to measurements of the pressure coefficient for a cube. The results of the measured pressure coefficient for the cube are listed in [Seifert et al., 2006] .

In figure 12.26 are showed the pressure coefficient for model 3 compared to the measured values.
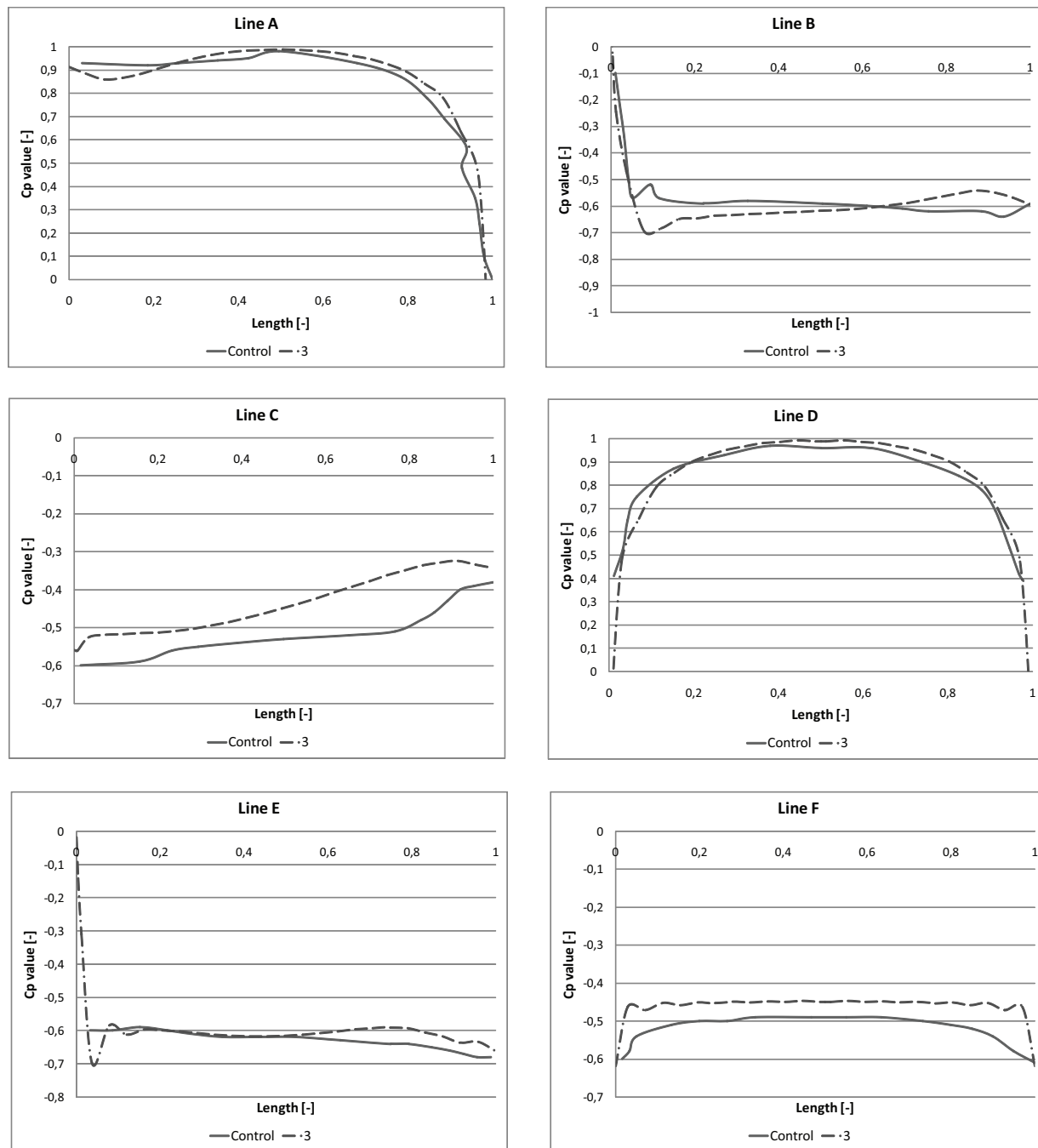
Figure 12.26: *Pressure coefficient for line A-F showed in figure 12.20 for model 3 compared to the benchmark model.*

From figure 12.26 it is seen that the greatest variation between the benchmark model and model 3 is for line C for the other lines the variation is less than $0, 05$.

In figure 12.27 are showed CFD calculation of the pressure coefficient for the 6 lines compared to the measurements of the pressure coefficient. The CFD calculation are done for two different models; the RNG $k-\epsilon$ model and the standard $k-\epsilon$ model. [Seifert et al., 2006]
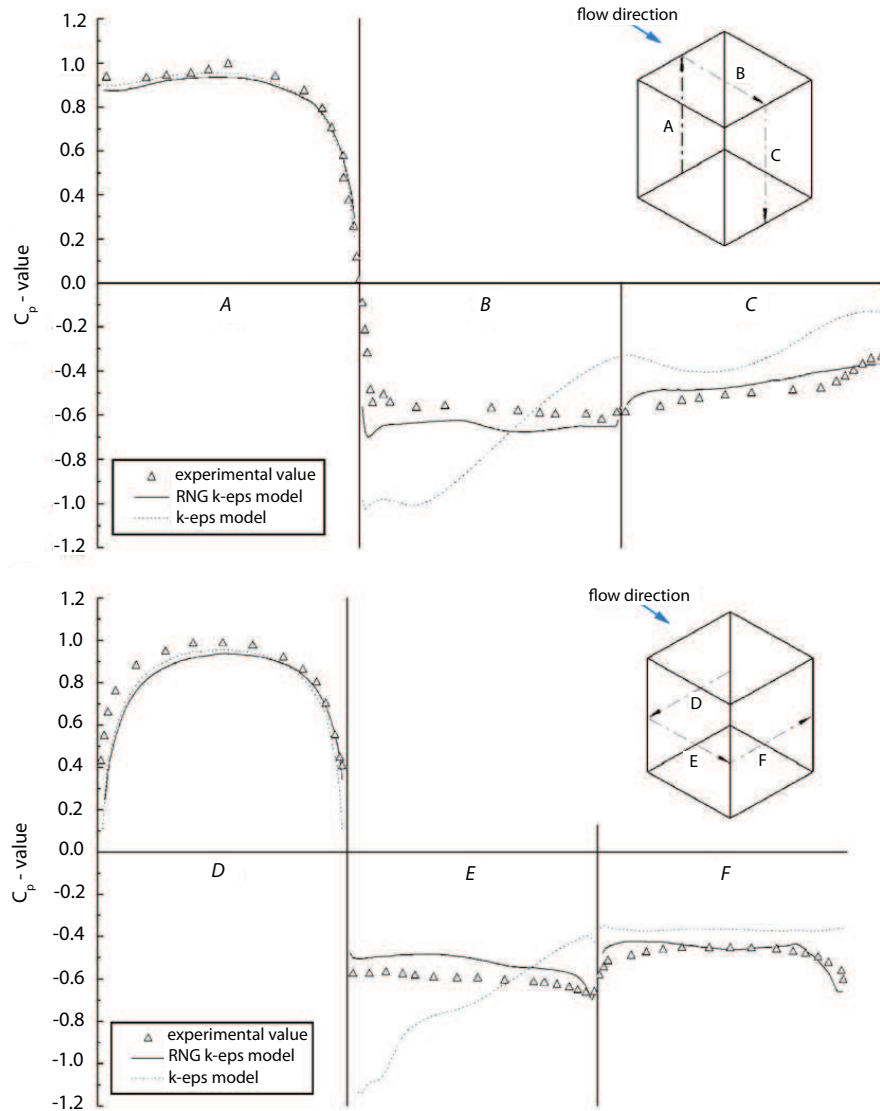
Figure 12.27: *CFD calculation of the pressure coefficient compared to measured values [Seifert et al., 2006] .*

From figure 12.27 it is seen that there also is a small variation between the measured pressure coefficient and the pressure coefficient calculated by CFD. It is seen that the smallest variation to the measured pressure coefficient is for the RNG $k - \epsilon$ model and the standard $k - \epsilon$ model varies more.

For the further simulations are therefore used the results for model 3. In table 12.13 are listed the grid distance for the benchmark model, the domain size and the turbulence model. For the final model are used the information from the benchmark model listed in table 12.13.

Table 12.13: *Setup for the benchmark model.*

Grid distance to first grid point	$0,02 \ m$
Distance in front of building	$5 \cdot H$
Distance behind building	$10 \cdot H$
Distance on either side of building	$3 \cdot H$
Turbulence model	RNG $k - \epsilon$
	Turbulence and length scale
Wall function	Enhanced wall treatment
Solution control	Body force weighted
	SIMPLE
	Second order upwind

12.3   3D model of Grantham hospital

In the following is the setup for the 3D model described. For the 3D model is used the setup from the 3D benchmark model listed in table 12.13. The purpose of the 3D model is to calculate the pressure on the surfaces of the hospital for the two cases daytime and nighttime.

12.3.1   Identification and formulation of the problem

The purpose of the model is to calculate the pressure on the surfaces of the hospital. The pressure on the surfaces of the hospital are used to calculate the airflow for the isolation room. From the calculation of the pressure on the surfaces of the building it is also discussed where the optimal location of the isolation room in the building is.

12.3.2   Specification of geometry and grid

The setup for the 3D model of the hospital is showed in figure 12.28.
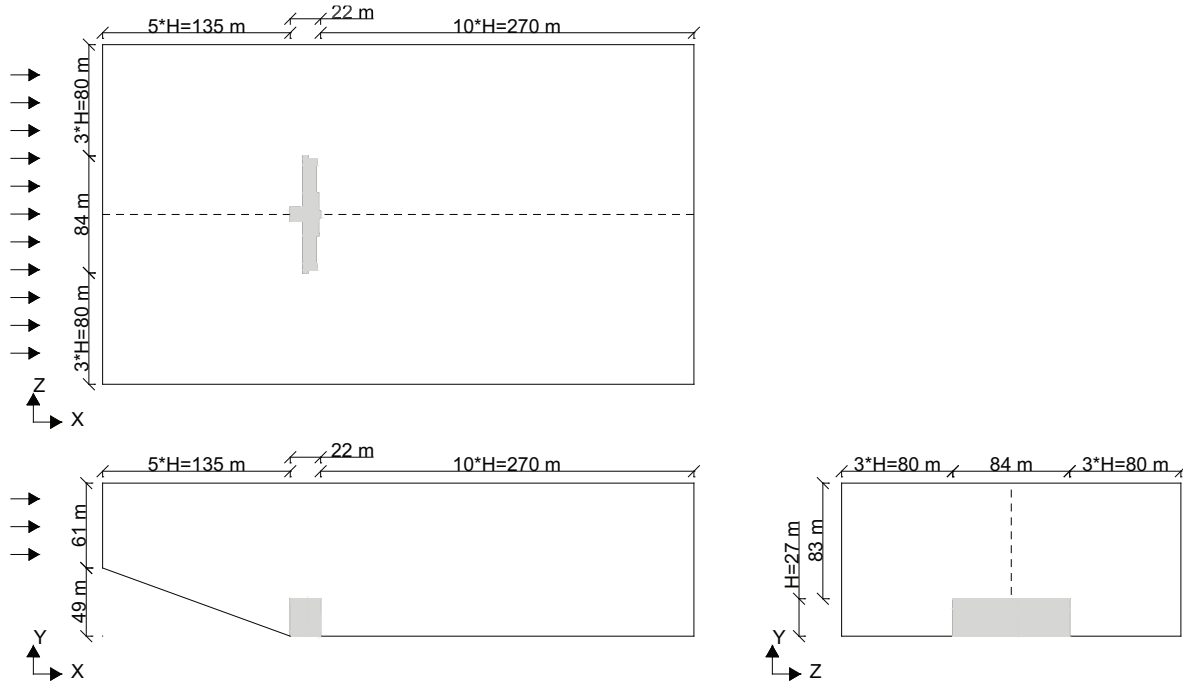
Figure 12.28: *Outline of the 3D model for the nighttime. Measurements in* [m].

In figure 12.28 is the outline of the 3D model for the nighttime case is shown. In front of the hospital the length is 5 times the height of the hospital. Behind the hospital the length is 10 times the height of the hospital. The distance of 10 times the height of the building behind the hospital is to ensure that the fluctuations behind the building is in the domain. On either side of the hospital the length of the domain is 3 times the height of the hospital. In the $y - z$ plane the hospital constitute of about 8 % of the domain. From figure 12.28 it is seen that the model is symmetric around the dotted line why only one half of the model is used.

The setup for the 3D model for the daytime is showed in figure 12.29.
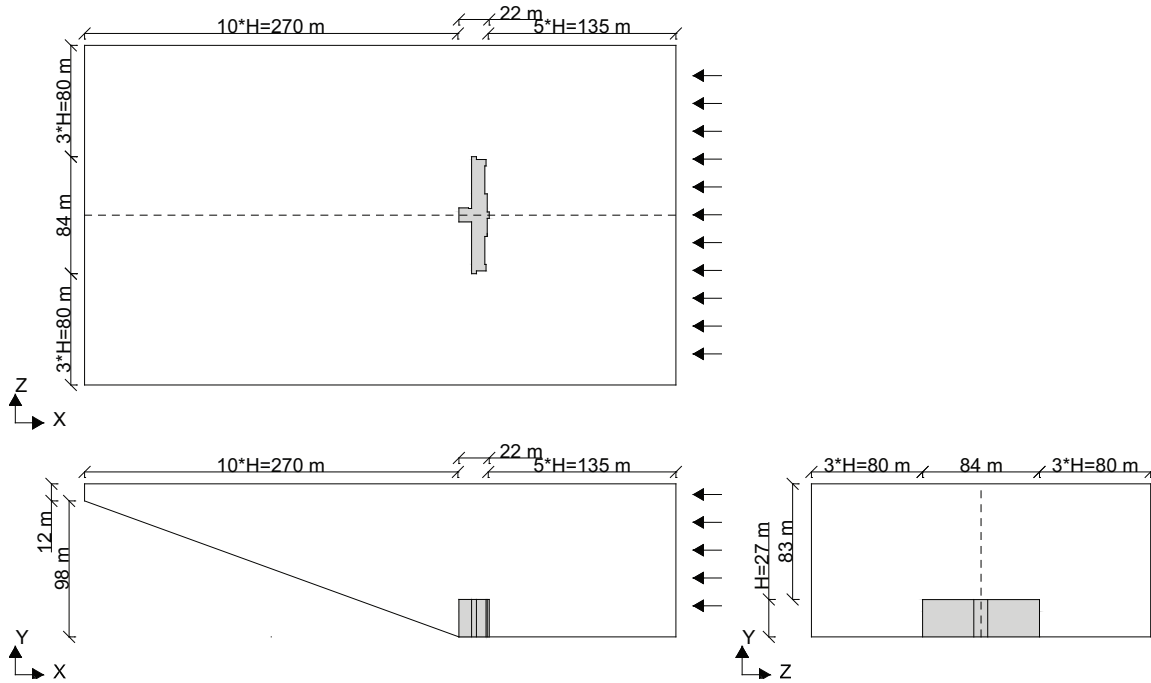
Figure 12.29: *Outline of the 3D model for the daytime. Measurements in millimeter.*

From figure 12.29 it is seen that the dimensions in front of the hospital and behind the hospital is the same for the daytime case as for the nighttime case.

As for the simulation of the velocity profiles the surfaces are smooth, this means that the thickness of the boundary layer is smaller than in the real situation. For the model surrounding obstacles are not taken into consideration either which means that the airflow around the hospital may vary to the real airflow for the hospital. Specially on the northern side of the hospital are located another building close to the hospital. This means that there might be greater parts for the northern side of the hospital where there are some circulation of the air. The building behind the hospital are not modeled because of the simulation time.

For the model the BFC grid is used.

To check the model the y^+ value is calculated. For the model thermal buoyancy is taken into consideration why the y^+ value close to the ground have to be below 5 and close to the hospital in the range of $y^+ > 30 \sim 60$.

12.3.3 Specification of physical models and boundary conditions

The RNG $k - \epsilon$ turbulence model and the enhanced wall treatment is used for the model. This is the same setup as for the 2D model and the benchmark model. As for the 2D model and the benchmark model the solution is steady state. The operation pressure is set to 101325 Pa and the gravitational acceleration is 9, 82 $\frac{m}{s^2}$.

Boundary condition

The boundary conditions used for the two cases are listed in table 12.14 and table 12.15.

Table 12.14: *Boundary condition for the daytime case.*

Surface	Boundary condition
Ground	Wall, stationary wall, no slip, temperature 28 $^\circ C$
Hill	Wall, stationary wall, no slip, temperature 33 $^\circ C$
Inflow	Velocity inlet, intensity and length scale, turbulent intensity 10 %, turbulent length scale 8 m
Outflow	Pressure outlet, intensity and length scale, turbulent intensity 10 %, turbulent length scale 1 m
Top	Pressure outlet, intensity and length scale, turbulent intensity 10 %, turbulent length scale 30 m
Side	Pressure outlet, intensity and length scale, turbulent intensity 10 %, turbulent length scale 30 m
Middle	Symmetry
Air	Boussinesq model, temperature 25 $^\circ C$, density $1,225 \frac{kg}{m^3}$, thermal expansion coefficient $0,00343 \ K^{-1}$

Table 12.15: *Boundary condition for the nighttime case.*

Surface	Boundary condition
Ground	Wall, stationary wall, no slip, temperature 18 $^\circ C$
Hill	Wall, stationary wall, no slip, temperature 15 $^\circ C$
Inflow	Velocity inlet, intensity and length scale, turbulent intensity 10 %, turbulent length scale 8 m
Outflow	Pressure outlet, intensity and length scale, turbulent intensity 10 %, turbulent length scale 1 m
Top	Pressure outlet, intensity and length scale, turbulent intensity 10 %, turbulent length scale 30 m
Side	Pressure outlet, intensity and length scale, turbulent intensity 10 %, turbulent length scale 30 m
Middle	Symmetry
Air	Boussinesq model, temperature 20 $^\circ C$, density $1,205 \frac{kg}{m^3}$, thermal expansion coefficient $0,00343 \ K^{-1}$

As listed in table 12.14 and table 12.15 the setup of the two cases is a bit different. For the daytime case the velocity inlet is at the right side while for the nighttime case the velocity inlet is at the left side. For both situations are used the calculated velocity profile from the 2D model. The velocity profiles in the two cases are showed in figure 12.13 and 12.14.

Solution control

The discretization scheme and the under-relaxation factors for the solution control are listed in table 12.3 and 12.4. Both the discretization scheme and the under-relaxation factors are the same as for the 2D model and the benchmark model.

12.3.4 Solution

For initial guess in the two cases are used the values for the velocity inlet boundary listed in table 12.16. The used Fluent files are located in the subfolder 'CFD\Fluent files\3D\Grantham' on the cd.

Table 12.16: *Values for the initial guess for the two cases.*

	Value	
	Daytime	**Nighttime**
Gauge pressure	$0\ Pa$	$0\ Pa$
X velocity	$-0,35\ \frac{m}{s}$	$0,77\ \frac{m}{s}$
Y velocity	$0\ \frac{m}{s}$	$-0,31\ \frac{m}{s}$
Z velocity	$0\ \frac{m}{s}$	$0\ \frac{m}{s}$
Turbulent kinetic energy	$0\ \frac{m^2}{s^2}$	$0\ \frac{m^2}{s^2}$
Turbulent dissipation rate	$0\ \frac{m^2}{s^3}$	$0\ \frac{m^2}{s^3}$
Temperature	$298\ K$	$293\ K$

The criteria for convergency is the same as for the 2D model and the benchmark model that the residuals have to decrease with a factor 3 or more and stay constant.

The residuals for the nighttime case is showed in figure 12.30.
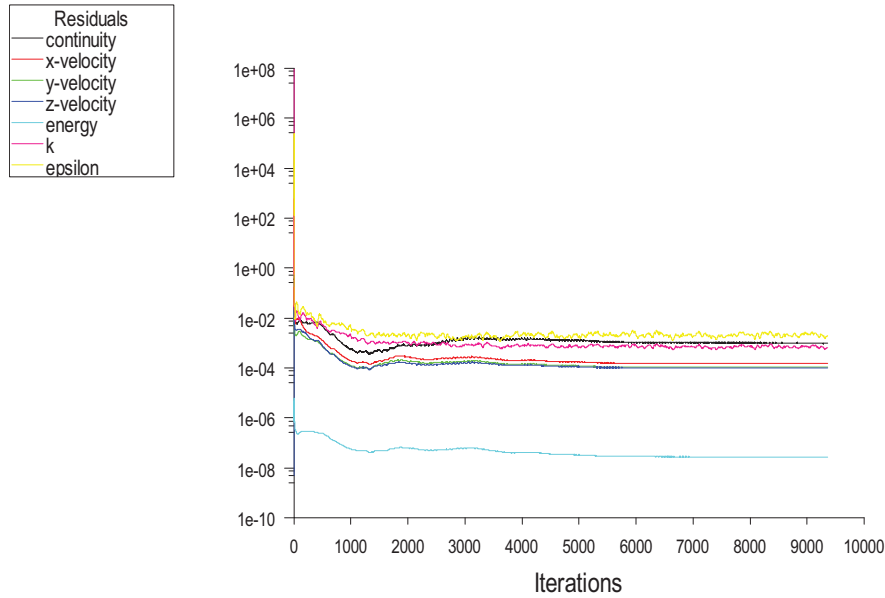
Figure 12.30: *Residuals for the nighttime case.*

From figure 12.30 it is seen that the residual for x-velocity, y-velocity, z-velocity and energy all decreases with a factor 3 or more. The continuity, k and epsilon stays at a level of $1^{-2} - 1^{-3}$. After about 3500 iterations all the residuals stays at a constant level. Because the continuity, k and epsilon residual has not decreased with a factor 3 the convergence criteria is not met.

For the model is made two monitoring points to control the convergency. The monitoring points for the nighttime case are for the outlet and the top of the model and are shown in figure 12.31.
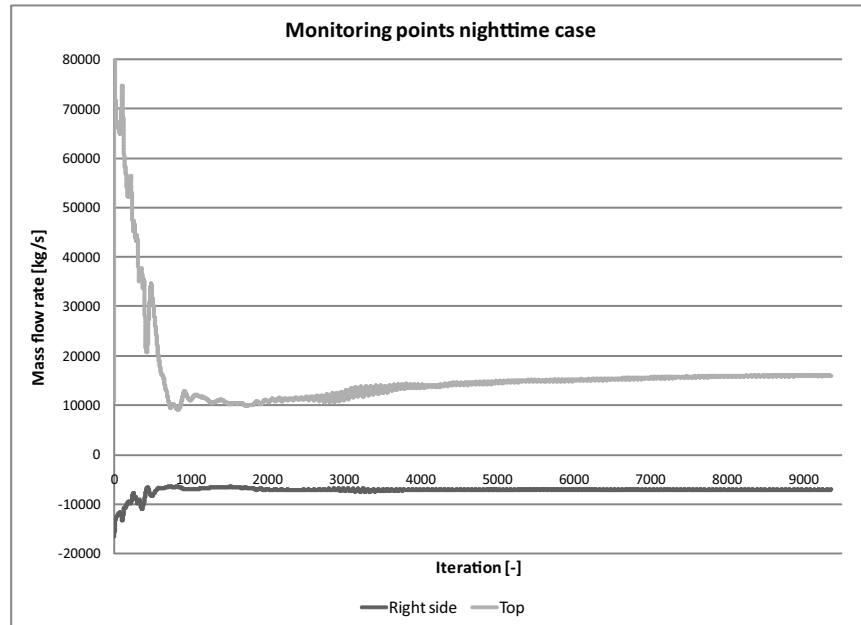
Figure 12.31: *Monitoring points for the nighttime case.*

The monitoring points in figure 12.31 shows that the model is converged after about 8000 iterations because the monitoring points stays stable. In table 12.17 are listed the mass flow rates for the model.

Table 12.17: *Mass flow rates for the different sides for the 3D model for the nighttime case.*

Side	Mass flow rate $[\frac{kg}{s}]$
Side	-1530,4
Inflow	6970,0
Outflow	-7043,9
Top	1605,0
Net	0,6

It is seen from table 12.17 that the net mass flow rate is not 0, but compared to the mass flow rate for the other sides it is low. It is therefore stated that the solution is converged.

To check the grid independency the total pressure for 6 different points for the hospital are calculated. The location of the 6 different points are showed in figure 12.32.
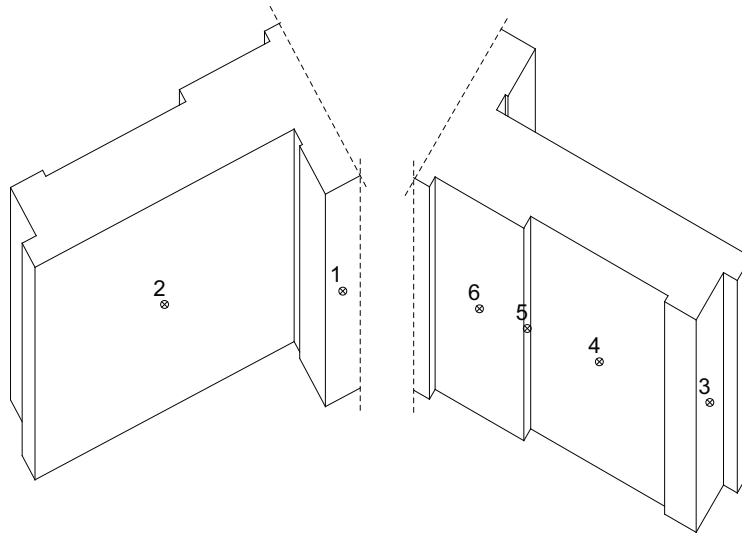
Figure 12.32: *Location of the 6 check points for the hospital.*

The calculated total pressure for the different models are showed in figure 12.33. To check the grid dependency are used the nighttime case.
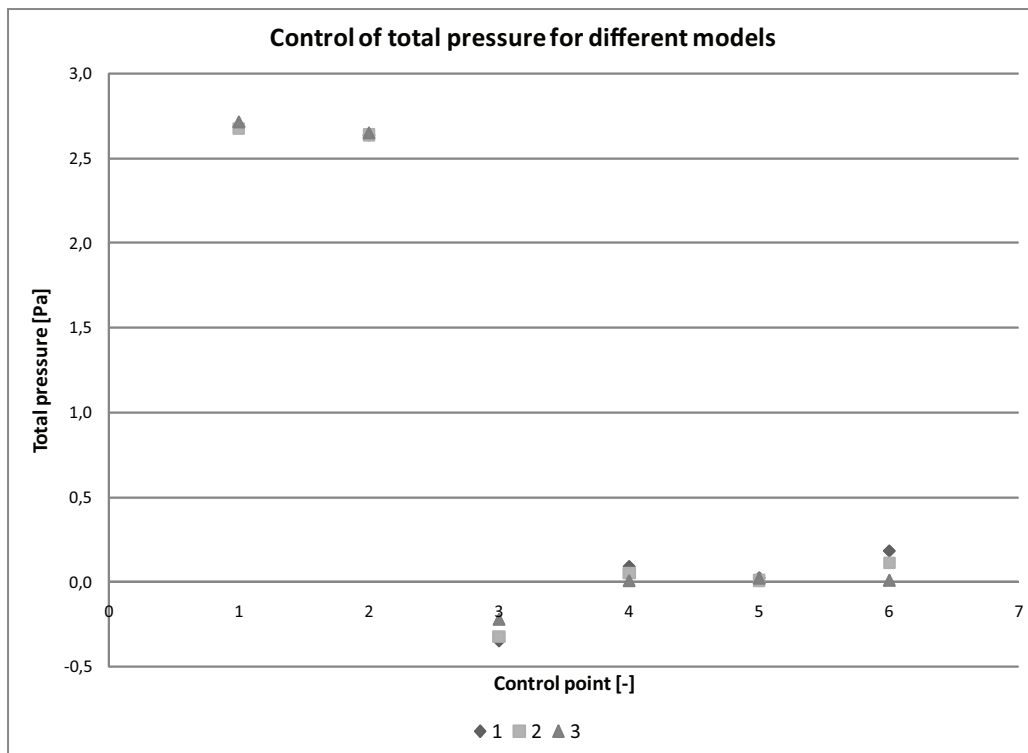
Figure 12.33: *Total pressure for the 6 points for the hospital for the different models.*

From figure 12.33 it is seen that the total pressure for all 3 models are almost the same for all 6 points.

The grid size for the different model are shown in figure 12.34.
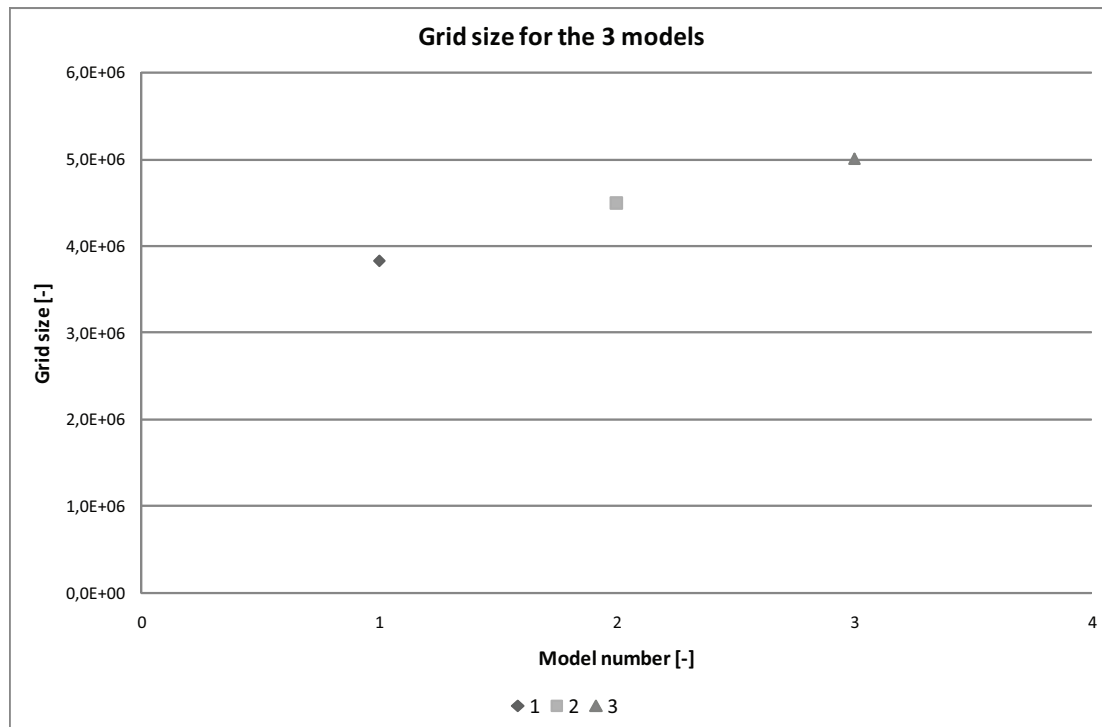
Figure 12.34: *Grid size for the different models.*

As showed in figure 12.34 the grid size from the different models increases with about 500000 cells or about ± 10 %. To ensure that the model is grid independent the results from 3 model with a grid size that increase with 500000 has to be the same it also has to be ensured that a model with a even lower grid size does not vary from the other models. From figure 12.33 and figure 12.34 it is seen that the difference of the grid for all 3 models are about 500000 and the results are close to each other. For the simulation are not made a model with an even lower grid size, therefore it is not possible to ensure that the model is total grid independent. The total pressure for all 3 models is almost the same it is therefore stated that the 3 models are grid independent and according to the simulation time with the available computer power there is not made a model with a higher grid size than model 3.

For further calculations the results from model 2 are used. This is chosen because the results from model 2 and 3 are close to each other and the time for an iteration for the 2 models are lowest for model 2 according to the grid size. The grid size for model 2 are used for both the nighttime and daytime case.

For the model the airflow around the hospital is calculated. This is done to investigate circulation of airflow and the airflow near to the isolation room.

Nighttime case

In figure 12.35 is showed the streamlines for the hospital in the nighttime case for a plane through the z-axis.

Figure 12.35: *Streamlines of the airflow around the hospital in the nighttime case through a plane in the z-axis.*

From figure 12.35 it is seen that there is some circulation at the bottom of the hospital on both the windward and the leeward side. It is also seen that on the top of the hospital there is some circulation of the air. On the leeward side of the hospital the direction of the airflow is opposite the direction of the airflow on the windward side, this means that

according to the airflow on the windward side the airflow on the leeward side is negative. It is also seen that in a distance of about 100 meter from the back side of the hospital, this means after the air circulation on the leeward side of the hospital, the airflow change direction and become positive in the x-axis direction.

The vectors of the velocity of the airflow for the same plane as above through the z-axis is showed in figure 12.36.

Figure 12.36: *Vectors of the airflow around the hospital in the nighttime case through a plane in the z-axis.*

It is seen from figure 12.36 that the magnitude of the velocity is highest on the windward side of the hospital and decreases on the leeward side. On the windward side of the hospital the magnitude of the velocity is highest close to the ground and decreases with the height.

The streamlines for a plane through the y-axis is showed in figure 12.37.
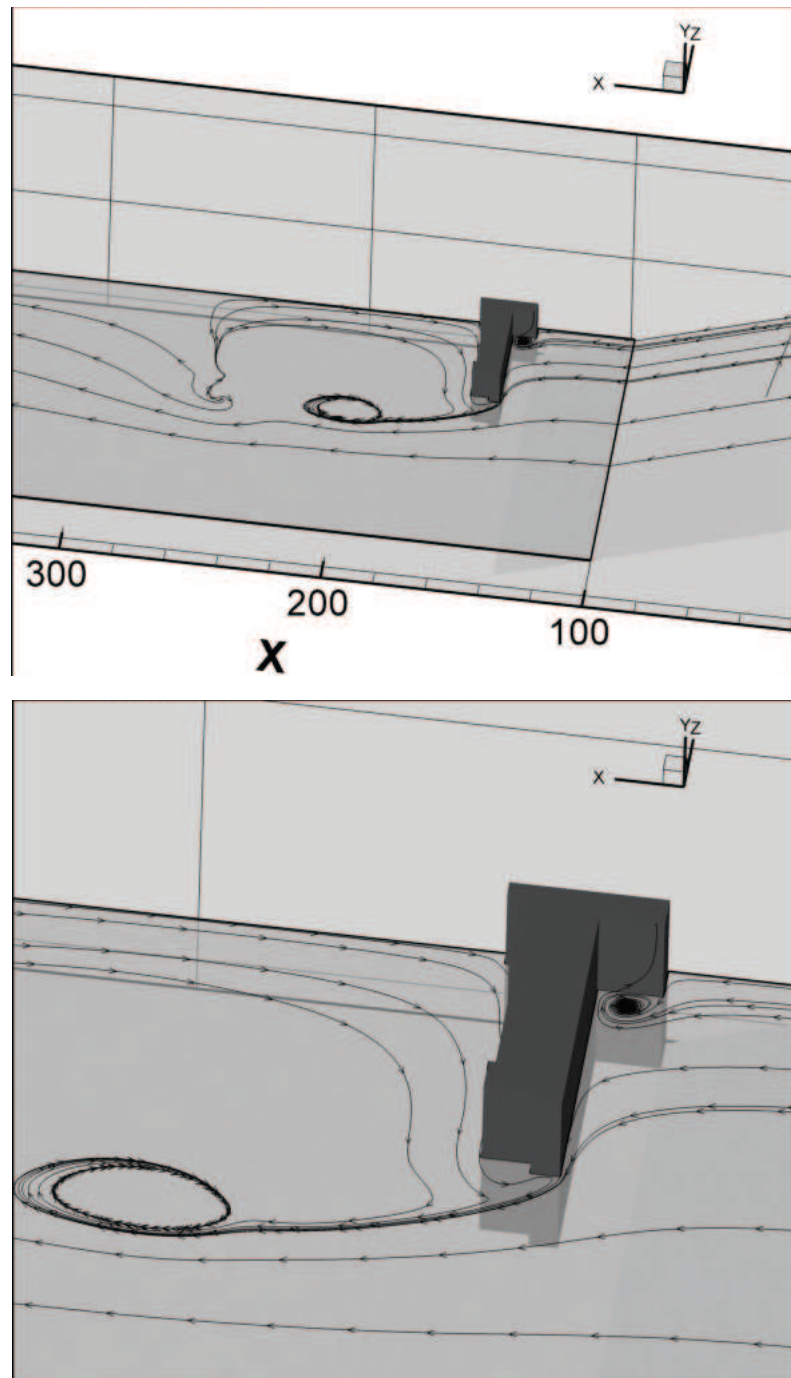
Figure 12.37: *Streamlines of the airflow around the hospital in the nighttime case through a plane in the y-axis.*

From the streamlines for the plane through the y-axis it is seen that in the corners on the windward side of the hospital there is some circulation. Some of this circulation is close to the location of the isolation room in the building, while it might have influence on the airflow for the isolation room. As for the streamlines for the plane in the z-axis the velocity is positive in the x-axis direction on the windward side of the hospital and negative until a distance of about 100 meter away from the hospital on the leeward side of the hospital. Further away from the hospital the velocity becomes positive in the x-axis again.

In figure 12.38 is showed the vectors of the velocity for the plane through the y-axis.
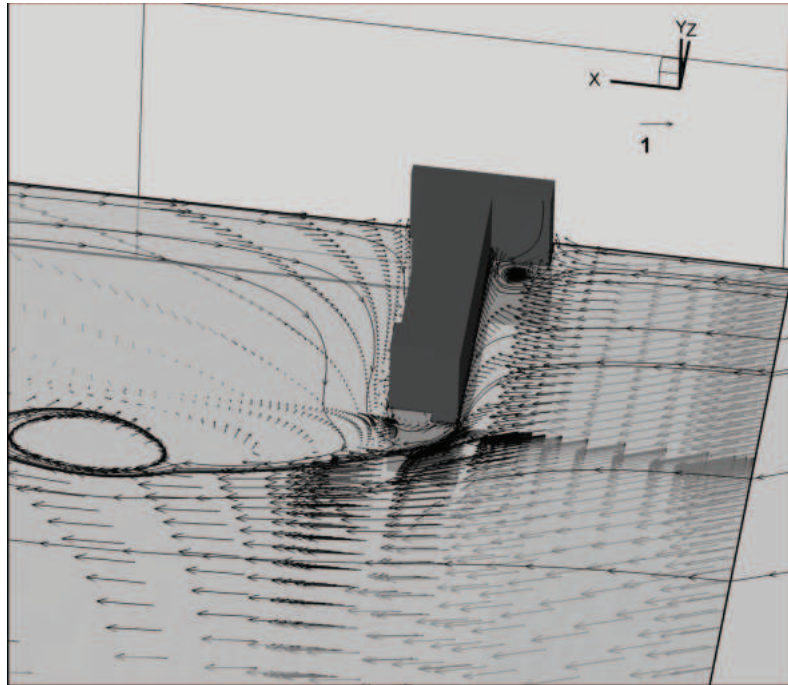
Figure 12.38: *Vectors of the airflow around the hospital in the nighttime case through a plane in the y-axis.*

The vector plot of the velocity for the plane through the y-axis shows that the magnitude of the velocity is highest on the windward side of the hospital. On the leeward side of the hospital the magnitude of the velocity is close to 0.

The dynamic, static and total pressure for the windward side of the hospital for the nighttime case is showed in figure 12.39. The pressure is defined by:

$$P + \frac{1}{2}\rho V^2 = P_0 \qquad (12.11)$$

where

$$
\begin{array}{lll}
P & : & \text{Static pressure } [Pa] \\
\frac{1}{2}\rho V^2 & : & \text{Dynamic pressure } [Pa] \\
P_0 & : & \text{Total pressure } [Pa]
\end{array}
$$

Static pressure

Dynamic pressure
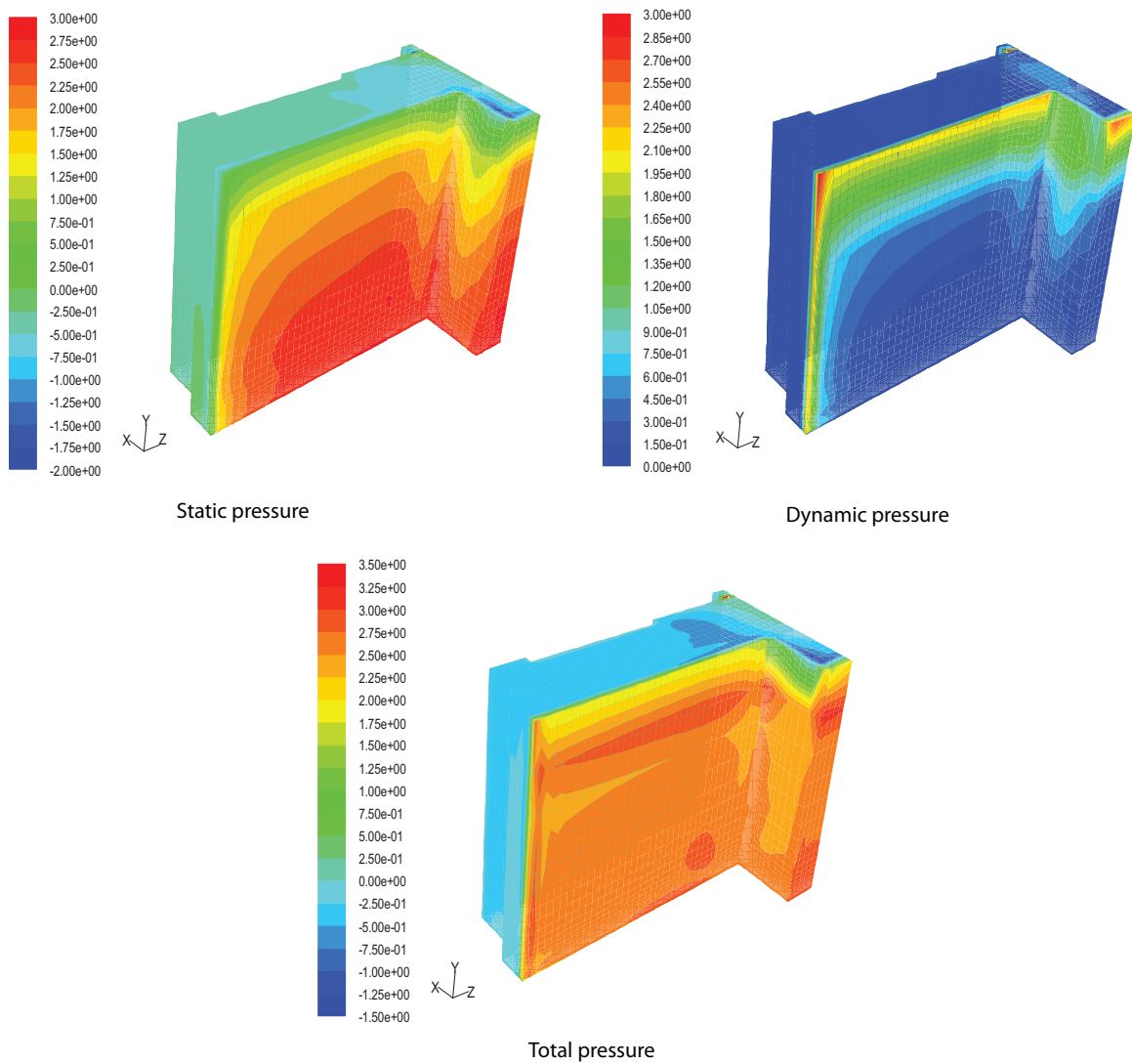
Total pressure

Figure 12.39: *Static, dynamic and total pressure for the windward side of the hospital for the nighttime case. Measurement in* $[Pa]$*.*

It is seen in figure 12.39 that for the windward side the static pressure is highest on the front of the building because the airflow is stagnated. The static pressure is highest for the lower half of the hospital and decreases with the height due to the acceleration of the airflow around the corners of the building. The dynamic pressure is highest for the upper part of the building and decreases downwards. According to the higher velocity around the corners the dynamic pressure is highest at the top of the building and at the sides. For the total pressure this is highest in a height of $\frac{2}{3}$ from the bottom of the surface. This is according to the sum of the static pressure and the dynamic pressure.

The static, dynamic and total pressure for the leeward side of the hospital is showed in figure 12.40

Static pressure

Dynamic pressure
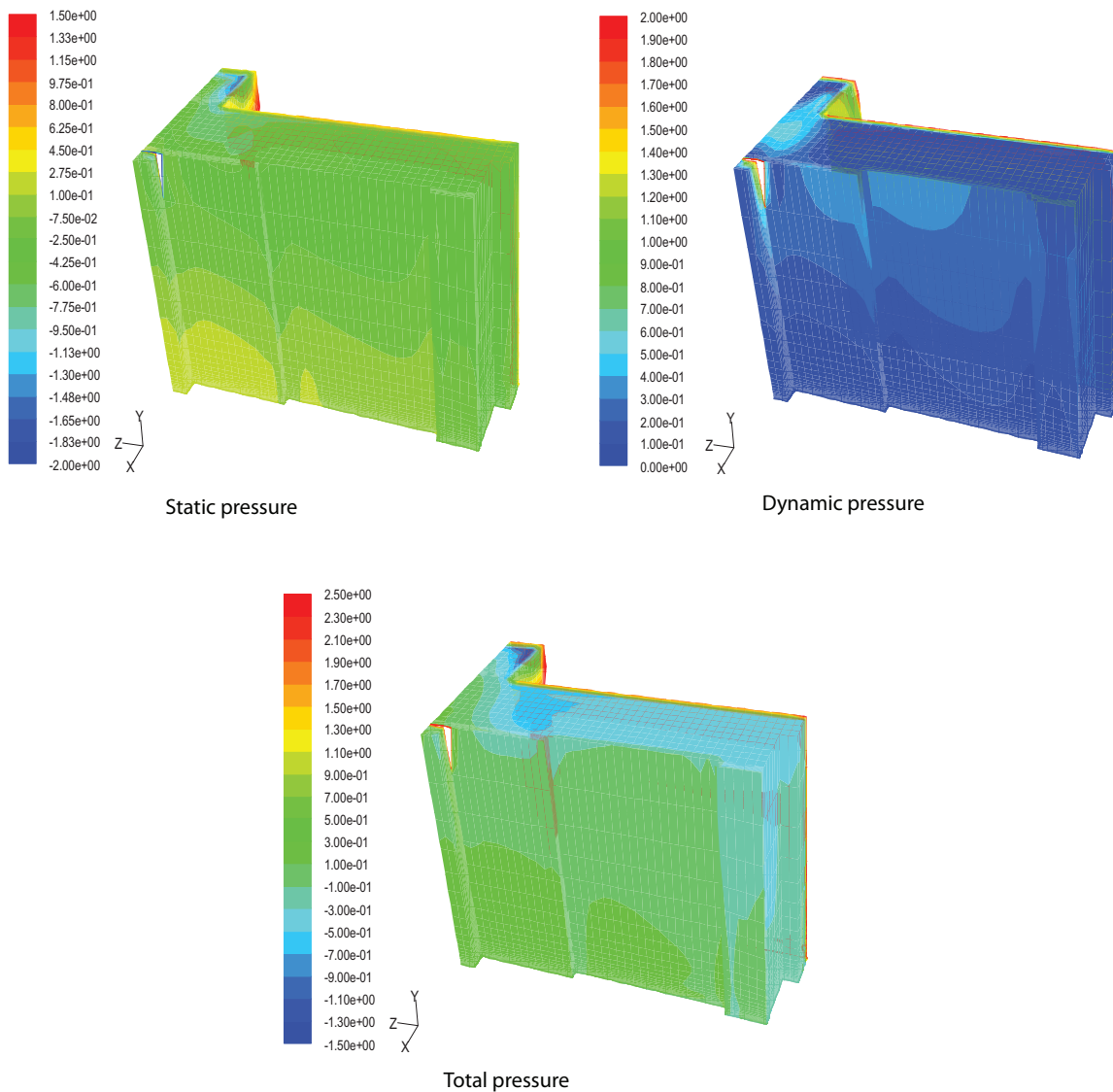
Total pressure

Figure 12.40: *Static, dynamic and total pressure for the leeward side of the hospital for the nighttime case. Measurement in* $[Pa]$.

From figure 12.40 it is seen that both the static, dynamic and total pressure is lower on the leeward side of the building compared to the windward side of the building. The static pressure on the surfaces of the building on the leeward side is highest at the bottom of the building according to stagnation of the wind and the hydrostatic pressure distribution and decreases with the height. As for the windward side the dynamic pressure is highest at the top of the building and decreases at the bottom according to the higher speed at the top. The total pressure on the surfaces of the building on the leeward side is highest at the bottom. From the figure it is also seen that for the upper left corner of the building both the static, dynamic and total pressure is very high. Since the wind accelerates at the top of the building the static pressure should be lowest at this point. From the figure it is seen that this is not the case. It is also seen that both the dynamic and total pressure is high in this corner. Because the pressure distribution at this corner is a lot different to the pressure distribution for the rest of the building there might be an error in this corner and the values for this corner is not used for further calculations.

Daytime case

In figure 12.41 are showed the streamlines for the hospital in the daytime case for a plane through the z-axis.
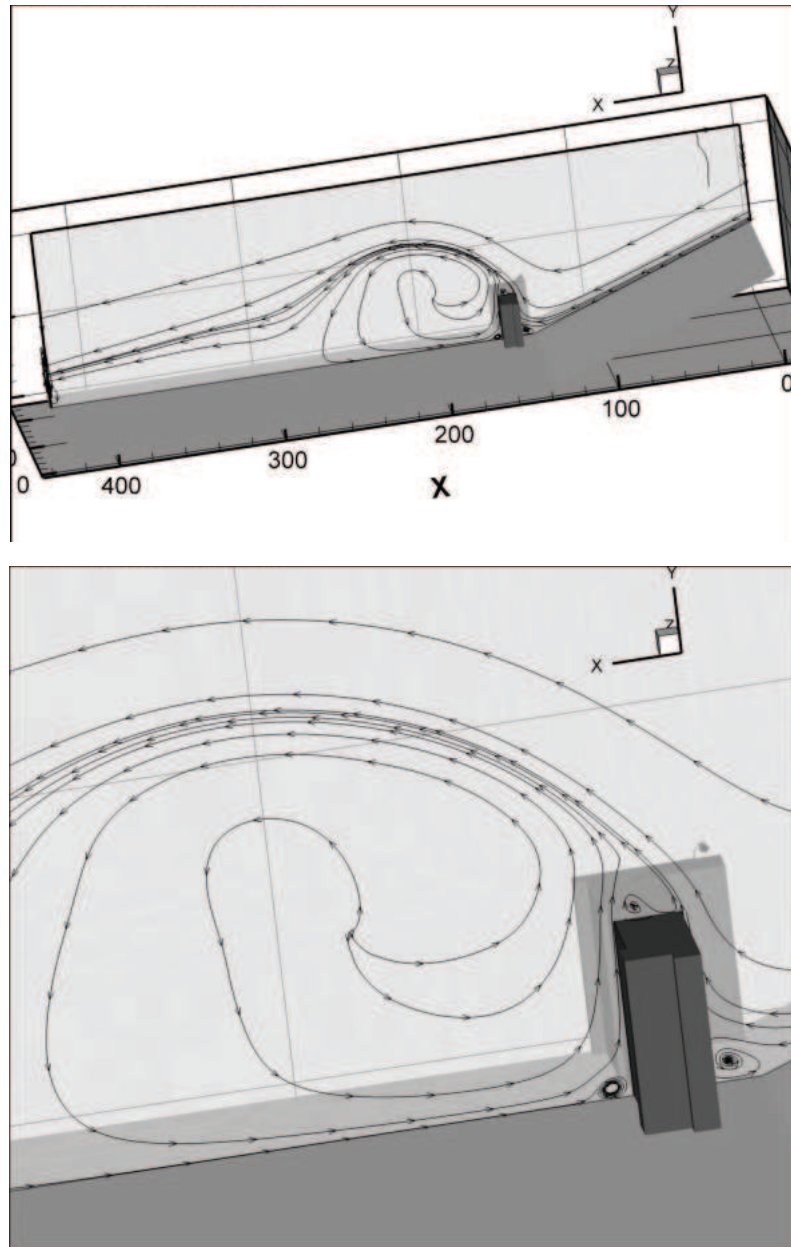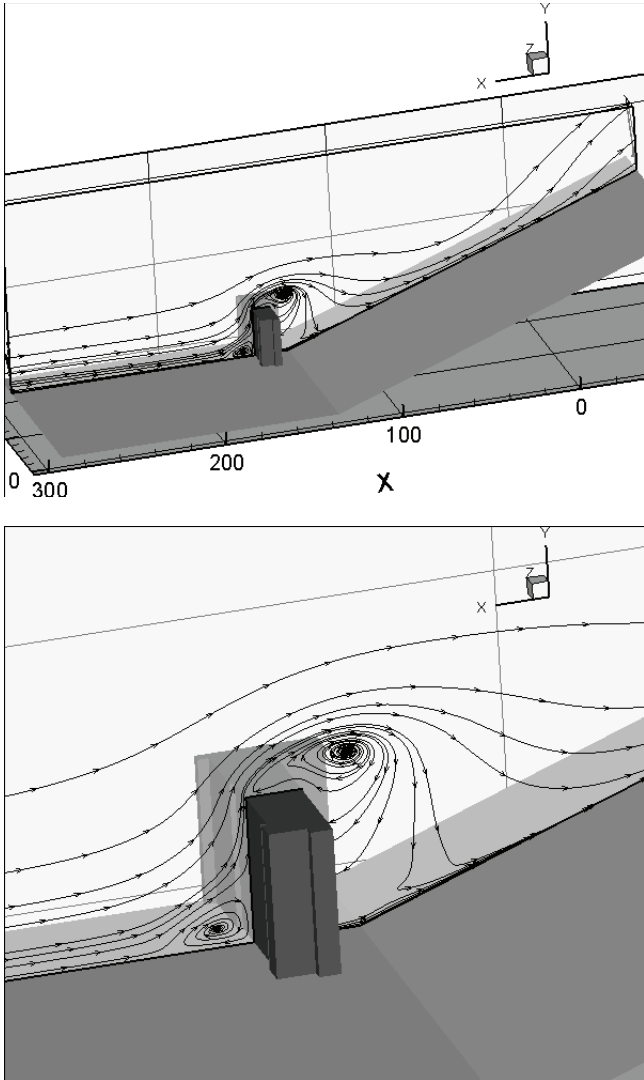
Figure 12.41: *Streamlines for the airflow around the hospital in the daytime case through a plane in the z-axis.*

From figure 12.41 it is seen that the airflow is from the left to right. On the windward side of the hospital are created some circulation at the bottom of the hospital. When the wind hits the hospital it changes direction and flows upwards. At the end of the roof of the hospital is again created some circulation because of the change in the geometry. It is seen that when the wind has passed the circulation at the roof it is going inwards against the leeward side of the hospital. Because of this airflow there will be created a positive pressure in the lower part of the facade for the hospital on the leeward side. When the wind hits the ground on the leeward side it flows towards right again.

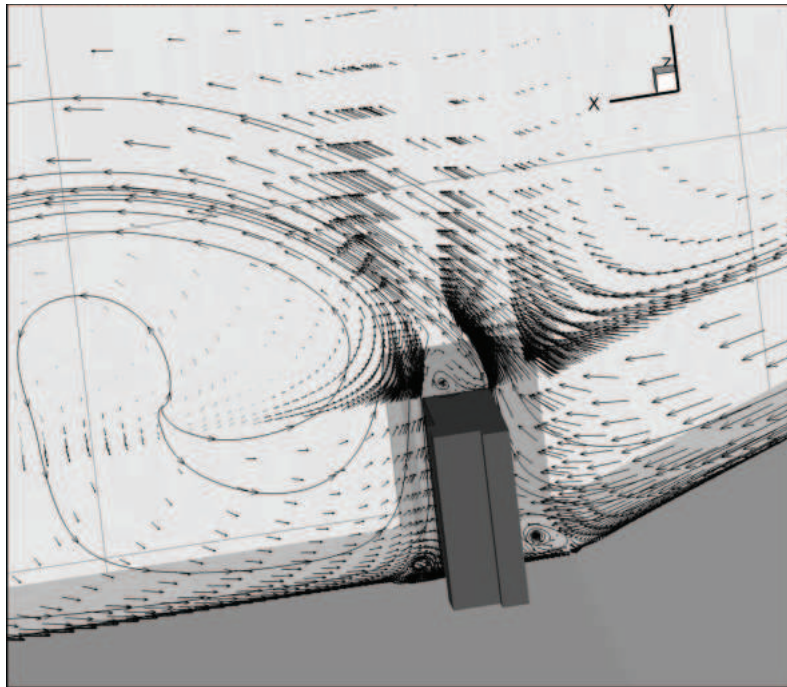The vectors of the velocity of the airflow for the same plane as above through the z-axis is showed in figure 12.42.
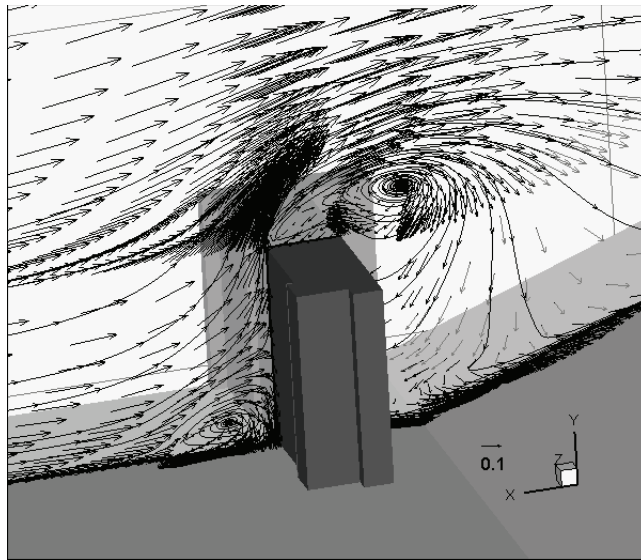
Figure 12.42: *Vectors of the airflow around the hospital in the daytime case through a plane in the z-axis.*

From figure 12.42 it is seen that the magnitude of the velocity is highest at the top of the hospital according to the acceleration of the wind because of the change in geometry. It is also seen that the magnitude of the velocity is higher on the windward side of the hospital compared to the leeward side. The lowest value of the velocity is for the leeward side of the hospital close to the ground.

The streamlines for a plane through the y-axis is showed in figure 12.43 and 12.44.
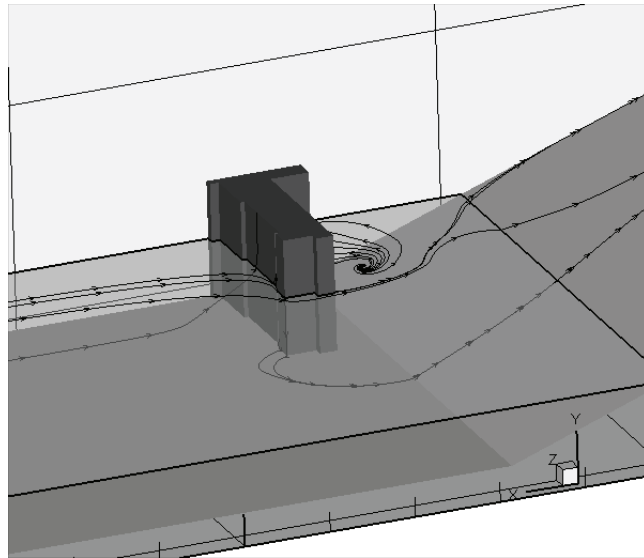
Figure 12.43: *Streamlines for the airflow around the windward side of the hospital in the daytime case through a plane in the y-axis.*

In figure 12.43 is the streamlines on the windward side of the hospital showed. From the figure it is seen that on the windward side of the hospital the streamlines hit the hospital almost perpendicular to the hospital. When the wind hits the hospital the direction of the wind change and flows around the corner of the hospital.

The streamlines on the leeward side of the hospital are showed in figure 12.44.
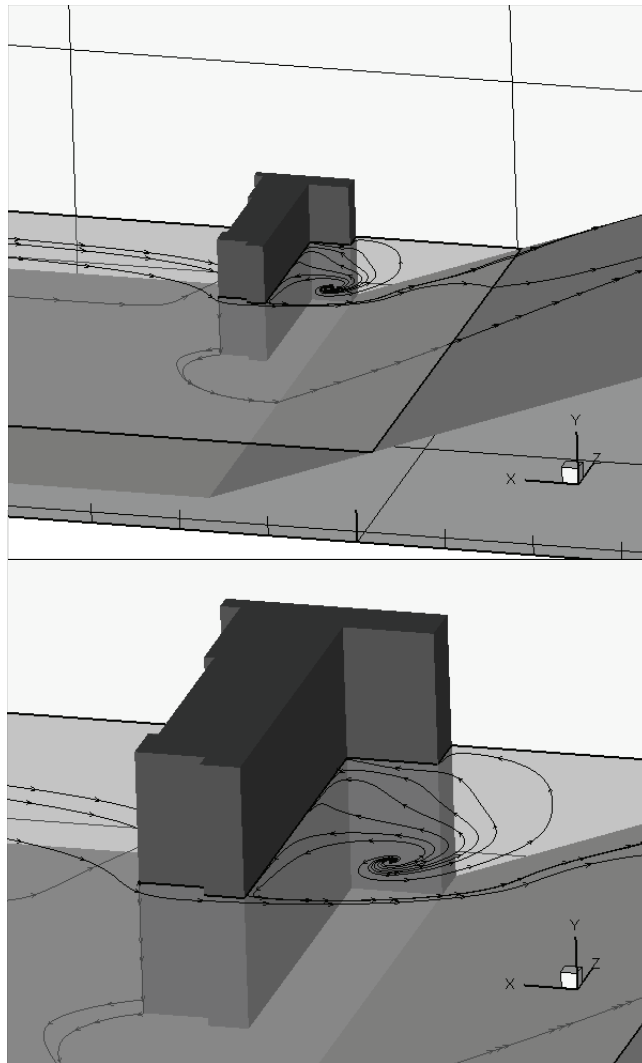
Figure 12.44: *Streamlines for the airflow around the leeward side of the hospital in the daytime case through a plane in the y-axis.*

From figure 12.44 it is seen that there is some circulation on the leeward side of the hospital. When the wind passes from the windward side of the hospital around the corner of the hospital it changes direction and flows along the leeward side of the hospital. Depending on the speed of the wind the wind follow the facade of the hospital in a determined distance and then leaves the facade and flows towards the hill and into a turbulent region. Because of the change in the geometry of the flow path some circulation of the air is created after it passes the hospital.

The velocity vectors for the plane through the y-axis is showed in figure 12.45 and 12.46.
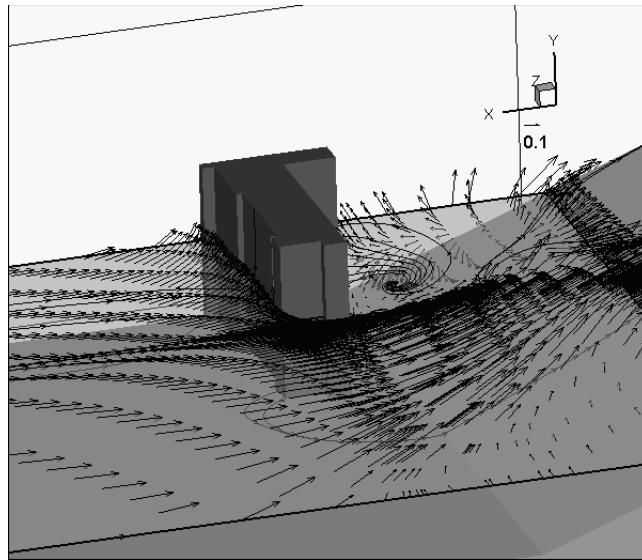
Figure 12.45: *Vectors of the airflow around the hospital on the windward side in the daytime case through a plane in the y-axis.*
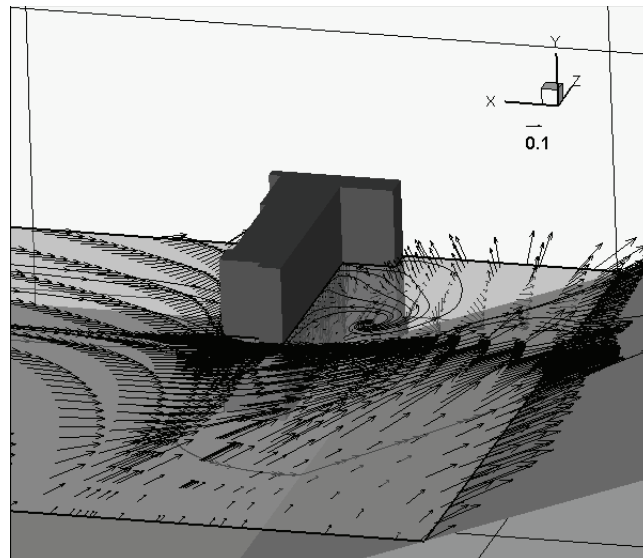
Figure 12.46: *Vectors of the airflow around the hospital on the leeward side in the daytime case through a plane in the y-axis.*

From figure 12.45 and 12.46 it is seen that the magnitude of the velocity for the daytime case is highest in a short distance away from the hospital. Close to the hospital are some circulation why the magnitude of the velocity in these places are lower than in a distance away from the hospital. From figure 12.46 it is seen that the direction of the wind changes for the leeward side compared to the windward side and further away from the building. On the leeward side of the hospital the wind speed is low compared to the windward side. In the daytime case the surface temperature of the hospital is lower than the air and because of the lower wind speed on the leeward side the temperature difference have greater influence on the leeward side than on the windward side.

The static, dynamic and total pressure on the surfaces of the windward side of the hospital for the daytime case is showed in figure 12.47.
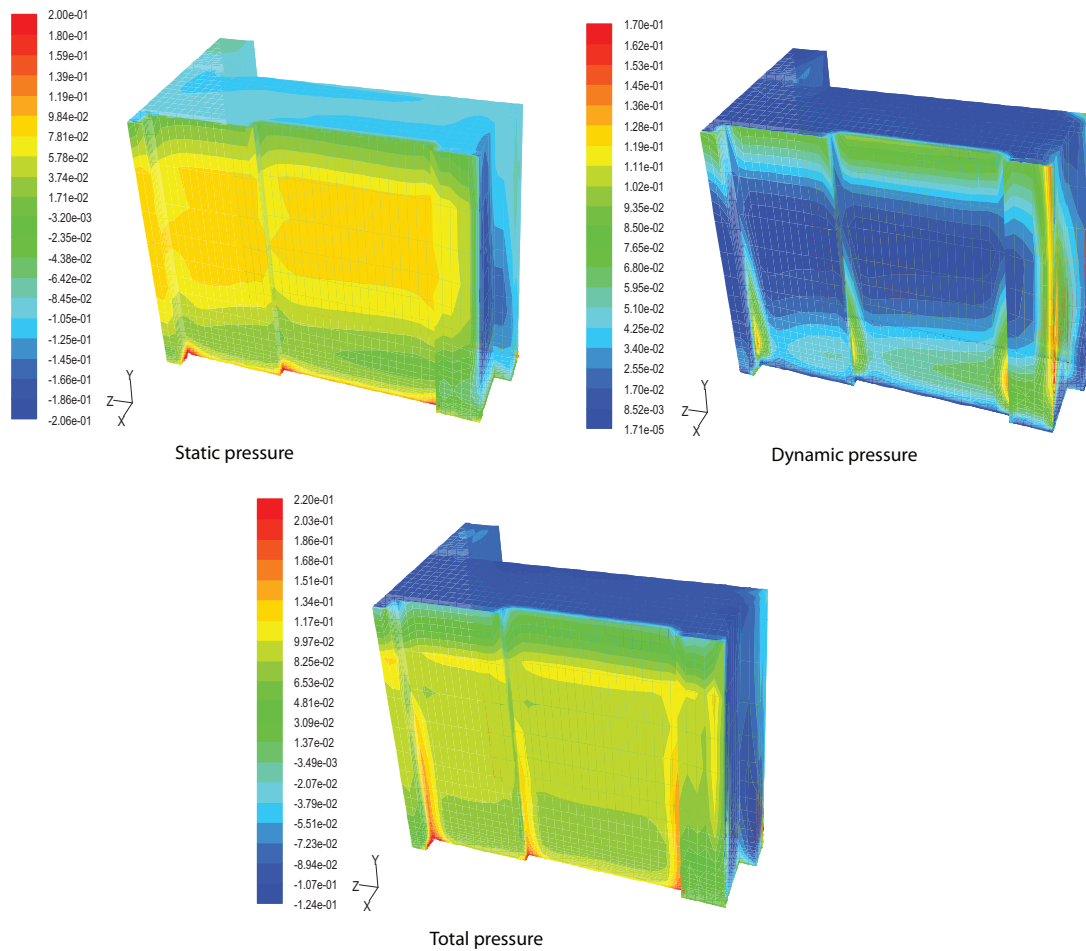
Figure 12.47: *Static, dynamic and total pressure on the surfaces of the windward side of the hospital in the daytime case. Measurement in* [*Pa*].

In figure 12.47 it is seen that for the windward side of the building the static pressure is highest at the bottom of the facade. This is due to the stagnation of the wind in this part and the hydrostatic pressure distribution. With the height the increases in the first $\frac{1}{4}$ part of the hospital hereafter the pressure decreases again. For the middle part of the facade the pressure is the highest level after the bottom. Hereafter the pressure decreases again. At the top of the hospital the lowest value of the static pressure is. This is because of the acceleration of the wind around the corner at the top of the building. The high static pressure in the middle part of the facade is according to the low velocity of the wind in this place.

The dynamic pressure is highest at the top of the building and at other corners of the building. When the geometry of the building changes the wind speed accelerates. From equation 12.11 it is seen that with a higher wind speed the dynamic pressure rises.

According to equation 12.11 the total pressure is the sum of the static pressure and the dynamic pressure. Therefore the highest total pressure is for the corners of the building and for the upper middle part of the facade of the hospital.

In figure 12.48 are showed the pressure on the surfaces of the leeward side of the hospital in the daytime case.
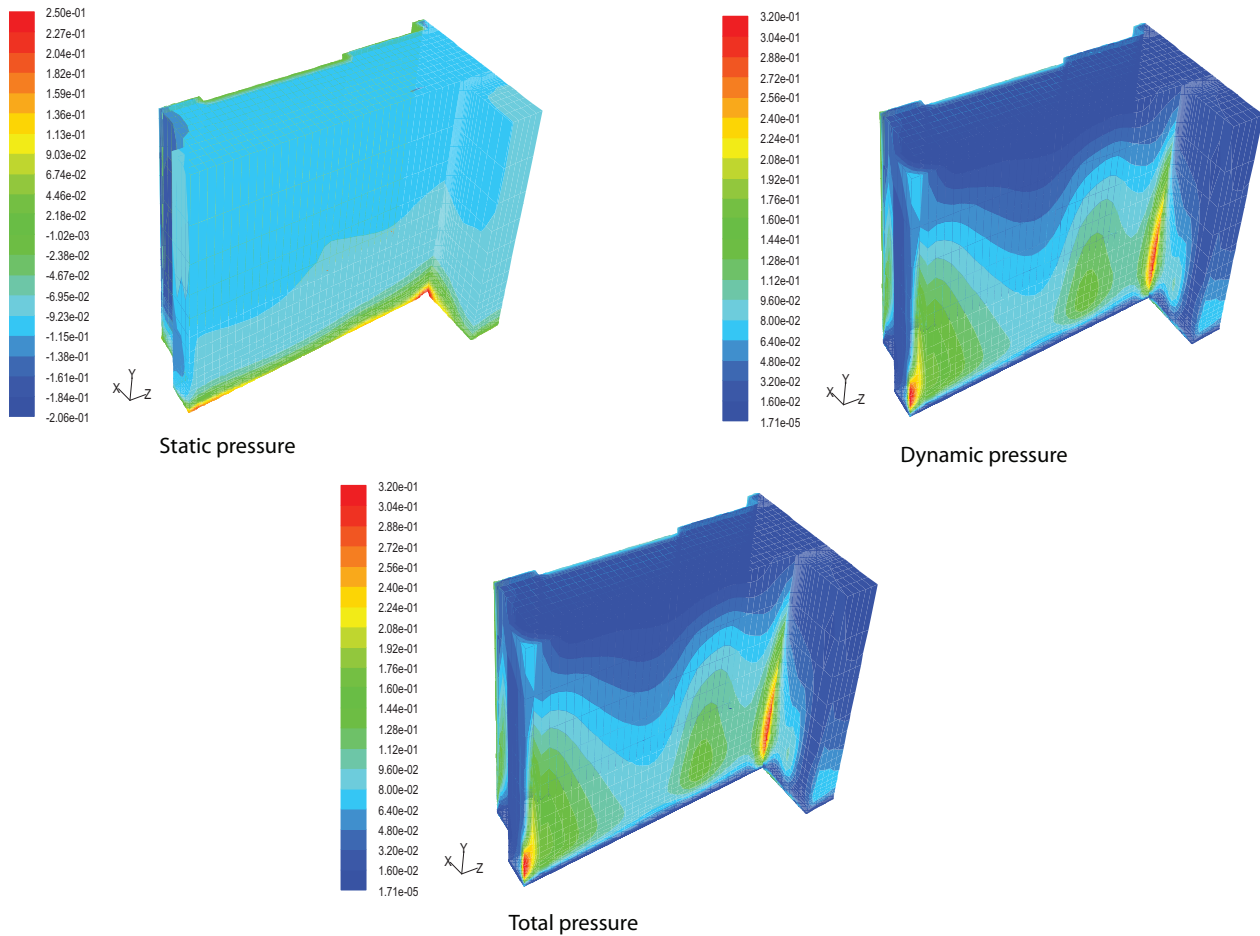
Figure 12.48: *Static, dynamic and total pressure on the surfaces of the leeward side of the hospital in the daytime case. Measurement in* [*Pa*].

It is seen from figure 12.48 that the static pressure on the leeward side of the hospital is the same for almost the hole facade. This might be because the change in wind speed for the leeward side is close to $0 \frac{m}{s}$.

The dynamic pressure on the surfaces of the leeward side is highest for the corners of the lower part of the facade. From figure 12.41 it is seen that for the upper half of the building there is a turbulent part and after the wind has passed this part the direction of the wind is towards the facade. Because of the change in direction and speed of the wind the velocity of the wind is highest for the lower part of the hospital. Therefore the dynamic pressure is higher for the lower part of the hospital compared to the upper part of the hospital.

It is seen that of the static pressure and the dynamic pressure, the dynamic pressure has the greatest influence on the hospital. Therefore the distribution of the total pressure is almost the same as for the dynamic pressure.

Pressure for isolation room

As stated in chapter 4 the pressure for the isolation room depends on the decease of the patient in the room. For a patient with an airborne infection the isolation has to have a negative pressure so the droplets are not spread into other parts of the hospital. For a patient that are particular week and vulnerable to diseases the pressure in the isolation room have to be positive so the patient is not infected. From figure 12.39 and 12.40 it is seen that the pressure is highest on the windward side of the hospital according to the wind direction. It is also seen that the highest total pressure is for the top half of the building in the nighttime case. In figure 12.49 are showed the location of the isolation room in the building and the total pressure on the facade where the isolation rooms are located.
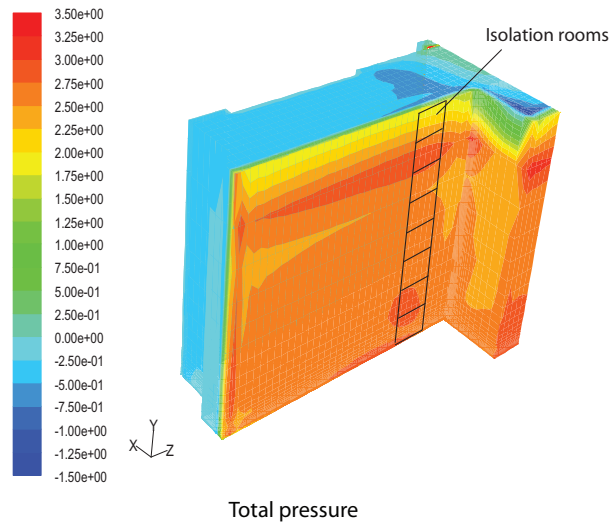
Figure 12.49: *Location of isolation rooms in the hospital and the total pressure on the facade for the nighttime case. Measurement in* [Pa].

From figure 12.49 it is seen that with the location of the isolation rooms as showed the total pressure on the facade for all the isolation rooms are about $2,5\ Pa$. It is seen that for the isolation room on the 6th floor the total pressure is higher than for the other rooms and for the isolation room on the top floor the total pressure is lower than for the other rooms.

In figure 12.50 are showed the total pressure for the location of the windows for the isolation rooms on the different floors in the nighttime case.
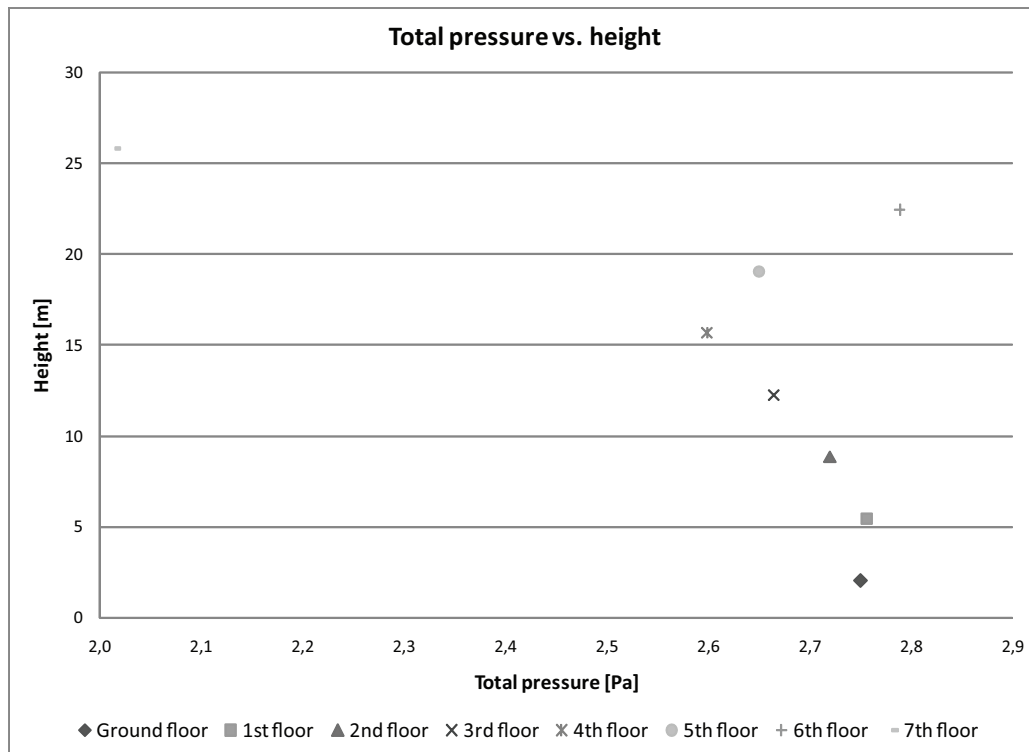
Figure 12.50: *Total pressure for the location of the windows on the different floors in the nighttime case.*

In figure 12.51 are showed the total pressure on the facade where the isolation rooms are located in the daytime case.
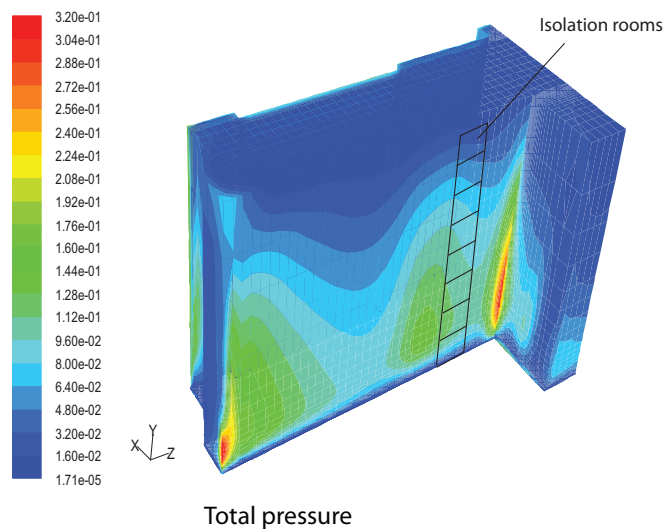
Figure 12.51: *Location of isolation rooms in the hospital and the total pressure on the facade for the daytime case. Measurement in* [*Pa*].

It is seen from figure 12.51 that the total pressure for the location of the isolation rooms

is close to 0 Pa. The highest pressure for the location of the isolation rooms is for the lower part of the hospital. Compared to the nighttime situation the pressure in the daytime situation is lower with more than 2 Pa, this means that there might be problems with creating the necessary pressure in the daytime case.

In figure 12.52 are showed the total pressure on the windows on the different floors in the daytime situation.
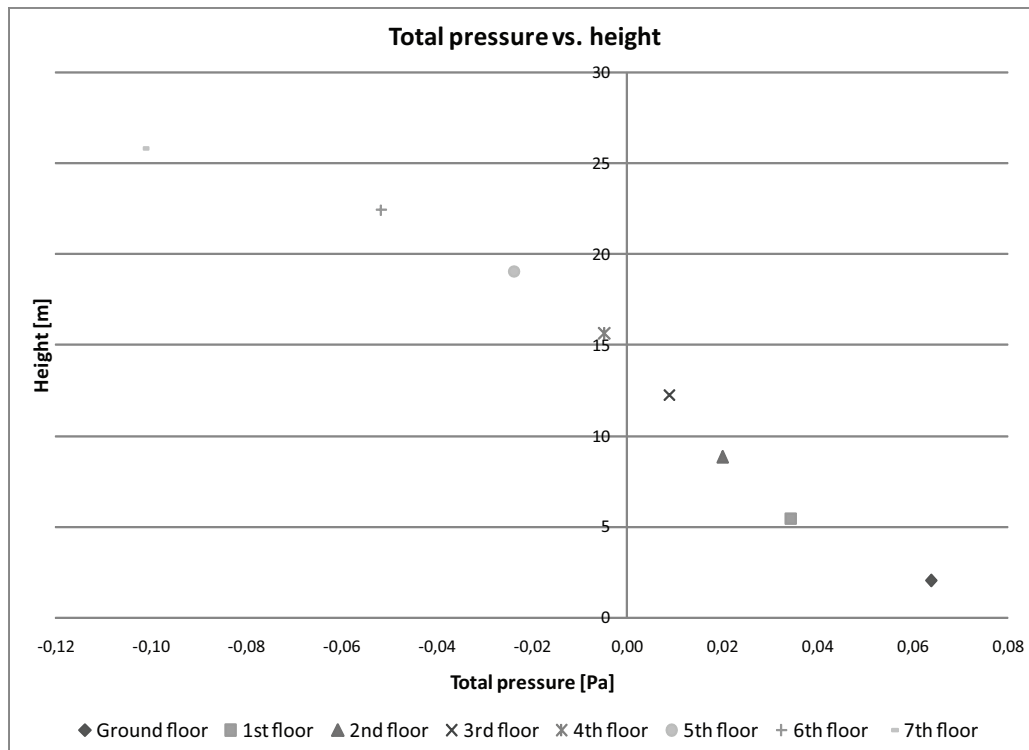
Figure 12.52: *Total pressure for the location of the windows on the different floors in the daytime case.*

From figure 12.52 it is seen that for the ground floor to the 3rd floor the total pressure is positive. For the floors above the 3rd floor the total pressure is negative. This is because of the circulation of the air at the top of the hospital and the change in direction of the wind. As shown above it is also seen that the total pressure in the daytime case is lower than for the nighttime case. Because of the negative pressure for the upper floors this does influence the airflow for the isolation room too.

To investigate the airflow for the isolation room are used the total pressure showed in figure 12.50 and 12.52.

12.4 Isolation room

To investigate the airflow for the isolation room are made a model that consist of one isolation room. For the model are used the calculated pressure for the hospital from the 3D model as showed above.

12.4.1 Identification and formulation of the problem

To investigate the airflow for the isolation room are made 3 different models which are listed below with different purpose:

Isolation room: Investigate the airflow and the air change rate for the isolation room when it is not influenced by other rooms. This is to ensure that when there are no infiltration to other rooms then the air change rate is high enough for the room.

Isolation room and corridor: Investigate the direction of the airflow between the isolation room and the corridor. To ensure the right pressure between the isolation room and the corridor to get the airflow in the desired direction.

Isolation room with an anteroom: Investigate the airflow between the isolation room and the anteroom and check the pressure between the two rooms. Ensure the right air change rate for the isolation room.

12.4.2 Specification of geometry and grid

The outline for the 3 different models listed above are showed in figure 12.53, 12.54 and 12.55.
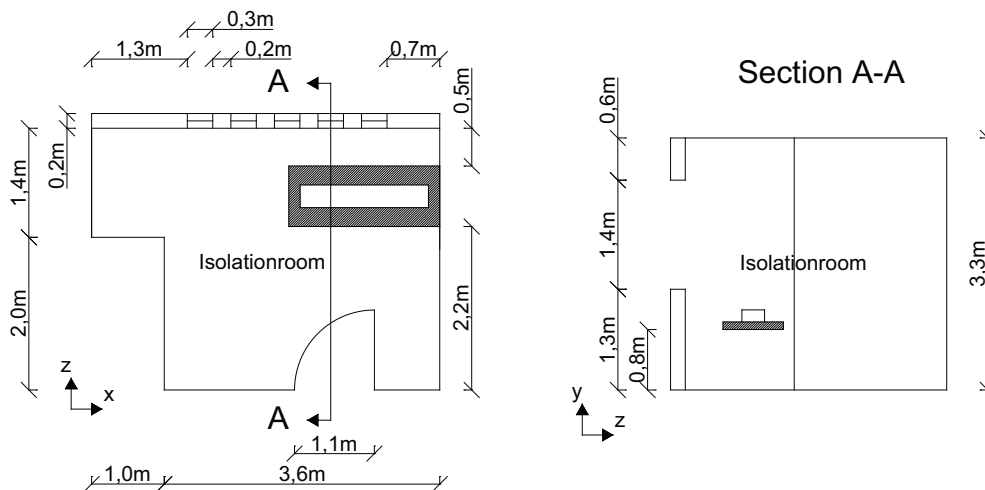
Figure 12.53: *Outline of the isolation room.*

The first model consists of only the isolation room as showed in figure 12.53. The door from the isolation to the corridor is closed and it is assumed that there is no infiltration
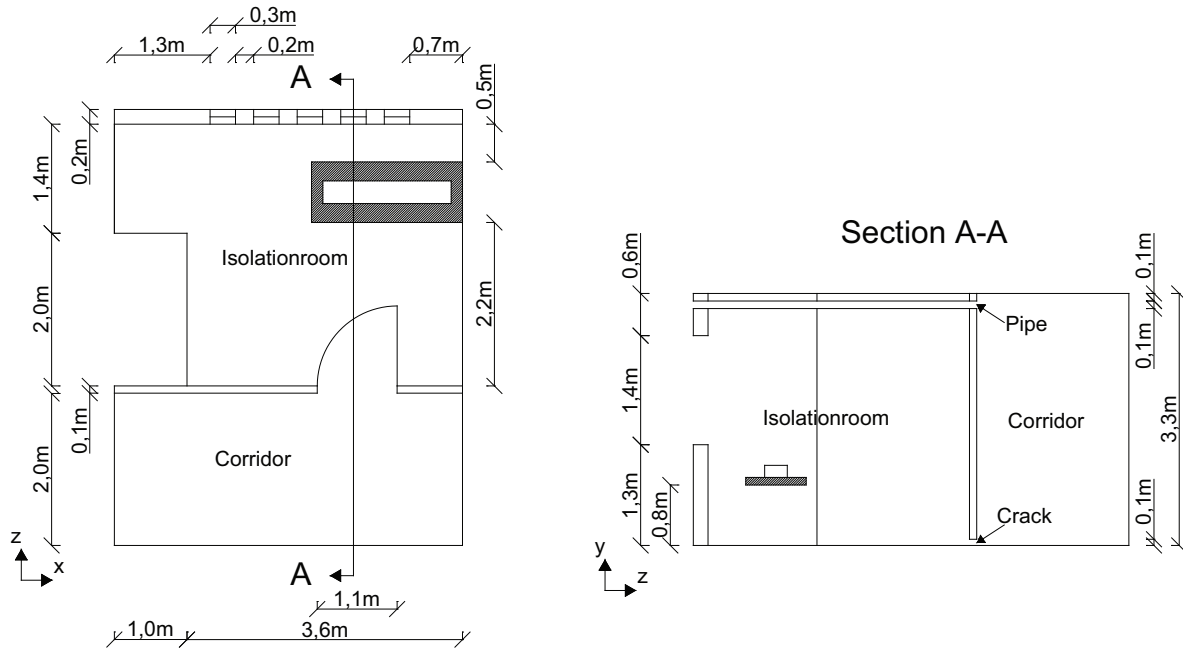
Figure 12.54: *Outline of the isolation room and the corridor.*

to and from the isolation room. For the first model the airflow for the isolation room is therefore only influenced from the windows.

For the second model is added a connection between the isolation room and the corridor as showed in figure 12.54. For the corridor is added a pipe in the top of the room that connect the corridor with the outside. Under the door between the isolation room and the corridor is also located a gap. The cross section of the pipe in the top of the room is $0,15\ m^2$ with a height and a length of $0,1\ m$ and $1,5\ m$ respectively. The area of the crack under the door is $0,11\ m^2$ with a height and a length of $0,1\ m$ and $1,1\ m$ respectively. The dimensions of the pipe and the crack are estimated from the analytical calculation of the airflow for the isolation room in chapter 9.2.
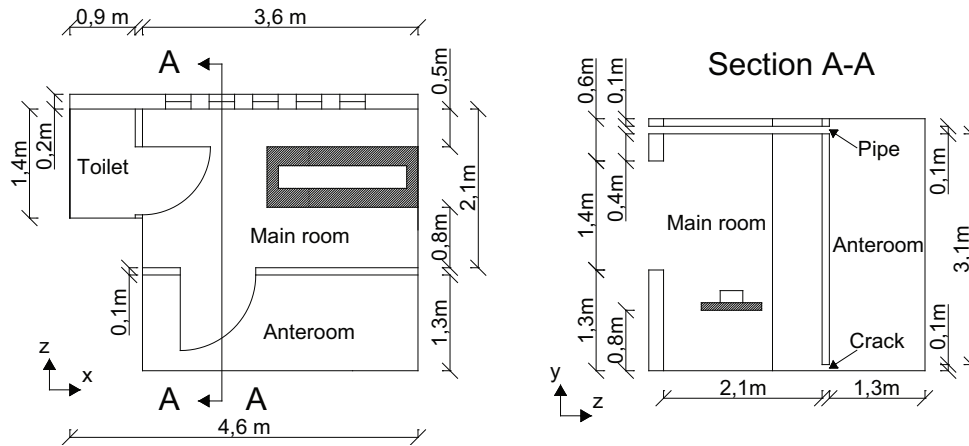
Figure 12.55: *Outline of the isolation room and the anteroom.*

The third model consists of the isolation room or the main room and an anteroom as showed in figure 12.55. Between the main room and the anteroom are two connections as for the corridor. In the top is located a pipe from the outside into the anteroom and under the door between the main room and the anteroom is a crack. The dimensions of the two openings are the same as for the corridor.

For the three models infiltration is not included. This means that the influence from the infiltration on the airflow path in the isolation room is not taken into consideration. Also the mass flow for the isolation room may differ from the real situation because infiltration is not taken into consideration. It assumed that compared to the modeled openings the influence from the infiltration is small.

The idea with the pipe in the top of the room is to let fresh outside air into the corridor or anteroom and from the corridor or anteroom into the isolation room. In situations where the outside air is colder than the inside air the airflow will be in the other direction where it is letting into the corridor or anteroom through the crack under the door from the isolation room and out through the pipe in the top. To ensure the right direction of the airflow in this situation a fan in the corridor or isolation room needs to be installed. The two situations are showed in figure 12.56.
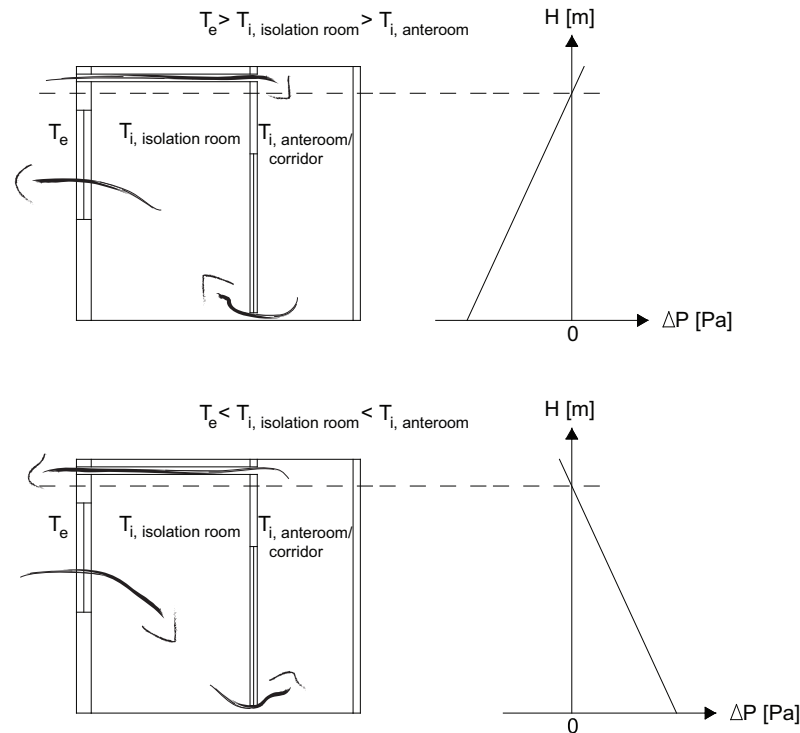
Figure 12.56: *Direction of airflow in the two situations where the outside air is warmer than inside and opposite.*

For the isolation room are placed 5 windows in the facade as showed in figure 12.53, 12.54 and 12.55. For the windows are used a discharge coefficient of 0,7. In the isolation room are located a patient on a bed. The dimensions of the patient and the bed are showed in figure 12.57.
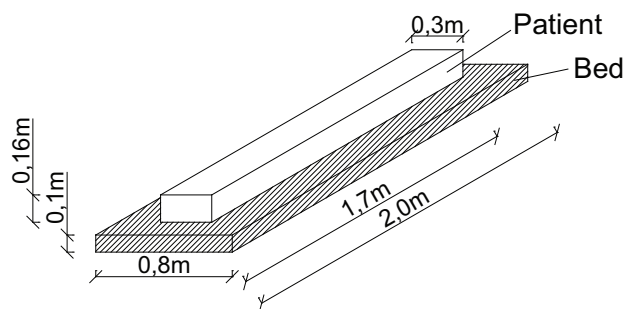
Figure 12.57: *Dimensions of the bed and the patient [Brohus and Nielsen, 1996] .*

The heat flux for the person is set for 76 W which correspond to an adult at rest. For the ceiling in the isolation room are attached a heat flux from lighting of 10 $\frac{W}{m^2}$. The heat loss from a person can be divided into 3 different categories:

Sensible heat loss $\sim$ 75 % Consists of convection and radiation heat losses that approximately account for one half each.

Latent heat loss ~ 25 % The insensible water loss range from approximately equals amounts from respiration and skin surface to a dominating evaporation heat loss from the skin surface.

Conduction Heat transfer by conduction is usually less than $1-2$ % of total and is normal ignored.

[Brohus, 1997]

For the ceiling in the isolation room is added a heat flux of $37,5$ % of the total heat flux of the person corresponding to $2 \frac{W}{m^2}$.

For the model is used the enhanced wall treatment to get a more accurate airflow near the walls. For the model the y^+ value is checked to be $y^+ > 30 \sim 60$ close to the person and the walls.

12.4.3 Specification of physical models and boundary conditions

For the simulation the RNG $k - \epsilon$ turbulence model and the enhanced wall treatment is used. The solution is steady state. The operational pressure is set to $101325 \ Pa$ and the gravitational acceleration to $9,82 \ \frac{m}{s^2}$.

Boundary condition

The boundary conditions used for the model are listed in table 12.18.

Table 12.18: *Boundary condition.*

Surface	Boundary condition
Window 1	Pressure inlet, intensity and length scale, turbulent intensity 10 %, turbulent length scale $0,1 \ m$
Window 2	Pressure inlet, intensity and length scale, turbulent intensity 10 %, turbulent length scale $0,1 \ m$
Window 3	Pressure inlet, intensity and length scale, turbulent intensity 10 %, turbulent length scale $0,1 \ m$
Window 4	Pressure inlet, intensity and length scale, turbulent intensity 10 %, turbulent length scale $0,1 \ m$
Window 5	Pressure inlet, intensity and length scale, turbulent intensity 10 %, turbulent length scale $0,1 \ m$
Patient	Wall, stationary wall, no slip, heat flux 66 $\frac{W}{m^2}$
Roof isolation room	Wall, stationary wall, no slip, heat flux 12 $\frac{W}{m^2}$
All other surfaces	Wall, stationary wall, no slip
Air	Boussinesq model, temperature 24 °C, density $1,184 \ \frac{kg}{m^3}$, thermal expansion coefficient $0,00343 \ K^{-1}$

According to the location of the isolation room there are used different pressure. The pressure for the different floors are listed in table 12.19.

Table 12.19: *Pressure for the different floors.*

Floor	Total pressure $[Pa]$	
	Daytime	**Nighttime**
Ground	0,06	2,75
1st	0,03	2,76
2nd	0,02	2,72
3rd	0,01	2,66
4th	0,0	2,60
5th	-0,02	2,65
6th	-0,05	2,79
7th	-0,10	2,02

For both the daytime and nighttime situation are used the same setup of the model only the total pressure for the windows are changed.

Solution control

The discretization scheme and under-relaxation factors used are the same as for the previous models and listed in table 12.3 and 12.4.

12.4.4 Solution

As listed above there are used pressure inlets as boundary condition for the windows. For the initial guess for the model are used the values for the middle window. For the different models the initial guess depend on the pressure on the window. The values for the initial guess for the first model with a location of the isolation room at the ground floor for the nighttime case are listed in table 12.20.

The used Fluent files are located in the subfolders 'CFD\Fluent files\3D\Isolation room', 'CFD\Fluent files\3D\Isolation room + Corridor' and 'CFD\Fluent files\3D\Isolation room + Anteroom' on the cd.

Table 12.20: *Values for the initial guess for the first model with a location of the isolation room at the ground floor for the nighttime case.*

	Value
Gauge pressure	$0\ Pa$
X velocity	$0\ \frac{m}{s}$
Y velocity	$0\ \frac{m}{s}$
Z velocity	$2,155\ \frac{m}{s}$
Turbulent kinetic energy	$0\ \frac{m^2}{s^2}$
Turbulent dissipation rate	$0\ \frac{m^2}{s^3}$
Temperature	$293\ K$

For all the models it is checked that the residuals have decreased with a factor 3 or more from the starting point to ensure that the models have converged. Also it is checked that the residuals stays stable. In the cases where the residuals have not decreased with a factor 3 or more it is checked that the monitoring points are stable and that the sum of the mass flow rate for the model is close to $0\ \frac{kg}{s}$.

To investigate the grid independence for the first model are made 3 different models with different grid. The grid size for the different models are listed in table 12.21.

Table 12.21: *Grid size for the first model.*

Model	**Grid size**
1	754 924
2	1 064 548
3	1 396 898

To check the grid independence for the model the total pressure is calculated in 7 different points. In figure 12.58 are showed the location of the different points.
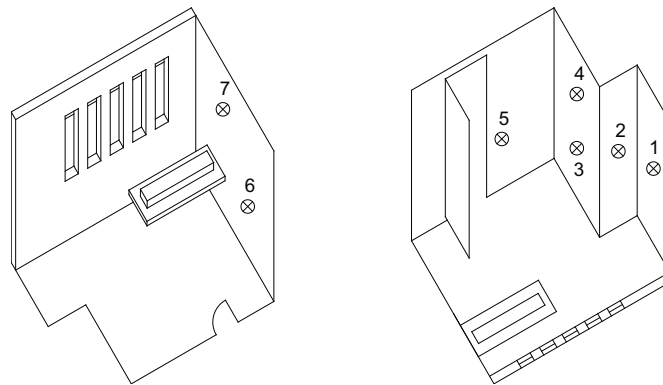
Figure 12.58: *Location of the 7 points where the total pressure is calculated.*

The total pressure for the 3 different models for the check points are showed in figure 12.59.
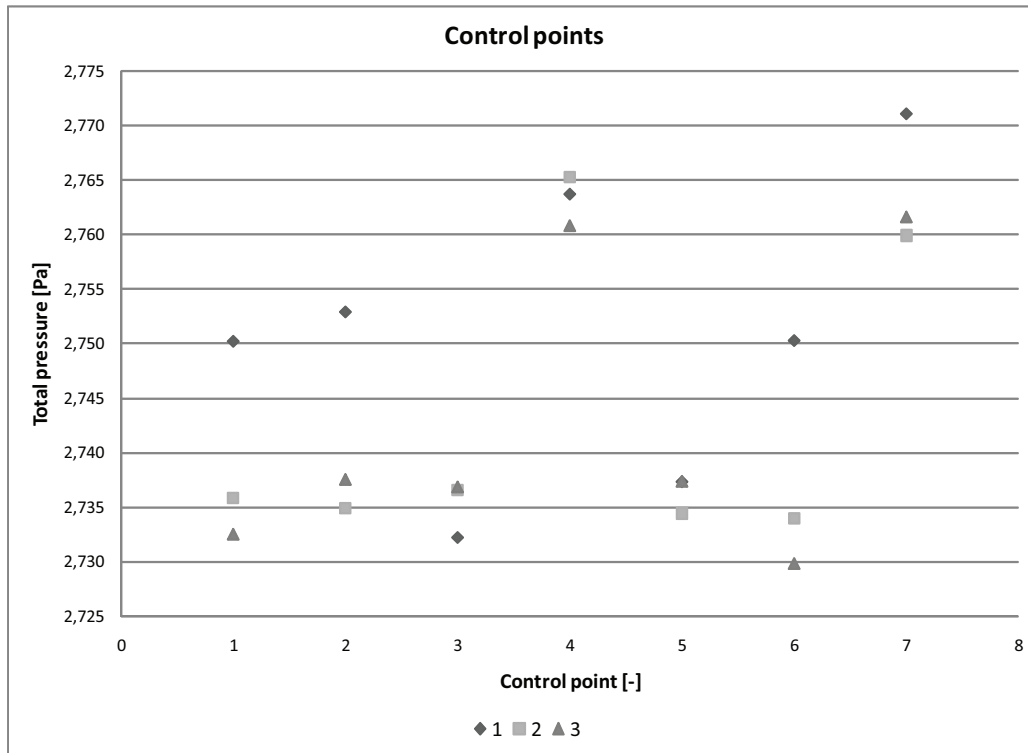
Figure 12.59: *Total pressure for the 3 different models for the check points.*

From figure 12.59 it is seen that there is a small variation in the total pressure for the different models. It is also seen that the greatest variation is about $0,015\ Pa$. For the 3 different models it is seen that the greatest variation between the models is for model 1 compared to model 2 and 3. Because of the small variation between the models it is chosen not to decrease the grid even further. Since the results from model 2 and 3 are close to each other and the greatest variation between the two models are $0,005\ Pa$ model 2 are used for further simulations according to the simulation time. The grid size from the first model are used for the 2 other models too.

The first model is used to investigate the air change rate and the airflow for the isolation room when it is not influenced by other rooms.

According to the location of the windows on only one side for the isolation room single sided ventilation is used for the room. Depending on the temperature of the inside air and the outside air the airflow will be different. Below are described the airflow and air change rate in the two situations; daytime and nighttime.

Nighttime case, model 1

In the nighttime case the outside temperature is set to 20 $°C$ as listed in chapter 12.1. For the isolation room is used an air temperature of 24 $°C$. For the nighttime case the inside temperature is therefore higher than the outside temperature therefore the air will be getting into the isolation room in the bottom of the window and out in the top of the window. The principle for the airflow in the nighttime case is showed in figure 12.60.
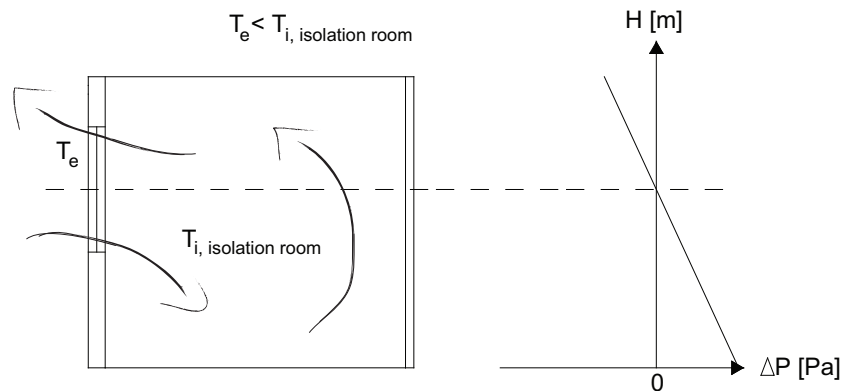
Figure 12.60: *Principle for the airflow in the nighttime situation where the indoor temperature is higher than the outside temperature.*

In figure 12.61 are showed the airflow for a plane through the first window for the isolation room.
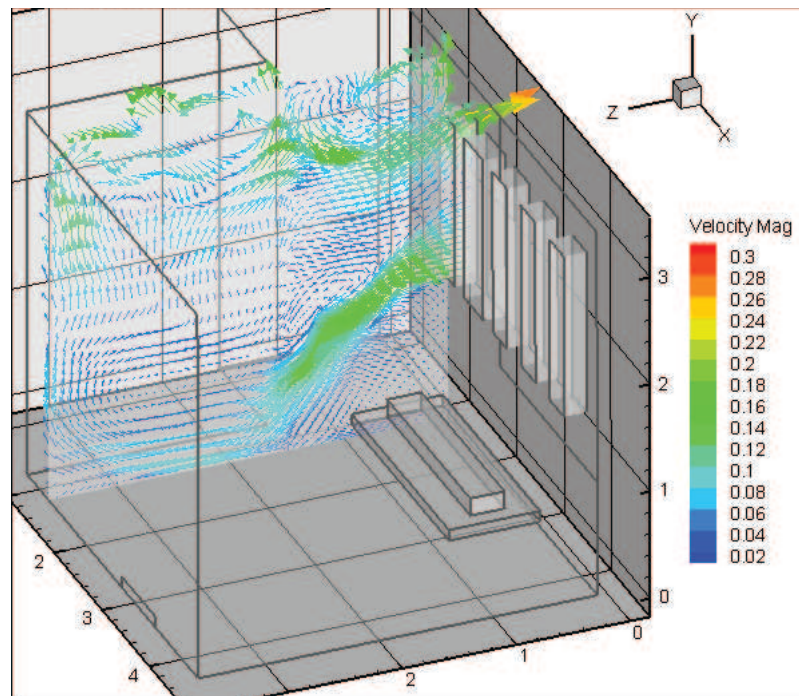
Figure 12.61: *Airflow for the isolation room for a plane through the first window.*

From figure 12.61 it is seen that there is an inflow for the room in the bottom of the window and an outflow through the top of the window because of the higher inside temperature than outside temperature. It is also seen that the direction of the air coming into the room is downwards because of the lower temperature of the outside air than inside. When the air is reaching the floor it changes direction and flows along the floor until the opposite wall. At the wall the air changes direction and flow upwards towards the ceiling. At the ceiling the direction of the air is different in different places. In the ceiling is installed light with a heat flux, the light is assumed to be on 24 hours a day. This means that the air at the ceiling gets heated up more than for the rest of the room and therefore the direction of the air at the ceiling is not constant. It is seen that for the room the lowest velocity of the air is in the lower left part of the plane and the highest velocity is at the window opening and the ceiling. Because the airflow is influenced thermal buoyancy the highest velocity is where the highest temperature difference is.

In figure 12.62 are showed the airflow close to the person and the window.
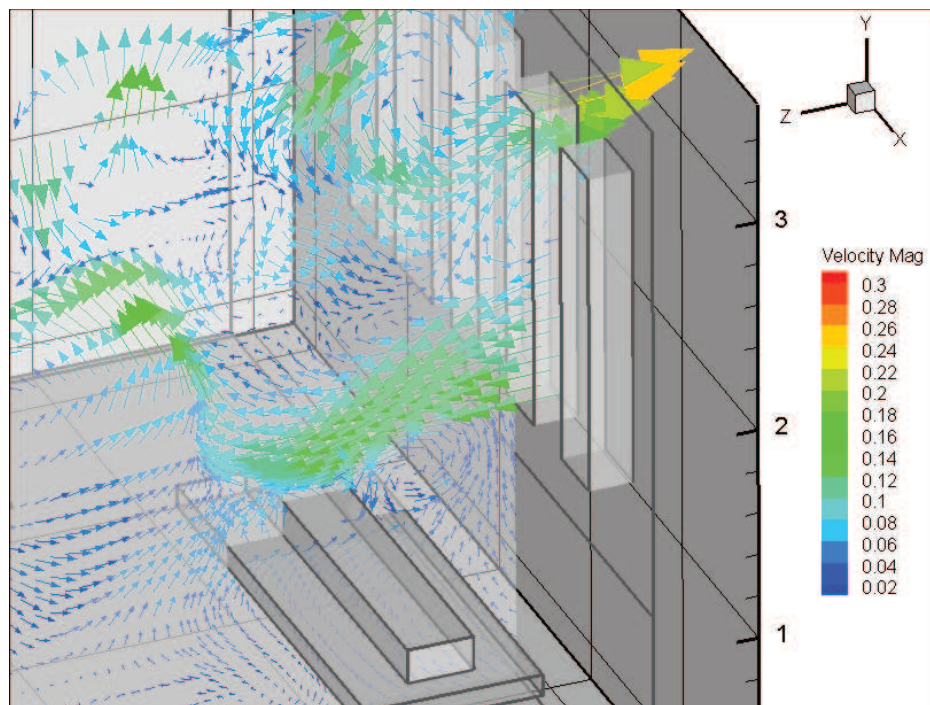
Figure 12.62: *Airflow for the isolation room for a plane through the fourth window around the person.*

From figure 12.62 it is seen that when the air reaches the person it gets heated up and change direction towards the ceiling. It is also seen that the air around the person also gets heated up and have a direction upwards. At the right side of the person it is seen that there is some circulation because of the cold air that flows into the room and the warmer person.

With the location of the windows and the person as showed in the figures above the fresh air is let into the room through the bottom of the window and hits the person. After it hits the person it does flow either further into the room or towards the ceiling. In the situation where the person is infected with an airborne infection the air will be infected when it passes the person and thereafter the air will flow further into the room. To ensure that no other people are being infected from the person the air should get out of the room after it has passed by the person and not further into the room. In the night situation there might therefore be a risk for other people in the room getting infected because of the airflow as showed above.

To investigate the influence from both the wind pressure on the windows and the effect from the temperature difference between inside and outside are made two calculations. For the first calculation the indoor temperature is set as the same as the outside temperature which is 20 $°C$. This is to investigate the influence of the wind pressure only. In the other situation the indoor temperature is set to 24 $°C$ and the outside temperature to 20 $°C$. In this case both the effect from the wind pressure and the temperature difference is taken into consideration. To ensure an air temperature of 24 $°C$ in the isolation when the outside temperature is 20 $°C$ it might be necessary to heat the room because the cooler outside air will cool the room.

For the isolation room all the windows are located in the same height and with the same area. In figure 12.64 are showed the z-velocity for the first window for 7 different locations. The 7 different locations are showed in figure 12.63.
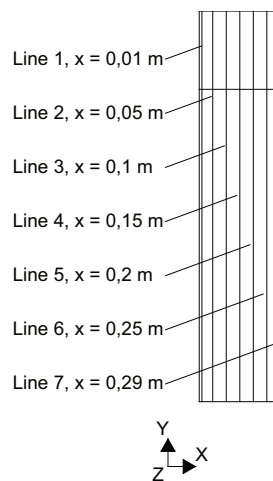
Figure 12.63: *Different locations for the window for calculation the velocity.*
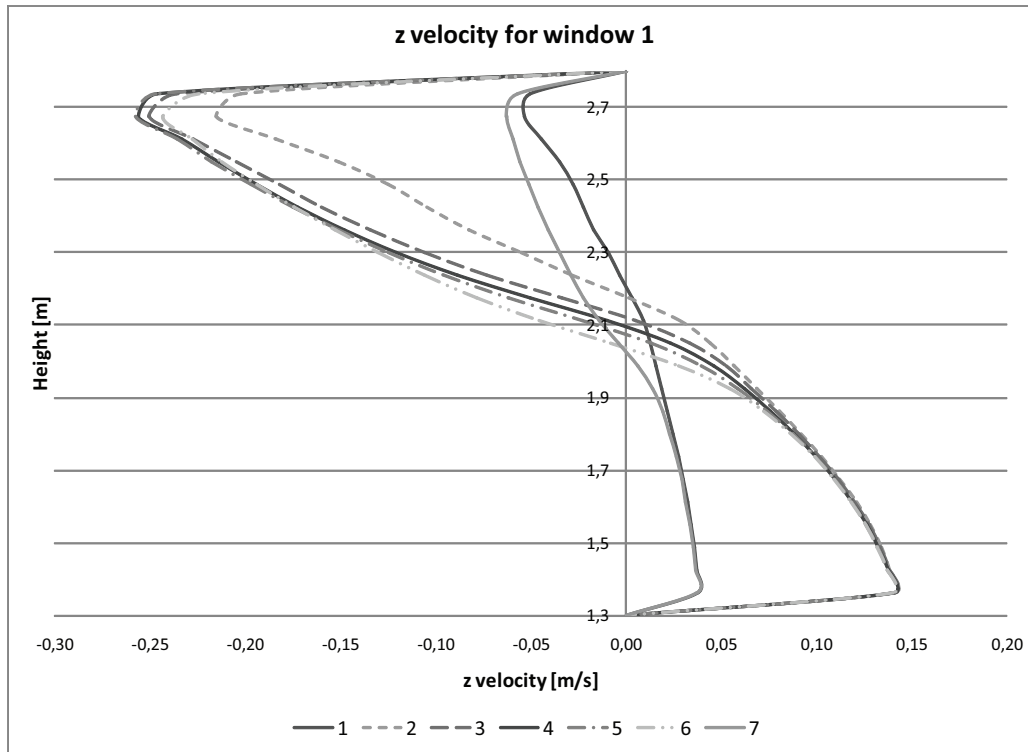
Figure 12.64: *z-velocity for the first window for the 7 different locations showed in figure 12.63.*

In figure 12.64 it is seen that the z-velocity varies for the different locations. The velocity is lowest for line 1 and 7. For the lines 2-6 the velocity are almost the same. It is seen that there is a variation for line 2 compared to the lines 3-6. Line 2 is located $0,05\ m$ from the side of the window, so this variation might be because the close location to the side. The same variation is not seen for line 6 even though this line is also located $0,05\ m$ from the side of the window. Since the two lines are located in the same distance from the window the velocity profile for these two should be the same. A reason why this might not be happening is that both the interior and exterior and the heat fluxes are not symmetric. Also line 7 is closer located to the next window which might have influence on the airflow too.

The neutral point for the window is found where the z-velocity is 0. From figure 12.64 it is seen that for the different lines the z-velocity is 0 in different heights. The location of the neutral point according to the velocity profile for the different lines are listed in table 12.22.

Table 12.22: *Location of neutral point for the 7 different lines.*

Line	Neutral point $[m]$
1	2,21
2	2,18
3	2,12
4	2,09
5	2,07
6	2,04
7	2,03

From table 12.22 it is seen that the location of the neutral point for the different lines does vary a bit. The neutral point is located in the highest position for line 1 and gets lower for the other lines. The middle of the window is located in a height of $2,05\ m$ from the floor. It is seen that the neutral point for the lines 1, 2, 3, 4 and 5 are located over the middle of the window while the neutral point for the lines 6 and 7 are located below. The reason why the neutral point for the different lines are not located in the middle of the window might be according to the influence on the airflow from the heat flux from the person and the light in the ceiling. Also the theoretical location of the neutral point might be displaced from the middle of the window according to density differences of the air. So the theoretical neutral point might be located lower than the middle of the window. Because of the wind influence the neutral point might also be displaced. The difference in the location of the neutral point for the different lines might also be according to the influence on the airflow because of the person and the temperature difference around the person, the ceiling and the windows. The person in the room is located closest to line 7 and furthest away from line 1. It is also seen that the variation in the location of the neutral point for the different lines is less than $0,2\ m$. To calculate the location of the neutral point for the room the neutral point for all 5 windows for line 4 is calculated. The location of the neutral point for the different windows are listed in table 12.23.

Table 12.23: *Location of neutral point for the 5 windows.*

Window	Neutral point $[m]$
1	2,09
2	2,16
3	2,28
4	2,28
5	2,30

Again it is seen that there is a small variation in the location of the neutral point for the 5 different windows as listed in table 12.23. For all the windows the neutral point is also located above the theoretical neutral point. It is therefore seen that for the room the location of the neutral point does vary according to the location.

The airflow rate for the room is calculated by:

For airflow through the bottom of the window:

$$q = (H_n - H_b) \cdot W_{win} \cdot U_{m,b} \tag{12.12}$$

For airflow through the top of the window:

$$q = (H_t - H_n) \cdot W_{win} \cdot U_{m,t} \tag{12.13}$$

where

q	:	Airflow rate $[\frac{m^3}{s}]$
H_n	:	Location of neutral point $[m]$
H_b	:	Height of bottom of window $[m]$
H_t	:	Height of top of window $[m]$
W_{win}	:	Width of window $[m]$
$U_{m,b}$	:	Mean air velocity below the neutral point $[\frac{m}{s}]$
$U_{m,t}$	:	Mean air velocity above the neutral point $[\frac{m}{s}]$

The mean air velocity and the airflow rate for the 5 windows are listed in table 12.24.

Table 12.24: *Mean air velocity and airflow rate for the 5 windows. Positive values are airflow into the room and negative values is airflow out of the room.*

Window	Location	Mean air velocity $[\frac{m}{s}]$	Airflow rate $[\frac{m^3}{s}]$
1	Bottom	0,089	0,021
	Top	-0,144	-0,031
2	Bottom	0,080	0,027
	Top	-0,114	-0,029
3	Bottom	0,077	0,030
	Top	-0,117	-0,024
4	Bottom	0,084	0,025
	Top	-0,132	-0,021
5	Bottom	0,081	0,024
	Top	-0,136	-0,020
Total	Bottom	0,082	0,128
	Top	-0,128	-0,125

From the airflow rate for the different windows the air change rate for the room is calculated. The air change rate for the room is calculated from:

$$n = \frac{q}{V} \cdot 3600 \tag{12.14}$$

From the total airflow rate listed in table 12.24 the air change rate for the isolation room with a volume of $47,6\ m^3$ is calculated from equation (12.14) to $9,6\ h^{-1}$.

The calculation of the air change rate is made for the situation where the isolation room is located at the ground floor and is not influenced by any other rooms. The calculation is made in the nighttime case where the isolation room is located on the windward side of the building which is the side facing towards the mountain and the temperature difference between inside and outside is not taken into consideration. In this situation it is seen that the air change rate does not satisfy the requirements for the air change rate of an isolation room of $12\ h^{-1}$. The air change rate for the isolation room located on the different floors are listed in table 12.25.

Table 12.25: *Air change rate in the nighttime case for the isolation room located on different levels in the hospital.*

Location	Neutral point $[m]$	Air change rate $[h^{-1}]$
Ground floor	2,22	9,6
1st floor	2,22	9,6
2nd floor	2,27	10,0
3rd floor	2,26	10,1
4th floor	2,20	9,8
5th floor	2,26	10,1
6th floor	2,22	10,2
7th floor	2,24	8,6

From table 12.25 it is seen that the air change rate for the isolation room located on either of the different floors does not satisfy the requirements of $12\ h^{-1}$. The highest air change rate is for the isolation room located on the 6th floor with an air change rate of $10,2\ h^{-1}$.

From the calculations it is therefore seen that with the used layout of the isolation room it is not possible to create a satisfying air change rate for the room in the nighttime situation where only wind pressure is taken into consideration.

In figure 12.65 are showed the air change rate as a function of the pressure for the different floors.
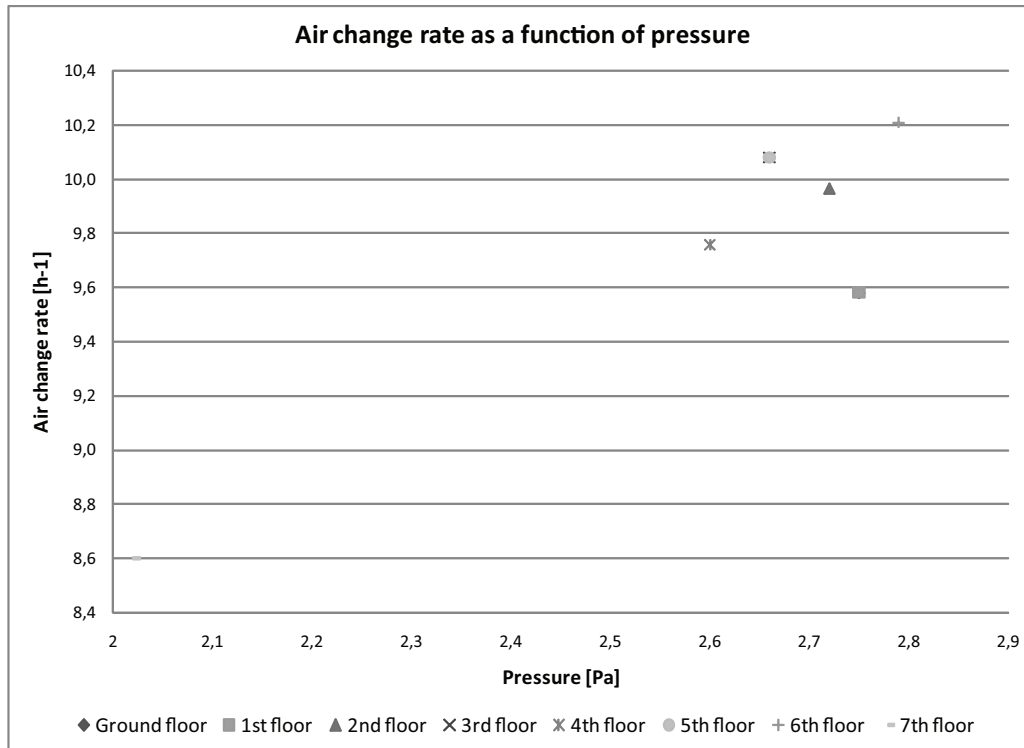
Figure 12.65: *Air change rate as a function of pressure for the different floors.*

From figure 12.65 it is seen that the highest air change rate is for the 6th floor where also the highest pressure are. The lowest air change rate is for the 7th floor where also the lowest pressure are. According to the pressure for the ground and 1st floor the air change rate is too low and for the 3rd and 5th floor the air change rate is too high compared to the pressure. A reason why the data from the ground, 1st, 3rd and 5th floor varies can be according to the way the air change rate is calculated. For the calculation is used the average velocity for a slice in the middle of the window. Since the room and the heat fluxes for the room is not symmetric the velocity varies for the window. Another reason might be that because the variation is small, a small inaccuracy for the calculation will create a great variation.

As stated above it is therefore not possible only by wind pressure created by the mountain breeze to ensure a high enough air change rate for the isolation room. In the following is investigated the influence from both the wind pressure and the temperature difference for the isolation room. The calculations of the air change rate for the isolation in the situation with both temperature difference and wind pressure are done in the same way as for the situation only with wind pressure.

The location of the neutral point and the air change rate for the different floors are listed in table 12.26. The calculation of the neutral point is the average value of the neutral point in the middle of the 5 windows.

Table 12.26: *Location of neutral point and air change rate in the nighttime case with both temperature difference and wind pressure for the isolation room located on different levels in the hospital.*

Location	Neutral point $[m]$	Air change rate $[h^{-1}]$
Ground floor	2,13	23,6
1st floor	2,13	23,6
2nd floor	2,11	23,4
3rd floor	2,14	23,6
4th floor	2,15	23,7
5th floor	2,14	23,6
6th floor	2,14	23,4
7th floor	2,14	23,6

Compared to the situation with only wind pressure it is seen in table 12.26 that when the temperature difference is taken into consideration it is possible to create an air change rate for the room that is higher than 12 h^{-1}. When the temperature difference between inside and outside is taken into consideration the air change rate for the room is about twice as high as when only the wind pressure is taken into consideration. It is also seen that when both the temperature difference and wind pressure is taken into consideration the location of the neutral point is about $0, 1$ m lower than for the situation with only the wind pressure as listed in table 12.25. The lower location might be because of the higher increase in the inlet velocity compared to the outlet velocity from the situation with only wind pressure to the situation with both wind pressure and temperature difference.

The air change rate as a function of the pressure is showed in figure 12.66.
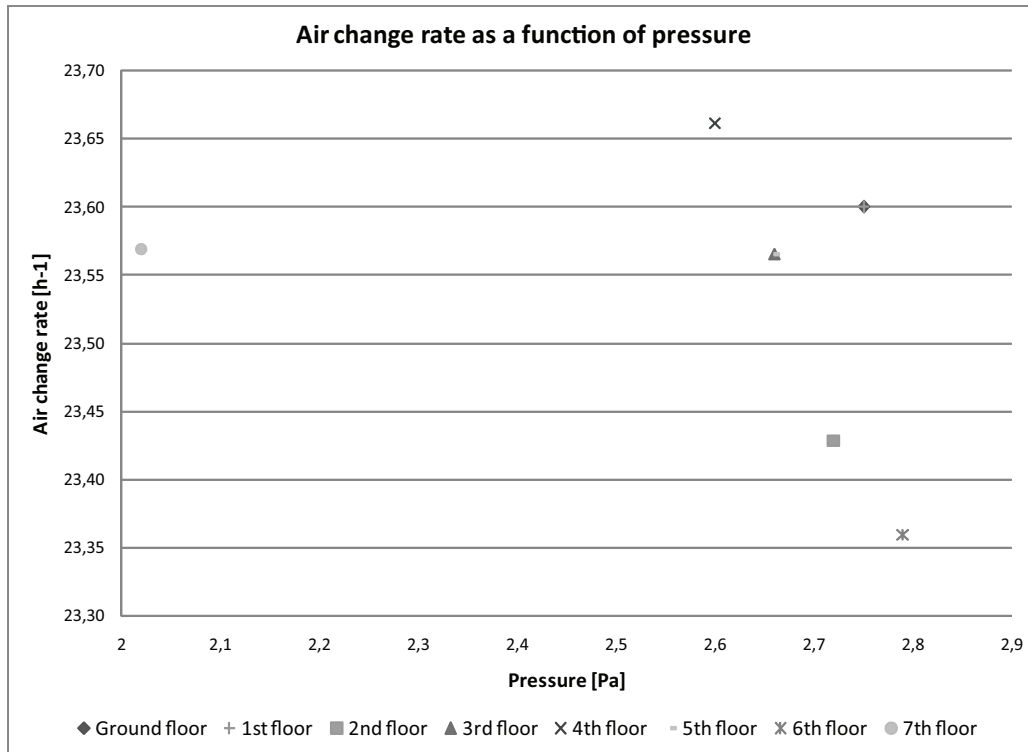
Figure 12.66: *Air change rate as a function of pressure in the nighttime case where the temperature difference is taken into consideration.*

It is seen from figure 12.66 that the air change rate does not depend as much on the pressure for the opening as in the situation without any temperature difference. From the figure it is seen that the highest air change rate is for the 4th floor with an air change rate of $23, 6 \ h^{-1}$. It is also seen that the air change rate is lowest for the 2nd floor with an air change rate of $23, 4 \ h^{-1}$. From the figure it is also seen that the variation in the air change rate for the different floors is small.

A reason why the air change rate does not depend as much on the pressure as for the situation without the temperature difference might be because the influence of the temperature. As stated above the air change rate with both temperature difference and wind pressure is about twice the air change rate with only wind pressure. Therefore the pressure does not have as great an influence as in the case with only wind pressure. For the situation the thermal buoyancy is dominating.

In the situation listed above the temperature difference between inside and outside is about $4 \ ^{\circ}C$ and the average air change rate is about $23, 6 \ h^{-1}$. It is therefore seen that in the case with both temperature difference and wind pressure the air change rate satisfy the requirement of an air change of minimum $12 \ h^{-1}$ for an isolation room. To ensure this air change rate it is also seen that with the wind pressure alone it is not possible to create the desired air change rate. Therefore it need to be ensured that there is an temperature difference between inside and outside to create the desired air change rate for the nighttime

case or cross ventilation need to be used.

Daytime case, model 1

For the daytime case are used an outside temperature of 25 $°C$ and an inside temperature of 24 $°C$. Because of the higher outside temperature than inside temperature the direction of the airflow will be opposite the direction of the airflow in the nighttime case. The principle of the airflow in the daytime case is showed in figure 12.67.
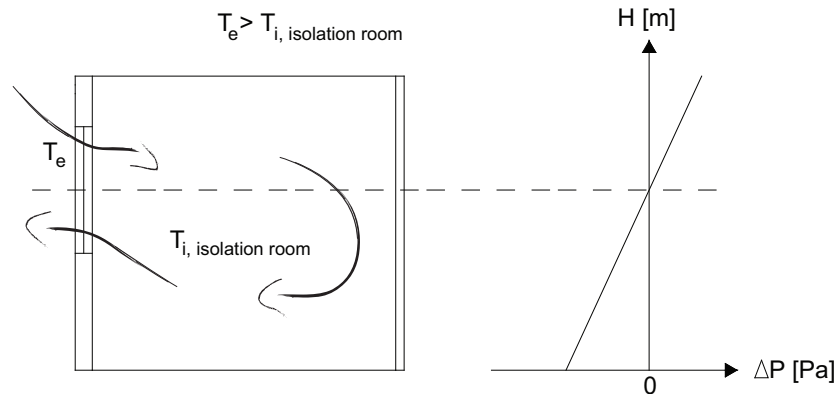
Figure 12.67: *Principle for the airflow for the isolation room in the daytime case.*

From the principle of the airflow showed in figure 12.67 it is seen that for the daytime case the air is getting into the room through the top of the window and out through the bottom because of the temperature distribution.

As showed in figure 12.52 the pressure for the isolation room in the daytime case varies between being positive for the lower floors and negative for the upper floors. In the situation where the pressure for the isolation room is positive this will create an airflow opposite the direction showed in figure 12.67 when only the wind pressure is taken into consideration. This means that in the case where the pressure is positive this will act against the airflow created because of the temperature difference where the inflow is in the top of the window. In figure 12.52 it is also seen that compared to the night situation the wind pressure is low. For the night situation it is investigated that it is not possible to create a high enough air change rate only with wind pressure and since the pressure is lower in the daytime case it is concluded that it is not possible for this situation to create a satisfying air change rate only according to the wind pressure. In the following are therefore investigated the airflow according to both temperature difference and wind pressure.

In figure 12.68 is showed the airflow for a plane through the first window in the isolation room.
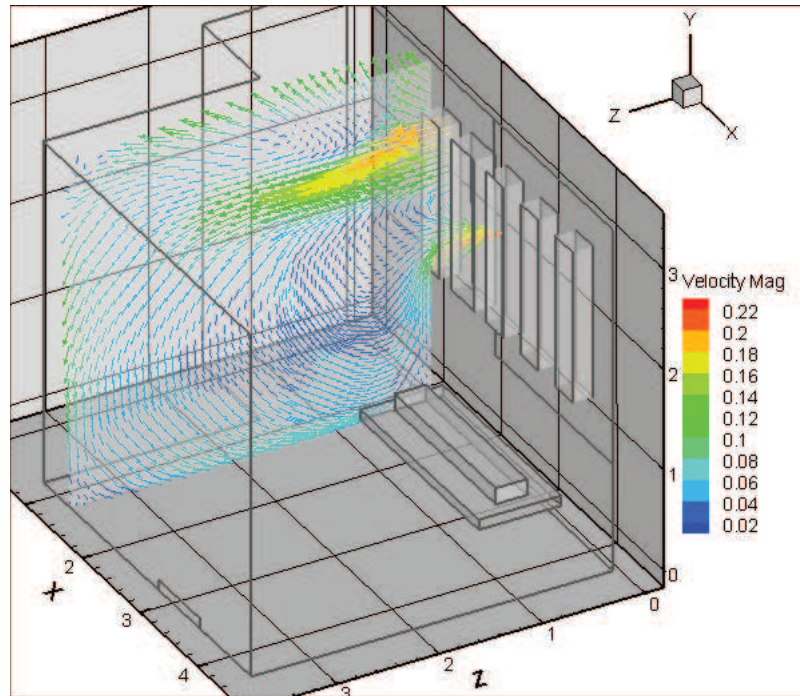
Figure 12.68: *Airflow for the isolation room for a plane through the first window.*

From figure 12.68 it is seen that the air is getting into the room through the top part of the window and out through the bottom. Depending on the height in which the air is getting into the room it creates a loop that flows into the room with different depths. In the top of the room the direction of the wind is upwards because of the higher temperature at the ceiling.

In figure 12.69 is showed the airflow closer to the 4th window.
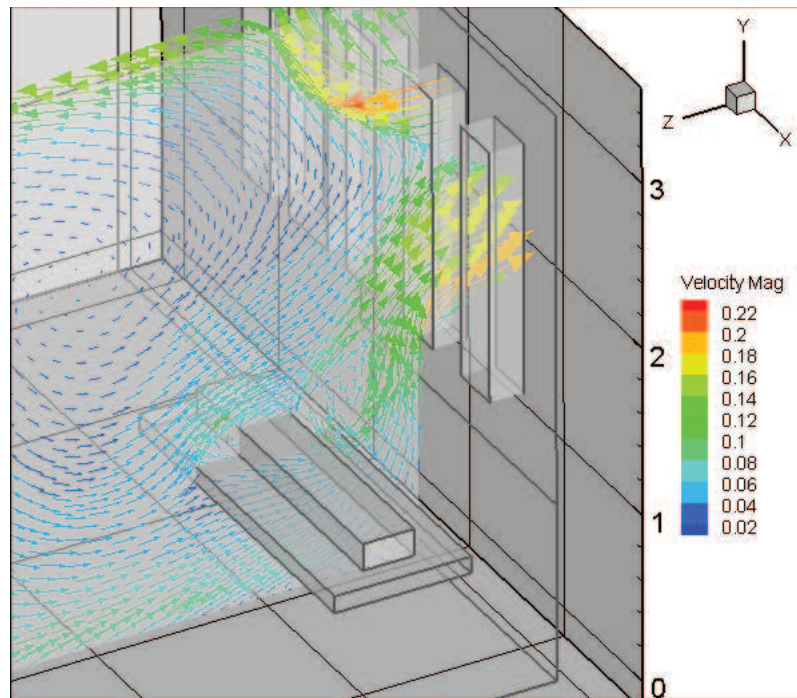
Figure 12.69: *Airflow around the patient in the isolation room.*

From figure 12.69 it is seen that the air hits the patient in the bed at the side furthest away from the window. When the air hits the bed it separate into two directions, where some of the air passes above the bed and the patient and some of the air passes by under the bed. At the side of the patient closest to the window there is some circulation because of the lower pressure on this side of the person. When the air has passed the patient it flows out through the window.

For the airflow through all the windows it is seen that the air is letting into the room through the top and out through the bottom. With the airflow shown in the figures above it is seen that the air is getting into the room before it hits the person. When it has passed by the person it leaves the room straight after. Because the air leaves the room straight after it has passed by the patient any deceases spread by the patient is not letting into the room. With this airflow it is therefore possible to have other people in the room without they are getting infected by the patient.

For calculating the air change rate for the room are used the same method as for the nighttime case where the neutral point and the average wind speed for the windows are calculated. To investigate the variation of the location of the neutral point for a single window are used the first window for the isolation room. The z-velocity for the window for the 7 lines showed in figure 12.63 are showed in figure 12.70.
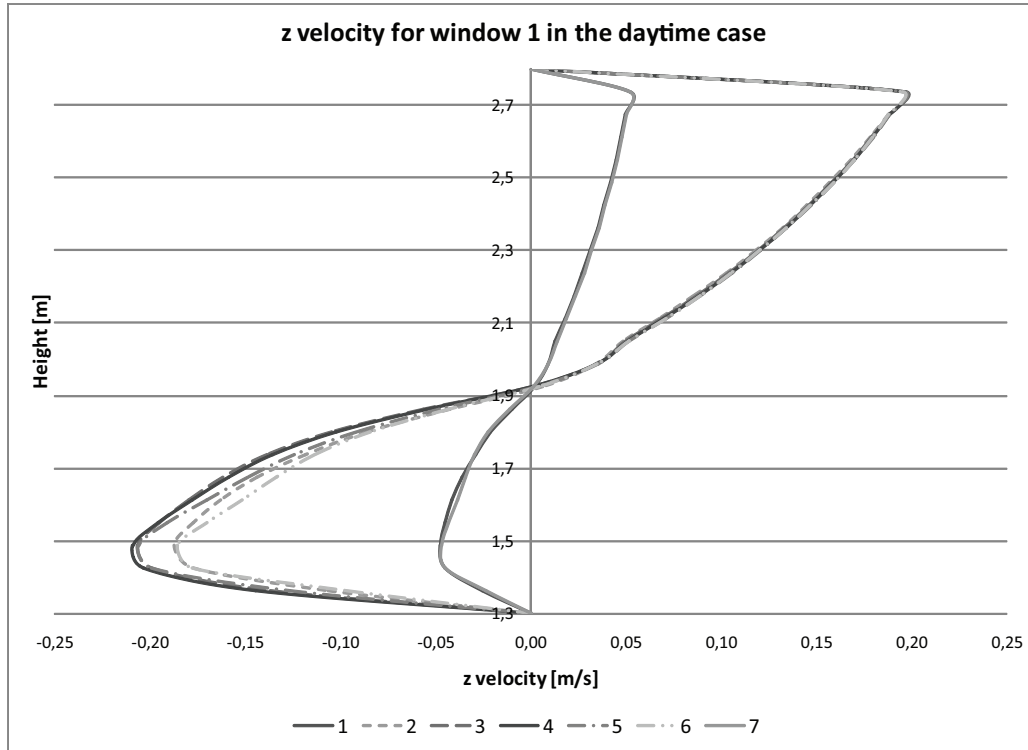
Figure 12.70: *z-velocity through the first window for the isolation room located on the ground floor in the daytime case.*

From figure 12.70 it is seen that for the 7 different lines the neutral point is located in almost the same height this is because the thermal buoyancy is dominating. Compared to the nighttime the variation in the location of the neutral point is small. Because the dominance of the thermal buoyancy in the daytime case the variation is smaller than for the nighttime case.

The location of the neutral point for the 7 different lines are listed in table 12.27.

Table 12.27: *Location of neutral point for the 7 different lines for the first window for the isolation room located on the ground floor in the daytime case.*

Line	Neutral point $[m]$
1	1,915
2	1,917
3	1,924
4	1,924
5	1,921
6	1,919
7	1,920

From table 12.27 it is seen that the variation in the location is small and for all the

different lines the neutral point is located in almost the same level.

Because of the small variation in the location of the neutral point for the different lines the location of the neutral point for the different windows are calculated in the middle of the window for line 4. The location of the neutral point for the different windows are listed in table 12.28.

Table 12.28: *Location of neutral point for the the different windows for the isolation room located on the ground floor in the daytime case.*

Line	Neutral point $[m]$
1	1,92
2	1,95
3	2,03
4	2,34
5	2,20

The airflow rate for the isolation room is calculated from equation (12.12) and equation (12.13). The mean air velocity and airflow for the 5 windows for the isolation room on the ground floor is listed in table 12.29.

Table 12.29: *Mean air velocity and airflow rate for the 5 windows for the isolation room on the ground floor in the daytime case.*

Window	Location	Mean air velocity $[\frac{m}{s}]$	Airflow rate $[\frac{m^3}{s}]$
1	Bottom	-0,14	-0,03
	Top	0,11	0,03
2	Bottom	-0,12	-0,03
	Top	0,12	0,04
3	Bottom	-0,13	-0,04
	Top	0,12	0,04
4	Bottom	-0,13	-0,03
	Top	0,10	0,02
5	Bottom	-0,12	-0,03
	Top	0,08	0,02
Total	Bottom	-0,13	-0,16
	Top	0,11	0,14

From the airflow listed in table 12.29 the air change rate for the room is calculated from equation (12.14). The air change rate for the isolation room located on the different floors are listed in table 12.30.

Table 12.30: *Air change rate in the daytime case for the isolation room located on different levels in the hospital.*

Location	Air change rate $[h^{-1}]$
Ground floor	11,4
1st floor	11,4
2nd floor	11,4
3rd floor	11,4
4th floor	11,2
5th floor	11,6
6th floor	11,5
7th floor	11,4

It is seen from table 12.30 that the air change rate for any of the floors does not satisfy the desired air change rate of 12 h^{-1}. For the daytime case the temperature between inside and outside is only 1 $^\circ C$. From table 12.19 it is seen that for the daytime case the wind pressure is both positive and negative for the windows but for all situations close to 0 Pa. It is seen in table 12.30 that in the situations with a positive pressure the air change rate is lower than in the situations with a negative pressure. This is according to the airflow direction created by the temperature difference, where a positive wind pressure will create an inflow in the top of the window and therefore act against the inflow direction created by the temperature difference.

With the location of the isolation rooms in the hospital as showed in figure 12.51 it is therefore not possible with the used setup to create a high enough air change rate. Because of the low wind pressure for the daytime case it is necessary to create a greater temperature difference between inside and outside to ensure a high enough air change rate.

Nighttime case, model 2

For the second model it is seen in figure 12.54 that the isolation room is connected to the corridor with a door. To get an airflow into the corridor only by using natural ventilation are made a pipe in the top of the room that connect the corridor with the outside. Under the door are located a crack that connect the isolation room and the corridor. The principle is shown in figure 12.54.

The boundary condition for the opening of the pipe is set for pressure outlet as for the windows. In figure 12.71 are showed the airflow through the pipe and into the corridor for the nighttime case.
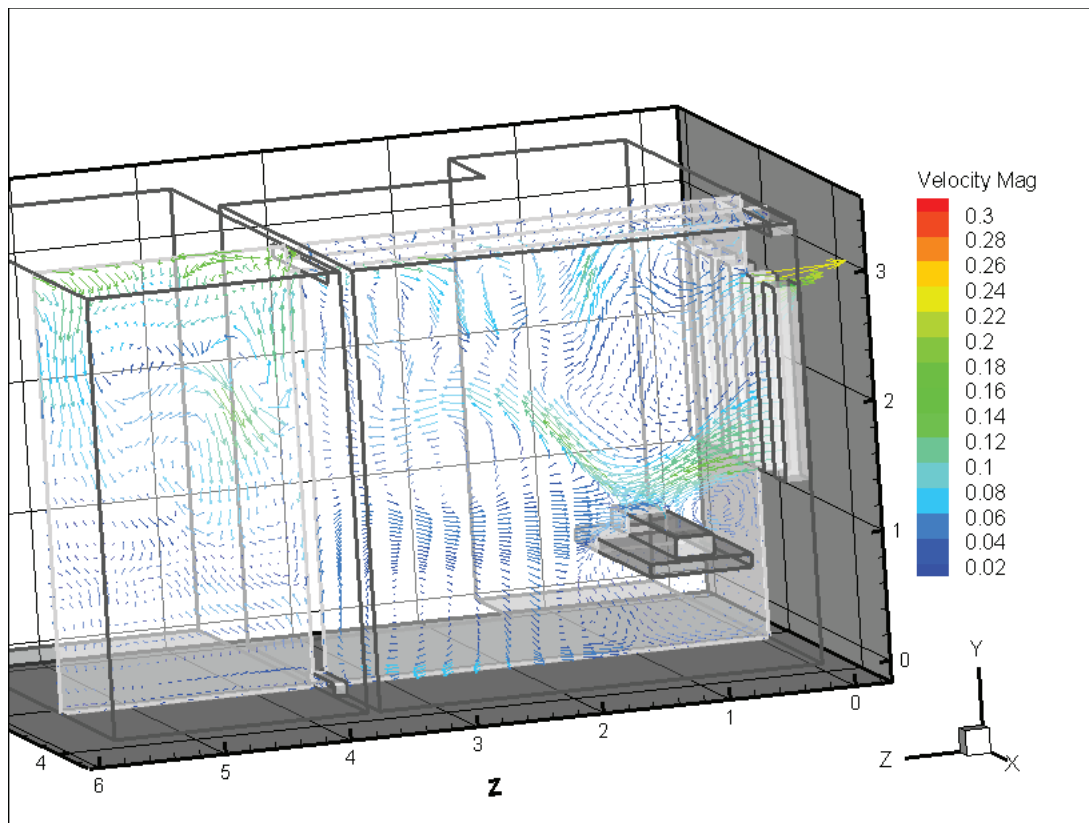
Figure 12.71: *Airflow through the pipe between the outside and the corridor.*

It is seen from figure 12.71 that there almost are no airflow through the pipe. In figure 12.72 are showed the airflow at the inlet and outlet of the pipe and through the crack under the door. The temperature for the isolation room and the anteroom is set for the same temperature, for the connection between the anteroom and the isolation room under the door the pressure difference is 0 Pa this means that only the pressure difference at the inlet for the pipe should drive the flow. From figure 12.71 it is seen that this pressure difference is not high enough to create the desired airflow.

Pipe opening into corridor

Pipe inlet
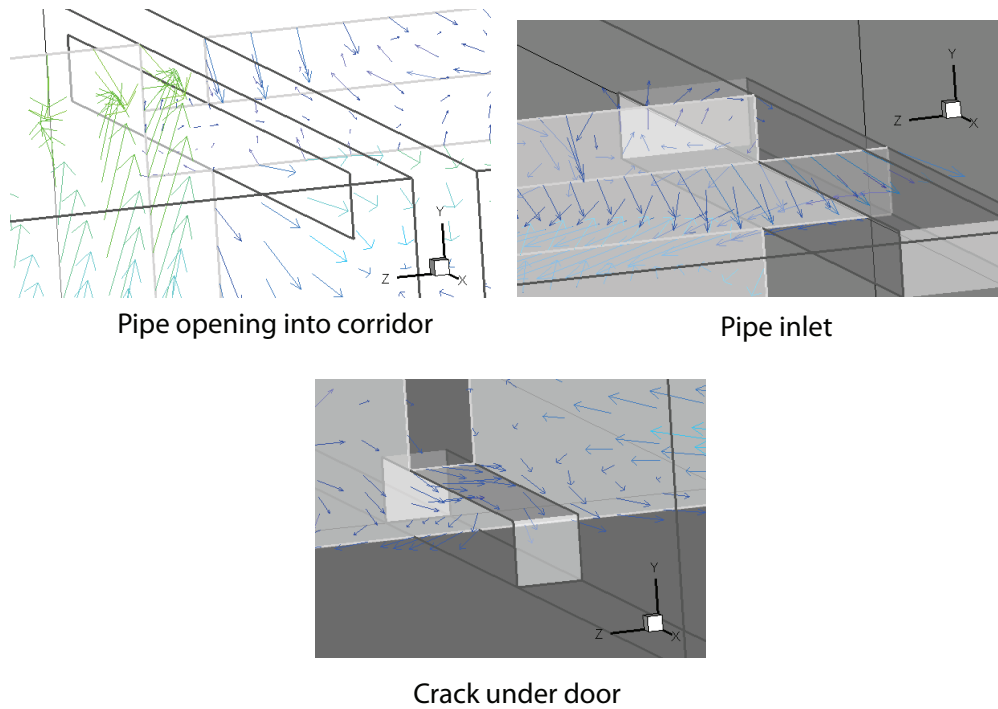
Crack under door

Figure 12.72: *Airflow through the pipe openings for the pipe and the crack under the door.*

For the pipe inlet it is seen in figure 12.72 that there both is a small inflow and outflow. It is also seen that in a short distance from the opening there is almost no airflow. For the pipe opening into the corridor it is seen that the airflow is smaller than for the inlet opening. It is also seen that the airflow in the corridor does almost not influence on the opening in the pipe.

From the crack under the door it is seen in figure 12.72 that the airflow for the crack both is going into and out of the corridor. It is also seen that the airflow through the crack does almost not influence the airflow in the isolation room.

Because the small airflow for both the pipe and the crack under the door it is not possible to create the desired airflow for the corridor only through the pipe in the top and the crack under the door with the used setup.

To create a higher airflow for the corridor are tried to install a fan in the ceiling of the corridor. For the fan the speed is set for $0,5 \frac{m}{s}$ and the opening to $0,025 \ m^2$. With the fan an air change rate of about $1,5 \ h^{-1}$ is created for the corridor. The corridor is still connected to the outside with the pipe in the top of the room and to the isolation room through the crack under the door. The airflow for the room in this case is showed in figure 12.73.
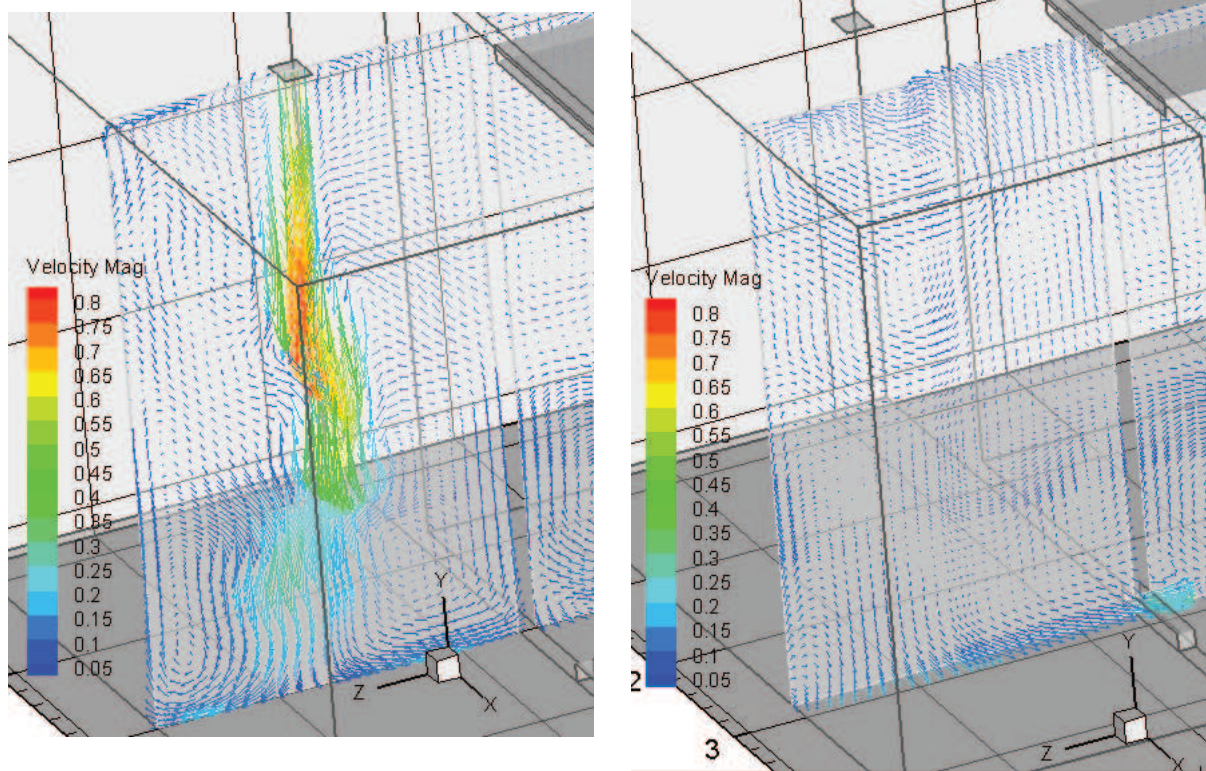
Figure 12.73: *Airflow for the corridor when a fan is installed in the ceiling.*

From figure 12.73 it is seen that there is an inflow for the corridor through the fan in the top of the ceiling. On the right picture in figure 12.73 the airflow for the opening for the pipe in the top of the room and the airflow for the crack under the door is seen. From the figure it is seen that the fan does almost not influence the airflow for the pipe and there is still almost no airflow through the pipe. For the crack under the door it is seen that the fan have a great influence on the airflow compared to the airflow through the crack without any fan. It is seen that with the fan there is created an airflow through the crack from the corridor and into the isolation room. It is seen that with the fan the airflow is from the corridor and into the isolation room, this means that there is created a higher pressure for the corridor than for the isolation room in this situation.

From the above calculations it is investigated if it is possible to create a satisfactory airflow and air change rate for the corridor by only using natural ventilation and by using hybrid ventilation. It is seen that only by using natural ventilation for the corridor it is not possible to supply the corridor with a satisfactory airflow with the used conditions. It is also seen that the airflow through the pipe and the crack is close to nothing. In this way also the airflow between the corridor and the isolation room is almost nothing.

To create a satisfactory air change rate and airflow for the corridor for the used conditions a fan need to be installed. By installing a fan in the ceiling in the corridor it is possible to create a satisfactory air change rate for the corridor. It is also seen that with

this setup the airflow between the corridor and the isolation room is from the corridor into the isolation room. In this way it is ensured that particles from the isolation room is not spread into the corridor and other parts of the hospital.

Nighttime case, model 3

In chapter 3.2 it is stated that for an isolation room there should be installed an anteroom to create a buffer zone between the corridor and the isolation room. In the following are investigated the airflow path between the anteroom and the isolation room and the air change rate for the isolation room. The layout for the isolation room with the anteroom is showed in figure 12.55.

For the model with the corridor and the isolation room, where the corridor is connected to the outside through a pipe in the top of the room, it is investigated that it is not possible to create an airflow with natural driving forces only for the corridor for this setup. To create the desired airflow for the anteroom is installed a fan in the anteroom. The anteroom and the isolation room is still connected through a crack under the door. The fan for the anteroom is made so the air change rate for the anteroom is $12\ h^{-1}$ which will create an average velocity for the opening of $0,48\ \frac{m}{s}$. For the toilet is installed an exhaust fan so the air is led from the isolation room into the toilet and out. The air change rate for the toilet is set to $9\ h^{-1}$ with an average velocity through the crack of $0,1\ \frac{m}{s}$. The toilet and the isolation room is also connected through a crack under the door.

The airflow between the anteroom and the isolation room is showed in figure 12.74.
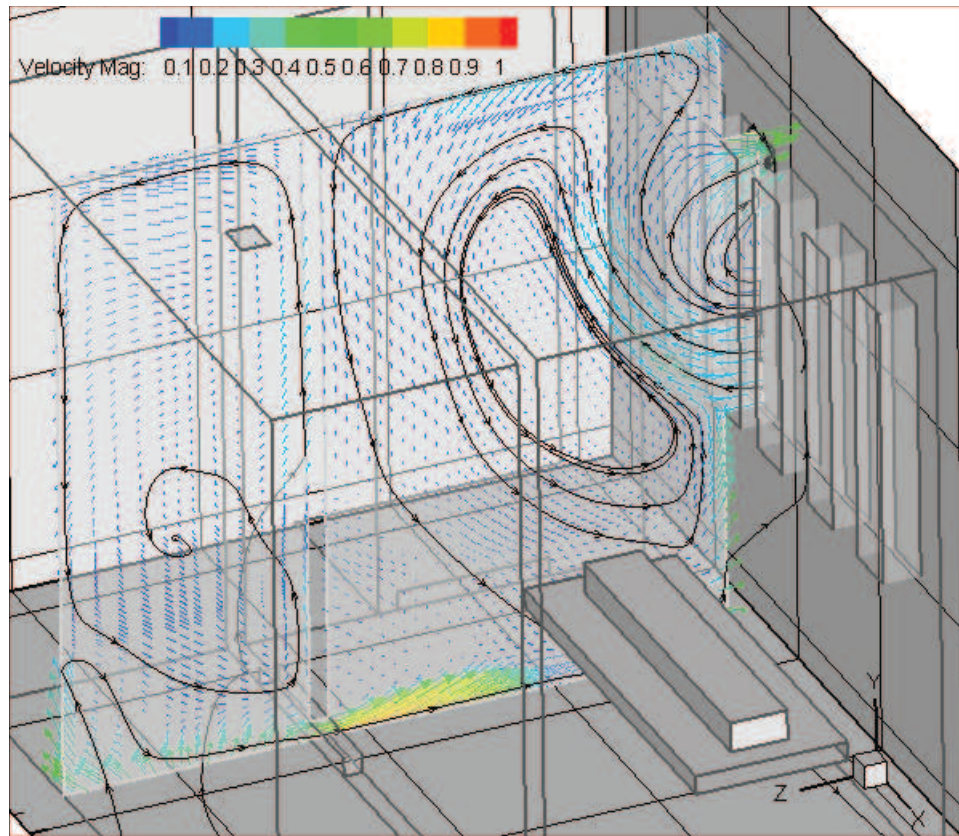
Figure 12.74: *Airflow for the anteroom and isolation room in the nighttime case.*

From figure 12.74 it is seen that the airflow between the anteroom and the isolation room is from the anteroom into the isolation room. Because of the inlet fan in the anteroom it is ensured that the air passes from the anteroom into the isolation room and not the other way around. For the anteroom it is also seen that there is some circulation of the air in the room. For the isolation room it is seen that through the window the air is getting in at the bottom and out through the top as for the situation stated above with only the isolation room.

When the air is getting from the anteroom into the isolation room it is seen that it follows the floor until it reaches the opposite wall. When the air reaches the wall it changes direction to upwards. At the bottom of the window it gets influenced from the inlet from the window and follows the flow path from the inlet air from the window. The pressure at the wall is about $0,5\ Pa$.

In figure 12.75 are shown the airflow between the toilet and the isolation room.
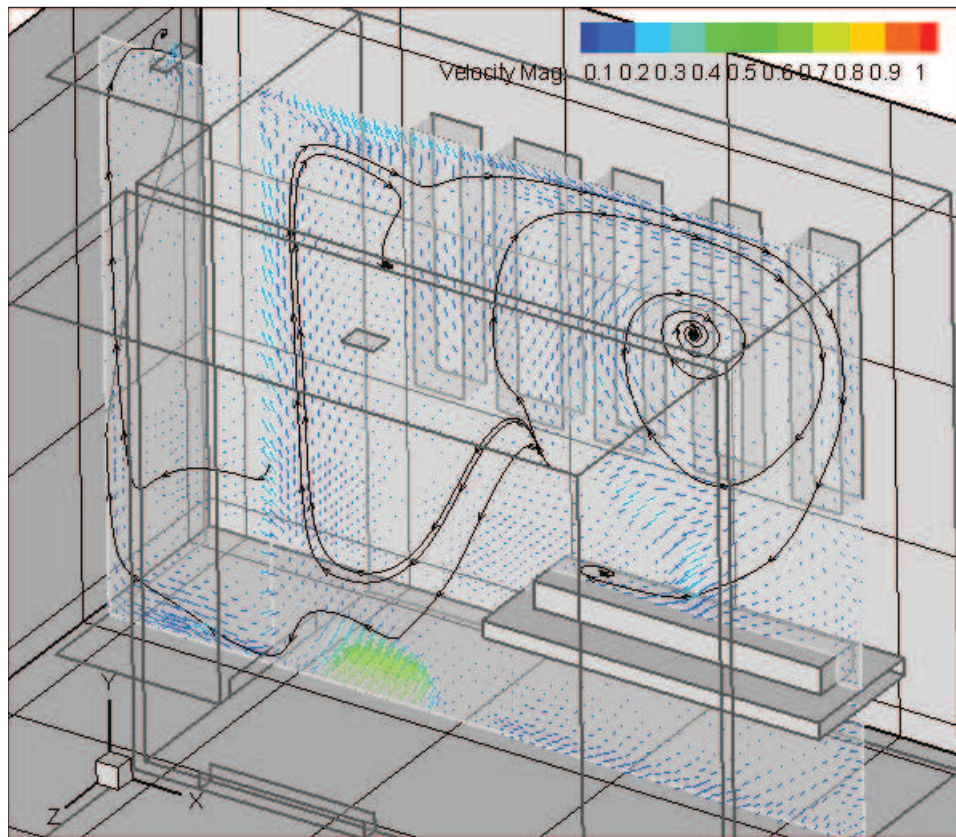
Figure 12.75: *Airflow for the toilet and isolation room in the nighttime case.*

It is seen from figure 12.75 that the airflow between the toilet and the isolation room is from the isolation room through the crack under the door and into the toilet. This is ensured because there is installed an exhaust fan in the toilet. By letting the air out from the toilet it is ensured that any smell from the toilet is not getting into the anteroom. From the figure the airflow for the isolation room is also shown where it is seen that there is a circulation of air between the ceiling and the patient. The airflow for the isolation room is created because of temperature difference therefore there is a circulation in the middle.

The mass flow rate for the different openings and the air change rate for the different rooms for the different floors are listed in table 12.31. The calculation of the air change rate is done as for the first model with only the isolation room.

Table 12.31: *Mass flow rate for the different openings and air change rate for the different rooms in the nighttime.*

Location	Room	Opening	Mass flow rate $[\frac{m^3}{s}]$	Air change rate $[h^{-1}]$
Ground floor	Isolation room	Window	0,26	35,3
			-0,30	-41,6
	Anteroom	Fan	0,06	14,4
		Crack	0,07	14,9
	Toilet	Fan	-0,01	-8,8
		Crack	-0,01	-8,6
1st floor	Isolation room	Window	0,26	35,3
			-0,30	-41,6
	Anteroom	Fan	0,06	14,4
		Crack	0,07	14,9
	Toilet	Fan	-0,01	-8,8
		Crack	-0,01	-8,6
2nd floor	Isolation room	Window	0,26	35,6
			-0,31	-42,1
	Anteroom	Fan	0,07	14,4
		Crack	0,07	14,9
	Toilet	Fan	-0,01	-8,8
		Crack	-0,01	-8,4
3rd floor	Isolation room	Window	0,24	32,4
			-0,30	-41,8
	Anteroom	Fan	0,06	14,4
		Crack	0,07	14,8
	Toilet	Fan	-0,01	-8,8
		Crack	-0,01	-8,6
4th floor	Isolation room	Window	0,26	35,7
			-0,31	-42,3
	Anteroom	Fan	0,06	14,4
		Crack	0,07	14,9
	Toilet	Fan	-0,01	-8,8
		Crack	-0,01	-8,1
5th floor	Isolation room	Window	0,24	32,4
			-0,30	-41,8
	Anteroom	Fan	0,06	14,4
		Crack	0,07	14,8
	Toilet	Fan	-0,01	-8,8
		Crack	-0,01	-8,6
6th floor	Isolation room	Window	0,26	35,6
			-0,30	-41,9
	Anteroom	Fan	0,06	14,4
		Crack	0,08	14,8
	Toilet	Fan	-0,01	-8,8
		Crack	-0,01	-8,5
7th floor	Isolation room	Window	0,26	35,4
			-0,31	-42,3
	Anteroom	Fan	0,06	14,4
		Crack	0,07	15,9
	Toilet	Fan	-0,01	-8,8
		Crack	-0,01	-8,5

From table 12.31 it is seen that with the setup of the isolation room with an anteroom and a toilet where there is a supply fan for the anteroom and an exhaust fan for the toilet the air change rate is a lot higher than the necessary air change rate of 12 h^{-1}. From the table it is also seen that for the windows the inlet mass flow rate is lower than the outlet mass flow rate. This is according to the higher inlet mass flow rate for the anteroom compared to the outlet for the toilet. For the setup is used hybrid ventilation where the isolation room is only natural ventilated and there is installed fans in the anteroom and the toilet. For this setup under the used conditions it is seen that it is possible to create a satisfying air change rate and pressure for the room.

Daytime case, model 3

The airflow between the anteroom and the isolation room in the daytime case is showed in figure 12.76.
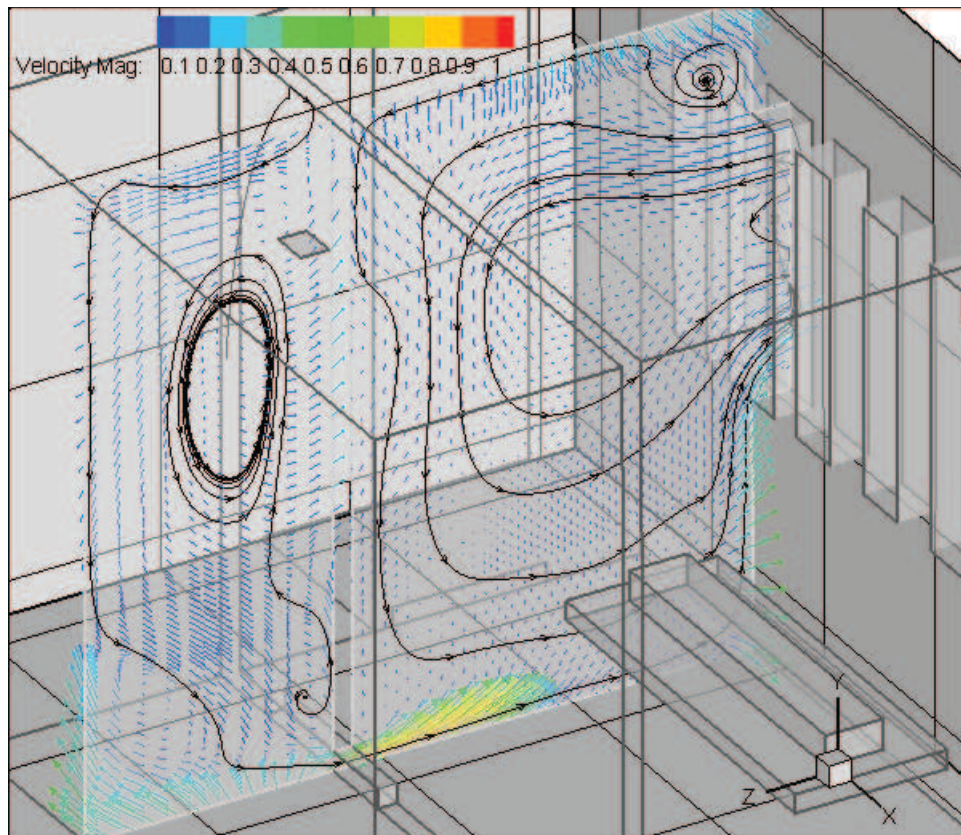
Figure 12.76: *Airflow for the anteroom and isolation room in the daytime case.*

As for the nighttime case it is seen that the airflow between the anteroom and the isolation room is from the anteroom into the isolation room. For the anteroom there is a circulation of the air in the room. For the isolation room it is seen that the airflow for the room is almost the same as for the case without the connection to the anteroom. The air is letting into the room in the top of the window and out through the bottom. It is seen

that the air from the anteroom into the isolation room follows the floor as for the nighttime case and when it hits the wall it change direction to upwards. Because of the lower inside temperature than outside temperature the air is getting out through the bottom of the window. In this situation the inlet air from the anteroom does almost not influence the airflow for the isolation room.

In figure 12.77 are showed the airflow between the toilet and the isolation room.
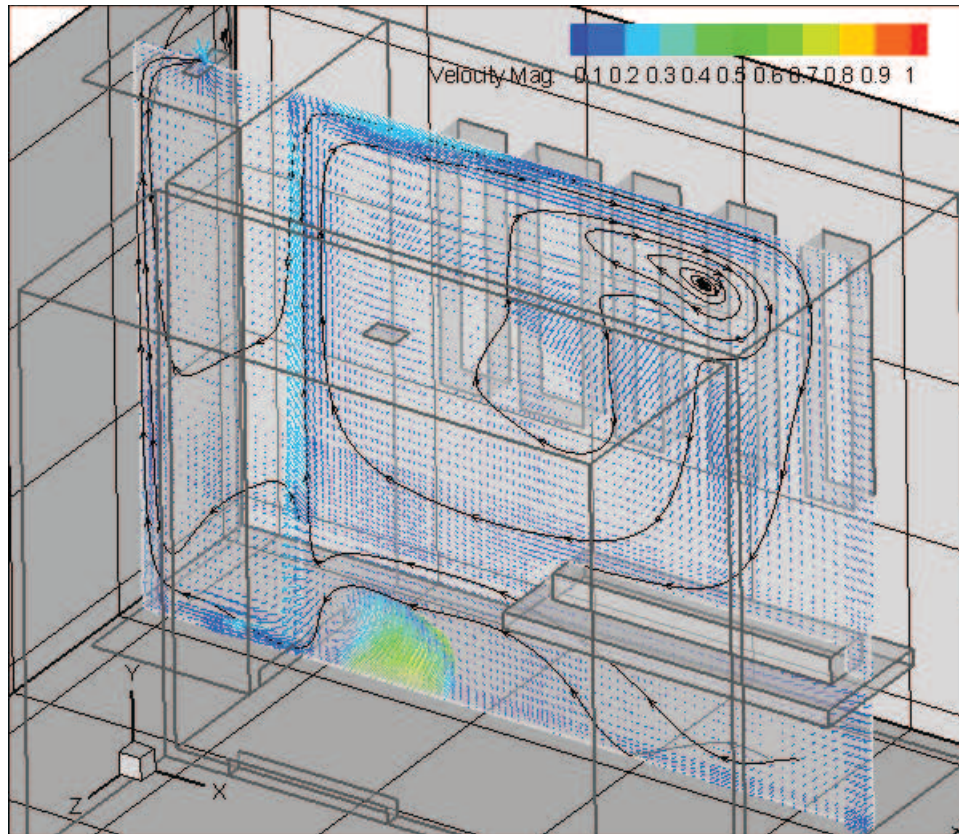
Figure 12.77: *Airflow for the toilet and isolation room in the daytime case.*

From figure 12.77 it is seen that the airflow between the toilet and the isolation room is from the isolation room into the toilet as for the nighttime case. This is because of the exhaust fan installed in the toilet. It is seen from figure 12.75 and figure 12.77 that the airflow for the isolation room is almost the same in the nighttime and daytime case. The reason for this might be because of the influence from the exhaust fan in the toilet. In both situations the air is getting from the isolation room into the toilet therefore the airflow in this part is the same for the two situations and does not influence the airflow for the rest of the room.

The mass flow rate for the different openings and the air change rate for the rooms are in the daytime case are listed in table 12.32.

Table 12.32: *Mass flow rate for the different openings and air change rate for the different rooms in the daytime.*

Location	Room	Opening	Mass flow rate $[\frac{m^3}{s}]$	Air change rate $[h^{-1}]$
Ground floor	Isolation room	Window	0,11	15,6
			-0,15	-21,1
	Anteroom	Fan	0,06	14,4
		Crack	0,08	14,9
	Toilet	Fan	-0,01	-8,8
		Crack	-0,01	-8,5
1st floor	Isolation room	Window	0,11	15,6
			-0,15	-21,1
	Anteroom	Fan	0,06	14,4
		Crack	0,07	14,5
	Toilet	Fan	-0,01	-8,8
		Crack	-0,01	-8,4
2nd floor	Isolation room	Window	0,12	15,9
			-0,15	-20,7
	Anteroom	Fan	0,06	14,4
		Crack	0,07	14,4
	Toilet	Fan	-0,01	-8,8
		Crack	-0,01	-8,3
3rd floor	Isolation room	Window	0,12	15,9
			-0,15	-21,1
	Anteroom	Fan	0,06	14,4
		Crack	0,07	14,6
	Toilet	Fan	-0,01	-8,8
		Crack	-0,01	-8,0
4th floor	Isolation room	Window	0,12	15,8
			-0,16	-21,5
	Anteroom	Fan	0,06	14,4
		Crack	0,07	14,9
	Toilet	Fan	-0,01	-8,8
		Crack	-0,01	-7,9
5th floor	Isolation room	Window	0,12	15,8
			-0,16	-21,5
	Anteroom	Fan	0,06	14,4
		Crack	0,07	14,8
	Toilet	Fan	-0,01	-8,8
		Crack	-0,01	-8,3
6th floor	Isolation room	Window	0,12	15,9
			-0,15	-20,7
	Anteroom	Fan	0,06	14,4
		Crack	0,07	14,8
	Toilet	Fan	-0,01	-8,8
		Crack	-0,01	-8,3
7th floor	Isolation room	Window	0,11	15,6
			-0,16	-21,4
	Anteroom	Fan	0,06	14,4
		Crack	0,07	14,9
	Toilet	Fan	-0,01	-8,8
		Crack	-0,01	-8,2

It is seen from table 12.32 that when the isolation room is connected with the anteroom, where there is installed an inlet fan, and the toilet, where there is added an exhaust fan, the air change rate for the room is higher than 12 h^{-1}. Also for the new design of the isolation room the volume of the room is smaller compared to the first model why the air change rate is higher.

12.5   Concise conclusion

The above simulations are done for Grantham hospital on Hong Kong Island in two situations; nighttime and daytime. For both the situations only the thermal buoyancy is taken into consideration. It is stated that there is no wind. The purpose with the simulations was to investigate the possibility of using natural ventilation for an isolation room according to mountain and sea breeze.

Because of temperature differences between the surfaces and the air it is investigated in chapter 12.1 that for the daytime case there is created a sea breeze and for the nighttime case is created a mountain breeze. The calculation of the sea and mountain breeze is done for a 2D model where the hole mountain is simulated. The simulation is done in this way to ensure the right airflow for the mountain. The simulation is done in 2D because it is assumed that the airflow is not influenced of any obstacles at any of the sides therefore the results does not differ from a 2D simulation to a 3D simulation. Because of the size of the model the simulation time is reduced by doing the simulation for a 2D case compared to a 3D case. It is investigated that for both the sea and mountain breeze the Grashof number is higher than $Gr = 10^9$ which means that both flows have transferred into a turbulent region. According to the Grashof number and Reynolds number it is calculated that the sea breeze is dominated of free convection and the mountain breeze is dominated of forced convection.

From the setup the velocity profile for the sea and mountain breeze is calculated. The velocity profiles are used to calculate the pressure for the hospital in the two situations. It is seen that the speed of the air is highest in the nighttime case compared to the daytime case. Because of the slope of the hill the gravity force increase the speed of the mountain breeze.

In chapter 12.3 the pressure for the hospital is calculated. Because of the higher speed of the air in the nighttime case from the mountain breeze the pressure for the building is higher in the nighttime case compared to the daytime case. The simulation of the pressure for the hospital is done in a 3D case where the domain is smaller than for the simulation of the velocity profiles. For the simulation it is ensured that the domain is big enough so any circulation around the hospital is not cut off.

For the daytime case the isolation rooms in the hospital are located on the leeward side of the hospital. This means that for the daytime case the pressure for the location of the isolation rooms are close to 0 Pa and therefore the airflow for the isolation rooms

are mainly driven of temperature differences. For the nighttime case the isolation rooms are located on the windward side and it is almost possible to ensure the right airflow only according to wind pressure.

The airflow and air change rate for the isolation rooms located on different floors are calculated in chapter 12.4. To investigate the influence of the wind pressure and the effect of different temperatures between inside and outside are first made simulations only with the isolation room without it is influenced by other rooms or airflows. For the simulations are used the layout of the isolation room as it is for Grantham hospital without any changes. It is investigated that for the nighttime case it is almost possible to ensure the right airflow only according to wind pressure. When there is a temperature difference of 4 $^\circ C$ between inside and outside the airflow is about twice the necessary airflow. It is therefore investigated that for the nighttime case it is possible to create the desired airflow only by natural ventilation. For the daytime case the isolation rooms are located on the leeward side and the temperature difference is only 1 $^\circ C$. In this case it is calculated that the air change rate is not high enough. For the daytime case there is no wind pressure as for the nighttime case therefore the airflow for the room is only created by temperature differences. To create the right airflow in the daytime case the temperature difference therefore need to be higher. Another solution is to place the isolation rooms on the other side of the building. In this way the wind pressure is higher for the daytime case but lower in the nighttime case. But because of the greater temperature difference in the nighttime case than for the daytime case it might be possible to create the necessary air change rate in both situations.

For the isolation room the airflow for the room is also investigated. For the nighttime case the air is letting into the room in the bottom of the window and out through the top. For the daytime case the airflow is the other way around. This means that for the nighttime case the air passes by the patient when it gets into the room and then it passes further into the room and out. In this situation particles from the patient is transferred further into the room. In the daytime case the fresh air gets into the room and passes the patient just before it leaves the room. In this way particles from the patient is not letting further into the room. Therefore in the nighttime case the risk of transmission is higher than in the daytime for this case.

In chapter 3.2 it is stated that the optimal design of an isolation room is with an anteroom. For the isolation room the design is therefore changed. The outer dimensions for the isolation room is still the same but there is installed an anteroom and a toilet in the room. It is investigated that it is not possible to create a high enough airflow only by natural ventilation for the anteroom because of the location of the anteroom. Therefore there is installed an supply fan in the anteroom and an exhaust fan in the toilet. For the isolation room is still used natural ventilation. For both the daytime and nighttime case it is investigated that the airflow in this case between the anteroom and the isolation room is from the anteroom into the isolation room. In this way particles from the isolation room is not transmitted away from the isolation room. When the layout of the isolation room is changed it is seen that both for the daytime and nighttime case it is possible to create a high enough air change rate for the isolation room with natural ventilation.

With the setup of the isolation room with a fan it is possible to create both a negative and a positive pressure isolation room. To create a negative pressure isolation room the fan in the anteroom should be a supply fan and to create a positive pressure isolation room the fan should be an exhaust fan. In this way it is possible to change the pressure for the isolation room without any influence on other rooms.

Above are investigated the air change rate for the isolation room according to mountain and sea breeze. To investigate the air change rate during a year according to the weather data for Hong Kong are made a single zone model in BSim in the following.

Chapter 13

Single zone modeling of Grantham hospital

In chapter 12.4 are the airflow for the isolation room for Grantham hospital investigated according to mountain and sea breeze. It is concluded that with a layout of the isolation room with an anteroom with a supply fan and a toilet with an exhaust fan it is possible to use natural ventilation for the isolation room to create a sufficient air change rate with the used weather conditions. To investigate the air change rate through the year for the isolation room for Grantham hospital are made a BSim simulation. For the BSim simulation are used weather data from Hong Kong, therefore the mountain and sea breeze are not taken into consideration. The BSim simulation is also used to investigate the temperature difference between the inside and outside and the humidity for the isolation room.

BSim is a building simulation program developed by The Danish Building Research Institute. With the program it is possible to calculate and analyze indoor climate and effect need and power use of the building for a selected period. The program uses the control volume method. [Wittchen et al., 2004]

13.1   Model of isolation room

The purpose of the simulation is to calculate the air change rate and the indoor climate for the isolation room for Grantham hospital. For the model therefore only the isolation room and the neighboring rooms are modeled. The neighboring rooms are modeled because these have influence on the airflow and the indoor climate for the isolation room. The layout of the isolation room is the same as used in the CFD calculations and showed in figure 13.1.
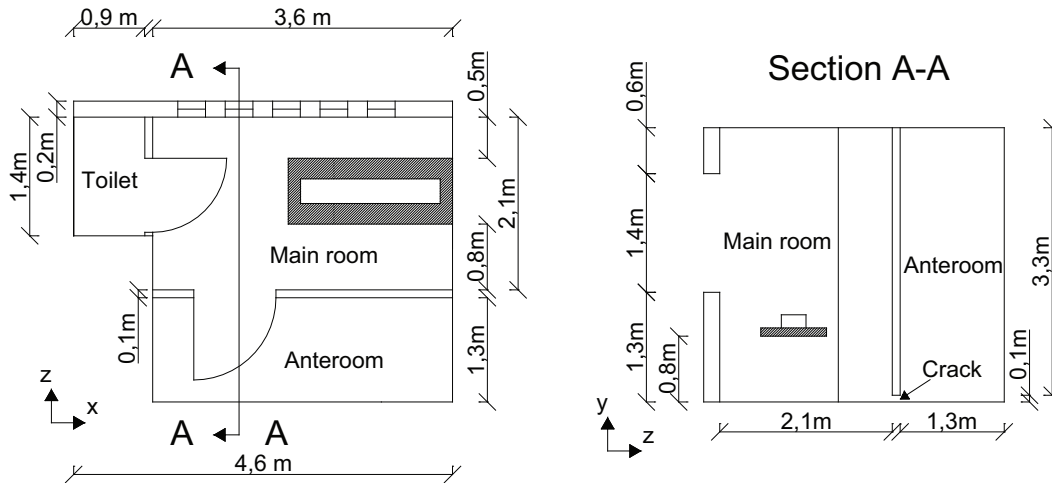
Figure 13.1: *Outline of the isolation room.*

It is seen in figure 13.1 that the isolation room consists of a main room or the isolation room, a toilet and an anteroom. The isolation room is connected to the anteroom and the toilet through a crack under the door. In the anteroom is located a supply fan while there in the toilet is located an exhaust fan.

In chapter 12.4 it is investigated that with the setup showed above it is ensured that the airflow between the anteroom and the isolation room is from the anteroom into the isolation room and the airflow between the toilet and the isolation room is from the isolation room into the toilet. For the isolation room are located 5 windows facing north.

The BSim model of the isolation room is showed in figure 13.2.
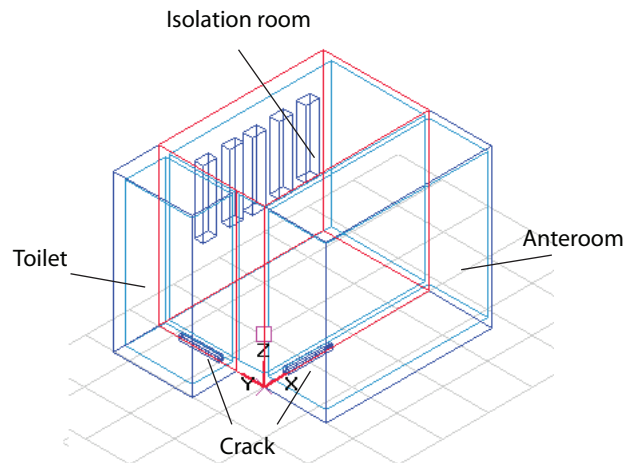
Figure 13.2: *BSim model of the isolation room and anteroom and toilet the neighboring rooms are not shown. The isolation room is marked with red.*

From figure 13.2 it is seen that the isolation room is connected to the toilet and anteroom through a crack. For the neighboring rooms there are no connections. The neighboring

rooms are modeled so the internal sides for the isolation room does not face the outside air.

The used construction elements for the model are listed in table 13.1. The real construction of the hospital is not known therefore are used U-values for the different constructions according to a reference building in Hong Kong.

Table 13.1: *U-values for construction elements.* *[Electrical and Mechanical Services Department, 2005]*

Element	Material layer	Thickness [mm]	Thermal conductivity U $[\frac{W}{m^2 \cdot ^\circ C}]$	Resistance R $[\frac{m^2 \cdot ^\circ C}{W}]$
Roof	Concrete tiles	25	1,1	0,023
	Asphalt	20	1,15	0,017
	Cement/sand screed	50	0,72	0,069
	Polystyrene insulation	50	0,034	1,471
	Concrete	150	2,16	0,069
	Gypsum plaster	10	0,38	0,026
	Total			1,675
Outside wall	Cement/sand render	10	0,72	0,014
	Concrete	150	2,16	0,069
	Gypsum plaster	20	0,38	0,053
	Total			0,136
Inside wall	Lightweight concrete	100	0,35	0,286
Window (fixed)	Single glazing	10	6,93	
Window (operable)	Single glazing	10	7,21	

For the simulation are used weather data from Hong Kong as listed in chapter 7.

The systems for the different rooms used for the simulations are listed in table 13.2.

Table 13.2: *Systems for BSim.*

Room	System	Description	Time
Isolation room	People load	1 patient, activity level: at rest	Always
	Equipment	Hospital equipment, effect equal to two computers, 140 W [Andersen et al., 2002]	Always
	Moisture	Cleaning one hour, water load: 0,45 kg water [Wittchen et al., 2004]	One hour each day (6-7 hour)
	Lighting	12 $\frac{W}{m^2}$	Daytime (7-21 hour)
	Ventilation	Natural ventilation	Always
Anteroom	People load	1 person, activity level: medium	Every 4th hour in daytime
	Moisture	Cleaning one hour, water load: 0,45 kg water [Wittchen et al., 2004]	One hour each day (6-7 hour)
	Lighting	10 $\frac{W}{m^2}$	Daytime (7-21 hour)
	Ventilation	Supply fan 0,053 $\frac{m^3}{s}$	Always
Toilet	People load	1 person, activity level: medium	Every 8th hour
	Moisture	Cleaning one hour, water load: 0,45 kg water [Wittchen et al., 2004]	One hour each day (6-7 hour)
	Lighting	10 $\frac{W}{m^2}$	Daytime (7-21 hour)
	Ventilation	Exhaust fan 0,012 $\frac{m^3}{s}$	Always

In table 13.3 are listed the regulation for the different systems.

Table 13.3: *Regulation of systems for BSim.*

Room	System	Regulation
Isolation room	Ventilation	Max air change: 100 h^{-1}, max wind: 0 $\frac{m}{s}$, single sided ventilation, set point: 8 °C
Anteroom	Ventilation	Set point 1: -12 °C supply air temp.: 24 °C, Set point 2: 20 °C supply air temp 17 °C

The air change rate for the natural ventilation system is set for 100 h^{-1}, this is done to ensure that there is no limit in the air change rate for the isolation room. The max wind is set for 0 $\frac{m}{s}$ in this way natural ventilation is possible no matter the wind speed.

For the supply fan for the anteroom is made a function for the temperature of the supply air. For the fan are not installed either a heating or a coiling coil therefore the supply

temperature of the air will be the temperature of the outside air even though this function is made. If there later are installed a heating or a coiling coil the temperature of the supply air is regulated by the function.

The isolation room is ventilated by natural ventilation while the anteroom and the toilet is mechanical ventilated. Since the isolation is connected to the anteroom and the toilet the airflow between the rooms is a multi zone. For the simulation it has not been possible to use the multi zone function implemented in BSim therefore the single zone model is used. To ensure the right airflow between the zones the airflow between the zones are ensured by the mixing function in BSim. The airflow between the zones are listed in table 13.4.

Table 13.4: *Airflow between zones.*

Mixing between zone	Volume flow rate $\left[\frac{m^3}{s}\right]$
Anteroom → Isolation room	0,053
Isolation room → Toilet	0,01

13.2 BSim simulation

With the setup listed above are made a year simulation in BSim to investigate the air change rate during a year for the isolation room. For the isolation room also the indoor temperature and the moisture load for the room is investigated.

The simulation is located in the BSim file 'IsoC1.dis' on the cd.

For the simulations are used weather data for Hong Kong. For the weather data are both the outside temperature, wind direction and speed, moisture load and sun radiation used. Compared to the CFD simulations of Grantham hospital the simulations are made for the weather data for a year where all the weather information from the weather data are used and not only for two situations. For the BSim simulation therefore the wind speed is also taken into consideration and not only the influence from the temperature as for the CFD simulations. For the BSim simulations are not made a simulation only with the influence from the temperature. For the BSim simulations the indoor temperature depend on the outdoor temperature and is therefore not set as a constant temperature.

In figure 13.3 are seen the indoor temperature for the isolation room, anteroom and toilet and the outdoor temperature of the air.
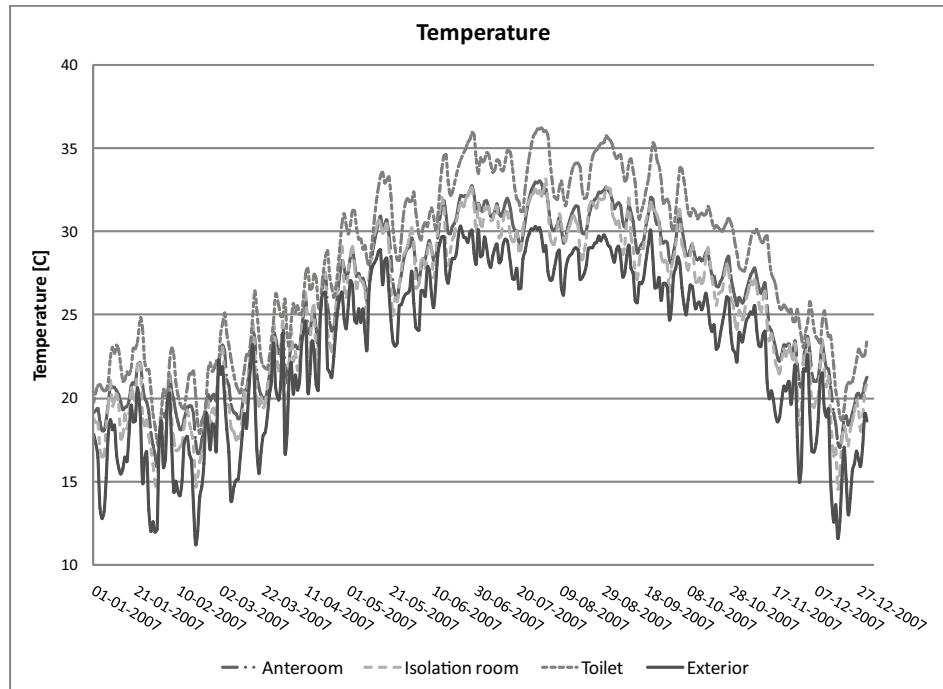
Figure 13.3: *Indoor temperature during a year for the isolation room, anteroom and toilet and exterior temperature.*

It is seen from figure 13.3 that for the hole year the indoor temperature for all the rooms are higher than the outdoor temperature. For the rooms there are not installed any form for heating or coiling as stated above. Therefore the heat supply for the rooms are only according to the people and equipment in the rooms and sun radiation. From the graph it is also seen that the indoor temperature for the anteroom and the isolation room are almost the same while the temperature for the toilet is higher. For the anteroom is installed an supply fan that supply the room with fresh air while for the toilet the air is extracted from the isolation room and exhausted in the toilet. Therefore the temperature of the supply air for the toilet is higher according to the air temperature for the isolation room than for the anteroom. From the figure it is also seen that the highest indoor temperature is in the end of June and beginning of August with a temperature for the isolation room of about $33\,°C$.

In figure 13.4 and figure 13.5 are showed the temperature variation over a week for January and August.
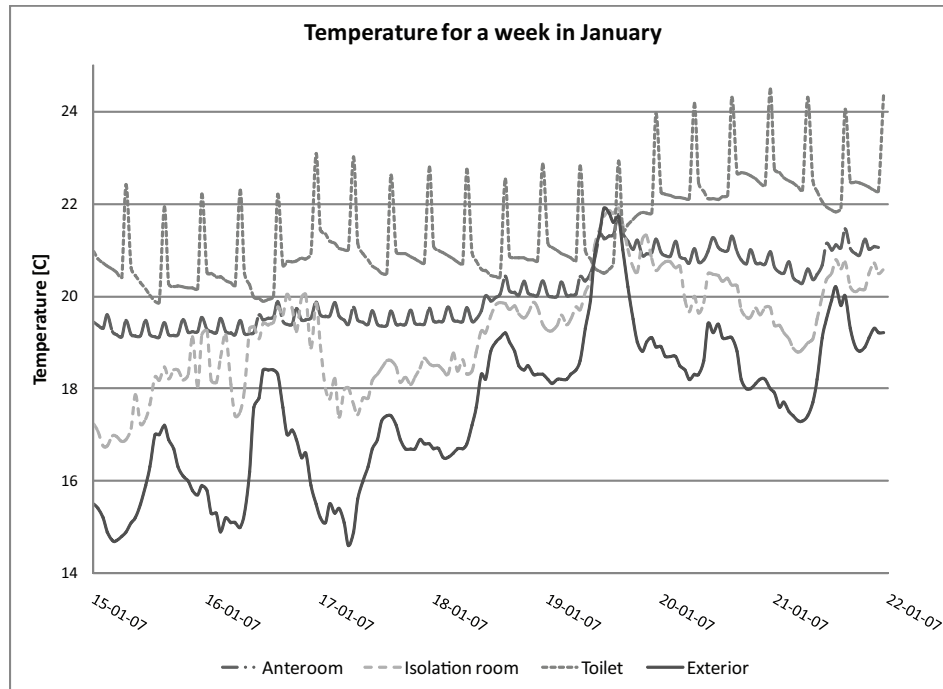
Figure 13.4: *Indoor temperature during a week in January for the isolation room, anteroom and toilet and exterior temperature.*
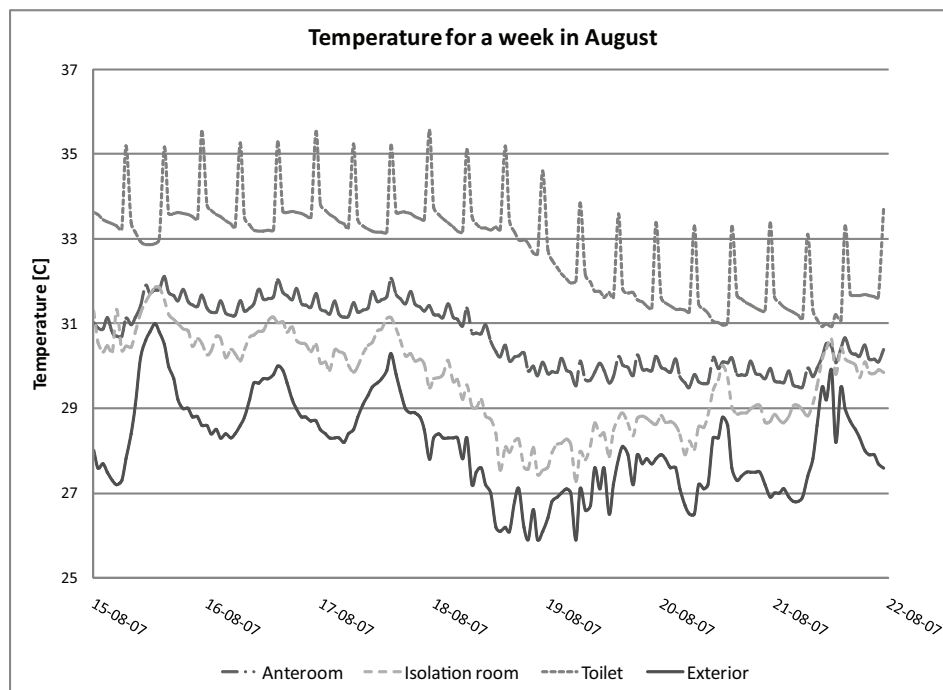
Figure 13.5: *Indoor temperature during a week in August for the isolation room, anteroom and toilet and exterior temperature.*

It is seen from both figure 13.4 and figure 13.5 that for both situations the temperature

of the exterior air is the coldest. It is also seen that there is a temperature difference between the anteroom and the isolation room where the temperature for the isolation room is lower than for the anteroom. This might be because of the higher air change rate for the isolation room compared to the anteroom.

The variation over the day for both the anteroom and the toilet is according to the person load and the lighting that are not contentious through the day as listed in table 13.2.

In table 13.5 are listed the minimum, maximum and average temperature for the rooms during the year and for the week in January and August.

Table 13.5: *Minimum, maximum and average temperature for the different rooms during the year and for a week in January and August.*

	Minimum temperature [$°C$]	Maximum temperature [$°C$]	Average temperature [$°C$]
Year			
Isolation room	14,5	33,2	25,2
Anteroom	15,9	33,1	25,8
Toilet	17,1	36,2	28,1
Exterior	11,2	30,3	23,1
Week January			
Isolation room	16,8	21,9	19,2
Anteroom	19,1	21,8	20,1
Toilet	19,9	24,5	21,4
Exterior	14,6	21,9	17,6
Week August			
Isolation room	27,3	31,9	29,6
Anteroom	29,5	32,1	30,7
Toilet	30,9	35,6	32,8
Exterior	25,9	31,0	28,1

From table 13.5 it is seen that the highest temperature is for the toilet. For the anteroom and the isolation room it is seen that the average temperature is just above 25 $°C$ through the year. The operative temperature depends on the outdoor temperature. The design temperature for an office building where it is possible to open the windows and the people are dressed according to the outside weather are showed in figure 13.6.
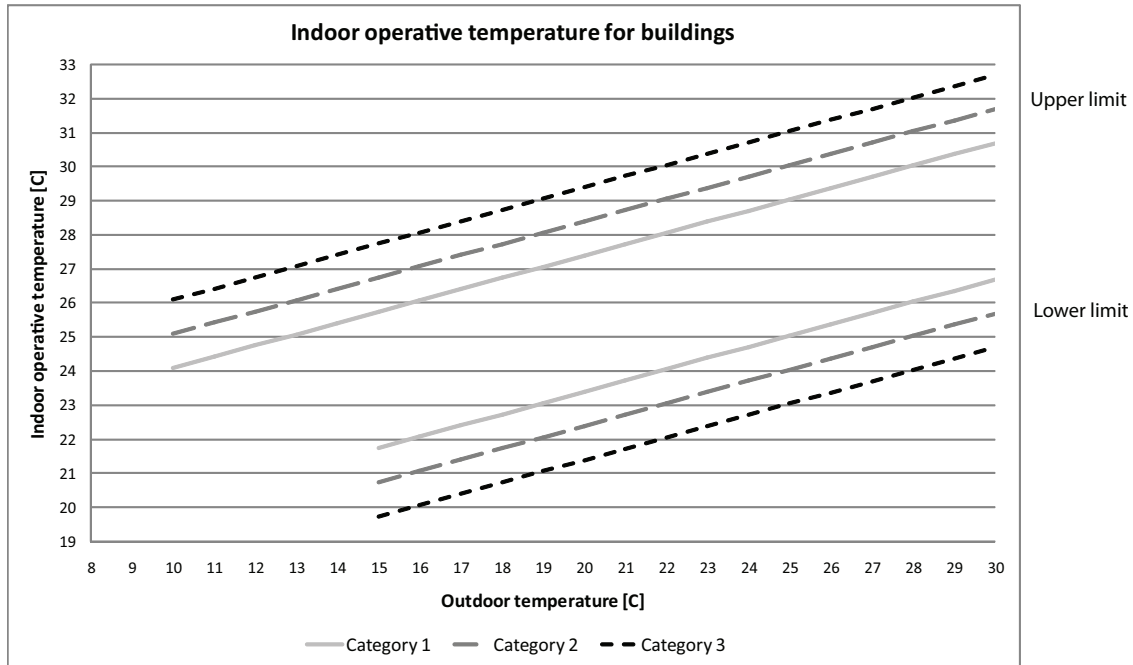
Figure 13.6: *Indoor operative temperature for a building without mechanical cooling.* *[DS/EN 15251, 2007]*

According to category 2 in figure 13.6 the average indoor temperature for the isolation room is inside the intervals. From table 13.5 and figure 13.6 it is also seen that for the week in January the average temperature is lower than the design temperature while it is inside the interval for the week in August. To get an indoor temperature according to the design temperature it might therefore be necessary to install a heater and an air conditioner. For the project there is not installed a heater or an air conditioner because it is only wished to investigate the airflow for the room and the pressure distribution.

The air change rate for the isolation room throughout the year is listed in table 13.7.
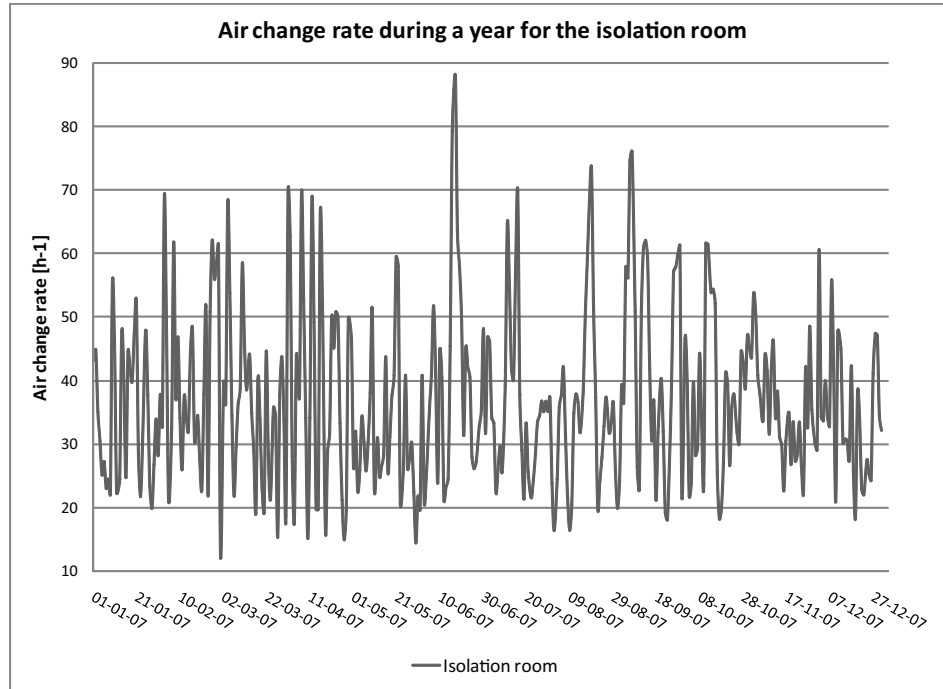
Figure 13.7: *Air change rate for the isolation room during a year.*

From figure 13.7 it is seen that the air change rate for the isolation room does vary a lot during the year. The lowest value of the air change rate is about $12\ h^{-1}$ and the highest air change rate about $88\ h^{-1}$. It is therefore seen that the air change rate is sufficient for the isolation room.

It is not possible to see from figure 13.7 in which situation the air change rate is highest only that it does vary during the year. To investigate the influence on the air change rate according to the wind speed and the temperature difference the air change rate is plotted against the wind speed and the temperature difference. For the calculation of single sided natural ventilation in BSim the wind direction is not taken into consideration. Therefore it is not possible to investigate the influence of the wind direction on the air change rate.

In BSim the volume flow rate according to natural ventilation is calculated from:

$$q_v = |\pm q_{Vv}^2 \pm q_{VT}^2|^{\frac{1}{2}} = \left| \frac{c_v}{|c_v|}(c_v v_{10})^2 + \frac{\Delta T}{|\Delta T|}\left(c_T |\Delta T|^{\frac{1}{2}}\right)^2 \right|^{\frac{1}{2}} \tag{13.1}$$

[Wittchen et al., 2004]

where

q_v : Total airflow rate $[\frac{m^3}{s}]$

q_{Vv} : Airflow rate from wind $[\frac{m^3}{s}]$

q_{VT} : Airflow rate from thermal buoyancy $[\frac{m^3}{s}]$

c_v : Constant depending on the building and wind conditions, calculated from equation (13.2) $[-]$

c_T : Constant depending on the building and temperature conditions, calculated from equation (13.3) $[-]$

v_{10} : Metrological wind speed for open country in 10 meters height $[\frac{m}{s}]$

ΔT : Temperature difference between inside and outside $[K]$

$$\text{For single sided ventilation in one level:} \qquad c_v = 0,03 \cdot A \qquad (13.2)$$

[Wittchen et al., 2004]

where

A : Area of opening $[m^2]$

$$\text{For single sided ventilation in one level:} \qquad c_t = 0,05 \cdot h^{\frac{1}{2}} \cdot A \qquad (13.3)$$

[Wittchen et al., 2004]

where

h : Height above reference level $[m]$

It is seen that equation (13.1) does not depend on the wind direction for the building. Therefore by using single sided natural ventilation in BSim it is not possible to investigate the influence of the wind direction for the building.

The influence of the wind direction for the airflow rate by using single sided natural ventilation is shown in equation (13.4).

$$q_v = \pm C_D \frac{1}{2} A \sqrt{ \underbrace{f(\beta)^2 \cdot |C_p| \cdot U_{ref}^2}_{P_{wind}} + \underbrace{\frac{(T_i - T_e) \cdot g \cdot (H_t - H_b)}{\overline{T}}}_{\Delta P_{thermal}} + \underbrace{\frac{\Delta C_{p,opening} \cdot (T_i - T_e)}{U_{ref}^2}}_{\Delta P_{fluct}} }$$

$$(13.4)$$

[Larsen and Heiselberg, 2007]

where

$f(\beta)$: Incidence angle [°]
U_R : Reference wind speed [$\frac{m}{s}$]
$\overline{T}$: Average temperature [K]

From equation 13.4 it is seen that the wind direction does influence on the airflow for the opening in the case of single sided natural ventilation.

From BSim this influence is not possible to investigate.

In figure 13.8 and 13.9 are showed the air change rate for the isolation room compared to the temperature difference between inside and outside and the wind speed for a week in January and August. The air change rate is divided by a factor 10.
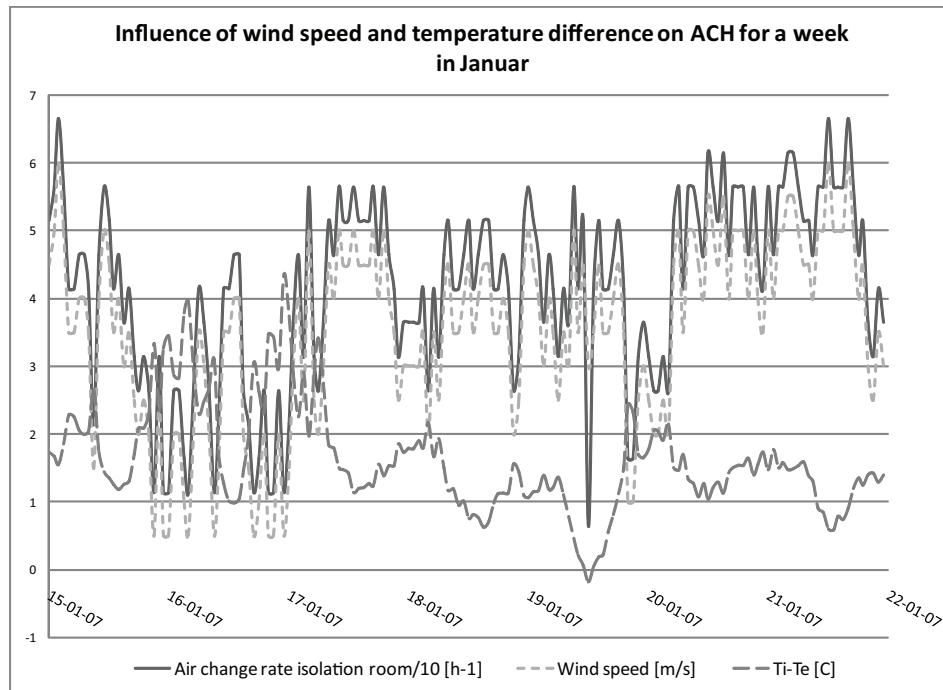
Figure 13.8: *Air change rate compared to wind speed and temperature difference between inside and outside for a week in January. The air change rate is divided by a factor 10.*
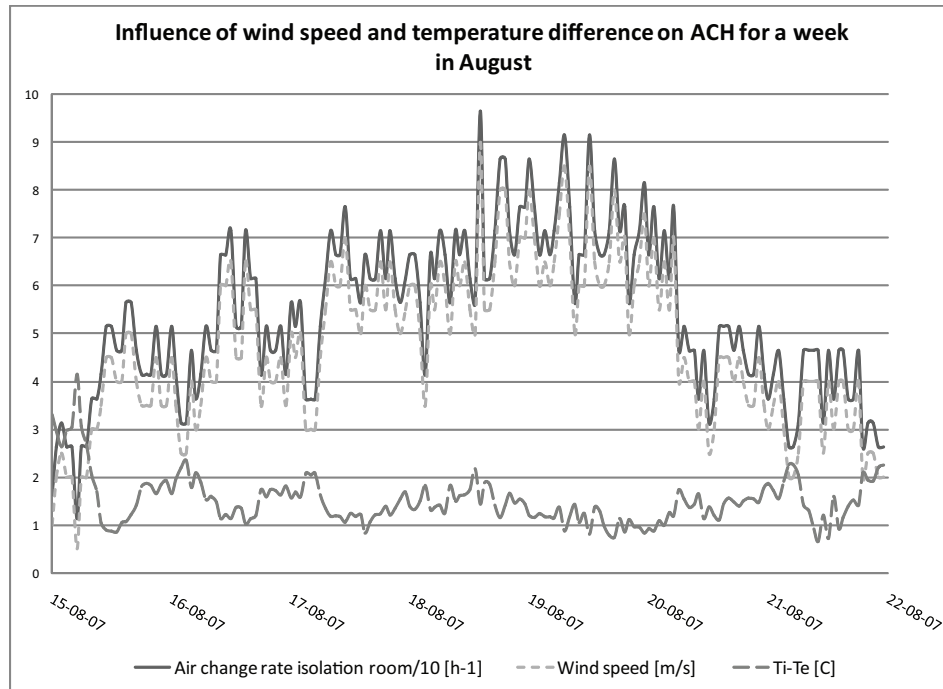
Figure 13.9: *Air change rate compared to wind speed and temperature difference between inside and outside for a week in August. The air change rate is divided by a factor 10.*

From both figure 13.8 and figure 13.9 it is seen that the air change rate does depend more on the wind speed than the temperature difference between inside and outside. It is seen that for both the week in January and the week in August the graph of the air change rate does follow the graph of the wind speed exactly. The only difference is that the two graphs are displaced from each other.

It is therefore seen that for the air change rate the wind speed have the highest influence and the difference in the temperature between inside and outside does almost not influence the air change rate.

In figure 13.10 are showed the relative humidity for the isolation room compared to the relative humidity of the outside air during a year.
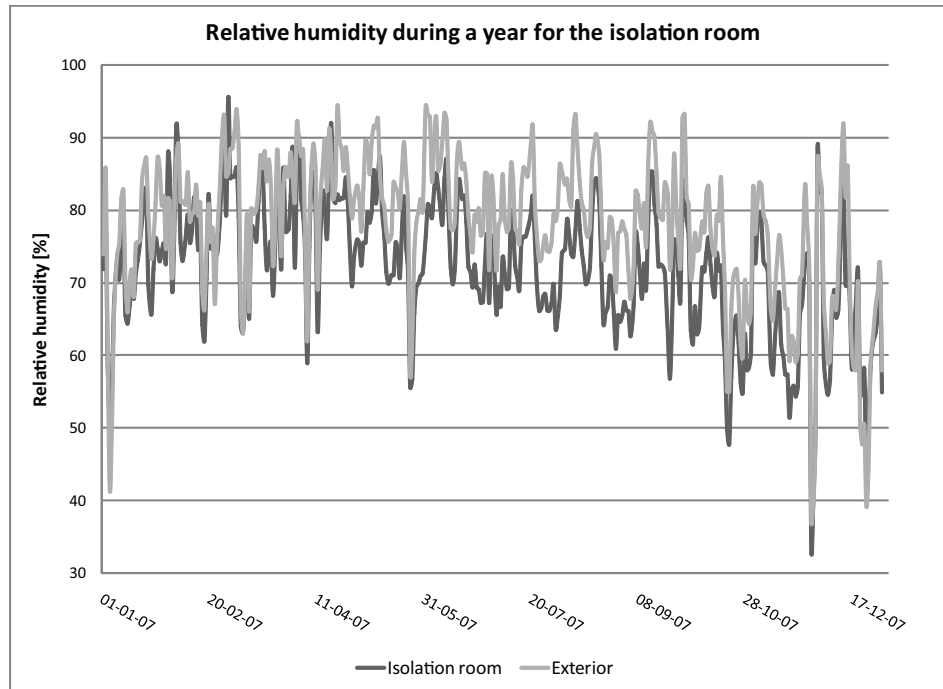
Figure 13.10: *Relative humidity for the isolation room during a year compared to the relative humidity of the outside air.*

From figure 13.10 it is seen that the relative humidity for the isolation room follows the relative humidity of the outside air. It is also seen that the relative humidity for the isolation room is lower than the relative humidity of the outside air. In table 13.6 are listed the minimum, maximum and average value of the relative humidity for the isolation room and outside during a year.

Table 13.6: *Minimum, maximum and average values of the relative humidity for the isolation room and outside during a year.*

	Minimum RH [%]	**Maximum RH** [%]	**Average RH** [%]
Isolation room	33,4	95,6	72,2
Exterior	37,0	94,4	78,0

The limit for the relative humidity is about $30 - 70$ %. If the relative humidity is too low it can be a nuisance for the respiratory passages and induce dried mucosa. On the other side if the relative humidity is too high it can induce the growth of house-dust mites and mould. From table 13.6 it is seen that the average value of the relative humidity is above 70 % which might increase the number of house-dust mites and mould. A reason for the high relative humidity is because of the high relative humidity of the outside air. The isolation room is ventilated by natural ventilation which means that the outside air is let directly into the isolation room. Because of the high relative humidity for the isolation room it might be necessary to install a dehumidifier for the room.

13.3 Check of BSim calculation

To verify the results from the BSim calculation are made a check of the results. The results from BSim are compared to a simple hand calculation of the air change rate.

For the verification are made some simplifications compared to the situation stated above. The simplifications are listed below:

- No connections between the isolation room and the anteroom and the toilet

- No systems for the isolation room except natural ventilation

With the simplifications it means that the isolation room is only influenced by the natural ventilation through the 5 windows. For the calculation the anteroom and the toilet are not taken into consideration. There are no other loads for the isolation room. For the calculation of the airflow rate are used the principles of a single zone.

For the isolation room are made two different calculations of the air change rate of the room. For the first calculation are used equation (13.1) to check the air change rate. Equation (13.1) is the equation used by BSim to calculate the airflow rate. For the second calculation are used equation (A.12) in appendix A.1. This equation is an empirical equation estimated from field measurements. For both the two equations the wind direction is not taken into consideration.

For the check calculation are used the weather data for the 28th of January and 17th of June. The calculations are made for these two days because for the 28th of January the temperature difference is high compared to the wind speed and for the 17th of June the wind speed is high compared to the temperature difference. The wind speed and temperature difference for the two days are showed in figure 13.11 and 13.12.
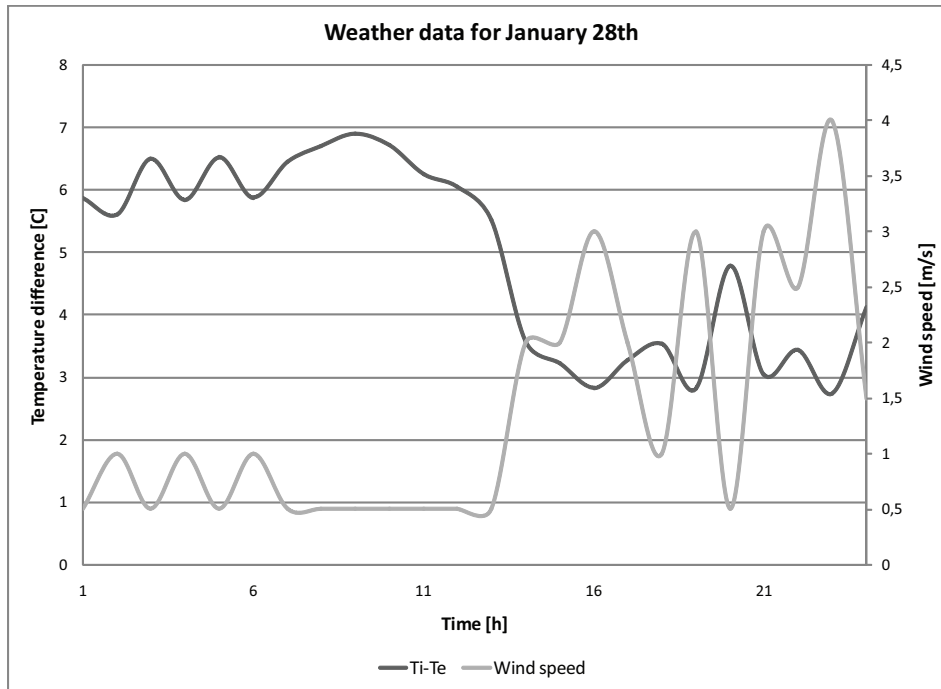
Figure 13.11: *Weather data for the 28th of January.*
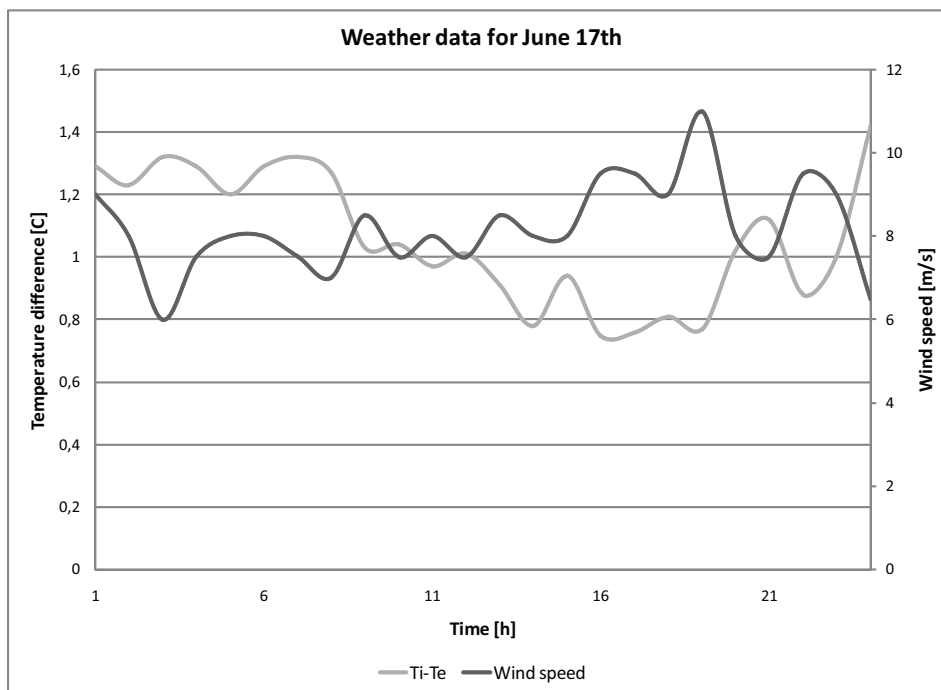
Figure 13.12: *Weather data for the 17th of June.*

The dimensions of the isolation room used for the hand calculation are the same as used for the BSim calculation. For the hand calculation the anteroom and the toilet are not taken into consideration.

In figure 13.13 and 13.14 are showed the volume flow rate and air change rate calculated for the 28th of January.
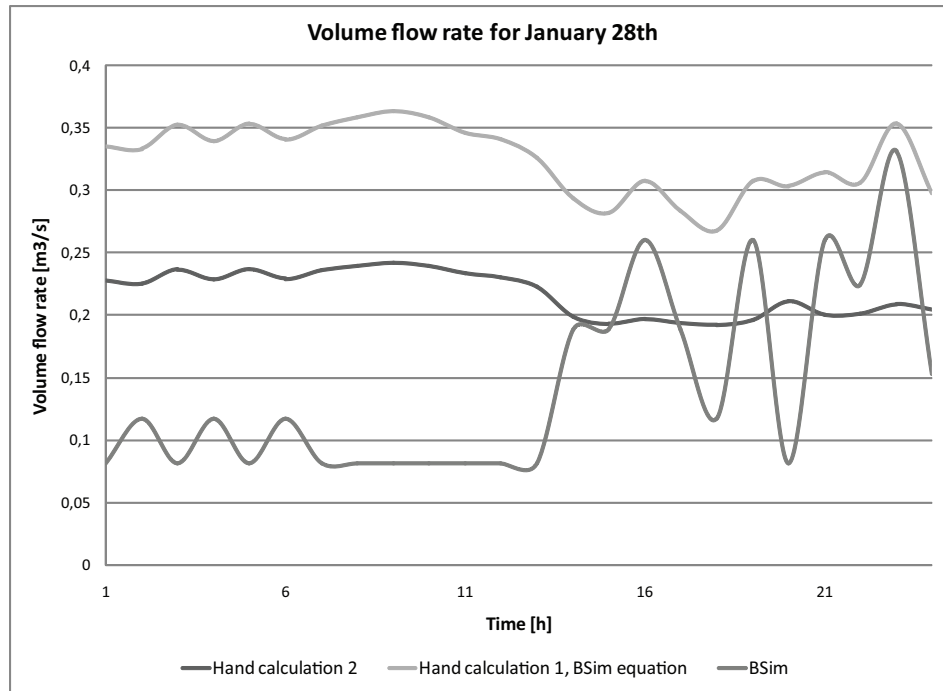
Figure 13.13: *Volume flow rate for the isolation room for the 28th of January.*
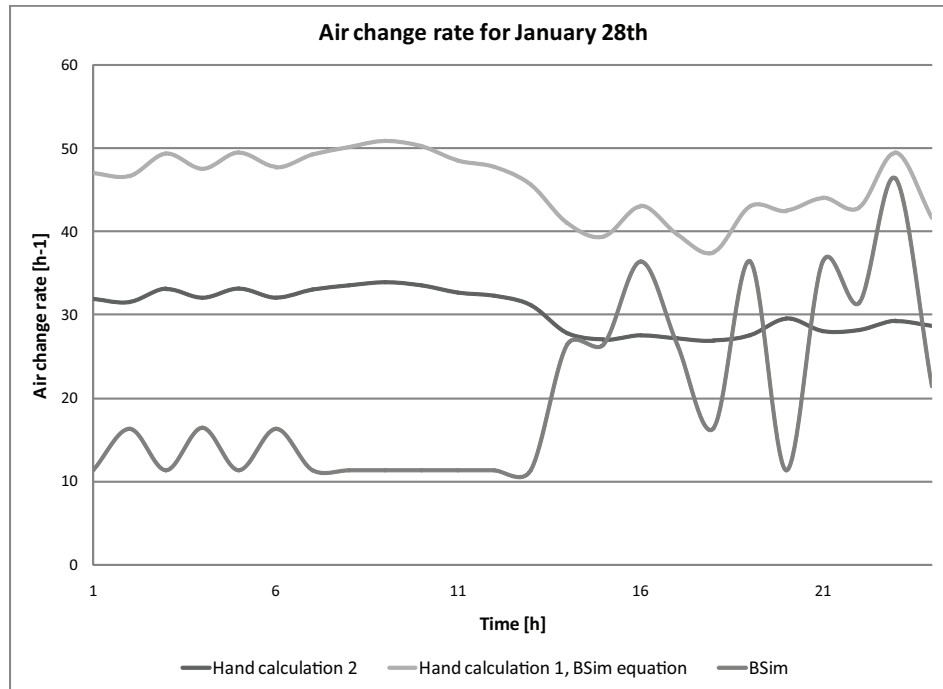
Figure 13.14: *Air change rate for the isolation room for the 28th of January.*

From the volume flow rate and air change rate for the isolation room for the 28th of January showed in figure 13.13 and 13.14 it is seen that the values varies for all the calculations. The highest values is for the first hand calculation and the lowers for the BSim values. It is also seen that there are a difference from the first hand calculation and the BSim values even though they uses the same equation for calculating the airflow.

BSim uses the control volume method where the real happenings are discretised. The calculations for BSim are made on an hourly basis where the input for the calculations might change every hour. This change might also have influence on the calculation of the airflow and therefore the results from the BSim calculation compared to the hand calculation from equation (13.1) may differ. The hand calculations are stationary and does not consider any changes through time. Another reason for the variation between the BSim calculation and the hand calculation from equation (13.1) might be according to a small difference in the room volume.

From figure 13.13 and 13.11 it is seen that the curve of the volume flow for the isolation room follows the curve of the wind speed. The curve of the temperature difference does almost not influence the volume flow for the room. It is also seen even though the temperature difference is higher for the first half of the day the volume flow rate is lowest for this time. For the first half of the day the wind speed is the lowest and rises at the end of the day. The volume flow also rises at the end of the day. It is therefore concluded that the BSim calculation mostly depends on the wind speed and that the temperature difference does not influence the volume flow rate as much.

In figure 13.15 and 13.16 are showed the volume flow rate and air change rate for the isolation room on the 17th of June.
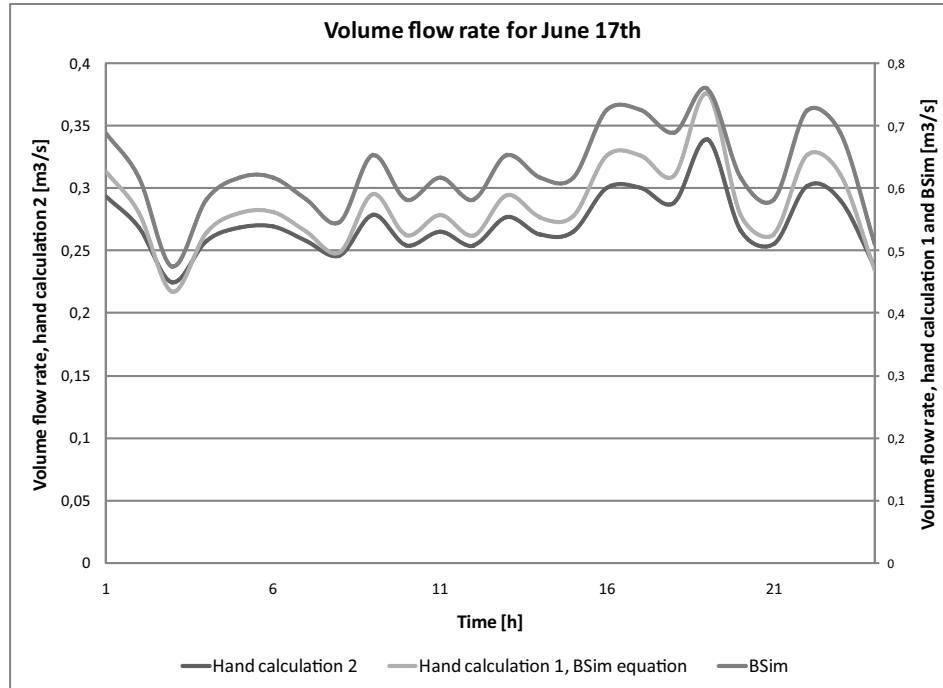
Figure 13.15: *Volume flow rate for the isolation room for the 17th of June.*
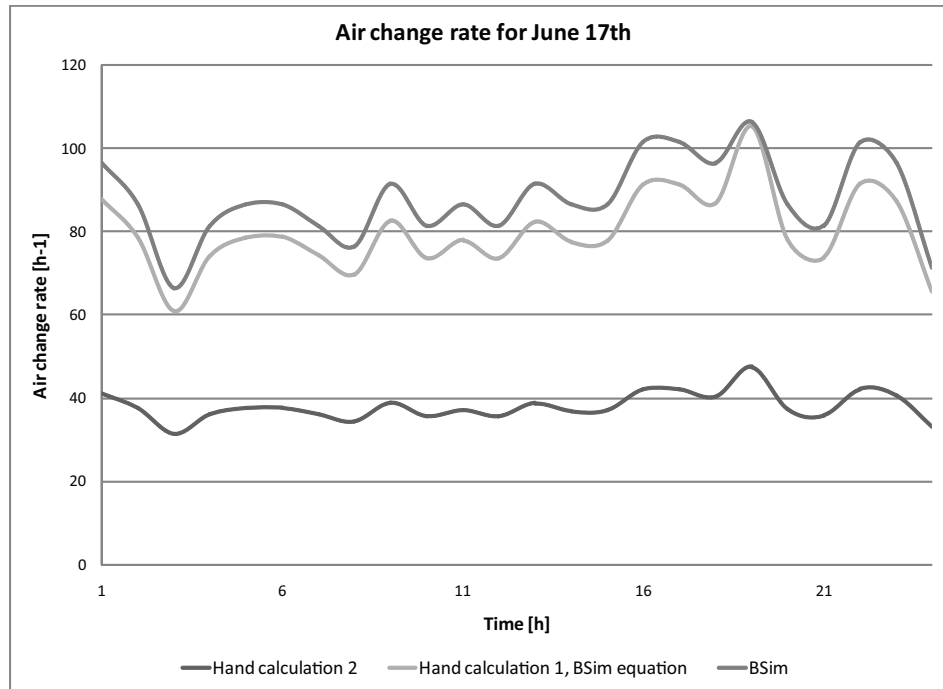
Figure 13.16: *Air change rate for the isolation room for the 17th of June.*

From figure 13.15 and 13.16 it is seen that the difference between the calculation of the volume flow and air change rate for the isolation room from hand calculation 1 and BSim is small and the values of these are about twice as high as the calculation of the volume flow and air change rate from hand calculation 2.

BSim uses equation (13.1) to calculate the airflow rate therefore the variation between these two calculations are small. A reason for the great variation to the hand calculation from equation (A.12) might be due to the development of the equations. Equation (A.12) is empirical and estimated from measurements as stated above. From BSim it is not possible to figure out the development of equation (13.1) so it is not possible to compare the requisite for the two equations.

Compared to the calculations for the 28th of January the variation between the first hand calculation and BSim are small. It is seen in figure 13.12 that for the 17th of June there are a high wind speed and that the temperature difference is small compared to the 28th of January.

Because of the high wind speed compared to temperature difference the variation between the first hand calculation and BSim are small.

From the control calculation it is concluded that the calculation of the airflow rate from BSim and equation (13.1) is about twice as high as the calculation of the airflow rate from equation (A.12). This might mean that the calculated airflow rate from BSim is too

high. It is also concluded that for the BSim calculations the temperature differences does not have as great influence as the wind speed. Since it is not possible to investigate the development of equation (13.1) the requisite of the two equations can not be discussed. To investigate the results even further another calculation of the airflow rate for another method need to be done.

To investigate the airflow for the isolation room further are made a COMIS simulation of the isolation room.

Chapter 14

Multi zone modeling of Grantham hospital

To investigate the airflow and the air change rate for the isolation room even further are made a multi zone simulation of one floor for Grantham hospital.

In chapter 12.4 the flow path for the isolation room according to mountain and sea breeze are investigated in Fluent. For the simulation of the isolation room in Fluent also the air change rate is investigated. In the simulations different setups for the isolation room are tried and the air change rate for the setup are calculated. It is concluded that the most efficient of the different setups are an isolation room connected to an anteroom where there is installed a supply fan. The isolation room is also connected to a toilet where there is installed an exhaust fan. The setup is showed in figure 14.1.
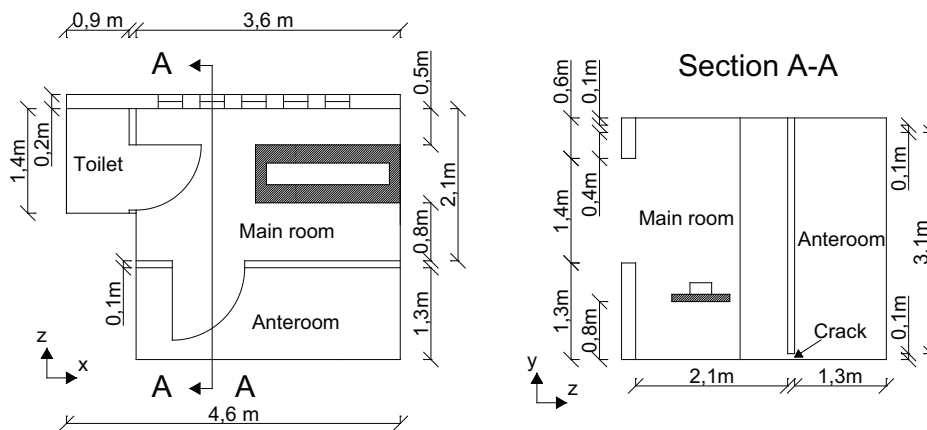
Figure 14.1: *Outline of the isolation room and the anteroom.*

From the CFD calculations in Fluent it is checked that in the two different situations with mountain and sea breeze with the setup showed in figure 14.1 the air change rate fulfill the requirement for an isolation room. From the CFD calculations also the flow path for the isolation room is checked. The air change rate for the isolation room is only investigated in two cases in the CFD simulations; daytime and nighttime, both cases only include the

wind from the sea and mountain breeze.

To investigate the air change rate for the isolation room during a year are made a single zone simulation in BSim in chapter 13. The BSim calculation showed that, with the same setup of the isolation room as for the CFD simulation but with weather data during a year for Hong Kong instead of only two situations with mountain and sea breeze, the air change rate fulfill the requirement for an isolation room during a year. For the BSim simulation only the isolation room with the anteroom and toilet is simulated therefore the influence from the other rooms are not calculated. The BSim calculation are made with the weather data from Hong Kong during a year.

Above are the air change rate therefore investigated in two different situations and with two different methods. To investigate the air change rate for the isolation room even further under different weather conditions are made a multi zone simulation in COMIS. In the COMIS simulation all the rooms for the floor are simulated so it is possible to investigate the airflow between the different rooms.

14.1   Layout of the multi zone model

For the multi zone model only one floor is simulated, this means that connections and thereby airflow between the floors are not taken into consideration. Therefore for the simulations the simulated floor is isolated from the other floors. Especially for rooms that are connected to other floors the airflow may differ from the real situation. It also means that infiltration from the rooms on the other floors are not taken into consideration. Compared to the airflow through the openings the infiltration is assumed to be small and therefore the error is small too. The main purpose is to investigate the airflow for the isolation room. This room is not direct connected to the other floors and therefore the airflow for these floors does not influence the airflow for the isolation much.

The layout of the floor is showed in figure 14.2.
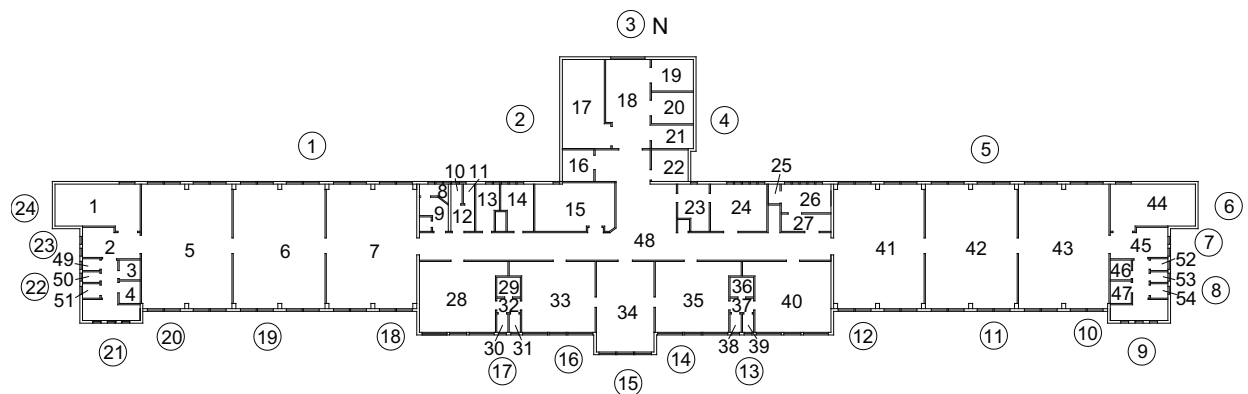
Figure 14.2: *Floor plan for the 4th floor of Grantham hospital.*

The numbers for the different zones showed in figure 14.2 and the zone names are listed in table 14.1 and 14.2.

Table 14.1: *Number and zone name for the different rooms showed in figure 14.3.*

Number	Room	Zone name
1	Staircase	z3_Stair1a
2	Lavatory	z2_Lav1a
3	Bath	z2_Bath1a
4	Bath	z2_Bath2a
5	Third class ward (8 people)	z1_3classA
6	Third class ward (8 people)	z1_3classB
7	Third class ward (8 people)	z1_3classC
8	Toilet	z2_WC2
9	Soiled linen	z4_Lin1
10	Toilet	z2_WC3a
11	Toilet	z2_WC3b
12	Staff lavatory	z2_Lav2
13	Linen store	z4_Lin2
14	Utility (dirty)	z4_Lin3
15	Dishwashing, ward servery	z4_Serv
16	Service lift	z3_Lift2
17	Staircase	z3_Stair2
18	Corridor	z6_CorLift
19	Lift	z3_Lift1a
20	Lift	z3_Lift1b
21	Nurses changing room	z5_Nurs
22	Sisters room	z5_Sis1
23	Sisters room	z5_Sis2
24	Treatment room	z5_Treat
25	Toilet	z2_WC4
26	Isolation room (1 person)	z1_Iso
27	Anteroom	z1_Ante

Table 14.2: *Number and zone name for the different rooms showed in figure 14.3.*

Number	Room	Zone name
28	Second class ward (4 people)	z1_2classA
29	Bath	z2_Bath3a
30	Toilet	z2_WC1a
31	Toilet	z2_WC1b
32	Lavatory	z2_Toil1a
33	Second class ward (4 people)	z1_2classB
34	Day room	z4_Day
35	Second class ward (4 people)	z1_2classC
36	Bath	z2_Bath3b
37	Lavatory	z2_Toil1b
38	Toilet	z2_WC1c
39	Toilet	z2_WC1d
40	Second class ward (4 people)	z1_2classD
41	Third class ward (8 people)	z1_3classD
42	Third class ward (8 people)	z1_3classE
43	Third class ward (8 people)	z1_3classF
44	Staircase	z3_Stair1b
45	Lavatory	z2_Lav1b
46	Bath	z2_Bath1b
47	Bath	z2_Bath2b
48	Corridor	z6_Cor
49	Toilet	z2_WC5a
50	Toilet	z2_WC5b
51	Toilet	z2_WC6a
52	Toilet	z2_WC5c
53	Toilet	z2_WC5d
54	Toilet	z2_WC6b

For the floor there are 3 staircases and 3 lifts that connect to the other floors. Since only one floor is simulated these staircases and lifts are not connected to the other floors.

The floor is divided into different zones that each consists of one room. Each zone is defined by the dimensions of the zone, the temperature of the zone and a reference height that is chosen as the floor level above ground level. The zones are divided into different zone groups that define the type of the room. The zone groups are listed in table 14.3.

Table 14.3: *Zone groups used for the simulation in COMIS.*

Zone group	Room type
z1	Bed ward
z2	Toilet and bath
z3	Lift and staircase
z4	Service room
z5	Nursing room
z6	Corridor

The connections between the different rooms are showed in a nodal network in figure 14.3. The black filled circles represent a nodal to the outside wile the white circles represent a nodal inside a zone in the building. The squares represent a resistance where there will be either a pressure increase or decrease. The white squares symbolize an opening while the grey squares symbolize a fan.
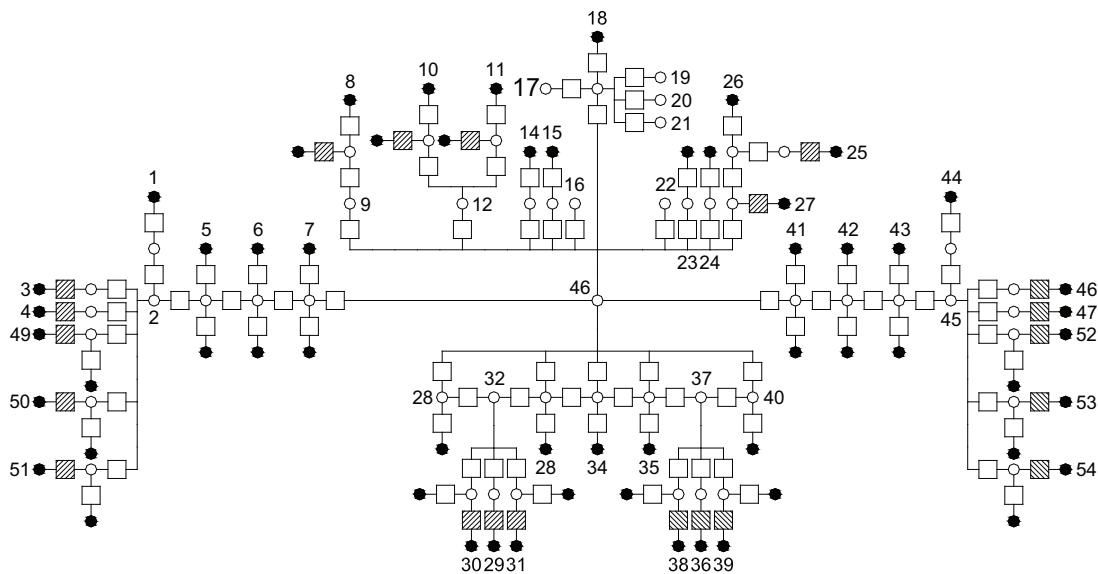
Figure 14.3: *The multi zone model for the 4th floor of Grantham hospital represented in a 2D nodal network.*

From figure 14.3 it is seen that the model consists of 54 zones. In the middle of the floor are located a corridor where most of the rooms are connected to.

14.1.1   The building and the environment

As listed in chapter 6.2 the hospital is located on the south side of Hong Kong Island at the bottom of a mountain. To the north of the building are the mountain to the other sides are located other buildings. The location of the building are listed in table 14.4.

Table 14.4: *Geographic position of Grantham hospital [Google Maps, 2007b] .*

Latitude $[°N]$	Longitude $[°E]$	Altitude $[m]$
22,15	114,10	21

For the simulation were both used pressure coefficients from literature and pressure coefficients calculated for the hospital in Fluent.

For the calculation of the pressure coefficients for the hospital is used a real wind profile. This is done to get the most accurate values because the airflow depend on the height. For the simulation are used a wind profile calculated by equation (9.1) in chapter 9.1.

For the wind profile are used terrain factors of $k = 0,35$ and $\alpha = 0,25$ corresponding to suburban area. From equation (9.1) the influence of the terrain layout and the building density is taken into consideration.

The pressure coefficient is a relationship between the given point and the wind pressure given by equation A.3, therefore the magnitude of the wind does not have any influence. For the simulation are used a reference wind speed of $3,1\ \frac{m}{s}$ corresponding to the average wind speed for Hong Kong listed in chapter 7.

The used C_p values calculated from Fluent are listed in table 14.5.

Table 14.5: C_p values for the different sides for the building calculated from Fluent. The facade element number are showed in figure 14.2.

Facade element no.	Wind angle [°]			
	0	**90**	**180**	**270**
1	0,15	-0,27	-0,07	-0,05
2	0,13	-0,29	-0,09	-0,09
3	0,15	-0,43	0,04	-0,43
4	0,13	0,29	-0,09	-0,29
5	0,15	-0,05	-0,07	-0,27
6	-0,17	0,65	-0,14	-0,26
7	-0,15	0,59	-0,16	-0,09
8	-0,15	0,43	-0,17	-0,09
9	-0,09	-0,48	0,48	-0,13
10	-0,10	-0,39	0,77	-0,08
11	-0,10	-0,48	0,79	-0,07
12	-0,08	-0,52	0,70	-0,10
13	-0,07	-0,34	0,77	-0,15
14	-0,07	-0,30	0,74	-0,16
15	-0,06	-0,22	0,78	-0,22
16	-0,07	-0,16	0,74	-0,30
17	-0,07	-0,15	0,77	-0,34
18	-0,08	-0,10	0,70	-0,42
19	-0,10	-0,07	0,79	-0,48
20	-0,10	0,08	0,77	-0,39
21	-0,09	-0,13	0,48	-0,48
22	-0,15	-0,09	-0,17	0,43
23	-0,15	-0,09	-0,16	0,59
24	-0,17	-0,26	-0,14	0,65
Roof	-0,03	-0,24	-0,16	-0,24

14.1.2 Links

To create an airflow between the different zones the zones are connected with links. The links define how the air can get from one zone into another, and the characteristic of the air passage. To characterize the airflow between the zones are used the power law. The power law defines the relation between pressure drop and airflow and is listed in equation 10.4 in chapter 10.

For the power law a flow exponent, n, of 0,5 correspond to fully turbulent flow and a flow exponent of 1 correspond to laminar flow. For the model are used different links depending on the opening type. The different links are described below.

External walls

To calculate the flow exponent for the links through the external walls are used the power law. To calculate the flow coefficient for the external walls the requirements from the Danish Building Regulations according to the maximum leakage through a wall is used. It is stated that the maximum acceptable leakage through a wall is $1,5 \ \frac{l}{s \cdot m^2}$ with an internal pressure of $50 \ Pa$ where the m^2 refer to the heated floor area.   [Erhvervs- og Byggestyrelsen, 2008] .

With the requirements from the Danish Building Regulation about leakage for a building the flow exponent for the links through the walls are calculated from the power law in equation 10.4. The flow coefficient and flow exponent are listed in table 14.6. For the calculation of the flow coefficient are used the floor area and height of the one floor and the perimeter for the hole building.

Table 14.6: *Flow coefficient and flow exponent for the links through the external walls.*

Flow coefficient $[\frac{kg}{s}$@1 $Pa]$	Flow exponent $[-]$
0,00015	0,66

For the external walls are made two links for each wall. This is done to simulate that both inflow and outflow is possible through one wall at the same time. The two links are located on the middle top half of the wall and the middle bottom half of the wall respectively.

Internal walls

For the internal walls the flow coefficient is calculated as for the external walls. For the internal walls are only used one link between the rooms. This is done because it is expected that the flow between the two rooms does not vary much from the top to the bottom of the wall. The flow coefficient and flow exponent for the internal walls are listed in table 14.7.

Table 14.7: *Flow coefficient and flow exponent for the links through the internal walls.*

Flow coefficient $[\frac{kg}{s}$@1 $Pa]$	Flow exponent $[-]$
0,00017	0,7

Large openings

The flow coefficient for the windows are calculated from the orifice model from equation 10.5 in chapter 10. Different from the power law the orifice model is defined using a discharge coefficient and the opening area of the window. For the large openings are used a discharge coefficient of 0,9.

The flow coefficient and flow exponent for the internal walls are listed in table 14.8.

Table 14.8: *Flow coefficient and flow exponent for the links through large openings.*

Flow coefficient $[\frac{kg}{s}@1\ Pa]$	Flow exponent $[-]$
1,17	0,5

Internal doors

For the doors the flow coefficient is calculated from the power law. For the door it is also possible to set the door to either open or closed. This is done by adding an orifice power law description to the link. In this way the door works as a crack in the wall when closed and an orifice opening when open.

The opening factor for the door can be set between 0 that correspond to closed and 1 corresponding to fully open. The opening area of the door is then calculated from the door area and the opening factor. Depending on whether the door is open or closed different values need to be defined. In the closed situation the flow coefficient and flow exponent need to be defined. For the situation where the door is open the door area, a discharge coefficient and an opening factor need to be defined. The discharge coefficient is calculated by COMIS therefore only the door area and opening factor need to be defined for the open door. The flow coefficient and flow exponent for the internal doors are listed in table 14.9.

Table 14.9: *Flow coefficient and flow exponent for internal doors.*

Flow coefficient $[\frac{kg}{s}@1\ Pa]$	Flow exponent $[-]$
0,0034	0,6

Windows

For the windows the same principle as for the doors are used. For the windows it is also possible to state the opening factor.

The windows therefore also uses both the power law and the orifice model dependent if it is open or closed.

For the model are used 8 different types of windows with different opening areas. Therefore the flow coefficient for the different windows vary. The flow coefficient and flow exponent for the different windows are listed in table 14.10.

Table 14.10: *Flow coefficient and flow exponent for the different windows.*

Window type	Flow coefficient $[\frac{kg}{s}$@1 $Pa]$	Flow exponent $[-]$
1	0,00041	0,6
2	0,00090	0,6
3	0,00067	0,6
4	0,00113	0,6
5	0,00016	0,6
6	0,00048	0,6
7	0,00062	0,6
8	0,00022	0,6

14.1.3 Air change rate

For the simulation are specified an air change rate for the toilets, bath and lavatory and the anteroom. The specified air change rate for the different rooms are ensured by installing mechanical ventilation for these rooms. For all other rooms are only used natural ventilation.

Toilets, bath and lavatory

For the toilets, bath and lavatory are used an air change rate of 9 h^{-1} as calculated in chapter 10.1.2. This will ensure that only 1 % pollution is left in the toilet 30 minutes after a person have left the toilet. In the Danish Building Regulation it is stated that for a toilet the airflow rate need to be 10 $\frac{l}{s}$ and for a toilet and bath 15 $\frac{l}{s}$ [Erhvervs- og Byggestyrelsen, 2008] . This correspond to an air change rate for the toilets between $4 - 9$ h^{-1}. For the toilets it is wished to ensure that no pollutant is left after 30 minutes therefore an air change rate of 9 h^{-1} is used.

Anteroom

For the anteroom are used an air change rate of 12 h^{-1} corresponding to the minimum air change rate for an isolation room as listed in chapter 5.

14.1.4 Fan characteristics

To ensure the described air change rate for the toilets, bath and lavatory are installed extract fans in these rooms. For the anteroom are installed an supply fan. The used fans are created as described in chapter 10.1.8 with the desired air change rate for the different rooms.

14.2 Check of model

To check the model the mass balance is checked for the isolation room and a third class ward. For the calculation are used average weather data for Hong Kong from chapter 7 and listed in table 14.11.

Table 14.11: *Average weather data for Hong Kong used for the check calculation.*

Ambient temperature $[°C]$	Wind speed $[\frac{m}{s}]$	Wind direction $[°]$	Humidity $[\frac{g}{kg}]$	Barometric pressure $[kPa]$
23,1	3,08	124	14,5	101

In figure 14.4 are showed the two rooms for which the mass balance is checked.
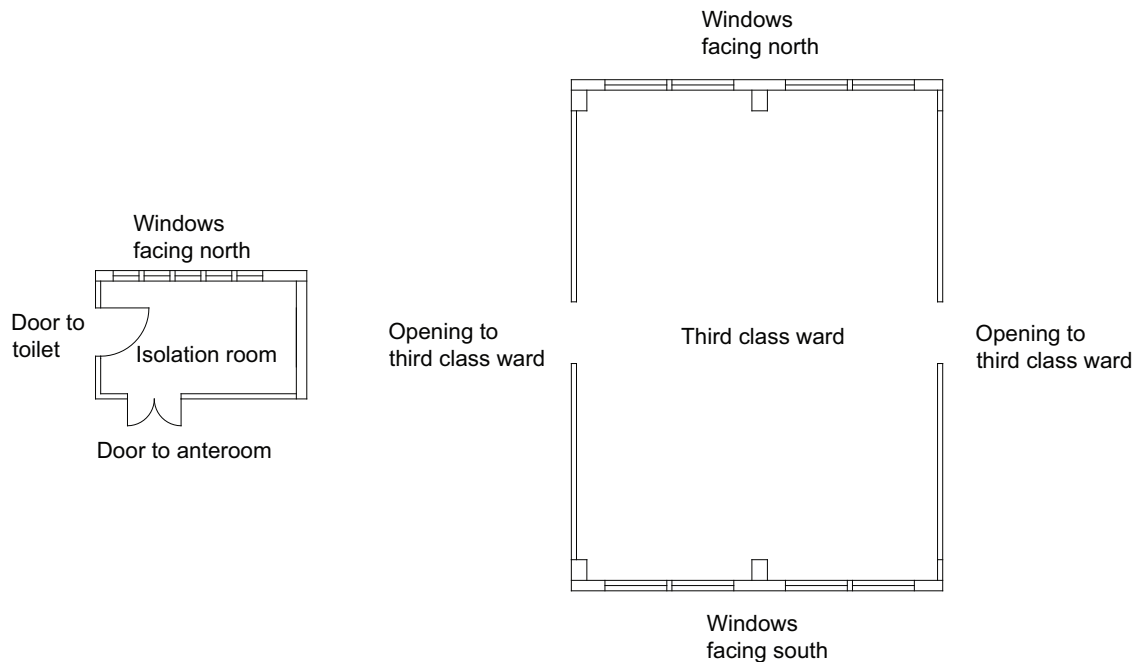
Figure 14.4: *Layout of the isolation room and a third class ward.*

For the rooms the mass balance need to be equal to 0. For the check the two doors for the isolation room are closed but there are created a crack under the doors for an airflow. For the calculation airflow through openings and infiltration are taken into consideration. Positive airflows equal airflow into the room while negative airflows equal airflow out of the room.

The mass balance for the the two rooms are listed in table 14.12. The airflow rates are calculated from COMIS.

The calculations are located in the subfolder 'COMIS\Grantham\Control' on the cd.

Table 14.12: *Mass balance for the two rooms.*

	Isolation room	Third class ward
Infiltration to outside		
North $[\frac{m^3}{s}]$	-0,004	-0,122
South $[\frac{m^3}{s}]$		0,116
Infiltration to other rooms		
Toilet $[\frac{m^3}{s}]$	0	
Anteroom $[\frac{m^3}{s}]$	0,004	
Third class ward $[\frac{m^3}{s}]$	0,017	
Corridor $[\frac{m^3}{s}]$	0	
Third class ward left side $[\frac{m^3}{s}]$		0
Third class ward right side $[\frac{m^3}{s}]$		0
Window		
In $[\frac{m^3}{s}]$	0,150	14,514
Out $[\frac{m^3}{s}]$	-0,174	-14,514
Crack between rooms		
Toilet $[\frac{m^3}{s}]$	-0,001	
Anteroom $[\frac{m^3}{s}]$	0,012	
Openings between rooms		
Third class ward left side		0,027
Third class ward right side		-0,025
Total mass balance $[\frac{m^3}{s}]$	0,003	-0,004
Error $[\%]$	1,50	0,03

From the mass balance for the two rooms listed in table 14.12 it is seen that the mass balance for the two rooms are not equal to 0. Compared to the magnitude of the mass airflow for the other openings the magnitude of the mass balance is low. The error for the two rooms are $1,50$ % for the isolation room and $0,03$ % for the third class ward. It is therefore concluded that the results from the model are right.

14.3 Airflow path

For the selected floor the airflow path is calculated. This is done to investigate the airflow in the building and the air change between the rooms. To calculate the airflow path are first made a monte carlo simulation for the floor with the weather data listed in chapter 7. From the simulation are used the mean values of the flow path and the pressure for the rooms. This is done to give an overview of the most frequent airflow path for the floor. For the following simulations are used C_p values from literature.

The used COMIS files are located in the subfolder 'COMIS\Grantham\Floor' on the cd.
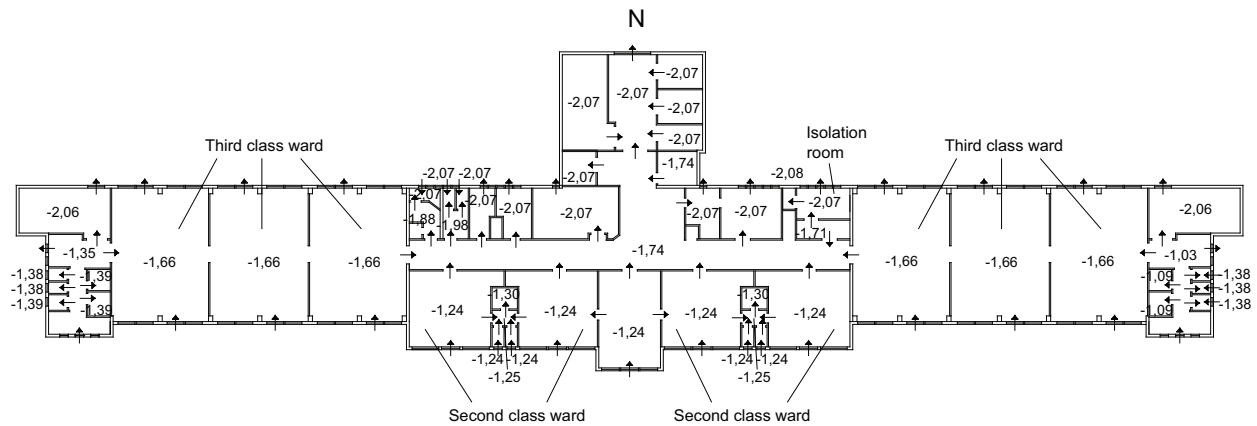
Figure 14.5: *Airflow path for the 4th floor of Grantham hospital and internal pressure for the different rooms. Pressure in [Pa].*

From figure 14.5 the airflow path for the 4th floor in the hospital is showed together with the internal pressure. It is seen in the figure, that the internal pressure is highest for the rooms facing north and lowest for the rooms facing south. It is also seen that the airflow for the floor is from south towards north. In table 14.13 are listed the frequency of the different wind directions for the simulation.

Table 14.13: *Frequency of wind direction for simulation.*

Wind direction	Frequency [%]
0	6,1
45	11,2
90	16,3
135	20,4
180	19,4
225	14,3
270	7,1
315	5,1

It is seen in table 14.13 that the most often wind direction for the simulation is the wind direction from 135 ° and 180 ° which means the wind from south east and south. Therefore the pressure is highest for the rooms facing south and lowest for the rooms facing north in the building.

For all the toilets, baths and lavatory are installed exhaust fans. From figure 14.5 it is also seen that there is an inflow to all the toilets, baths and lavatory which was desired.

For the floor are located one isolation room for one patient therefore the airflow for this room is calculated. For the isolation room the airflow is from the anteroom and into the isolation room. In the isolation room the air either flows into the toilet through the crack under the door between the rooms or out through the windows. With the higher pressure in the anteroom compared to the isolation room it is therefore ensured that the air from the isolation room is not spread into the rest of the hospital. Because the air is let out through the window it has to be ensured that it is not flowing into an other room through another inlet. For all the rooms located in the northern part of the floor it is seen from figure 14.5 that there is an outflow through the windows. Therefore the air from the isolation room is not getting into another room.

For the second class ward the inlet air is flowing from both the southern windows and the day room. From the wards the air is let into the corridor. Therefore if the air from the second class ward are polluted it will be spread to the rest of the hospital.

The inlet for the third class wards are from the southern windows and out through the northern windows. Because the internal pressure for the third class ward and the corridor are almost the same there will not be a high airflow between these two rooms. The third class ward are therefore mainly cross ventilated.

14.3.1 Northern wind

In figure 14.6 are showed the average airflow path for the 4th floor and the average internal pressure for the different rooms with northern wind.

Figure 14.6: *Airflow path for the 4th floor of Grantham hospital and pressure for the different rooms in the case with northern wind. Pressure in [Pa].*

Because of the wind direction from north the airflow for the building is from north towards south as seen in figure 14.6.

For the toilets, baths and lavatories the airflow is into the rooms where it is let out through an exhaust fan, except for the toilets facing north. Because of the northern wind

the air is let into the toilets through the windows but not all the air is let out through the exhaust fan. It is seen that for the toilets facing north the air is lead from the toilets and further into the neighboring rooms. This means that the pollutant from the toilets are spread further into the hospital and not all exhausted in the toilet. Therefore in the case with a strong northern wind it might be necessary to install a more powerful exhaust fan in the toilet to prevent an airflow from the toilets further into the hospital.

For the anteroom next to the isolation room was installed an inlet fan to ensure the right airflow direction between the anteroom and the isolation room. With the inlet fan in the anteroom it was desired that the airflow would be from the anteroom and into the isolation room so pollutant air from the isolation room was not spread into the rest of the hospital. From figure 14.6 it is seen that this airflow is not happening. With the northern wind it is seen that the air is let into the isolation room through the windows and further into the anteroom. This means that the air is going the opposite direction as desired and there is a possibility of pollutant air from the isolation room is spread into the rest of the hospital. Because of the inlet fan in the anteroom the air is spread further into the hospital. To prevent this airflow a stronger fan in the anteroom might therefore be needed.

For the third class wards it is seen from figure 14.6 that the airflow is flowing from the bed wards towards the lavatory in the two ends. With northern wind it is therefore ensured that air from the third class wards are not spread into the corridor and the other rooms.

14.3.2   No wind

In figure 14.7 are showed the average airflow path and internal pressure for the floor in the case where there are no wind.
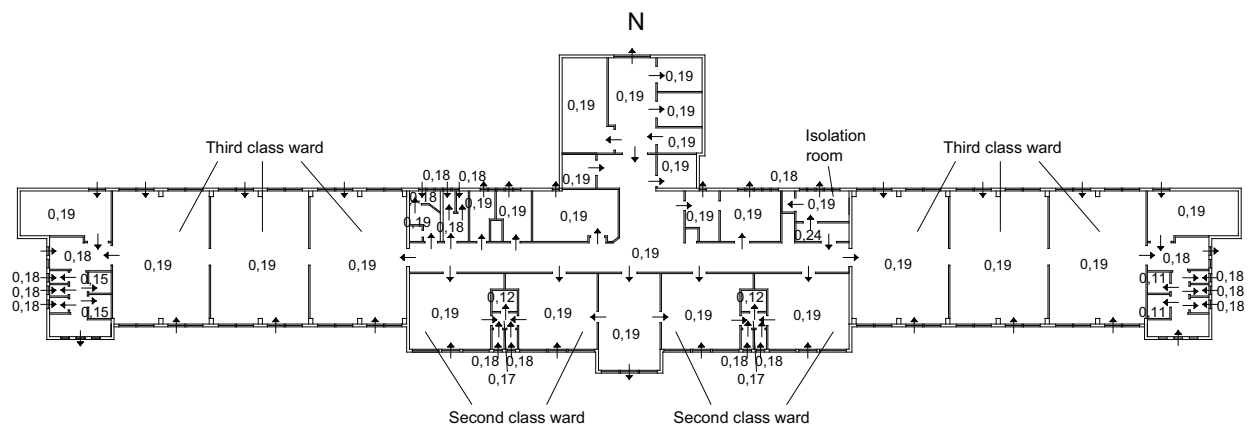
Figure 14.7: *Airflow path for the 4th floor of Grantham hospital and pressure for the different rooms in the case without wind. Pressure in [Pa].*

From figure 14.7 it is seen that the internal pressure does not vary much for the different rooms. This means that the created pressure according to thermal buoyancy is low compared to the situation with both thermal buoyancy and wind pressure. The greatest

variation is for the rooms where there are installed a fan. Because the small variation in the internal pressure for the rooms the driving force between the rooms are small too.

For the floor it is seen that most of the windows are used as inlet and the outlet for the floor is through the exhaust fans in the toilets.

Because of the inlet fan for the anteroom it is secured that the air flowing from the isolation room is not spread into the rest of the building but let out through the fan in the toilet or through the windows.

14.4   Air change rate

To ensure a high air quality and that polluted air is not spread it is stated that the minimum air change rate for an isolation room is $12 \ h^{-1}$ according to chapter 5.

The air change rate for the isolation room in Grantham hospital is calculated by CFD methods and by using BSim. For the CFD method was calculated the air change rate where only thermal effects were taken into consideration, for the BSim calculation was made a year simulation to calculate the air change rate.

For both the CFD calculation and the BSim calculation only the single room was simulated with the toilet and the anteroom, the influence from other rooms was not taken into consideration. For both the calculations the infiltration was not taken into consideration either.

To get a more accurate picture of the air change rate for the isolation room are made a COMIS calculation where the influence from other rooms and infiltration are taken into consideration too.

The used COMIS files are located in the subfolder 'COMIS\Grantham\Isolation room' on the cd.

First are made a monte carlo simulation with the weather data distributions listed in chapter 7 as for the calculation of the airflow path above. From the simulation the average air change rate for the room is calculated.

The average airflow path and volume flow for the hospital is showed in figure 14.8.
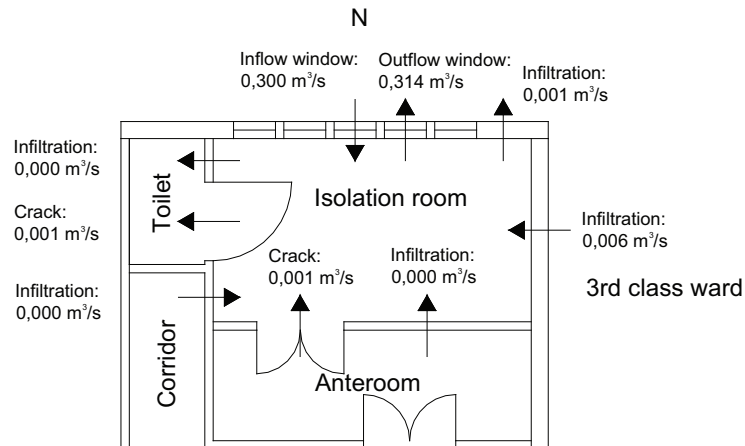
Figure 14.8: *Average airflow path and volume flow for the isolation room.*

From figure 14.8 it is seen that the main inflow and outflow for the isolation room is through the windows. For the crack under the two doors there are a small airflow.

The air change rate for the isolation room with the airflows showed in figure 14.8 is calculated for 45 h^{-1}. This shows that the average air change rate for the isolation room is higher than the necessary air change for an isolation room.

In figure 14.9 are showed the frequency of the air change rate.
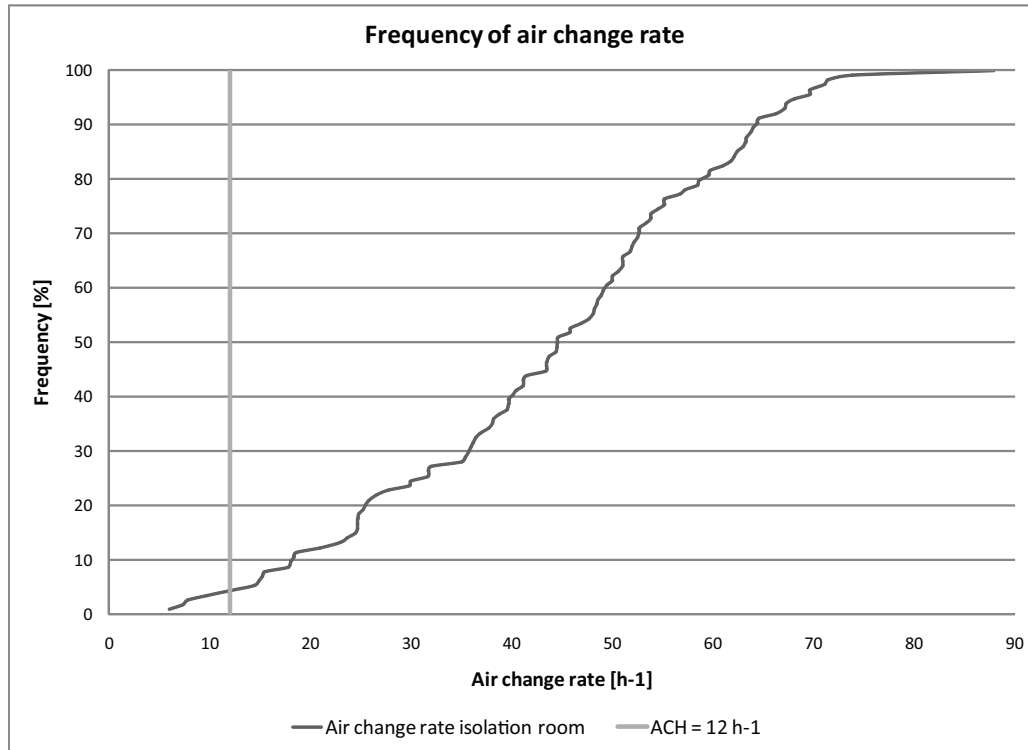
Figure 14.9: *Frequency of the air change rate for the isolation room.*

With the weather distribution stated in chapter 7 it is seen from figure 14.9 that it is not possible to create a high enough air change rate in about 5 % of the time, in this situation the air change rate is below 12 h^{-1}.

To investigate the influence of the thermal buoyancy and the wind pressure for the air change rate for the room are made simulations only with thermal buoyancy and with wind pressure.

14.4.1 Thermal buoyancy

In figure 14.10 are showed the airflow for the isolation room where only thermal buoyancy is taken into consideration. The local sea and mountain breeze is not taken into consideration.

N

Inflow window:
0,272 m³/s

Outflow window:
0,287 m³/s

Infiltration:
0,002 m³/s

Infiltration:
0,000 m³/s

Toilet

Isolation room

Infiltration:
0,000 m³/s

Crack:
0,001 m³/s

Crack:
0,004 m³/s

Infiltration:
0,002 m³/s

Infiltration:
0,000 m³/s

3rd class ward

Infiltration:
0,000 m³/s

Corridor

Anteroom
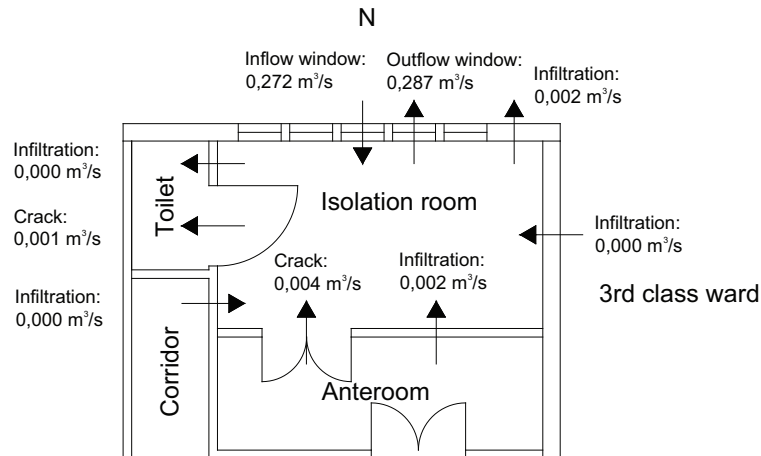
Figure 14.10: *Average airflow path and volume flow for the isolation room with thermal buoyancy.*

As for the average situation also for the situation with only thermal buoyancy the main inlet and outlet for the isolation room is through the windows. For the situation with only thermal buoyancy the airflow path for the isolation room is almost the same as for the average situation with both thermal buoyancy and wind pressure listed above. Compared to the average situation the airflow is a bit smaller when only thermal buoyancy is taken into consideration.

The air change rate for the isolation room is calculated to 39 h^{-1}, which is higher that the necessary air change rate. It is therefore seen that in the situation with no wind the thermal buoyancy is enough to create a sufficient air change rate. To investigate the influence of the temperature difference on the air change rate are showed the air change rate for the isolation room as a function of the temperature difference between inside and outside in figure 14.11.
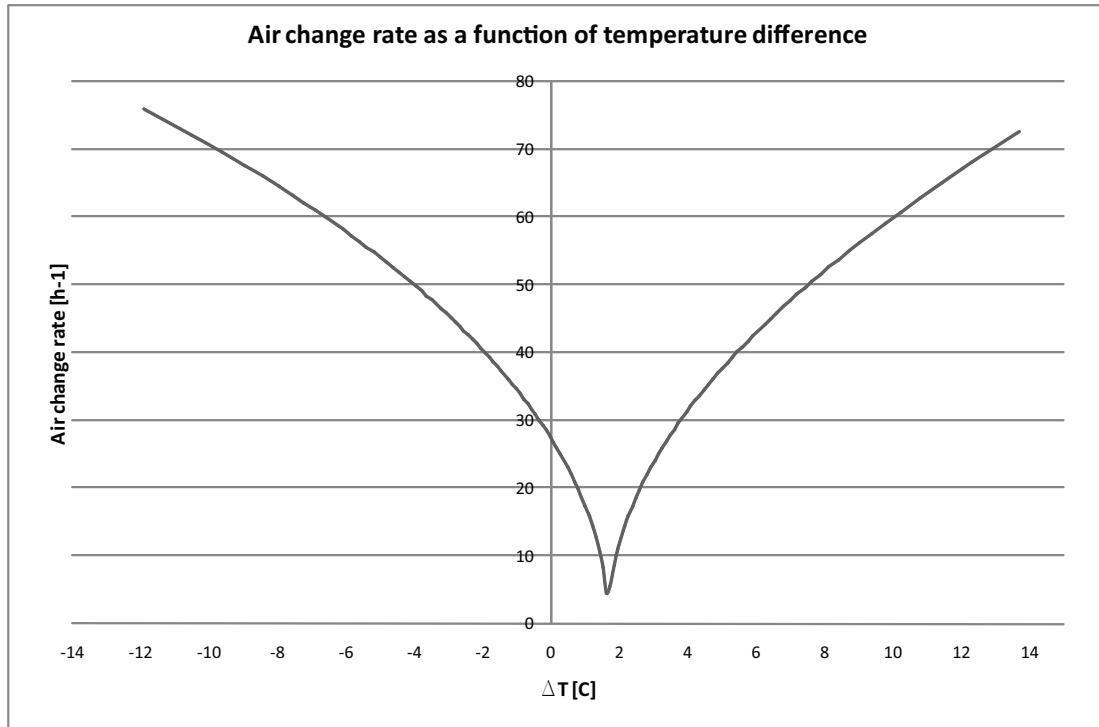
Figure 14.11: *Air change rate for the isolation room as a function of temperature difference.*

It is seen from figure 14.11 that with a temperature difference between $1\ °C\ -\ 3\ °C$ the air change rate for the isolation room is below $12\ h^{-1}$. A reason why the air change rate is not lowest for a temperature difference of $0\ °C$ might be because of the fans in both the anteroom and the toilet. Because the pressure created by the fans the natural driving forces need to create the opposite pressure to equal the airflow, therefore the lowest air change rate might be for a temperature difference of $1\ °C\ -\ 3\ °C$.

The frequency for the air change rate in the situation with only thermal buoyancy is showed in figure 14.12.
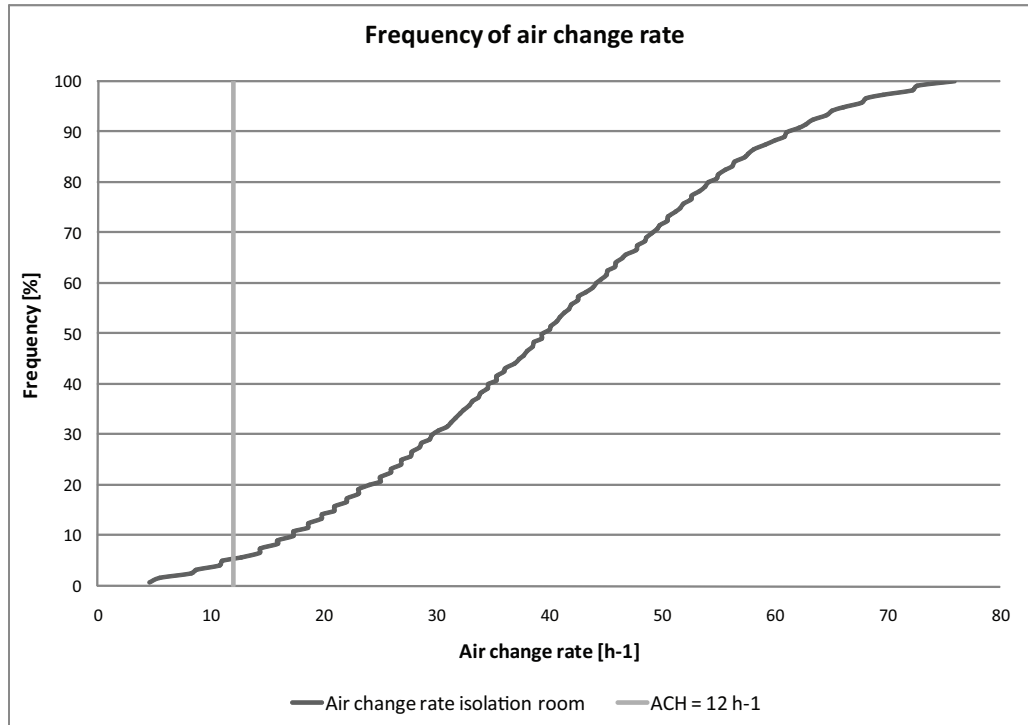
Figure 14.12: *Frequency of the air change rate for the isolation room with only thermal buoyancy.*

From figure 14.12 it is seen that for about 7 % of the time the air change rate is lower than 12 h^{-1} in the case where only thermal buoyancy is taken into consideration.

14.4.2 Wind pressure

To investigate the influence of the wind pressure on the air change rate are made two different simulations. For the first simulation the wind speed is changed and for the second simulation the wind direction is changed. In the case where the wind speed is changed are used a wind direction of 124 ° and in the case where the direction is changed are used a wind speed of 3, 1 $\frac{m}{s}$, corresponding to the average values for Hong Kong listed in chapter 7.

In figure 14.13 are showed the airflow path for the isolation room in the situation with different wind speed.
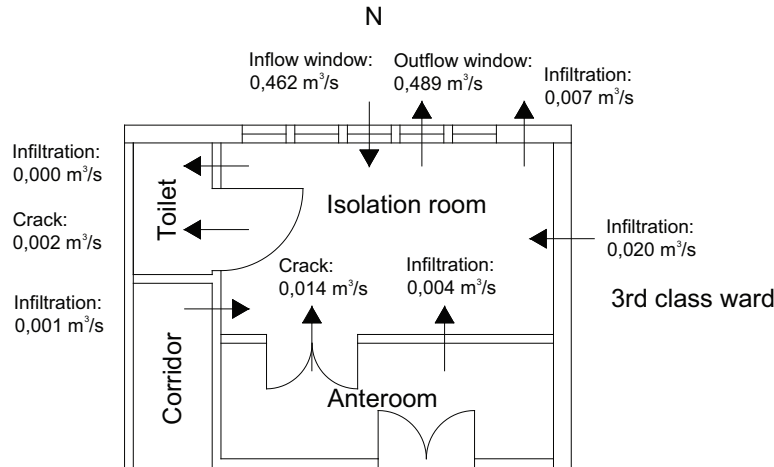
Figure 14.13: *Average airflow path and volume flow for the isolation room with different wind speed.*

It is seen from figure 14.13 that for the situation where only the wind speed is varied the main airflow directions are the same as for the other two cases. Compared to the first situation where both the temperature, wind speed and wind direction is varied the airflow shown in figure 14.13 for the situation where only the wind speed is varied is higher than for the other cases. A reason for this might be that the wind pressure and the thermal buoyancy does not always act in the same direction but in some cases against each other depending on the temperature difference and the wind speed and direction.

For most wind directions when wind is acting alone the airflow from wind pressure will be in at the top of the opening and out at the bottom of the opening. Depending on the inside and outside temperature the airflow according to thermal buoyancy will flow through the opening in the top when the inside temperature is lower than outside and the other way when the inside temperature is higher than outside. This means that in the case where the inside temperature is higher than outside the thermal buoyancy and wind pressure will act against each other. The principles are showed in figure 14.14.
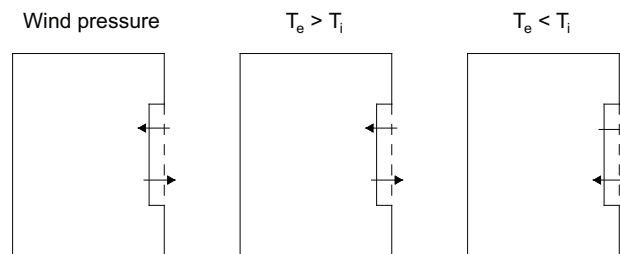
Figure 14.14: *Inflow direction for wind pressure and thermal buoyancy.*

For the situation with different wind speed it is seen from figure 14.13 that the main in- and outflow for the isolation room is through the windows as for the other two situations. The average air change rate in this situation is calculated for 69 h^{-1} which is higher than

the necessary air change rate rate.

The dependency of the air change rate on the wind speed is showed in figure 14.15.
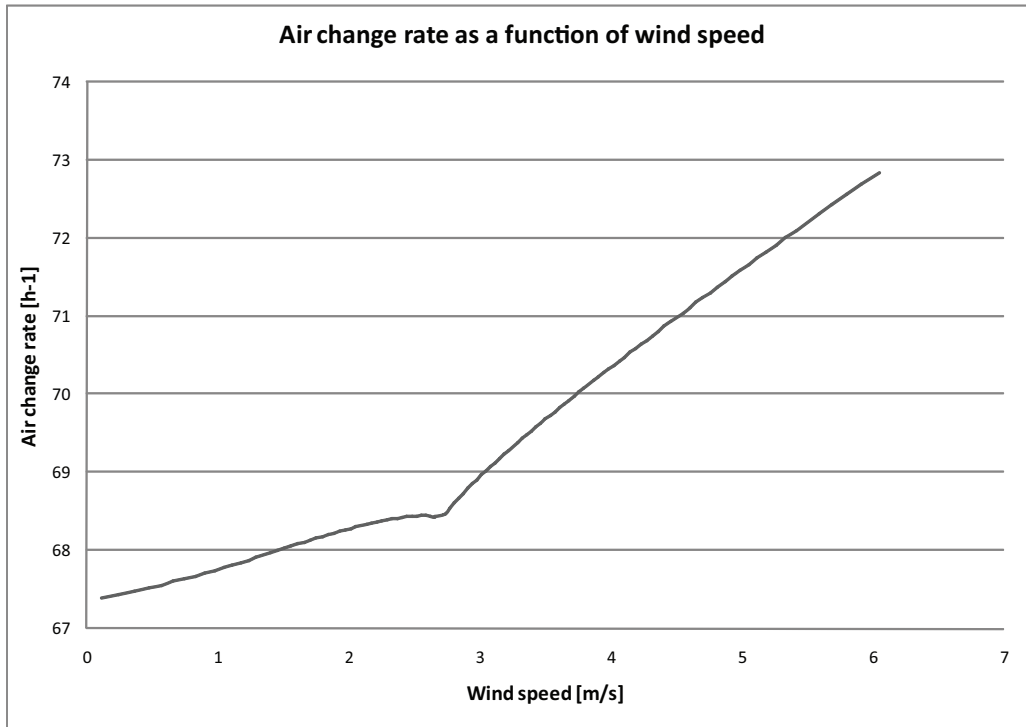
Figure 14.15: *Air change rate for the isolation room as a function of wind speed.*

From figure 14.15 it is seen that even with a low wind speed it is possible to create an air change rate higher than 12 h^{-1}.

The frequency of the air change rate for the isolation room when the wind speed differ is showed in figure 14.16.
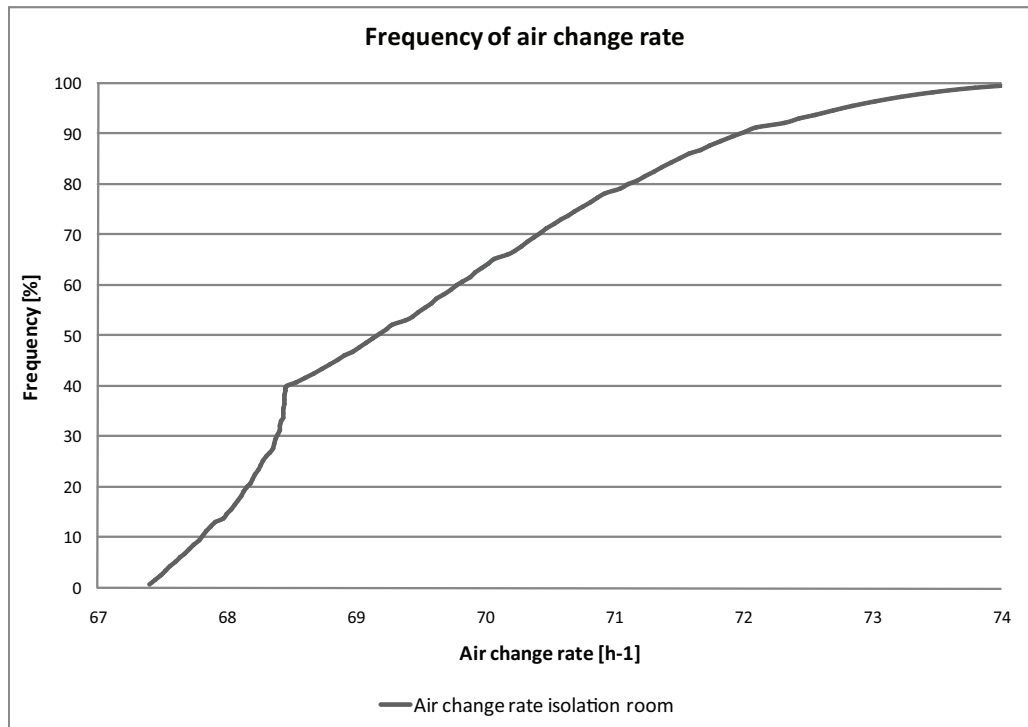
Figure 14.16: *Frequency of the air change rate for the isolation room with different wind speed.*

From figure 14.16 it is seen that when only the wind speed is taken into consideration the air change rate for the isolation is higher than $12\ h^{-1}$.

The airflow for the isolation room where only the wind direction is taken into consideration is showed in figure 14.17.
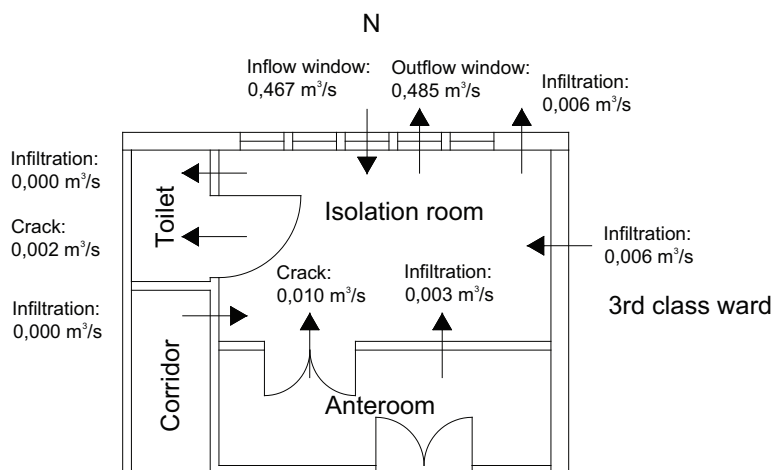
Figure 14.17: *Average airflow path and volume flow for the isolation room with different wind directions.*

Also for the situation where the wind direction does variate the main inflow and out-

flow for the isolation room is through the windows. For the situation with different wind direction it is seen from figure 14.17 that the inflow and outflow is higher than for the other situations. The average air change rate for this situation is calculated for 69 h^{-1}.

The air change rate as a function of wind direction is showed in figure 14.18.
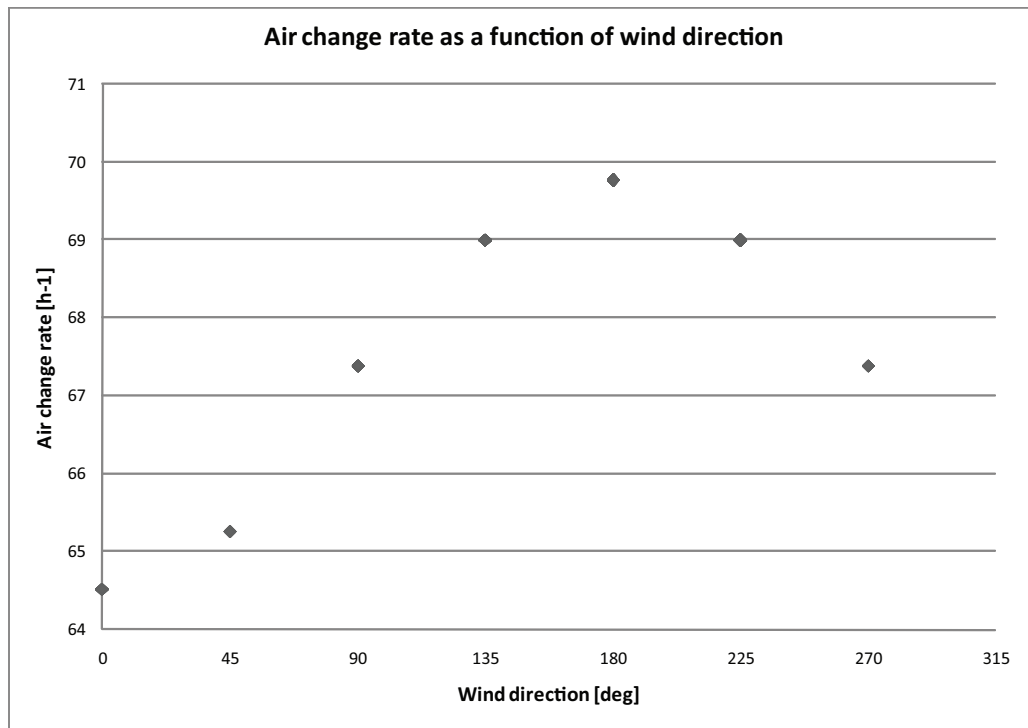
Figure 14.18: *Air change rate for the isolation room as a function of wind direction.*

It is seen from figure 14.18 that the highest air change rate is for a wind direction of 180 ° from south. The highest air change rate for the isolation room is therefore not created when the wind hits perpendicular to the isolation room. This is because the higher pressure in the anteroom. When the wind hits perpendicular to the isolation room this acts against the pressure between the anteroom and the isolation room.

In figure 14.19 are showed the frequency of the air change rate with the different wind directions.
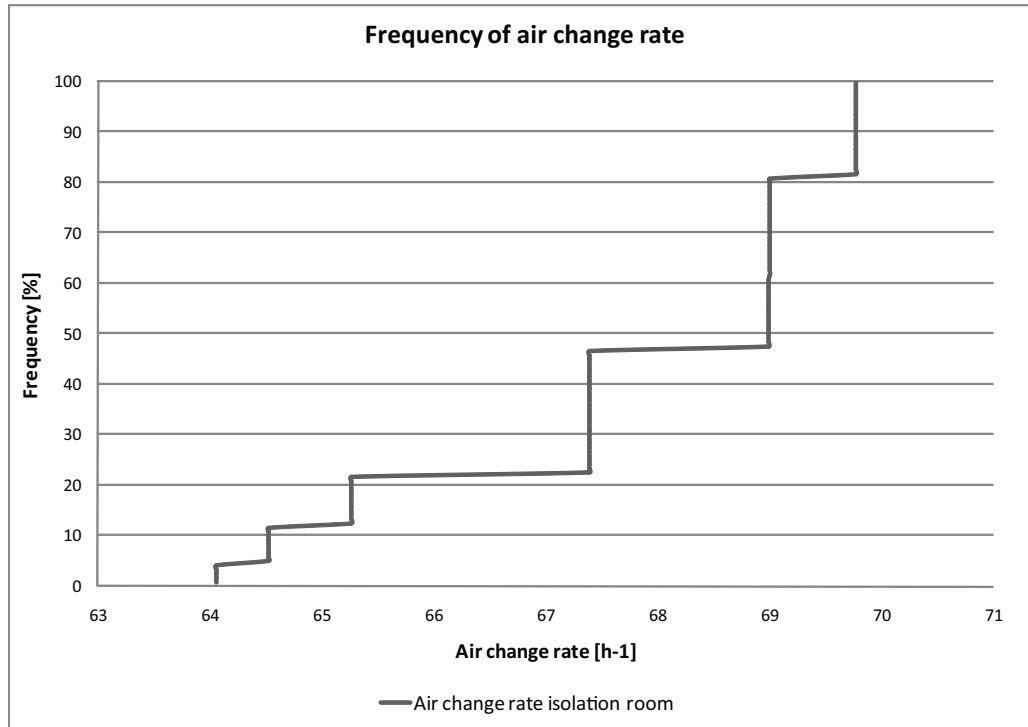
Figure 14.19: *Frequency of the air change rate for the isolation room with different wind direction.*

From figure 14.19 it is seen the the air change rate does not get below 12 h^{-1} for the different wind directions with a wind speed of 3, 1 $\frac{m}{s}$.

14.5 Pressure for isolation room

In the above calculation are used an inlet fan for the anteroom to create a negative pressure isolation room for patient infected with airborne diseases. For situations where the patient is particular week and vulnerable to diseases the isolation room should be positive pressurized to keep out the pathogenic microorganisms from the surrounding areas.

A way to create a positive pressurized isolation room instead of a negative pressurized isolation room is to install an exhaust fan in the anteroom instead of an inlet fan. In this way the air will be let from the isolation room into the anteroom instead of the other way around.

The airflow path for the positive pressurized isolation room with the average weather data from Hong Kong are showed in figure 14.20.
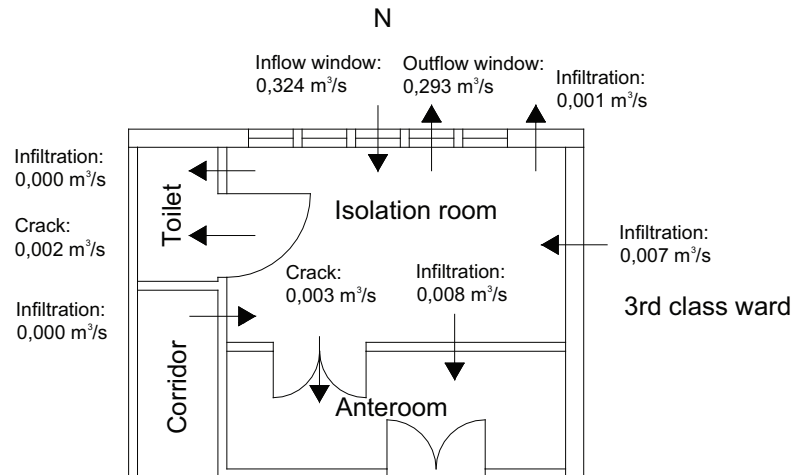
Figure 14.20: *Average airflow path and volume flow for the positive pressurized isolation room.*

It is seen from figure 14.20 that by installing an exhaust fan in the anteroom the airflow between the isolation room and the anteroom is from the isolation room into the anteroom.

From figure 14.20 it is also seen that there is an infiltration from the third class ward into the isolation room, this means that the pressure in the third class ward might be higher than for the isolation room. To ensure that this airflow is not happening it might be necessary to install an extract fan in the third class ward or to ensure that the infiltration between the rooms are lowered.

As for the negative pressurized isolation room the main inlet and outlet for the isolation room is through the windows.

In figure 14.21 are showed the frequency of the air change rate for the positive pressurized isolation room.
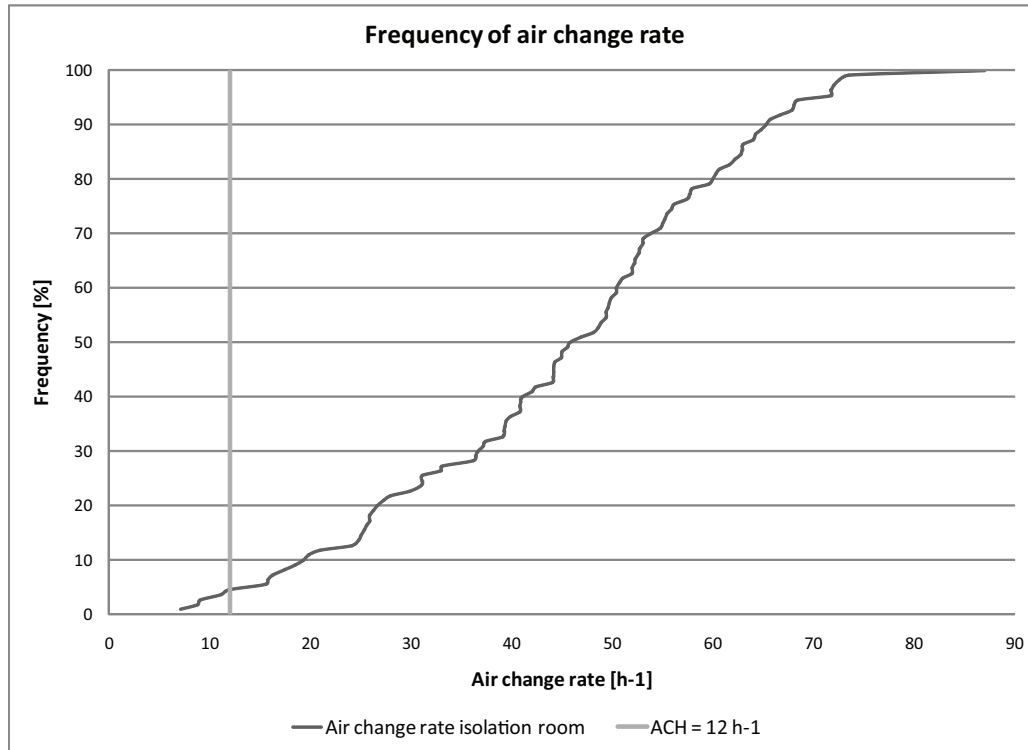
Figure 14.21: *Frequency of the air change rate for the positive pressurized isolation room.*

As for the negative pressurized isolation room it is seen from figure 14.21 that only for about 5 % of the time the air change rate is below 12 h^{-1}.

14.6 Calculated pressure coefficients

The above calculations are made with pressure coefficients from literature, in the following calculations are used calculated pressure coefficients from CFD simulation of Grantham hospital. The used pressure coefficients are listed in table 14.5.

Compared to the pressure coefficients from literature the variation of the calculated pressure coefficients for the hospital is higher. This means that the positive value of the calculated pressure coefficients are higher than the value of the pressure coefficients from literature and the negative values are lower. Because of the higher and lower values of the pressure coefficients for the hospital compared to the literature values this means that there will be a higher airflow for the floor. In the following are made two calculations the first for the airflow for the whole floor and the second of the volume flow for the isolation room. These two calculations are made to state the difference by using pressure coefficients from literature and pressure coefficients calculated for the building.

The used COMIS files are located in the subfolder 'COMIS\Grantham\CFD Cp' on the cd.

In figure 14.22 are showed the airflow for the floor with pressure coefficients from the CFD calculations.

Figure 14.22: *Airflow path for the 4th floor of Grantham hospital and pressure for the different rooms with pressure coefficients calculated for the hospital. Pressure in [Pa].*

As for the situation with pressure coefficients from the literature the airflow for the floor is from south towards north, where the lowest internal pressure is for the rooms facing north.

Compared to the situation with pressure coefficients from the literature the variation in the internal pressure for the floor is higher with pressure coefficients calculated for the hospital. A reason for the higher variation might be because of the higher variation in the calculated pressure coefficients compared to the pressure coefficients from literature.

The higher pressure coefficients calculated for the hospital compared to literature also means that the airflow for the hospital is higher with the calculated pressure coefficients.

From figure 14.22 it seen that the airflow for the third class room is from the third class room into the lavatory. This is the opposite direction of the airflow with the pressure coefficients from literature.

In figure 14.23 are showed the volume flow for the isolation room with the calculated pressure coefficients.

Figure 14.23: *Average airflow path and volume flow for the isolation room with calculated pressure coefficients.*

It is seen from figure 14.23 that the airflow direction for the isolation room with the calculated pressure coefficients are the same as for the simulation with pressure coefficients from literature. It is also seen that the volume flow are a bit higher for the isolation room showed in figure 14.23 compared to the volume flow for the isolation room with pressure coefficients from the literature as showed in figure 14.8. This is again because of the higher pressure coefficients for the isolation room in figure 14.23.

The frequency of the air change rate for the isolation room for the situation with calculated pressure coefficients are showed in figure 14.24.
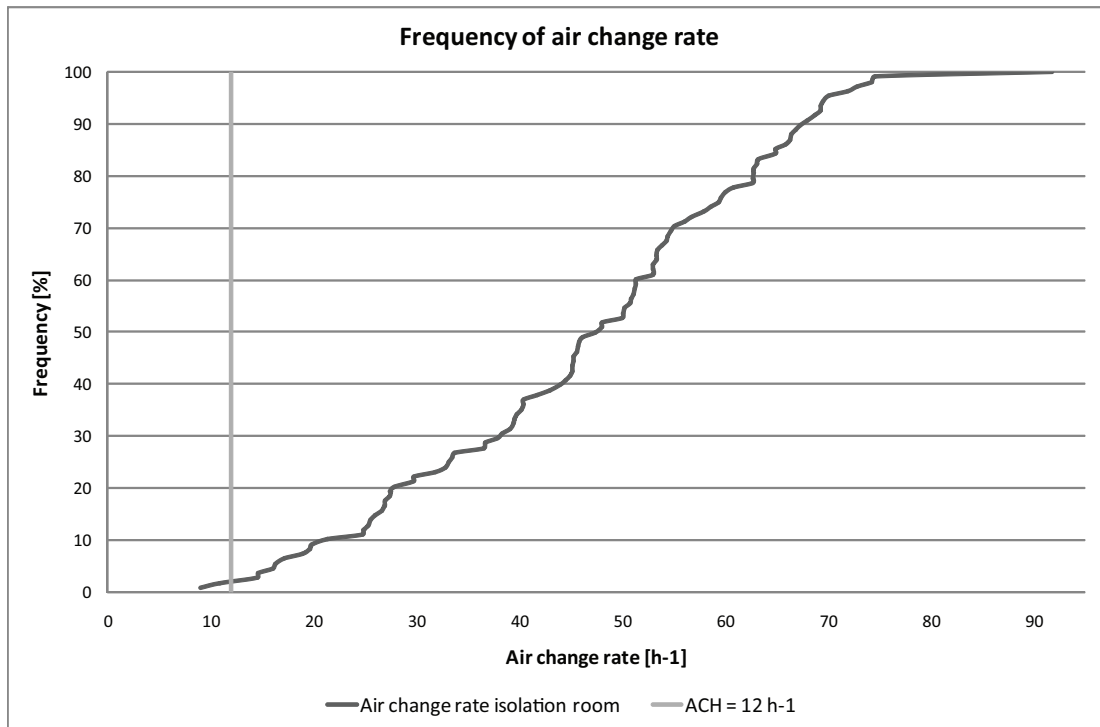
Figure 14.24: *Frequency of the air change rate for the isolation room with calculated pressure coefficients.*

Compared to the situation with pressure coefficients from literature the frequency of the air change rate below 12 h^{-1} is lower for the situation with calculated pressure coefficients. The frequency of the air change rate below 12 h^{-1} is about 2 %.

14.7 Concise conclusion

Above are made calculations of the airflow for both the whole floor and for the isolation room. From the calculations of the airflow for the floor it is seen that by installing exhaust fans in the toilets, bath and lavatories it is possible to get an airflow into the toilets where the air is exhausted. For the anteroom is installed an inlet fan to prevent an airflow from the anteroom into the isolation room to avoid spread of pollutant air into the rest of the hospital. From the calculations with a strong northern wind it is investigated that the inlet and exhausts fans are not strong enough to prevent the undesired airflow direction.

The most often wind direction for Hong Kong is from south to south east which means that most often the airflow direction is in the predicted direction, only with strong northern wind there is some problems.

From the calculation of the volume flow for the isolation room it is seen that with pressure coefficients calculated for the building the air change rate is below 12 h^{-1} for about 2 % of the time. In the case where there is no wind it is calculated that the air change rate

is below 12 h^{-1} for about 7 % of the time. For the situation where the indoor temperature is the same as outdoor temperature it is investigated the the air change rate is higher than 12 h^{-1} all the time.

It is therefore seen from the calculations that there are some problems with the airflow in the case of strong northern wind, and for about 2 % of the time with both wind pressure and thermal buoyancy the air change rate is below 12 h^{-1}.

With the setup used it is therefore not possible to ensure the right air change rate 100 % of the time.

Chapter 15

Energy and comfort

In the chapters above are solutions for using natural ventilation for the two hospitals stated. For the solution for both hospitals are not looked further into the energy use and comfort for the rooms. To get an idea about these two aspects for the hospitals this is discussed in the following.

Because of the use of natural ventilation the outside weather conditions have great influence on the indoor climate for the isolation rooms. In the solutions for both Aabenraa and Grantham hospital the main inflow to the rooms are through openings connected to the outside, this means that outside air is let directly into the rooms. Because of the different location of the two hospitals the indoor climate differ a lot from each other.

In chapter 7 it is stated that the average ambient temperature for Denmark is $7,8\ °C$ and for Hong Kong $23,1\ °C$. The ambient temperature during a year for both Denmark and Hong Kong are showed in figure 15.1.
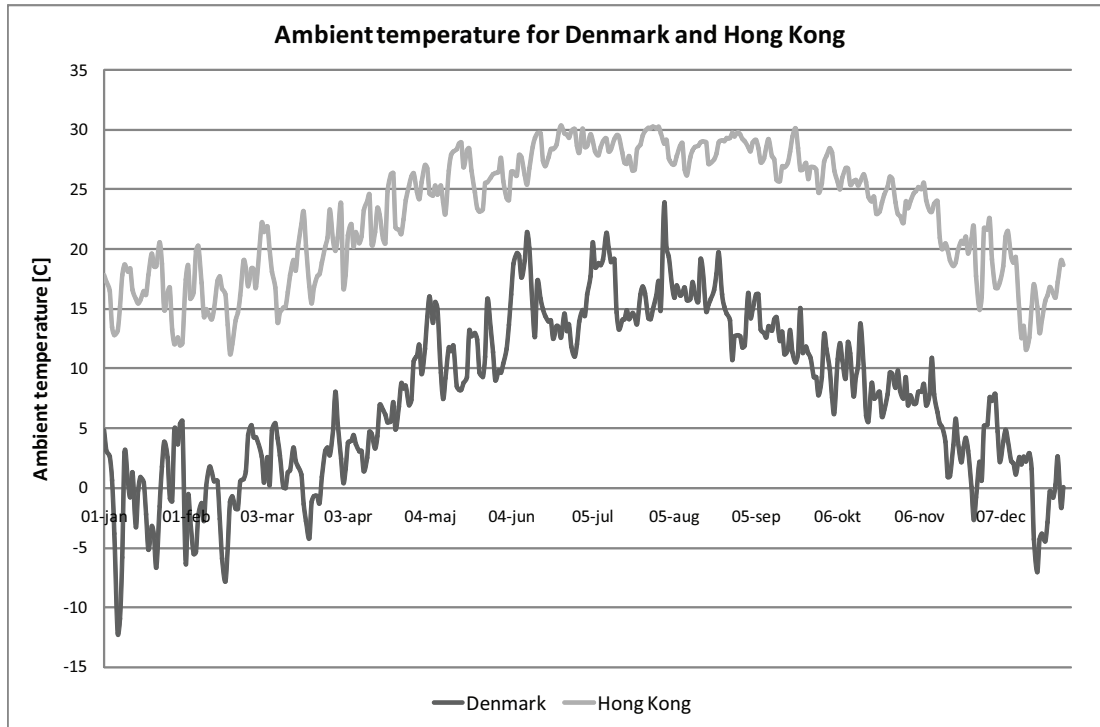
Figure 15.1: *Ambient temperature for Denmark and Hong Kong during a year. [Jensen, 2007]
, [EnergyPlus, 2007]*

From figure 15.1 it is seen that the ambient temperature for Denmark is about $10-15\,^{\circ}C$ lower than for Hong Kong. It is also seen that for Denmark the average temperature for the winter period is about $0-5\,^{\circ}C$. This means that when natural ventilation is used without any preheating of the air the inlet air is cold compared to comfort temperature.

For Hong Kong the opposite is happening where it is seen in figure 15.1 that the ambient temperature during summer rises to a temperature of $25-30\,^{\circ}C$. For the summer period there are therefore a possibility of overheating for the rooms using natural ventilation.

In figure 15.2 are showed the indoor temperature for an isolation room in Aabenraa hospital compared to the ambient temperature and in figure 13.3 in chapter 13.2 are showed the indoor temperature compared to the ambient temperature for an isolation room of Grantham hospital. For both situations it is assumed that the windows are fully open.
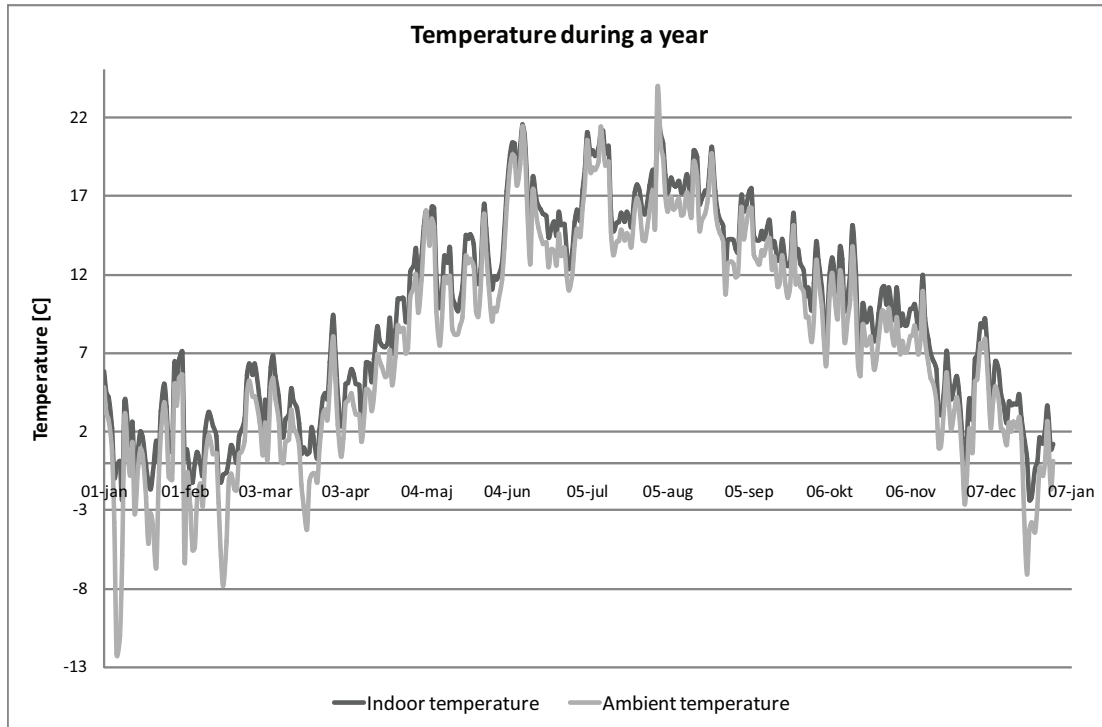
Figure 15.2: *Indoor temperature for an isolation room in Aabenraa hospital compared to the ambient temperature.*

For both isolation rooms it is seen that the indoor temperature follows the ambient temperature during a year but is about $1 - 3\ ^\circ C$ higher. This means that for Aabenraa hospital the indoor temperature get low during winter and for Grantham hospital the temperature get high during summer. The indoor temperature for the two rooms compared to the design temperature from figure 13.6 in chapter 13.2 are showed in figure 15.3 and 15.4.

The design temperature are empirical calculated from:

$$\text{Upper limit:} \qquad \Theta_{i,max} = 0,33 \cdot \Theta_{rm} + 18,8 + 3 \qquad (15.1)$$

$$\text{Lower limit:} \qquad \Theta_{i,min} = 0,33 \cdot \Theta_{rm} + 18,8 - 3 \qquad (15.2)$$

[DS/EN 15251, 2007]

where

Θ_i : Limit value of indoor operative temperature $[^\circ C]$
Θ_{rm} : External running mean temperature $[^\circ C]$
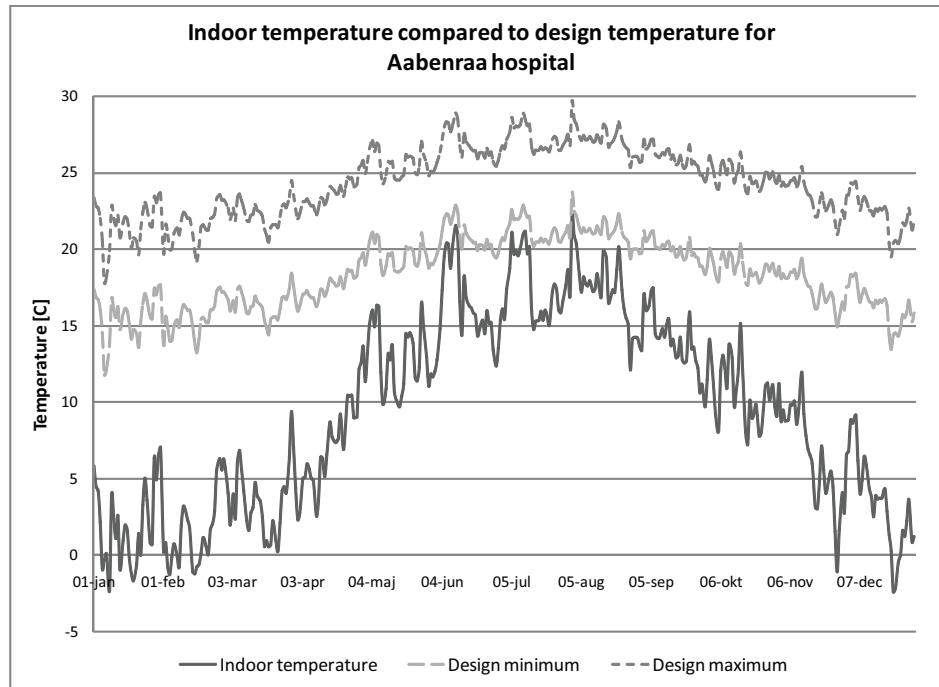
Figure 15.3: *Indoor temperature for an isolation room in Aabenraa hospital compared to the design temperature.*
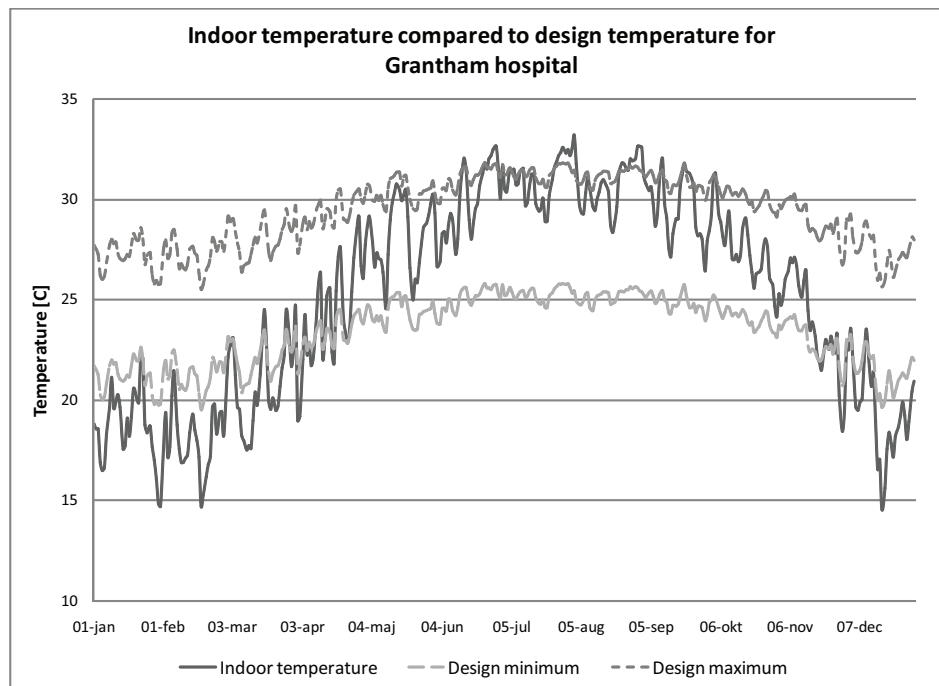
Figure 15.4: *Indoor temperature for an isolation room in Grantham hospital compared to the design temperature.*

It is seen from figure 15.3 and 15.4 that specially for Aabenraa hospital there are problems with a low indoor temperature. From the figure it is seen that also during the summer

period the temperature does not rise to the minimum design temperature. For Grantham hospital the indoor temperature is not as low as for Aabenraa but it is still seen that there are some problems with a too low indoor temperature during winter and a too high temperature during summer. Compared to Aabenraa hospital the temperature difference to the design temperature for Grantham hospital are not high.

To get a comfortable indoor temperature specially for Aabenraa hospital preheating of the air is needed.

The power needed for heating the air is calculated by:

$$P = c \cdot m \cdot \Delta t \tag{15.3}$$

where

P : Power $[kW]$
c : Specific heat capacity $[\frac{kJ}{kg \cdot °C}]$
m : Mass flow $[\frac{kg}{s}]$
Δt : Temperature difference $[°C]$

The average and minimum and maximum temperature difference for Aabenraa hospital compared to the design temperatures are listed in table 15.1.

Table 15.1: *Temperature difference for Aabenraa hospital compared to the design temperature.*

		Temperature difference to	
		Design minimum $[°C]$	Design maximum $[°C]$
Summer period	Average	5,5	11,5
	Minimum	1,3	7,3
	Maximum	10,4	16,4
Winter period	Average	12,4	18,4
	Minimum	6,1	12,1
	Maximum	16,8	22,8
Hole year	Average	8,9	14,9

From table 15.1 it is seen that the average temperature difference for the indoor temperature for the isolation room at Aabenraa hospital to the design temperature is between $1,3 \; °C \; - \; 10,4 \; °C$ in the summer period and between $6,1 \; °C \; - \; 16,8 \; °C$ in the winter period. The average air change rate and mass flow for an isolation room at Aabenraa hospital is listed in table 15.2.

Table 15.2: *Average air change rate and mass flow rate for an isolation room at Aabenraa hospital.*

	Air change rate $[h^{-1}]$	Mass flow rate $[\frac{kg}{s}]$
Summer period	26,4	0,71
Winter period	32,7	0,87

With the temperature difference listed in table 15.1 and the average mass flow rate listed in table 15.2 the power for heating the air to a comfortable temperature is calculated from equation (15.3) and listed in table 15.3.

Table 15.3: *Power for heating.*

		Power $[kW]$	
		Minimum	Maximum
Summer period	Average temperature difference	3,9	8,2
	Minimum temperature difference	0,9	5,2
	Maximum temperature difference	7,4	13,1
Winter period	Average temperature difference	10,8	16,1
	Minimum temperature difference	5,3	10,6
	Maximum temperature difference	14,7	19,9

From table 15.3 it is seen that the needed power for heating special for the winter period is high. The power needed for the winter period is listed in table 15.3 for between $5,3\ kW - 14,7\ kW$. For the summer period the needed power is lower than for the winter period and about $0,9\ kW - 7,4\ kW$. Therefore to ensure a comfortable temperature in the isolation room during the year a minimum power for heating needs to be $14,7\ kW$.

Because of the high power needed for heating the pressure drop over the heating coil needs to be high. With a high pressure drop over the heating coil this might cause problems according to the airflow for the isolation room because the natural driving forces might not be strong enough to create the desired airflow then.

A way to preheat the air before it is let into the room is by installing a radiator in front of the opening. The maximum power for a radiator is about $2000\ W$ this means that for the room are needed about 8 radiators. It is therefore argued that it is not a solution. To use heat recovery it is possible to install a air-to-liquid heat exchanger. The problem with the heat exchanger is again that for the situation for Aabenraa hospital the mass flow is high and therefore the pressure drop over the heat exchanger is too high.

The average energy for heating for a day during a year is calculated for $177\ kWh$ with a total effect during the year of $65\ 500\ kW$. The yearly cost with a district heating price of $0,32\ \frac{dkk}{kWh}$ is therefore about $21\ 000\ dkk$ [Århus Kommune, 2008] .

As stated above the price for heating the air is high and it is almost impossible to create the needed effect for heating. A way to lower the needed effect and thereby also the cost is by lowering the mass flow for the room. It is stated that for an isolation room the minimum air change rate has to be 12 h^{-1} therefore the air change rate for the room can be lowered with $14,4$ h^{-1} for the summer period and $20,7$ h^{-1} for the winter period. This means that the energy needed will be lowered with 61 %.

Because it is not possible to use heat recovery according to the high pressure drop there might be an advantage by using mechanical ventilation. For mechanical ventilation it is possible to create the desired pressure because of the mechanical driving forces and therefore heat recovery can be used.

In table 15.4 are listed the energy use for heating and transportation for the different ventilation systems. The calculations are made with an air change rate of 12 h^{-1} and a temperature difference between interior and exterior of $8,9$ $°C$ corresponding to the average temperature difference during the year as listed in table 15.1.

The power needed for heating is calculated from equation (15.3) while the power needed for transportation is calculated from:

$$P = \frac{\Delta p \cdot q}{\eta} \tag{15.4}$$

where

$$
\begin{array}{lll}
P & : & \text{Power } [W] \\
\Delta p & : & \text{Pressure loss } [Pa] \\
q & : & \text{Volume flow } [\frac{m^3}{s}] \\
\eta & : & \text{Useful effect for the ventilator } [-]
\end{array}
$$

Table 15.4: *Power use for heating and air transportation for different ventilation systems. The pressure losses for the different systems are from [Heiselberg, 2008].*

Ventilation system	Average net power use $[kW]$	
	Heat	Transportation
Natural ventilation	2,9	0
Hybrid ventilation Pressure loss < 10 Pa, useful effect 0,8	2,9	0,004
Hybrid ventilation with heat recovery Pressure loss $30 - 100$ Pa, useful effect 0,8, heat recovery of 50 %	1,6	$0,01 - 0,04$
Mechanical ventilation with heat recovery Pressure loss 2100 Pa, useful effect 0,8, heat recovery of 65 %	1,1	0,8

The yearly costs in *dkk* is listed in table 15.5. For electricity is used a price of $1,95 \frac{dkk}{kWh}$ [Energitilsynet, 2007] .

Table 15.5: *Yearly energy costs for heating and air transportation for different ventilation systems.*

Ventilation system	Energy costs [*dkk*]		
	Heat	Transportation	Total
Natural ventilation	8 100	0	8 100
Hybrid ventilation	8 100	100	8 200
Hybrid ventilation with heat recovery	4 500	400	4 900
Mechanical ventilation with heat recovery	3 100	13 700	16 800

From table 15.4 and 15.5 it is seen that the best solution according to power use and the costs is the solution with hybrid ventilation with heat recovery. This solution utilizes the advantages of both natural and mechanical ventilation. Because it is possible to use heat recovery for the solution the energy use for heating is lower than for the natural ventilation solution and the hybrid ventilation solution without heat recovery. Compared to the mechanical ventilation system the energy costs is higher because of the lower useful efficiency compared to the mechanical ventilation system.

Hybrid ventilation uses the natural driving forces in situations where they are strong enough to create the desired airflow. Because of the utilization of the natural driving forces the energy use and specially the costs is lower for hybrid ventilation compared to mechanical ventilation. In situations where the natural driving forces are not strong enough to create the desired airflow mechanical ventilation is used, therefore the higher energy use for hybrid ventilation compared to natural ventilation.

Specially in the winter situation with a high temperature difference between inside and outside there is a great advantage of heat recovery.

From table 15.5 it is also seen that the costs for the different ventilation systems does not vary much. For the calculations are used a relative low price for district heating. In areas with a high costs for district heating the total costs for the natural ventilation systems rises more than for the mechanical ventilation system because of the higher power use for the natural ventilation systems. The best solution therefore also depend on the price for district heating for the area where the ventilation system is installed. The price for electricity does not vary as much for Denmark.

Chapter 16

Conclusion

In the resent years there have been great focus, that for the modern society there is a risk that a local epidemic easy can evolve to a global pandemic. The greater risk of a global disease means that health care systems all over the world have to be able to handle an eventual outbreak of for instance SARS or other airborne diseases. However in most countries this is not the case and this goes for rich countries as well as poor countries. A reason is that there are not enough isolations rooms. This is because isolations rooms are expensive to construct and they are costly to have running.

Therefore the problem stated for the project in chapter 1 is, if it is possible to use natural ventilation for isolation rooms in hospitals.

The Performance of natural ventilation for isolations rooms is investigated based on two cases; Aabenraa hospital in Denmark and Grantham hospital in Hong Kong.

For both Aabenraa and Grantham hospital are made calculations for the airflow path and air change rate for an isolation room. For both situations the calculations showed that it was not possible only by natural ventilation to ensure the right airflow path and air change rate for 100 % of the time. It were therefore concluded for both situations that to ensure the right airflow all the time hybrid ventilation were installed.

By installing hybrid ventilation the natural driving forces are still used but in situations where these were too low to create the desired airflow a mechanical driven fan were used. Even though a mechanical fan need to be used the costs by using hybrid ventilation might still be lower than by using mechanical ventilation because of the use of the natural driving forces.

For the two hospitals are used different solutions for the ventilation strategy according to the location and layout of the hospital. Aabenraa hospital is a flat squared building located in a temperate climate while Grantham hospital is a 8 stories high narrow building located in a tropical climate.

According to the location and layout of Aabenraa hospital the solution for the ventila-

354 Chapter 16. Conclusion

tion system is to use a combination of cross and stack ventilation. Compared to single sided ventilation cross ventilation can create a greater airflow therefore this system is chosen. To increase the effect of the thermal buoyancy are placed an opening in the roof. To increase the effect of the thermal buoyancy for the negative pressurized isolation room even more were placed a chimney on the top of the room. Because Aabenraa hospital is located in Denmark where the interior temperature most often is higher than the exterior temperature the chimney will increase the effect of the thermal buoyancy to create a negative pressurized isolation room.

Grantham hospital is located in a tropical climate where the exterior temperature often is higher than the interior temperature. Therefore it is not possible to use the effect of the thermal buoyancy in the same way as for Aabenraa hospital to create a negative pressurized isolation room.

Compared to Aabenraa hospital the isolation room for Grantham hospital does only have one side facing the outside, therefore single sided ventilation is used for this situation. In the situation with a higher exterior temperature compared to the interior temperature this will increase the airflow for the room when it is placed on the windward side of the building.

For both hospitals were made minor changes to the layout of the isolation room compared to the real layout to optimize the use of the room. For Aabenraa hospital there were not already an isolation room therefore an one-bed bed ward were changed for an isolation room. For both the isolation room for Aabenraa and Grantham hospital were therefore installed an anteroom between the isolation room and the corridor. The purpose of the anteroom is to ensure the right airflow between the isolation room and the rest of the hospital and for masking and unmasking of personnel.

To create the highest airflow for both the situations it is investigated that the best location of the isolation room is for the windward side of the hospital. The problem with placing the isolation room on the windward side is that for this location there is a high possibility that the pressure for the isolation will be higher than for connecting rooms, and therefore it might be difficult to create a negative pressurized isolation room. The best location for a negative pressurized isolation room is therefore on the leeward side of the hospital but because of the lower wind pressure for this side the airflow might not be as high as for the location on the windward side. For the location of the isolation room on the leeward side of the hospital the thermal buoyancy does therefore have greater influence in this situation compared to a location of the room on the windward side.

16.1 Methods

Because of the different location and the different layout of the two hospitals different solutions are investigated. For both hospitals it is investigated that with the listed solutions it is possible to create a sufficient air change rate and to ensure the right airflow direction

except for about 5 % of the time. For both situations it is also listed that hybrid ventilation is necessary to ensure this airflow and air change rate.

For both hospitals the air change rate and airflow for the isolation room were calculated for different methods, and the results for the methods did differ from each other. The different calculations uses different methods and different requisite for calculating therefore the results may vary. Depending on the purpose of the calculating different methods may be used.

Because of the influence of the surroundings the isolation room is a part of a multi zone. For both hospitals where therefore made a multi zone model of the hospital to calculate the airflow path and air change rate for the isolation room. In table 16.1 are listed some characteristics for the single zone and multi zone model.

Table 16.1: *Single zone model compared to multi zone model.* *[Brohus, 2007b]*

Single zone model	Multi zone model
Airflow rate and direction through separate openings are determined	Airflow rate and direction through external routes are determined
Zone air change rate is determined as the sum of all airflows through "supply"-openings	Airflow rate and direction through internal routes are determined
The total mass inflow equals the total mass outflow of the building	The total mass flow into each zone equals the total mass flow out of the zone
All leakage flows must be identified	The total air change rate into each zone is determined
	The total building air change rate is determined

A reason for the difference between the analytical calculations and the multi zone might therefore be because the multi zone consider the influence from the surroundings which is not included in the single zone model. Because of the layout of the hospitals the multi zone model is determined as more correct than the single zone.

To calculate the airflow path for both hospitals are used CFD methods. Compared to the multi zone model, which is a macroscopic model, the CFD model is a microscopic model. Where the multi zone model uses control volumes to build and calculate the non linear equations, CFD uses Navier-Stokes equations to determine the airflow. Because the CFD methods is a microscopic model it is possible to calculate the airflow for the domain

more accurate than for the multi zone model.

To get the most accurate results for the airflow around the building CFD methods are therefore used.

The most accurate result for the airflow is found by experiments, which is not done for the project. Therefore to validate the results experiments need to be done.

For the calculations it is assumed that the windows are fully opened and the doors are closed. In the situation where it is possible for the people in the room to control the openings the opening sizes will differ depending to the people. In situations with cold outdoor climate there is a possibility that the people inside the room might close the windows and therefore the airflow is minimized.

16.2   Solutions

For both Aabenraa and Grantham hospital were made minor changes to the actual layout of the isolation room to achieve the desired air change rate and airflow for the room. For all the solutions it were desired to keep the outer dimensions of the actual room.

To create a buffer zone between the isolation room and the corridor where installed an anteroom for the isolation rooms. The purpose of the anteroom is to ensure the right air pressure between the rooms and to help reduce the escape of droplets during opening and closing of the isolation room door. The anteroom may also be used for masking and unmasking. For both Aabenraa and Grantham hospital the anterooms where used to ensure the right pressure distribution between the isolation room and the rest of the hospital. With the anteroom it is possible to create the desired pressure for the isolation room without a high influence of the pressure for the rest of the hospital.

The ventilation principles for the two hospitals differ from each other where Aabenraa hospital utilizes cross ventilation and Grantham hospital utilizes single sided ventilation. The reason for chose of ventilation system depend on the layout of the isolation room, the location in the building and the weather conditions. For Aabenraa hospital are used a combination between cross ventilation and stack ventilation to create a negative pressure at the floor for the isolation room. The chimney is installed to increase the effect from the thermal buoyancy. For Denmark the indoor temperature is often higher than the outside temperature than the opposite. This means that by using thermal buoyancy the airflow will be from the lowest opening to the highest position, in this way are created a lower pressure at the floor compared to a higher location in the room. For Hong Kong the outside temperature is often higher than the inside temperature therefore it is not possible to create the same airflow path for Hong Kong and thereby use the thermal buoyancy in the same way.

Because of the location of the isolation room in the middle of the hospital for Grantham

hospital were used single sided ventilation. For Aabenraa hospital it were possible to use cross ventilation. The advantage of cross ventilation is that the airflow rate is higher than for single sided ventilation.

Therefore the strategies used for the natural ventilation system for the hospital depends on the location and the layout. In table 16.2 are listed some strategies for ventilation depending on the circumstances for the hospital.

Table 16.2: *Ventilation strategies for natural ventilation.*

Ventilation principle	Main natural driving forces	Most sufficient for	Less sufficient for
Natural ventilation	Thermal buoyancy Wind pressure	Climate with exterior temperatures close to the design temperature for the room Climates with a relatively high wind pressure	Hot and humid climates Cold climates Climate with high pollution
Single sided ventilation	Thermal buoyancy Wind pressure	Rooms with openings in only one side Climate with higher exterior temperature than interior temperature	Locations with low wind pressure and small temperature difference
Cross ventilation	Wind pressure	Rooms with openings in more than one side Rooms where single sided ventilation is not able to create a sufficient airflow Rooms that require a high airflow	Climate with low wind pressure
Stack ventilation	Thermal buoyancy	Rooms with openings in one facade and in the roof Higher interior temperature than exterior temperature to create a negative pressure	Climate with higher exterior temperature than interior temperature
Hybrid ventilation	Thermal buoyancy Wind pressure Mechanical forces	Rooms where natural driving forces are not able to create the sufficient airflow alone Hot and humid climates and cold climates where the possibility of closing the windows are high because of the exterior climate	Climates close to the design temperature for the room where the natural driving forces are able to create the sufficient airflow

16.3   Discussion

The disadvantages with natural ventilation is the controlling of the airflow and to secure the right air change rate for the room. Natural ventilation relay on natural driving forces that depends on the weather conditions. Because the weather conditions are not stable

at the same level throughout the hole year, the airflow and air change rate for the room changes. Specially on completely still days it might be impossible to create the desired airflow.

From the calculations it is seen that with only natural ventilation it is not possible to ensure the right airflow and air change rate 100 %. For about 5 % of the time the airflow is below the desired value. It is also seen from the calculations that with big openings to the outside the average air change is about three times the size of the necessary air change rate.

An other disadvantage for natural ventilation is the costs for heating or cooling to ensure the right indoor temperature. For natural ventilation the outside air is used for ventilation. In situations with either very low or high outside temperature this will influence the inside temperature too when no preheating or cooling is used. To create a comfortable temperature in cold and hot climates preheating or cooling is therefore needed. Because of the high temperature difference between exterior temperature and design temperature, this can be quiet costly. For natural ventilation it is not possible to use heat recovery as for hybrid ventilation or mechanical ventilation therefore the costs for heating in situations with natural ventilation is higher than for hybrid or mechanical ventilation.

The solution by using natural ventilation might therefore be the greatest advantage for poor countries compared to rich countries. For poor countries it might not be possible to install mechanical ventilation because of the high costs and they may also be more willing to accept a poor comfort level in the isolation rooms, therefore natural ventilation might be a solution. With the right setup of the system for natural ventilation it is possible to ensure the right pressure and airflow for about 95 % of the time. Compared to no ventilation and no control of the airflow this is a great improvement.

A probability of the right airflow of 95 % might not be good enough for rich countries because of the higher demand for the safety according to the spread of pollution. Also with the demands for the comfort level for the isolation rooms natural ventilation is not a good solution because of the high costs for heating or cooling. Therefore for rich countries only natural ventilation might not be a solution. To ensure the right airflow 100 % of the time and a comfortable indoor climate mechanical ventilation might be used.

Another doubt about installing natural ventilation is the possibility to ensure the right opening areas. For Grantham hospital the openings used for natural ventilation are the windows. With manually controlled windows the opening area therefore depend on the people in the room. With cold temperatures there is a tendency to close the windows to avoid a low indoor temperature. In this situations the openings sizes might therefore be too low to ensure the right airflow. For hot and humid climates the same tendency might be happening to avoid a high humidity in the room. In these situations automatic controlled windows might therefore be necessary to ensure the right opening sizes.

Because the influence of the exterior climate on the interior climate for natural ventilated rooms these solutions might not be comfortable in cold or very hot and humid

climates. For these situations it can be discussed what is most important; high airflow rate to ensure that pollutant are not spread or comfort temperature to ensure that the people in the room are in thermal comfort.

The advantage of natural ventilation compared to mechanical ventilation is therefore specially for resource limited countries where the costs of mechanical ventilation are too high and it is possible with natural ventilation to create the desired airflow.

For rich countries where the demands for the right airflow and indoor climate is high natural ventilation is not a solution. To ensure the right conditions mechanical ventilation might be the best solution because it is more reliably and it is possible to create the exactly airflow as wished and use heat recovery therefore the costs for preheating is lower than with natural ventilation.

Since a pandemic is relatively rare it is costly to create isolation rooms that are not used. Therefore isolation rooms are often not installed in hospitals. In these situations natural ventilation can be used as an emergency preparedness. The demands for bed wards in hospitals is an air change rate of 6 h^{-1} whereas for isolation rooms the demand is 12 h^{-1}. Therefore the installed mechanical ventilation systems for the bed wards might not be able to handle a higher air change rate. To create a higher air change rate temporary natural ventilation might be used. With only a small effort it is possible to create a high air change rate using natural ventilation. Even that it is not possible to ensure the right air change rate of minimum 12 h^{-1} 100 % of the time with natural ventilation the solution is better than an air change rate of 6 h^{-1} with only mechanical ventilation. For hospitals it might therefore be a solution to create rooms that can be used for normal one-bed bed wards in the situation of no pandemic and isolation rooms in the case of an outbreak of a pandemic. Such an isolation room can be created as listed above for an isolation room and in normally situations still be used as a one-bed bed ward. Because of the anteroom the area for the isolation room might be smaller than for a normal bed ward, and therefore it might be difficult to manoeuvre with a wheelchair or other wide hospital equipments in the room.

It is therefore concluded that for emergency preparedness where the right airflow is more important than the indoor climate natural ventilation can be used, but for permanent situations mechanical ventilation is the best solution.

Chapter 17

Sammendrag på dansk

I det moderne samfund har der i de senere år været stor fokus på hvordan en lokal epidemi kan udvikle sig til en global pandemi. Specielt efter udbruddet af SARS i sydøst Asien i 2003 har fænomenet fået stor bevågenhed.

Den øgede risiko for en global pandemi betyder at sundhedsvæsenet over hele verden skal være i stand til at handle overfor et sådant udbrud af for eksempel SARS eller andre luftbårne sygdomme. Imidlertid er dette ikke tilfældet for de fleste lande hvilket gælder for både rige som fattige lande. En af grundene er at der ikke er installeret nok isolations rum på sygehusene på grund af både anlægs omkostningerne og de løbende omkostninger for disse.

En måde at nedbringe omkostningerne for isolations rum er ved at bruge naturlig ventilation i stedet for mekanisk ventilation. I dette projekt er mulighederne for anvendelse af naturlig ventilation for isolations rum derfor undersøgt. Projektet tager udgangspunkt i to hospitaler; Aabenraa sygehus i Danmark og Grantham hospital i Hong Kong.

Aabenraa sygehus er en flad firkantet bygning hvorimod Grantham hospital er en 8 etagers smal bygning. På grund af den forskellige udformning for de to hospitaler er der undersøgt forskellige løsningsstrategier.

For begge hospitaler er udført mindre ændringer i indretningerne for at skabe de bedste betingelser for et isolations rum. Der er således i begge situationer tilføjet et forværelse. For ændringerne af udformningen af isolations rummet er de ydre dimensioner af rummet bibeholdt.

De fundne løsninger er beregnet ud fra analytiske beregninger, multizone modeller samt CFD simuleringer.

For Aabenraa sygehus er det valgt at udføre ventilations systemet som en kombination af krydsventilation og opdriftsventilation. For at skabe et positivt tryk i isolations rummet er lavet en åbning i taget med samme størrelse som vindues åbningerne på $0,5 \ m^2$. Med denne udformning er det sikret at for kun 5 % af tiden er luftskiftet mindre end $12 \ h^{-1}$. I

sommermånederne er det undersøgt at der kan være problemer med luftstrømmen mellem isolations rummet og forværelset hvor denne er i den modsatte retning af ønsket. For at sikre den rette luftstrømning og retning er der derfor installeret en indblæsnings ventilator i isolations rummet således der benyttes hybrid ventilation.

For at skabe et negativt tryk i isolations rummet er placeret en 10 meter høj skorsten på toppen af isolations rummet. I toppen af skorstenen er der placeret en åbning på $1,5\ m^2$. Åbningsstørrelsen for vinduerne er $0,25\ m^2$. Med denne udformning er den rette luftstrøm mellem isolations rummet og forværelset sikret med undtagelse af nogle få timer i sommer perioden og for et isolations rum der vender mod nord. Derfor er der i denne situation placeret en udsugnings ventilator i toppen af skorstenen for at sikre den rette luftstrøm. Med denne udformning er det rette luftskifte sikret i vinter perioden men lavere end $12\ h^{-1}$ for ca. 3 % af tiden i sommer perioden.

I modsætning til isolations rummet på Aabenraa sygehus er isolations rummet på Grantham hospital placeret med kun en facade til omgivelserne. Derfor er det ikke muligt at bruge krydsventilation i dette tilfælde.

For isolations rummet er udført forskellige beregninger for at undersøge luftstrømmen for dette. På grund af placeringen af Grantham hospital ved foden af et bjerg og tæt på vandet optræder der en lokal land- og søbrise under vindstille forhold. Tryk påvirkningen for hospitalet på grund af denne luftstrøm er undersøgt ved CFD modellering og med det aktuelle design af rummet er det gennemsnitlige luftskiftet beregnet til $18\ h^{-1}$ under forudsætning af landbrise og $18\ h^{-1}$ under søbrise. Grunden til det højere luftskifte under landbrise skyldes den højere vindhastighed samt rummets placering i bygningen. For at sikre den rette luftstrømning mellem forværelset og isolations rummet er placeret en indblæsnings ventilator i forværelset.

Med samme udformning af isolations rummet som ved CFD modelleringen er ligeledes udført en enkelt zone model for at lave en års beregning af indetemperaturen, den relative fugtighed samt luftskiftet. Fra modellen er den gennemsnitlige indetemperaturer over året beregnet til $25,2\ °C$ med en gennemsnitlig relativ luftfugtighed på 72,2 %. Luftskiftet for modellen er beregnet til mellem $12 - 88\ h^{-1}$ med et gennemsnitligt luftskifte på $37\ h^{-1}$.

For rummet er der endelig lavet en multizone model hvori der er lavet en Monte Carlo simulering. Fra modellen er det gennemsnitlige luftskifte beregnet til $45\ h^{-1}$. Ca. 5 % af tiden vil luftskiftet være mindre end $12\ h^{-1}$. I situationer med vindstille vejr hvor kun temperatur forskelle vil have indflydelse på luftskiftet er det gennemsnitlige luftskifte $39\ h^{-1}$ det laveste luftskifte er fundet for en temperatur forskel på $1\ °C\ -\ 3\ °C$. I tilfælde med kun vind og ingen temperatur forskel er det gennemsnitlige luftskifte $69\ h^{-1}$.

Appendix A

Calculation of airflow

According to the available information and the accuracy of the calculated airflow for a room or a building there are different methods to predict the airflow rate. The most simple methods are empirical algorithms while the most advanced are computerized fluid-dynamics (CFD) techniques to solve the Navier-Stokes equation. The airflow according to natural ventilation in buildings can be estimated with the following three methods:

- Analytical and empirical methods

- Measurement

- CFD methods

The analytical and empirical methods are based on simplified equations and assumptions that often do not correspond to the actual case. Therefore the analytical and empirical methods should only be used to get an estimate of the airflow. To get a more accurate estimate of the airflow it is necessary to make experiments or CFD-calculations.

A.1   Analytical and empirical methods

In the following section the analytical and empirical methods are described. The methods are described from [Heiselberg, 2006] .

A.1.1   Natural driving forces

Natural ventilation uses the natural driving forces to create an airflow through the building. The natural driving forces are:

- Thermal buoyancy

- Wind pressure

- Combined thermal buoyancy and wind pressure

After a while a steady-state condition will happen with a balance between heat supply, temperature difference, the resulting ventilation capacity and heat losses. For the calculations of the airflow with analytical and empirical methods steady-state conditions are used.

Thermal buoyancy

Airflow through the building according to thermal buoyancy is created because of difference in temperature and/or moisture contents between two or more zones. To create an airflow through the building one or more openings may be applied between the zones. The difference in temperature can be according to heating one zone or because difference in indoor and outdoor conditions.

The internal and external pressure distribution when there are no wind can be calculated from:

$$P = P_0 - \rho_0 g H \tag{A.1}$$

where

P : Internal or external pressure $[Pa]$
P_0 : Pressure at a reference level $[Pa]$
ρ_0 : Internal or external air density at a reference level $[\frac{kg}{m^3}]$
g : Gravitational acceleration $[\frac{m}{s^2}]$
H : Height above reference level $[m]$

From equation (A.1) the pressure difference across an opening at the height z are given by:

$$\Delta p_t = P_{e0} - P_{i0} - gz(\rho_e - \rho_i) \tag{A.2}$$

The indexes refer to internal and external conditions.

For calculating the neutral plane above the floor the pressure difference is equal to zero. For openings below the neutral plane the pressure difference is positive and for openings above the neutral plane the pressure difference is negative as shown in figure A.1.
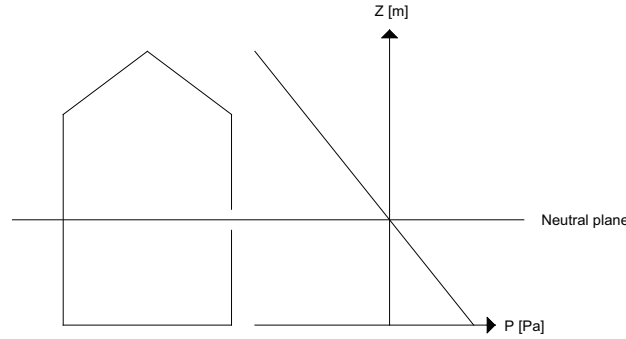
Figure A.1: *Pressure difference according to the neutral plane*

Wind pressure

Airflow through the building according to wind pressure is created because of different wind pressure on the building facade. According to the wind pressure there will be an over pressure on the windward side and under pressure on the other sides. As for thermal buoyancy ventilation with wind pressure require at least one opening between the zones.

The pressure according to wind is given by the following equation:

$$P_w = C_p \frac{1}{2} \rho_e v_{ref}^2 \tag{A.3}$$

where

$$
\begin{array}{lll}
P_w & : & \text{Wind induced pressure } [Pa] \\
C_p & : & \text{Pressure coefficient } [-] \\
\rho_e & : & \text{External air density } [\frac{kg}{m^3}] \\
v_{ref} & : & \text{Reference wind speed } [\frac{m}{s}]
\end{array}
$$

The pressure coefficient depends on the wind direction, the building surface orientation and the topography and roughness of the terrain in the wind direction. The pressure coefficient accounts for the changes in wind-induced pressure because of the surrounding obstacles on the wind characteristics.

The pressure difference across an opening is given by:

$$\Delta p_w = P_w - P_i = \frac{1}{2} C_p \rho_e v_{ref}^2 - P_i \tag{A.4}$$

where

$$P_i \quad : \quad \text{Internal pressure in the building } [Pa]$$

Combined thermal buoyancy and wind pressure

The pressure difference according to both thermal buoyancy and wind pressure is given by the sum of the pressure difference according to thermal buoyancy and wind pressure

respective, given by:

$$\Delta p = \Delta p_t + \Delta p_w = \frac{1}{2}C_p \rho_e v_{ref}^2 - P_i + \frac{\rho_e \Delta T}{T_i}g(H_0 - H) \tag{A.5}$$

A.1.2   Single side ventilation

According to the openings in the room the ventilation can be either single sided ventilation or cross ventilation. Single sided ventilation occur in the building when there are only one opening in the building and the ventilation flow can be driven by either thermal buoyancy, wind pressure or a combination of both.

Single sided ventilation according to thermal buoyancy

To calculate the flow rate according to thermal buoyancy in a case with single sided ventilation the orifice model is used. For the calculations the pressure difference is determined according to the airflow through the opening. For the calculations with the orifice model there are made some assumptions:

- Close to and within the aperture there is no mixing or heat transfer between the contra-flowing air streams

- At the height of the neutral plane the pressures in both zones are equal

- Streamlines are parallel and horizontal at the large opening. Vertical velocity component are small compared to the horizontal component

- The viscous forces are small in comparison with those due to buoyancy

- The pressure in the flow as it enters the receiving zone is equal to the hydrostatic pressure in that zone

The pressure difference over an opening due to thermal buoyancy is given by:

$$\Delta p = P_{i0} - P_{e0} + (\rho_e - \rho_i)gz = \rho_i \frac{u_i(z)^2}{2} \tag{A.6}$$

where

$u_i(z)$:   Velocity in the indoor air leaving the room $\left[\frac{m}{s}\right]$

For the opening the neutral plane is calculated by letting the pressure difference be equal to zero. When the neutral plane is known the velocities in the inside and outside airstreams are calculated by:

$$u_i(z) = C_v\sqrt{\frac{2g}{\rho_i}(\rho_e - \rho_i)(z - H_n)} \qquad (z \geq H_n) \tag{A.7}$$

$$u_e(z) = C_v \sqrt{\frac{2g}{\rho_e}(\rho_e - \rho_i)(H_n - z)} \qquad (z \le H_n) \qquad \text{(A.8)}$$

where

C_v :   Velocity coefficient $[-]$
$u_i(z)$:   Velocity in the indoor air flowing out of the room $[\frac{m}{s}]$
$u_e(z)$:   Velocity in the outdoor air flowing into of the room $[\frac{m}{s}]$

When mass conservation is assumed the neutral height can be calculated from:

$$\frac{H_n - H_b}{H_t - H_n} = \left(\frac{\rho_i}{\rho_e}\right)^{\frac{1}{3}} \qquad \text{(A.9)}$$

where

H_n :   Height of the neutral plane $[m]$
H_b :   Height above ground for the bottom of the opening $[m]$
H_t :   Height above ground for the top of the opening $[m]$

When the neutral plane is located in the middle of the opening and the temperatures are used instead of densities the airflow can be calculated by:

$$q = \frac{1}{3}AC_d \sqrt{\frac{g(T_i - T_e)(H_t - H_b)}{T_i}} \qquad \text{(A.10)}$$

where

C_d :   Discharge coefficient $[-]$
q :   Total airflow rate through the opening $[\frac{m^3}{s}]$
A :   Opening area $[m^2]$

Single sided ventilation according to wind pressure

The airflow according to the wind pressure can be divided into three components:

- Steady-state ventilation

- Ventilation by turbulent eddy penetration

- Ventilation by pulsation flow

The ventilation according to wind pressure through a single opening in the building depends on the following parameters:

- Reference wind speed, v_{ref}, wind direction, θ and turbulence

- Opening area, A, opening geometry and position of the opening in the building facade

- The shape and surroundings of the building

Single sided ventilation according to both thermal buoyancy and wind pressure

The airflow rate with a combination of both thermal buoyancy and wind pressure is a function of temperature difference, wind velocity and fluctuating terms. The effect of thermal buoyancy and wind pressure on the flow through a window has been investigated by de Gids and Phaff and are given by:

$$v_{eff} = \frac{q}{\frac{A}{2}} = \sqrt{\frac{2}{\rho}(\Delta p_{wind} + \Delta p_{stack} + \Delta p_{turb})} \tag{A.11}$$

where

$$v_{eff} \quad : \quad \text{Effective velocity } \left[\frac{m}{s}\right]$$

Equation (A.11) leads to the form:

$$v_{eff} = \frac{q}{\frac{A}{2}} = \sqrt{C_1 v_{ref}^2 + C_2(H_t - H_b)(T_i - T_e) + C_3} \tag{A.12}$$

where

$$
\begin{aligned}
C_1 \quad &: \quad \text{Coefficient depending on the wind } [-] \\
C_2 \quad &: \quad \text{Constant depending on thermal buoyancy } [-] \\
C_3 \quad &: \quad \text{Constant depending on wind turbulence } [-]
\end{aligned}
$$

From the effective velocity in equation (A.11) the airflow rate is given by:

$$q = \frac{A}{2} v_{eff} \tag{A.13}$$

From 33 measurements de Gids and Paff has obtained values for the three constants as shown in table A.1.

Table A.1: *Values for the constants for equation* (A.12).

C_1	0,001
C_2	0,0035
C_3	0,01

Single side ventilation through a horizontal opening

When it is colder outside than inside there will be an airflow through a horizontal opening. The airflow is driven by difference in density between the inside air and the outside air. The heavier outside air make a buoyancy driven downflow whereas the lighter inside air makes a buoyancy driven upflow. Unlike the flow through a vertical opening the characteristic for this flow is that it gives rise to oscillatory of the air across the hole opening. The airflow rate through an horizontal opening depends on the relation between the height and the diameter of the opening. Based on model experiments there are developed

relations for an airflow rate through an opening. One of the relations is: [Heiselberg, 2006]

$$q = 0,093 \cdot \sqrt{\frac{g(T_i - T_u)D^5}{T_i}} \frac{1}{\sqrt{1 + 0,084 \left(\frac{h}{D} - 0,4\right)}} \quad \text{for} \ \ 0,4 < h \backslash D < 3,25 \qquad (A.14)$$

where

T_i : Indoor temperature $[°C]$
T_o : Outdoor temperature $[°C]$
g : Gravitational acceleration $[\frac{m}{s^2}]$
h : Height of the opening $[m]$
D : Diameter of the opening $[m]$

For a square opening with the side length S, the diameter can be found as:

$$q = \sqrt{\frac{4}{\pi}S^2} \qquad (A.15)$$

A.1.3 Single zone ventilation

As for the single sided ventilation single zone ventilation is influenced by thermal buoyancy and wind pressure.

Single zone ventilation by thermal buoyancy

To calculate the airflow by thermal buoyancy the mass-balance has to be fulfilled. The mass-balance state that the total flow into the building has to be the same as the total flow out of the building.

The most simple case of single sided ventilation is a room with two openings placed above each other and where the inside temperature is constant. Because of pressure difference for the lower and higher opening there will be an inflow for the lower opening because of under pressure and an outflow for the higher opening because of an over pressure. In between the two openings there will be a neutral plane where the inside and outside pressure is equal.

The pressure difference across an opening can be calculated from:

$$\Delta p = P_{e0} - P_{i0} - gH(\rho_e - \rho_i) \qquad (A.16)$$

The location of the neutral plane is calculated by putting the pressure difference equal to zero:

$$P_{e0} - P_{i0} = \rho_e g H_0 \frac{T_i - T_e}{T_i} \qquad (A.17)$$

When the pressure difference is known the airflow rate can be calculated from:

$$q = C_d A v_{theo} = C_d A \sqrt{\frac{2|\Delta p|}{\rho} \frac{\Delta p}{|\Delta p|}} \tag{A.18}$$

When the area of the openings are known the location of the neutral plane can be calculated from:

$$\rho_e q_{v1} - \rho - i q_{v2} = 0 \tag{A.19}$$

$$\rho_e C_{d1} A_1 \left(\frac{2\Delta T g (H_0 - H_1)}{T_i} \right)^{\frac{1}{2}} - \rho_i C_{d2} A_2 \left(\frac{2\Delta T g (H_0 - H_2)}{T_e} \right)^{\frac{1}{2}} = 0 \tag{A.20}$$

where

ρ_e, ρ_i	:	Density of outdoor and indoor air $[\frac{kg}{m^3}]$
q_{v1}, q_{v2}	:	Airflow rates through inlet and outlet $[\frac{m^3}{s}]$
C_{d1}, C_{d2}	:	Discharge coefficient of inlet and outlet openings $[-]$
A_1, A_2	:	Inlet and outlet area $[m^2]$
ΔT	:	Temperature difference between inside and outside $[°C]$
T_i, T_e	:	Absolute indoor and outdoor temperature $[°C]$
H_1, H_2	:	Height of the inlet and outlet opening $[m]$
H_0	:	Height of neutral plane $[m]$

When the location of the neutral plane is known, the pressure difference, air velocities and ventilation capacity can be calculated from equation (A.20). If there are more than two openings in the room equation (A.20) may still be used if the openings are located only in two heights.

When there are more than two openings located at different heights the mass balance is given by:

$$\rho_u q_{v1} + \rho_u q_{v2} - \rho_i q_{v3} - \rho_i q_{v4} = 0 \tag{A.21}$$

Single zone ventilation by wind

When only wind is acting on the building the pressure difference across an opening can be calculated from:

$$\Delta p = P_w - P_i \qquad \Leftrightarrow \qquad \Delta p = \frac{1}{2} C_p \rho_u v_{ref}^2 - P_i \tag{A.22}$$

where

P_i : Internal pressure in the building $[Pa]$

For the building the internal pressure is found from the mass balance:

$$\Sigma \rho_o C_{d1} A_1 v_{theo,1} = \Sigma \rho_i C_{d2} A_2 v_{theo,2} \tag{A.23}$$

The index 1 refer to inlet openings and the index 2 refer to outlet openings.

The theoretical velocity where the friction loss is not taken into consideration can be calculated from:

$$v_{theo,i} = \sqrt{\frac{2\Delta p}{\rho}} \tag{A.24}$$

where

ρ : Density of outside air for inlet openings and density of inside air for outlet openings $[\frac{kg}{m^3}]$

With the theoretical velocity equation (A.23) can be written as:

$$\sum \rho_e C_{d1} A_1 \left(\frac{|C_{p1}\rho_e v_{ref}^2 - 2P_i|}{\rho_e} \right)^{\frac{1}{2}} = \sum \rho_i C_{d1} A_2 \left(\frac{|C_{p2}\rho_e v_{ref}^2 - 2P_i|}{\rho_i} \right)^{\frac{1}{2}} \tag{A.25}$$

The general form of the mass balance is given by:

$$\sum_{j-1}^{n} C_{d,j} A_j \rho_j \left(\frac{|\Delta p_j|}{\frac{1}{2}\rho_j} \right)^{\frac{1}{2}} \frac{\Delta p_j}{|\Delta p_j|} = 0 \tag{A.26}$$

The last factor in equation (A.26) denotes if it will be an inlet or outlet opening. It will be 1 for an inlet opening and -1 for an outlet opening.

When the internal pressure is known the ventilation airflow through all openings can be calculate from:

$$q_v = \frac{1}{2} \sum_{j-1}^{n} C_{d,j} A_j \left(\frac{|\frac{1}{2}C_{p,j}\rho_u v_{ref}^2 - P_i|}{\frac{1}{2}\rho_j} \right)^{\frac{1}{2}} \tag{A.27}$$

To use equation (A.27) it is stated that the wind flow is steady, which is normally not the case. Natural wind is normally turbulent and because the pressure will be fluctuating investigations shows that this can cause a considerable increase in ventilation capacity compared to a situation with steady state.

Single zone ventilation with a combination of thermal buoyancy and wind

Normally thermal buoyancy and wind pressure acts on the building at the same time therefore it is necessary to calculate the airflow rate as a combination of both. To calculate the airflow rate it is necessary to know the location of the natural plane and the internal pressure. The location of the neutral plane can be found from the mass balance:

$$\sum_{j-1}^{n} A_j |H_0 - H_j|^{\frac{1}{2}} \frac{H_0 - H_j}{|H_0 - H_j|} = 0 \tag{A.28}$$

The total pressure difference across an opening is the sum of the pressure difference by thermal buoyancy and the pressure difference by wind pressure:

$$\Delta p = \Delta p_w + \Delta p_T = \frac{1}{2} C_p \rho_e v_{ref}^2 - P_i + \left(\frac{\rho_e \Delta T}{T_i} \right) g(H_0 - H) \tag{A.29}$$

The internal pressure can be found from equation (A.26) when the location of the neutral plane is known.

The airflow rate for the openings can then be calculated from:

$$q_v = \frac{1}{2} \sum_{j-1}^{n} C_{d,j} A_j \left(\frac{|\frac{1}{2} C_{p,j} \rho_e v_{ref}^2 - P_i + \frac{\rho_e \Delta T}{T_i} g(H_0 - H_j)|}{\frac{1}{2} \rho_j} \right)^{\frac{1}{2}} \tag{A.30}$$

A.1.4   Loop equations

For single zone ventilation for a system containing of different openings it is possible to use loop equations to calculate the pressure difference for the different openings. The principle for the loop equation method is to divide the ventilation system into smaller volumes. These volumes are connected through different components or airflow paths. In figure A.2 is showed the room divided into smaller volumes and connected by different airflow parts.
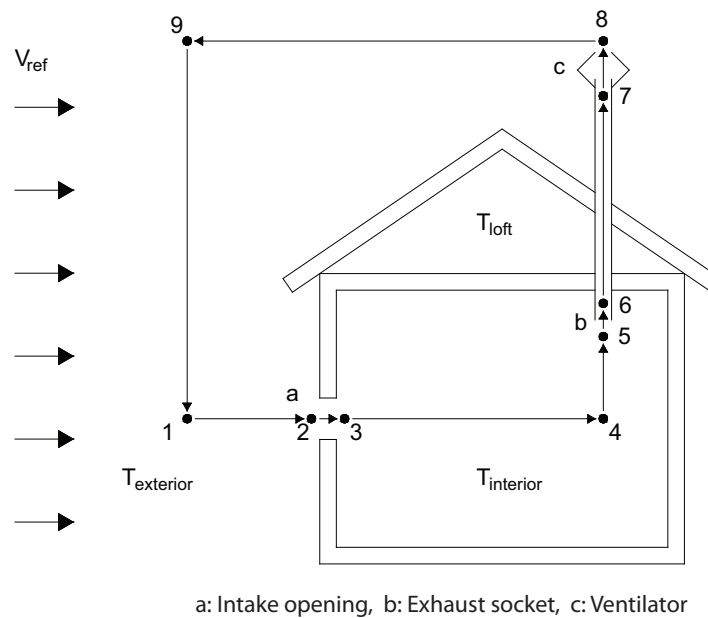

a: Intake opening, b: Exhaust socket, c: Ventilator

Figure A.2: *Principle for the ventilation system where the room consist of an intake opening (a), an exhaust socket (b), an exhaust pipe (b-c) and a ventilator. [Heiselberg, 2006]*

The control volumes for the room is the room and the exhaust pipe while the airflow parts is the intake, the exhaust socket and ventilator.

For the different control points the temperature and pressure is set. For the different control volumes the temperature is constant while the pressure varies. To calculate the pressure difference for the openings a loop is created for the room. The loop is created so it follows a possible flow path. The total pressure for the loop is 0. The loop for the building is showed in figure A.2. For the building the loop starts in the control point 1 and ends in the same point. For the different control points the equations for the pressure distribution and pressure difference is calculated. The pressure distribution and pressure difference for all the control points is summed up and set equal to 0. For the building in figure A.2 the final loop equation is listed below:

$$\frac{1}{2}C_{p,2}\rho_e v_{ref}^2 - \Delta p_a - \rho_i g \Delta H_{45} - \Delta p_b - \rho_s g \Delta H_{58} + \Delta p_m - \Delta p_c - \frac{1}{2}C_{p,8}\rho_e v_{ref}^2 + \rho_e g \Delta H_{91} = 0$$
$$(A.31)$$

Equation A.31 consists of the pressure distributions for the different components. In a general form the equation can be written as:

$$\sum \Delta p_{ij} = g \sum \rho_{ij} \Delta H_{ij} + \Delta C_p \frac{1}{2}\rho_e v_{ref}^2 \qquad (A.32)$$

A.2 Multi zone

The multi zone model is an extension of the single zone model and like the single zone model it is a macroscopic model that uses control volumes to calculate the airflow in a building. The control volumes are in the model linked together by discrete airflows. These airflows leads to governing conservation expressions. [Axley, 2003]

The possibility of idealizing the model with more than one control volume, makes it possible to take the internal resistance of the airflow into account, and hereby make the model more correct. A multi zone model is however still not as accurate as a CFD simulation, also known as a microscopic model. The reason is that a microscopic model has a different approach to calculate the airflows and hereby also take the continuum descriptions of momentum and energy conservation into account to create the governing partial differential equations. [Axley, 2003]

A.2.1 Multi zone theory

For a multi zone model there are two methods to find the airflows through the different zones in the buildings.

The first option take the approach in the continuity of mass flows for each zone:

$$\left(\sum_{in} m - \sum_{out} m \right)_i = \frac{dM_i}{dt} \qquad \text{(A.33)}$$

[Axley, 2003]
where

m : Mass flow $[\frac{kg}{s}]$
M : Total air mass accumulated $[kg]$
t : Time $[s]$
i : Index for the zone $[-]$

Normally the airflows are modeled as steady state, and the accumulation term is assumed to be zero.

After the mass balances are set up the equations that describe the correlation between the mass flows and the pressure drops across the openings are substituted into the equations. By assuming a hydrostatic pressure distribution inside and outside the building there are the same amount of governing equations as there are unknown pressure nodes inside the building.

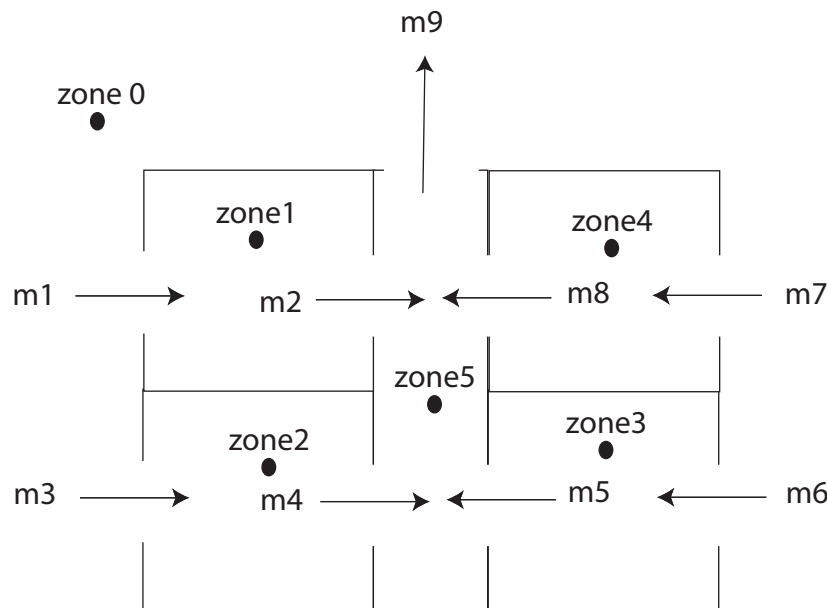An example of this approach is shown figure A.3.

Figure A.3: *Simple 2d model with 5 zones inside the building.*

In the model there are 5 zones inside the building and it is therefore possible to set up 5 governing equations.

Zone 1   :   m1 - m2 = 0
Zone 2   :   m3 - m4 = 0
Zone 3   :   m6 - m5 = 0
Zone 4   :   m7 - m8 = 0
Zone 5   :   m2 + m4 + m5 + m8 - m9 = 0

It is seen that there are too few governing equations, compared to the amount of unknown mass terms. The correlation between the mass flows and the pressure drops across the openings are substituted into the equations. With the field assumptions for the indoor and outdoor pressure distributions there are only five unknown corresponding the pressure node in each zone. It is therefore now possible to solve the system of governing equations.

The second option for setting up the system of equations is to use the compatibility of pressure changes as one follows a flow path around a continues loop, as showed in equation A.34. This method corresponds to the loop equation from section A.1.4. Like for the first option it is necessary to assume a hydrostatic pressure indoor and outdoor to be able to find the pressure drops in the loops.

$$\sum_{k,l}(p_k - p_l) = 0 \tag{A.34}$$

[Axley, 2003]
where

p :   Pressure in a intermediate node $[Pa]$
k :   Index for the first node $[-]$
l :   Index for the second node$[-]$

It is however not all loops that can be used, the loops have to be independent of each other. It goes that the amount of independent loops in a multi zone model can be found as:

$$O - Z + 1 = independent\ loops \tag{A.35}$$

where

O :   Numbers of openings $[-]$
Z :   Numbers of zones $[-]$

When the independent lops have been set up the pressure drops are substituted with equations for the correlations between the pressure drops and the mass flow through the openings. By setting up the mass balances for the building there are enough equations to solve the systems of equations.

Like for the continuity of mass approach there are made an example to illustrate how the compatibility of pressure changes in a loop works, as shown in figure A.4.
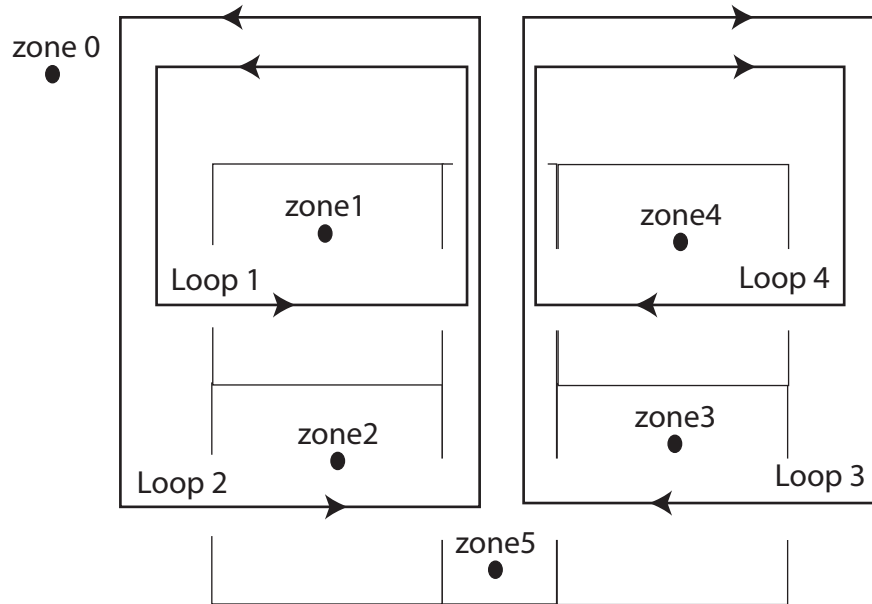
Figure A.4: *Simple 2d model with 5 zones inside the building.*

$$
\begin{array}{llll}
\text{Loop 1} & : & \sum \Delta P_1 = 0 \\
\text{Loop 2} & : & \sum \Delta P_2 = 0 \\
\text{Loop 3} & : & \sum \Delta P_3 = 0 \\
\text{Loop 4} & : & \sum \Delta P_4 = 0
\end{array}
$$

In the example there are four independent loops and when the masses are substituted into the equations there are 9 unknown values. By setting up a mass balance for the system there are gained 5 equations more. There are therefore the same amount of unknown as there are equations and the system of equations can be solved.

General in the past the primary choice has been to use the continuity approach to set up the governing system of equations for the airflows in the building. There have only been a few people in the building simulation community who have used the compatibility approach to analyze the airflows in the building. However an example of where the compatibility approach has been used is in BSim. [Axley, 2003]

Models of passive air components

No matter which of the approaches that is chosen, it is necessary to be able to describe the airflows through the different airflow components. If the continuity approach is chosen the description of the airflows is on the forward form and the mass flow is a function of the pressure drop across the opening and the component characteristics:

$$
m = f(\Delta P, \vartheta) \tag{A.36}
$$

[Axley, 2003]

where

m :   Mass flow $[\frac{kg}{s}]$
ΔP :   Pressure drop $[Pa]$
ϑ :   Component characteristics $[-]$

Is it instead the compatibility approach that is chosen, then it is the inverse form that is used where the pressure drop is a function of the mass flow and the component characteristics:

$$\Delta P = f^{-1}(m, \vartheta) \tag{A.37}$$

[Axley, 2003]

To create the correlations between the mass flow, the pressure drop and the component characteristics there are used either theoretical, semi-empirical, or fully empirical component relations. [Axley, 2003]

Often used models to describe the airflow components are for instance the simplified orifice model in equation (A.38) or the power law in equation (A.39). Both models are nonlinear models:

$$m = C_d \cdot A\sqrt{2\rho \cdot \Delta p} \tag{A.38}$$

where

m :   Mass flow $[\frac{kg}{s}]$
C_d :   Discharge coefficient $[-]$
A :   Area $[m^2]$
ρ :   Density $[\frac{kg}{m^3}]$
Δp :   Pressure drop $[Pa]$

$$m = \rho \cdot C \cdot \Delta p^n \tag{A.39}$$

where

m :   Mass flow $[\frac{kg}{s}]$
ρ :   Density $[\frac{kg}{m^3}]$
C :   Flow coefficient $[-]$
Δp :   Pressure drop $[Pa]$
n :   Measured component exponents $[-]$

No matter which model are used to describe the airflow through the components, it is assumed that the pressure across the components opening is spatially uniform and equal to the intermediate node values. For larger opening this is however not a good assumption.

[Axley, 2003]

A problem with the models is that they are purely pressure driven and therefore do not account for the kinetic energy , which has a great importance at high air velocities. It can therefore be argued that there in these cases should be used models based on Bernoulli's equation, and hereby ensure the conservation of mechanical energy through the airflow component. [Axley, 2003]

The choice of which airflow model that should be used depends on the component the air is going through. If the component is a large opening like a window or a door the orifice model should be used. Is the component instead a component in the ventilation system like a filter, heating coil etc., then it is most correct to use the power law or the quadratic model. If the airflow is through a ventilation duck or is infiltration then it is most correct to use a third and a fourth model. [Heiselberg, 2006]

Models of active air components

Of active air components a fan can be mentioned. In the macroscopic models there are used a polynomial approximation to the fan performance curve:

$$\Delta p = a_0 + a_1 \cdot m + a_2 \cdot m^2 + a_3 \cdot m^3 + ... \quad (A.40)$$

[Axley, 2003]

where

m : Mass flow $[\frac{kg}{s}]$
$a_0, a_1, a_2, a_3...$: Empirical determined coefficients $[-]$

By using the fan laws geometric simpler fans are model from one fan performance curve. The extended polynomial of the fan performance curve:

$$\frac{\Delta p}{(\frac{D}{D_0})^2 \cdot (\frac{N}{N_0})^2} = a_0 + a_1 \cdot \frac{m}{(\frac{D}{D_0})^3 \cdot (\frac{N}{N_0})} + a_2 \cdot \frac{m^2}{(\frac{D}{D_0})^6 \cdot (\frac{N}{N_0})^2} + a_3 \cdot \frac{m^3}{(\frac{D}{D_0})^9 \cdot (\frac{N}{N_0})^3} + ... \quad (A.41)$$

[Axley, 2003]

where

D_0 : Fan size for which the fan curve is made $[-]$
D : Fan size of the geometrically similar fan $[-]$
N_0 : Rotational speed of the fan for which the fan curve is made $[-]$
N : Rotational speed for the geometrically similar fan $[-]$

Field assumption

The models that describes the airflows through the components and the fans are not enough to be able to solve the system of equations for the building. To make sure that the system of equations can be solved it is necessary to assume that there is a hydrostatic pressure in the building. When the hydrostatic assumption is used it can either be chosen to use a nonuniform zone density or constant zone density, as in equation (A.42) and (A.43), none of these are a problem to include in the multi zone model.

$$p(z) + \int_0^z \rho(z)_i \cdot g dz = p_i \tag{A.42}$$

where

$$
\begin{array}{lll}
p(z) & : & \text{Pressure at a reference height } [Pa] \\
\rho(z)_i & : & \text{Density of the indoor air } [\frac{kg}{m^3}] \\
p_i & : & \text{Indoor pressure } [Pa]
\end{array}
$$

$$p(z) + \rho_i \cdot z \cdot g = p_i \tag{A.43}$$

The assumption of a hydrostatic pressure distribution in the building is only true when there is no airflow in the building. In the building there will be airflows and therefore the assumption is not correct and the conservation of mechanical energy in the system will not be fulfilled either. [Axley, 2003]

Solving

It is not easy to solve the equations systems because they contains non linear terms. To solve these systems it necessary to take a numerical approach. A way to do this is to use Newton's method. When the continuity approach is used the mass balances for the different zones are first set up, the mass flows are a function of the unknown pressure. [Brohus et al., 2002]

$$\overline{m}(\overline{P}) = 0 \tag{A.44}$$

where

$$
\begin{array}{lll}
\overline{m}(\overline{P}) & : & \text{Vector that contains the sum of the mass flows to and from each of the} \\
& & \text{zones in the model } [\frac{kg}{s}] \\
\overline{P} & : & \text{Vector that contains unknown pressure } [Pa]
\end{array}
$$

To find a numerical solution there is made a first order Taylor series expansion of the function based on vector, $\overline{P}_0$, the following expression is obtained:

$$\overline{m}(\overline{P}) \approx \overline{m}(\overline{P}_0) + \left.\frac{d\overline{m}}{d\overline{P}}\right|_{\overline{P}_0} (\overline{P} - \overline{P}_0) = 0 \tag{A.45}$$

[Brohus et al., 2002]

where

$\overline{P_0}$: A vector that contains a guess of the pressure values $[Pa]$

This equation can be rewritten as:

$$dP = \overline{P} - \overline{P}_0 = - \left(\left. \frac{d\overline{m}}{d\overline{P}} \right|_{\overline{P}_0} \right)^{-1} \cdot \overline{m}(\overline{P}_0) \tag{A.46}$$

[Brohus et al., 2002]

A new guess can then be for the pressure:

$$\overline{P}_{0,new} = d\overline{P} + \overline{P}_{0,old} \tag{A.47}$$

[Brohus et al., 2002]

This value can then be used in a new iteration in equation (A.46) where it will replace $\overline{P}_0$ vector as a better guess. This loop of iterations will continue until a converged pressure vector is obtained.

Test of the Newton method indicate that it sometimes convergence very slow. It can therefore in some case be an advantages to use another iteration method. [Brohus et al., 2002]

A.3   CFD methods

In the following section are described the calculations methods and procedure for calculating the airflow by CFD methods.

The calculation procedure includes the following points:

1. Identification and formulation of problem

2. Specification of geometry and grid

3. Specification of physical models and boundary conditions

4. Solution

5. Results

[Brohus, 2007a]

A.3.1   Identification and formulation of problem

For the identification and formulation of the problem detailed knowledge of the problem has to be defined. The details include:

- Geometry

- Physics

- Processes

[Brohus, 2007a]

For the formulation of the problem the expected outcome and results have to be stated and the effort for the calculations have to be discussed. For the problem the simplifications and the assumptions also have to be discussed and the influence of the simplifications for the result has to be stated.

A.3.2   Specification of geometry and grid

For the CFD simulation the model have to be specified and drawn in the simulation program or imported from other programs. The ideas on how to create the model and the conditions for the model as specified in section A.3.1 have to be modeled in the program and different details for the model have to be specified. When the model is created the grid for the model has to be taken into consideration.

Grid

To get the most accurate solution the grid does have great influence. A coarse grid means that only a few values for the solution is calculated while a fine grid means that a high level of details is available. To get an overview of the solution a course grid can be used because the accuracy is not as good as a finer grid but the time the simulation takes is shorter than for a finer grid. Therefore a course grid is used in the beginning to get an idea of the solution whereafter the grid is getting finer to improve the solution and get a more accurate result.

The grid can be defined in different ways:

- Cartesian grid

- BFC grid

- Block-structured grid

- Unstructured grid

- Adaptive grid

[Jones and Whittle, 1992]

Cartesian grid Cartesian grid is defined as rectilinear rectangles. For this kind of grid the cells are often concentrated around the inlet and the walls for the model to get the most accurate result. To get an accurate result the grid type is often too course and therefore should only be used to get an estimate of the result. In figure A.5 are showed a model of a typical cartesian grid.
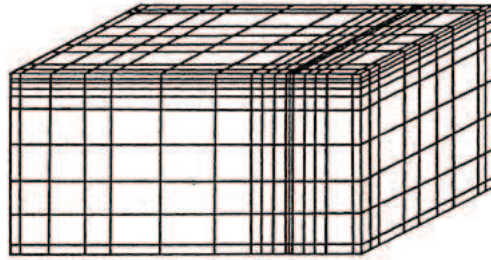

Figure A.5: *Typical cartesian grid. [Jones and Whittle, 1992]*

For the grid the aspect ratio has to be as close to unity as possible. This means that the length and width of the cells should be as close to the same dimension as possible. An aspect ratio greater than 5:1 will in some cases slow the rate of convergence. [Jones and Whittle, 1992]

In table A.2 are listed some advantages and some disadvantages for the cartesian grid.

Table A.2: *Advantages and disadvantages for the cartesian grid. [Jones and Whittle, 1992]*

Advantages	Disadvantages
Relatively easy to generate and use	The finer grid for the supply openings are also carried in each direction into other areas where it is not required
Calculations are preformed very efficiently by the finite element method	Calculations are not as accurate as by other grids
Easy to use to represent flow in cylindrical polar co-ordinates	Not easily able to correctly represent irregularly shaped rooms, comprising slopes or curved surfaces

BFC grid For the BFC grid the Cartesian grid structure is maintained but the cells are formed from four-sided or six-sided elements according to 2D or 3D. This means that the two sides opposite each other does not need to be the same length as for the Cartesian grid.

Therefore by using BFC grid it is possible to model a sloped surface as shown in figure A.6.
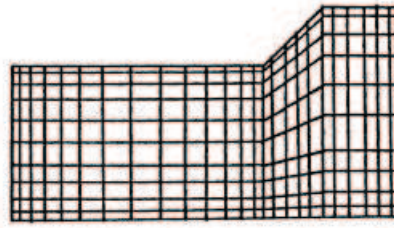

Figure A.6: *BFC grid for a sloped surface.   [Jones and Whittle, 1992]*

Compared to the Cartesian grid it is possible with the BFC grid to change the grid dimensions in the two directions. In this way a fine grid can be located close to the opening and further away it is getting more course. The principle is showed in figure A.7.
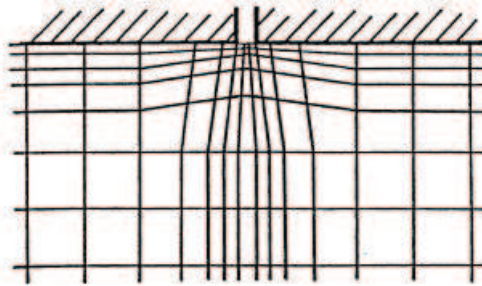
Figure A.7: *BFC grid for an inlet where the grid dimensions change away from the opening. [Jones and Whittle, 1992]*

In table A.3 are listed some advantages and some disadvantages for the BFC grid.

Table A.3: *Advantages and disadvantages for the BFC grid.   [Jones and Whittle, 1992]*

Advantages	Disadvantages
Possible to model sloped surfaces more accurate than with Cartesian grid	The grid structure is not linear
More accurate calculations than with Cartesian grid	Require more CPU time than for Cartesian grid
Possible to change the grid structure away from the opening	

Block-structured grid   The Block-structured grid combines one or more individual grid structures. This means that for the Block-structured grid it is possible to combine different grid structures. The Block-structured grid has an advantages when modeling an atrium compared to the BFC grid as showed in figure A.8.
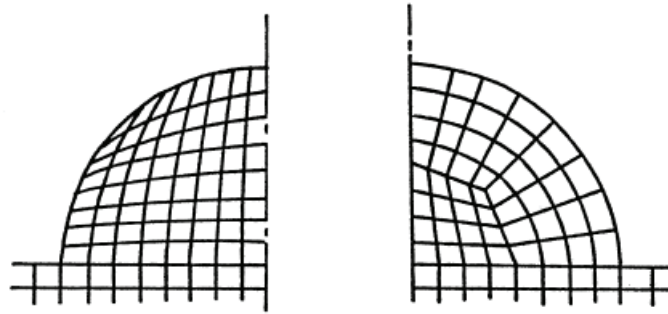
Figure A.8: *BFC grid and Block-structured grid for an atrium. To the left the BFC grid to the right the Block-structured grid.   [Jones and Whittle, 1992]*

From figure A.8 it is showed that the advantage with the Block-structured grid compared to the BFC grid is that it is possible to combine to individual structures and get a more accurate grid modeling of the structure.

Also for a cross-section of triangular shape the Block-structure does fit better than the BFC grid as showed in figure A.9 again because it is possible to combine two individual grids.
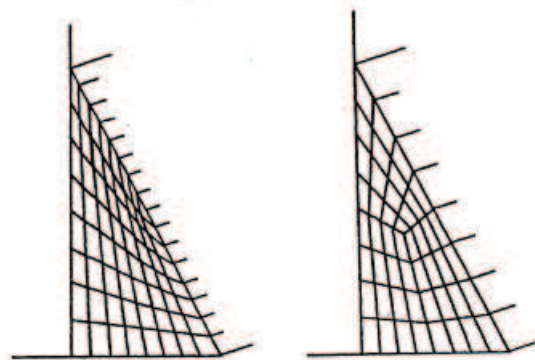

Figure A.9: *BFC grid and Block-structured grid for an cross-section of triangular shape. To the left the BFC grid to the right the Block-structured grid.   [Jones and Whittle, 1992]*

In table A.4 are listed some advantages and some disadvantages for the Block-structured grid.

Table A.4: *Advantages and disadvantages for the Block-structured grid. [Jones and Whittle, 1992]*

Advantages	Disadvantages
More flexibility because of the combination of one or more BFC grids	Use more CPU time than BFC grid because the grid is not structured in an Cartesian notation anymore
Possible to create more accurate grid for difficult constructions	More complicated calculations than for the BFC grid

Unstructured grid   With the unstructured grid it is possible to use elements as triangular elements and wedges as four- and six-sided elements. The grid can be structured in all possible ways. Because it is possible to structure the grid so it fits exactly to the figure the calculations are more accurate but it also demands even higher CPU time than the Block-structured grid.

Adaptive grid   The adaptive grid is more accurate than the unstructured grid because it makes it possible to adjust the grid geometry to optimize local shapes against specified criteria based on a combination of a measure of solution gradient, grid orthogonality and grid smoothness.   [Jones and Whittle, 1992]

A.3.3   Specification of physical models and boundary conditions

To calculate the airflow for the model the turbulence model have to be taken into consideration and the type of turbulence model has to be decided. For the turbulence model there are different kind of models:

- Zero-equation RANS model

- $k - \varepsilon$ model

- Reynolds Stress equation Model

- Large Eddy Simulation

- Direct Numerical Simulation

All the models are based on an airflow model that consist on the continuity equation, Navier-Stokes equation, energy equation and concentration equation [Gan, 1994] .

The time averaged equations for an incompressible steady-state flow are listed below.

Continuity equation

The continuity equation state the mass balance for a control volume in the air where the incoming mass equals the outgoing mass. The equation is given by:

$$\frac{\partial(\rho u_i)}{\partial x_i} = 0 \tag{A.48}$$

[Gan, 1994]

where

ρ :   Density of the air $[\frac{kg}{m^3}]$
u_i :   Mean velocity in the i direction $[\frac{m}{s}]$
x_i :   Co-ordinate direction i $[m]$

Navier-Stokes equation

The Navier-Stokes equation is also given by the momentum equation. The equation is expressing Newtons second law of motion for a fluid. Navier-Stokes equation is given by:

$$\overbrace{\frac{\partial(\rho u_i u_j)}{\partial x_j}}^{Convection\ term} = \overbrace{\frac{\partial}{\partial x_j}\left((\mu_l + \mu_t)\left(\frac{\partial u_i}{\partial x_j} + \frac{\partial u_j}{\partial x_i}\right)\right) - \frac{\partial}{\partial x_j}\left(p + \frac{2}{3}\rho k \delta_{ij}\right)}^{Diffusion\ term}$$

$$- \overbrace{\frac{\partial p}{\partial x_i}}^{Pressure\ gradient\ term} + \overbrace{B_i + S_u}^{Buoyancy\ term} \tag{A.49}$$

[Gan, 1994]

where

μ_l :   Laminar dynamic viscosity $[\frac{kg}{m\dot{s}}]$
μ_t :   Turbulent viscosity (eddy viscosity) $[\frac{kg}{m\dot{s}}]$
u_i' :   Fluctuating velocity component in the i direction $[\frac{m}{s}]$
k :   Turbulent kinetic energy $[\frac{J}{kg}]$
δ_{ij} :   Kronecker delta $[-]$
p :   Pressure $[Pa]$ or $[\frac{N}{m^2}]$
B_i :   Volume force in the i direction $[\frac{N}{m^2}]$
S_u :   Source term $[\frac{N}{m^3}]$

On the left side of equation (A.49) is the convection term that describe the net supply of momentum from the surroundings. The first term on the right side is the diffusion term that describes the influences from the shear forces. The second term is the pressure gradient term that is due to the normal forces and the last term is the buoyancy term which describes the volume forces acting on the air and the source term which is used to implement the boundary conditions. [Brohus, 1997]

Energy equation

To calculate the temperature distribution the energy equation is used. The energy equation is derived from the basic law of conservation of energy and given by:

$$\frac{\partial(\rho c_p u_j t)}{\partial x_j} = \frac{\partial}{\partial x_j}\left(\lambda_{eff}\frac{\partial t}{\partial x_j}\right) + S_t \tag{A.50}$$

[Brohus, 1997]

where

c_p :   Specific heat at a constant pressure $[\frac{J}{kg^\circ C}]$
t :   Mean temperature of the air $[^\circ C]$
λ_{eff} :   Effective conductivity $[\frac{W}{m^\circ C}]$
S_t :   Source term $[\frac{W}{m^3}]$

The effective conductivity is given by:

$$\lambda_{eff} = \lambda_l + \lambda_t \tag{A.51}$$

where

λ_l :   Laminar thermal conductivity $[\frac{W}{m^\circ C}]$
λ_t :   Turbulent conductivity $[\frac{W}{m^\circ C}]$

The laminar conductivity is constant for the domain and is a property for the fluid. The turbulent conductivity depends on the local flow field and is normally found by the turbulent Prandtl number given by:

$$\sigma_t = \frac{\nu_t}{\alpha_t} = \frac{c_p \mu_t}{\lambda_t} \tag{A.52}$$

where

σ_t :   Turbulent Prandtl number $[-]$
ν_t :   Turbulent kinetic viscosity $[\frac{m^2}{s}]$
α_t :   Turbulent thermal diffusivity $[\frac{m^2}{s}]$

The turbulent kinematic viscosity describes the rate of which momentum may diffuse through the fluid because of turbulent motion. The turbulent thermal diffusivity explains the rate of which momentum may diffuse through the fluid because of diffusion of heat. [Brohus, 1997]

Concentration equation

To calculate the transport of contaminant the concentration equation is used. The equation is based on the mass conservation and given by:

$$\frac{\partial(u_j c)}{\partial x_j} = \frac{\partial}{\partial x_j}\left(D_{eff}\frac{\partial c}{\partial x_j}\right) + S_c \tag{A.53}$$

[Brohus, 1997]

where

c :   Concentration of contaminant $[\frac{kg}{kg}]$
D_{eff} :   Effective diffusivity $[\frac{m^2}{s}]$
S_c :   Source term $[\frac{kg}{kgs}]$

The effective diffusivity is given by:

$$D_{eff} = D_l + D_t \tag{A.54}$$

where

D_l :   Mass molecular diffusivity $[\frac{m^2}{s}]$
D_t :   Turbulent diffusivity $[\frac{m^2}{s}]$

Zero-equation RANS model

The zero-equation RANS model is the zero-equation Reynolds Averaged Navier-Stokes model. The model is also called the mixing length model and is the most simple of the turbulence models because the eddy viscosity is given as a constant number or from an analytical equation without involving any transport equations [?] . For 2D cases the model uses a single algebraic function to calculate the turbulent viscosity which is given by a product of the velocity scale and length scale:

$$\mu_t = k\rho u_0 H \tag{A.55}$$

[?]

where

k :   Constant $[-]$
u_0 :   Characteristic velocity $[\frac{m}{s}]$
H :   Characteristic length $[m]$

In table A.5 are listed some advantages and disadvantages for the zero-equation RANS model.

Table A.5: *Advantages and disadvantages for the zero-equation RANS model.* *[Brohus, 2007a]*

Advantages	Disadvantages
Easy to implement	Cannot determine flow with separation and recirculation
Cheap in terms of computer power	Determines only properties for mean flow and turbulent shear stress
Good results for jets, mixing layers, wakes and boundary layers	
Robust	
Well established	

$k - \varepsilon$ model

Different from the zero-equation RANS model the $k - \varepsilon$ model is a two equation model where two transport equations are solved. The transport equations are for turbulent kinetic energy k and dissipation of turbulent kinetic energy ε.

The turbulent kinetic energy is defined as:

$$k \equiv \frac{1}{2}\overline{u_i' u_i'} = \frac{1}{2}(\overline{u'^2} + \overline{v'^2} + \overline{w'^2}) \tag{A.56}$$

The dissipation of turbulent kinetic energy is defined as:

$$\varepsilon \equiv -2\nu\overline{s_{ij}s_{ij}} \tag{A.57}$$

where

$s_i j$: Strain rate of the fluctuating flow $[-]$

The transportation equation for the turbulent kinetic energy is given by:

$$\frac{D}{Dt}(\rho k) = \frac{\partial}{\partial x_j}\left[\left(\mu + \frac{\mu_t}{\sigma_k}\right)\frac{\partial k}{\partial x_j}\right] + G_k - \rho\epsilon \tag{A.58}$$

[Brohus, 2007a]

where

G_k : Buoyancy term $[-]$
σ_k : 1,0

The transport equation for the dissipation of turbulent kinetic energy is given by:

$$\frac{D}{Dt}(\rho\epsilon) = \frac{\partial}{\partial x_j}\left[\left(\mu + \frac{\mu_t}{\sigma_\epsilon}\right)\frac{\partial\epsilon}{\partial x_j}\right] + C_1\frac{\epsilon}{k}G_k - \rho c_2\frac{\epsilon^2}{k} \tag{A.59}$$

[Brohus, 2007a]

$$
\begin{array}{lll}
\sigma_\epsilon & : & 1,3 \\
C_1 & : & 1,44 \\
C_2 & : & 1,92
\end{array}
$$

The $k - \varepsilon$ model is the most used model in CFD programs. To use the model the flow has to be fully turbulent.

In table A.6 are listed some advantages and disadvantages for the $k - \varepsilon$ model.

Table A.6: *Advantages and disadvantages for the $k - \varepsilon$ model. [Brohus, 2007a]*

Advantages	Disadvantages
Most simple turbulence model where only initial and boundary conditions must be prescribed	More expensive (according to CPU power) to implement than the mixing length model (two extra differential equations)
Good results for many industrial flows	Poor performance for a number of important flow types:
Well established, most widespread turbulence model	1. Some internal flows
Robust	2. Flow with large shear stresses (e.g. curvilinear boundary layers, swirl flow)
	3. Flow with rotation
	4. Fully developed flows in non-circular channels

Reynolds Stress equation Model

The Reynold stress equation model is a seven-equation model that solves transport equations for the Reynolds stresses together with an equation for the dissipation rate. With the Reynold Stress equation model it is possible to get an accurate prediction for a complex flow compared with the one and two-equations models. The Reynold stress equation model

is more accurate than the $k - \varepsilon$ model. [Sørensen and Nielsen, 2003]

In table A.7 are listed some advantages and disadvantages for the Reynold stress equation model.

Table A.7: *Advantages and disadvantages for the Reynold stress equation model.* *[Brohus, 2007a]*

Advantages	Disadvantages
Potentially the most general of all classical turbulence models	Expensive in terms of computer power (seven extra differential equations), typically 2 - 3 times more CPU-time than $k - \varepsilon$ model
Only initial and/or boundary conditions must be prescribed	Not as widely validated than the mixing length model and the $k - \varepsilon$ model
Very accurate results for the mean flow properties and all the Reynolds stresses for many simple and complex flows	As poor as the $k - \varepsilon$ model for some flow types

Large Eddy Simulation

The simulations with large eddy simulation is 3D and transient. The large eddy simulation is used to obtain details about the turbulence that is not possible with other models. With the model the turbulence is predicted in detail. For the calculations with the large eddy simulation the turbulence is made time dependent. [Sørensen and Nielsen, 2003]

In table A.8 are listed some advantages and disadvantages for the large eddy simulation model.

Table A.8: *Advantages and disadvantages for the large eddy simulation model.   [Brohus, 2007a]*

Advantages	Disadvantages
Provides knowledge about the turbulence in the flow (e.g. quantities which at present cannot be measured)	More expensive (according to CPU power) than other turbulence models
Good results for free turbulent flows for all Re	Near a wall (boundary) all vortices are small, which implies that: 1. Either one must perform DNS simulations near the wall (= expensive) 2. Or use a coarser grid and a model (= practice $\Rightarrow$ Re-dependence, dependence of empirical data) Fluctuating inlet boundary conditions may cause problems Not as widely validated as the other models for industrial flows Relatively new in "indoor environmental engineering", cf. boundary conditions

Direct Numerical Simulation

For the direct numerical simulations the Navier-Stokes equations are numerically solved without any turbulence model.

In table A.9 are listed some advantages and disadvantages for the direct numerical simulation model.

Table A.9: *Advantages and disadvantages for the direct numerical simulation model.* *[Brohus, 2007a]*

Advantages	Disadvantages
No approximations or turbulence models required	Much more expensive than turbulence models
Provides substantial new knowledge about turbulence and other flow characteristics (e.g. quantities which at present cannot be measured in the laboratory)	Only applicable in case of simple, low Re flows - in practise

Specification of boundary conditions

When the boundary conditions have to be specified the following points have to be taken into consideration:

- Available symmetry or axis symmetry

- Steady or unsteady

- Isothermal or thermal

- Two-dimensional or three-dimensional

- Selection of discretisation schemes

- Selection of algorithm for pressure-velocity coupling

[Brohus, 2007a]

Because of the friction near a wall the velocity of the air passing by will change from free stream away from the wall to zero velocity near the wall. The velocity profile for the flow near a wall is showed in figure A.10.
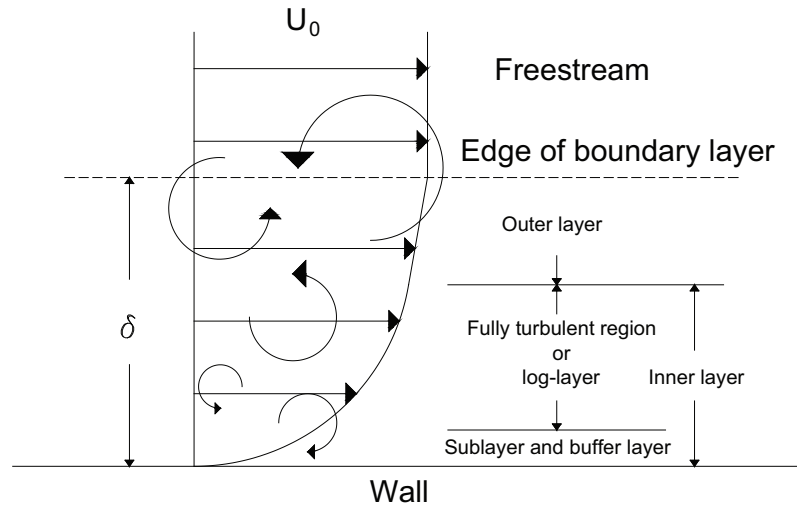
Figure A.10: *Flow structure near a wall.*

As showed in figure A.10 the friction near the wall have great influence on the velocity profile near the wall. To ensure a good description of the velocity profile close to the wall there have to be a fine grid close to the wall.

To evaluate the friction between the wall and the air the wall functions are used. For the standard wall functions the boundary layer or inner layer is divided into two layers, a viscous sub-layer and a fully turbulent region as showed in figure A.10.

For the description of the wall function are used the two dimensionless functions for the velocity and the length. The dimensionless velocity is given by:

$$u^+ = \frac{u}{u_\tau} \tag{A.60}$$

where

u^+ : Dimensionless velocity $[-]$
u : Velocity in the x-direction $[\frac{m}{s}]$
u_τ : Friction velocity $[\frac{m}{s}]$

The dimensionless length is given by:

$$y^+ = \frac{\rho y u_\tau}{\mu} \tag{A.61}$$

where

y^+ : Dimensionless length $[-]$
ρ : Density of air $[\frac{kg}{m^3}]$
y : Coordinate in y direction $[m]$
μ : Laminar dynamic viscosity $[\frac{kg}{ms}]$

The friction velocity is given by:

$$u_\tau = \sqrt{\frac{\tau_w}{\rho}} \tag{A.62}$$

where

τ_w : Wall shear stress $[\frac{N}{m^2}]$

The wall shear stress is given by:

$$\tau_w = \sqrt{c_\mu} \rho k_p \tag{A.63}$$

where

c_μ : Constant $(= 0,09)$ $[-]$
k_p : Turbulent kinetic energy at first grid node adjacent to surface $[\frac{J}{kg}]$

From equation (A.61) it is seen that the dimensionless height also can be defined as a local Reynolds number.

The dimensionless height locate the difference between the viscous sub-layer and the fully developed turbulent regime as showed in figure A.10.

The viscous sub-layer is given for $y^+ < 11,5$ [Flovent, 2005] where the dimensionless velocity is:

$$u^+ = y^+ \qquad for \qquad (y^+ < 11,5) \tag{A.64}$$

The fully developed turbulent regime is given for $y^+ \geq 11,5$ [Flovent, 2005] where the dimensionless velocity is:

$$u^+ = \frac{1}{0,435} \ln(9y^+) \qquad for \qquad (y^+ \geq 11,5) \tag{A.65}$$

The numerical wall shear stress τ_w is calculated from the value of the velocity in the first grid node at a distance y from the wall. [Brohus, 1997]

Because of the dependency of the wall function on the velocity profile the grid layout in the boundary layer is important. The first grid note should be located so the relative error for the measurement is as low as possible. The relative error also depend on the location on the first grid node.

Discretization

For the calculations are used the Finite Volume Method where the model is divided into finite number of volumes with a related grid point. For the temperature calculation the temperature is calculated in the grid point for the cell and used as the value for the whole

volume.

For each cell the differential equations are calculated and the profiles expressing the variation over the grid points are used to evaluate the integral. [Brohus, 1997]

The general form of the solved equation is given by:

$$\overbrace{\frac{\partial(\rho u_j \phi)}{\partial x_j}}^{Convection\ term} = \overbrace{\frac{\partial}{\partial x_j}\left(\Gamma_\phi \frac{\partial \phi}{\partial x_j}\right)}^{Diffusion\ term} + \overbrace{S_\phi}^{Souce\ term} \qquad (A.66)$$

[Brohus, 1997]

where

ϕ : Dependent variable
Γ_ϕ : Diffusion coefficient
S_ϕ : Source term

The meaning of ϕ, Γ_ϕ and S_ϕ depend on the respective equations.

The convection and diffusion term in equation (A.66) can be calculated from the following differencing schemes:

- Central Differencing Scheme

- Upwind Differencing Scheme

- Hybrid Differencing Scheme

[CFD Online, 2005]

With the differencing schemes the variable ϕ is calculated. In figure A.11 is showed the division into different volumes and grid notes.
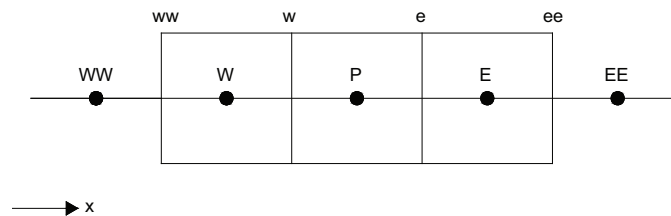

Figure A.11: *Principle for division of control volumes and grid notes for a 1D case.*

Central Differencing Scheme Second order accurate scheme. The central differencing scheme is used for low Reynold number flow where diffusive elements dominate over convection. The convected variable of the cell face is calculated from:

$$\phi_w = 0,5(\phi_W + \phi_P) \tag{A.67}$$

[CFD Online, 2005]

Upwind Differencing Scheme Unconditionally bounded and highly stable. Because it is only a first order accurate scheme it might produce severe numerical diffusion. The convected variable of the cell face is calculated from:

$$\phi_w = \phi_W \tag{A.68}$$

[CFD Online, 2005]

Hybrid Differencing Scheme Switches between discretisation of the convective term between the central differencing scheme and the upwind differencing scheme according to the local cell Peclet number. The Peclet number for thermal diffusion is defined as:

$$Pe_L = \frac{LV}{\alpha} = Re_L \cdot Pr \tag{A.69}$$

[Hansen et al., 1997]

where

$$
\begin{array}{lll}
Pe_L & : & \text{Peclet number } [-] \\
L & : & \text{Characteristic length } [m] \\
V & : & \text{Velocity } [\frac{m}{s}] \\
\alpha & : & \text{Thermal diffusivity } [\frac{m^2}{s}] \\
Re_L & : & \text{Reynolds number } [-] \\
Pr & : & \text{Prandtl number } [-]
\end{array}
$$

The convected variable of the cell face is calculated from:

$$\phi_w = 0,5(\phi_W + \phi_P) \qquad for \qquad Pe < 2 \tag{A.70}$$

$$\phi_w = \phi_W \qquad for \qquad Pe > 2 \tag{A.71}$$

[CFD Online, 2005]

The source term is most often dependent on the variable ϕ. The dependence of the variable is described in a linear form even that it is not always linear. [Brohus, 1997]

The pressure is calculated indirectly from the continuity equation by using the SIMPLE algorithm. [Brohus, 1997]

A.3.4 Solution

For the solution the following points has to be stated:

- Start up procedure (initial field, generation of intermediate solution, etc.)

- Underrelaxation or false time step

- Multigrid, grid adaption, etc. (if available)

- Convergence monitoring (residuals, monitoring points)

- Convergence criteria

[Brohus, 2007a]

To get the best result of the simulation the points listed above have to be discussed and decided for the single problem. For different problems the different criteria may differ according to the different models.

The convergence criteria depends on the accuracy of the calculation and on the used software for the calculation. For a simple model that only are used to get an estimate of the result a not-well converged solution might be good enough. When the interesting point of the calculation is a small area of the flow a high level of convergence might be required.

A.3.5 Results

The last point for the CFD modeling is the results. For this point the result of the simulation has to be analyzed. This also means that it has to be decided what kind of plots that shows the calculations in the best way eg. vector plots or contour plots. To control the calculation the results has to be validated and and maybe a revision to the numerical or physical model has to be done.   [Brohus, 2007a]

Appendix B

Measurements at The Peak in Hong Kong

In the following chapter is described the measurements of the temperature at The Peak in Hong Kong.

B.1 Purpose

The purpose of the measurements was to measure the mountain's surface temperature, the ground temperature and the temperature of the building. The measurements of the temperature were used as input for the simulation of the mountain and sea breeze Grantham hospital.

For the simulations were needed the surface temperature of the mountain located behind the hospital, the ground temperature for the location of the hospital, the sea temperature and the air temperature.

B.2 Equipment

For the experiment were used the infrared camera ThermaCAM S40 as showed in figure B.1.

Figure B.1: *ThermaCAM S40.*

The technical data for the camera is listed in table B.1.

Table B.1: *Technical data for the infrared camera ThermaCAM S40. [Flir Systems, 2002]*

Temperature range	$-40\ °C$ to $+120\ °C$	Range 1
	$0\ °C$ to $+500\ °C$	Range 2
	$+350\ °C$ to $+1500\ °C$	Range 3
	Up to $+2000\ °C$	optional
Accuracy (% of reading)	$\pm2\ °C$ or ±2 %	

For controlling the measured temperature with the infrared camera were used k-type thermocouple and a datalogger CENTER 309, as showed in figure B.2.

Figure B.2: *CENTER 309 datalogger.*

The technical data for the datalogger is listed in table B.2.

Table B.2: *Technical data for the datalogger CENTER 309. [Center Technology Corp., 2007]*

Temperature range	$-200\ °C$ to $+1370\ °C$
Accuracy	$\pm 3\ \%$ rdg $+1\ °C$

B.3 Theory

For the infrared camera the emitted infrared radiation from an object is measured. Because the radiation is a function of the temperature it is possible for the camera to calculate the temperature. [Flir Systems, 2003]

The measured radiation is not only dependent on the temperature of the object but also the radiation from the object. The radiation from the object and the reflected radiation is also influenced by absorption of the atmosphere. [Flir Systems, 2003]

To measure the temperature accurately it is necessary to compensate for the effects of a number of different radiation sources. To get the correct temperature, the following points have to be defined for the camera:

- The emissivity of the object

- The relative humidity

- The temperature of the atmosphere

- The distance between the camera and the object

- The effective temperature of the object surroundings, or the reflected ambient temperature

[Flir Systems, 2003]

B.4 Performance

The experiment was carried out Wednesday the 14th of November 2007 from 8 o'clock to 24 o'clock. The location for the experiment was at The Peak in Hong Kong as shown in figure B.3.
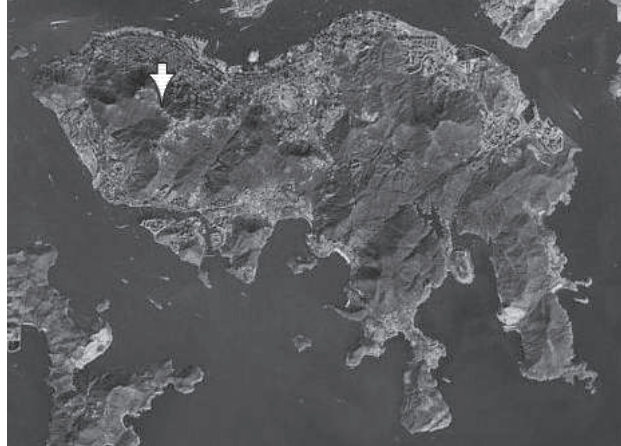
Figure B.3: *The location for the experiment at the Peak in Hong Kong.*

For the experiment there were taken pictures of the following surfaces:

1. The mountain facing north

2. Buildings in the central of Hong Kong Island

3. The mountain facing south

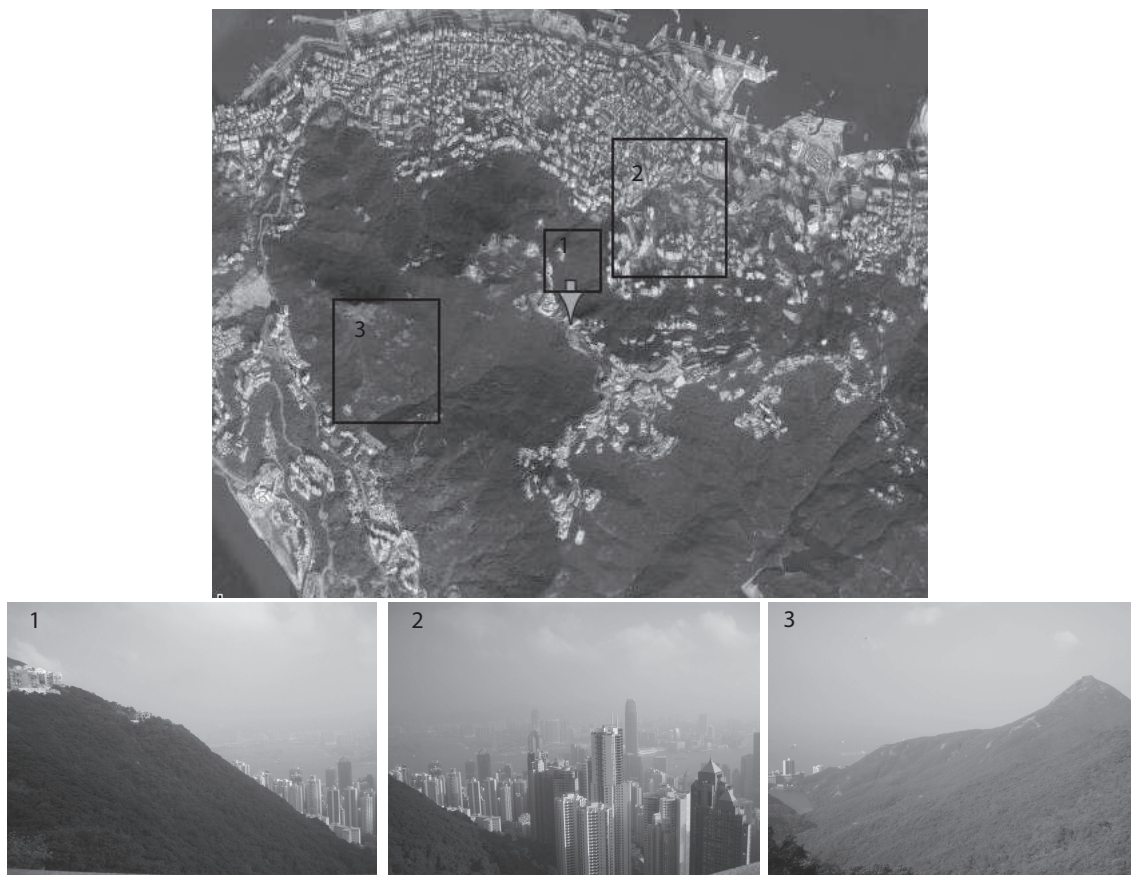The three directions are showed in figure B.4.

Figure B.4: *The three directions for the picture.*

The temperature for the three directions were measured every second hour starting at 8 o'clock. For every measurement were taken 10 pictures with an interval of 30 seconds. To get the same direction for the pictures for the different time steps there were used a tripod for every location. The tripod were located in the same position all the time. The setup of the camera is showed in figure B.5.

Figure B.5: *The setup for the experiment.*

The object parameters used for the measurements are listed in table B.3.

Table B.3: *Object parameters.*

Emissivity	0,9
Distance	500 m
Ambient temperature	20, 0 $^\circ C$
Atmospheric temperature	20, 0 $^\circ C$
Relative humidity	75 %

B.5   Results

From the pictures it is possible to measure the temperature of the surfaces. In figure B.6 are shown the picture of the hill facing north at 10 o'clock.
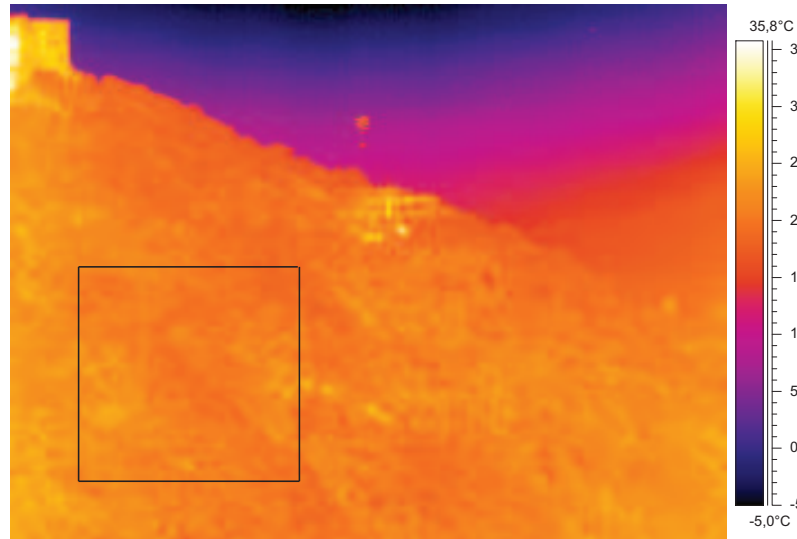
Figure B.6: *Infrared picture of the mountain facing north at 10 o'clock.*

From figure B.6 it is possible to define the temperature for the mountain. The temperature is defined as a mean value from the temperature of the mountain. The mean value is calculated from the square showed in figure B.6. For every time step are made 10 pictures. For all the pictures the mean temperature is calculated and the actual temperature is calculated as the mean value of the 10 pictures. The same procedure is used for all the picture. In figure B.7 and B.8 are shown the a picture of the central of Hong Kong and of the mountain facing south at 10 o'clock.

Figure B.7: *Infrared picture of the central of Hong Kong at 10 o'clock.*

Form figure B.7 it is seen that the surface temperature for one of the building rises to at temperature of about 50 °C. This might be because the reflectance from the sun in the

glass of the building. Because of the reflectance the temperature therefore might be too high. For the calculating of the temperature of the building this temperature is not used.
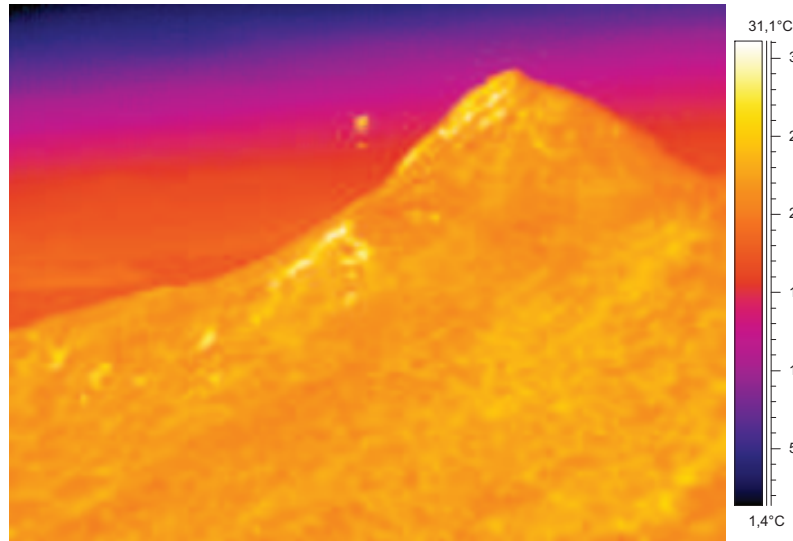

Figure B.8: *Infrared picture of the mountain facing south at 10 o'clock.*

B.6 Data analysis

In figure B.9 is showed the temperature distribution for the three different location. Besides is also showed the air temperature at The Peak and at Wong Chuk Hang which is located close to the hospital.
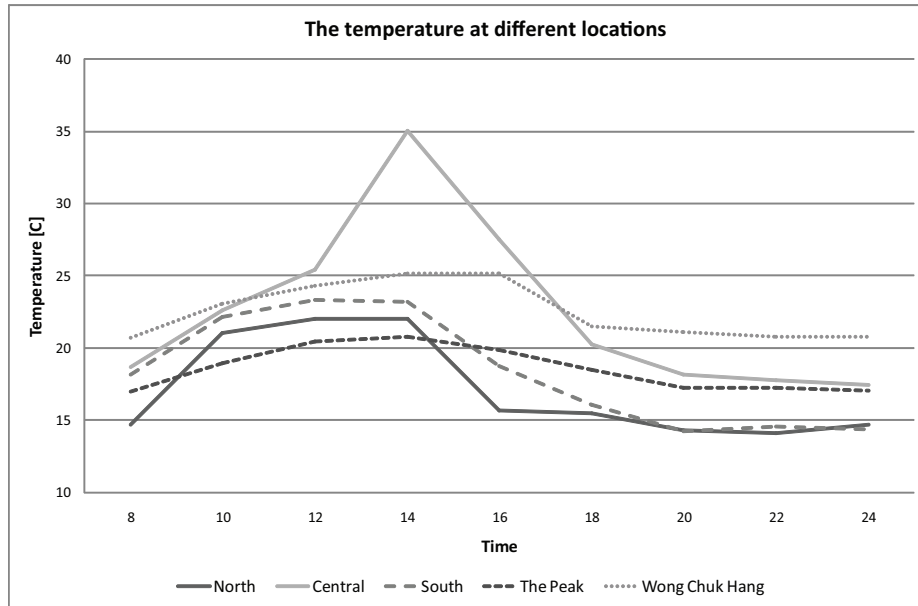
Figure B.9: *Temperature distribution for the three different locations; mountain facing north, central of Hong Kong, mountain facing south and the air temperature at The Peak and Wong Chuk Hang.*

From figure B.9 it is showed that the air temperature at Wong Chuk Hang is about $3-4\ °C$ higher than at The Peak. It is also shown that the temperature of the mountain facing south is about $1-3\ °C$ higher than the northern side. The temperature of the buildings in central rises to the highest point in the afternoon.

At Wong Chuk Hang the air temperature is at all the time higher than the surface temperature of the mountain both facing north and south. For The Peak the air temperature between about 9 o'clock to 14 o'clock is lower than the surface temperature of the mountain. The rest of the time the air temperature is higher than the surface temperature. The temperature of the buildings in central rises to a higher point from about 11 o'clock to 17 o'clock than the air temperature at Wong Chuk Hang.

B.7 Uncertainty

Because of the vegetation of the mountain it where not possible to measure the correct surface temperature of the mountain. The measured temperature were instead the temperatures of the threes at the mountain. This is an uncertainty for the calculation of the temperature of the mountain. To get the right temperature it has to be measured for a mountain without vegetation. The mountain behind Grantham hospital is also planted with threes. Therefore the measured temperature is used for the simulations.

Another uncertainty for the experiment is the direction for the picture. Even though it where tried to get the same direction for all the pictures by letting the tripods stay in the

same place for the hole time, the tripods got moved a bit according to people going into it.

For the measuring of the temperature of the buildings this also depends on the surface of the buildings. The temperature is calculated from the radiation from the surface. Because the radiation depends on the surface of the building the different buildings have different temperature.

In figure B.10 is showed the temperature of a building measured with the infrared camera compared to the measured temperature of the Yam Pak building close to The University Of Hong Kong measured with the thermocouple and the datalogger.
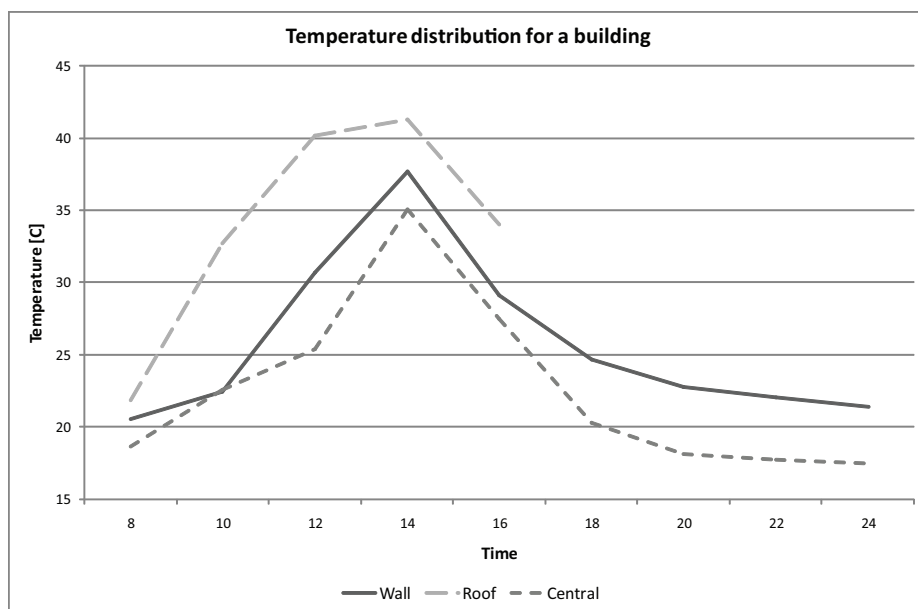
Figure B.10: *Temperature distribution for a building measured with the infrared camera and the thermocouple and the datalogger. The Central measurements are done with the infrared camera and the wall and roof measurements are done with the thermocouple and the datalogger.*

From figure B.10 it is showed that the temperature measured with the two different measurements differ from each other. A reason for this could be that the temperature is not measured for the same building for the two graphs and the calculating methods for the two measurements are different. To be able to compare the two methods the measurements should be for the same location and the equipment should be calibrated for the same reference point. Therefore the comparison can only be used to get an idea of the accuracy measured with the infrared camera.

For the measurements with the infrared camera the radiation from the buildings have great influence. Because of the radiation from the buildings, the measured temperature depend on the surface material of the buildings. For the thermocouple and the datalogger this do not have any influence. This might be an other reason for the difference in the

temperature.

Another reason for the difference might be according to the shading factors. The thermocouple on the roof of the Yam Pak building is exposed to the sun all the time. The wall for the thermocouple is facing south so they will be direct in the sun at noon. For the buildings in the central of Hong Kong they might shade for each other. The different shading factors could also be a reason for the difference in the measurements.

B.8 Conclusion

As showed in figure B.9 the temperature for both the mountain and the buildings varies more than the air temperature and rises to the highest point in the afternoon.

From figure B.10 it is seen that there is a difference between the temperature of the building measured with the infrared camera and the thermocouple. This might be because the temperature were not measured for the same building in the two situations. For the infrared camera the uncertainty is high and therefore the measurements is not exactly correct but can only be used to get an estimate of the temperature of the different surfaces.

For the simulations is used the measured temperature as a starting point. The variation for the measured temperature is set to $\pm 10\ ^{\circ}C$.

Bibliography

Aalborg Sygehus (2007). Hvad laver infektionsmedicinsk afdeling. `http://www.aalborgsygehus.rn.dk/Afdelinger/Medicinske+afdelinger/Medicinsk+Center/Afdelinger/Infektionsmedicinsk+Afdeling/For+borgere/Hvad+laver+Infektionsmedicinsk+Afdeling/`.

Ables, M. A. F., Ajero, M. M., Fabian, M. H., and Ramirez, M. N. (2006). City synthesis report on urban air quality management, hong kong sar. Discussion draft, Asian Development Bank and the Clean Air Initiative for Asian Cities (CAI-Asia) Center.

Andersen, K. T., Heiselberg, P., and Aggerholm, S. (2002). *Naturlig ventilation i erhvarvsbygninger*. By og Byg, Statens Byggeforskningsinstitut, 1 edition.

ASHRAE (2003). *HVAC design manual for hospitals and clinics*. W. Stephen Comstock. ISBN 1-931862-26-5.

Asian Intensive Care (2007). Isolation rooms. `http://www.aic.cuhk.edu.hk/web8/isolation.htm`.

avisen.dk (2007). Her grædes af lykke og skriges af smerte. `http://avisen.dk/popprint.aspx?postID=252590&appID=artikel`.

Axley, J. W. (2003). Loop design method, preliminary draft. Technical report.

Beggs, C. (2002). Engineering the control of airborne pathogens.

Brohus, H. (1997). Personal exposure to contaminant sources in ventilated rooms. Ph.d.-thesis, Aalborg University. ISSN 0902-7953 R9741.

Brohus, H. (2003). Example2. xls file.

Brohus, H. (2007a). Cfd in ventilation. `http://www.civil.aau.dk/~i6hb/cfd/`. Lecture notes from the cource CFD on 9th semester at Indoor Environmental Engineering at Aalborg University.

Brohus, H. (2007b). Multizone modeling. Lecture notes from the course Multizone Modeling on 8th semester at Indoor Environmental Engineering at Aalborg University.

Brohus, H., Frier, C., and Heiselberg, P. (2002). Stochastic single zone and multizone models of a hybrid ventilated building – a monte carlo simulation approach. Technical

report. Annex 35 Technical Report TR19, Department of Building Technology and Structural Engineering, Aalborg University,.

Brohus, H. and Nielsen, P. V. (1996). Cfd models of persons evaluated by full-scale wind channel experiments. Technical Report Paper no. 60, Aalborg University. ISSN 1395-7953 R9652.

Brorsen, M. (2005). *Strømningslære*. Aalborg Universitet.

Canossa Hospital (2004). General ward. `http://www.canossahospital.org.hk/eng/eng_index.htm`.

Center Technology Corp. (2007). Center 309 four channel thermometer. `http://www.centertek.com/309.htm`. Thenical specifications CENTER 309.

CFD Online (2005). Approximation schemes for convective term. `http://www.cfd-online.com/Wiki/index.php?title=Approximation_Schemes_for_convective_term`.

Chaddock, J. B. (1986). Ventilation and exhaust air requirements for hospitals - part 1: Standards. *ASHRAE transactions*.

DMI (2007a). `http://www.dmi.dk/dmi/klima_ref_kbh.htm`.

DMI (2007b). `http://www.dmi.dk/dmi/index/verden/verdensvejr.htm?city=800852001&country=Hong+Kong`.

DMI (2007). Tekniske rapporter. `http://www.dmi.dk/dmi/index/viden/dmi-publikationer/tekniskerapporter.htm`.

DS474 (1994). *Norm for specifikation af termisk indeklima*.

DS/EN 15251 (2007). *Input-parametre til indeklimaet ved design og bestemmelse af bygningers energimæssige ydeevne vedrørende indendørs luftkvalitet, termisk miljø, belysning og akustik*, volume 1. Dansk standard. ICS: 91.040.01.

Electrical and Mechanical Services Department (2005). *Guidelines on performance-based building energy code*, 2005 edition.

ENERGINET.DK (2006). Landstal 2006: Elproduktion, brændselsforbrug og miljønøgletal. Spreadsheet.

Energistyrelsen (2006). Hovedtal fra energistyrelsens foreløbige energistatistik for 2006. Technical report.

Energitilsynet (2007). Elprisstatistik januar 2007. `http://www.energitilsynet.dk/prisstatistik/elektricitet/statistik-efter-januar-2007/elprisstatistik-januar-2007/`.

EnergyPlus (2007). Clima data for hong kong. `http://www.eere.energy.gov/`
`buildings/energyplus/cfm/weather_data3.cfm/region=2_asia_wmo_region_2/`
`country=CHN/cname=China`.

Environmental Protection Department (2007a). Air pollutants and greenhouse gas
emission inventory (1990-2005). `http://www.epd.gov.hk/epd/english/`
`environmentinhk/air/data/emission_inve.html`.

Environmental Protection Department (2007b). Legislative council panel on
environmental affairs. Progress report.

Erhvervs- og Byggestyrelsen (2008). *Bygningsreglement 2008*.

Esbensen Consulting Engineers A/S (2005). Hospitals - exemplar energy conscious
european hospitals and health care buildings, full final report, the country of south
jutland. Project No: NNE5-2001-00295.

Escombe, A. R., Oeser, C. C., Gilman, R. H., Navincopa, M., Ticona, E., Pan, W.,
Martý´nez, C., Chacaltana, J., Rodrý´guez, R., Moore, D. A. J., Friedland, J. S., and
Evans, C. A. (2007). Natural ventilation for the prevention of airborne contagion.
PLOS MEDICINE, 4(2).

European Commission (2005). Results. EU Proj. No: NNE5-2001-00295.

Flir Systems (2002). *ThermaCAM S40*. Thenical specifications ThermaCAM S40.

Flir Systems (2003). *ThermaCAM Researcher, User's manual*, 2.7 edition. Publ. No. 1
557 773 Rev. A – ENGLISH (EN).

Flovent (2005). On-line manuals. `http://www.flovent.com`.

Fluent Inc. (2005). The fluent user's guide. `http://www.engres.odu.edu/`
`Applications/fluent6.2/help/html/ug/node8.htm`.

Gan, G. (1994). Numerical method for a full assessment of indoor thermal comfort.
Indoor Air, 4:154–168. ISSN 0905-6947.

Google Maps (2007a). `http://maps.google.com/maps?q=aabenraa+sygehus&`
`ie=UTF-8&oe=utf-8&rls=org.mozilla:en-GB:official&client=firefox-a&um=1&`
`sa=N&tab=wl`. Seach result from Google Maps on Aabenraa Sygehus.

Google Maps (2007b). `http://maps.google.com/maps?tab=wl`. Seach result from
Google Maps on Grantham Hospital.

Grantham Hospital (2007). Grantham hospital. `http://www.ha.org.hk/hesd/nsapi/?`
`MIval=ha_visitor_index&`
`intro=ha%5fview%5ftemplate%26group%3dOSR%26Area%3dHNI`.

Hansen, H. E., Kjerulf-Jensen, P., and Stampe, O. B. (1997). *Varme- og Klimateknik,
Grundbog*, volume 2. Danvak, 1 edition. ISBN 87-982652-8-8.

Health, Welfare and Food Bureau (2003). Legco panel on health services, enhancement of infectious disease facilities in the public hospital system. Technical report. Paper No. CB(2)2658/02-03(02).

Heiselberg, P. (1994). Stratified flow in rooms with a cold vertical wall. Technical report. NO-94-16-1.

Heiselberg, P. (2002). *Principles of hybrid ventilation.* KOMMUNIK Grafiske Løsninger A/S, 1 edition. ISSN 1395-7953 R0207.

Heiselberg, P. (2006). *Modelling of natural and hybrid ventilation.* Aalborg University, Department of Civil Engineering. DCE Lecture Notes No. 004, ISSN 1901-7286.

Heiselberg, P. (2007a). Slides from the Modelling of natural and hybrid ventilation course.

Heiselberg, P. (2007b). Microclimate of buildings. pdf file.

Heiselberg, P. (2008). *Ventilation Systems: Design and performance / Edited by Hazim B. Awbi; Characteristics of natural and hybrid ventilation systems.* Taylor & Francis. ISBN: 978-0-419-21700-8.

Heisselberg, P. (2008). Teacher.

Helmut E. Feustel and Brian V. Smith (2001). *Comis 3.1 - User's Guide.*

Hong Kong Observatory (2007). The year's weather. `http://www.weather.gov.hk/wxinfo/pastwx/ywx.htm`.

Hoy, W. and Ross, T. (2005). Grashof number, a helpful way to look at convective effects. `http://www.owlnet.rice.edu/~chbe402/proj05/hoy/hoyroos/background/background.html`.

Indenrigs- og Sundhedsministeriet (2007). Sammenlign sygehuse og klinikker. `http://sundhedskvalitet.dk/Noegletal.aspx`.

Jensen, R. L. (2007). Dry. Spreadsheet. Spreadsheet with DRY weather data from the lecture IDBBS on 8th semestre.

Jones, P. J. and Whittle, G. E. (1992). Computational fluid dynamics for building air flow prediction - current status and capabilities. Technical report. Building and Environment, Vol. 27, No. 3.

Kowalski, W. J. (1996). Isolation rooms & pressurization control.

Larsen, K. (2007). Trenden i hospitalsdesign går i retning af enestuer. *Lægen i hovedstadsregionen*, (1):27.

Larsen, T. S. and Heiselberg, P. (2007). Single-sided natural ventilation driven by wind pressure and temperature difference. Technical report, Aalborg University.

LI, Y. (2007). Fresh air the key for isolation room ventilation. *Hong Kong Infection Control Nurses' Association*, (11):4.

Limb, M. (2002). An alternativ approach to infection control.

Nasjonalt medisinsk museum (2007). Ustanselige bronchnitter og blodspytninger. `http://www.tekniskmuseum.no/medisinskmuseum/sunn_sjel/tuberkulose.htm`.

National Environmantal Reseach Institute, Denmark (2007). Luftmålinger: Slå op i database. `http://www2.dmu.dk/1_Viden/2_miljoe-tilstand/3_luft/4_maalinger/5_database/HentData.asp#OverTabel`.

National Environmental Research Institute, Denmark (2005). The danish air quality monitoring programme. NERI Technical Report 584, Ministry of the Environment, `http://www.dmu.dk`. ISBN: 978-87-772-935-5.

Nielsen, P. V. (2008). Teacher.

Panel on Coastal Meteorology, Committee on Meteorological Analysis, Prediction and Research, Board on Atmospheric, Sciences and Climate, Commission on Geosciences, Environment and Resources, and National Research Council (1992). *Coastal Meteorology: A Review of the State of the Science*. NATIONAL ACADEMY PRESS. ISBN-10: 0-309-04687-4, ISBN-13: 978-0-309-04687-9, `http://books.nap.edu/openbook.php?record_id=1991&page=R1`.

PrivatHospitalet Skørping (2007). Privathospitalet skørping. `http://www.privathospitalet-skoerping.dk/index.htm`.

Qian, K. (2005a). Data recorded at the hong kong observatory headquarters (tsim sha tsui). txt file. Weather data measured from Keenwa Qian at The University of Hong Kong.

Qian, K. (2005b). Data recorded at wong chuk hang. txt file. Weather data measured from Keenwa Qian at The University of Hong Kong.

Region Nordjylland (2007). Ortopædkirurgisk Afsnit OK3. `http://images.google.dk/imgres?imgurl=http://www.ortopaedkirurgi.rn.dk/NR/rdonlyres/962C8F3B-5C39-4CD5-8560-148AD45B6288/0/K3_sengestue_l.jpg&imgrefurl=http://www.ortopaedkirurgi.rn.dk/Klinikker/Klinik%2BVendsyssel/AfsnitOK3.htm&h=150&w=225&sz=14&hl=da&start=4&tbnid=oPa6AXFL54WPOM:&tbnh=72&tbnw=108&prev=/images%3Fq%3Dsengestue%26gbv%3D2%26ndsp%3D18%26svnum%3D10%26hl%3Dda%26sa%3DN`.

Århus Kommune (2008). 2008 forbrugspriser for fjernvarme pr. 1. januar. `http://www.aarhuskommune.dk/view/borger/miljoe_energi/varme/borger_varme_priser_betaling/2008_priser_fjernvarme/view_col2_2008_priser_for_fjernvarme.htm?_page=4563736`.

Seifert, J., Li, Y., Axley, J., and Rosler, M. (2006). Calculation of wind-driven cross ventilation in buildings with large openings. *Journal of wind engineering and industrial aerodynamics.*

Sørensen, D. N. and Nielsen, P. V. (2003). Quality control of computational fluid dynamics in indoor environments. *Indoor Air*, (13):2–17. ISSN 0905-6947.

Vejle Amt (2003). *Den gode sengestue - retningslnier for indretning af sengestuer til plejekrævende patienter på sygehusene.*

Vejlefjord (2007). Vejlefjord dengang. `http://www.vejlefjord.dk/Vejlefjords%20historie-577.aspx`.

Wikipedia (2007). Earth cooling tubes. `http://en.wikipedia.org/wiki/Earth_cooling_tubes`.

Wikipedia (2008). Reynolds number. `http://en.wikipedia.org/wiki/Reynolds_number`.

Window Master (2007). Økonomi - naturlig vantilation er god økonomi. `http://www.windowmaster.dk/regado.jsp?type=page&id=52`.

Wittchen, K. B., Johansen, K., and Grau, K. (2004). *BSim Brugervejledning.* Statens Byggeforskningsinstitut, 5.6.3.8 edition.

World Health Organization (2007). Infection prevention and control of epidemic- and pandemic-prone acute respiratory diseases in health care - who interim guidlines. Who interim guidelines.

Yik, F. W., Lo, T. Y., and Burnett, J. (2003). Wind data for natural ventilation design in hong kong. Technical Report 24, Building Service Engineering Research and Technology.